CRANFIELD INSTITUTE OF TECHNOLOGY

SCHOOL OF MECHANICAL ENGINEERING

Ph.D. THESIS

ACADEMIC YEAR 1985-6

RAMIZ F. BABUS'HAQ

OPTIMAL HEAT TRANSFER DESIGN FOR DISTRICT-HEATING AND COOLING PIPELINES IN AIR-FILLED CAVITIES

Supervisors: Prof. S.D. PROBERT

Dr. M.J. SHILSTON

April 1986

TO MY FAMILY AND THE FUTURE

ACKNOWLEDGEMENTS

I am greatly indebted to Prof. S.D. Probert for his advice, guidance, continuous help and encouragement that made this study possible. Thanking him in this inadequate way leaves much to be desired.

I am grateful to Dr. M.J. Shilston, who paved the way and guided me whenever I needed direction.

I would like to express my special thanks and gratitude to the University of Technology and to the Ministry of Higher Education and Scientific Research, Baghdad, Iraq for providing the financial support and the award of a Research Fellowship.

I extend my gratitude to all members of the staff of the Photographic Department at Cranfield, since the present programme of work was heavily dependent upon their services.

I would also like to thank the staff of the School of Mechanical Engineering for their academic, experimental and administrative help during my course of study.

I gratefully acknowledge the typing of Mrs. D. Hoffman which was of the highest degree and to Mrs. B. Stalley who showed me how to use the word-processor.

ABSTRACT

District-heating and/or cooling systems are gradually becoming popular all over the world for heating and/or cooling of large premises.

Current conventional practice for the DHC underground distribution networks is to place the supply and the return pipelines side-by-side in air-filled trenches. However, the present investigation has shown that by optimising the location of the pipelines, the thermal insulation provided by the air around the pipes can be maximised. This is achieved by placing the hot pipeline above the cold one, the exact position depending upon the temperatures involved. For most purposes, it is recommended that the displacement ratio for the hot pipe is to be at -0.7 or -0.08 and that of the cold pipe at 0.05 or 0.67 for district heating or cooling respectively [i.e. the hot and cold pipes being placed in the upper and lower halves of the trench respectively].

Each chapter is presented in such a way that it can be read independently of the others as far as possible.

CONTENTS

CHAPTER 1

ENVOLVEMENT OF COMBINED HEAT AND POWER WITH DISTRICT HEATING OR COOLING

SUMMARY

Great Britain compares poorly with other European countries with respect to its rate of introduction of combined heat and power (CHP) together with district heating and/or cooling (DHC) systems. Sources of energy for such schemes, as well as developments in metering and control of CHP-DH systems are reviewed. Major governmental investments to encourage the wider adoption of these systems are needed urgently in the best interests of Britain.

ABBREVIATIONS

CEGB	Central Electricity Generating Board
CHP	Combined heat and power
DC	District cooling
DH	District heating
DHC	District heating and/or cooling
GLC	Greater London Council
ITOC	Intermediate take-off condensing turbines
SNG	Synthetic natural gas

GLOSSARY

Condensing boiler: A boiler with the ability to condense the water vapour in the combustion products by reducing the flue-gas temperature below its dew point.

Culm : Coal dust, especially of anthracite.

Discount rate : The rate of interest used in discounting costs and benefits with respect to investments.

Heliostat : A device consisting of a mirror which turns so as to always reflect the insolation, from the Sun, in a fixed selected direction.

Load factor : The average load divided by the designed maximum capacity of the installed system.

Operational pay - back period : Capital cost of the system divided by the savings achieved per hour by the installation of that system.

Premium fuel : A high-quality primary fossil fuel: electricity can be considered for some applications as the premium fuel.

Syncrude : Synthetic crude oil derived from coal or oil shale.

DISTRICT HEATING AND/OR COOLING SYSTEMS

An Overview

By these processes, a heated or cooled fluid (usually water) is distributed from a central source to residential, commercial or industrial consumers, usually in high intensity of demand areas (e.g. for well-occupied tall buildings) in which comfortable conditions need to be maintained. The central source may be either a chiller(1), a boiler(2), a refuse incinerator(3), a geothermal source(4), solar energy(5), or waste-heat, e.g. as a by-product of electricity generation(6). This latter approach is known generally as the combined heat and power (CHP) or cogeneration procedure. The extent of the delivery zone alone should not be regarded as the sole criterion for assessing the economic feasibilities of proposed district-heating or district-cooling schemes. A small project can be attractive financially if a sufficiently large heating or cooling demand exists, whereas it will probably be uneconomic to serve a large area having only low demands(7).

The History of CHP-DHC

A sufficient supply of heat is a basic human necessity. The Romans employed piped heating systems for dwellings as well as baths, whereas mediaeval castles had vast chimney-less fire-places, in which piles of logs were burned(8). Sir William Cook in 1745 used pipes for conveying steam to heat his home in

Manchester, England: he also attempted to warm a group of buildings in this same way from a single source of heat[9]. Subsequently, in 1748, Benjamin Franklin employed an underground iron-stove furnace to heat a row of houses, via a small district-heating scheme, at Philadelphia, USA[10].

Throughout the eighteenth century, in many places men were applying their wits, skills and hands to devise and improve heating services. Thomas Newcomen, a British mechanic, in 1712 took what in retrospect has been called "one of the longest steps in history" when he improved radically the primitive, steam-driven, water-lifting device invented by Thomas Savery[10].

James Watt in 1774 heated his upstairs workroom with heat derived from a basement boiler. Subsequently, in 1791, Hoyle of Halifax obtained a patent on a system involving pipes filled with steam to heat a building. In 1816, Jacob Perkins and the Marquis de Chambonne employed hot water as the heat-distribution medium for a system they introduced in England[10].

However, Birdsill Holly, in 1877, deserves the credit for being the first person to put district heating on a successful commercial basis[9]. By 1879, Holly's Corporation had nearly three miles of mains heating lines in service, and by 1880 the steam service had been extended to include several factories[11]. The potential for CHP was also evolving simultaneously: many small electric companies were set up to satisfy the eager appetite for electric supplies following Edison's pioneering

efforts at the end of 1870's. Electric generators, operated by reciprocating steam engines, were employed in plants sited in high population-density urban areas. Commonly the waste steam was exhausted to the atmosphere. However, as economies of scale began to be achieved in the generation of electricity during the early part of the twentieth century, the "total-energy" approach was abandoned, and so, at that time, district heating failed to gain in popularity.

By 1909, only about 150 district-heating systems existed in the United States, and many of these operated on low profit margins[11]. Significant numbers of district-heating installations were not installed in Europe until after World War Two. Since then, mainly in Northern European countries, the USSR (the largest user of district heating in the world) and the other communist block, centralised-planning, countries, DH systems have become common place. This was usually feasible and economic because of the building there of large (but compact) housing blocks: a policy which is favoured in many of these countries. District heating in the other European countries has grown in popularity less rapidly because of the low unit fuel costs during the last 40 years, and the abundance of available fossil fuels. Nevertheless, in the USA, district heating has been adopted frequently for college/university campuses , and for commercial multi- purpose buildings[12].

Due to the 1973/1974 and 1979/1980 oil crises, and the political reluctance to permit nuclear power to be substituted, in a

large way, for fossil fuels in the UK, the problem of energy thrift has, intermittently during the last decade, been regarded as urgent[13]. Thus the concepts of DH, DC, and CHP (or cogeneration) have become increasingly advocated as desirable in energy-thrift policies by many planners, architects, engineers and even some politicians[14-21]. For instance, DH is included in the US Government's energy-conservation programme and is now regularly commended in the British Parliament as an important means of reducing the national rate of fuel consumption[22-25]. Yet few of the good intentions have been translated into positive actions in the UK. However, in the USA, new systems (e.g. CHP/DHC systems in Trenton, New Jersey and St. Paul, Minnesota) have recently been brought into service as a direct consequence of the US Department of Energy and US Department of Housing and Urban Development grants and technical support[26-29].

DC is not so widely implemented as DH, but it is being advocated and adopted slowly as a financially-attractive process. One of the biggest systems in the world, outside Japan, is located in Hartford, Connecticut, USA: it was, in 1962, the first utility-operated district plant to market both chilled water and steam. Nevertheless fewer than sixty urban systems are in current use in the USA(12). Japan has been somewhat of a pioneer in the field of DC: even in 1981, it was estimated that about ninety different systems were in operation there. However, DC systems are already operating, or are being installed, in several cities of Europe and the USSR[30,31].

TECHNICAL CONSIDERATIONS

Basic Features

DHC systems usually consist of three major components[11]. The first is the production plant (i.e. the energy-release system) which provides either steam, hot water or chilled water. CHP is the production of heat as well as useful shaft power — see Fig. 1. However, recent thermodynamic availability studies applied to the processes involved in CHP plant, consider the optimal amounts of mechanical power and heat current as end-products[32]. CHP can involve topping cycles or bottoming cycles. In the more commonly-employed topping cycle, the generation of electricity is the prime aim, the exhaust stream heat being made available at various pressures and temperatures. In the bottoming cycle, heat is produced for process use, and relatively high-temperature and high-pressure waste heat is then recovered and used to generate electricity[33,34].

The second component in a CHP-DHC system is the transmission (i.e. the distribution) network, which conveys the heated or cooled fluid through pipes from the production plant to the consumers. DHC line-networks are expensive: they constitute at least 50% of the capital costs of the DHC supplies. The use of flexible pipelines, simplified fittings and compact measuring instruments could reduce the costs of distribution systems significantly[35,36]. Several design studies as well as behavioural tests have been undertaken, and computer-program packages for

predicting the performances of proposed CHP-DHC distribution networks have been devised[37-65]. Much time, effort and money have been devoted to producing reliable, cheap, well thermally-insulated underground pipelines, but unfortunately to date, these endeavours have not been completely successful[60].

Many CHP-DHC pipeline networks are buried; some of the available DH configurations being shown schematically in Figs. 2 –→ 9. The most frequently-recommended and widely-used design in the U.K. is that of two thermally-insulated pipelines, located side-by-side in an atmospheric-pressure, air-filled, rectangular trench -- see Fig. 10[29,66]. In the event of such a trench becoming flooded (which occurs intermittently in Britain, because of its maritime climate, high humidities and relatively high water-table levels), drainage and evaporation from around the pipelines can then ensue automatically. Otherwise, if the insulant is allowed to remain damp, the moisture reduces the insulant's effectiveness and mechanical strength (sometimes permanently), as well as promotes corrosion of the underlying steel pipelines, which are supposedly being protected by the insulant.

The third component of a CHP-DHC system is the "in-building" equipment. If steam is supplied by the DH system, it may be (i) employed directly for heating; (ii) directed through a pressure-reducing station for use in either a low-pressure steam space-heating system, a domestic water-heating system or an absorption-cycle refrigerating system; or (iii) passed through a steam-to-water heat exchanger in buildings employing hot-water heating

systems[11]. However in most hot-water systems, water-to-water heat exchangers are used[67].

Types of CHP-DHC Systems

DHC systems are classified according to the heat-transfer medium employed[11] :-

(a) Steam types

1: Heat-only systems, for which the boiler supplies only steam at the required design pressure to the distributio network[29].

2: CHP, cogeneration, or dual-energy use systems, in which the available steam is a by-product of the electricity-generation process. Back-pressure steam turbines, inter-mediate take-off condensing (ITOC) turbines, gas-turbines and diesel-engine driven generators are employed in such systems[34,68-72].

3: Supply or purchase systems, where steam surplus to the demands on other boiler plants, including refuse-incineration systems, is bought[73,74].

(b) Hot-water types

1: Hot water supplied from boilers at central locations in the system[75].

2: Hybrid systems, where there is a basic steam system which develops on-site hot water for a localised hot-water network[76].

3: CHP, cogeneration, or dual-energy use, where hot water is produced as part of an electricity - generation process[77].

4: Hot water obtained from geothermal sources[78,79].

5: Preheated water arising from refuse-burning operations; hot water extracted from an industrial waste-heat system (e.g. cooling water from a power station or a heating system return-pipe); or sea or lake water up-graded with respect to temperature by means of heat pumps [80-86].

(c) Chilled-water types

1: Chilled water produced at a central plant by steam-driven equipment[1].

2: Electrically-driven equipment producing chilled water at a central plant[87].

3: Absorption refrigerator (e.g. operating on a lithium bromide/water mixture)[11,88].

4: Natural cold-water direct-cooling systems, using fresh water sources such as lakes, reservoirs, rivers, ice ponds, and ground-water[34,89].

SOURCES OF ENERGY FOR CHP-DHC SCHEMES

Wood

Wood has a relatively low calorific value compared with those for bituminous coal and oil. Because cellulose (wood being its chief source) is the most abundant natural material on Earth, and we are not dependent upon it for food supplies, it is the logical choice for conversion to fuels. Several different procedures have been proposed in order to develop an economic process for the conversion of wood to liquid fuel. Such a process aims at maximising the rate of production of oil (which should have improved physical properties as a fuel relative to wood) and be achieved with the minimum consumption of heat and reducing gas[90,91].

Until the latter part of the nineteenth century, when it was replaced by coal, wood was the principal fuel for providing heat. However, it is no longer a major fuel source due to (i) forest depletion and (ii) the increasing demand for wood as lumber and for the production of paper, plywood, rayon and other products. Forest lands now comprise some 9.6×10^9 acres, which is equivalent to about 27% of the world's land area. The productive forest area is estimated to be 6.4×10^9 acres, some 4.0×10^9 acres of which being accessible economically[11].

Peat

It is desirable to avoid polluting the environment, and so one major advantage of peat as a fuel is its low sulphur content. However, the combustion of peat involves many difficulties and risks. The problems of operating peat-fuelled DH systems are due mainly to the impurities which occur in the peat, variations of its calorific value, and corrosion of the system's components. Ligneous matter, stones, pieces of metal, large lumps of peat and (even ice in winter), hamper the reception and handling. Their removal at the bog would reduce the combustion plant construction costs, but raise the unit price of peat appropriately. Mechanical handling of the peat is difficult: when used in silos, it is liable to arching, thereby possibly obstructing the feed mechanisms. The sand in the peat causes wear of the conveyors, and of the combustion and ash-removal equipment. Dry peat is extremely dusty, and so the risks of explosion (and fires) when using it are high.

For peat-fuelled DH schemes to be feasible commercially, peat must be cheap. However investment costs in the combuster equipment required are higher for peat than for oil or coal because the calorific value of peat per unit volume is lower and its handling problems are greater. The unit price of peat must therefore be correspondingly lower for it to be a commercial proposition as a fuel for DH systems. The competitiveness of peat is being improved continuously by technological development and standardisation of the DH plants using it.

Finland now has some 50 peat-fuelled heat-supply stations, with a total capability of delivering 230MW, as well as three peat-fuelled CHP plants: the combined thermal-power output of these three plants is 259 MW, together with 256 MW of electricity. In addition, a few peat-burning industrial plants also supply district heating alone[92,93].

Coal

Although the price of coal (in £ per kWh which is capable of being released) is generally lower than those for the other fossil fuels, and the UK national reserves of coal are substantially greater, coal consumption in the UK is unlikely to increase spontaneously during the next decade because of several technological reasons as well as some political ones. For direct combustion applications, coal is often less convenient to use, particularly with regard to storage and handling, than oil or natural gas. Also, combustion equipment, fired by coal, is often significantly more expensive than commensurate systems using premium fuels, and this off-sets the fuel price advantage of coal. In the case of electric-power generation, coal is facing increasing competition from non-fossil energy sources, namely nuclear and the "alternative" (e.g. hydro, wind, tidal and solar) powers. Furthermore, environmental protection standards are becoming increasingly more stringent, and this will lead to increased coal costs.

Technological improvements are required so that coal will make a greater contribution to future UK annual energy supplies. Many of the traditional markets for coal (e.g. railways or domestic open-fires) have almost completely declined and are unlikely to be reinstated. Therefore it is desirable to open-up new markets, such as those in CHP-DHC , where the economies of scale favour the use of coal. In Britain, the adoption of pneumatic coal-and-ash handling in a coal-fired CHP station at the Boots Co. Plc., Beeston, has resulted in a system that is both clean in operation and low in manpower requirements[94,95]. Nevertheless political leadership is required. As a further incentive in West Germany and France, coal - fired CHP - DHC plants benefit specifically from fiscal advantages and inducements arising out of national desires to substitute the use of coal for that of oil[30,96].

Coal-Derived Synthetic Fuels

The conversion of most types of coal (except anthracite) is directed primarily at producing synthetic low-sulphur, low-ash, liquid or solid fuels. Coal liquefaction shows promise for making commercially syncrude (a material suitable for use as a refinery feedstock) as well as petrochemicals. A wide range of liquid products, especially heavy fuels, distillate fuel oil, and gasoline, can be derived from coal by varying the operating conditions.

The Bergius single-stage process for direct liquefaction and hydrogeneration of coal was developed in the 1920's and proved to be viable, under the conditions of World War II in Germany. In the USA, there are three second-generation progenies of this process, none of which is predicted will be commercially successful before 1990. However, the chief means for indirect liquefaction of coal are the Sasol process and the Mobil-M process. Sasol-I, developed in the Republic of South Africa but based in part on German techniques, was in 1955 the only commercially-operating coal-liquefaction plant in the world. Sasol-II went into operation in the early part of 1980, and a site has been prepared for Sasol III. Both are modified and enlarged versions of Sasol-I. Notable improvements claimed for the Mobil-M process over Sasol-I are that it is much more selective in making gasoline, and its product has a higher octane number[97].

Coal gasification requires a higher chemical transformation (with gasification temperatures of about 1000 °C) than liquefaction, and achieves only a 60 –→ 70% energy conversion efficiency versus 78% for liquefaction. However, gasification is arguably the most versatile of the presently-available coal conversion processes, having applications in almost every sector of energy demand (e.g. industrial installations and power-generation systems). In most gasification processes, which are available for use or under development, the reactions are endothermic; air or oxygen being supplied to the gasifier. From the industrial user's viewpoint, the net result is a low or medium calorific-value gas. However, the medium calorific-value gas can be

up-graded to a high calorific-value gas -- called synthetic natural gas (SNG) -- by removing the sulphur compounds and carbon dioxide, and then passing the resulting gas to a catalytic methanation unit[97,98].

Fluidised beds have been developed, during the last 30 years, for achieving higher combustion efficiencies. The fuel (which, for instance, can be a mixture of anthracite coal and culm) is fed-in above the bed material, which is usually crushed limestone, sand, or crushed dolomite. Air is blown uniformly through the mix at a controlled rate: the resulting bubbling fluidised mixture acquires the free-flowing characteristics of a liquid and permits stable combustion to ensue throughout the whole bed. Moreover, the fluid-bed boiler is environmentally beneficial: it can satisfy existing air-pollution control regulations pertaining to SO_2 and particulate emissions[99,100].

Development studies on coal-water mixtures began in the 1970s. The main incentive is that the overall costs of using coal-water mixtures are widely expected to be substantially less than for coal-oil mixtures, because they avoid using the relatively expensive fuel oil component. Coal-water mixtures consist of a suspension of finely ground coal particles in water such that the resulting mixture may be pumped and generally regarded as a fluid fuel. The prospectively attractive economics of coal-water mixtures have encouraged the establishment of development programmes in several countries, the lead being taken by Sweden and the USA[98].

Refuse-Derived Energy

With landfill sites for burning refuse becoming scarcer, and environmental controls more costly to satisfy, some cities have built plants to recover artefacts and materials from refuse as well as to produce marketable energy from the residual municipal solid wastes. For example, Luxembourg uses 76% of its refuse for producing energy, while Denmark, Sweden and West Germany use 75%, 50% and 25% respectively for this purpose. In Japan, where refuse and sewage are increasingly used to make electricity, there are 63 energy-from-waste plants. Although some components of refuse are reclaimed and their valuable constituents recycled, vast tonnages per annum are still discarded, thereby incurring significant disposal costs.

It should be noted that cellulose is the most abundent chemical species in municipal refuse. Four tonnes of typical British refuse, could provide approximately the same amount of energy as one tonne of coal[101]. Nevertheless, three tonnes of pulverised waste a year could produce one tonne of waste-derived fuel pellets, with a specific calorific value about two-thirds that of coal[102]. At present, the UK produces about 30 million tonnes of household rubbish annually[103] and about 40% of this is combustible. It is reckoned that waste-derived fuels from refuse, have the potential to contribute 12 --> 14 million tonnes of coal equivalent per year to the British economy[104].

A British city with approximately 5×10^5 inhabitants, producing 150 kilo-tonnes of rubbish annually, spends about 1.5×10^6 £ each year on waste disposal. The calorific content of that rubbish is currently worth about 2.5×10^6 £: the energy saving alone would amount to approximately 30 kilo-tonnes of oil[102]. However the harnessing problem is compounded by the fluctuating amount and constituents of the refuse and the unit prices paid for energy. With the growing need to develop alternative sources of energy, municipal, commercial and industrial wastes are being actively explored as potentially useful sources of both materials and fuels[105-107]. DH from refuse incinerators is common in Europe, but it is only in recent years that it has been even contemplated or installed in Britain. Such schemes are now (1986) in service in London, Coventry, Sheffield, and Nottingham[88,108].

Refuse has been burnt successfully as a supplementary fuel in coal-fired boilers: for example, in the 100 MW unit at the Meramec station, of the Union Electric Company in the city of St. Louis, USA[88].

Oil

Before the 1973/1974 oil crises, oil-fired DHC plants were cheaper to run than coal-fired systems. Also coal has a much lower calorific value than oil, and it cannot be transported and stored as easily, neatly and cleanly. The plant required for the conveyance, storage and combustion of oil is simpler, requires less maintenance and can be operated more easily than the

commensurate coal plant. On the other hand, proven indigenous oil reserves are much smaller (~ 5% in tonnes) than those of indigenous coal in Britain, and there is an enormous competing oil demand to provide petrol, paraffin, plastics, ... etc. In consequence, the current price of oil per unit of heat content is far higher than that of coal, and this disparity is likely to increase. Oil is used to great advantage in transport systems. However, it is still sometimes financially advantageous to use the cheapest grade (i.e. the viscous heavy-fuel oils) in CHP-DHC systems. In this financial assessment, due allowance must be made for the expense of heating the oil to an optimal temperature (~ 60 °C), and maintaining at such a temperature, in order to reduce its viscosity, so permitting it subsequently to be pumped at the least total financial cost (i.e. for pumping power and heat losses)[30,109].

Oil Shale

Oil-shale deposits are widely distributed throughout the world, with the largest reserves being in the US and Canada[11]. The production of oil from oil shale has not progressed rapidly mainly because conventionally-obtained oil per gallon is usually still cheaper than that extracted from shale.

Natural Gas

This (i.e. predominantly methane) frequently occurs in the same geographic regions as petroleum. Due to its lower density, natural gas usually is found above the petroleum, trapped by a layer of non-porous rock. Such conditions create the high pressures which cause the gas to be discharged readily from a well[11].

The use of natural gas for stimulating CHP-DHC schemes is a relatively simple operation: the associated boiler plants can be straight forward and compact. The number of chimneys required can be deduced in accordance with the UK Clean Air Acts of 1956 and 1968 and their heights can be kept to a minimum, subject to standard and supply companies' codes[30].

Natural gas has captured major shares in each of the main energy markets in the UK excluding transport. Sales are expected to increase significantly during the late 1980s and then continue at approximately the same level at least to the end of the century.

By employing gas-fired condensing boilers significant improvements in the efficiency of combustion and performance are being made. Such boilers are now being designed to withstand the corrosive effects of condensation and these are capable of attaining practical efficiencies exceeding 90%. The condensing boiler is

now widely used on the European Continent and increasing numbers are being specified in Britain[110].

By 1984, over 30 gas-engine heat pumps had been, or were being installed in the UK, and their use achieves significant energy thrift. Design improvements and technological innovation for mass production are still required before the domestic heat pump is a more efficient alternative and a commercial competitor to conventional or condensing-gas boilers.

Small-scale CHP sets, based on gas-fired reciprocating engines, are becoming attractive in many circumstances and some 140 such units are now installed in the UK. However, it has been found that their operational pay-back period is 2×10^4 operating hours, which may ensue during two to five years, according to use[110].

Geothermal Energy

As a drill penetrates downwards through the Earth's crust, the temperature of the layer encountered generally increases: the magnitude of this rise depends upon the thermal conductivities of the rocks. Scientists now believe that heat is being produced continuously inside the Earth by radioactive disintegration; the interior of the Earth, like the Sun, being a continuously-operating nuclear furnace. The internal molten core of the Earth comprises an almost inexhaustible energy source. Usually when this energy reaches the surfaces layers of the

Earth, it is highly diffuse. However, in some regions it accumulates: from these it can be exploited more easily for direct (e.g. non-electric) uses or for the generation of electricity[11].

Extensive pertinent observations have been obtained in Iceland, New Zealand, Hungary, the Soviet Union (where the largest harn- essed geothermal heat source for DH exists) and elsewhere[30,111].

Several schemes occur in France for using subterranean hot water for DH purposes. One such successful scheme is at Carrieres sur Seine near Paris, which is not a volcanic region. The heat contained in the hot water has been supplied for over ten years to carry part of the heating load of a group-heating scheme for 800 dwellings(30). The Paris Basin DH system deliveres hot water (at 60 –→ 70 °C) for communities at Melun, Creil and Villeneuve la Garenne(97). Another geothermal DH scheme is at Creteil supplying a total of 5660 dwellings (including shops, offices, ...etc.)[78]. However, the Beauvais geothermal DH installation was the first in France to be designed for gas-engine driven heat pumps. The DH network there supplies floor heating for a development of over 1000 flats and commercial premises in 15 buildings, with a design load of 6.5 MW[79].

Parts of Great Britain have a similar geological structure to Northern France. Yet, there has been no direct commercial operating experience of geothermal installations in Britain since the Romans utilised such heat in the city of Bath almost 2000 years

ago. Experience from other countries suggests that the use of geothermal (including hot dry rock) resources has only a trivial adverse environmental impact[112].

Recent studies in the city of Ely, Minnesota, USA, led to the conclusion that the use of water-filled abandoned mines could be a potential heat source for district heating. The water so heated will be pumped from one of the shafts through a heat exchanger where the temperature is reduced by approximately 5 °C, after which it is either returned to the mine or discharged into an adjacent lake[113].

For many years, heat has been used to produce cooling[11]. However geothermal energy is rarely employed for this purpose. Nevertheless, space cooling is achieved by this means in Rotorua, New Zealand: a lithium bromide/water absorption unit (involving evaporation and condensation) produces the cooling. Highly corrosive contaminated water at about 150 °C from the geothermally hot strata is passed through a heat exchanger to raise the temperature of water in a piping circuit to 120 °C. This heated water is employed later to drive the absorption unit.

Recently, because of the growing interest in the use of solar energy and waste heat, there have been efforts to employ these energies to produce cooling. Achieving space cooling (via absorption units) of say a warehouse from the same geothermal resource that is used simultaneously for space heating of other buildings has the potential to improve the overall efficiency of use of the

geothermal energy. The potential for improvement is due primarily to a potentially increased load factor. Nevertheless, whether or not the provision of space cooling will actually increase the load factor depends on the temperature of the geothermal resource and the ratio of the cooling load to the heating load. It is expected that large-scale DHC systems will require geothermal resources with temperatures of exceeding 90 °C, and that the systems to be used will be designed to achieve a relatively large temperature-drop from the geothermal fluid. The first large geothermal space-cooling application is at present (1986) in the design phase: the city of El Centro, California is planning to use 115 °C fluid from the Heber resource area to provide about 230 kW of cooling via absorption units[11].

Solar Insolation

Heat from the Sun is potentially a major source of energy for stimulating DH systems. At present, only a small part of the solar insolation potential is being realized: the annual amount of solar energy which reaches the surface of the Earth is approximately 22,500 times as great as present world-wide total energy usage during a year[11]. Although the rising unit energy costs of more conventional sources have offset some of the barriers to the more widespread use of solar energy, other obstacles still remain. The principal ones include: the relatively low heat intensity of solar radiation; its daily intermittency and seasonal fluctuations, as well as it being subject to unpredictable

interruptions due to clouds, rain, snow, ...etc.; and the still relatively high cost of large solar collectors.

Many of the obstacles associated with central-station solar facilities are surmountable. For example, the Electric-Power Research Institute, USA, already has plans for solar electrical generation. These include the use of a large receiver, filled with helium, placed on an 80-storey high tower surrounded by 320 acres of reflectors. These reflectors will track the sun and be able to concentrate the radiant energy onto the receiver. Heated to 810 °C, the helium in the receiver will drive a turbine to produce electricity and then be passed through a cooling tower and reused[11].

As part of the Sunshine Project, the National Energy Development Organisation, Japan, completed two thermal electric-power generation plants, each with a capacity of 1,000 kW, in Nio-cho, Kanagawa Prefecture. While these installations have been put into use experimentally, the Organisation decided recently (1985) that because the commercial viability of these plants was contentious, they would henceforth be operated on a reduced budget. However, even though this particular project did not attain fully its expectations, it constitutes a significant step forward in the history of solar-stimulated power generation and has attracted world-wide attention. The central receiver's pilot plant has an output of 1,000 kW. Numerous heliostats, with plane mirrors, were installed around a 69-metre high solar-energy collection tower. The insolation reflected by these mirrors is concentrated at the

receiver on the top of the tower. This solar-heat receiver consists of numerous pipes coated with black paint. The water in these pipes is heated and vaporised, attaining a temperature of approximately 250 °C, by solar energy and temporarily stored in a steam drum at the uppermost part of the tower. From this, the steam is piped to five heat storage tanks (i.e. accumulators) on the ground, where the steam is compressed and stored in the form of hot pressurised water. These storage tanks have a combined capacity for storing heat equivalent to 3,000 kWh of energy. The necessary amount for power generation is then piped as saturated steam to drive a steam turbine (of rated output, 1 MW and rated steam temperature, 187 °C) and so generate electricity. The steam used for power generation is subsequently sent to a condenser and the reverted water is recycled to the heat receiver at the top of the tower[114].

For Japan, the theoretical availability of solar energy which is capable of being converted into electric power is estimated to be in the vicinity of 1.6×10^{14} kWh per annum. Of this, the practically usable amount has been predicted to be 6×10^{12} kWh. However, further efforts must be made to ensure a stable power supply by developing more efficient methods for collecting the solar power harnessed over vast sites. With present systems, only about 10% of the collected solar energy is converted into electricity, whereas the optimal conversion rate is expected to be about 20%. Technologies need to be developed to operate several such installations as one system through a commercial power network. Lof and Tybout[115,116] have developed a mathematical model

for predicting the costs of delivered solar energy for houses. This model has been validated by showing that the predictions agree with observations for two sizes of houses in eight US locations experiencing different climates. Several system design parameters were studied in addition to collector area, in order to determine the range of optimal values, including collector inclination, number of covers on the collectors, and heat storage capacity per unit collectors area.

During 1977, a research program was supported in Corsica, France for the conceptual design of a solar thermal-electric power plant for producing, continuously during daylight hours, 50 to 1,000 kW of electricity[117]. The design involved linear-focus collectors (operating at design temperatures from 180 to 250 °C), the heat store using stratification of the heat-transfer fluid itself, and the Rankine-cycle conversion loop, with a turbine expanding a heavy organic fluid (Fluorinert). The construction of an experimental prototype plant started at the beginning of 1980, and it is now connected to the local grid, i.e. it is one of the first major solar power plants in operation in the world, using this kind of collector and such high-efficiency turbines. Since October 1983, a solar-energy laboratory was associated with this power plant. The tests carried out there indicate that the plant can provide medium-temperature heat (at 150 -→ 300 °C), as well as mechanical and electrical power simultaneously.

A conceptual renewable-energy conversion system, suitable for industrial applications in the UK, was investigated[118]. A

computer program was developed to simulate the performances of the solar, wind and thermal storage sub-systems, either individually or in combination. The renewable heat and electricity system showed considerable advantages in performance over the equivalent single-source energy-conversion systems (i.e. a solar or wind only system). Typical improvements in heat output variability were noted. However, extensive further studies are needed to test the computer model for various system configurations and with a range of specified costs and investment conditions.

Nuclear Power

This appears, for the short term, to be the only large-scale realistic alternative to fossil fuels, even though solar energy will make an increasing contribution. Already it permits the generation of electricity at lower unit costs than those achieved using fossil fuels[119,120]. There are other advantages: in Switzerland, for example, reduced oil consumption and avoidance of air pollution (that accompanies the combustion of oil) were the main driving influences behind the nuclear CHP movement[121, 122]. Basically to be economic, a DH system fed from a nuclear-energy grid has to be very large (with a load exceeding 1000 MW) and so must usually supply many consumers: e.g. in West Germany, a DH grid network which covers the entire country is being constructed. In Switzerland, a reactor is intended to supply space heating to 65% of the population[30,123,124]. In the operation of such DH systems, it is necessary to vary the heat output drastically, yet keep the

plant running at a constant rate. Hence nuclear stations should not be used only for supplying heat: it is desirable that the heat and power generation should be combined using intermediate take-off condensing (ITOC) turbines to adjust the heat demand to the heat supply[30,125].

Although the capital investment required to develop a nuclear-based DH system is relatively high, the associated operating costs are usually low. This occurs partly because the cost of nuclear heat is affected only to a minor extent by the price of uranium (most of the costs being due to the purchase of equipment). The single most uncertain variable of such an approach is likely to be the financial outlay required to contend with the democratic opposition which all types of nuclear plant engender. In some cases, the emotionalism associated with such opposition may make the nuclear approach unfeasible politically[11,126,127].

Electricity

Using electricity to provide heat is relatively expensive per kWh. This occurs because, when electricity is produced from fossil fuels, only about one-third of the energy in the fuel is converted into electric power, and it requires a high capital investment plant to achieve this. Hence, even if domestic electric-heating appliances are taken as running at 100% efficiency, the overall thermal efficiency is less than 33%, i.e. much lower than the combustion efficiencies that can be achieved with fossil fuels[30]. However, in most circumstances in order to

achieve the higher electrical efficiency (even though it is still only ~ 37%) with nuclear generating plant, the heat is discarded at a temperature too low for most commercial applications.

In normal parlance, CHP is taken to imply cogeneration where commercial use can be made of both the electricity as well as the heat that would otherwise be rejected. It is also employed by industries who sell their excess electricity and/or heat to neighbouring facilities[11]. Nevertheless, industrial CHP schemes are well established in most industrialised countries including the UK, France, West Germany and Spain. There are (in 1986) more than 150 industrial CHP schemes operating in the UK, mostly privately owned, particularly in the paper, food and chemical industries[128,129].

DEVELOPMENTS IN THE METERING AND CONTROL OF CHP-DHC SYSTEMS

Obtaining revenue in the commercial operation of a DH and/or DC business usually occurs via the aid of meter readings, that record the amount of the product used. A meter is regarded as the impartial arbitrator between the supplier and the consumer. Thus meters should be sturdy, reliable, tamper-proof, and preferably cheap. These systems must be capable of sustained operation at a prescribed accuracy level to qualify as a measuring device in commercial service. No meter or metering system should be used to indicate the amounts of heat used if its accuracy cannot be tested in relation to standards (e.g. the National Bureau of Standards) [130].

It is interesting to note that Birdsill Holly's meter patent in 1880 preceded the first Edison electric meter by three years. Gas meters, however, were well-established devices, having been manufactured in the USA since 1832. The rate of progress in steam, and hot as well as chilled water, measurement during the past decade has been disappointing. If DHC is implemented rapidly, it will be a challenge for the instrument community to keep pace[11,131].

Current UK practice in the metering and control of heat-distribution systems is based largely on experience obtained with group-heating schemes in local authority housing and at various sites, particularly military, within Government estates. The nature of these market sectors has been particularly significant in determining the adopted control philosophy, which generally is a desire to limit the capital cost of group heating.

Heat-distribution systems, developed in conjunction with CHP, will differ from existing group-heating schemes in both technical and marketing features. CHP-DH will serve existing properties which already have their own heating systems of differing suitabilities for connection to a DH network. On the other hand, CHP-DH schemes will be installed progressively and on a larger scale than existing group heating systems -- potentially these could be city-wide. Moreover, the cost of CHP heat depends upon the temperature at which it is produced, and its unit fuel cost is relatively low. However, the capital costs of CHP-DH are high compared with the present alternatives[132].

The metering and control arrangements for a proposed CHP-DH system will form an integral part of the design. The standard of service desired by consumers in each market sector should be provided as cost effectively as possible, so as to achieve the maximum competitive advantage of CHP-DH over other heating systems. Not employing meters for the individual customers leads to the profligate use of at least 20% of the total energy consumed. In 1980, reliable electronic heat meters were introduced and proved to be acceptable. Currently, in the UK, only 300,000 dwellings, or 7% of total district-heating market, have any form of metering device[133].

A novel design has recently been proposed[134] for a heat meter: it (i) provides a direct connection across the consumer/network interface; (ii) controls the pressures in the consumer's system independently of the distribution system; (iii) measures accurately the water flow-rate taken by the consumer (and controls its maximum value); (iv) measures the temperatures of the water at the inlet and the outlet of the consumer's system; and (v) detects any leakage from or failure of the system. Nevertheless, the system should be controlled on the consumer's side entirely by two-way valves in order to enable (i) the lowest water-return temperature to be achieved, and (ii) the minimum volume of water to be taken. So a combination of the facilities offered by the normal direct system and by the heat exchanger system was needed. The requirements to measure the water flow accurately, and control the maximum volume rate, suggested the use of positive-displacement devices, such as rotary-vane meters

or piston meters. Arrangements have to be devised to deal with wear and the turn-down of the equipment. However, the performance of the proposed system[134] in the field has yet to be determined.

For a CHP-DH system, both the cost-effectiveness and acceptability of the chosen meter will vary between markets, and possibly even between individual consumers within the same sector. It is therefore likely that metering will be observed in some sectors, but not in others, and that different forms of metering, associated with different charging arrangements and tariff structures, will be applied in different sectors. For instance, as regards cost-effectiveness alone, the heat-metering of individual dwellings is unlikely in many situations to be cost-effective with CHP, because of the low marginal cost of the CHP heat which would be saved[135]. However, recent studies[136] suggest that metering would influence consumers and so result in a reduced peak heat demand, as well as a smaller annual consumption, thereby allowing other savings to be made in installed heating capacity. Nevertheless, this would not be the case for large consumers of heat,such as institutional buildings, because of their proportionally lower costs of metering. Alternatively, simpler and cheaper forms of metering could be adopted which would not measure heat consumption directly. An example, would be flow - metering alone, which has the additional advantage of encouraging low flow rates and low return-water temperatures[132].

At present it is the policy of many local authorities not to charge customers, on their group-heating schemes, according to metered consumptions. Sometimes the heating charge, often paid with the rent, is based on dwelling-design rate of heat loss or floor area, or number of bedrooms, and is set so as to recover the annual operating cost of the scheme (or of all the authority's schemes if it operates a "pooled" system of charges). This does not encourage, or result in, energy thrift by the individual customer. In some market sectors, the attractiveness of CHP-DH to consumers may well be enhanced by the provision of pre-payment facilities. Modern electronic pre-payments, coded onto magnetic cards, are flexible and can be programmed to take account of special requirements, such as charging OAPs at a lower rate, or providing a certain amount of free heat to 'look after' the building structure, or to reduce the likelihood of deaths from hypothermia[137-139]. Recently, an average saving of approximately 28% has been claimed for the Billingham DH scheme in which a package of metering, pre-payment, and time-clock, thermostatic controls has been installed[140].

Metering cannot be divorced from the question of financial charging arrangements, and of the tariff structure adopted for CHP heat supply. The tariff devised for each market sector should be such as to indicate to the consumers that they should use heat in such a way as to minimise the unit cost of its supply: the adopted charging procedure must also be perceived by consumers to be equitable. In the early years of CHP-DH development, tariff structures should also be designed to encourage the rapid take-up

of such schemes. One problem with the development of CHP-DH is that these requirements might sometimes be in conflict[132].

The UK 1983 Energy Act requires the Electricity Boards to publish tariffs for the purchase of electricity from private generators, and to state the principles upon which these tariffs are established. Tariffs have been published but principles have not, other than as informal statements[141,142]. However there is no statutory assurance that the widely-varying values of the Area Board tariffs are consistent with the principles that have been set down and discussed[143]. The principles, as can be deduced from informal statements by the Electricity Council, have not been related quantitatively to the Area Board tariffs and there are, in consequence, significant variations which affect adversely small CHP generation in particular. Tariffs supposedly based on these principles result in less than fair levels of remuneration for selling privately-generated electricity to the CEGB. Although the Electricity Supply Industry states that fully-harmonised tariffs will be made available equally to consumers, whether or not they are electricity generators, these have still to appear[142,144,145].

THE DEVELOPMENT OF CHP-DH IN GREAT BRITAIN

In Western Europe, more than three quarters of the currently existing 100 GW of DH load has been built since the end of the Second World War. Those countries in which DH supplies a significant proportion of the energy used for achieving warm comfortable

environments are West Germany (35% of the total load), France (20%) and Sweden (18%)[146]. But the prospects for CHP-DH in the UK contrast poorly with those in such countries, as well as in many Eastern European countries. Only the Nottingham system approaches the scope of even the smaller European ones. Essential extensive post-war reconstruction in Europe provided an excellent opportunity for introducing district heating; other contributory factors resulting in the relative lack of interest in DH in Britain include the major role of gas in the domestic sector and the different traditions in housing density between Britain and the rest of Europe[24,141,147-149].

At present, about two-thirds of the total energy used in electricity-producing power stations is dissipated wastefully as heat via cooling towers, rivers and/or the sea. The energy manager may wonder why he has to pay to heat the air or the sea directly. This 'wild heat' -- Britain's largest untapped energy source -- is equivalent to more than twice the amount of the electricity now generated. Annually (in 1985) it was equivalent to more than the total amount of natural gas brought ashore from the British sector of the North Sea and was enough to heat every home in Britain for that year. Denmark (one of the pioneers in CHP technology) satisfies 40% of its community heating needs via CHP. For Finland, the figure is 30%, whereas for Sweden the proportion is 25%. Europe has approximately 3000 such schemes. Many incorporate a refuse-incineration heat station, so satisfying the dual purpose of providing heat and/or electricity, as well as

reducing the volume of refuse needed to be transported to the declining number of suitable land-fill sites[150-152].

The first industrial CHP installation in the UK was at the Singer Factory on Clydebank in 1898. Early CHP - based district heating schemes soon followed. In 1911, a small power station was modified in Bloom Street, Manchester to supply steam to neighbouring shops, offices and factories. In 1920 and 1922 respectively, DH schemes were started at Dundee (the Logie scheme) and at Stirling. In the Dundee scheme, four blocks of buildings, divided into flats, were supplied with hot water. Since then, with the exception of a few housing blocks supplied with district heat on a small scale, there have been only a few notable developments. However, one is the Whitehall scheme which supplies all the government buildings in that area. Another, is the Pimlico DH undertaking in London, which was commissioned in 1950 to serve a community of about 11,000 people using waste heat from Battersea power station (which was closed down in 1983). In 1960, a scheme was introduced based on Spondon power station near Derby to supply steam to the adjoining Courtaulds Factory. Another municipal scheme (the largest UK coal-fired group-heating scheme) was introduced in 1965 at Billingham using a central- boiler plant and circulating hot water[8,129,153-155].

DH, has not been popular in the UK, partly because of the difficulties encountered, as might be expected with any new technological venture. In the early stages some schemes proved to be financially disastrous because of inexperience in the operation

of this new form of public utility service. Latterly there have been some failures due to the use of unproven methods for the design and installation of the transmission network. However, despite setbacks of this kind, interest in DH has grown steadily[8].

The oil-price shock in November 1973, and the subsequent fluctuations of the unit price of crude oil have encouraged UK interest in alternative energy systems, including CHP. A well-attended Institute of Fuel (now Energy) conference in December 1971 was devoted to "Total Energy" (subsequently called CHP) (156). On investigating such a scheme in detail, it became clear that there were grave disadvantages in Total Energy schemes as then practised(157). By the end of 1974, the Government established the CHP Group, under the aegis of the Secretary of State for Energy's Advisory Council on Research and Development to consider the economic role of CHP in the UK and to identify technological, institutional, planning, legal and other obstacles to the fulfilment of that role, and to make recommendations. Their report was published in 1977 as Energy Paper No. 20[158] by the Department of Energy in the form of a discussion document. It resulted in extensive discussions and has been largely accepted as one of the most comprehensive assessments attempted in the area of CHP-DH. The medium-term analysis of CHP assumed that both natural gas and oil would be available as fuels for heating for ~ 15 years. However, it was assumed that reserves of these fuels would, in the longer term (> 50 years), be severely depleted and so would not

be available for space-heating purposes: by then the energy economy would be nuclear and coal based.

In July 1979, the CHP Group produced the Marshall Report, which appeared as Energy Paper No. 35[159]. Relatively little use to that date had been made of CHP for domestic or commercial space and water heating purposes in the UK, by contrast to the situations in countries such as Sweden, Denmark and West Germany. They concluded that the major reason for this was the availability of a convenient and highly-competitive alternative, namely the use of natural gas, for which an elaborate distribution network already existed in the UK. Heat from CHP stations could be competitive with heat derived from burning natural gas only in densely-populated cities, where the heat loads are highly concentrated. However, in these areas, natural gas is already supplied to consumers as an established cheap and convenient fuel. Nevertheless, in the longer term, large CHP plant appears to be an attractive, economic and energy-thrift option compared with other developed forms of heating. The Group reported that energy savings by the adoption of CHP-DH economically - viable schemes[159] might amount to as much as 30 million tonnes of coal equivalent per year, a figure representing between 5% and 10% of the probable UK primary annual energy demand beyond the year AD 2000. The comparative economics of the alternatives at 5, 10, and 15% discount rates in 1976 money values were presented for the long term. The economics of CHP are very sensitive to the discount rate and the choice of the appropriate figure is a key issue. CHP has a clear advantage over other options at a 5%

discount rate, when the unit fuel prices double in real terms. However, at a 10% discount rate, CHP has only a small advantage even for high dwelling densities. At 15% discount rate, gas-fired central heating generally has the advantage over CHP. The standard Treasury discount rate is 7% (it stood for a long time at 10%). This is the rate used for public sector appraisal of investments in projects[160]. Figure 11 represents the situation for marginal costs of long-term (i.e. to persist beyond AD 2000) alternatives at a 10% discount rate.

The public responses to contemplated CHP schemes were regarded as probably the most important consideration to be settled before initiating a lead-city project. Financial assistance from the Government appeared to the Group to be highly desirable in order to help CHP schemes to 'get off-the-ground'.

The Marshall Report included the results of a survey of actual and potential CHP users. Of the 56 companies which had considered the use of a CHP scheme, 26 rejected it: the dominant reasons being given as unattractive overall economics and capital shortages. The tariffs for the supply of electricity and "buy-back" provisions offered to CHP operators by Electricity Boards were also quoted as obstacles. It was also clear that a high plant load-factor was a necessity for CHP to be commercially viable[141].

One reason for the apparent lack of interest in industrial CHP is the decline of British heavy industry relative to that of

our competitors. UK industrial energy demand peaked in 1973, and by 1980 had declined by 25%, and a further 5% by 1981. This undoubtedly has greatly lessened the scope for development and modernisation[157]. In 1983, for the first time ever, an adverse balance-of-trade in manufactured goods occurred for the UK, which now relies on oil to keep its current account in surplus[161]. This adverse trend with respect to manufactured goods appears unlikely to change for the immediate future.

In April 1981, a further report, produced by Members of the Building Research Establishment and the Atomic Energy Research Establishment, was published by the Department of Energy[135]. It deduced that for the conversion of an existing city to CHP-DH, where the cost of the mains network is important, estimates were around 30% less than those given in Energy Paper No. 20. The reduction in the estimates resulted mainly from an examination of the cost of a real network serving commercial and institutional property as well as housing. The study concludeded that the overall cost-effectiveness of converting an existing city to CHP-DH would not be greatly affected by: (i) the size and location of the CHP station, (ii) the cost-effective improvements to the thermal insulation of dwellings, and (iii) whether or not the supplies of heat to domestic customers were metered[24].

In response to the Marshall Report, the Government announced that it proposed to initiate investigations concerning the feasibility of CHP-DH schemes in particular locations in the UK. The first stage, which was undertaken by consultants, identified

possible locations where CHP-DH might be an economic proposition. The second stage was to involve a detailed examination of several locations with a view to using them as lead-city schemes. The Government took the view that a National Heat Board, as proposed by the majority of the Marshall Group,was unnecessary, at least at present, because in the early stages of any development programme the investigations and analyses would be carried out mainly by consultants, local government and local interests[154].

The first stage was carried out by the consultants W.S. Atkins and Partners, whose report was published in August 1982 (and as Energy Paper No. 53 in 1984) [162]. The report indicated that nine cities showed promise with respect to the economic feasibility of installing a major CHP-DH scheme: these were Belfast, Edinburgh, Glasgow, Leicester, Liverpool, London, Manchester, Sheffield and Tyneside. In these cities, high density heat load areas of 20 MW per square km or more were identified, with a peak heat requirement of 100 MW per square km or more[154]. The composition of domestic central-heating costs using electricity, coal or gas, and the derived price of DH, for four representative years was presented for Great Britain (i.e. excluding Northern Ireland) -- see Fig. 12. A separate assessment has been under-taken for Northern Ireland where unit fuel prices are higher than in the rest of the UK.

In April 1984, the Government's Department of Energy announced that it was initiating the second stage of the investigation, and would contribute £750,000 towards further detailed studies,

including engineering-design, financial and marketing plans for large scale CHP-DH schemes in up to three of the chosen cities. It invited applications from local consortia involving both the public and private sectors to obtain grants to prepare prospectuses for the implementation of CHP-DH systems[154].

Since the publication of the report, much has happened. Sheffield's City Council has refined its plans, and formed a consortium to implement them[163]. In Tyneside, a detailed programme of work was proposed to be undertaken by the consortium members, the CEGB and the financial advisers: the end-product would be a practical CHP scheme funded by the private sector. The first phase of the development -- representing about 20% of the final scheme -- was based on refuse incineration as the heat source[164].

In London, the Borough of Southwark has (i) examined the prospects for CHP-DH within its boundaries, (ii) considered the potential impacts of installing DH mains in an existing built-up area, and (iii) investigated the possibility of interconnecting its major existing DH schemes[165,166]. A GLC-sponsored study by Orchard Partners has concluded that a coal-fired CHP-DH development could ultimately meet half the heating requirements of London's Inner Boroughs[165-168]. The study also concluded that the proposed development would (i) benefit electricity consumers to the same extent as a new nuclear-power station, and (ii) make a real return of 5% per annum on its DH operation, which is the same as that required for the gas and electricity-supply

industries. Moreover, it would provide heat to customers at 20% less cost than otherwise would be incurred. The development as envisaged, would, by the year AD 2012, encompass a total connected heat load of 2895 MW. However, this capacity would be provided by a staged construction of six CHP sets all located on the CEGB's Barking site. The scheme is three times the size envisaged in the Atkins Report. Nevertheless, the Outer London Boroughs were also found to be suitable for DH.

There was a worry for the towns involved in the CHP-DH studies, that by involving suppliers of equipment or services to be members of the consortia, they will be allowing these companies to be in a very strong position even while the plans are being drawn up[166-168].

In January 1985, the Government announced the winners of the grants, of up to £250,000 (per city) to fund research study groups and their city's prospects for implementing a CHP-DH scheme. The three British cities were Belfast, Edinburgh and Leicester. This reflects the Department of Energy's fundamental aim to incorporate one city from each of Northern Ireland, Scotland and England in the overall investigation. Substantial private sector funding has provided additional capital to finance extensive analysis of CHP-DH prospects in all the three cities considered[169].

Belfast, whose award of £250,000 was a forgone conclusion, could also opt for conversion of a power station -- in particular

the site at Belfast West. Alternatively, the city may choose a CHP station close to the rich deposits of soft brown coal (i.e. lignite).

Members of the Edinburgh consortium while undertaking an 18-month feasibility study, are concentrating on developing the engineering procedures and economics for a CHP scheme, within an area containing the highest proportion of offices and public buildings and the lowest proportion of industrial floor space of any of the nine cities short-listed in the Atkins Report[162]. If the detailed study confirms the viability of using the Cockenzie Power Station as the prime source of heat, alterations will be made to the generating plant and to the operating regime to divert some of the heat produced through the district-heating system. Two additional sources of fuel have been considered in the design of a system for the city: namely refuse incineration and a coal-fired boiler station at Dalry[170,171].

A consortium of varied interests has come together in Leicester. The proposed CHP plants would generate heat in a useable form with electricity as a by-product. This would increase the efficiency of the fuel used from 35% to 75% approximately[172,173].

Despite only three cities out of the original list of nine having been chosen to feature in the prospectus, it is probable that CHP assessments will continue in the other cities despite, at this stage, their lacking Governmental support. For instance,

the consortium of businesses and local authorities, which submitted a plan to build a multi-million pound CHP plant on Tyneside has decided to press ahead. They were anxious not to waste the preparatory investigations that had already been completed, and which have led to considerable interest from potential customers for the "cheap" heat to be produced, and from other firms working in this area, who are not at present involved in the Tyneside scheme(174).

Given that London has consistently come out on top in the Department of Energy's recommendations for suitable venues for CHP, the GLC-led consortium is now independently funding further work on CHP for London with approval from the Department of the Environment. The Council is commissioning two engineering consultants, Orchard Partners and W. S. Atkins in the London Boroughs of Southwark and Tower Hamlets respectively, to undertake detailed studies and to investigate the potential for a core scheme or schemes. Reports will be due in February 1986 and are intended to encourage the early development of CHP in London after April 1986(169,175,176).

A research project into small-scale CHP, covering parts of South London, was officially launched during December 1985. The scheme uses equipment producing as little as 15 kW of electricity and 40 kW of heat. It was organised by London's South Bank Polytechnic with the help of the Inner City Partnership. Efficiencies of up to 85% are being attained(144).

However, the city which has probably achieved most progress towards realising its own CHP scheme is Sheffield: already it has received a grant from the EEC towards the cost of its study. The scheme has been designed to be implemented in two stages. The first stage will be based on an existing refuse incinerator and a new heat station using fluidised-bed technology with in-bed de-sulphurisation. The second stage will be based on a new CHP station using coal-gasification combined-cycle technology with de-sulphurisation. Many institutional and commercial buildings, with firm heating requirements, will be supplied, together with two large existing residential group-heating schemes[154,176,177].

Superficially this would appear to be a time of hope for advocates of CHP in the UK. However, in practice, the opposite is true: pessimism prevails because of the Government's requirement that approval for city-wide CHP will depend on the availability of private finance. Also there is a conflict of interests between CHP and the existing power utilities: the widespread introduction of CHP in the UK would contribute significantly to fuel thrift by reducing the demands for gas, electricity and coal whose suppliers each still compete to sell customers more of their fuel(see Fig. 13). Investment in a public utility, like a power station, is essentially long term and therefore is fundamentally less attractive to private investors. A further problem could arise from the shorter economic life assumed for privately-funded CHP and electricity generation stations. There is little likelihood of the private sector competing with the CEGB for large-scale electricity-only power stations. This is despite the

publication of the 1983 Energy Act, which was heralded as paving the way for competition from the private sector[29,154,178] — see Fig. 14. Currently, the CEGB has only one small CHP-DH scheme operating in Hereford: it uses two 7.5 MW diesel generators[179]. However, some of the older coal-fired DH schemes have been modernised with respect to the introduction of simplified (but more comprehensive) controls, which can be individually monitored by the user. This has resulted in lower overall costs, and particularly smaller running costs. The range of options for refurbishment, which an authority may wish to consider, can be very broad. Apart from fuel switching and/or a change of heat source, they include (i) installing consumer controls, heat emitters and heat meters as well as improving the thermal insulation in the dwellings, (ii) installing hydraulic controls and increasing the hot-water storage in the local plant rooms, and (iii) improving the scheme efficiency by 'tuning' the existing boiler plant. It is also important to be satisfied as to the cause of failure in the heat mains before contemplating replacement. For instance, Fig. 15 indicates a range of alternatives which can be adopted with respect to a DH scheme in the UK. It demostrates the projected costs of DH upgrading and refurbishment for the next 30 years[140]. Nevertheless, it is assumed that heat mains have an average service life of 25 years, and that mains repairs will increase at 0.085 repairs/km/annum. Conversion of firing from oil to coal is also assumed.

CHP linked to DH may yet become highly competitive. Many <u>small</u> CHP schemes are being installed in the UK, often driven by

modified automobile engines e.g. the Totem system[157,180-183]. However, in national macroeconomic terms, there is a serious disadvantage in biasing CHP development towards smaller schemes. Such schemes will generally be based on oil and gas, and so cannot offer the long term balance-of-payments benefits that would accrue from large city-wide schemes using coal and, eventually, nuclear energy[154].

DH will struggle to compete with off-peak electricity and domestic or imported natural gas. SNG produced from coal is estimated to be two to three times the price of today's natural gas, even given the availability of secure and relatively cheap coal supplies. Both coal and nuclear power, which provide the most immediate and substantial options for diversifying the energy economy, are the subjects of deep divisions of opinion in society. The miners' strike revealed significant differences about the future role of coal in the UK energy economy, and over the modernisation of the methods of coal excavation[24,161].

The introduction of CHP would reduce the rate of demand for coal in the UK. However, it would increase the overall percentage of coal in the UK's total annual energy consumption. Clearly this would not be universally welcomed, and there are those whose cynicism is such that they believe that the conditions attached to the funding of the lead-city schemes have been contrived to prevent such an outcome. Even if this depressing view is rejected, it is still hard to believe that the situation is fair or even remotely likely to provide a proper basis for the assessment

of the potential benefits of CHP. Without such an assessment, there is the distinct possibility that British society will be poorer because of the failure to implement CHP-DH and, for some, this will mean being very much colder[154]. The Government appears to have no energy policy. It prefers to interfere as little as possible, yet allegedly let market forces (with Government interference) control the development of the electricity, gas and coal industries. But this may not be the wisest approach to see us into the next century[184,185]. Nevertheless, the Energy Secretary, Peter Walker, has claimed[151] that he can make Britain the most energy-efficient country in Europe. To achieve this will require Government leads and investments with respect to CHP-DH and a more reasonable (i.e. what is in the best interest of Britain) approach from the Electricity Boards!

CONCLUSIONS

District heating (DH) and cooling (DC) are means of distributing heated or cooled fluid respectively, from a central source to highly occupied areas. Combined heat and power (CHP) or cogeneration is the production of heat as well as useful shaft power. The available sources of energy for CHP-DHC schemes have been discussed. With greater incentives to develop new sources of energy, municipal, commercial and industrial wastes are being explored actively as potentially-useful sources of both materials and fuels. Of the non-conventional fuels, nuclear energy, solar energy and coal-derived synthetic fuels show promise as large-scale realistic alternatives to fossil fuels for CHP-DHC.

The selection of metering and control arrangements for CHP-DHC systems will form an integral part of the design. Yet, the rate of progress in this field has been dissappointing. Avoiding the use of meters leads to the profligate use of at least 20% of the total energy consumed. However, at present, it is the policy of many local authorities not to charge customers according to metered heating consumptions. Nevertheless, modern electronic pre-payments, coded onto magnetic cards, are flexible and can be programmed to take account of special requirements.

While the use of CHP-DH may well be economic overall, tariffs must be so structured so as to make it financially attractive for as many individual consumers as possible. The electricity supply industry states that fully-harmonised tarrifs will be made available equally to consumers whether they are electricity generators or not. Unfortunately, these have still to appear!

The future development of the CHP-DH in Great Britain is uncertain. An analysis of the principal parameters indicating the major trends has been discussed in this paper. It would appear that large-scale CHP-DH schemes will not be developed, in the near future, without government financial support. However, in the mean time, the government has offered to contribute towards the cost of planning the CHP-DH supplies for three cities: namely Belfast, Edinburgh and Leicester. More encouragingly, the Electricity Supply Industry is working closely with the municipal authorities in the cities of London, Newcastle, and Sheffield to develop CHP schemes.

Many small CHP schemes, driven by modified automobile engines, are being installed in the UK. There is a serious disadvantage in biasing national policy towards the use of such systems. They are generally based on oil and gas, and so cannot offer the long-term balance-of-payments benefits that can accrue from large city-wide schemes using coal and eventually, nuclear energy.

ACKNOWLEDGEMENTS

The authors wish to thank the University of Technology, Baghdad, Iraq, for the award of a Research Fellowship to R.F. Babus'Haq to permit this review to be undertaken.

REFERENCES

1. G.S. Farkas, Energy conservation through technology in comfort cooling, ASME Winter Annual Meeting, Atlanta, USA, 1977, Heat Transfer in Energy Conservation, ed. by R.J. Goldstein, D. Didion, R. Gopal, K. Kreider and R. Schoenhals, ASME, New York, USA, 1977, pp. 121-126.

2. D. Neil, The role of the boiler in DH, Building Services Eng., 44, 1976, pp. 50-51, 53-55.

3. S. Griffin, Waste equals grist for the mill as Swiss take up recycling, Smithsonian, 11(8), 1980, pp. 143-148.

4. G.M. Reistad and T. Lawrence, Geothermal DH models: a review of compatibility and validity, ASHRAE Trans., 90 (1B), 1984, pp. 313-344.

5. P.D. Lund and J.T. Routti, An analysis of district solar ponds with heat pumps, Int. J. Ambient Energy, 4(4), 1983, pp. 187- 192.

6. R.T. Mahini and V.E. Schrock, The use of waste heat in district systems with consideration of seasonal heat-demand variations, Berkeley: University of California, USA, 1982, UCB-NE-4022.

7. A.S. Kennedy and J.F. Tschanz, DHC -- a 28 city assessment, Illinois: Argonne National Laboratory, USA, 1983, ANL/CNSV-TM-119.

8. F.B. Turpin, District heating, Haywood Books, London, England, 1966.

9. J.F. Collins,Jr., The history of DH, District Heating, 62 (1), 1976, pp. 18-23.

10. R. Meador, Cogeneration and DH - an energy-efficiency partnership, Ann Arbor Science Publishers, Inc., Michigan, USA, 1981.

11. IDHA, District heating handbook -- a design guide: vol.1, 4th. ed., International District-Heating Association, Washington DC, USA, 1983.

12. D.O. Meeker, Jr., DHC in the USA: prospects and issues, National Academy of Sciences, National Academy Press, Washington DC, USA, 1985.

13. J.T. McMullan, R. Morgan and R.B. Murray, Energy resources, 2nd. ed., Edward Arnold Publishers Ltd., London, England, 1983.

14. Anon, German DH progressing, Building Services and Environmental Eng., 7(6), 1985, p. 6.

15. L. Thornquist, Socio-economic, political and institutional aspects associated with the introduction of CHP-DH in Sweden, The Swedish Experience, Combined Heat and Power/District Heating, Swedish Council for Building Research, 1985, D16, pp. 48-73.

16. O. Lagerholm, The future role and characteristics of CHP-DH systems in Sweden, The Swedish Experience, Combined Heat and Power/District Heating, Swedish Council for Building Research, 1985, D16, pp. 98-107.

17. Anon, Norwegian plans to augment the DH networks, Heating and Air Conditioning, 55(635), 1985, p. 23.

18. Anon, The future of DH systems, Heating and Air Conditioning, 54(633), 1984, p. 15.

19. Anon, US Navy goes for CHP, Building Services and Environmental Eng., 7(2), 1984, p. 21.

20. Anon, Cogeneration: DH turns problem into profit, ASHRAE J., 27(1), 1985, p. 13.

21. Anon, Burroughs plans cogeneration units, ASHRAE J., 27(7), 1985, p. 11.

22. A.E. Haseler, DH and telethermics - new data on heat mains, Building Services Eng., 42, 1975, pp. 257-272, 42, 1975, pp. 273-285.

23. N. Jenkins, CHP -- the battle hots up, Consulting Eng., (Sep.), 1983, p. 32-35.

24. House of Commons,CHP, vol.1, 3rd. Report from the Energy Committee, Session 1982-1983, HMSO, London, 1983.

25. P. Rost, CHP-DH and the UK, The Swedish Experience, Combined Heat and Power/District Heating, Swedish Council for Building Research, 1985, D16, pp. 11-17.

26. C. Stein, Trenton's down-town system, ASHRAE J., 27(2), 1985, pp. 36-43.

27. Anon, St. Paul's DH completed early, ASHRAE J., 27(3), 1985, p. 16.

28. R.W. Porter, Economic distribution distance for cogenerated DHC, Energy, 10(7), 1985, pp. 851-859.

29. IEA, DH and CHP systems: a technology review, International Energy Agency, Paris, France, 1983.

30. R.M.E. Diamant and D. Kut, DHC for energy conservation, The Architectural Press, London, England, 1981.

31. Y. Suzuki, P.S. Pak and K. Ito, Total planning of combined district heating, cooling and power generation systems for a new town -- parts I and II, Energy Research, 8, 1984, pp. 61-75, and pp. 77-87, respectively.

32. J.H. Horlock and R.W. Haywood, Thermodynamic availability and its application to CHP plant, Proc. I. Mech. E., 199 (C1), 1985, pp. 11-17.

33. R.R. Hite and G.M. Fielding, A design concept for Caltech, ASHRAE J., 27(7), 1985, pp. 24-29.

34. Center for Renewable Resources, Renewable energy in cities, Van Nostrand Reinhold Co. Inc., New York, USA, 1984.

35. H.E. Brachetti, Studies and tests specific to requirements for avoiding construction faults, Fernwarme Int., 13, 1984, pp. 100-102.

36. H.E. Brachetti, Studies relating to specific demands in the further developments of DH lines, Haustechnik-Bauphysik-Umwelttechnik, 99(5), 1978, pp. 117-122; 99(10), 1978, pp. 285-291; and 101(11), 1980, pp. 317-319.

37. R.F. Babus'Haq, S.D. Probert and M.J. Shilston, Improved configuration for DC pipelines, Applied Energy, 16(1), 1984, pp. 67-76.

38. R.F. Babus'Haq, S.D. Probert, M.J. Shilston and A. Talati, Suggested design improvements concerning DH pipeline configurations, Applied Energy, 17(2), 1984, pp. 77-96.

39. R.F. Babus'Haq, S.D. Probert and M.J. Shilston, Optimal location of a single horizontal pipeline in a rectangular, horizontal, air-filled enclosure to achieve maximum thermal insulation, Applied Energy, 18(4), 1984, pp. 239-259.

40. R.F. Babus'Haq, S.D. Probert and M.J. Shilston, Improved pipeline configurations for DH in Great Britain, 6th. Nat. Conf. CHPA, CHP -- Developments and Decisions, Torquay, England, 1985.

41. R.F. Babus'Haq, S.D. Probert and M.J. Shilston, Steady-state heat losses from horizontal pipes in an air-filled rectangular concrete duct, Proc. I. Mech. E., 199(C3), 1985, pp. 203-213.

42. R.F. Babus'Haq, S.D. Probert, M.J. Shilston and S. Chakrabarti, Optimising the location of a DC pipeline in a rectangular trench, Applied Energy, 23(2), 1986, pp. 109-141.

43. R.N. Quade, J.D. Stanley and T.H. Van Hagen, A new pipeline design for high-temperature fluids, 18th. Intersociety Energy Conversion Eng. Conf., Orlando, USA, 1983.

44. A.G. Usher and P. Rouhiainen, Efficiency in sizing and analysing DH networks for city CHP schemes, 5th. Nat. Conf. DHA, Planning for CHP Heat, Torquay, England, 1983.

45. H.H. Bau, Convective heat losses from a pipe buried in a semi-infinite porous medium, Int. J. Heat Mass Transfer, 27(11), 1984, pp. 2047-2056.

46. V.S. Khokhlov, Operation of storage tanks for topping up DH networks, Energetik, (10), 1984, pp. 29-30.

47. N.I. Serebryanikov, E.K. Kuznetzov and V.A. Zakharov, Operating experience and basic ways of improving the heat-supply networks in Moscow, Energetik, (11), 1984, pp. 8-9.

48. Orchard Partners, The development of CHP with DH in London, Report No. 4: The costs of local heat distribution and building connections, Orchard Partners, London, England, 1983.

49. P.S. Woods, The design and costs of large-scale DH net-works, Pipework Design and Operation Conf., I. Mech. E., London, England, 1985.

50. Anon, Computer-aided planning method of DH systems, Energy Digest, 13(2), 1985, pp.11-16.

51. E. Figwer, Pre-insulated flexible piping system for DH net-works at a resonable price, Fernwarme Int., 13, 1984, pp. 11-12.

52. G. Ratschmann, Long-term behaviour of flexible plastic pipes for DH lines, Kunststoffe, 75(3), 1985, pp. 164-167.

53. Technologisches Gewerbemuseum, Heating pipe made from poly-butylene, Hohere Technische Bundes-Lehr-und Versuchsans-talt, Vienna, Austria, 1984, TGM/103-7/84.

54. T.P.M. Bontje, Insulated flexible plastic pipes in DH, 5th. Int. Plastic Pipes Conf., University of York, England, 1982.

55. M. Ball, Polybutylene-piping performance and application, Shell Chemical Int. Trading Co., London, England, 1985.

56. Anon, Finnish DH technology, The Finnish Foreign Trade Assoc., Helsinki, Finland, 1985.

57. A.G. Loudon, Heat loss from underground heating mains, J. IHVE, (Nov.), 1957, pp. 196-203.

58. W.R.H. Orchard, Thermal insulation in DH, Orchard Partners, London, England, 1982.

59. W.R.H. Orchard, The potential for optimisation of CHP systems -- the Heat Board's Role, 3rd. Nat. Conf. DHA, A National Plan for Heat, Eastbourne, England, 1979.

60. W.T Huber, Piping systems are the key, ASHRAE J., 27(2), 1985, pp. 27-35.

61. K.T. Linton, Chilled-water storage, Heating Piping and Air Conditioning, 50, 1978, pp. 53-56.

62. F.W. Carson, Economics of chilled-water storage, District Heating, 56(1), 1970, pp. 12-13.

63. Anon, Increase of the insulation capacity of Lebit ducts, Lebit District-Heating System, Lebit Ltd., Leicester, England, 1981.

64. Anon, Repair and renovation of DH pipes with a 10 -- year guarantee, Lebit District-Heating System, Lebit Ltd., Leicester, England, 1978.

65. R.M.E. Diamant, Microcomputer programs for HVAC designs, a series of articles, Heating and Air Conditioning, 54(627)-55(644), 1984/5/6.

66. J.R. Kell and P.L. Martin, Heating and air conditioning of buildings, 6th. ed., Architectural Press, London, England, 1984.

67. W.R.H. Orchard and P.J. Robinson, Optimisation of CHP through the use of heat exchangers, 2nd. Int. Total Energy Congress, Copenhagen, Denmark, 1979.

68. L.A. Kosla,Jr., S.H. Shepherd and H.S. Orbach, Cogeneration fills San Jose needs, ASHRAE J., 27(7), 1985, pp. 30-34.

69. M.E. McKay and A. Rabl, A case study on cogeneration, Energy, 10(6), 1985, pp. 707-720.

70. Anon, CHP scheme said to be largest, Building Services and Environmental Eng., 6(7), 1984, p. 11.

71. Anon, Largest of its type claim for US CHP installation, Building Services and Environmental Eng., 7(10), 1985, p. 14.

72. Anon, Looking at the options for gas-turbine CHP, Building Services and Environmental Eng., 7(11), 1985, p. 15.

73. G.M. Priest, Producing steam from the combustion of solid waste, Energy Recovery from Refuse Incineration Seminar, I. Mech. E., London, England, 1985.

74. R.W. Horton, Experience with steam and power generation from municipal waste, Energy Recovery from Refuse Incineration Seminar, I. Mech. E., London, England, 1985.

75. A. Kunzli, E. Grielka and A. Lasser, DH plant for Basle station area, Sulzer Technical Review, (1), 1983, pp. 3-7.

76. Anon, DH fuelled by waste, Building Services and Environmental Eng., 7(5), 1985, p. 6.

77. Anon, Animals warm to CHP in Utrecht, Building Services and Environmental Eng., 7(11), 1985, p. 14.

78. Anon, Geothermal at Creteil, France, Chauffage Ventilation Conditionnement, (Jan./Feb.), 1985, p.7.

79. Anon, Heat pump district-heating, Chaud Froid Plomberie, (Sep.), 1984, pp. 61-67.

80. B. Rukes, Large heat pumps in DH systems, Siemens Power Eng., 6(5), 1984, pp. 260-264.

81. P. Bailer, Heat pumps in Swedish DH, Sulzer Technical Review, (2), 1982, pp. 51-53.

82. A.W. Carter, Design, construction and first five-years operation of municipal-waste incinerator with energy recovery at Jersey, Channel Islands, Energy Recovery from Refuse Incineration Seminar, I. Mech. E., London, England, 1985.

83. N. Barnes, Operational performance of waste-to-energy plants, Energy Recovery from Refuse Incineration Seminar, I. Mech. E., London, England, 1985.

84. I.E. Eastham, DH for leisure at 28 pence/therm, Int. Energy Efficiency Conf., Combustion/Heating/CHP, National Energy Management Group, Brighton, England, 1985.

85. Anon, District-heat pump will reduce oil use by 70%, Building Services and Environmental Eng., 7(7), 1985, p. 6.

86. Anon, Geothermal heat pump for DH in Sweden, Building Services and Environmental Eng., 8(1), 1985, p. 14.

87. Anon, The quest for smaller units, ASHRAE J., 27(2), 1985, pp. 18-23.

88. J.M. Burnett, Recent developments in the use of municipal refuse as a fuel, Proc. I. Mech. E., 191(7), 1977, pp. 89-98.

89. J. Hirshman, Natural cold-water direct cooling systems, Specifying Eng., (39), 1978, pp. 140-146.

90. Anon, Cogeneration plant to burn wood waste, Building Services and Environmental Eng., 8(1), 1985, p. 15.

91. M. Tshiteya, Conversion of wood to liquid fuel, Energy, 10 (5), 1985, pp. 581-588.

92. J. Sarkava, Peat as a fuel for DH in Finland, Fernwarme Int., 13(3), 1984, pp. 117-120.

93. Anon, Peat pellets for Swedish power plants, Building Services and Environmental Eng., 8(2), 1985, p. 17.

94. Anon, Industrial solid fuel plant, The National Coal Board, London, England, 1985.

95. G.F. Grove-White and V.R. Johnson, The Beeston CHP scheme - the reintroduction and integration of coal firing, 6th. Nat. Conf. CHPA, CHP -- Developments and Decisions, Torquay, England, 1985.

96. Anon, France switches to coal for DH, Chauffage Ventilation Conditionnement, (Dec.), 1983, p. 39.

97. S.P. Parker, Encyclopedia of energy, 2nd. ed., McGraw-Hill Book Co., New York, USA, 1981.

98. D. Merrick, Future coal utilisation technologies, 6th. Nat. Conf. CHPA, CHP -- Developments and Decisions, Torquay, England, 1985.

99. Anon, Fluid-bed boiler provides DH, ASHRAE J., 27(6), 1985, p. 23.

100. Anon, Fluidised-bed furnaces and boilers, Babcock Worsley Ltd., St. Helens, England, 1985.

101. Anon, Refuse-burning CHP system, GEC Energy Systems Ltd., Leicester, England, 1985.

102. K. Cooper, Treasure Island, Energy Manager, 8(11), 1985, pp. 40-41.

103. Anon, The value of rubbish, Building Services CIBSE J., 7 (2), 1985, p. 3.

104. J. David, Cheap and easy, Building Services CIBSE J. 7(2), 1985, p. 59.

105. D.V. Jackson and A.R. Tron, Energy from wastes, Int. J. Ambient Energy, 6(1), 1985, pp. 31-43.

106. Anon, Heat from refuse -- Swiss DH scheme, Energy World, (126), 1985, p. 11.

107. Anon, Pelletise and burn, Energy Manager, 8(10), 1985, p. 24.

108. G.S. Hall and M.J.D. Knowles, Good design and operation reaps benefits for UK refuse incineration over the last ten years, Energy Recovery from Refuse Incineration Seminar, I. Mech. E., London, England, 1985.

109. A.R. Hatcher, A case history of a diesel-powered CHP plant, 6th. Nat. Conf. CHPA, CHP -- Developments and Decisions, Torquay, England, 1985.

110. E. Clatworthy, The future uses of gas, 6th. Nat. Conf. CHPA, CHP -- Developments and Decisions, Torquay, England, 1985.

111. Anon, Iceland geothermal plant uses frequency convertor, Building Services and Environmental Eng., 8(1), 1985, p. 15.

112. J.D. Garnish, Geothermal energy and the UK environment, Int. J. Ambient Energy, 5(3), 1984, pp. 115-130.

113. L. Leoni, Water-filled abandoned mines as a heat source for DH, Underground Space, 9(1), 1985, pp. 23-27.

114. Anon, A survey of the development of solar energy in Japan, Times Publishing Bhd., Tokyo, Japan, 1983.

115. G.O.G. Lof and R.A. Tybout, Cost of house heating with solar energy, Solar Energy, 14(3), 1973, pp. 253-278.

116. J.A. Duffie and W.A. Beckman, Solar Engineering of thermal processes, John Wiley and Sons, Inc., New York, USA, 1980.

117. J.L. Boy-Marcotte, M. Dancette, J. Bliaux, E. Bacconnet and J. Malherbe, Construction of a 100 kW solar thermal-electric experimental plant, Trans. ASME, 107(3), 1985, pp. 196-201.

118. S.S. Thabit and J. Stark, Renewable heat and electricity concept for industrial applications in the UK, Proc. I. Mech. E., 199(A3), 1985, pp. 193-202.

119. P. Silvennoinen, R. Tarjanne, J. Kuusi and P. Rouhiainen, Prospects for small nuclear-heating reactors in Finland, Urban DH Using Nuclear Heat, Proc. Advisory Group, Int. Atomic Energy Agency, Vienna, Austria, 1976, pp. 33-43.

120. Y. El Mahgary, P. Kinnunen, P. Salminen, P. Kortelainen and A. Nikkanen, On the economy and optimisation of nuclear-heat power plants and their heat-transport systems, Urban DH Using Nuclear Heat, Proc. Advisory Group, Int. Atomic Energy Agency, Vienna, Austria, 1976, pp. 69-81.

121. K. Kirvela, Possibilities of nuclear DH for the Swiss Canton of Basle, Urban DH Using Nuclear Heat, Proc. Advisory Group, Int. Atomic Energy Agency, Vienna, Austria, 1976, pp. 197-203.

122. K Handl, Refuna -- a case history of a nuclear powered CHP plant, 6th. Nat. Conf. CHPA, CHP -- Developments and Decisions, Torquay, England, 1985.

123. P. Kroehner and K. Reinhard, Main report on DH in the FRG for 1983, Fernwarme Int., 13(6), 1984, pp. 334-344.

124. V.P. Zoller, Nuclear heating plants for DH supply -- a possible alternative for the FRG, Fernwarme Int., 14(4), 1985, pp.131 -142.

125. W. Jaek, E. Sauer and G. Thissen, Problems in DH supply from a boiling-water reactor in a relatively sparsely populated area using the example of the KRB Gundremmingen nuclear power plant, Urban DH Using Nuclear Heat, Proc. Advisory Group, Int. Atomic Energy Agency, Vienna, Austria, 1976, pp. 137-150.

126. T. Beresovski, Studies relating to central nuclear-heat supply systems in the US, Urban DH Using Nuclear Heat, Proc. Advisory Group, Int. Atomic Energy Agency, Vienna, Austria, 1976, pp. 151-157.

127. J. Hooper, Few nuclear families and no nuclear heat, The Guardian, London, England, (15th. October), 1985, p. 26.

128. R.J.R. Budden and D.L. Tolley, The role of the electricity supply industry in CHP, CHP Bureau, The Electricity Council, London, England, 1984.

129. Anon, Power stations with a dual role -- the electricity supply industry and CHP, CHP Bureau, The Electricity Council, London, England, 1985.

130. P H. Tamm, Metering heat, 3rd. Nat. Conf. DHA, A National Plan for Heat, Eastbourne, England, 1979.

131. N.R. Taylor, Is revenue metering feasible?, ASHRAE J., 27 (2), 1985, pp. 44-52.

132. J.A. Macadam and P.S. Woods, Development in the metering and control of heat-distribution systems, 6th. Nat. Conf. CHPA, CHP -- Developments and Decisions, Torquay, England, 1985.

133. G.C. Towler, DH -- the way ahead, Int. Energy Efficiency Conf., Combustion/Heating/CHP, National Energy Management Group, Brighton, England, 1985.

134. W.R.H. Orchard and P.J. Robinson, The importance of a building's internal design in optimising the overall performance of DH schemes, 4th. Int. District Heating Conf., Sirmione, Italy, 1980.

135. J.A. Macadam, D.A. Jebson, R.G. Owen and R.J. Brogan, DH combined with electricity generation: a study of some of the factors which influence cost-effectiveness, Department of Energy, London, England, 1981.

136. D.J. Fisk and D.A. Jebson, Influence of heat metering on DH scheme consumption, Building Services Eng. Res. and Tech., 5(3), 1984, pp. 102-105.

137. Anon, The prepayment heat controller, The Mainmet Group of Companies, Bradford, England, 1985.

138. Anon, Swiss decide against heat metering, Clima Commerce Int., (May), 1984, p. 68.

139. D. Hutchinson, Who should market CHP heat?, 5th. Nat. Conf. DHA, Planning for CHP Heat, Torquay, England, 1983.

140. J.A. Macadam, Options for refurbishment DH: tackling the problems, Orchard Partners, London, England, 1985.

141. R. Bending and R. Eden, UK energy: structure, prospects and policies, Cambridge University Press, Cambridge, England, 1984.

142. B.C. Wilkins, Electricity tariffs and the 1983 Energy Act, 6th. Nat. Conf. CHPA, CHP -- Developments and Decisions, Torquay, England, 1985.

143. G. J. Fowler, Electricity tariffs for private generation, CHP Bureau, The Electricity Council, London, England, 1984.

144. J. Ross, CEGB running scared of CHP, Electrical Review, 217 (11), 1985, p. 9.

145. B. Barnes, The potential for recuperated gas-turbine CHP in the UK, Int. Energy Efficiency Conf., Combustion/Heating/ CHP, National Energy Management Group, Brighton, England, 1985.

146. Anon, Trends in DH in mainland Europe, Heating and Ventilating Eng., 58(671), 1985, pp. 6-7.

147. H. Harboe, There is a case for energy conservation through DH, Energy, (Autumn), 1975, pp. 24-26.

148. W.G.E. Rowe, The Nottingham combined refuse incineration and DH scheme: a review of its development, 3rd. Nat. Conf. DHA, A National Plan for Heat, Eastbourne, England, 1979.

149. J.M. Cassels, The CHP potential in British cities and towns, 'Whole City Heating' Conf., Planning Tommorrow's Energy Economy, London, England, 1979, CHP, ed. by W.R.H. Orchard and A.F.C. Sherratt, George Godwin Ltd., London, England, 1980.

150. Anon, Britain's untapped heat source: a missed apportunity?, CHPA, Bedford House, Caterham, Surrey, England, 1985.

151. T. Lancaster, Lost: enough energy to heat every home in Britain!, Warmer Bulletin, 2(6), 1985, p. 7.

152. P. Bonham, CHP: applying common sense to energy usage, Int. Energy Efficiency Conf., Combustion/Heating/CHP, National Energy Management Group, Brighton, England, 1985.

153. Anon, Billingham - largest coal-fired group heating scheme, Steam and Heating Eng., (May), 1965, pp. 44-49.

154. R. Dettmer, CHP: the cogeneration game, Electronics and Power, 31(10), 1985, pp. 735-739.

155. R.M.E. Diamant and J. McGarry, Space and district heating, Iliffe Books Ltd., London, England, 1968.

156. G. Payne, One and one > two, Energy Manager, 8(9), 1985, pp. 26-27.

157. G.T. Shepherd, CHP the UK situation, Heating and Ventilating Eng., 58(670), 1985, p. 19.

158. W. Marshall, DH combined with electricity generation in the UK, Department of Energy Paper No. 20, HMSO, London, England, 1977.

159. W. Marshall, Combined heat and electrical generation in the UK, Department of Energy Paper No. 35, HMSO, London, England, 1979.

160. J.W. Wallington, DH futures — economic or social?, 3rd. Nat. Conf. DHA, A National Plan for Heat, Eastbourne, England, 1979.

161. R. Belgrave and M. Cornell, Energy self-sufficiency for the UK?, Gower Publishing Co. Ltd., Cambridge, England, 1985.

162. W.S. Atkins and Partners, CHP-DH feasibility programme: stage 1, summary report and recommendations, Department of Energy Paper No. 53, HMSO, London, England, 1984.

163. Anon, Sheffield runs strongly in CHP race, Energy Manager, 7(5), 1984, p. 6.

164. Anon, Cities submit CHP proposals, Chartered Mech. Eng., 31 (9), 1984, p. 13.

165. W.R.H. Orchard, Combined heat, energy and power: the Southwark scheme, Orchard Partners, London, England, 1980.

166. Orchard Partners, The development of CHP-DH in London: summary report, Orchard Partners, London, England, 1984.

167. Anon, London -- wide CHP proposals, Building Services CIBSE J., 6(4), 1984, p. 7.

168. Anon, CHP moves one more step, Building Services CIBSE J., 6(5), 1984, p. 5.

169. Anon, London loses out on CHP cash, Building Services CIBSE J., 7(3), 1985, p. 5.

170. Anon, Edinburgh CHP on the move, Building Services CIBSE J., 7(7), 1985, p. 7.

171. B. Ried, Cheap heat study for Edinburgh, Press Release, Scottish Development Agency, Glasgow, Scotland, (May), 1985.

172. I. Jarvis, There's a plan in the pipeline for Leicester, Leicester Town Hall, Leicester, England, 1985.

173. Anon, CHP - Leicester chosen, Energy World, July, 1985, p. 15.

174. Anon, CHP - Tyneside to go ahead, Energy World, (126), 1985, p. 13.

175. Anon, GLC investigates CHP for Londoners, Press Release, Greater London Council, London, England, (October), 1985.

176. Anon, Losing CHP finalists press on regardless, Energy Manager, 8(3), 1985, p. 5.

177. D. Lawrence, A CHP scheme for Sheffield: technical, financial and social considerations, 6th. Nat. Conf. CHPA, CHP - Developments and Decisions, Torquay, England, 1985.

178. M.V. Murray, Who should market CHP heat?, 5th. Nat. Conf. DHA, Planning for CHP Heat, Torquay, England, 1983.

179. J. Ramage, Energy -- a guidebook, Oxford University Press, Oxford, England, 1983.

180. P. Millbank, CHP for everyman, Building Services CIBSE J., 6(12), 1984, p. 47-51.

181. Anon, Electricity bills slaughtered by the mini CHIP system, Applied Energy Systems Ltd., Watford, England, 1985.

182. R. Forrest, Small-scale CHP, Energy Technology Series No. 4, Energy Efficiency Office, Harwell, England, 1985.

183. S. Andrews, CHP and parallel operation with the grid, Int. Energy Efficiency Conf., Combustion/Heating/CHP, National Energy Management Group, Brighton, England, 1985.

184. F. Nash, CHP frustration, Electrical Review, 217(11), 1985, pp. 34-35.

185. J. Ross, Why we need an energy plan, Electrical Review, 217 (11), 1985, pp. 16-17.

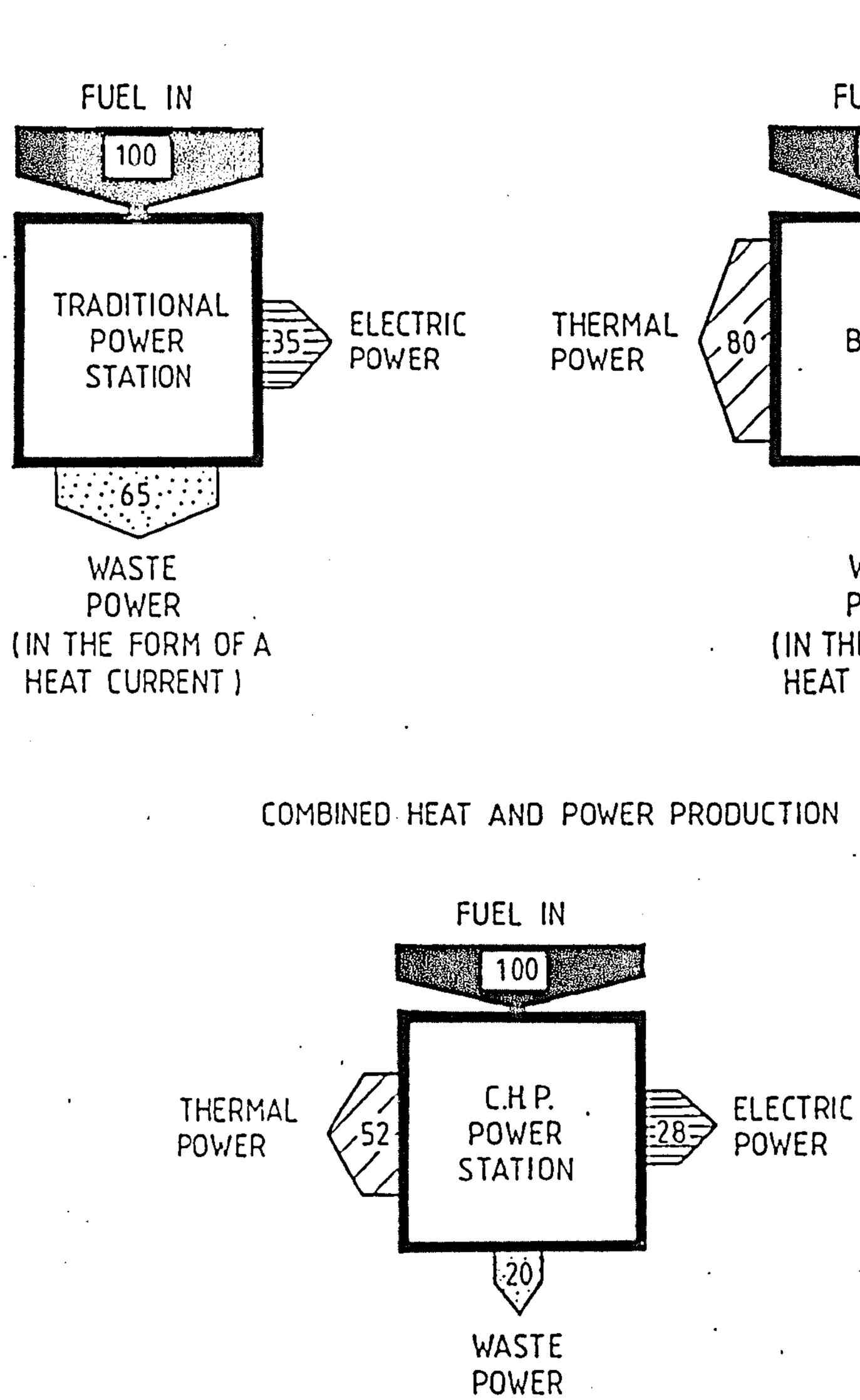

Fig. 1.1. Alternative methods of producing electricity and thermal power: for the numbers given as typical percentages it can be seen that the CHP option is likely to be the prefered method(24).

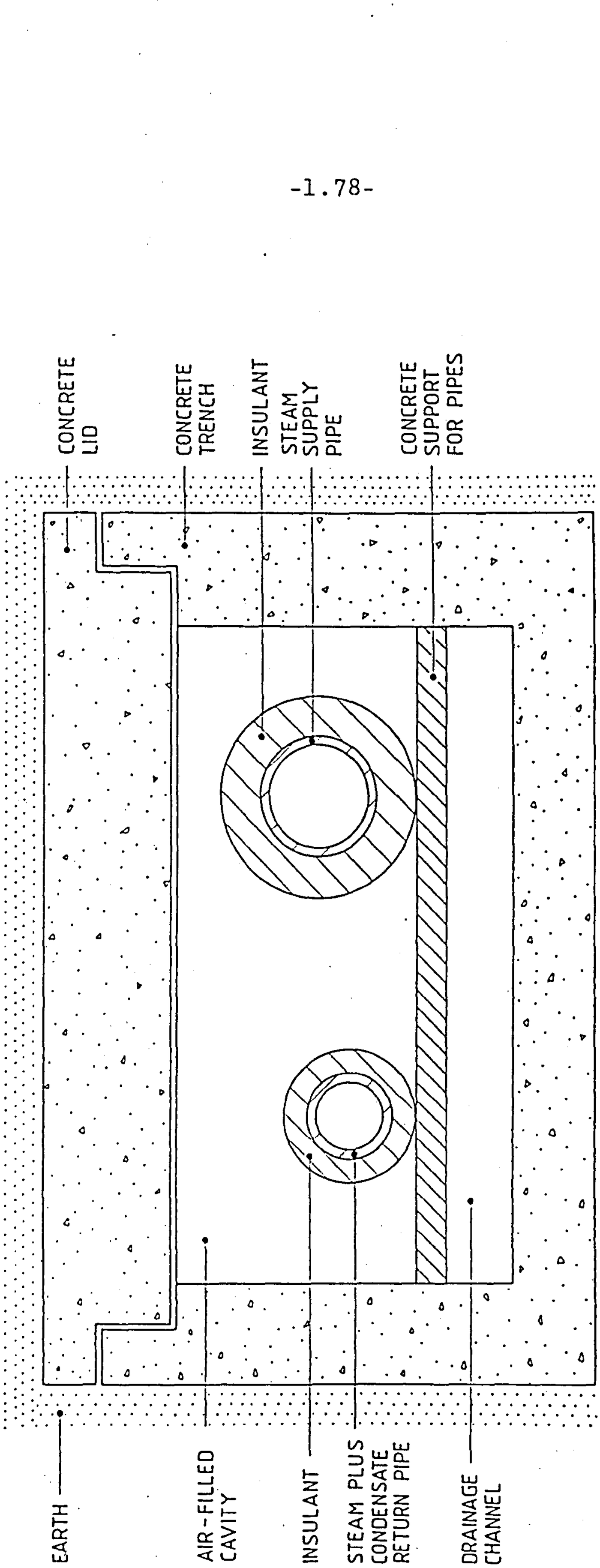

Fig. 1.2. Schematic cross-section through a concrete trench system for supply and return pipelines (60).

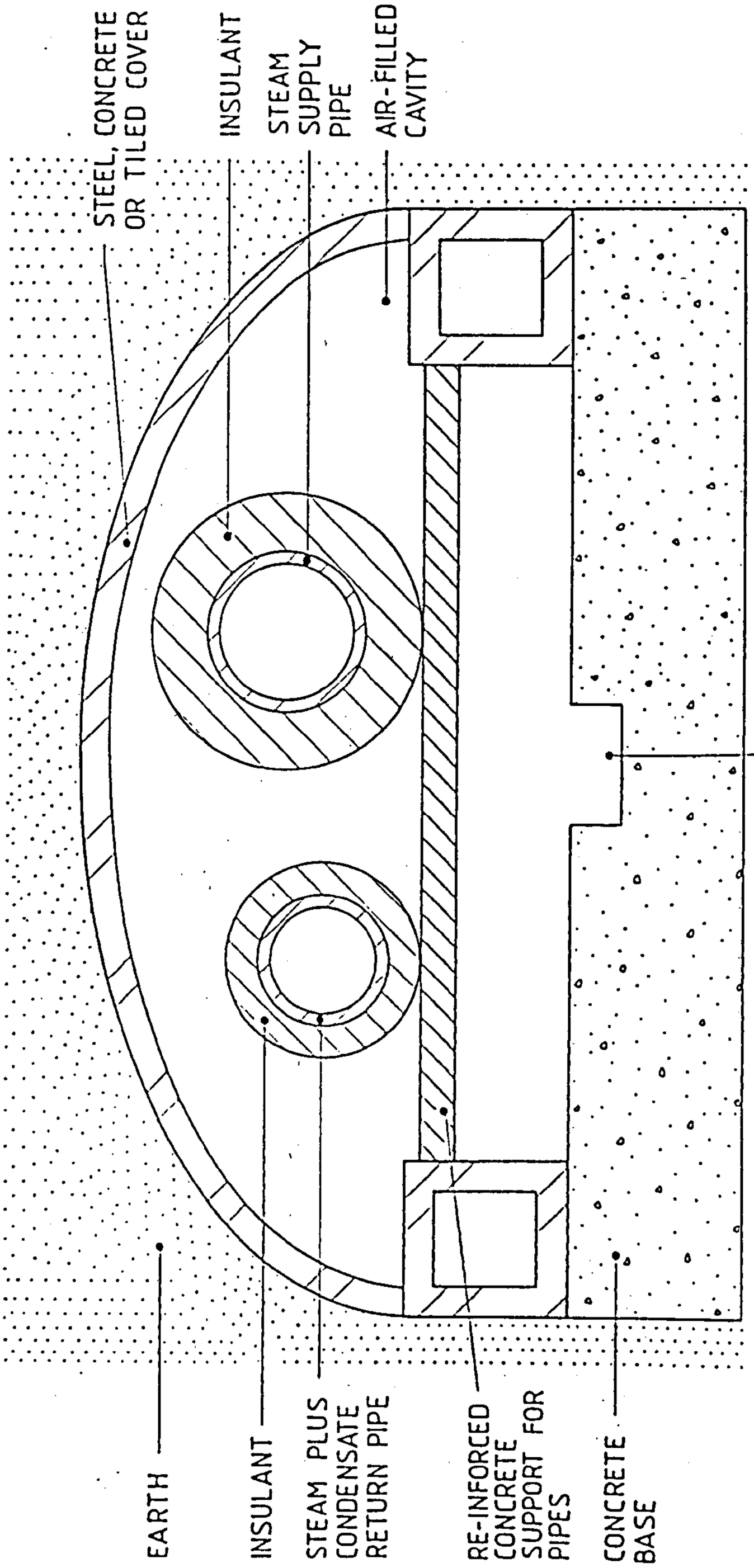

Fig. 1.3. Schematic cross-section through a half-round clay tile system for supply and return pipelines(60).

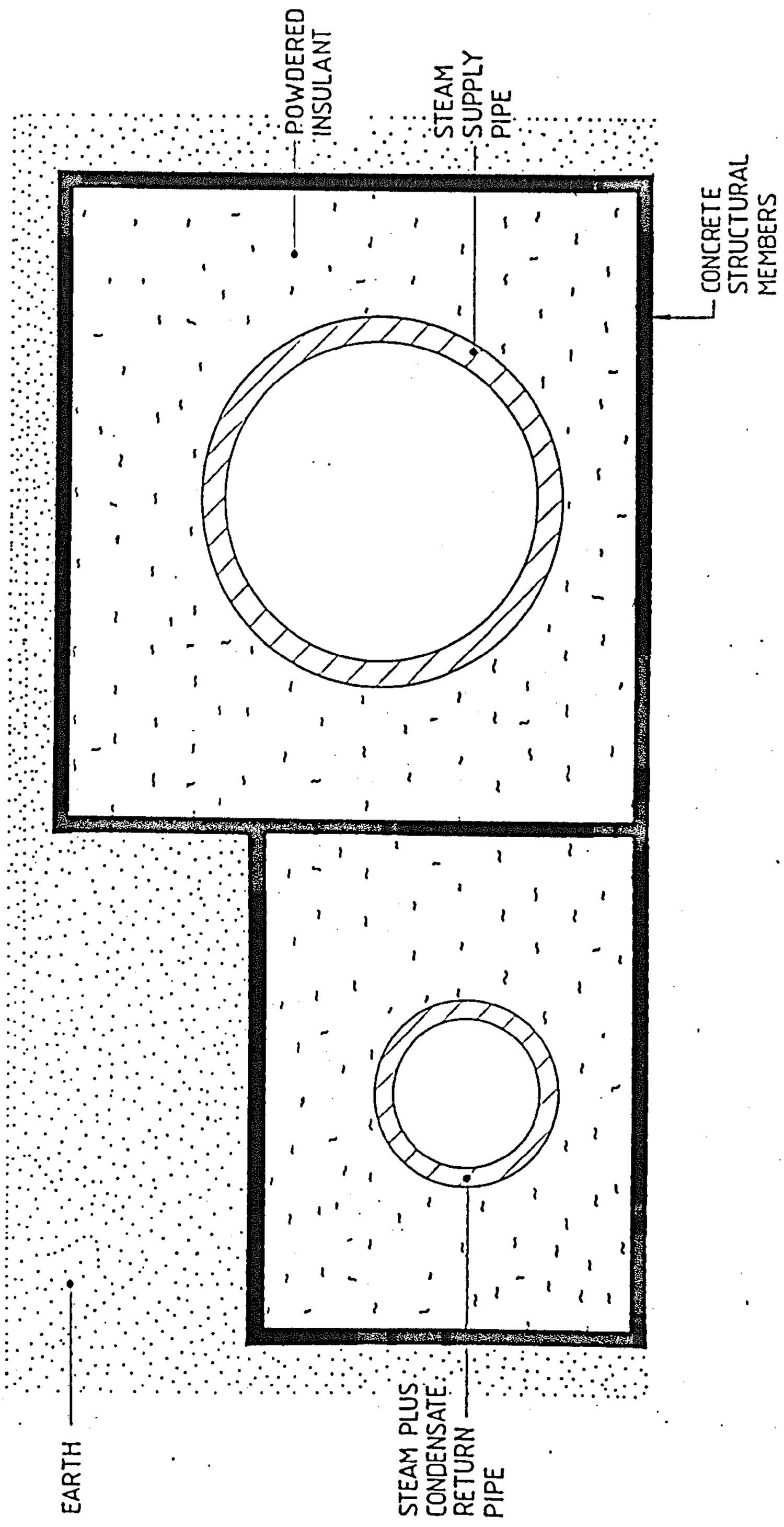

Fig. 1.4. Schematic cross-section through a poured-in-place, loose-fill, insulating-envelope type system for supply and return pipelines (60).

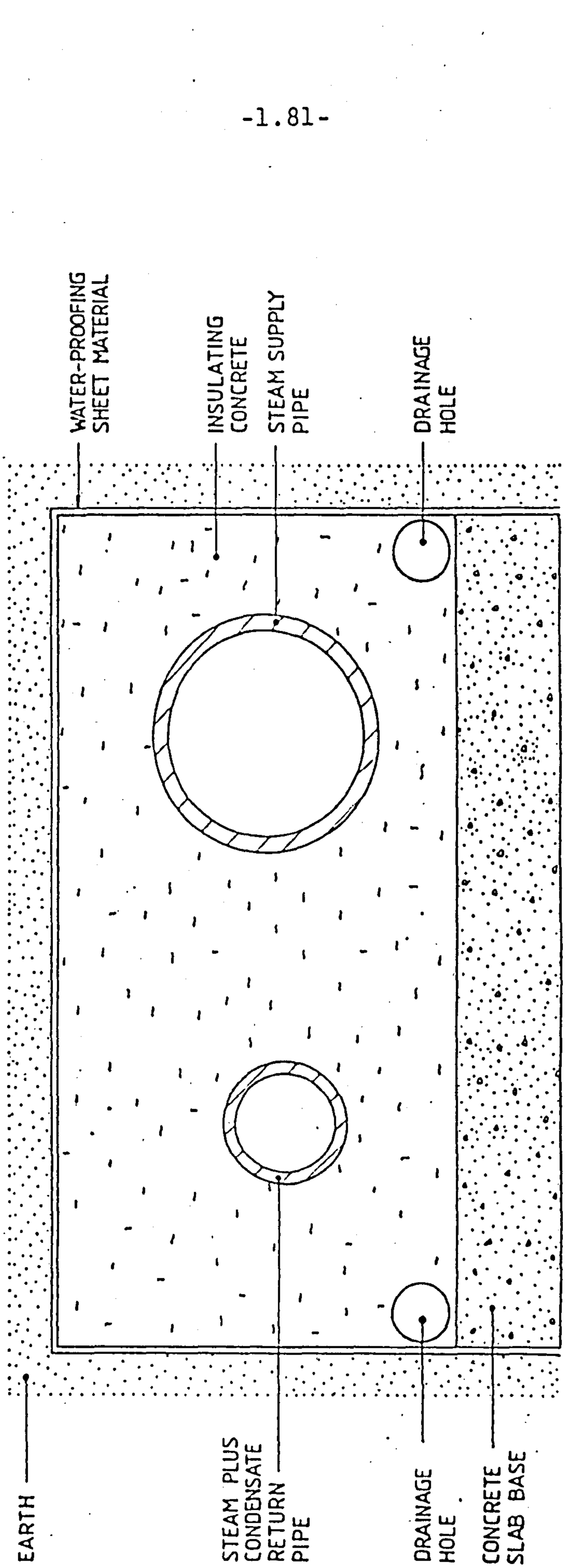

Fig. 1.5 Schematic cross-section through an insulating-concrete envelope system for supply and return pipelines (60).

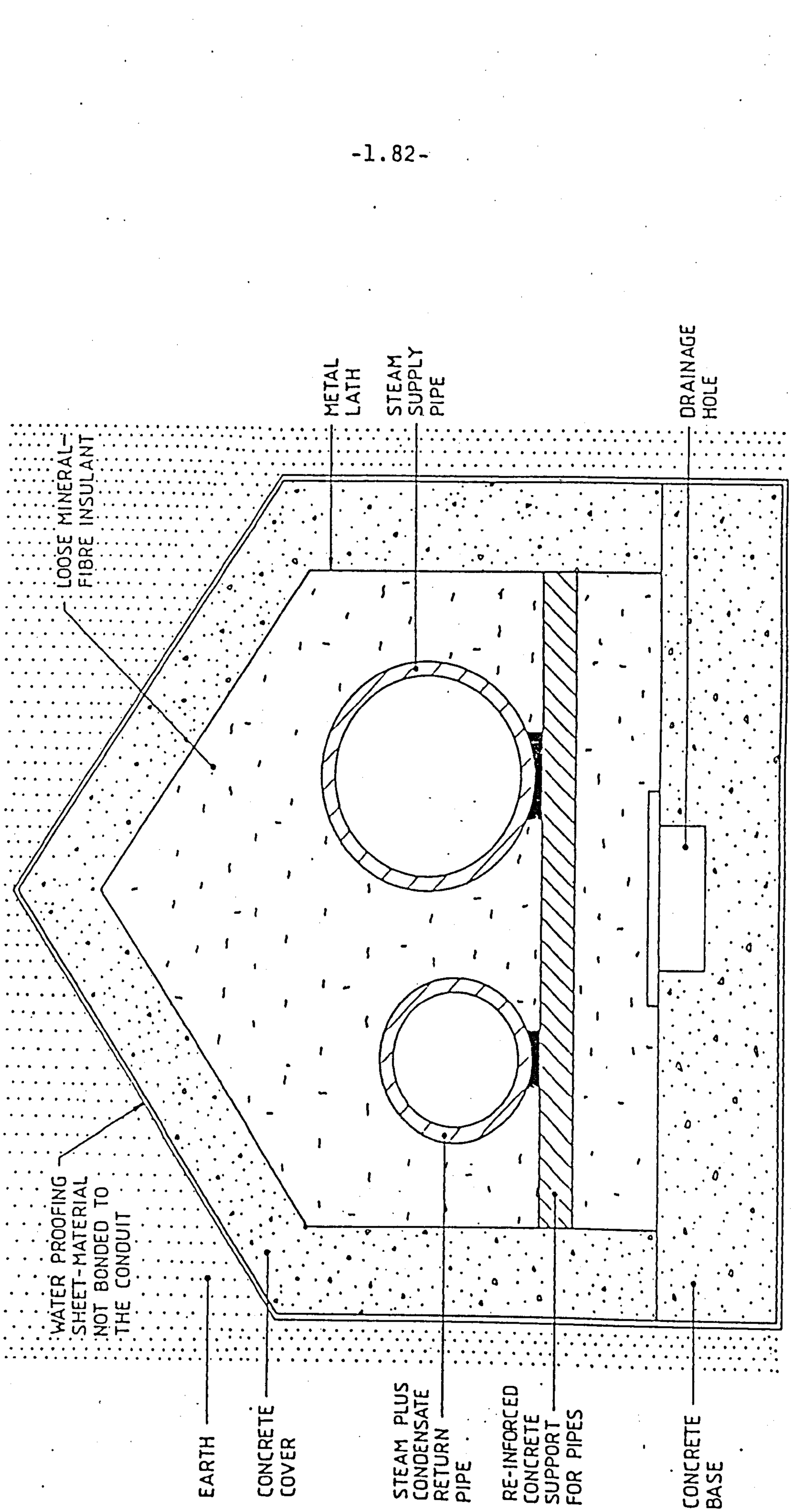

Fig. 1.6. Schematic cross-section through a concrete conduit system for supply and return pipelines(60).

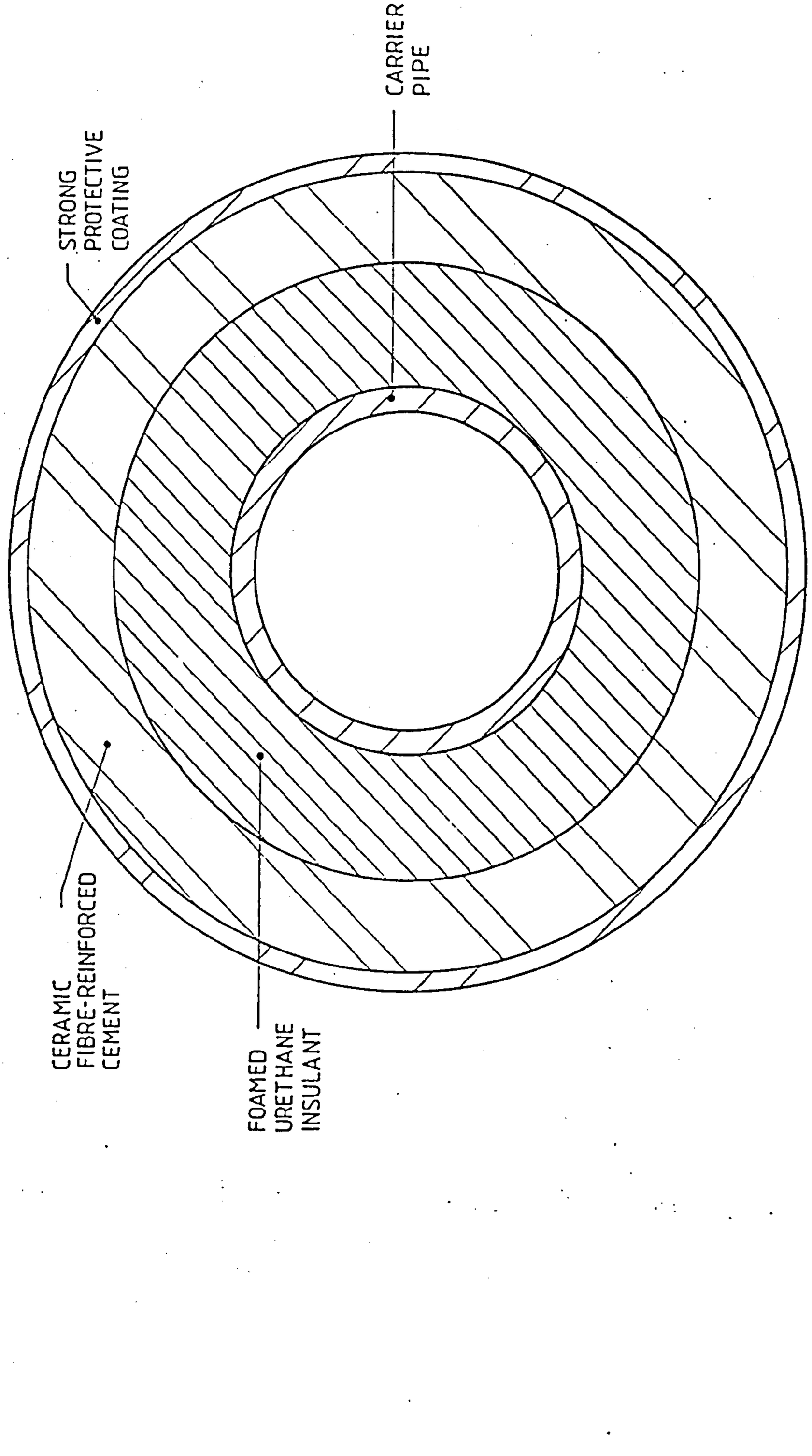

Fig. 1.7. Cross-section through a prefabricated pipeline for DH systems (60).

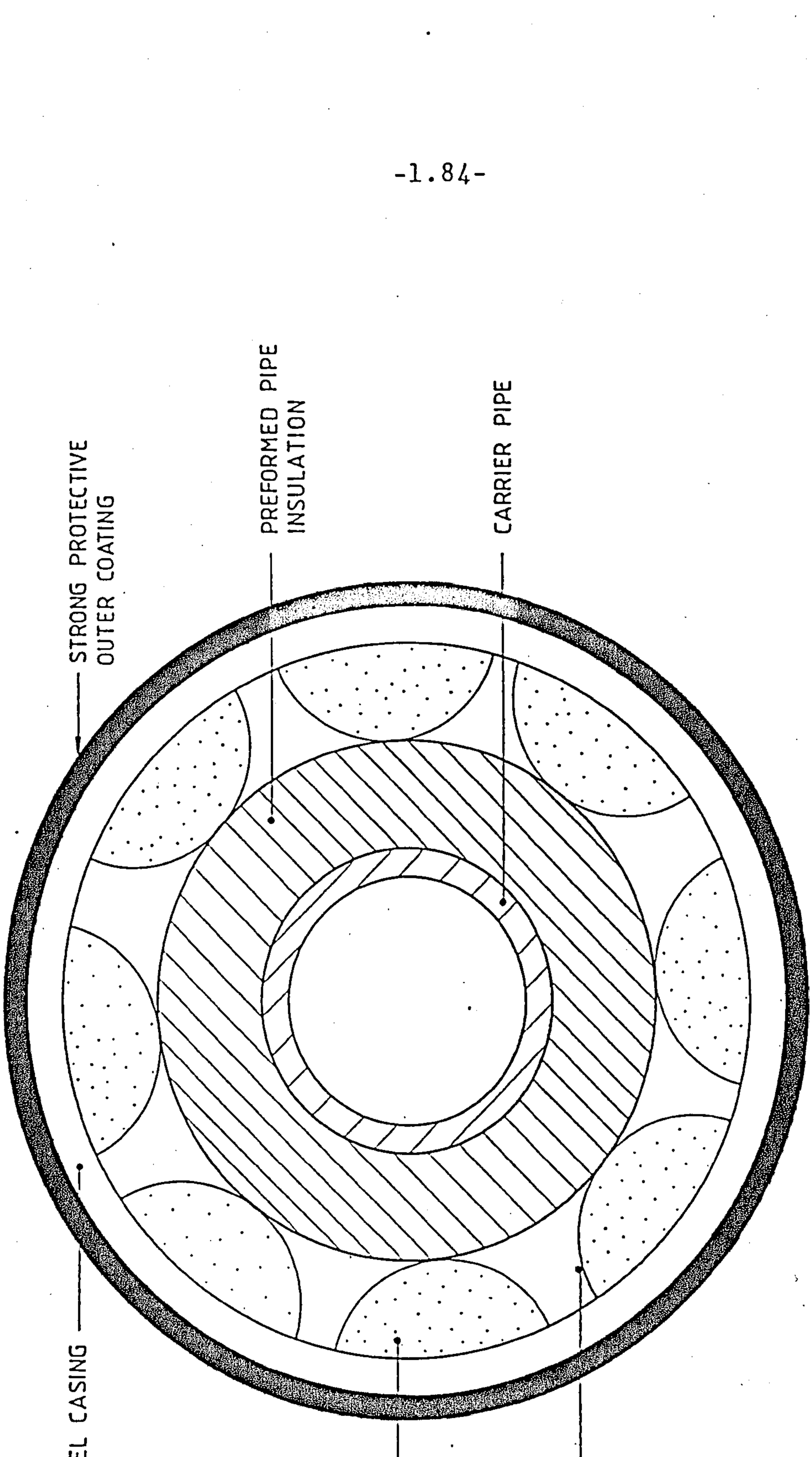

Fig. 1.8. Cross-section through a prefabricated pipeline with drainage channels and dryable interlinking air-filled cavities (60).

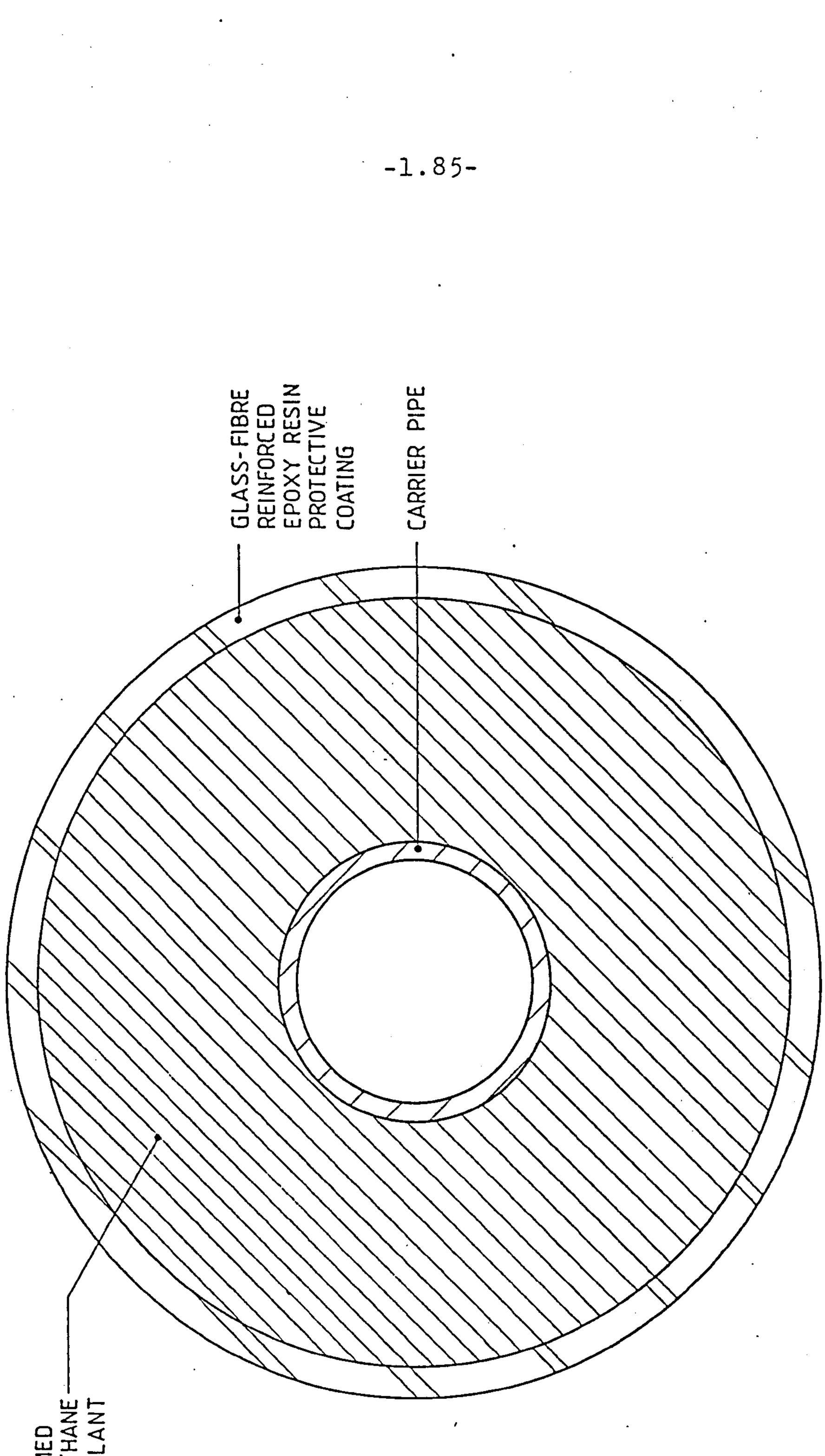

Fig. 1.9. Cross-section through a sealed insulation pipeline for DH systems (60).

Fig. 1.10. Recent conventional practice, i.e. the 'side-by-side' arrangement of the 'outward' and 'return' district-heating pipelines in an air-filled rectangular trench.

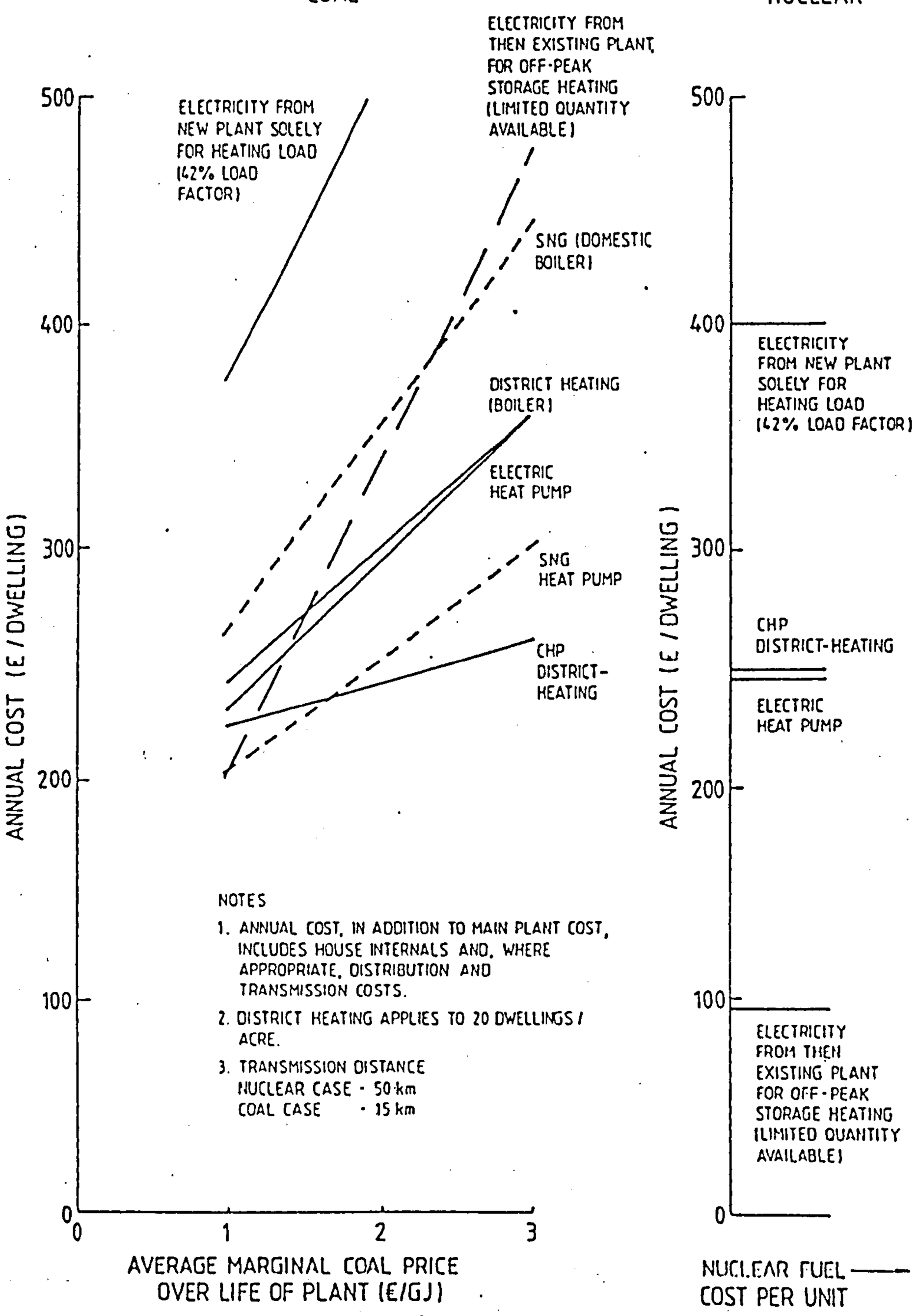

Fig. 1:11. Marginal costs of long-term (i.e. to persist beyond AD 2000) alternatives assuming a 10% discount rate(159).

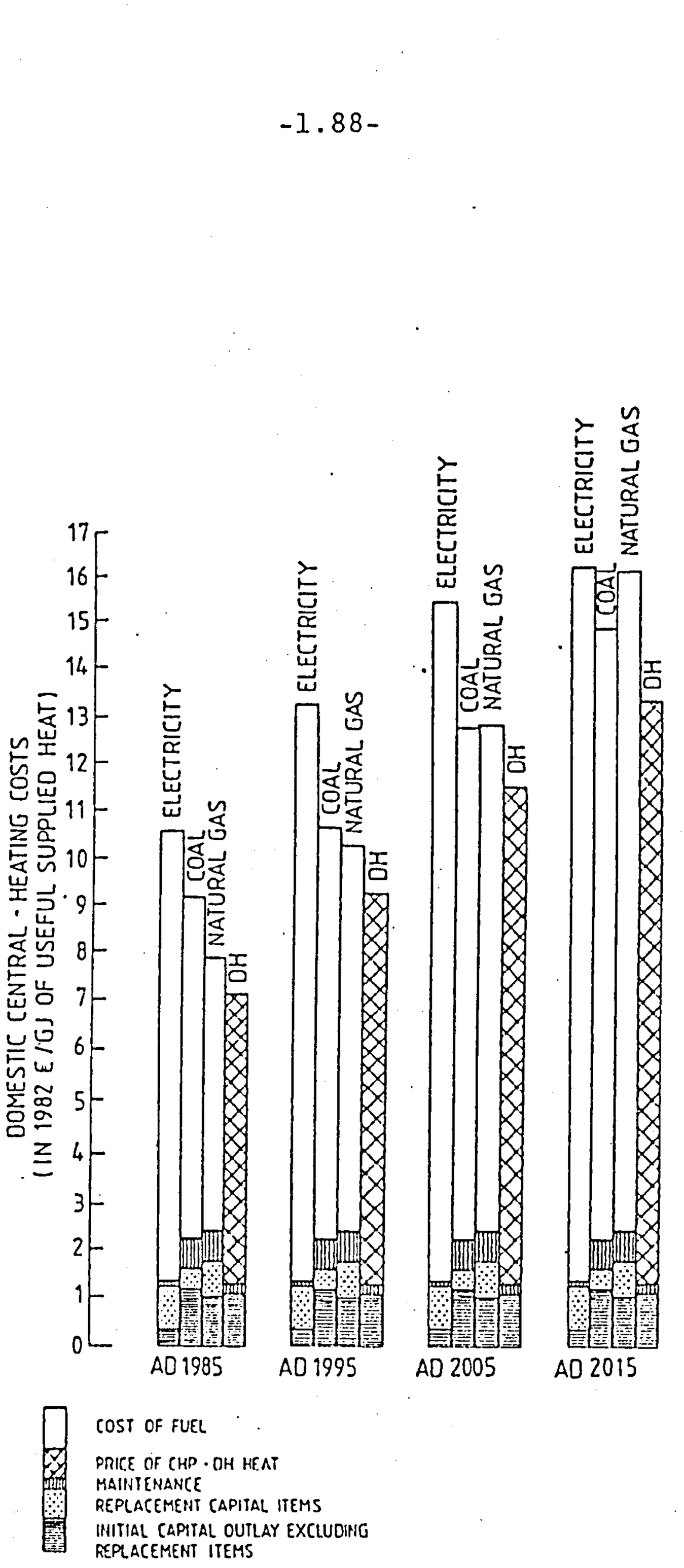

Fig. 1.12. The composition of present and predicted domestic central-heating costs using electricity, coal, or gas, and the derived price of district heating (data for England, Scotland and Wales) (162).

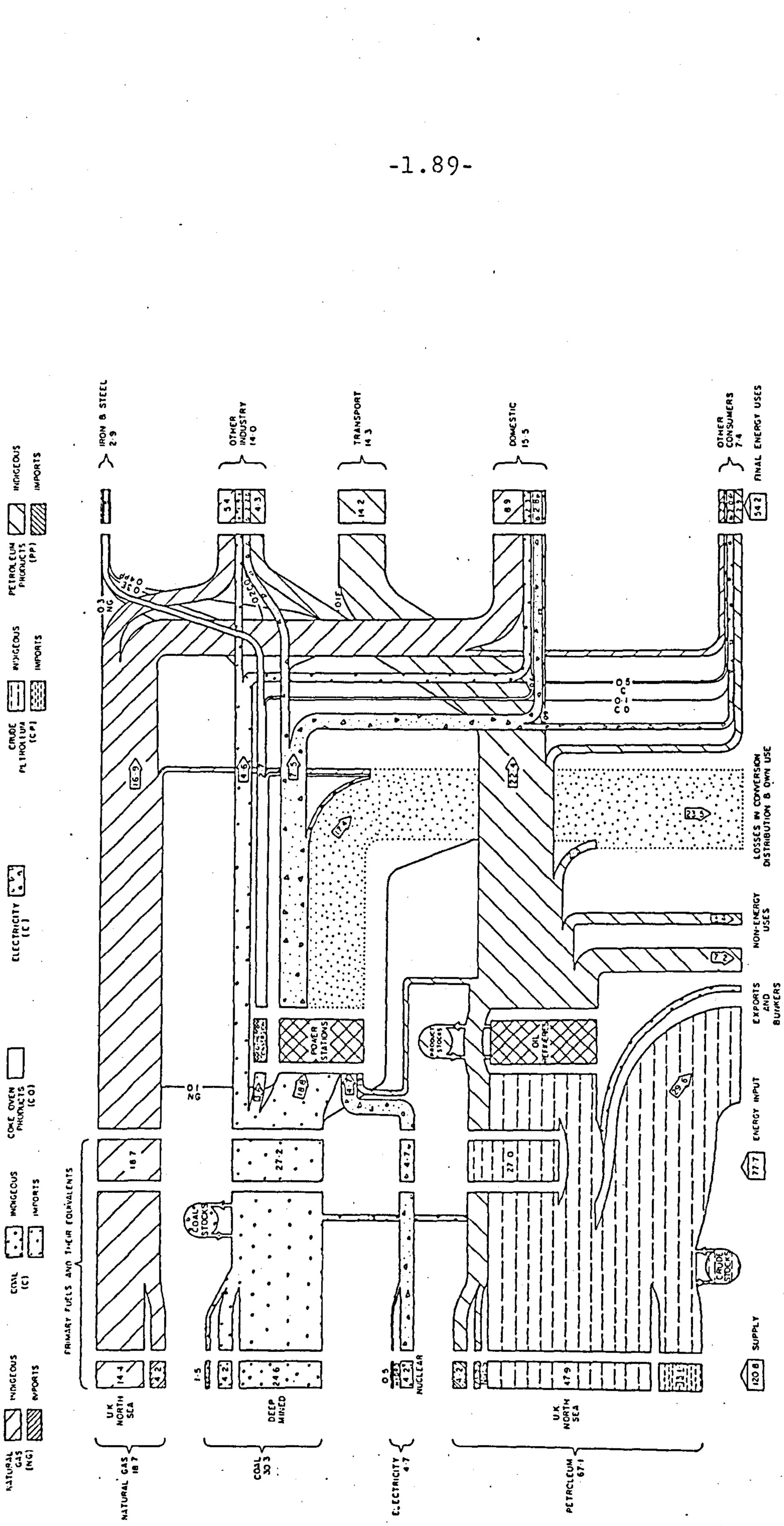

Fig. 1.13. The UK energy flows for AD 1983 (N.B. The figures displayed in this chart have been rounded off to the nearest single figure of decimals. Thus occasionally the sums of the contributions indicated differ by 0.1 x 10^9 therms from those indicated)

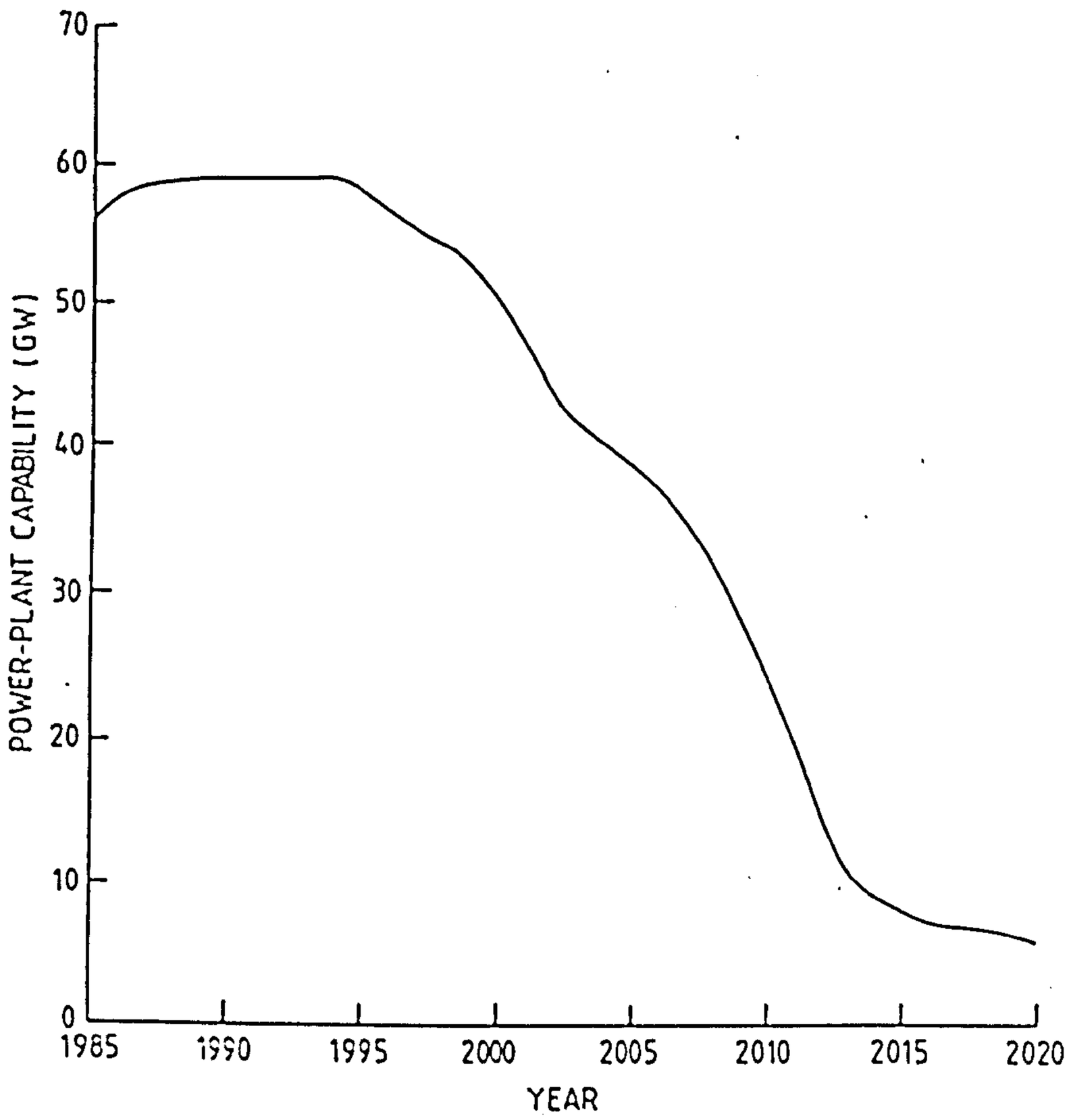

Fig. 1.14. How the total output of all existing power plant in the UK would decline if no new stations are built(185).

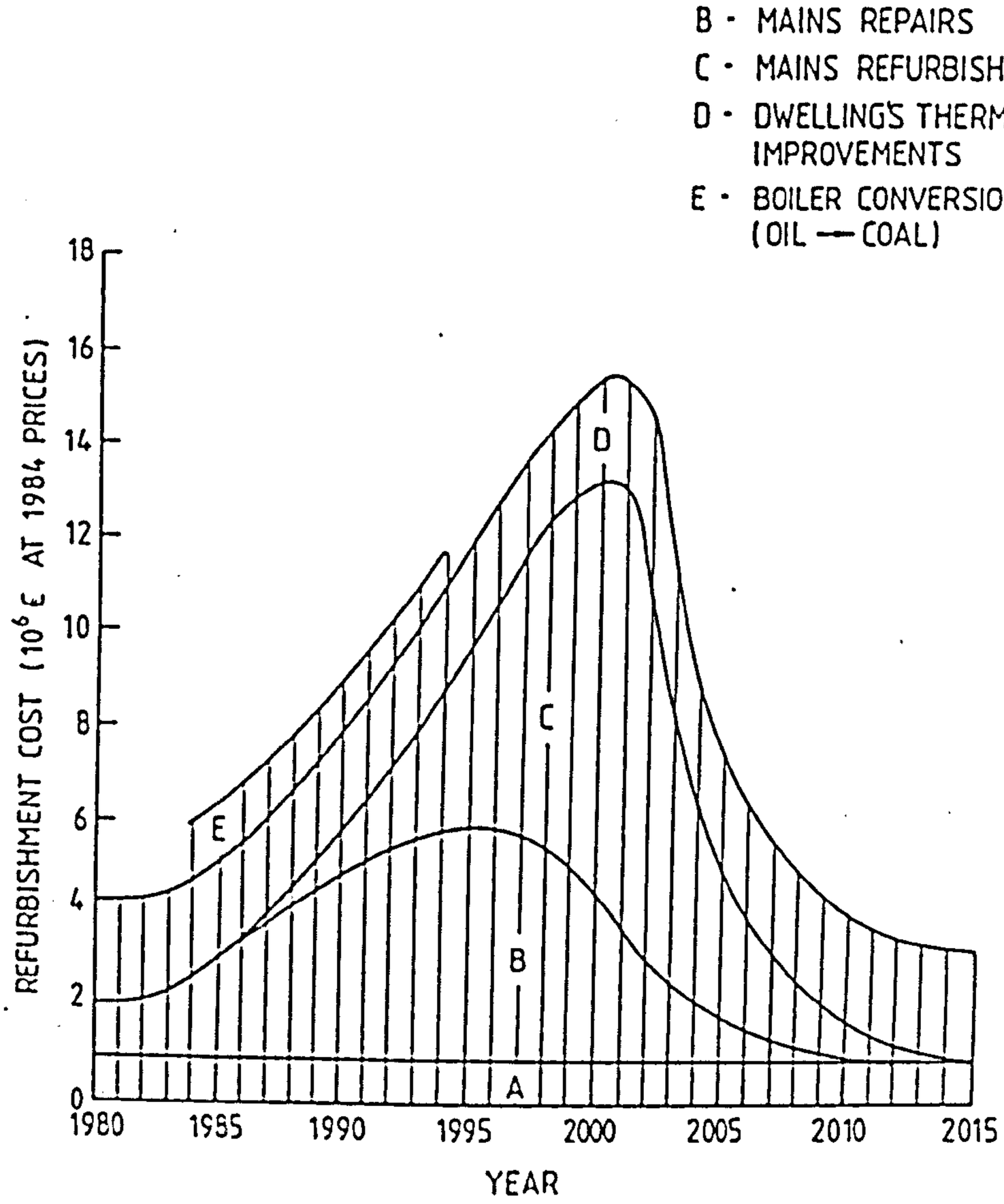

Fig. 1.15. Projected costs of district heating upgrading and refurbishment since 1980(140).

CHAPTER 2

NATURAL CONVECTION ACROSS CAVITIES: DESIGN ADVICE

Applied Energy 20 (1985)

Natural Convection Across Cavities: Design Advice

SUMMARY

Experimental measurements and theoretical predictions of steady-state heat transfers to or from horizontal single or double pipelines enclosed in horizontal circular or rectangular enclosures have been collated. The optimal configurations of the pipelines to achieve maximum thermal resistances of the air-filled cavities are identified. A recommended correlation for predicting the combined convective/conductive resistances provided by the contained air in a horizontal concentric annuli is presented.

NOMENCLATURE

d	Diameter of the inner pipe(s), see Figs 1 and 2 (mm).
D	Diameter of the outer pipe, see Fig. 1 (mm).
e	Vertical eccentricity $=(h/G)$, see Fig. 1.
E	Displacement ratio $=[1-2H_R/(Y-d)]$ or $[1-2H_S/(Y-d)]$ for the return or supply pipe, respectively, see Fig. 2.
G	Average vertical gap size $=[(D-d)/2]$ and $[(Y-d)/2]$ for the circular and rectangular enclosures, respectively (mm).
Gr	Local Grashof number.
h	Distance between the vertically displaced horizontal centrelines of the outer and inner pipes, see Fig. 1 (mm).

Applied Energy 0306-2619/85/$03·30

H_R, H_S Vertical distances between the return and supply horizontal pipes, respectively, and the upper horizontal internal surface of the enclosure, see Fig. 2 (mm).

k Thermal conductivity of the fluid contained in the cavity ($W m^{-1} K^{-1}$).

k_c Effective thermal conductivity due to combined convection and conduction through the air trapped in the cavity ($W m^{-1} K^{-1}$).

L Axial length of the considered horizontal cavity (mm).

M Dimensionless parameter dependent upon the geometry and temperature distribution of the system $= \overline{Nu}/Gr^n$.

n Power index of the Grashof number in the $\overline{Nu}$ versus Gr relationship.

Nu Local Nusselt number.

$\overline{Nu}$ Average Nusselt number.

Pr Prandtl number.

Ra Rayleigh number for the convecting fluid flow.

T_o Steady-state uniform temperature of the inner surfaces of the outer surrounding 'isothermal' enclosures, see Figs 1 and 2 (°C).

T_R, T_S Steady-state temperatures of the outer surfaces of the return and supply pipes, respectively, see Figs 1 and 2 (°C).

X, Y Horizontal width and vertical height, respectively, of the rectangular enclosure, see Fig. 2 (mm).

$\Delta( )$ Increment of the parameter ( ), e.g. ΔT represents the steady-state difference between the temperatures of the outer surface of the inner (supply) pipe, T_S, and the inner surface of the outer enclosure, T_o (°C).

θ Angular co-ordinate, measured from zero for the vertically downwards radius vector, emanating from the centre of the supply pipe; θ increases in a counter-clockwise rotation, see Fig. 3 (degrees).

Suffixes

d Based on the diameter of the inner pipe.

G Based on the gap size.

o Of the inner surfaces of the outer enclosure.

r Based on the inner characteristic radius for two-dimensional laminar natural convective heat transfer in a horizontal annulus.

R For the return pipe.
S For the supply pipe.

HEAT TRANSFERS AND FLUID FLOWS

The transfer of heat through a fluid is achieved by gaseous conduction, convection and radiation. If absorption of the latter occurs in the fluid, the radiation flux becomes a function of the properties of the enclosed fluid, as well as of the temperature distribution, surface finish and geometric configuration that affect the situation when the fluid is transparent to thermal radiation. Irrespective of whether the fluid is thermally transparent, radiation occurs independently of the presence of any simultaneous gaseous conduction and convection.

As convection never ensues without simultaneous fluid conduction, these modes of heat transfer are usually considered together. Fluid motion, due to buoyancy forces resulting from density variations within the fluid, is termed 'natural' (or free) convection.

Heat transfer data are conveniently expressed in dimensionless forms by an appropriate Nusselt number, Nu, which is a function of either the Grashof number, Gr, or the Rayleigh number, Ra. The Nusselt number is defined as the ratio of the actual steady-state heat transfer rate, by combined convection and conduction through the fluid, to the steady-state heat transfer had the conduction occurred alone.

By means of dimensionless analysis, it can be deduced that, when convection occurs, the rate of heat transfer across the enclosed fluid layer is a function of: the Grashof number, Gr, the Prandtl number, Pr, the aspect ratio, L/G, and the diameter ratio, D/d, for the circular enclosure (see Fig. 1); or the width ratio, X/G, the height ratio, Y/G, and the pipe ratio, d/G, for the rectangular enclosure (see Fig. 2). However, if L is sufficiently large, the Nusselt number will become independent of L/D. It is alleged[1] that the influence of the surface roughness on the natural convection heat transfer is negligible in practice.

For natural convection of the air between horizontal concentric pipes, with $T_o < T_s$ (see Fig. 1), two basic types of flow—depending on the gap size, G—have been observed,[2] namely the crescent-eddy pattern (see Fig. 4) and the kidney-shaped eddy pattern (see Fig. 5). For both vortex systems, the fluid flows up along the heated inner-pipe's outer surface and down along the outer-pipe's cooled inner surface with the fluid in the

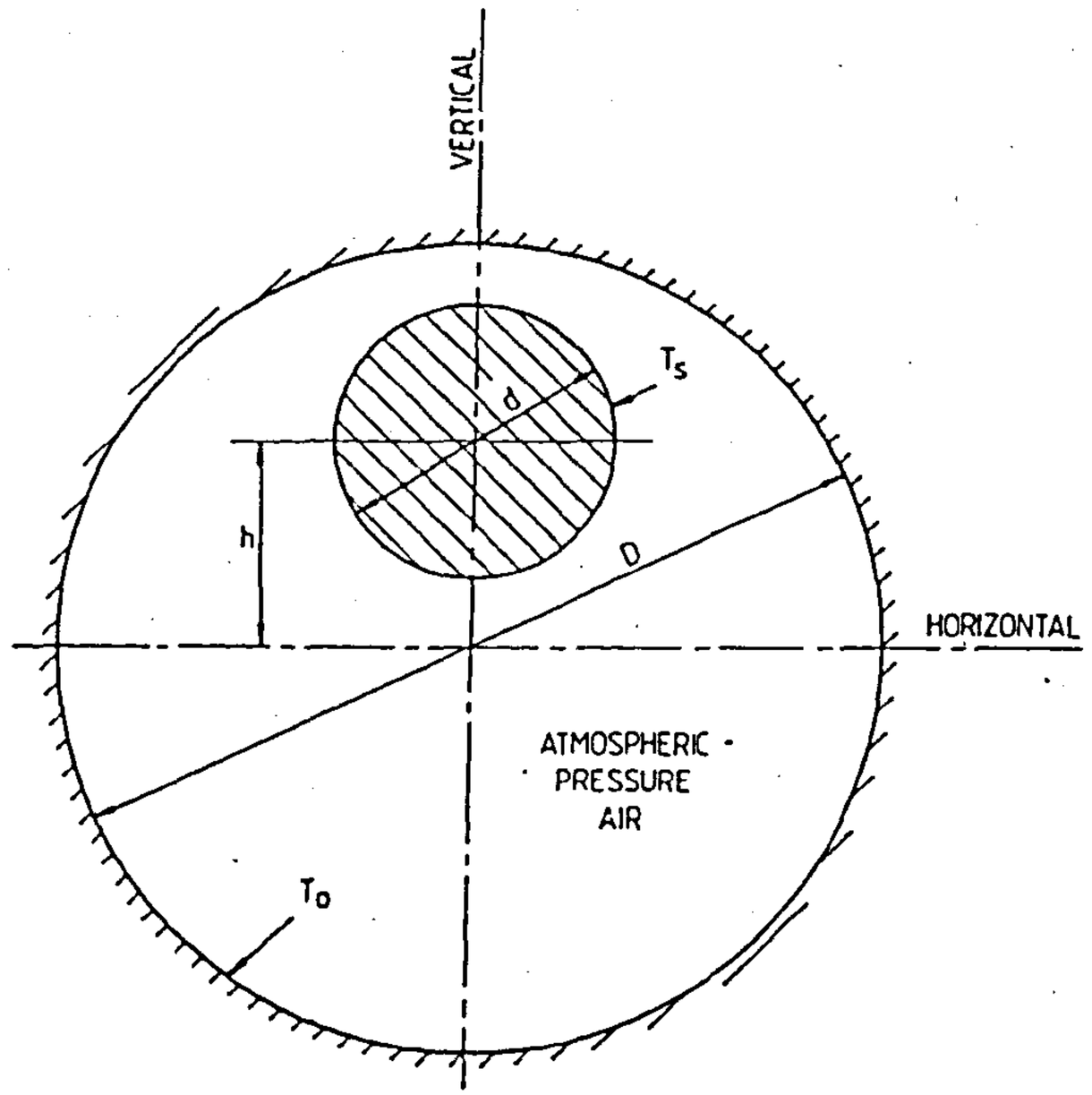

MEAN GAP SIZE, $G = (D-d)/2$
ECCENTRICITY, $e = h/G$
$-1 \leq e \leq 1$

Fig. 1. Schematic representation of a vertical section through the horizontal *eccentric* annulus between two horizontal pipes; a configuration with a positive eccentricity is illustrated.

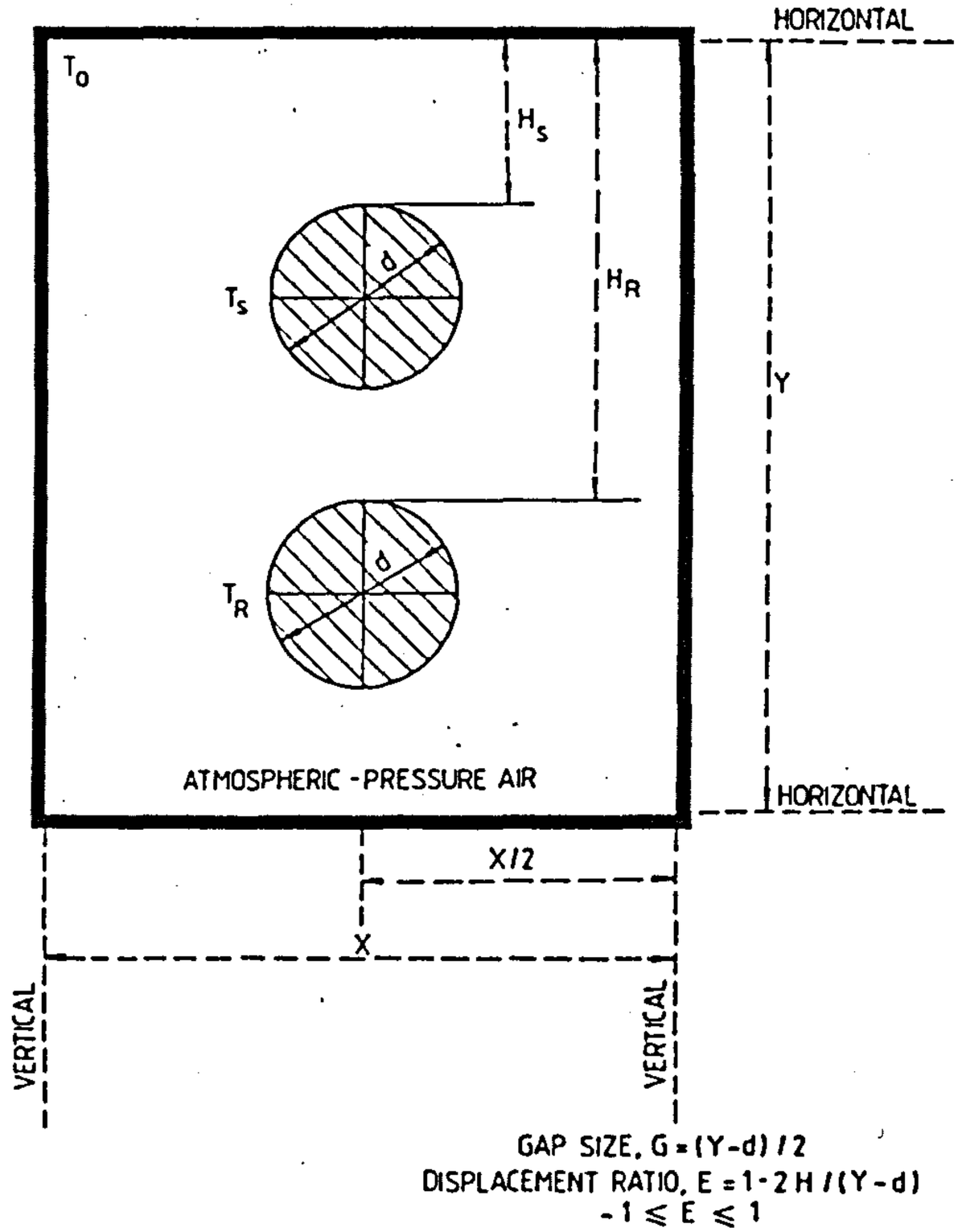

GAP SIZE, $G = (Y-d)/2$
DISPLACEMENT RATIO, $E = 1-2H/(Y-d)$
$-1 \leq E \leq 1$

Fig. 2. Schematic representation of a vertical section through the horizontal pipes in the horizontal rectangular enclosure.

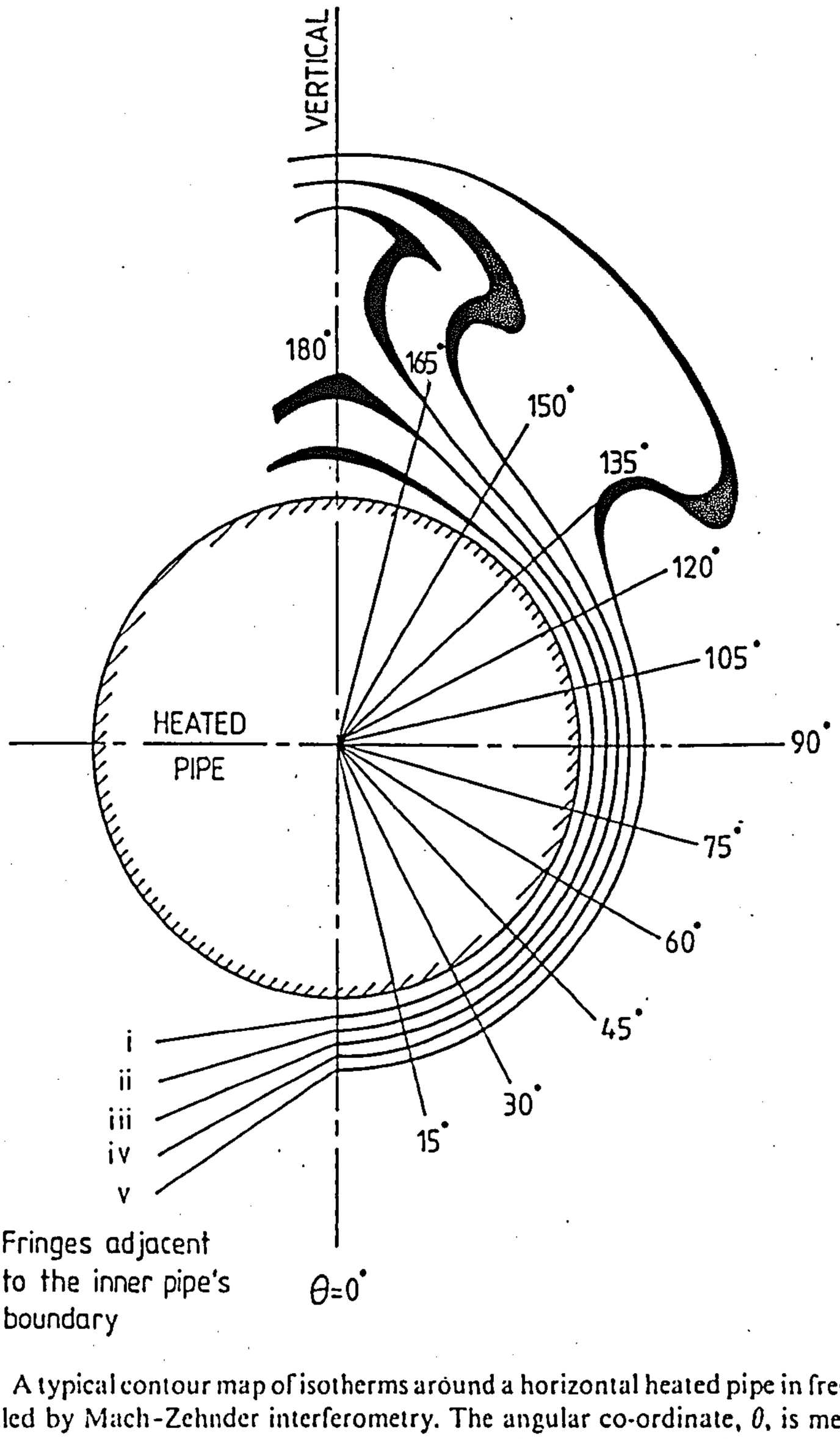

Fig. 3. A typical contour map of isotherms around a horizontal heated pipe in free space as revealed by Mach-Zehnder interferometry. The angular co-ordinate, θ, is measured from the vertically downwards radius vector from the centre of the pipe.

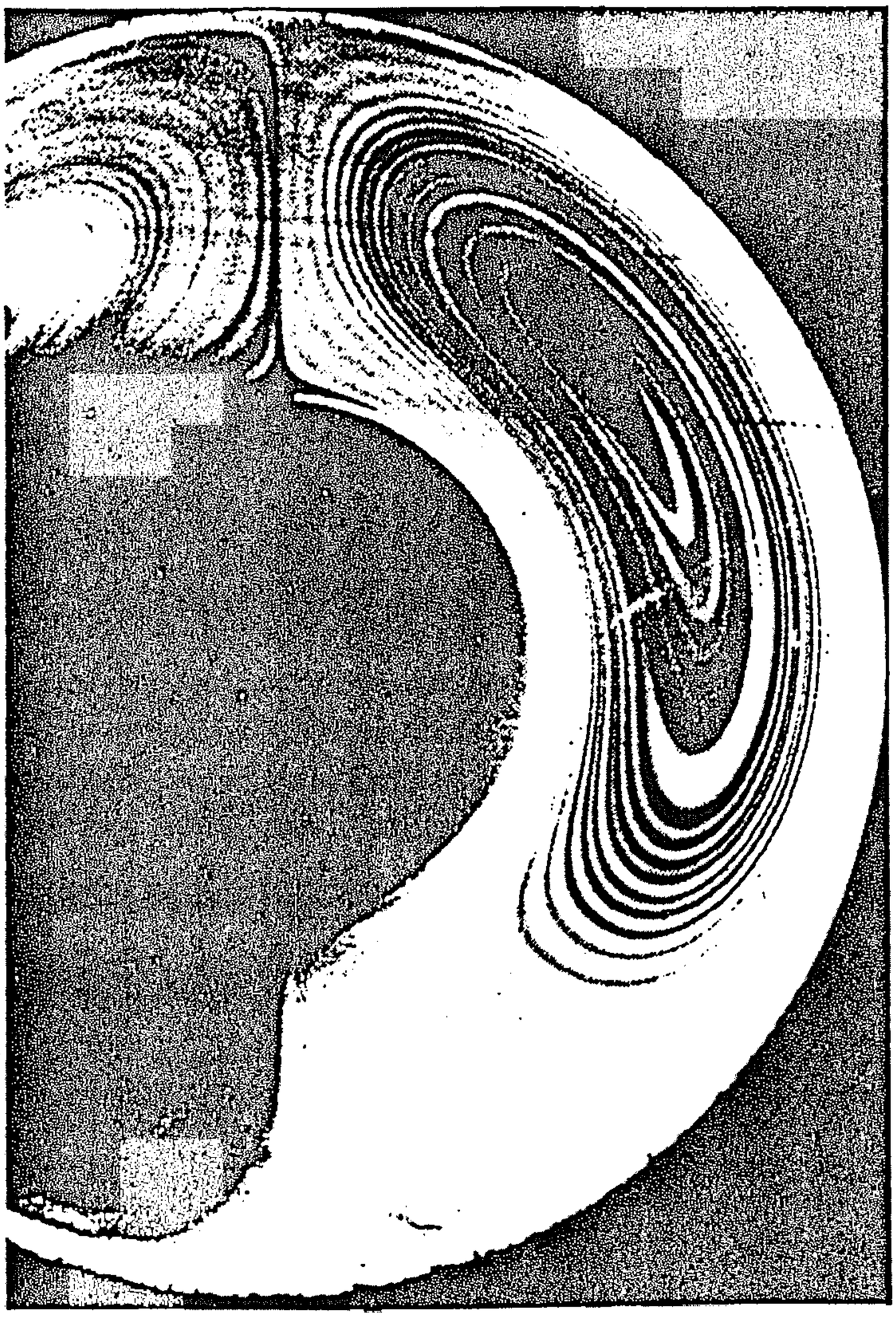

Fig. 4. Typical flow visualisation in a horizontal annulus; a stable crescent-eddy pattern, between a heated inner horizontal pipe *concentric* with a cooled outer horizontal pipe. $G/d = 0{\cdot}73$, $Gr_d < 1{\cdot}57 \times 10^5$.[2]

Fig. 5. As for Fig. 4 but with $G/d = 1{\cdot}35$, $Gr_d < 1{\cdot}57 \times 10^5$; a stable kidney-shaped eddy pattern then occurs.[2]

Fig. 6. As for Fig. 4 but with $G/d = 1{\cdot}35$, $Gr_d > 1{\cdot}57 \times 10^5$; an unstable (i.e. θ varying) oscillatory flow of the plume then ensues.[2]

central cores of the vortices being almost stagnant. However, for large gap sizes at a higher Grashof number, the stable kidney-shaped eddy pattern becomes unstable and begins to oscillate circumferentially (see Fig. 6). *Qualitatively* similar flow patterns were observed for $T_o > T_s$, but the air in this instance moved up as it was heated by the inner surface of the outer pipe and subsequently fell as it was cooled by the relatively cold inner-pipe surface forming the annulus.[3] The stability of the flow field within the annulus, in both cases, was dependent upon the Grashof number, Gr.

Extensive experimental and theoretical analyses of natural convections in horizontal cavities have been carried out to study the interaction between the hydrodynamic and thermal effects for a variety of parameters.[4] Most of these studies were concerned with concentric pipes;[5,6] only a few considered systems with the inner pipe mounted eccentrically with respect to the outer one.[7,8] Many different techniques for correlating the typical heat transfer behaviours have been proposed.[9,10] Analysis of steady-state isotherm maps and flow visualisations has been helpful, both quantitatively and conceptually.[11,12] Recent studies have focused attention upon rectangular enclosures,[13] effects of spacers,[14] non-circular geometric pipes,[15] and the rotation of the inner[16] or the outer[17] pipe while the other pipe remains at rest.

APPLICATIONS

Stagnant, or near stagnant, atmospheric-pressure air is the most common thermal insulant. By judicious design, it can be incorporated within assemblies to reduce the rates of heat exchange. For example, the use of pores of less than 1·8 mm tends to suppress natural convection within insulants at near normal ambient temperature.[18] A 19 mm air gap is recommended for vertical double-glazing for housing,[19] and ~15 mm is the optimal air-filled gap width size for vertical, concentric, annular-cavity lined chimneys.[20] An air gap was initially recommended[21] between horizontal concentric pipes as a means of protecting any insulant attached to the inner pipe, because the cavity acts as an emergency drainage and ventilation channel in the event of flash flooding or other temporary rise of the water table.

Natural convection heat transfers to or from a pipe (or pipes) enclosed in a circular or rectangular enclosure have received much

attention[12,13,17,22-35] because of applications in superconducting AC generators,[17] aircraft cabin insulation,[22] electronic equipment,[23] compressed-gas insulated electric-power cables,[24] underground electric transmission cables,[25] solar collectors,[26] nuclear reactors,[27] fusion reactor blankets,[28] as well as in many industrial processes such as district cooling,[12] district heating,[13] heat storage,[29] density inversion of water,[30-32] reactor-spent fuel cooling,[33] radioactive waste-heat removal,[34] and geological and astrophysical problems.[35] Besides air, other fluids have been used to inhibit or enhance heat transfers across cavities: for instance, hydrogen, carbon dioxide,[36] water, transformer oil, machine oil,[37] silicone fluid,[38] nitrogen, sulphur hexafluoride[39] and argon.[40] Thus data are available for the range $0{\cdot}7 < Pr < 6000$.

THE EXPERIMENTAL STUDIES

The circular enclosure

The earliest reported systematic study of heat transfers from a horizontal pipe across a horizontal cylindrical annular cavity was by Beckmann[36] in 1931. He simulated the pipeline situation, for which the thermal insulation is provided by multilayered, thermally floating aluminium foil shields forming a series of annular, air-filled cavities around a pipe. The parameters involved in this study were the Grashof number, Gr_d (based on the inner pipe diameter, d), the Prandtl number, Pr, and the diameter ratio, D/d. The resulting correlation was stated as:

$$k_c/k = f(\mathrm{Gr}, \mathrm{Pr}, D/d) \qquad (1)$$

where k_c is the effective thermal conductivity due to combined convection and conduction through the air trapped in the cavity (and therefore $k_c \geq k$). The values of the thermal conductivity ratio, k_c/k (a form of Nusselt number), for air and carbon dioxide were determined in the ranges $1{\cdot}2 < D/d < 8{\cdot}1$ and $10^3 < Gr_d < 10^7$. The Nusselt number was found to rise with an increase of the gap size, G, for a fixed diameter hot inner pipe. However, failure to compensate for the heat losses from the ends of the inner pipe led to axial conduction errors and introduced significant three-dimensional convective currents in the flow field.

Voigt and Krischer[41] analysed an experimental system similar to that of Beckmann[36] for $1{\cdot}4 < D/d < 4{\cdot}29$ and corroborated Beckmann's

conclusions. By presenting k_c/k graphically as a function of the Grashof number, Gr_d, it was found that the correlating equation holds for geometrically similar systems, irrespective of the actual pipe sizes. This enables one to simulate large-scale practical pipe-in-pipe systems cheaply in the laboratory.

Kraussold[37] extended Beckmann's investigation using water, transformer oil and machine oil, and was able to account for the Prandtl number variations. He considered diameter ratios of 1·2, 1·5 and 3·0 and proposed a correlation which included both his and Beckmann's results to within an estimated error of $\pm 20\,\%$. However, this did not account for the independent effects of either the Grashof or the Prandtl number.

Interest in this topic subsequently declined and no significant further study was reported until 1961 when Liu *et al.*[38] considered both the fluid flow and the corresponding temperature distribution in the cavity. They examined the steady-state heat transfers between concentric pipes across annuli of air, water or silicone fluid. The overall rate was expressed as:

$$\overline{Nu}_G = f(Pr, Gr_G, G/d) \qquad (2)$$

for the range $1{\cdot}154 < D/d < 7{\cdot}50$ and $2{\cdot}41 \times 10^2 < Ra_G < 4{\cdot}22 \times 10^7$. They observed different types of stable and unstable flow depending on: (1) the diameter ratio, D/d; (2) the fluid properties; and (3) the geometry of the arrangement. With air in annuli with large diameter ratios, the fluid moved rapidly in a thin layer near each surface whilst remaining practically stationary near the gap centre, the flow pattern having a kidney shape (see Fig. 5). Maximum velocities occurred near the top of the inner pipe. The central slow-speed region gradually reduced in extent if the gap size was decreased, until a crescent-shaped pattern formed (see Fig. 4). For large temperature differences across the cavity, slow sideways oscillations were experienced for diameter ratios in the range $1{\cdot}5 < D/d < 7{\cdot}5$ (see Fig 6). Convection gradually increased as the Rayleigh number, Ra_G, rose and at very high values ($Ra_G > 5 \times 10^5$) a temperature gradient inversion (i.e. opposite in sign from that which would be expected initially in view of the temperatures of the immediate boundaries) occurred for $90° < \theta < 150°$. This is caused by the fast moving thin layer of fluid near the outer pipe wall. (A somewhat similar behaviour was also observed for a closed-ended vertical, plane-walled cavity by Brooks and Probert[42] and between infinite parallel plates by Lietzke.[43])

The observations of Liu *et al.*[38] were later confirmed by Bishop *et*

al.[2.11] for diameter ratios of 1·23, 1·85, 2·45 and 3·69, and by Lis[39] using the schlieren method with $Ra_d < 2 \times 10^5$ for annuli with $2 < D/d < 4$. Motion pictures of the flow pattern were made[11] to assist in accurately describing the flows. Kidney-shaped, crescent-shaped and cellular flow patterns were also observed by Bishop *et al.*,[44] and by Yin *et al.*[45] in their investigations of natural convection between concentric *spheres*.

Apart from the stable kidney- and crescent-eddy-shaped flows under steady conditions, Powe *et al.*[46,47] observed a two-dimensional oscillatory flow, a three-dimensional spiral flow and a two-dimensional multi-cellular flow for different values of the inverse relative gap size $1{\cdot}43 < d/G < 10{\cdot}0$. The Grashof number, Gr_d, for which the flow becomes unstable varied inversely with the radii of curvature of the bounding pipes. Huetz and Petit[48] observed multi-cellular flows when a constant heat flux was imposed on one wall and a fixed temperature on the other; a mixture of sodium and potassium was used as the working fluid.

However, Grigull and Hauf[5] proposed a different categorisation of the atmospheric-pressure air flow patterns for diameter ratios in the ranges $1{\cdot}3 < D/d < 6{\cdot}3$ and $3{\cdot}2 \times 10^2 < Gr_G < 71{\cdot}6 \times 10^4$. They identified three different flow regimes:

1. *Pseudo-conductive (i.e. two-dimensional) regime*, for $Gr_G < 2{\cdot}4 \times 10^3$, mainly characterised by conductive heat transfers as indicated by near-concentric interference fringes, and $\overline{Nu}_G$ being almost independent of Gr_G: convection effects were noticed as ΔT increased. Liu *et al.*[38] also observed that convection was present at such low Grashof numbers.
2. *Transition regimes*, for $2{\cdot}4 \times 10^3 < Gr_G < 3{\cdot}0 \times 10^4$, showing three-dimensional vortices in oscillation about the vertical longitudinal plane and restrained to relatively smaller values of the relative gap size, G/d.
3. *Fully developed two-dimensional laminar convection regime*, for $Gr_G > 3{\cdot}0 \times 10^4$, when the flow field was much more steady. However, upon increasing Gr_G the flow patterns became more kidney-shaped and the centre of the closed flow loops moved upward in the annulus.

A comparison of the results of Grigull and Hauf[5] with those of others is presented in Fig. 7 which suggests the type of flow that is expected to occur in the annuli when $0{\cdot}3 < d/G < 12{\cdot}5$ and $25 < Gr_G < 6 \times 10^6$. The multicellular flows observed[46] at $d/G = 10{\cdot}0$ were similar to those

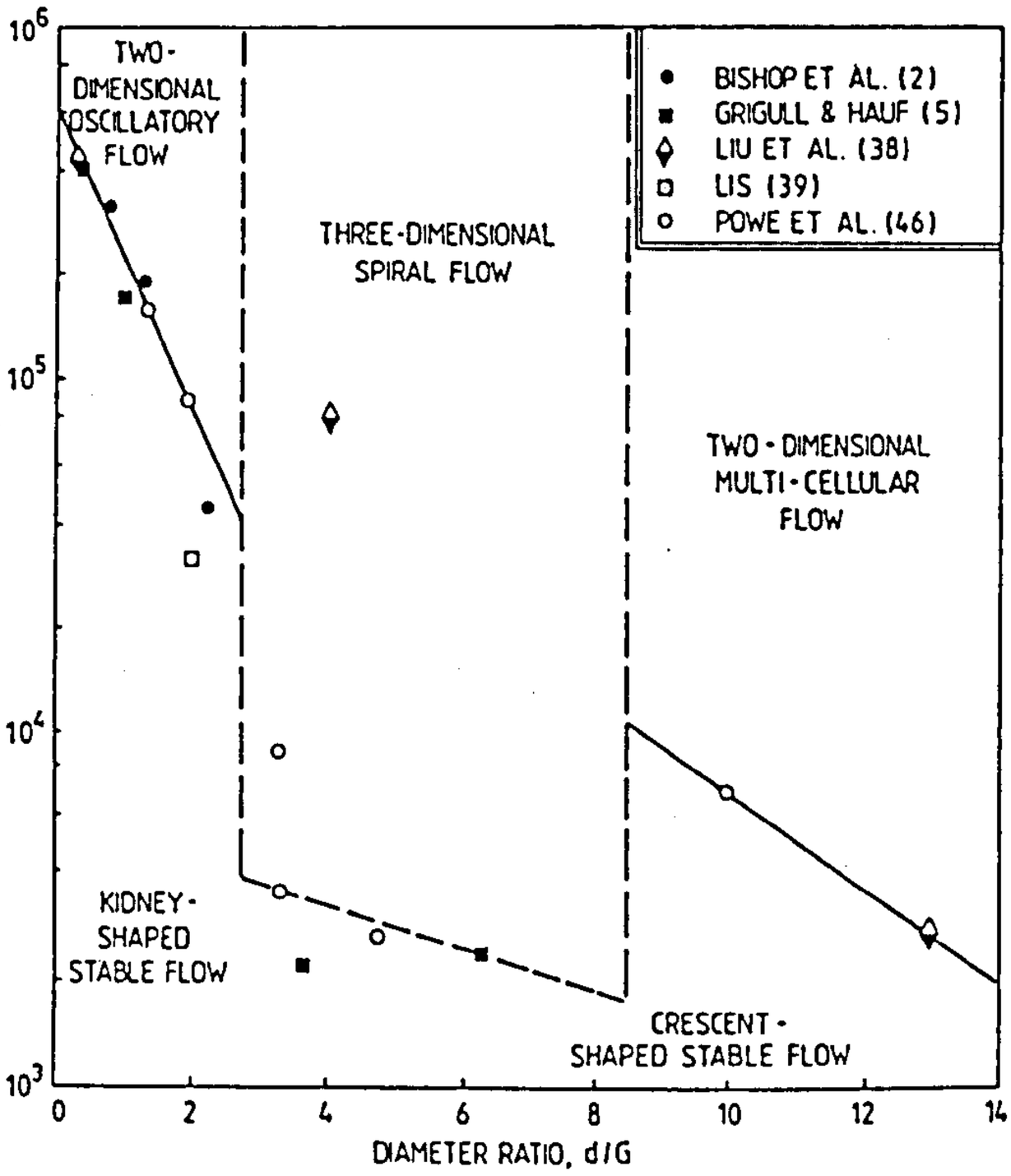

Fig. 7. Categorisation of the natural convection flow patterns in horizontal *concentric* annuli,[46] the heat flowing outwards from the central pipe.

reported by Liu *et al.*[38] at $d/G = 4{\cdot}76$ and $3{\cdot}33$; these appear to be similar to the flows described by Grigull and Hauf in the transition regime.[49] Powe *et al.*[46] concluded that, although the diameter ratio did not significantly affect the flow-patterns in an annulus, the radii of curvature of the cylinders influenced the value of the transition Grashof number, Gr_G, i.e. the value at which instabilities first appeared. This indicates that, even for the same diameter ratio, flows in larger systems would tend to have higher values of Grashof number.

However, by relating the Rayleigh number, Ra_G, and the average Nusselt number, $\overline{Nu}_d$, Liu *et al.*[38] obtained a lower value of $\overline{Nu}_d$ from that of McAdams[50] for steady-state natural-convection heat transfers from a single horizontal pipe to an infinite plane boundary. This difference can be attributed to the fact that a simple correction for gap size, G, or Prandtl number, Pr, cannot be used to reconcile data due to the

complicated flow phenomena encountered. Senftleben and Gladisch[51] set an upper limit of 500 for the diameter ratio, whereas Powe[52] suggested a limiting range of $4 < D/d < 25$ for Nusselt number versus Rayleigh number relations to be applicable. The minimum limit is determined by the conductive heat transfer, whereas the upper limit is dictated by the criterion of natural convection in a fluid of infinite extent.

Grigull and Hauf[5,53] using a Mach–Zehnder interferometer measured the local heat transfer coefficients on the boundaries of a horizontal annulus containing atmospheric-pressure air by means of a technique similar to that of Eckert and Soehngen.[54] Their results corroborated those of Beckmann,[36] and the computer predictions of Crawford and Lemlich.[55] Unlike the apparatus used by Beckmann, that employed by Grigull and Hauf achieved a constant outer pipe temperature. The latter measurements did not agree so well with those of Liu *et al.*,[38] which were consistently smaller (by ~20%). The data obtained for the fully convective flow regime could be represented by the equation:

$$\overline{\mathrm{Nu}}_G = 0{\cdot}2 + 0{\cdot}145(G/d)\,\mathrm{Gr}_G^{0{\cdot}25\exp(-0{\cdot}02G/d)} \qquad (3)$$

for $2{\cdot}1 < D/d < 6{\cdot}3$.

Soviet studies[40,56] obtained overall heat transfer data for diameter ratios, D/d, of 1·9, 4·7 and 9·4 at Grashof numbers $10^{-9} < \mathrm{Gr}_d < 10^5$, including results for the rarefied-gas regime.[40] Their experimental results were in good agreement with other published data[5,36,39,41,55] at $\mathrm{Gr}_d > 10^4$.

Kuehn and Goldstein[6] extended the existing knowledge of velocity, temperature distribution and local heat transfer coefficients as well as the overall heat transfer coefficients by using a Mach–Zehnder interferometer. For air and water at atmospheric pressure, with $G/d = 0{\cdot}8$ ($D/d = 2{\cdot}6$) at $2{\cdot}1 \times 10^4 < \mathrm{Ra}_G < 9{\cdot}8 \times 10^5$, their results were correlated using a least-squares regression analysis. It was deduced that for:

air, $k_c = 0{\cdot}159\,\mathrm{Ra}_G^{0{\cdot}272}$ over the range $2{\cdot}1 \times 10^4 < \mathrm{Ra}_G < 9{\cdot}6 \times 10^4$

water, $k_c = 0{\cdot}234\,\mathrm{Ra}_G^{0{\cdot}238}$ over the range $2{\cdot}3 \times 10^4 < \mathrm{Ra}_G < 9{\cdot}8 \times 10^5$

These conclusions agree well with the experimental correlation of Bishop,[57] the conduction-boundary-layer model developed by Raithby and Hollands,[58] and the experimental correlation given by Itoh *et al.*,[9] but the curves from Kraussold[37] and Liu *et al.*[38] were deemed to be too low. Those of Lis,[39] Shibayama and Mashimo,[59] and Barelko and

Shtessel[60] were better but the slopes of these curves do not correspond to those of Kuehn and Goldstein.[6]

Several authors[5,6,9,37-39,41,58] tried to achieve a correlation, by using a modified form of Nusselt number and/or by the introduction of a further parameter. Thus each investigation appears to have analysed their own and other results in their own way. In practice, to achieve a comprehensive correlation is extremely difficult. Kuehn and Goldstein[61] developed a semi-empirical theoretical solution, but this led to an excessively complicated correlation. However, Shilston and Probert[10] suggested a simpler correlation for the steady-state rate of heat transfer outwards by combined laminar, natural convection and conduction through the atmospheric-pressure air contained within horizontal concentric annuli.

The evolved equation was:

$$\overline{Nu}_G = [0{\cdot}181(D/d) - 0{\cdot}215]\,Gr_d^{0{\cdot}25} \qquad (4)$$

for the ranges $3 \times 10^3 < Gr_d < 10^8$ and $1{\cdot}3 < D/d < 7{\cdot}5$. This correlation obtained from an analysis of their own and other published experimental information enables designers to predict the combined convective/conductive resistance provided by the contained air for the range of concentric pipes likely to be encountered in practice. Figure 8 shows a cross-plot for the variation of 'M' in the standard equation describing the combined steady-state convection plus conduction through the air (i.e. $\overline{Nu}_G = M\,Gr_d^n$) with the diameter ratio D/d assuming $n = 0{\cdot}25$. Shilston and Probert[10] suggested that an analogous correlating equation would exist for turbulent boundary-layer flows.[39] However, insufficient experimental data have, as yet, been obtained to determine the coefficients for the turbulent situations. The shapes of the temperature profiles were dependent primarily upon the geometry of the system, i.e. upon the eccentricity, and were comparatively insensitive to the temperature difference. This corroborates the findings of Liu *et al.*[38] for the concentric arrangement.

The suggestion of Zagromov and Lyalikov[23] and Lis[39] that a vertical or horizontal eccentric displacement would influence the rate of heat transfer across a horizontal cylindrical annulus was substantiated experimentally by Probert and co-workers.[7,62] They found an optimal eccentricity, e, of 0·24 (i.e. in the upper half of the cavity) for a diameter ratio of 1·33. This position of the inner pipe reduced the overall steady-state outward heat transfer rate by ~10% compared with that for the

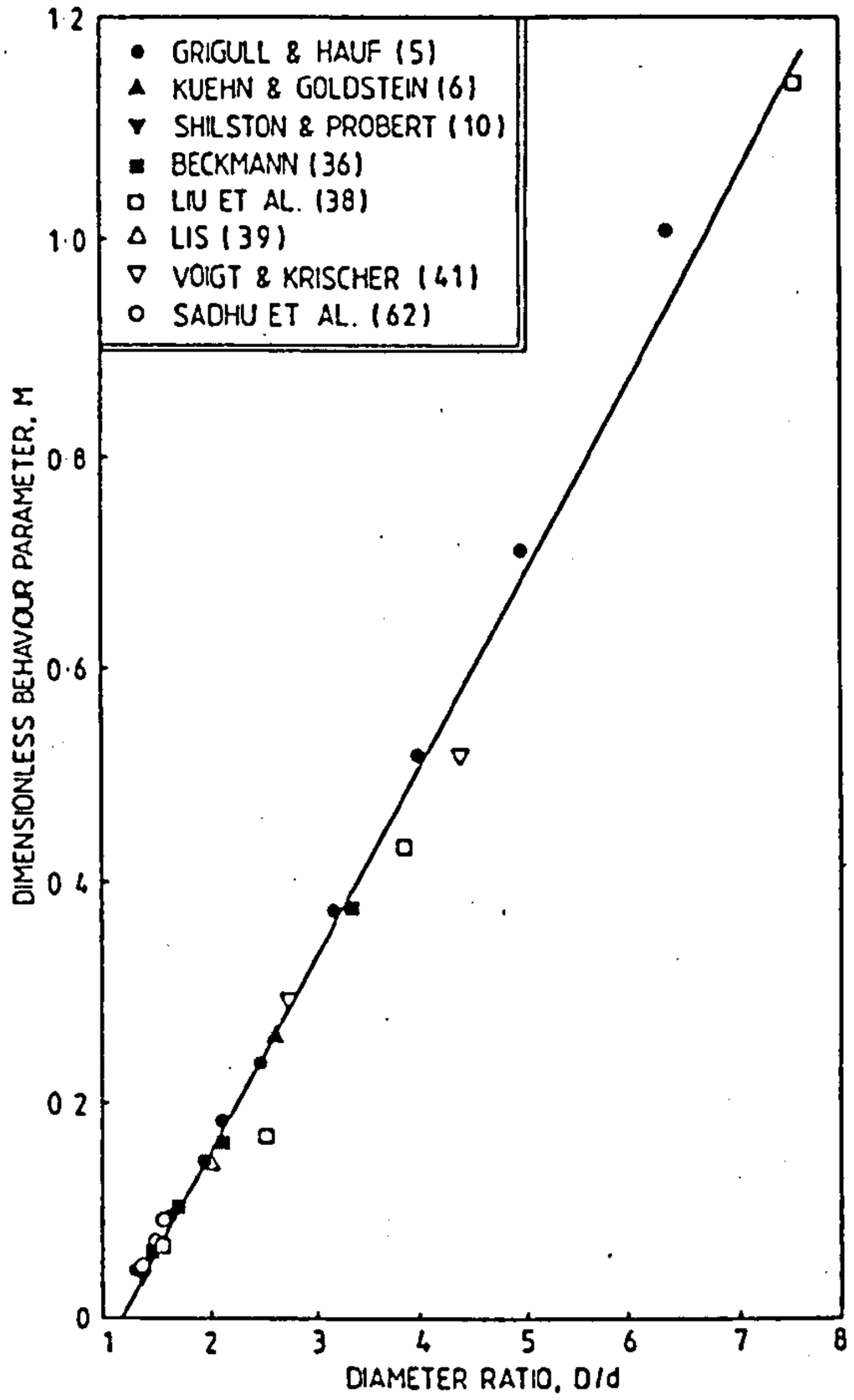

Fig. 8. Correlation of the combined steady-state convective/conductive heat transfers across horizontal, air-filled, *concentric* annular cavities, from a heated central pipe.[10]

concentric configuration. Similar observations were later confirmed by Shilston and Probert,[10] but Kuehn and Goldstein[63] stated that the overall heat transfer coefficient changed by less than 10% over the range of eccentricities investigated. Ratzel *et al.*[26] also suggested that the downward displacement of the hot inner pipe marginally enhanced the rate of convection.

Experiments by Shilston and Probert[10] and Kuehn and Goldstein[63] showed that a horizontal sidewise displacement of the inner horizontal pipe increased the rate of convective/conductive heat transfer, whereas Van de Sande and Hamer[25] did not find any change in the rate for such a displacement.

The flow patterns do not change appreciably with eccentricity for any particular set of pipes, but depend largely on the actual pipe sizes—particularly their radii, the diameter ratio and the gap size of the cavity.

Convective heat transfers in spherical annuli showed very similar basic flow patterns in spite of the entirely different bounding geometries. Weber *et al.*[64] noted that, for a given diameter ratio and test fluid, the rate of heat transfer could be increased by an eccentric displacement of the inner sphere; a negative eccentricity enhanced the convective motion and a positive value always stabilised the flow field and promoted conduction.

Considering the effects of obstructing the fluid flow in a concentric annulus, Lis[39] investigated turbulent flows at diameter ratios of 2, 3 and 4 by using either six evenly-spaced, longitudinal splitters or one helical splitter. Both spacer designs reduced the natural-convection heat-transfer rate by ~20%. The flow velocities were not appreciably affected. Shilston and Probert[65] suggested a reduction of the convective/conductive rate of heat flow by ~11% by using two horizontal radial co-planar spacers (at $\theta = \pm 90°$)—see Fig. 3—and an increase of ~8% by using two vertical radial co-planar spacers ($\theta = 0°$, 180°) for a diameter ratio of 1·5. Kwon *et al.*[14] used three equally spaced low-conductivity axial spacers ($\Delta\theta = 120°$) for diameter ratios 1·56 and 1·96; a reduction of ~20% in the convective/conductive heat leak was achieved. However, high-conductivity spacers lead to relatively large heat leaks, which overwhelm the reductions in natural convection between the pipes.

All the previously mentioned studies have been concerned with *outward* natural convection heat transfer across the cavity. Chakrabarti *et al.*[3] carried out an investigation for an *inward* heat transfer where the inner pipe was cooled by cold fluid within a relatively warm pipe. They determined the local and average heat transfer coefficients for diameter ratios of 1·57, 2·60 and 7·28. A simple correlation was presented for concentric systems. Different behaviours were observed if the heat transfer was inwards rather than outwards across the gap (see Fig. 9). However, it can be seen that the two lines describing the inwards and outwards heat transfer behaviours cross at $\overline{Nu}_G = 1$, i.e. this implies that if conduction through the air is the only heat transfer mechanism, the thermal resistance of the air cavity is the same in both directions as expected. However, when convection is present, the inwards and outwards behaviour differ increasingly as the strength of the convective currents increases. Chakrabarti *et al.* deduced an optimal eccentricity for each diameter ratio tested. The choice of the optimal value (with the inner

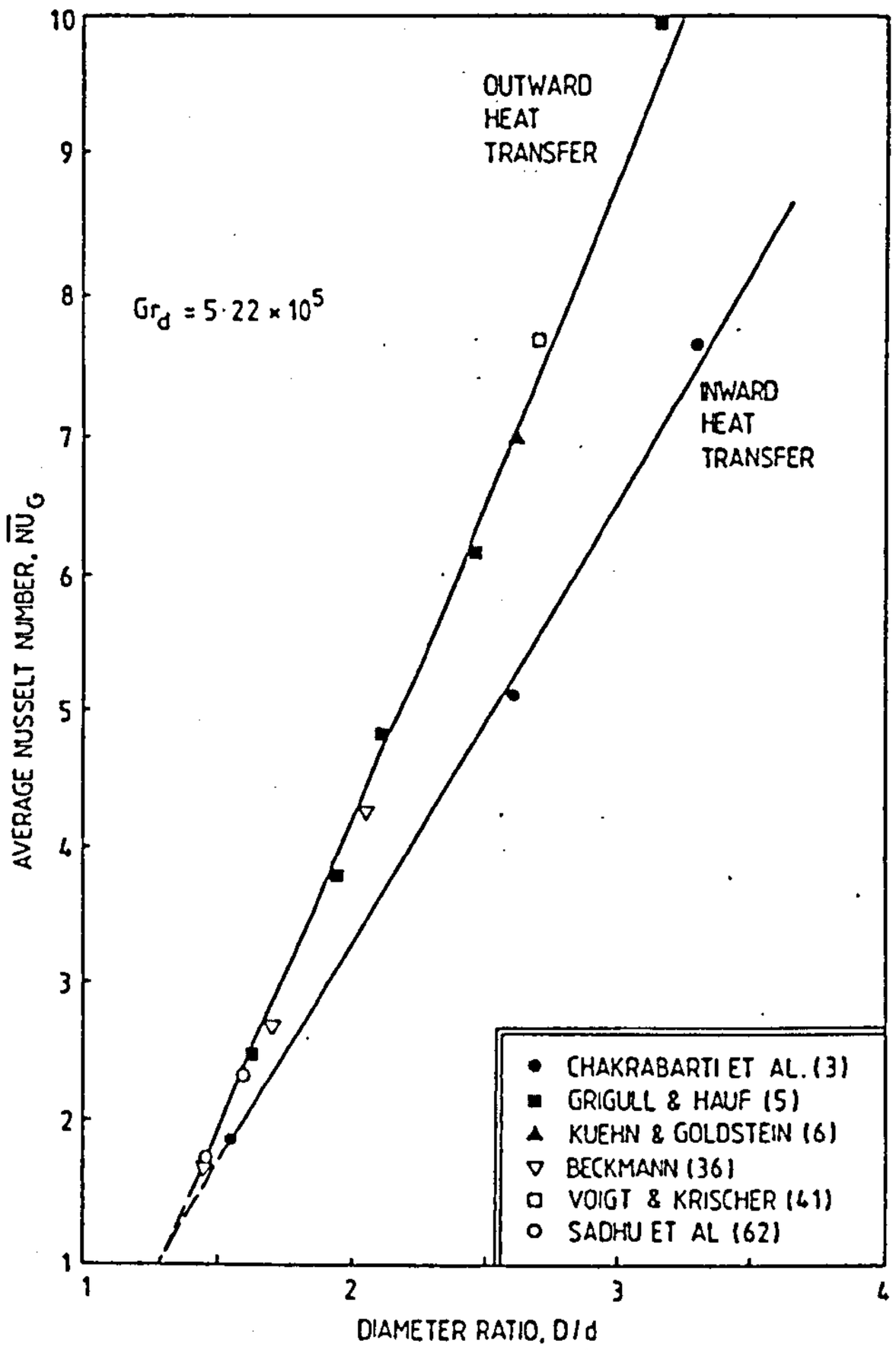

Fig. 9. Correlation of experimental data for the combined steady-state rates of convective/conductive heat transfers inwards or outwards across the horizontal, air-filled, *concentric* annuli.[3]

pipe in the lower half of the cavity) for any considered configuration led to an increase of ~15% in the combined convective/conductive component of the thermal resistance of the air in the annulus compared with that for the appropriate concentric geometry.

Babus 'Haq *et al.*[12] studied the steady-state natural convection flow visualisations of the air around two horizontal pipes: one was relatively cold and the other slightly warmer, representing the supply and return pipelines of a district-cooling system, respectively, within a slightly heated

horizontal pipe. An improvement of ~35% of the total heat transfer was achieved in the insulating performance *of the air* by adopting the 'warm-above-cold' configuration rather than the current conventional practice ('side-by-side' configuration).

The rectangular enclosure

Babus 'Haq *et al.*[66] studied experimentally the effect of the displacement ratio, E (see Fig. 2), of a heated horizontal pipe within an atmospheric-pressure, air-filled, relatively cold, horizontal rectangular enclosure. An optimal position, at a displacement ratio approximately equal to 0·7, i.e. in the upper region of the cavity, was deduced. Using this optimal value, a reduction of ~13% was obtained in the convective/conductive thermal resistance of the air compared with current conventional practice, i.e. for systems with $E = 0$.

Babus 'Haq *et al.*[13,67] considered the factors influencing the heat loss behaviour of a horizontal, *double-pipe* system (e.g. the supply and return hot water pipes of a district-heating system) within a relatively cold rectangular enclosure. Flow visualisation photographs were needed to supplement and corroborate conclusions drawn from the interferometric observations of the steady-state isotherms in the air gap. The supply (i.e. the hot) pipe was kept constant at the optimal displacement ratio[66] $E_S = 0{\cdot}7$ and an optimal displacement ratio, E_R ($= -0{\cdot}05$) was determined experimentally for the return (i.e. the relatively cooler) pipe. A reduction of ~14% was obtained in the *total* rate of heat loss through the air by using this optimal geometry of the 'hot-above-cooler' configuration compared with that for the 'side-by-side' arrangement.

Shimmel[68] employed laser holographic interferometry to investigate natural convection from a heated horizontal pipe in an isothermal rectangular enclosure.

ANALYTICAL AND NUMERICAL STUDIES

The first numerical solution of the equations describing natural convective atmospheric-pressure air flows in a cylindrical annulus was obtained by Crawford and Lemlich[55] for several diameter ratios and Grashof numbers. The solutions, achieved using a Gauss–Seidel iteration, were in good qualitative agreement with the results of Beckmann[36] and Liu

et al.[38] The numerical treatment also produced the characteristic kidney-shaped flow, with the centre of rotation of the cores in the upper half of the annulus.

Abbott's[22] matrix inversion technique led to similar but not identical results as he considered a relatively large cold pipe in a hot outer one (i.e., *inwards* heat transfer). No comments were presented for the difference in the behaviour of the inwards and outwards heat transfer across the gap, as was observed experimentally by Chakrabarti *et al.*[3]

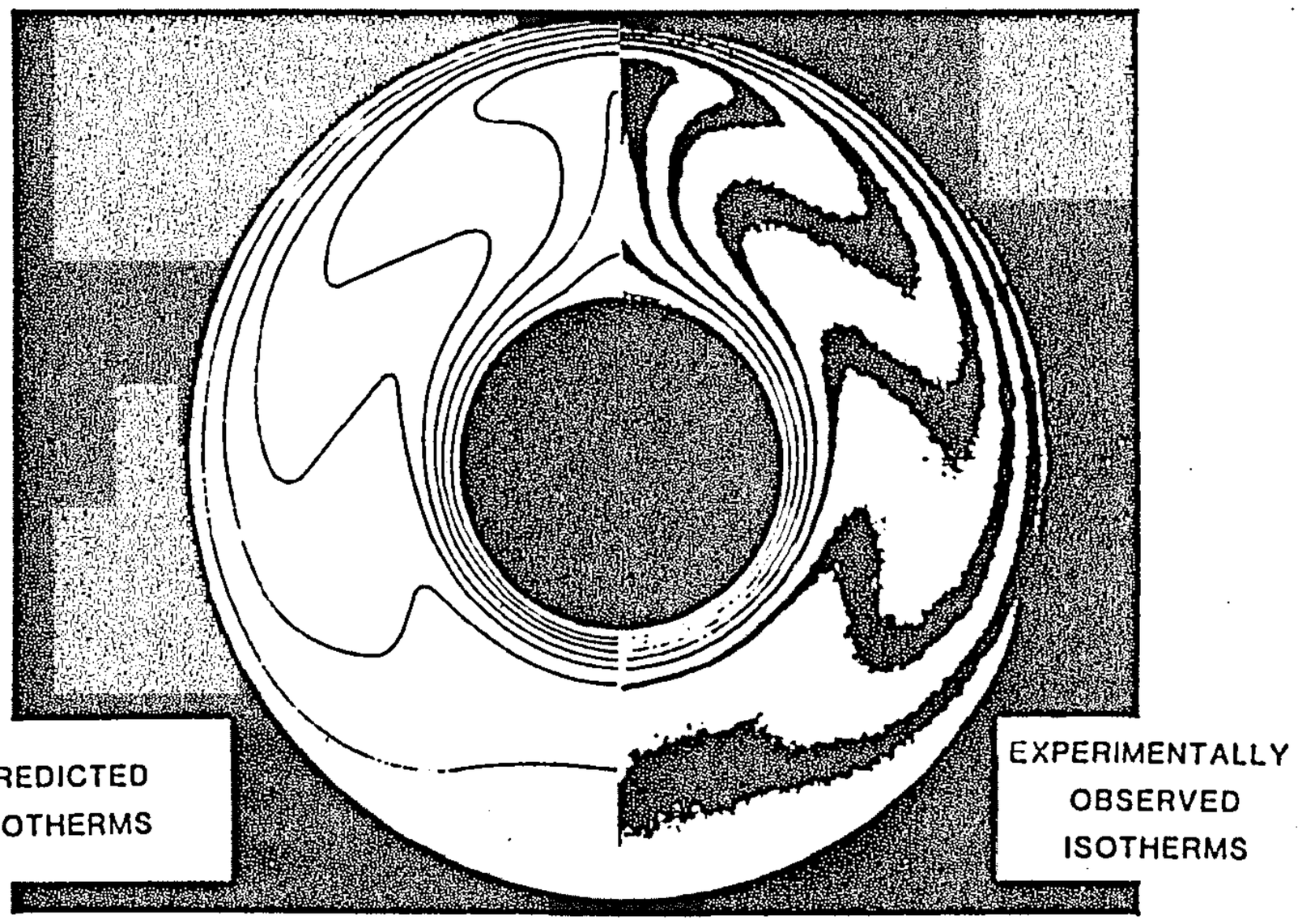

Fig. 10. Comparison of the experimental observations (for $Ra_G = 4{\cdot}7 \times 10^4$, $Pr = 0{\cdot}706$, $G/d = 0{\cdot}8$) with the numerical predictions (for $Ra_G = 5{\cdot}0 \times 10^4$, $Pr = 0{\cdot}700$, $G/d = 0{\cdot}8$) for the steady-state isotherms in an air-filled annular cavity.[6]

Extensive theoretical studies followed[4,6,29,48,59,69–76] concerning the flows and heat transfers due to natural convection between concentric pipes. Various methods were adopted, for example the finite-difference technique,[6] the power expansion for the Rayleigh number,[48,69] the perturbation expansion for temperature and velocity,[71,72] the boundary-layer approximation and integral methods,[75] and the method of series truncation.[76] They all produced numerical predictions in good agreement with experimental results (see, for example, Fig. 10).

Although correlations for the mean heat transfer coefficients have been presented,[3,10,52,58,61] no parametric studies have been reported that investigate the effects of Prandtl number and diameter ratio over the ranges needed for many practical applications. Kuehn and Goldstein[77] employed an explicit, successive over-relaxation, finite-difference technique to solve the governing equations for steady laminar flows in two dimensions between two horizontal, concentric, isothermal pipes. However, their solution did not satisfy these equations at various Prandtl numbers as well as the correlation given in Ref. 61. However, Boyd[15,78] developed a correlation of two-dimensional natural-convection heat-transfer data for horizontal concentric annuli, i.e.

$$Nu_G = 0{\cdot}794\,Ra_r^{0{\cdot}25} \tag{5}$$

This correlation applies for two different two-dimensional annuli geometries: (1) concentric circular pipes, and (2) a regular hexagonal pipe inside a concentric circular pipe in the ranges $0{\cdot}7 < Pr < 3100$, $10 < Ra_r < 10^7$ and the gap size to diameter of inner pipe ratio $0{\cdot}25 < G/d < 1{\cdot}0$.

Yao[79] developed the regular perturbation heat-transfer solution for slightly eccentric annuli at small Rayleigh numbers; eccentric effects were more important for wider gaps. But Ratzel *et al.*,[26] in their analytical study, concluded that large eccentricities caused only a slight increase in natural convective heat transfers.

However, the numerical analysis by Projahn *et al.*,[4] employing Stone's strongly implicit method, indicated that by increasing the Rayleigh number, Ra_G (i.e. with convection gradually becoming the dominant mode of heat transfer), the rate of heat transfer decreased for positive eccentricities whereas it increased substantially for negative configurations, compared with the rate across the concentric annulus. Similar conclusions were presented numerically by Prusa and Yao[8] for a diameter ratio of 2·6. Detailed predictions of the temperature and flow fields, and local heat transfer rates were given for representative cases. However, no comments on the existence of an optimal geometry were made.

In addition to their experimental study, Kwon *et al.*[14] used an approximation to model the thermal boundary condition of the spacers in the two-dimensional finite-difference numerical computations. The numerical and experimental temperature distributions and local convective heat transfer coefficients showed good agreement.

CONCLUSIONS

Experimental studies of natural convective heat transfers across horizontal circular or rectangular enclosures around single or double pipe systems suggest that the steady-state rate of free-convective heat transfer is a function of Grashof number, Gr, Prandtl number, Pr, and some other geometrical parameters in addition to the diameter ratio, D/d; the exact nature of this function is not, as yet, fully established. A recommended correlation (see eqn. (4)) for the range $3 \times 10^3 < Gr_d < 10^8$ and $1{\cdot}3 < D/d < 7{\cdot}5$ is presented to enable designers to predict the combined convective/conductive resistance provided by the air contained in the cavity.

The basic flow pattern of air is of a kidney shape or a crescent-eddy shape. For relatively narrow gap sizes, a three-dimensional cellular or spiral flow also occurred above the inner pipe. However, different shapes of flow patterns were observed for enclosures around double-pipe systems.

Optimal eccentricities and displacement ratios for the inner pipes relative to the outer enclosure for each air-filled cavity have been deduced. Eccentricity has possibly less than a 20% effect on increasing the thermal resistance of the cavity, but axial spacers may suppress the convection even further. However, by using the optimal displacement ratios ($E_S = 0{\cdot}7$, $E_R = -0{\cdot}05$), a reduction of $\sim 14\%$ in the *total* rate of heat loss across the cavity for the considered boundary temperatures was obtained.

As the boundary layer approximations and simplifying assumptions regarding the pressure gradients normally made for convection from simple bodies in a free atmosphere are invalid for enclosed spaces,[80] the problem of the analytical or numerical treatment of natural convection in a finite enclosure becomes more complicated. Still, the qualitative similarity between the theoretically predicted and experimentally observed flow patterns and the quantitative agreement of the predicted and experimental values of the heat-transfer coefficients observed have been remarkably good.

This survey has been solely concerned with natural convection and conduction heat transfer through the fluid. However, in practice, if the total heat leak is required, the corresponding radiative contribution must be determined and added to the convective/conductive value for the appropriate temperature difference. It was not felt apposite to do this

at this juncture because the radiation contribution in such a situation will depend upon the emissivities of the bounding surfaces. For totally enclosed, infinitely long systems, the radiation contribution remains constant irrespective of the position of the inner pipe relative to the outer one, and so does not affect the optimal position of that pipe provided the same surfaces are involved.[81]

REFERENCES

1. N. Heya, M. Takeuchi and T. Fujii, Influence of surface roughness on free-convection heat transfer from a horizontal cylinder, *J. Chem. Eng.*, 23 (1982), pp. 185-92.
2. E. H. Bishop, C. T. Carley and R. E. Powe, Natural convective oscillatory flow in cylindrical annuli, *Int. J. Heat Mass Transfer*, 11 (1968), pp. 1741–52.
3. S. Chakrabarti, S. D. Probert and M. J. Shilston, Optimal eccentric annuli (containing atmospheric-pressure air) for thermally-insulating, horizontal, relatively cold pipes, *Applied Energy*, 14 (1983), pp. 257-93.
4. U. Projahn, H. Rieger and H. Beer, Numerical analysis of laminar natural convection between concentric and eccentric cylinders, *Numerical Heat Transfer*, 4 (1981), pp. 131-46.
5. U. Grigull and W. Hauf, Natural convection in horizontal cylindrical annuli, *Proc. 3rd. Int. Heat Transfer Conf., Chicago*, Paper 60, 2 (1966), pp. 182–95.
6. T. H. Kuehn and R. J. Goldstein, An experimental and theoretical study of natural convection in the annulus between horizontal concentric cylinders, *J. Fluid Mech.*, 74 (1976), pp. 695-719.
7. S. D. Probert, D. Sadhu and D. Syed, Thermal insulation provided by annular air-filled cavities, *Applied Energy*, 1 (1975), pp. 145–53.
8. J. Prusa and L. S. Yao, Natural convection heat transfer between eccentric horizontal cylinders, *Trans. ASME, J. Heat Transfer*, 105 (1983), pp. 108–16.
9. M. Itoh, T. Fujita, N. Nishiwaki and M. Hirata, A new method of correlating heat-transfer coefficients for natural convection in horizontal cylindrical annuli, *Int. J. Heat Mass Transfer*, 13 (1970), pp. 1364–8.
10. M. J. Shilston and S. D. Probert, Thermal insulation provided by plain horizontal annular cavities containing atmospheric-pressure air, *Applied Energy*, 5 (1979), pp. 61-80.
11. E. H. Bishop and C. T. Carley, Photographic studies of natural convection between concentric cylinders, *Proc. Heat Transfer Fluid Mech. Inst., University of Santa Clara*, Paper 5, Stanford University Press, Palo Alto, 1966, pp. 63-78.
12. R. F. Babus 'Haq, S. D. Probert and M. J. Shilston, Improved configuration of district-cooling pipelines, *Applied Energy*, 16 (1984), pp. 67–76.
13. R. F. Babus 'Haq, S. D. Probert, M. J. Shilston and A. Talati, Suggested

design improvements concerning district-heating pipeline configurations, *Applied Energy*, 17 (1984), pp. 77-96.
14. S. S. Kwon, T. H. Kuehn and T. S. Lee, Natural convection in the annulus between horizontal circular cylinders with three axial spacers, *Trans. ASME, J. Heat Transfer*, 104 (1982), pp. 118-24.
15. R. D. Boyd, A correlation theory for steady natural convection heat transport in horizontal annuli, *Trans. ASME, J. Heat Transfer*, 105 (1983), pp. 144-50.
16. T. S. Lee, Numerical experiments with laminar fluid-convection between concentric and eccentric heated rotating cylinders, *Numerical Heat Transfer*, 7 (1984), pp. 77-87.
17. Y. Brunet and M. Renard, Heat transfer between two horizontal concentric cylinders: the outer cylinder rotating, the inner at rest, *Cryogenics*, July (1977), pp. 423-7.
18. S. D. Probert, Honeycomb structures as thermally-insulating supports, *J. Inst. Fuel*, 45 (1972), pp. 259-61.
19. S. D. Probert, M. Dixon and N. M. Pediaditakis, The optimal separation of hot and relatively cool parallel walls, *J. Inst. Fuel*, 44 (1971), pp. 104-10.
20. D. Sadhu and S. D. Probert, Thermal insulation provided by vertical annular, air-filled cavities, *J. Mech. Eng. Sci.*, 15 (1973), pp. 11-16.
21. B.S. 5970, Code of practice for thermal insulation of pipework and equipment (in the temperature range −100°C → 870°C), British Standards Institution, London, 1981.
22. M. R. Abbott, A numerical method for solving the equations of natural convection in a narrow concentric cylindrical annulus with a horizontal axis, *Quart. J. Mech. Appl. Math.*, 17 (1964), pp. 471-81.
23. Y. A. Zagromov and A. S. Lyalikov, Free-convection heat transfer in a horizontal cylindrical layer with variable source location, *Inzh.-Fiz. zh.*, 10 (1966), pp. 577-83.
24. J. A. Hitchcock and M. J. Thelwell, The cooling of underground EHV transmission cables, *IEEE Trans., Power Apparatus and Systems*, 87 (1968), pp. 129-34.
25. E. Van de Sande and B. J. G. Hamer, Steady and transient natural convection in enclosures between horizontal circular cylinders (constant heat flux), *Int. J. Heat Mass Transfer*, 22 (1979), pp. 361-70.
26. A. C. Ratzel, C. E. Hickox and D. K. Grantling, Techniques for reducing thermal conduction and natural convection heat losses in annular receiver geometries, *Trans. ASME, J. Heat Transfer*, 101 (1979), pp. 108-13.
27. K. L. Preddicord, B. D. Granapol and R. Henninger, A consistent algorithm for the study of heat transfer in eccentric annuli, *Trans. Am. Nucl. Soc.*, 22 (1975), pp. 572-3.
28. P. J. Gierszewski, B. Mikic and N. E. Todreas, *Natural circulation in fusion-reactor blankets*, ASME Paper 80-HT-69, 1980.
29. S. N. Singh and J. M. Elliott, Free convection between horizontal concentric cylinders in a slightly-thermally stratified fluid, *Int. J. Heat Mass Transfer*, 22 (1979), pp. 639-46.

30. N. Seki, S. Fukusako and M. Nakaoka, Experimental study on natural convection heat transfer with density inversion of water between two horizontal concentric cylinders, *Trans. ASME, J. Heat Transfer*, 97 (1975), pp. 556-61.
31. N. Seki, S. Fukusako and M. Nakaoka, An analysis of free-convective heat transfer with density inversion of water between two horizontal concentric cylinders. *Trans. ASME, J. Heat Transfer*, 98 (1976), pp. 670-2.
32. P. Vasseur, L. Robillard and B. Chandra Shekar, Natural convection heat-transfer of water within a horizontal cylindrical annulus with density inversion effects, *Trans. ASME, J. Heat Transfer*, 105 (1983), pp. 117-23.
33. B. B. Klima, *LMFBR spent fuel transport: single assembly heat transport test*, Oak Ridge National Laboratory TM-4936, 1975.
34. P. Vasseur, T. H. Nguyen, L. Robillard and V. K. Tong Thi, Natural convection between horizontal concentric cylinders filled with a porous layer with internal heat generation, *Int. J. Heat Mass Transfer*, 27 (1984), pp. 337-49.
35. G. N. Facas and B. Farouk, Transient and steady-state natural convection in a porous medium between two concentric cylinders, *Trans. ASME, J. Heat Transfer*, 105 (1983), pp. 660-3.
36. W. Beckmann, Die Wärmeübertragung in zylindrischen gasschichten bei natürlicher konvektion, *Forsch. Geb. d. Ingenieurwesen*, 2 (1931), pp. 165-78.
37. H. Kraussold, Wärmeabigabe von zylindrischen flüssigkeitschichten bei natürlicher konvektion, *Forsch. Geb. d. Ingenieurwesen*, 5 (1934), pp. 186-91.
38. C. Y. Liu, W. K. Mueller and F. Landis, Natural-convection heat transfer in long horizontal cylindrical annuli, *Int. Developments in Heat Transfer, Int. Heat Transfer Conf., University of Colorado*, Paper 117, 5, 1961, pp. 976-84.
39. J. Lis, Experimental investigation of natural convection heat transfer in simple and obstructed horizontal annuli, *Proc. 3rd. Int. Heat Transfer Conf.*, Chicago, Paper 61, 2, 1966, pp. 196-204.
40. Y. A. Koshmarov and A. Y. Ivanov, Experimental study of heat transfer through a rarefied gas between coaxial cylinders, *Heat Transfer—Soviet Research*, 5 (1973), pp. 29-36.
41. H. Voigt and O. Krischer, Die Wärmeübertragung in zylindrischen luftschichten bei natürlicher konvektion, *Forsch. Geb. d. Ingenieurwesen*, 3 (1932), pp. 303-6.
42. R. G. Brooks and S. D. Probert, Heat transfer between parallel walls: an interferometric investigation, *J. Mech. Eng. Sci.*, 14 (1972), pp. 107–27.
43. A. F. Lietzke, *Theoretical and experimental investigation of heat transfer by laminar natural convection between parallel plates*, NACA Report 1223, 1956.
44. E. H. Bishop, R. S. Kolflat, L. R. Mack and J. A. Scanlan, Convective heat transfer between concentric spheres, *Proc. Heat Transfer Fluid Mech. Inst., University of California*, Paper 5, Stanford University Press, Palo Alto, 1964, pp. 69-80.

45. S. H. Yin, R. E. Powe, J. A. Scanlan and E. H. Bishop, Natural-convection flow patterns in spherical annuli, *Int. J. Heat Mass Transfer*, 16 (1973), pp. 1785–95.
46. R. E. Powe, C. T. Carley and E. H. Bishop, Free convective flow patterns in cylindrical annuli, *Trans. ASME, J. Heat Transfer*, 91 (1969), pp. 310-14.
47. R. E. Powe, S. H. Yin, E. H. Bisop, C. T. Carley and J. A. Scalan, Flow visualisation of free convection in confined spaces, *Proc. 4th. Canadian Congress of Appl. Mech., Montreal*, 1973, pp. 797–8.
48. J. Huetz and J. P. Petit, Natural and mixed convection in concentric annular spaces—experimental and theoretical results for liquid metals, *5th. Int. Heat Transfer Conf., Tokyo*, Paper NC4.9, 3, 1974, pp. 169–72.
49. U. Grigull and W. Hauf, Authors' rebuttal, natural convection in horizontal cylindrical annuli, *3rd. Int. Heat Transfer Conf., Chicago*, Discussion Volume, 1966, pp. 157-8.
50. W. H. McAdams, *Heat transmission*, 3rd edn, McGraw-Hill Book Co. Inc., New York, 1954, pp. 176-8.
51. H. Senftleben and H. Gladisch, Wärmeübergang in gasen zwischen koaxialen zylindern, *Zeitschrift für Physik*, 125 (1949), pp. 629-52.
52. R. E. Powe, Bounding effects on the heat loss by free convection from spheres and cylinders, *Trans. ASME, J. Heat Transfer*, 96 (1974), pp. 558-60.
53. W. Hauf and U. Grigull, Optical methods in heat transfer, *Advances in Heat Transfer*, Vol. 6, Academic Press, New York, 1970, pp. 133-366.
54. E. R. G. Eckert and E. E. Soehngen, *Studies on heat transfer in laminar free-convection with the Zehnder-Mach interferometer*, Wright-Patterson Air Force Base, AF Technical Report 5747, 1948.
55. L. Crawford and R. Lemlich, Natural convection in horizontal concentric cylindrical annuli, *I & EC Fundamentals*, 1 (1962), pp. 260-4.
56. A. A. Berkengeim, An investigation of natural convection in cylindrical liquid layers, *Inzh.-Fiz. zh.*, 10 (1966), pp. 459-64.
57. E. H. Bishop, Discusser, natural convection in horizontal cylindrical annuli, *3rd. Int. Heat Transfer Conf., Chicago*, Discussion Volume, 1966, pp. 155-7.
58. G. D. Raithby and K. G. T. Hollands, A general method of obtaining approximate solutions to laminar and turbulent free-convection problems, *Advances in Heat Transfer*, Vol. 11, Academic Press, New York, 1975, pp. 265-315.
59. S. Shibayama and Y. Mashimo, Natural-convection heat-transfer in horizontal concentric cylindrical annuli, *Papers JSME Nat. Symp.*, 196 (1968), pp. 7-20.
60. V. V. Barelko and E. A. Shtessel, On a heat-transfer law for free convection in cylindrical and spherical layers, *Int. Chem. Engrs.*, 13 (1973), pp. 479-83.
61. T. H. Kuehn and R. J. Goldstein, Correlating equations for natural convection heat transfer between horizontal circular cylinders, *Int. J. Heat Mass Transfer*, 19 (1976), pp. 1127-34.

62. D. Sadhu, S. D. Probert, J. Medwell and D. Syed, Thermal resistance of a closed-ended, annular, air-filled cavity: inclination and eccentricity dependence, *J. Mech. Eng. Sci.*, 17 (1975), pp. 313–22.
63. T. H. Kuehn and R. J. Goldstein, An experimental study of natural convection heat transfer in concentric and eccentric horizontal cylindrical annuli, *Trans. ASME, J. Heat Transfer*, 100 (1978), pp. 635–40.
64. N. Weber, R. E. Powe, E. H. Bishop and J. A. Scanlan, Heat transfer by natural convection between vertically eccentric spheres, *Trans. ASME, J. Heat Transfer*, 95 (1973), pp. 47–52.
65. M. J. Shilston and S. D. Probert, Effects of horizontal and vertical spacers on the heat transfer across a horizontal, annular, air-filled cavity, *Applied Energy*, 4 (1978), pp. 21–37.
66. R. F. Babus 'Haq, S. D. Probert and M. J. Shilston, Optimal location of a single horizontal pipeline in a rectangular, horizontal, air-filled enclosure to achieve maximum thermal insulation, *Applied Energy*, 18 (1984), pp. 239–59.
67. R. F. Babus 'Haq, S. D. Probert and M. J. Shilston, Steady-state heat losses from horizontal pipes in an air-filled rectangular trench, *Proc. I. Mech. E, Eng. Sci.*, in press.
68. W. P. Shimmel, Jr, *Application of laser holographic interferometry to natural convection in enclosures*, Sandia Laboratories, Fluid Mech. Heat Transfer Div. Albuquerque, 1979, pp. 41–8.
69. L. R. Mack and E. H. Bishop, Natural convection between horizontal concentric cylinders for low Rayleigh numbers, *Quart. J. Mech. Appl. Math.*, 21 (1968), pp. 223–41.
70. R. E. Powe, C. T. Carley and S. L. Carruth, A numerical solution for natural convection in cylindrical annuli, *Trans. ASME, J. Heat Transfer*, 93 (1971), pp. 210–20.
71. Z. Rotem, Conjugate free-convection from horizontal, conducting circular cylinders, *Int. J. Heat Mass Transfer*, 15 (1972), pp. 1679–93.
72. P. F. Hodnett, Natural convection between horizontal heated concentric circular cylinders, *J. Appl. Math. Physics*, 24 (1973), pp. 507–16.
73. J. R. Custer and E. J. Shaughnessy, Thermo-convective motion of low Prandtl number fluids within a horizontal cylindrical annulus, *Trans. ASME, J. Heat Transfer*, 99 (1977), pp. 596–602.
74. M. C. Charrier-Mojtabi, A. Mojtabi and J. P. Caltagirone, Numerical solution of a flow due to natural convection in horizontal cylindrical annulus, *Trans. ASME, J. Heat Transfer*, 101 (1979), pp. 171–235.
75. M. C. Jischke and M. Farshchi, Boundary-layer regime for laminar free convection between horizontal circular cylinders, *Trans. ASME, J. Heat Transfer*, 102 (1980), pp. 228–35.
76. Y. T. Shee and S. N. Singh, Natural convection from a horizontal cylinder at small Grashof numbers, *Numerical Heat Transfer*, 5 (1982), pp. 479–92.
77. T. H. Kuehn and R. J. Goldstein, A parametric study of Prandtl number and diameter ratio effects on natural convection heat transfer in horizontal cylindrical annuli, *Trans. ASME, J. Heat Transfer*, 102 (1980), pp. 768–70.

78. R. D. Boyd, A unified theory for correlating steady laminar natural-convective heat-transfer data for horizontal annuli, *Int. J. Heat Mass Transfer*, 24 (1981), pp. 1545-8.
79. L. S. Yao, Analysis of heat transfer in slightly eccentric annuli, *Trans. ASME, J. Heat Transfer*, 102 (1980), pp. 279-84.
80. R. E. Powe, R. O. Warrington and J. A. Scanlan, Natural-convective flow between a body and its spherical enclosure, *Int. J. Heat Transfer*, 23 (1980), pp. 1337-50.
81. A. Feingold and K. G. Gupta, New analytical approach to the evaluation of configuration factors in radiation from spheres and infinitely-long cylinders. *Trans. ASME, J. Heat Transfer*, 92 (1970), pp. 69-76.

CHAPTER 3

OPTIMAL LOCATION OF A SINGLE HORIZONTAL PIPELINE IN A RECTANGULAR, HORIZONTAL, AIR-FILLED ENCLOSURE TO ACHIEVE MAXIMUM THERMAL INSULATION

Applied Energy 18 (1984)

Optimal Location of a Single Horizontal Pipeline in a Rectangular, Horizontal Air-filled Enclosure to Achieve Maximum Thermal Insulation

SUMMARY

An experimental investigation into the effect of the displacement ratio of a heated horizontal pipeline within an atmospheric pressure air-filled, relatively cold, horizontal rectangular cavity was made. The optimal position of the pipeline to achieve maximum energy thrift occurred at a displacement ratio approximately equal to 0·7, *i.e. in the upper region of the cavity. This result is of significance with respect to the reduction of distribution heat losses from underground district-heating pipelines.*

NOMENCLATURE

D	Diameter of the supply (i.e. the hot) pipe (mm).
E	Displacement ratio $\{=1-2U/(Y-D)$, see Fig. 1$\}$: $-1 \leq E \leq 1$.
G	Average vertical gap size $\{=(Y-D)/2\}$ (mm).
L	Axial length of the considered horizontal air-filled cavity, see Fig. 2 (mm).
M	Dimensionless parameter dependent upon the geometry and temperature distribution of the system $\{=\overline{Nu_0}/Gr_0^n\}$.
n	Power index of the Grashof number in the $\overline{Nu_0}$ versus Gr_0 relationship.

Applied Energy 0306-2619/84/$03·00

R Radius of the circle enclosing the rectangular outer cavity $\{=\frac{1}{2}\sqrt{X^2+Y^2}\}$(mm).

T Steady-state temperature of the air corresponding to the considered interference fringe (°C).

U Minimum vertical gap for the chosen configuration, i.e. the shortest vertical distance between the pipe and the *upper* horizontal internal surface of the enclosure, see Fig. 1 (mm).

X Horizontal width of the rectangular cavity, see Fig. 1 (mm).

Y Vertical extent of the rectangular cavity, see Fig. 1 (mm).

Gr_0 Local Grashof number, based on the diameter, D, of the pipe.

Nu_0 and $\overline{Nu_0}$ Local and average Nusselt numbers, respectively, for the steady-state heat transfers from the supply (i.e. the hot) pipe, based on the average gap size, G.

β Coefficient of the thermal expansion of the air contained in the cavity ($\approx 1/T_m$), (K^{-1}).

ΔN Fringe shift, i.e. number of fringes moved.

ΔT Steady-state temperature difference between the outer surface of the supply (i.e. the hot) pipe and the inner surface of the enclosure: $\Delta T = T_s - T_o$ (°C).

λ Wavelength of light ($=0{\cdot}6328\,\mu$m) for the He–Ne laser used.

μ Refractive index of air.

θ Angular co-ordinate, measured from zero for the relatively upwards radius vector emanating from the centre of the supply (i.e. the hot) pipe and increasing in a clockwise rotation, see Fig. 7 (degrees).

Suffixes

m Mean value.

o For the outer enclosure.

R At the reference temperature.

S For the hot pipe.

v In vacuum.

0 Value at angle θ.

Abbreviations

CHP Combined heat and power.

DH District heating.

SNG Synthetic natural gas.

Glossary

Utilidor — A duct (including a walkway) through which the mains supplies (e.g. heated water) pass, and which facilitates inspection of those distribution mains. This term is used primarily in the USA.

DISTRICT-HEATING

Much attention has been devoted to investigating heat transfers across annular cavities,[1-7] but there is a dearth of information concerning the corresponding heat leaks across rectangular horizontal air-filled cavities containing cylindrical pipes.[8] However, in practice, this geometry is frequently adopted, especially for ground-level and underground pipeline systems, where a rectangular trench carries a hot water or steam pipe for district-heating schemes[9] or for industrial processes.

Well designed district-heating systems can be found in many towns and cities in Europe and in the Asian part of the Soviet Union.[10] For Europe, about 55 per cent of the population could be supplied economically from central district-heating plants and this figure will most probably rise significantly in the next two decades, because the world's urban population is growing much faster than the total population.[11] However, currently less than 1 per cent of the UK space-heating demand is supplied by district-heating compared with more than 10 per cent in countries such as Denmark and Sweden.[12] The UK is at least 20 years behind Europe with respect to the widespread adoption of district-heating.[13] This has arisen partly because the installation of large heat-distribution pipeworks in cities presents particular disruption problems due to space limitations in UK highways, the configuration of buildings and customers insistence upon a high standard of operational reliability.[14] The control over each of the water, gas, electricity and telephone services remains in the hands of separate nationalised industries, each with its own bureaucracy. This makes it excessively frustrating even to try to get accepted the techniques of pipeline laying commonly adopted in many other countries.[10]

Following the Marshall report[15] which recommended the introduction in the UK of a large-scale CHP/DH plant and a 'lead city' to be chosen, and later the Atkins & Partners report[16] which concluded that large-scale CHP/DH schemes for nine selected cities may now be commercially viable in the UK, no candidate cities have, as yet, been chosen by the Government. Recent studies[17] suggest that, by the time natural gas prices have risen sufficiently for coal-derived synthetic natural gas to become

available commercially, combined heat and power, together with district-heating, would have the potential to economically serve almost 30 per cent of the existing buildings. However, pertinent experience to date[18] has been unsatisfactory, although these predominantly employ mains systems not conforming to the relevant British Standards.

It is normal practice for district-heating pipes to be clad with insulants, located in an atmospheric pressure air-filled rectangular trench: this arrangement is sometimes referred to as the 'free-draining' system.[19] Then, in the event of a leak, flooding or a high water table (which occurs intermittently in Britain's maritime climate), drainage and evaporation from around the pipe would ensue automatically.[20] Otherwise, dampness in the insulant can (i) lead to leaching and hence promote corrosion of the underlying steel pipe, (ii) reduce the system's insulating effectiveness and (iii) in many instances damage the insulant permanently. However, this ventilation lowers the effective thermal resistance of the cavity, and so usually should be limited to the minimum necessary to disperse the moisture.[21] However, such ventilation may be used to avoid overheating of a hot surface. Many large buried utilidors in Siberia are ventilated once a year in the winter to refreeze the surrounding soil.[22]

District-heating has been introduced in some situations which are not economically viable—for example, on low density of demand 'new' university campuses in the 1960s. There, quite often, the architect wished to avoid a plethora of chimneys, preferring to have only one for a central boiler house, i.e. architectural considerations took excessive precedence over engineering economics. Also, the heat pipelines installed were sometimes inadequately designed and poorly insulated, so it is not surprising that the opinion on several university campuses is now forcibly propagated that it is always better to use separate boilers in individual buildings. However, this need not necessarily be so on a high density site (for example, the City University, London).

THE PRESENT INVESTIGATION

As the air-filled cavity configuration is frequently adopted, it appears desirable to optimise the position of the pipe within the cavity in order to minimise the rate of heat loss from the pipe via conduction, convection and radiation through the surrounding air. By using this optimal

geometrical arrangement, the thermal insulation afforded by the surrounding air is maximised: this can be achieved without any additional material costs and without the need for special constructional skills.[23,24]

The present study investigated the steady-state rate of heat transfer across a horizontal rectangular cavity containing a horizontal hot pipe (representing the supply pipeline of the district-heating system). The aim was to optimise the position of the pipe in order to achieve the minimum rate of heat loss for a specified steady-state temperature difference, ΔT, between the pipe and its rectangular enclosure.

THE EXPERIMENTAL RIG (see Fig. 1)

The values of the experimental parameters chosen for this investigation were:

$$X = 100\,\text{mm}, \qquad Y = 100\,\text{mm}, \qquad L = 630\,\text{mm}, \qquad D = 28{\cdot}5\,\text{mm}$$

$$-0{\cdot}5 < E < 0{\cdot}9$$

$$17\,^{\circ}\text{C} < T_S < 40\,^{\circ}\text{C}$$

$$4\,^{\circ}\text{C} < \Delta T < 25\,^{\circ}\text{C}$$

For all the tests undertaken in this investigation, the centre of the pipe was maintained at $X/2$ ($=50\,\text{mm}$) from both vertical walls of the enclosure.

Hauf and Grigull[25] stated that the length, L, of the test cavity should exceed 500 mm in order to justify disregarding the three-dimensional effects in the air near the end plates (see Fig. 2). This implied that, for $L/R > 8$, three-dimensional motions in the annular cavity had only negligible influences upon the recorded steady-state rates of heat transfer.[2] For the present system, taking R as the least radius of the circle enclosing the rectangular section perpendicular to the outer cavity, $L/R = 8{\cdot}9$ and so complies with this criterion.

The walls of the cold outer enclosure (representing the district-heating trench in practice) were manufactured from Perspex and were water cooled, each wall containing a series of enclosed channels through which water ran at mains pressure. Each wall was cooled independently so as to avoid an appreciable rise in the temperature of the water, which would thereby lead to a significantly non-uniform temperature distribution of the rectangular walls. Thirty-six copper-constantan thermocouples were sealed into holes so that the thermojunctions were flush with the cavity's

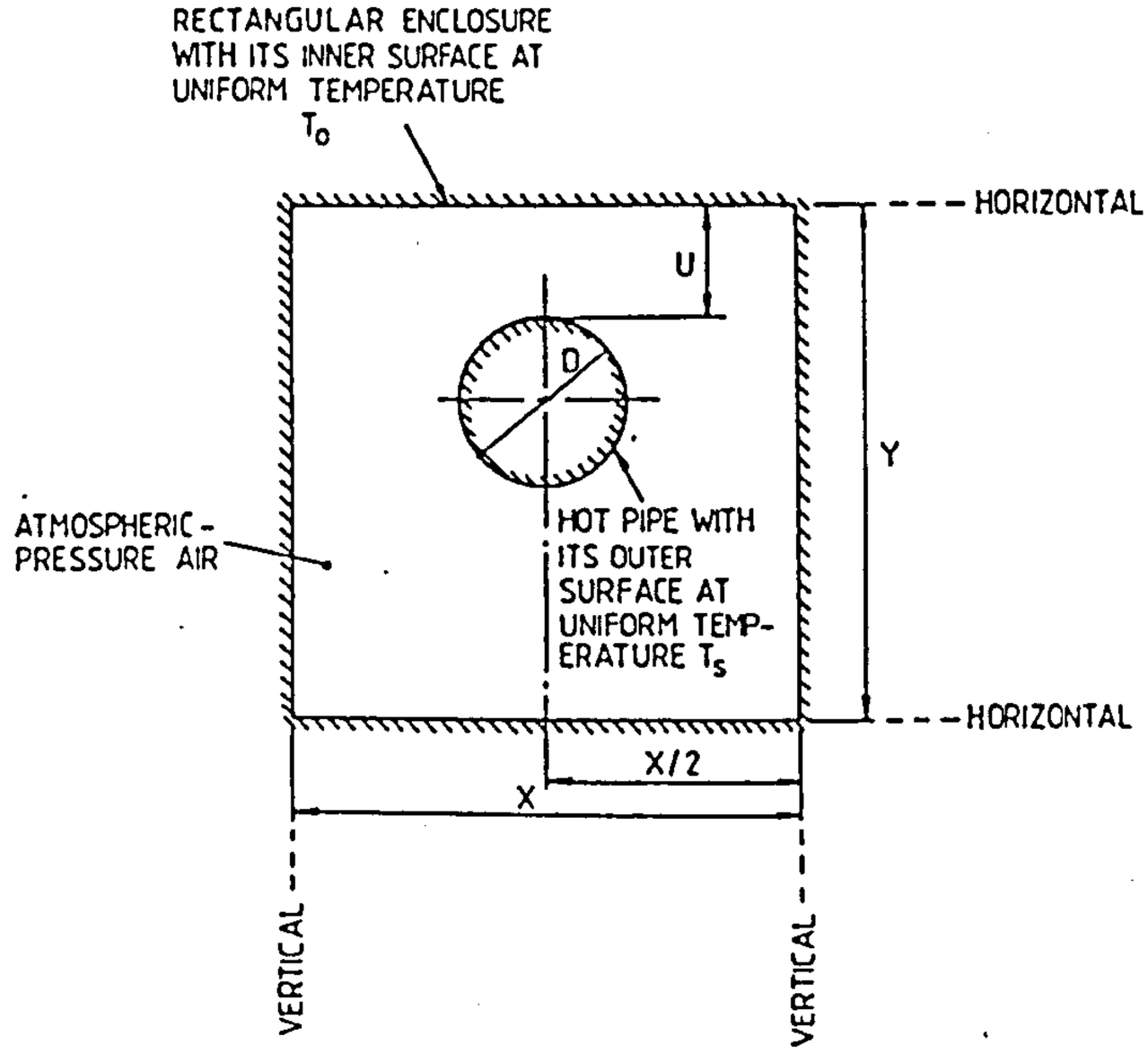

Fig. 1. Schematic representation of a vertical section perpendicular to the length of the horizontal pipe in its rectangular enclosure.

inner surface to avoid tripping the boundary layer air flows within the cavity. The leads of these thermocouples were passed horizontally, and parallel with the cavity's surfaces, through the cavity wall to avoid conductive heat leaks affecting the recorded observations. The ends of the cavity were insulated with expanded polystyrene collars to insulate the small amount of inner pipe which protruded at each end. Vertical optically flat, uniformly thick, homogeneous glass plates, i.e. the end plates, were fixed flush to the collars in order to seal the cavity from the surrounding ambient air.

The ends of the copper pipe (i.e. representing the supply pipeline) were closed with brass spigots, which were drilled and tapped to take a drilled bolt. Twelve copper-constantan thermojunctions were fixed flush with the outer surface of the pipe in small drilled holes. The thermojunction leads, being inside the pipe, were passed through the drilled bolts at either end. The pipe was fixed at each end to a copper bus-bar, which was attached to a support stand, so that the pipe could be set at any position along the symmetrical vertical plane running the length of the duct. The pipe was

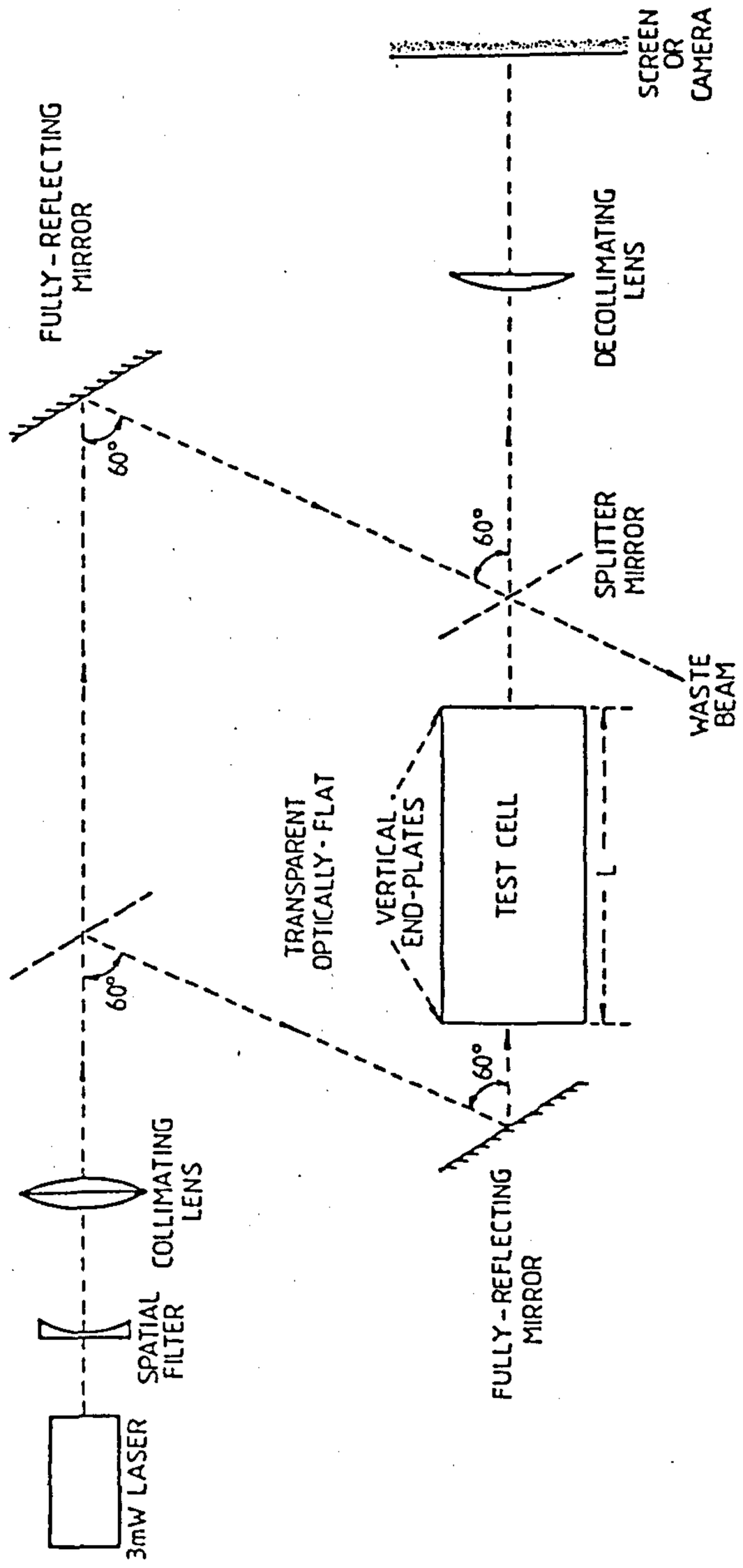

Fig. 2. Schematic plan view of the Mach-Zehnder interferometer.

heated by passing a low-voltage high-amperage alternating current between its two ends. The eddy current dissipation resulted in uniform heating along the pipe, the ends of the bus-bar being secured at the centre of each pipe end with a drilled bolt and washer. The transformer was equipped with a control dial so that the amount of current passing through the pipe, and hence the amount of heating, could be varied by known amounts as desired.

An 18 cm field-of-view, 3 mW He–Ne laser-stimulated Mach-Zehnder interferometer[26]—see Appendix 1—was used to produce a distinctive characteristic interferogram for each two-dimensional steady-state temperature distribution in the cavity examined. These interferograms indicated the refractive index variations integrated over the axial length of the considered cavity. The map of interference fringes so obtained indicated the isothermal contours within the cavity. It was recorded on an Ilford FP4 film, with a single-lens reflex camera (fitted with a 135 mm, f2·8 telephoto-lens). The effects of image distortion due to refraction of the beam through the cavity, and also at the ends of it, were reduced by focusing the camera on a vertical plane (at 0·33 L) from the end-plate nearer to the camera, as recommended by Mehta and Black.[27]

OBSERVATIONS AND RECOMMENDATIONS

Enlarged prints of the interferograms (see Fig. 3) were developed for analysis (see Appendix 2). A travelling microscope was used to aid accurate measurement of the separations between the centres of fringes. The fringe displacements from the pipe wall were recorded at 15 degree ($=\Delta\theta$) increments around the pipe, generally the first five fringe displacements being measured except where there were less fringes in the pipe's boundary layer. Readings were only necessary for half of each interferogram because the pipe was always equi-distant from the two vertical walls of the enclosure, i.e. vertical symmetry appertained.

A plot of the local Nusselt number, Nu_θ, versus the angular co-ordinate, θ, is shown in Fig. 4 for selected values of the displacement ratio, E. The minimum value of the local Nusselt number occurred near the top of the pipe (i.e. at $\theta = 0°$) for $-0{\cdot}5 < E < 0{\cdot}5$. The angular position of the minimum local Nusselt number increases from $\theta = 0°$ for $E = 0{\cdot}5$ to $\theta = 45°$ for the largest positive displacement ratio of 0·9. This 'minimum'

angular position was also temperature dependent: as the temperature difference, ΔT, increased, the angular position of the minimum local Nusselt number decreased. This occurred because the fluid velocity in the boundary layer increased as ΔT rose, and the flow penetrated further into the relatively stagnant region near the top of the cavity. The influence of the temperature difference on the position corresponding to the minimum local Nusselt number for a pipe-in-pipe system with eccentric displacement is much less (than for the present configurations with the rectangular enclosure) because of the greater restriction imposed on the fluid flow by the outer cylinder wall.

Grigull and Hauf[2] noticed three regions of flow in an annular cavity, and these could be differentiated by their distinct curves for the combined steady-state convective/conductive heat leaks versus Gr, although all are of the form $\overline{\mathrm{Nu}}_0 = M\,\mathrm{Gr}_0^n$. The pseudo-conductive region, where the Nusselt number is essentially independent of the Grashof number, has a slope (corresponding to 'n') of virtually zero. The fully developed convective region has a slope of $n = 0{\cdot}25$ for laminar flow, and between these two regions is the transition region. Thus, for this investigation, stable convective flow was observed to occur over the whole Grashof number range tested. However, the slope of the $\log_{10}\overline{\mathrm{Nu}}_0$ versus $\log_{10}\mathrm{Gr}_0$ plot (see Fig. 5) does not remain invariant at 0·25, as would be expected for cylindrical annuli. For small temperature differences, a large area of relatively stagnant fluid exists at the bottom of the cavity. As the temperature difference increases, the flow penetrates further into this region. Thus, a large initial increase in the steady-state convective heat transfer across the cavity occurs with a small change in ΔT for low values of ΔT. For higher values of ΔT, the effect of the same change in temperature difference is reduced. When fully developed flow occurs throughout the cavity, it is anticipated that the slope of the $\log_{10}\overline{\mathrm{Nu}}_0$ versus $\log_{10}\mathrm{Gr}_0$ plots would tend to 0·25 (see Fig. 5).

The radiative component of the steady-state rate of heat flux across the cavity is independent of the displacement ratio for a configuration composed of infinitely long pipe and enclosure.[28] For this configuration, therefore, the optimal displacement ratio, determined from the conduction–convection data, will also be the optimum for the combined radiation, conduction and convection contributions through the air.

Figure 6 is a plot of 'M' (an indication of the steady-state rate of heat transfer) versus the displacement ratio, E. The value of 'M' is a maximum

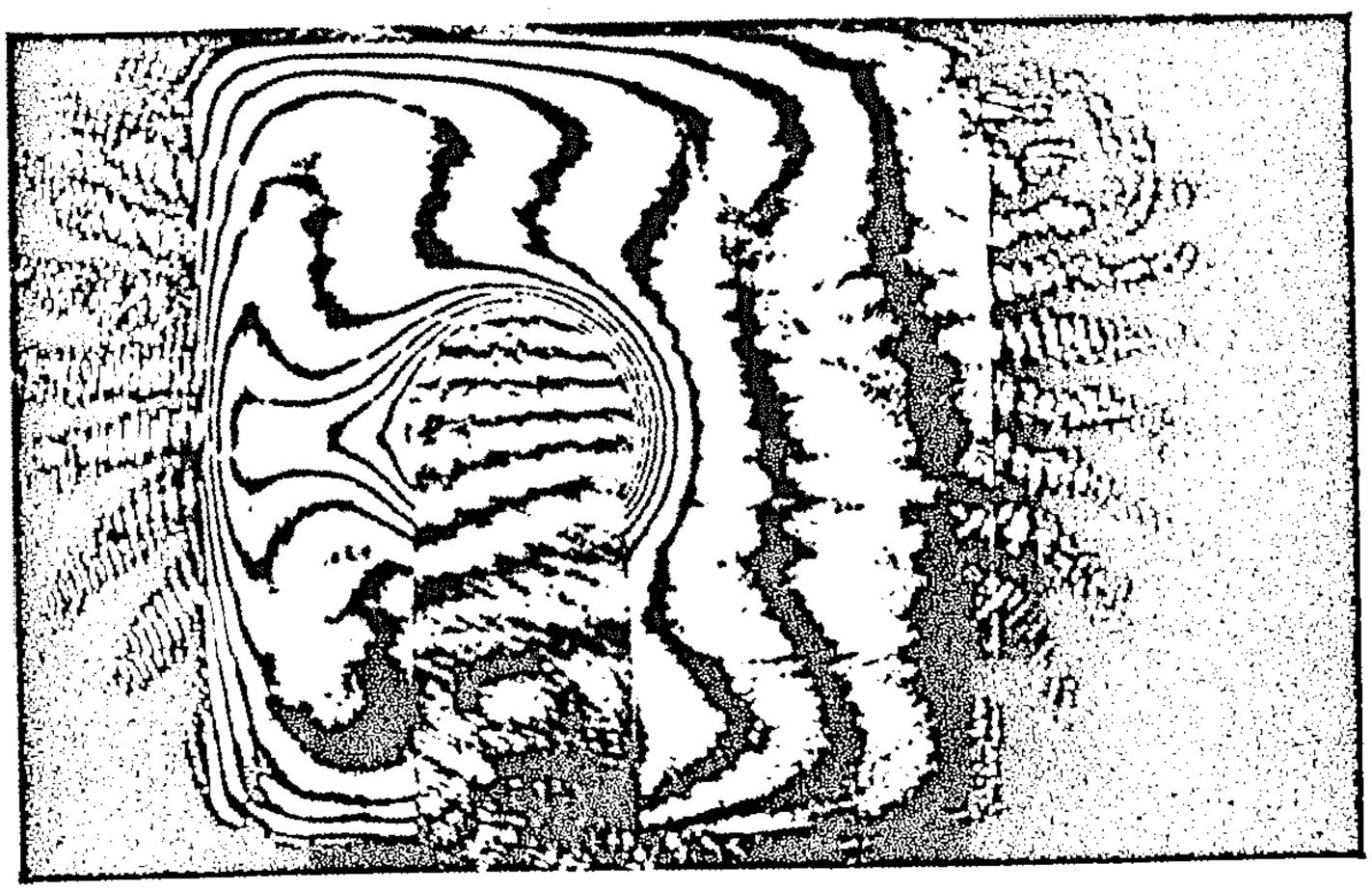

(iii)

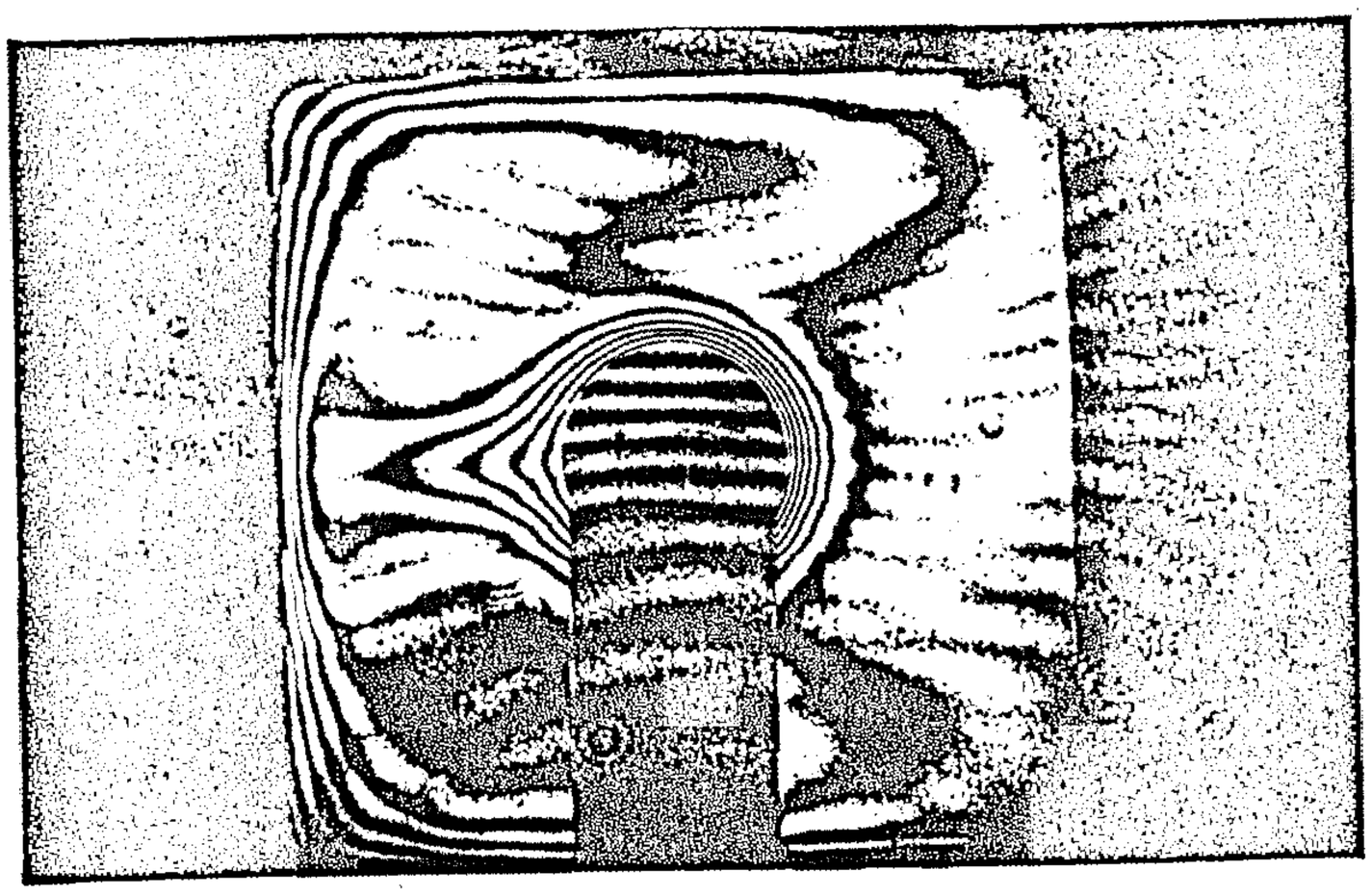

(iii)

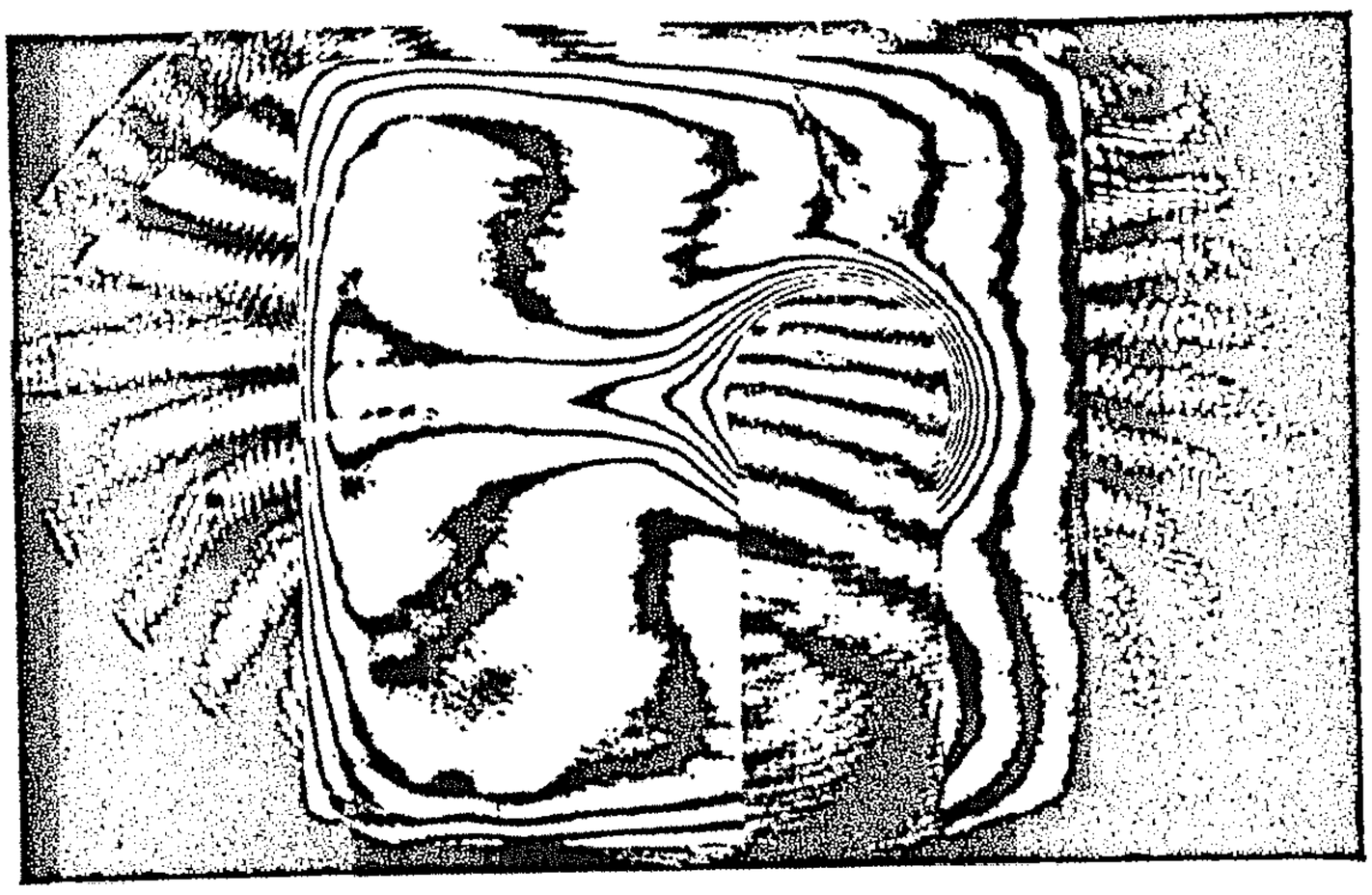

(ii)

(i)

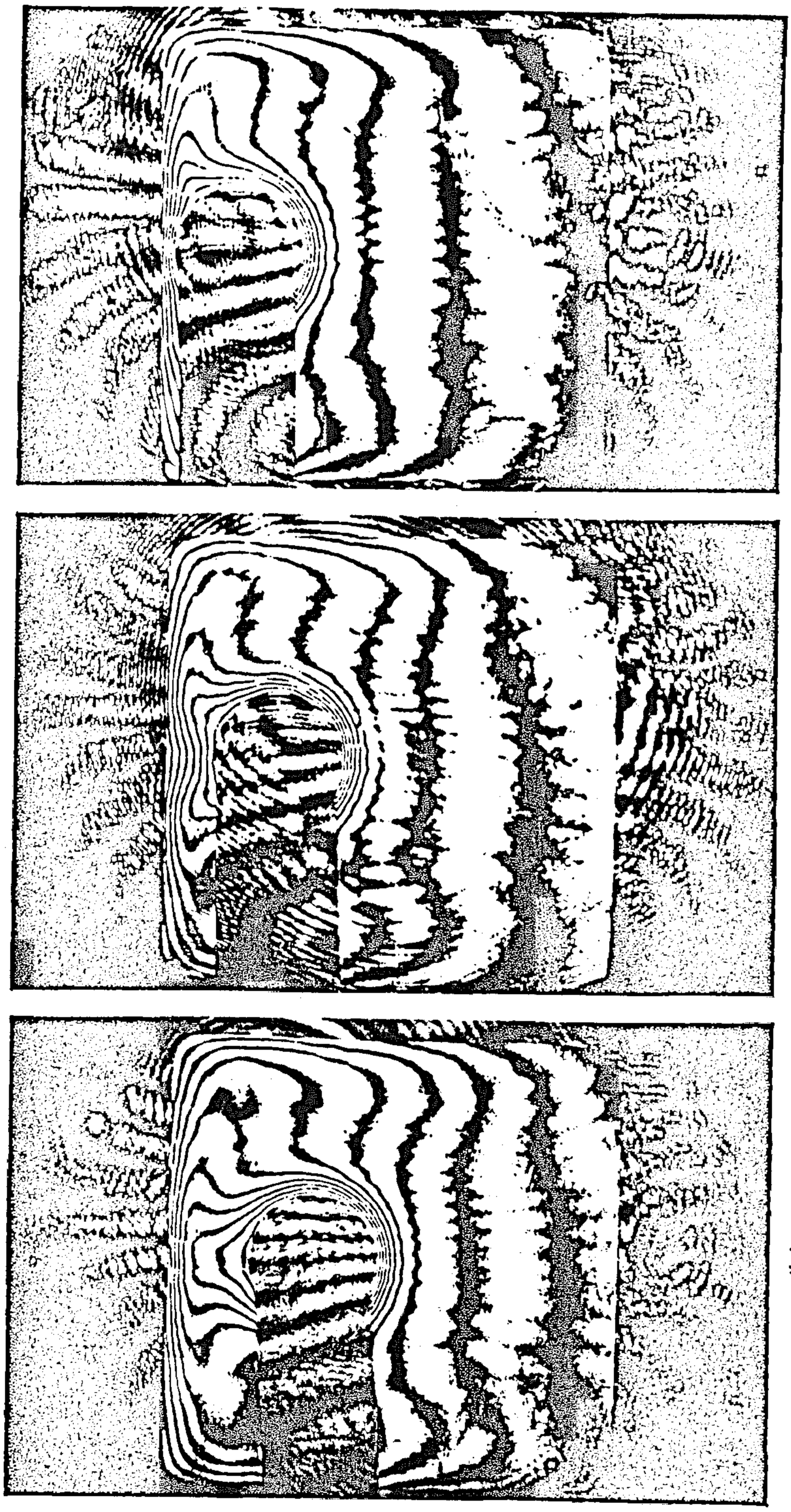

(vi)

(v)

(iv)

Fig. 3. Typical Mach-Zehnder interferograms, indicating the steady-state isotherms in the air cavity. For the particular systems presented: (i) $E = -0{\cdot}3$, $\Delta T = 9{\cdot}6$°C; (ii) $E = 0$, $\Delta T = 9{\cdot}0$°C; (iii) $E = 0{\cdot}5$, $\Delta T = 9{\cdot}9$°C; (iv) $E = 0{\cdot}5$, $\Delta T = 10{\cdot}0$°C; (v) $E = 0{\cdot}7$, $\Delta T = 9{\cdot}2$°C; (vi) $E = 0{\cdot}9$, $\Delta T = 9{\cdot}4$°C. The darkened band stretching horizontally across the interference field (from the left) to the pipe under consideration indicates the filler and outlet system for that considered pipe. These connections occur outside the enclosure and so do not disrupt the natural convective flows therein.

a.

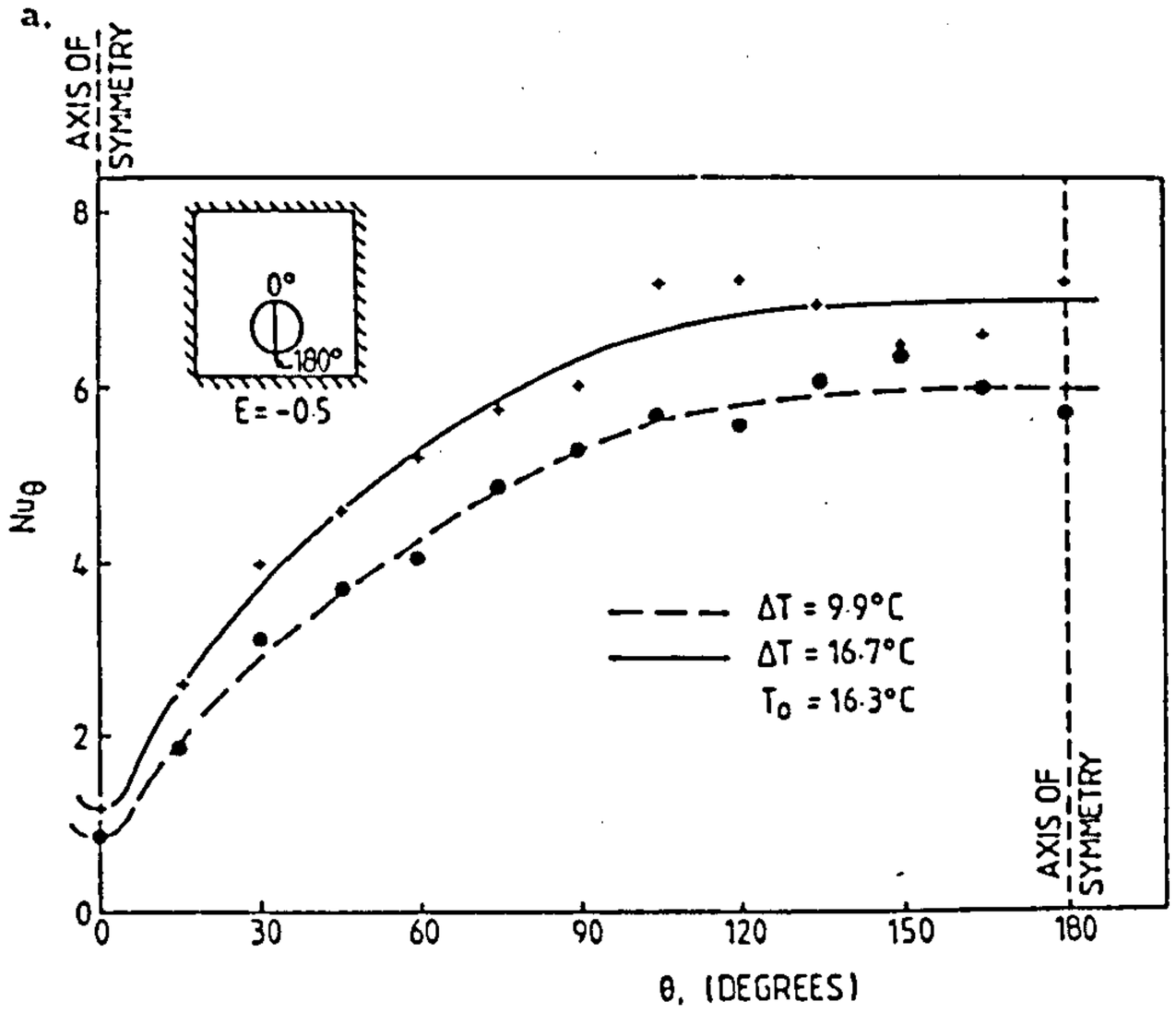

b.

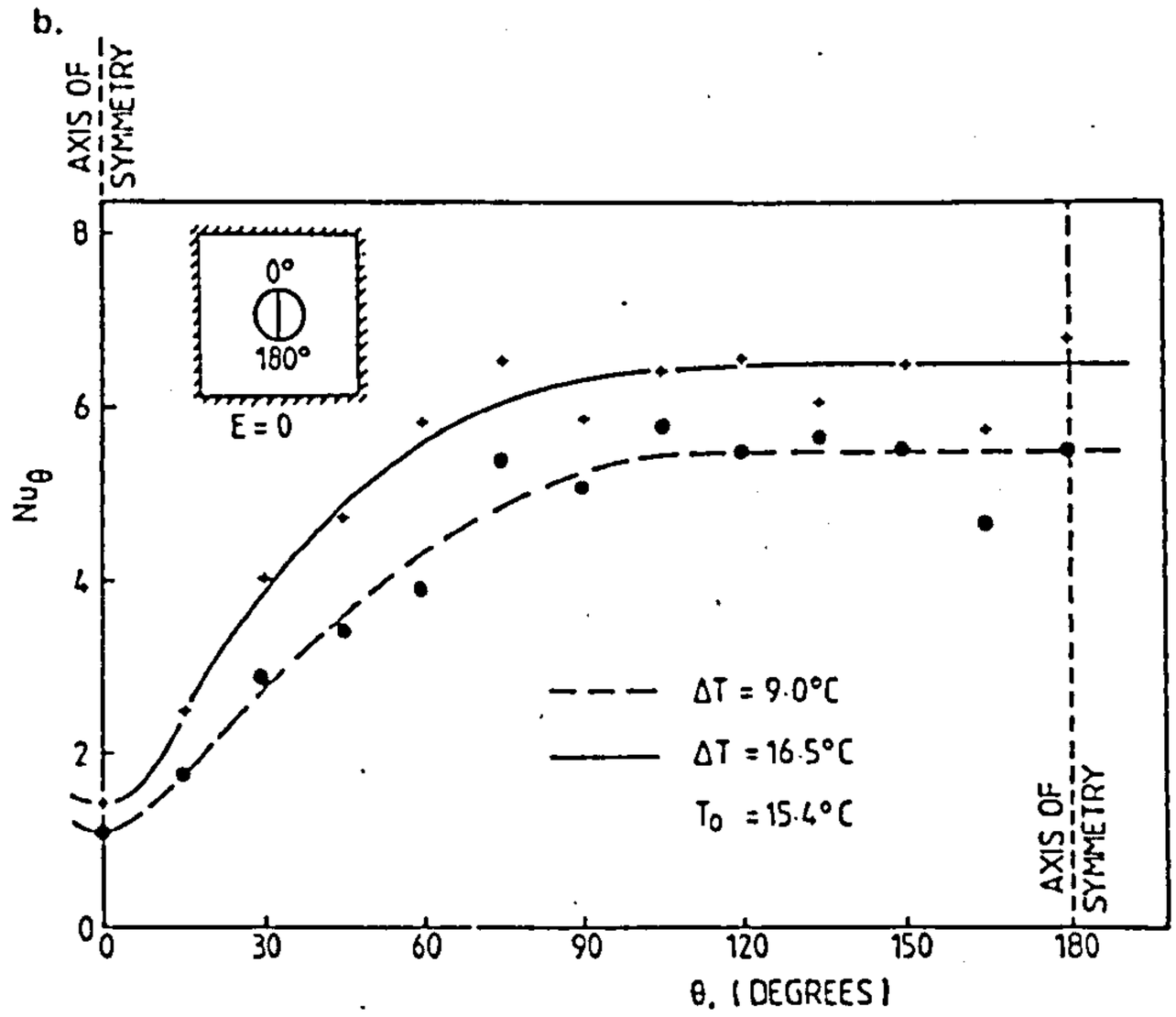

Fig. 4. Variations of the local Nusselt number, Nu_θ, versus angular co-ordinate, θ, for the supply pipeline. (a) $E = -0{\cdot}5$; (b) $E = 0$; (c) $E = 0{\cdot}3$; (d) $E = 0{\cdot}5$; (e) $E = 0{\cdot}7$; (f) $E = 0{\cdot}9$.

c.

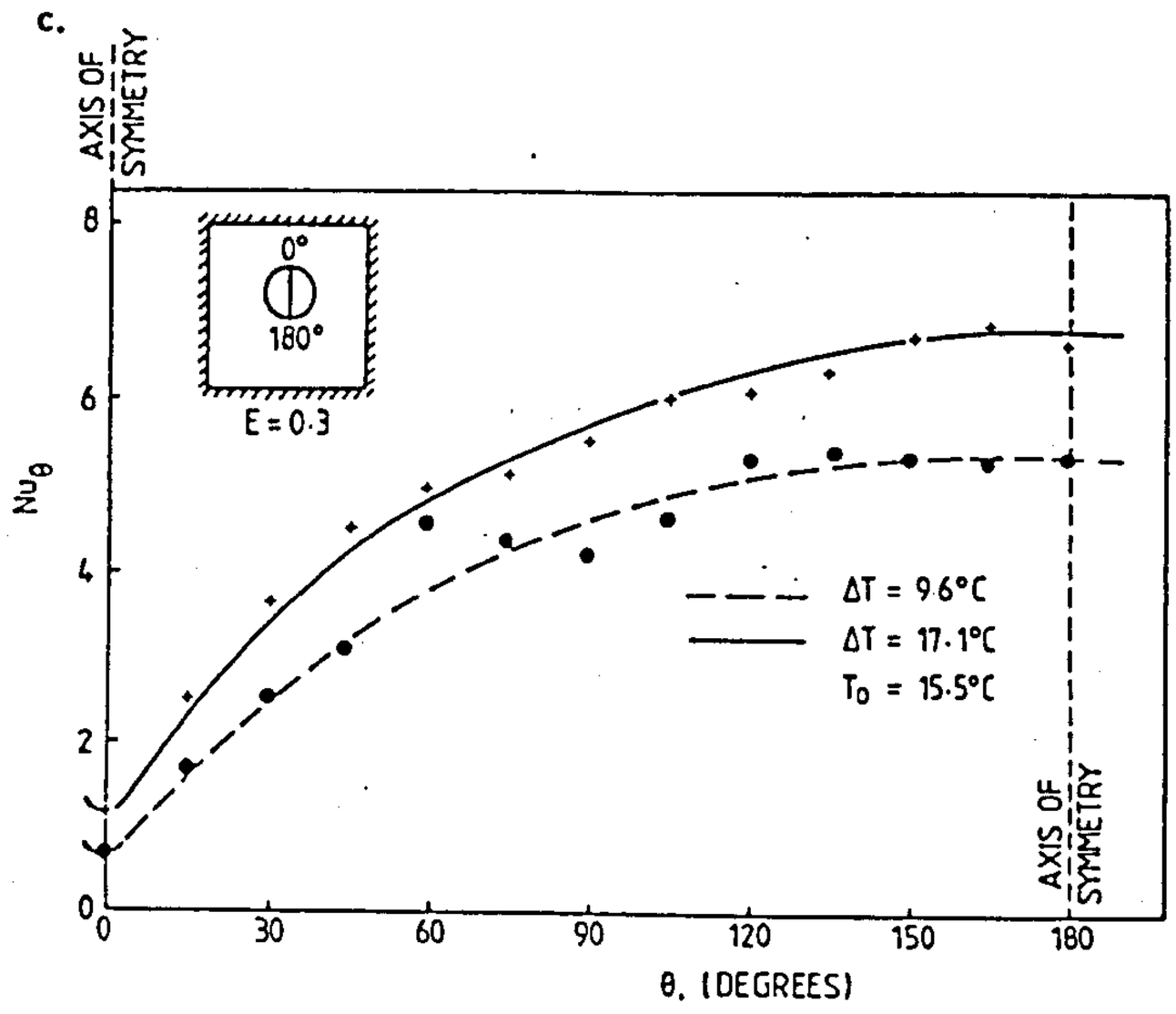

d.

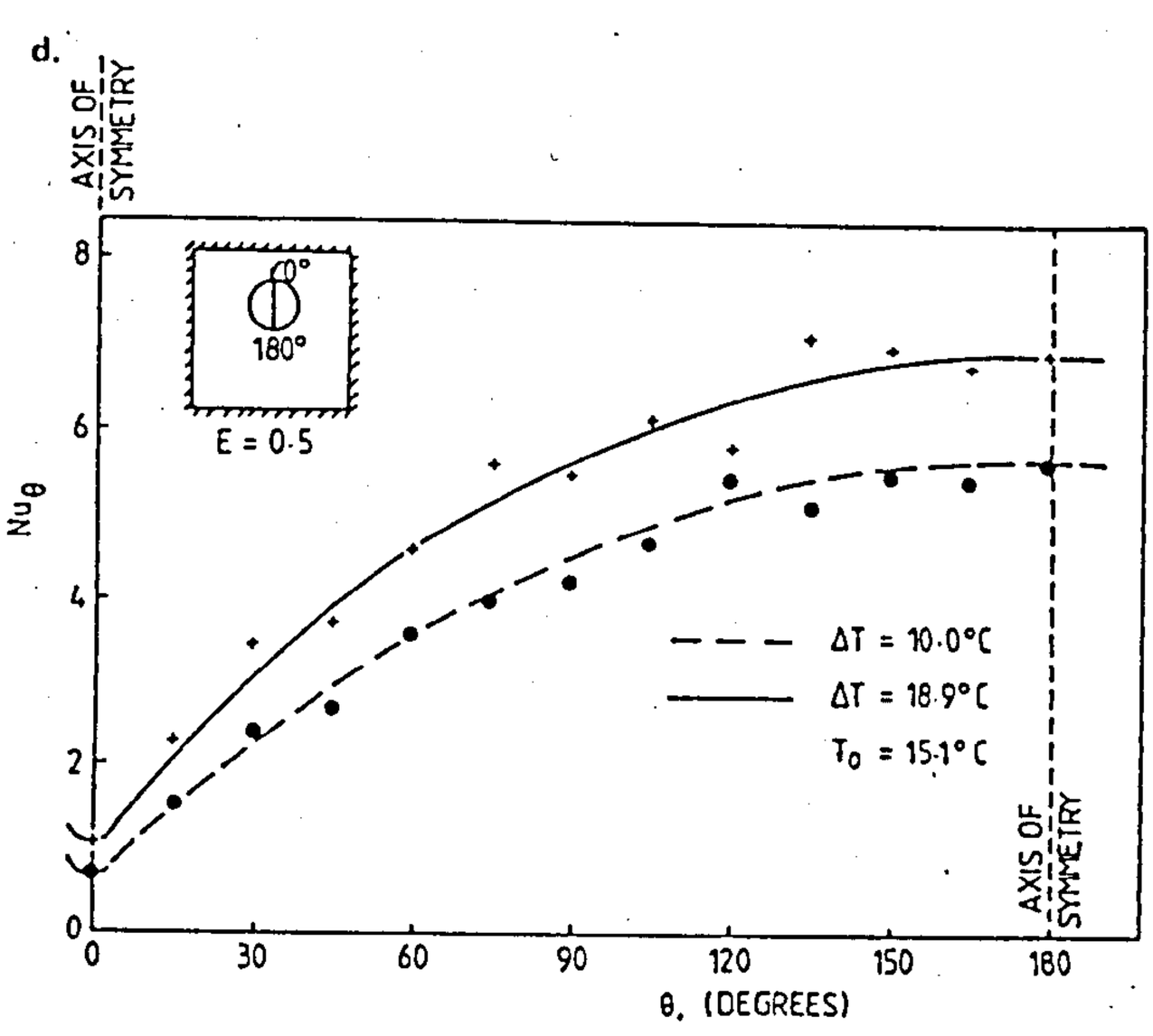

Fig. 4.—*Contd.*

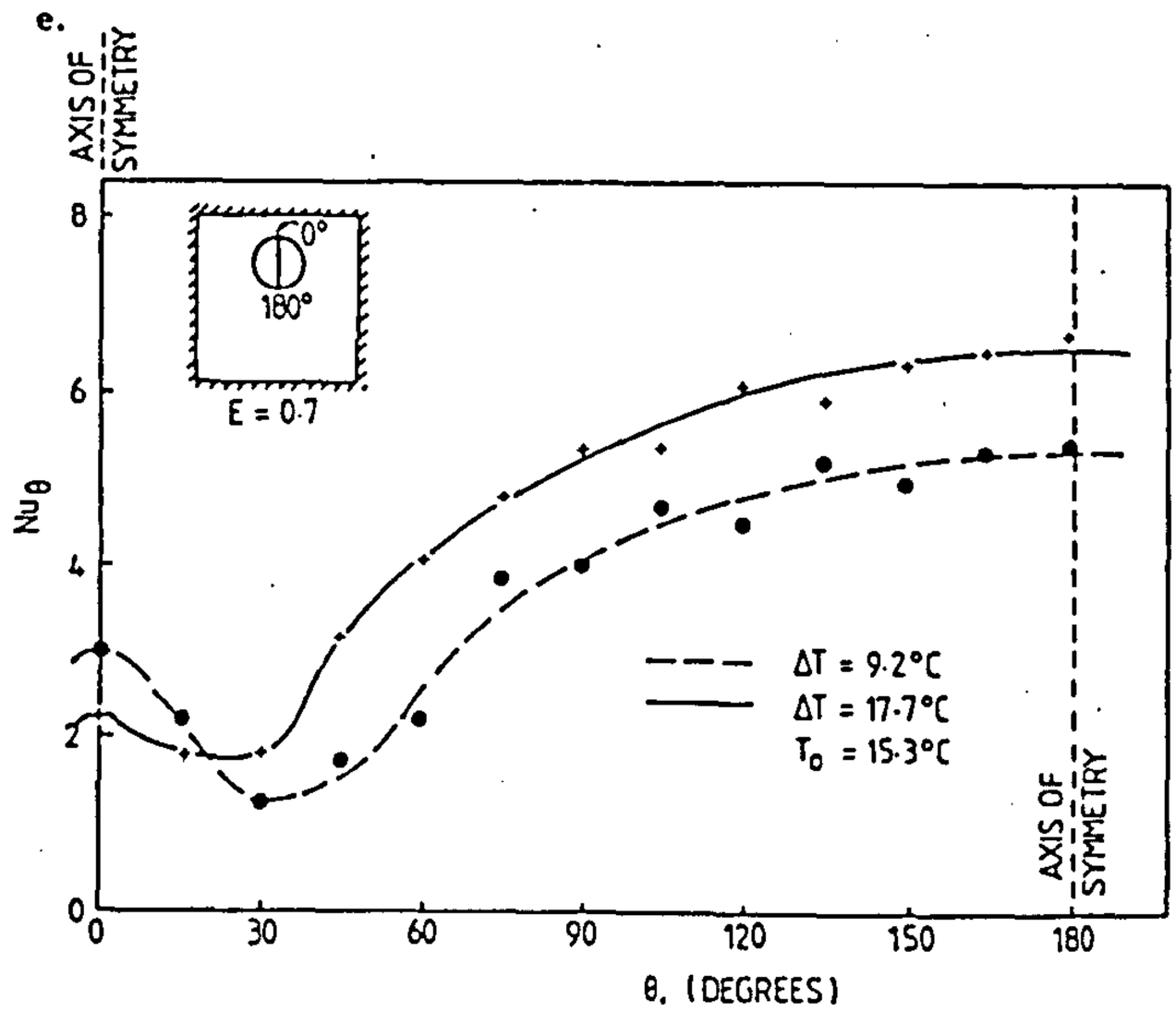
e.
AXIS OF SYMMETRY
0°
180°
E = 0·7
Nuθ
ΔT = 9·2°C
ΔT = 17·7°C
T0 = 15·3°C
AXIS OF SYMMETRY
θ, (DEGREES)
f.
AXIS OF SYMMETRY
0°
180°
E = 0·9
Nuθ
ΔT = 9·4°C
ΔT = 17·5°C
T0 = 15·2°C
AXIS OF SYMMETRY
θ, (DEGREES)

Fig. 4.—*Contd.*

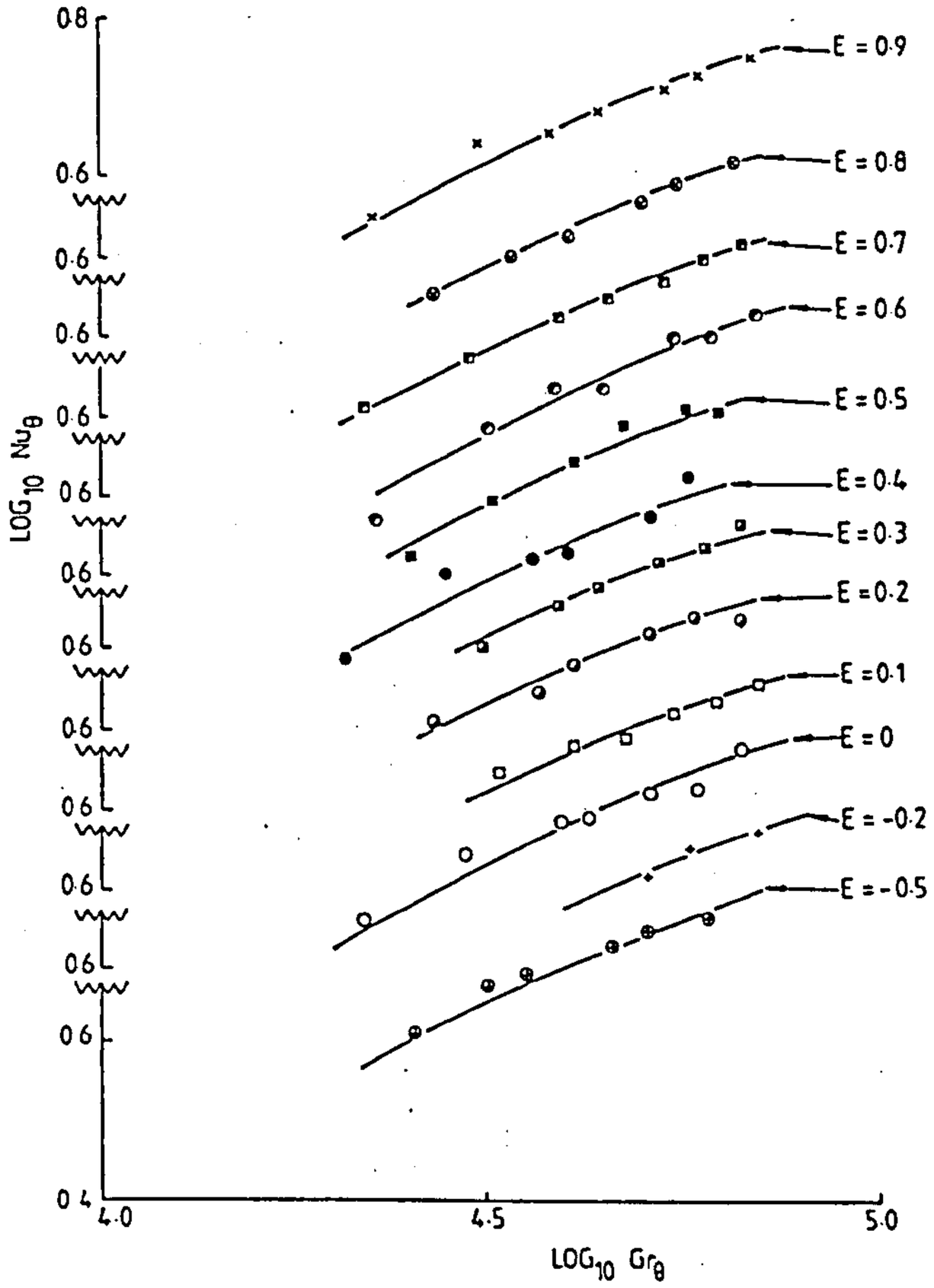

Fig. 5. Dependence of the average Nusselt number for steady-state heat flows outwards across the cavity upon the Grashof number for various displacement ratios.

at the lowest displacement ratio, i.e. $E = -0{\cdot}5$, and decreases slowly to its value at $E = 0{\cdot}3$, where it begins to decrease more rapidly. The minimum occurs at approximately $E = 0{\cdot}7$, although the value of 'M' does not change significantly throughout the region $0{\cdot}55 < E < 0{\cdot}8$. In a parallel investigation, a displacement ratio of $E = -0{\cdot}7$ was found to be approximately the optimal displacement ratio for a horizontal cold pipeline in a cylindrical, horizontal air-filled rectangular enclosure, i.e. as might be used for district-cooling.[23]

At $E = 0{\cdot}7$, an improvement of 13 per cent in the thermal resistance of the air-filled cavity is obtained compared with current conventional

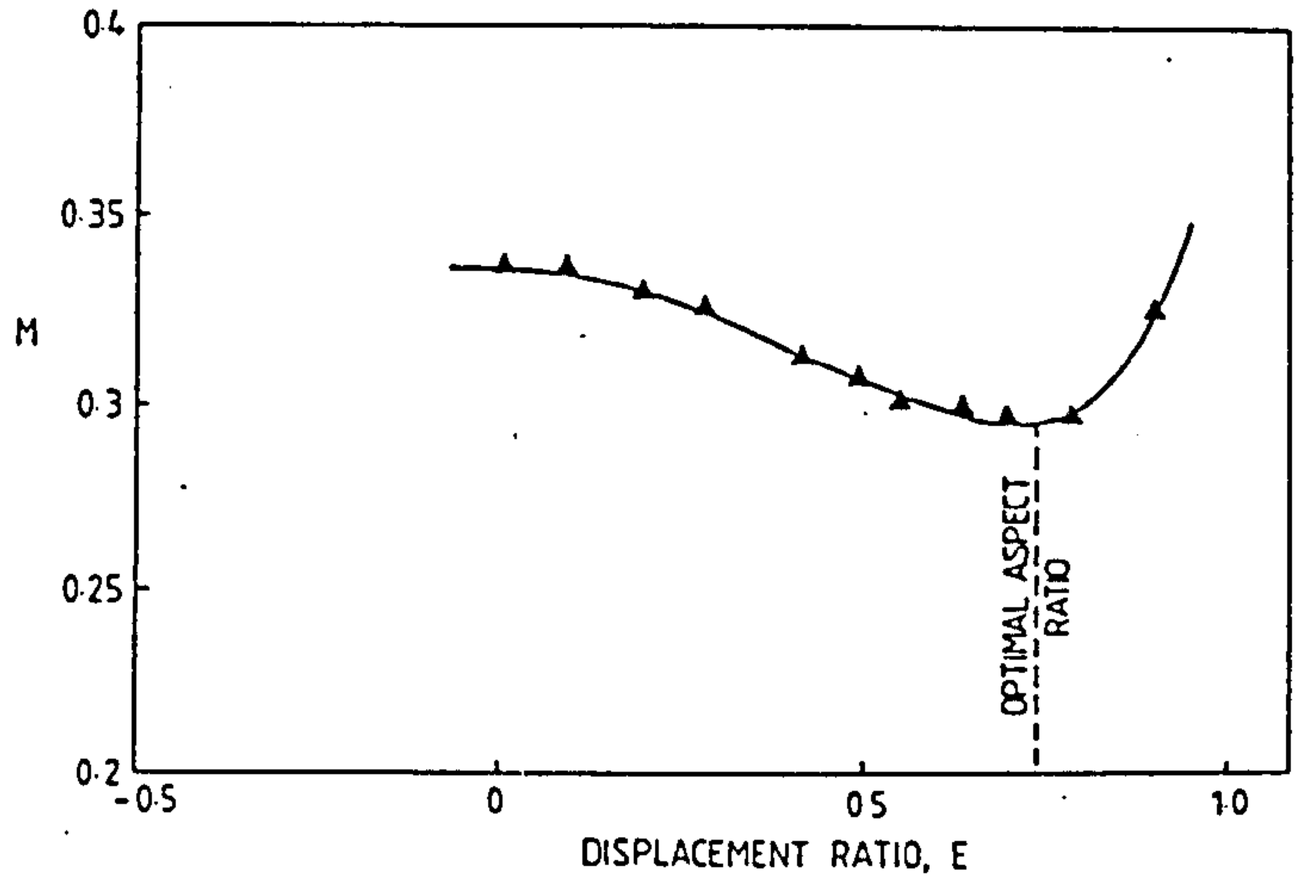

Fig. 6. Variation of M (an indication of the steady-state rate of heat transfer) versus the displacement ratio, E, for the hot pipe in the rectangular sectioned enclosure.

practice, i.e. the use of systems with $E = 0$ (see Fig. 6). This improvement is smaller than that achieved for a similar sized pipe-in-pipe system. This difference is due to the influence that the shape of the external enclosure has on the fluid flow. The upward vertical displacement of a pipe-in-pipe system restricts the convective flow in the region $90° < \theta < 180°$, the degree of this restriction being dependent upon the eccentric upward displacement. In the rectangular enclosure, the flow zone is substantially affected only near $\theta = 180°$ by this eccentric displacement. This fact emphasises the importance of the vertical separation between the tops of the inner and outer surfaces of the cavity on the steady-state rate of convective heat transfer across the cavity.

This optimal design knowledge is most relevant for underground pipeline systems, for which distribution losses should, if the operation of the district-heating system is to become more economically attractive, be minimised. There is no additional cost incurred by installing the pipeline at the optimal position as compared with the current conventional practice, and the precise optimal displacement ratio need not be strictly adhered to as there is a relatively wide region where the heat transfer coefficient is near to its minimum value. In reality, for typically insulated pipelines, the 13 per cent improvement in the thermal resistance of the air-filled cavity would amount to only ~2 per cent improvement in the

overall insulation of the system (i.e. allowing for the presence of the insulant and the insulation provided by the surrounding air and earth), but over the lifetime (> 30 years) of pipeline this is still very worth while.

REFERENCES

1. C. Liu, W. K. Mueller and F. Landis, Natural convection heat transfer in long horizontal cylindrical annuli. (Paper 117). *Proc. 'International Developments in Heat Transfer', Int. Heat Transfer Conf., University of Colorado*, V (1961), pp. 976–84.
2. U. Grigull and W. Hauf, Natural convection in horizontal cylindrical annuli. (Paper 60). *Proc. 3rd Int. Heat Transfer Conf., Chicago*, 2 (1966), pp. 182–95.
3. R. E. Powe, G. T. Carley and S. L. Carruth, A numerical solution for natural convection in cylindrical annuli, *Trans. ASME, J. Heat Transfer*, 93 (1971), pp. 210–20.
4. T. H. Kuehn and R. J. Goldstein, An experimental study of natural convection heat transfer in concentric and eccentric horizontal cylindrical annuli, *Trans. ASME, J. Heat Transfer*, 100 (1978), pp. 635-40.
5. M. J. Shilston and S. D. Probert, Thermal insulation provided by plain, horizontal annular cavities containing atmospheric pressure air, *Applied Energy*, 5 (1979), pp. 61-80.
6. L. S. Yao, Analysis of heat transfer in slightly eccentric annuli, *Trans. ASME, J. Heat Transfer*, 102 (1980), pp. 279-84.
7. U. Projahn, H. Rieger and H. Beer, Numerical analysis of laminar natural convection between concentric and eccentric cylinders, *Numerical Heat Transfer*, 4 (1981), pp. 131-46.
8. W. P. Schimmel, Jr., *Application of laser holographic interferometry to natural convection in enclosures*, Sandia Laboratories, Fluid Mechanics and Heat Transfer Division 1261, Albuquerque, NM 87115 (1979), pp. 41-8.
9. R. G. Courtney and P. J. Hobson, The performance of 15 district-heating schemes. *The Heating and Ventilating Engineer* (November, 1977), pp. 4–11.
10. R. M. E. Diamant and D. Kut, *District heating and cooling for energy conservation*, The Architectural Press, London, 1981, pp. 390-1 and pp. 162–3.
11. J. E. Mesko, Economic advantages of central heating and cooling systems, *Proc. Symposium on Underground Heat and Chilled Water Distribution Systems, Washington, DC*, 1973, Report No. NBS-BSS-66, May, 1975, pp. 9-17.
12. A. F. Postlethwaite, *Combined heat and power activities in the UK*. Central Electricity Generating Board, Generation Development and Construction Division, Barnwood, Gloucestershire, 1981, pp. 1-6.
13. A. E. Haseler, District heating progress in UK—Past, present and future.

(Paper 22). *Proc. Conf. 'District Heating for the Community', Bristol, UK*, District Heating Association, 1969, pp. 1–7.
14. W. G. E. Rowe, Arterial mains systems to supply U.K. city heat loads, *Proc. The District Heating Association's 4th National Conf., Torquay*, 1981.
15. Anon., *Combined heat and electric power generation in the United Kingdom*, Combined Heat and Power Group (Marshall Committee), Energy Paper 35, Department of Energy, HMSO, London, 1979.
16. W. S. Atkins & Partners, *CHP/DH feasibility programme: Stage 1. Summary report and recommendations*. A report prepared for the Department of Energy, July, 1982.
17. W. R. H. Orchard and J. A. MacAdam, The potential of CHP/DH as a major energy supply option for the U.K. (Paper 14). *Proc. The District Heating Association's 5th National Conf., Torquay*, 1983.
18. Anon., Planning for CHP heat, *The Heating and Ventilating Engineer* (September, 1983), pp. 22–4.
19. H. A. Borger, Available types of underground heat distribution system, *Proc. Symposium on Underground Heat and Chilled Water Distribution Systems, Washington, DC, 1973*. Report No. NBS-BSS-66 (May, 1975), pp. 52–9.
20. BS 4508, Specifications for thermally-insulated underground piping systems: Part 1: steel-cased systems with air gap, British Standards Institution, London, 1969.
21. BS 5970, Code of practice for thermal insulation of pipework and equipment (in the temperature range −100 °C to 870 °C), British Standards Institution, London, 1981.
22. W. Tobiasson, Experience with central heat distribution systems in cold regions, *Proc. Symposium on Underground Heat and Chilled Water Distribution Systems, Washington, DC, 1973*. Report No. NBS-BSS-66 (May, 1975), pp. 122–35.
23. S. Chakrabarti, S. D. Probert and M. J. Shilston, Optimal eccentric annuli (containing atmospheric pressure air) for thermally-insulating, horizontal, relatively cold pipes, *Applied Energy*, 14 (1983), pp. 257–93.
24. R. F. Babus'Haq, S. D. Probert and M. J. Shilston, Improved configurations for district-cooling pipelines, *Applied Energy*, 16 (1984), pp. 67–76.
25. W. Hauf and U. Grigull, Optical methods in heat transfer, *Advances in Heat Transfer* (Hartnett, J. P. and Irvine, Jr., T. F. (Eds)), Academic Press, New York, 6 (1970), pp. 133–66.
26. R. G. Brooks, S. D. Probert and J. Maxwell, 18 cm field of view Mach-Zehnder interferometer for heat transfer studies, *Trans. Institute of Measurement and Control*, 1 (1968), pp. T9–16.
27. J. M. Mehta and W. Z. Black, Errors associated with the measurement of convective heat transfer coefficients, *Applied Optics*, 16(6) (1977), pp. 1720–6.
28. A. Feingold and K. G. Gupta, New analytical approach to the evaluation of configuration factors in radiation from spheres and infinitely-long cylinders, *Trans. ASME, J. Heat Transfer*, 92 (1970), pp. 69–76.

APPENDIX 1: THE MACH-ZEHNDER INTERFEROMETER

This instrument consists of two light splitters and two mirrors, all of which are optically flat and parallel. Monochromatic light ($\lambda = 0{\cdot}6328\ \mu m$) from a nominally 3 mW He–Ne laser passes through a spatial filter and a collimating lens (see Fig. 2). The parallel beam is then incident upon a vertical, partially silvered, optically flat splitter-plate, S_1, which is inclined at 60° to the light beam. About half of the light in the incident beam is reflected at S_1, then strikes a fully reflecting mirror, M_1, and travels to the second splitter plate, S_2. The other part of the incident beam passes through S_1, is reflected at mirror, M_2, and is again reflected by S_2. Thus, two separate, coherent, monochromatic light beams, of approximately equal intensities, originating from a single source, recombine via a decollimating lens, L_2, after travelling almost equal optical path lengths. A uniformly bright or dark field on a screen or at the focal plane of the camera should then ensue provided that the plates are optically flat and of homogeneous glass.

As the system under test involves disturbances (e.g. a temperature gradient) being introduced orthogonally to the beam between M_1 and S_2, the corresponding optical path for the laser light is affected. The two coherent beams thus become out of phase. So, on their recombination, the field of view contains interference fringes whose numbers and spacings are dictated by the temperature distribution across the test section perpendicular to the mean direction of the light beam.

APPENDIX 2: INTERPRETING THE INTERFEROGRAMS

The interferograms were printed, at as great a contrast as could be achieved, on glossy paper (thereby obtaining sharply defined fringes). Because of symmetry, only the right half of each interferogram was analysed.

In the situation depicted schematically in Fig. 7, the thermal boundary layer adjacent to the inner cylinder is indicated by five fringes (i to v). The separations between fringes i, ii, iii and the inner cylinder boundary were measured at 15° radial intervals by means of a travelling microscope. As the 180° radius vector (i.e. vertically downwards) is approached, the fringes become closer, i.e. the local heat transfer coefficient at the cylinder's surface increases.

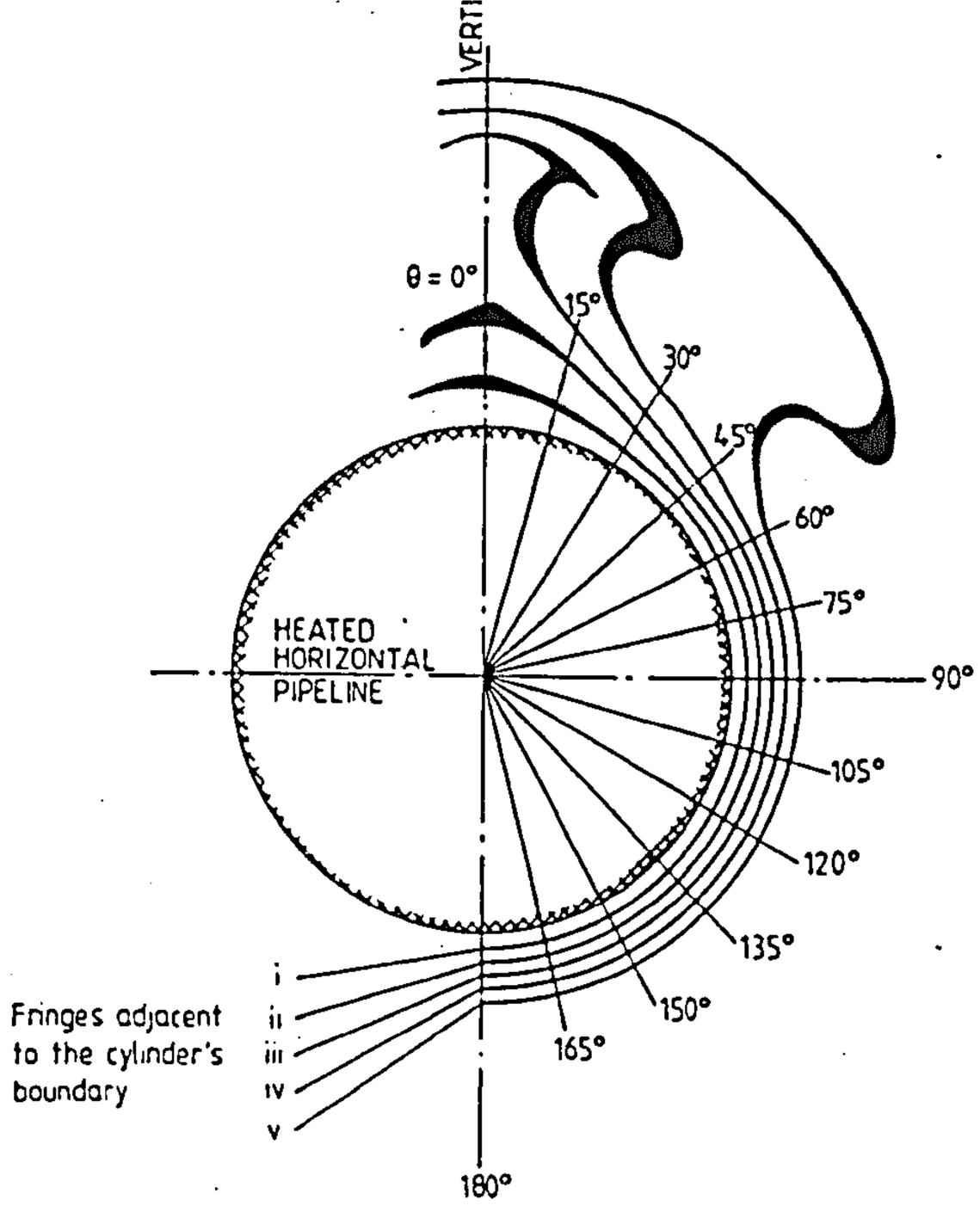

Fig. 7. Isotherms around a horizontal heated pipeline as revealed by Mach-Zehnder interferometry. The angular co-ordinate, θ, is measured from the top of the supply pipe in a clockwise rotation.

From the following three standard interferometric equations, the 'fringe' temperature, T, was calculated, taking the temperature of the cold wall as the reference:

$$\mu = \mu_R - \frac{\lambda}{L}\Delta N$$

$$\mu_R = 1 + \left(\frac{\mu_r - 1}{1 + \beta T_R}\right)$$

$$T = \frac{1}{\beta}\left(\frac{\mu_r - \mu}{\mu - 1}\right)$$

The distances of the first three fringes from the hot wall along a radial

(i.e. constant θ) line were plotted against the temperatures corresponding to the fringes. A least-squares straight-line fit was employed to deduce the gradient (dT/dx) of this line at the reference wall, i.e. the hot inner cylinder, using only those fringes contained within the inner cylinder's boundary layer. This value of dT/dx was used in conjunction with the average gap size, G, and the overall mean value of ΔT across the cavity, to deduce the local Nusselt number, Nu_θ, for that particular polar angle: $Nu_\theta = (G/\Delta T)(dT/dx)$. The local Nusselt numbers at other radial positions were evaluated in a similar manner. By an appropriate integration over the surface of the inner cylinder, a mean value for the overall Nusselt number, $\overline{Nu_\theta}$, for each configuration tested was determined.

CHAPTER 4

STEADY-STATE HEAT LOSSES FROM HORIZONTAL PIPES IN AN AIR-FILLED RECTANGULAR CONCRETE DUCT

Steady state heat losses from horizontal pipes in an air-filled rectangular concrete duct

Factors influencing the steady state heat loss behaviours of horizontal 'supply' and 'return' hot-water pipes, within an atmospheric pressure air-filled, relatively cold, horizontal rectangular trench, are considered. An experimental investigation concerning the effects of the displacement ratios for the two pipes revealed the optimal configuration, that is one which achieves a minimum steady state rate of heat loss from the supply pipe. For one set of temperatures for the pipes and trench walls, the optimal configuration of the supply and return pipes occurred at displacement ratios of +0.70 and −0.05, that is with the supply pipe in the upper region of the cavity and the return pipe vertically below it, the pipes being equidistant from the vertical walls of the trench. This configuration is of significance with respect to achieving maximum energy thrift for district heating pipelines, because it differs radically from the 'side-by-side' arrangement of pipes conventionally adopted in district heating practice.

NOTATION

D	diameter of both the considered supply (that is the hot) and return (that is the *relatively* cooler) pipes (mm)
E	displacement ratio: $=\{1-2H_R/(Y-D)\}$ or $\{1-2H_S/(Y-D)\}$ for the return or supply pipe respectively (see Fig. 1)
G	average vertical gap size: $=(Y-D)/2$ (mm)
Gr_D	local Grashof number, based on the diameter D of the supply pipe
H_R, H_S	minimum gaps, that is the shortest vertical distances between the return and supply horizontal pipes respectively and the upper horizontal internal surface of the trench (mm) (see Fig. 1)
L	axial length of the considered horizontal air-filled cavity (mm) (see Fig. 2)
M	dimensionless parameter dependent upon the geometry and temperature distribution of the system: $=\overline{Nu}/Gr^n$
Nu_G and Nu_X	local Nusselt number for the steady state heat transfers from the *supply* pipe, based respectively on the average gap size G and the width of the rectangular cavity X; — above the symbol implies the average value over the surface of the supply pipe
n	power index of the Grashof number in the $\overline{Nu}$ versus Gr relationship
$Q_{conv+cond}$, Q_{rad}	contributions to the total steady state rate of heat leak *through the air* from the horizontal supply pipe due to, respectively, convection + conduction, and radiation (W)

The MS was received on 19 June 1984 and was accepted for publication on 16 January 1985.

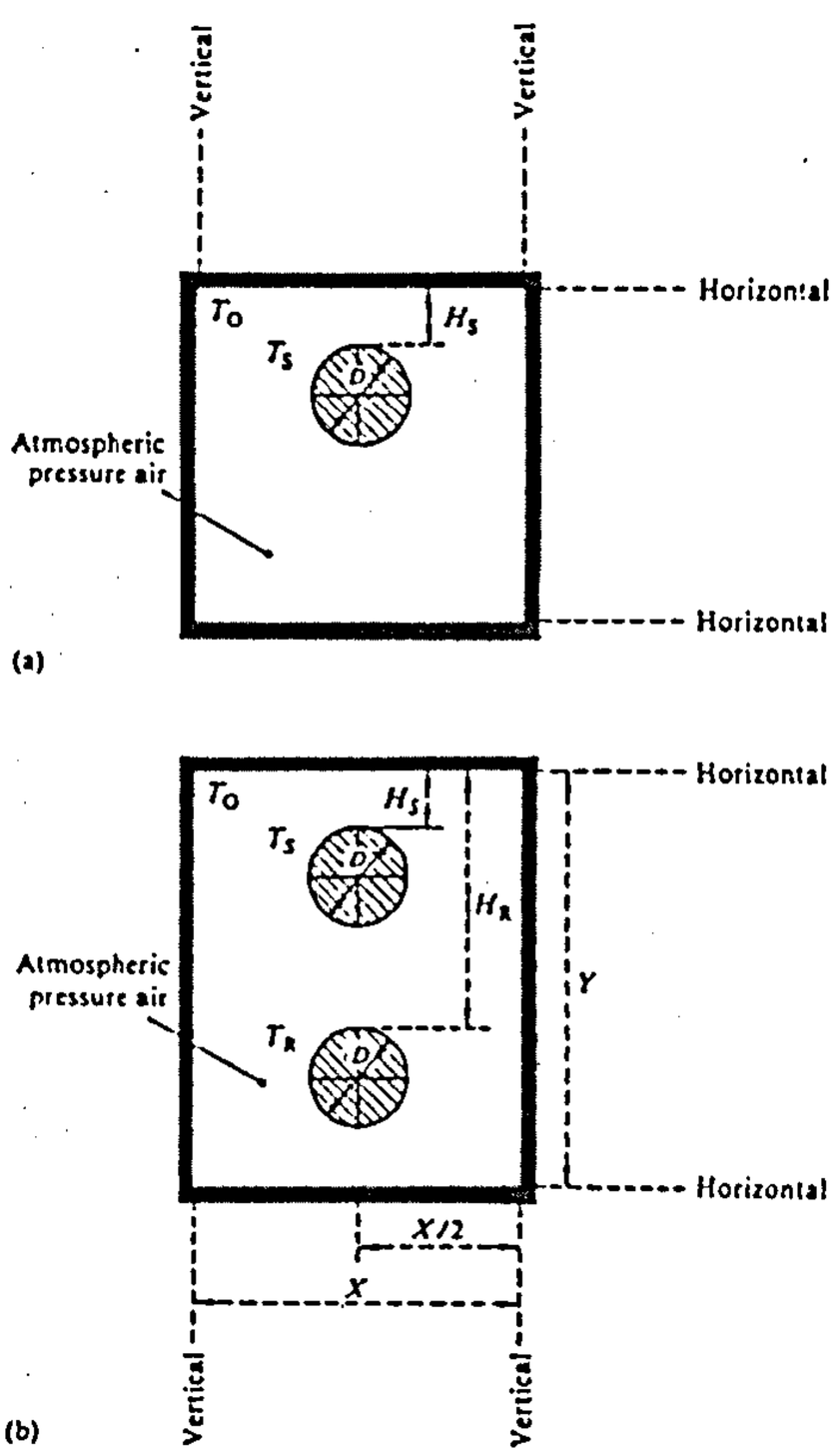

Fig. 1 Schematic representation of vertical sections through the considered horizontal pipes in the rectangular trenches for (a) the single-pipe system and (b) the double-pipe system

0263-7154/85 $2.00 + .05

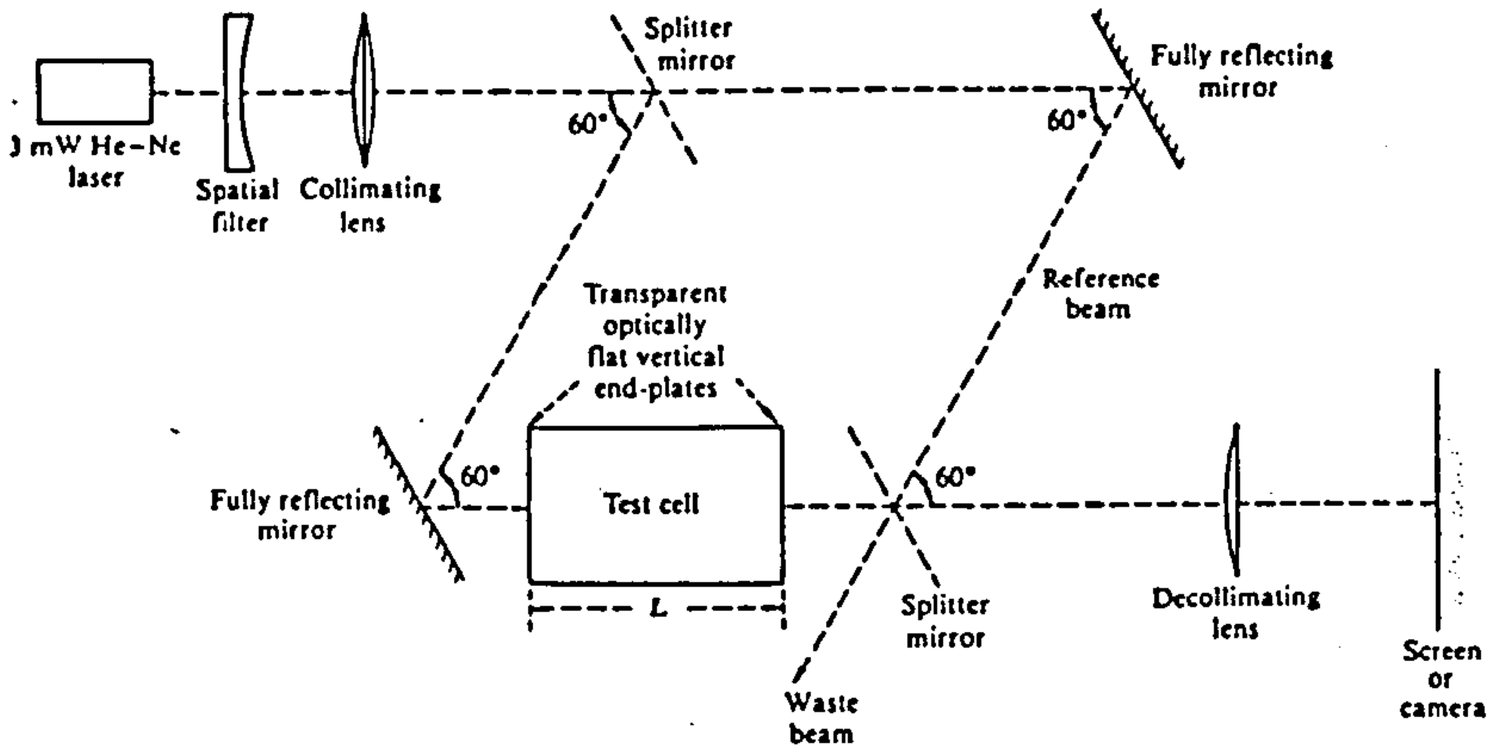

Fig. 2 Schematic plan-view of the Mach–Zehnder interferometer employed in this investigation

Q_{total} total steady state rate of heat loss *from the supply* (that is the hotter) pipe (W)

R radius of the circle passing through the four inner corners of a cross-section of the outer rectangular duct perpendicular to its length: $=\frac{1}{2}\sqrt{(X^2 + Y^2)}$ (mm)

T_0 steady state temperature of the inner surfaces of the outer surrounding isothermal model rectangular trench, as used in the present set of experiments (°C) (see Fig. 1)

T_R, T_S steady state temperatures of the outer surfaces of the return and supply pipes respectively (°C) (see Fig. 1)

X, Y horizontal width and vertical extent respectively of the rectangular cavity (mm) (see Fig. 1)

ΔT steady state difference between the temperatures of the outer surface of the supply pipe and the inner surface of the trench: $\Delta T = T_S - T_0$ (°C)

ε emissivity of the appropriately identified surface

θ angular coordinate measured from zero for the relatively upwards radius vector emanating from the centre of the supply pipe, and increasing in a counterclockwise rotation (degrees) (see Fig. 3)

Suffixes

cond due to conduction through the air

conv due to convection of the air

G for the average gap size

O of the inner surface of the rectangular trench

R for the pipe along which the hot water returns

rad due to net radiation loss from the supply pipe

S for the hot-water supply pipe

total referring to the total steady state heat leak through the air

X with respect to the horizontal width of the rectangular cavity

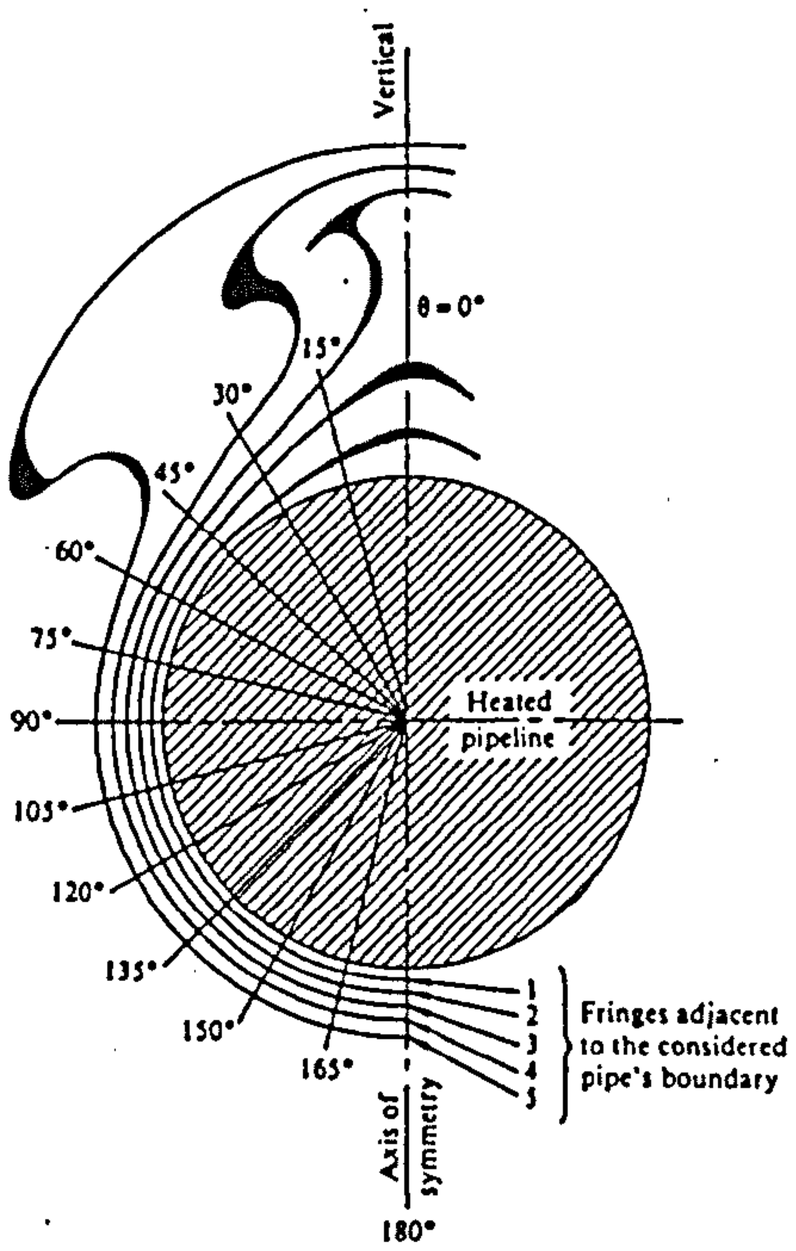

Fig. 3 A typical contour map of isotherms around a horizontal heated pipe, as revealed by Mach–Zehnder interferometry. The angular coordinate θ is measured from the upwards vertical radius vector of the supply pipe

1 THE DESIGN PROBLEM

Much attention has been devoted to studying steady state heat transfers across annular cavities (1–4). However, there is a dearth of information concerning the corresponding heat leaks across rectangular horizontal air-filled cavities containing cylindrical pipes, even though they are more frequently encountered in practice (5–7). Employing a single pipeline for a district heating distribution network is usually unsatisfactory, both technically and economically. It is preferable to use double-pipe systems, comprising a 'supply' pipe conveying the hot water (at ~90°C) to the customer and a 'return' pipe taking the water from which heat has been extracted, but which is still much higher in temperature than the environment, back to the central boiler. This configuration is often adopted, especially for ground-level and underground pipeline systems, where a rectangular duct or trench protects the hot-water pipes for district heating schemes (8) or for industrial processes. Most hot-water distribution systems nowadays are based on the two-pipe, side-by-side, layout. Unfortunately, attention has not so far been devoted to the financial savings which can be achieved by reducing the heat losses as a result of choosing the optimal configuration for such pipes in the duct.

The most frequent practice is for the district heating pipelines to be clad with insulants and located in an atmospheric pressure air-filled rectangular trench (9, 10). This assembly is sometimes referred to as the 'free-draining' system (11) because in the event of a leak, flooding or a temporary high water table, drainage and evaporation from around the insulated pipe would ensue automatically (12). Otherwise moisture may enter the insulant, which might then:

(a) damage the insulant permanently,
(b) reduce the system's insulating effectiveness and
(c) lead to leaching, and hence promote corrosion of the underlying steel pipe.

However, ventilation of this air trench lowers the effective thermal resistance of the air cavity, and so usually should be constrained to the minimum which is likely to be necessary to permit the moisture to disperse readily from the cavity (13).

Because controllers of district heating schemes aim to distribute the maximum amount of heat to their customers, they are *primarily* concerned with reducing the heat losses from the *supply* pipelines during transmission. Therefore only losses from these pipes were considered in the present experimental investigation. Nevertheless, in practice, the return pipe would also be well insulated thermally. For a combined heat and power/district heating (CHP/DH) system, there is probably less concern as to the losses from the return pipe as the cost of CHP heat is low. (Also there is a small compensating effect from having a low mean condensing temperature, thereby increasing the power output slightly.)

2 THE EXPERIMENTS

The present investigation involved measuring the steady state rates of heat transfer across the atmospheric pressure air-filled gap between an isothermal 'cold' horizontal, rectangular sectioned, trench enclosing:

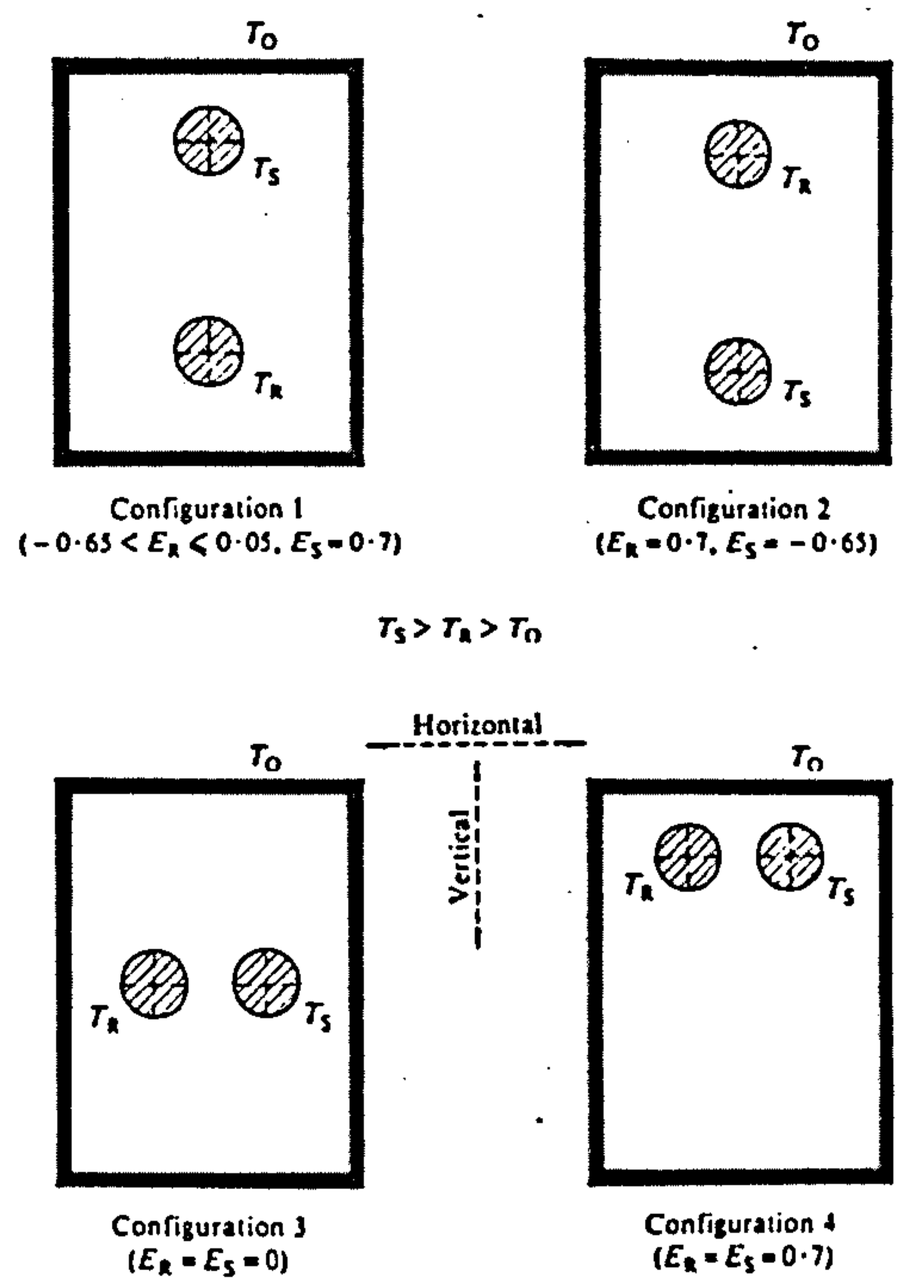

Fig. 4 Schematic vertical sections perpendicular to the lengths of the experimental 'district heating' horizontal pipeline systems tested

(a) initially a single horizontal hot pipe (that is the supply pipeline; see Fig. 1), and subsequently
(b) two horizontal pipes, the first carrying hot water (that is the supply pipe) and the other, slightly cooler water (that is the return pipe; see Fig. 4).

With system (a), the aim was to determine the optimal position of the hot (that is the supply) pipe which results in the minimum rate of heat loss for a specified steady state temperature difference, ΔT, between the pipe and the rectangular trench. Then for system (b), using the optimal position of the *supply* pipe, as identified from experiments with system (a), the optimal position of the *return* pipe was identified experimentally, so that the least steady state rate of heat loss from the supply pipe for a prescribed ΔT occurs.

The convective flow patterns within the enclosed air space were observed by injecting smoke particles *very* slowly into the illuminated rectangular trench. Flow visualizations for different steady state temperatures of the pipes and trench, and for different geometric configurations, were needed to stimulate, supplement and corroborate conclusions being drawn from interferometric indications of the steady state isotherms in the air gap.

In practice, there is likely to be a lower temperature on the upper surface of the trench because, when the district heating system is in operation, ambient air temperatures will be low compared with the temperature at

the base of the trench, say 1 m down where the temperature would be relatively constant. However, the temperature gradient along the vertical surfaces of an actual trench in such circumstances will be relatively small due to two contrary processes: (a) convection in the air of the trench leading to the upper top strata being warmer and (b) the heat loss by conduction to the horizontal surface of the ground in cold weather. Thus the isothermal assumption is a reasonable first approximation for the present design optimization exercise. In practice there would be a small vertical temperature gradient along the sides of the concrete duct, but the effect of this would have to be assessed as a separate investigation when the magnitude of this gradient for each particular application is known.

3 THE EXPERIMENTAL RIG

The values of the experimental parameters (see Figs 1 and 4) chosen for this investigation were:

1. *For the single-pipe system:*
   $X = 100$ mm, $Y = 100$ mm, $L = 630$ mm, $D = 28.5$ mm
   $-0.5 \leqslant E_S \leqslant 0.9$
   $17°C \leqslant T_S \leqslant 40°C$
   $4°C \leqslant \Delta T \leqslant 25°C$
2. *For the double-pipe system:*
   $X = 100$ mm, $Y = 125$ mm, $L = 650$ mm, $D = 28.5$ mm
   $-0.6 \leqslant E_R$ or $E_S \leqslant 0.7$
   $10°C \leqslant T_0 \leqslant 20°C \leqslant T_R \leqslant 30°C \leqslant T_S \leqslant 50°C$

Hauf and Grigull (14) concluded that the length L of the test cavity (see Fig. 2) should exceed 500 mm in order to be justified in disregarding axial heat transfers through the air to the end-plates. This implied that, for $L/R > 8$, three-dimensional convections in the annular cavity had only negligible influences upon the recorded steady state rates of heat transfer across the cavity (2). For the present systems, taking R as the radius of the circle passing through the inner corners of the rectangular section perpendicular to the length of the outer rectangular duct, then $L/R > 8$ and so complies with this criterion.

The walls of the cold outer duct (representing the district heating trench in practice) were manufactured from transparent Perspex. These were painted matt black except for a peripheral thin (~5 mm wide) slit one-third the way along the duct to facilitate the introduction of adequate illumination from three projectors positioned around the slit, so enabling the convecting airflows, within the trench, to be observed by viewing along the horizontal pipe direction. The walls were water-cooled, each wall containing a series of enclosed channels, through which water from the mains passed. Each wall was cooled by an independent line from the mains, so as to avoid an appreciable rise in the temperature of the water, which could thereby lead to significant differences in the average temperatures of the rectangular walls. Thirty-six copper-constantan thermocouples were sealed into holes drilled through the Perspex in directions in which, when the system is in operation, would be expected to be isotherms. The thermojunctions were arranged to be flush with the cavity's inner surface, thereby avoiding tripping the boundary layer airflows within the cavity. This permitted the temperature distribution over the inner surface of the cavity wall to be determined. Vertical, optically flat, uniformly thick, homogeneous glass plates, that is the end-plates, were fixed flush to the ends of the cavity, thereby sealing it from the surrounding ambient air.

The copper pipe (in the single-pipe system) was heated by passing a low-voltage, high-amperage, alternating current between its two ends. The eddy current dissipation resulted in uniform heating along the length of the pipe. The transformer was equipped with a control dial so that the magnitude of the steady state current passing through the pipe, and hence the rate of heating, could be varied by known amounts as desired. However, in the other tested assembly—the double-pipe system—the two contained horizontal copper pipes were heated by passing separate streams of hot water through them at their respective steady temperatures, T_R and T_S, so that $T_0 < T_R < T_S$. The pipes were always aligned with the length of the horizontal trench. Wide ranges of values of the displacement ratios, E_R or E_S, were adopted.

The main instrument used in this investigation was the 18 cm field-of-view, 3 mW He–Ne laser-stimulated, Mach–Zehnder interferometer (15) (see Fig. 2). This, when employed in the infinite-fringe mode, produced a distinctive pattern of isotherms for each two-dimensional steady state temperature distribution in the cavity examined. These interferograms indicated the refractive index (and hence density and consequently temperature) variations integrated over the axial length of the considered cavity. The effects of image distortion due to refraction of the beam through the cavity, and also at the ends of it, were reduced by focusing the camera on a vertical plane within the cavity, at $0.33L$ from the end-plate nearer to the camera, as recommended by Mehta and Black (16).

4 THE OBSERVATIONS

4.1 Single-pipe system

A4 enlarged photographic prints of the steady state interferograms (see Fig. 5a) were produced for analysis. The fringe displacements from the pipe wall were recorded at 15° ($=\Delta\theta$) increments (see Fig. 3) around each pipe. Generally the displacements (that is the true distances between the centres of adjacent fringes) for each of the first five fringes adjacent to the wall and the separations of the first fringes from the wall were deduced, except where there were fewer fringes in the pipe's boundary layer. Readings were only necessary for half of each recorded interferogram, because the pipe was always equidistant from the two vertical walls of the trench, that is vertical symmetry existed. This was always checked visually via the obtained interferograms: if it did not apply, the resulting interferograms were not analysed numerically.

A plot of the local Nusselt number Nu_G versus the angular coordinate θ is shown in Fig. 5b for a selected value ($=0.7$) of the displacement ratio E_S. The minimum value of the local Nusselt number occurred near the top of the pipe (that is at $\theta = 0°$) for $-0.5 < E_S < 0.5$. The angular position of the minimum local Nusselt number increased from $\theta = 0°$ for $E_S = 0.5$

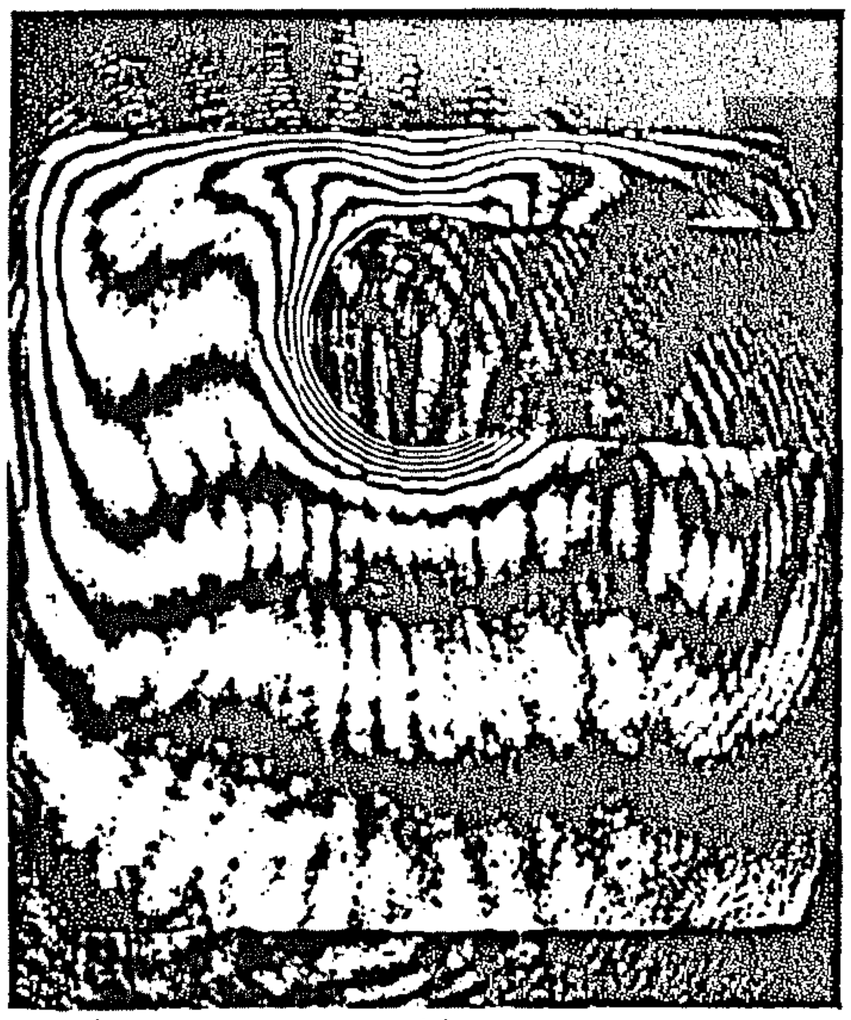

(a)

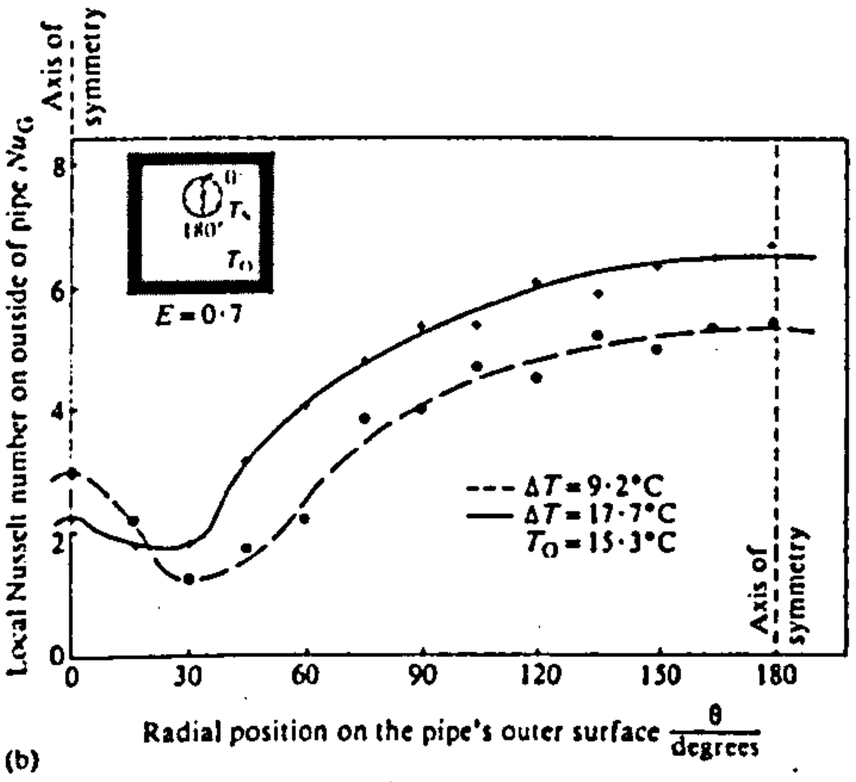

(b)

Fig. 5 Single-pipe system with $E_s = 0.7$:
(a) Typical steady state Mach–Zehnder interferogram for the system with $\Delta T = 9.2$ C
(b) Variation of the local Nusselt number Nu_G versus the angular coordinate θ for the supply pipe

to $\theta = 45°$ for the largest positive displacement ratio of 0.9 (7). This 'minimum' angular position was temperature dependent: as the temperature difference ΔT increased, the angular position θ of the minimum local Nusselt number decreased. This occurred because the fluid velocity in the boundary layer increased as ΔT rose, and the flow penetrated further into the relatively stagnant region near the top of the cavity. The influence of the temperature difference on the position corresponding to the minimum local Nusselt number for a single horizontal pipe eccentrically mounted within another horizontal pipe was much less than for configu-

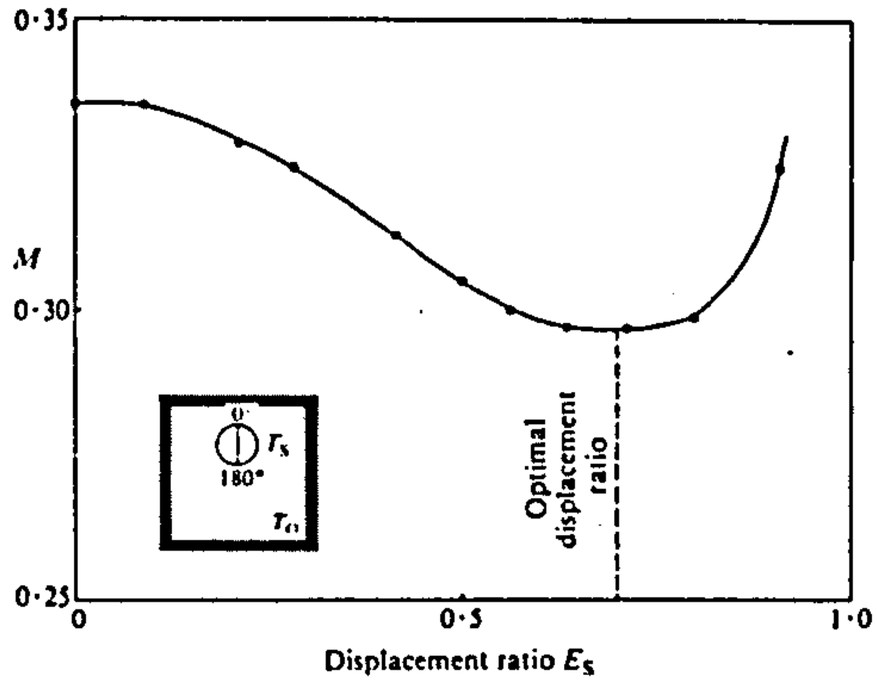

Fig. 6 Variation of $M(=\overline{Nu}/Gr_D^*)$, versus the displacement ratio E_s for the horizontal supply pipe in the horizontal rectangular-sectioned trench

rations with the rectangular trench because of the greater restriction imposed on the fluid flow by the outer, approximately comparable size, cylindrical wall in the former case.

The value of M in the standard equation describing the combined steady state conduction plus convection through the air, that is $\overline{Nu}_G = M(Gr)_D^*$, for this system was deduced and plotted versus the displacement ratio E_S (see Fig. 6). The value of M was a maximum at the lowest displacement ratio, that is at $E_S = -0.5$, and decreased slowly to its value at $E_S = 0.3$, where it began to decrease more rapidly. The minimum occurs at $E_S = 0.70 \pm 0.03$, which represents the approximate value for the optimal location for the single horizontal pipe in the rectangular trench considered, and for the temperature distributions tested.

The radiative component of the steady state rate of heat flux across the cavity is independent of the displacement ratio for an infinitely long pipe and trench (17). Therefore the optimal position, as deduced from the 'conduction plus convection through the air' data, is also that, even if the total heat leak had been considered.

4.2 Double-pipe system

Flow visualization was undertaken for several different geometrical configurations (see Fig. 4). A small amount of smoke was injected very slowly into the cavity and photographs were taken of the resulting steady state flow patterns. These flow visualizations also indicated the presence of any flow instabilities, so that the conditions under which the latter occurred could be ascertained.

Flow patterns for the hot-above-cooler pipe arrangement (that is configuration 1 of Fig. 4) exhibited two stable counter-rotating, approximately triangular-shaped, eddies, which were symmetrical about the vertical plane, through the horizontal axes of the pipes, bisecting the trench (see Fig. 7a).

For the warm-above-hot pipe arrangement (that is configuration 2 of Fig. 4), the flow pattern was of an irregular shape. It also exhibited severe instabilities with

Fig. 7 Typical steady state flow visualizations and Mach-Zehnder interferograms for the double-pipe system:
(a) Configuration 1 ($E_R = -0.65$, $E_S = 0.7$, $\Delta T = 17.5$ C)
(b) Configuration 2 ($E_R = 0.7$, $E_S = -0.65$, $\Delta T = 17.5$ C)
(c) Configuration 3 ($E_R = E_S = 0$, $\Delta T = 17.5$ C)
(d) Configuration 4 ($E_R = E_S = 0.7$, $\Delta T = 17.5$°C)
(e) Configuration 1 ($E_R = -0.05$, $E_S = 0.7$, $\Delta T = 21.5$ C)
(f) Configuration 2 ($E_R = 0.7$, $E_S = -0.65$, $\Delta T = 21.7$ C)
(g) Configuration 3 ($E_R = E_S = 0$, $\Delta T = 21.5$°C)
(h) Configuration 4 ($E_R = E_S = 0.7$, $\Delta T = 20.4$°C)

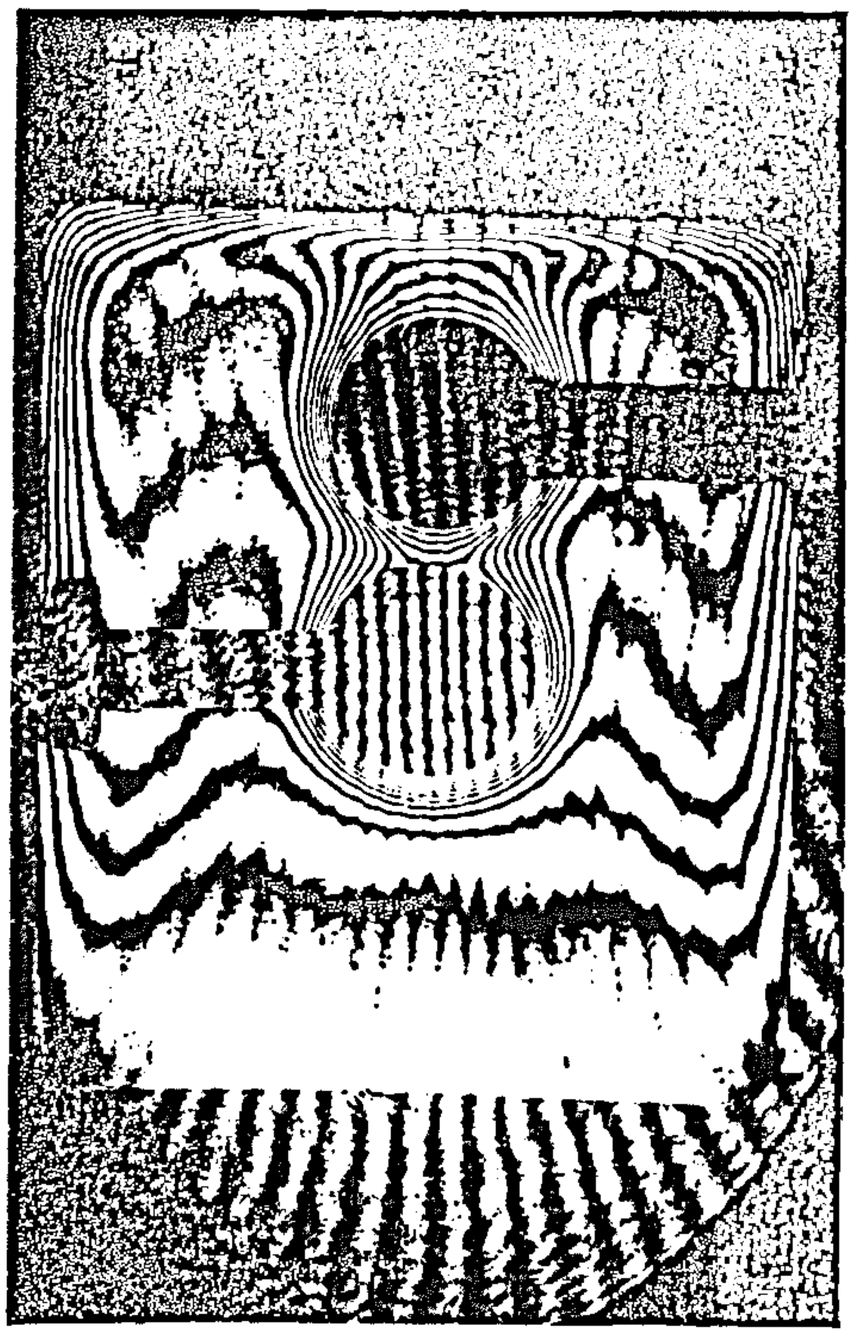

(c)

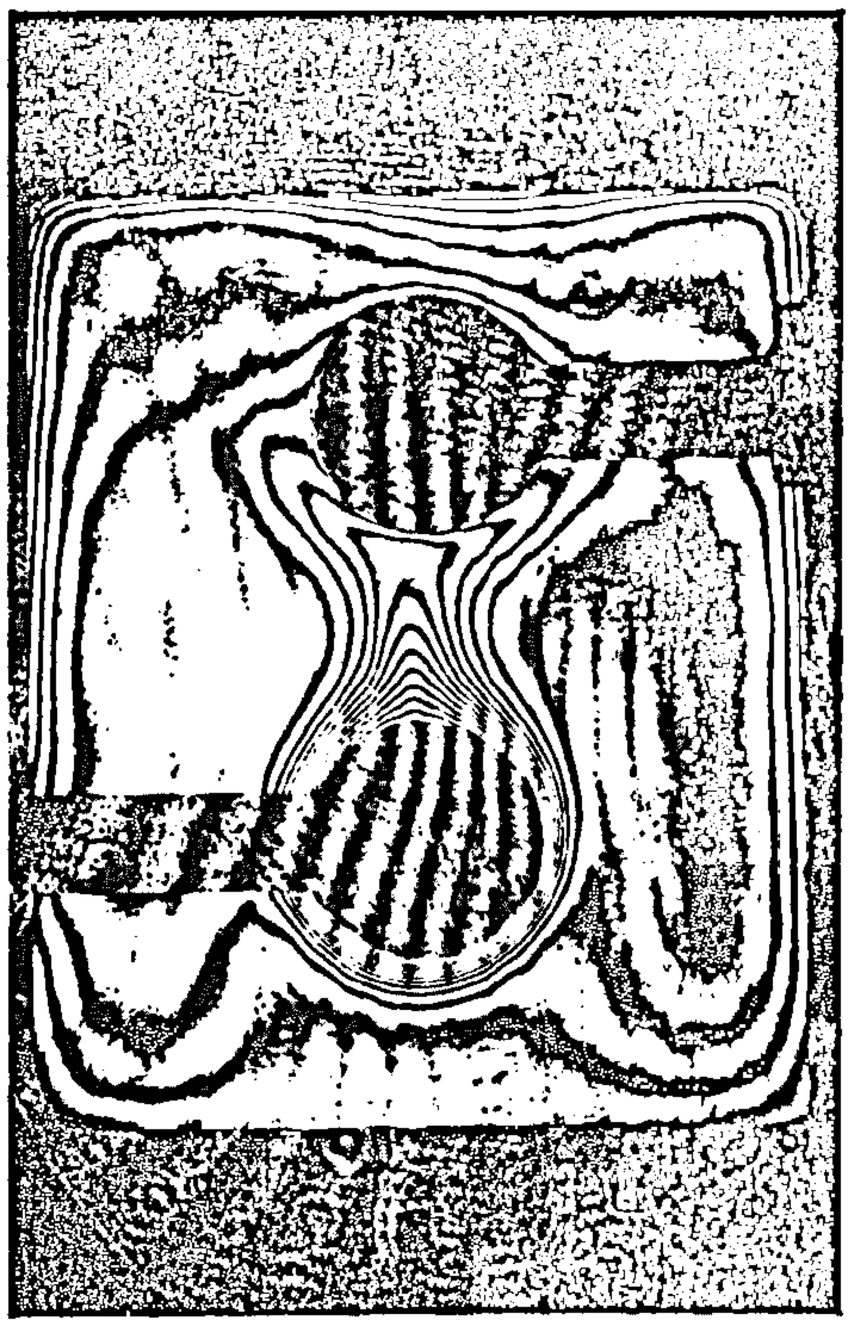

(f)

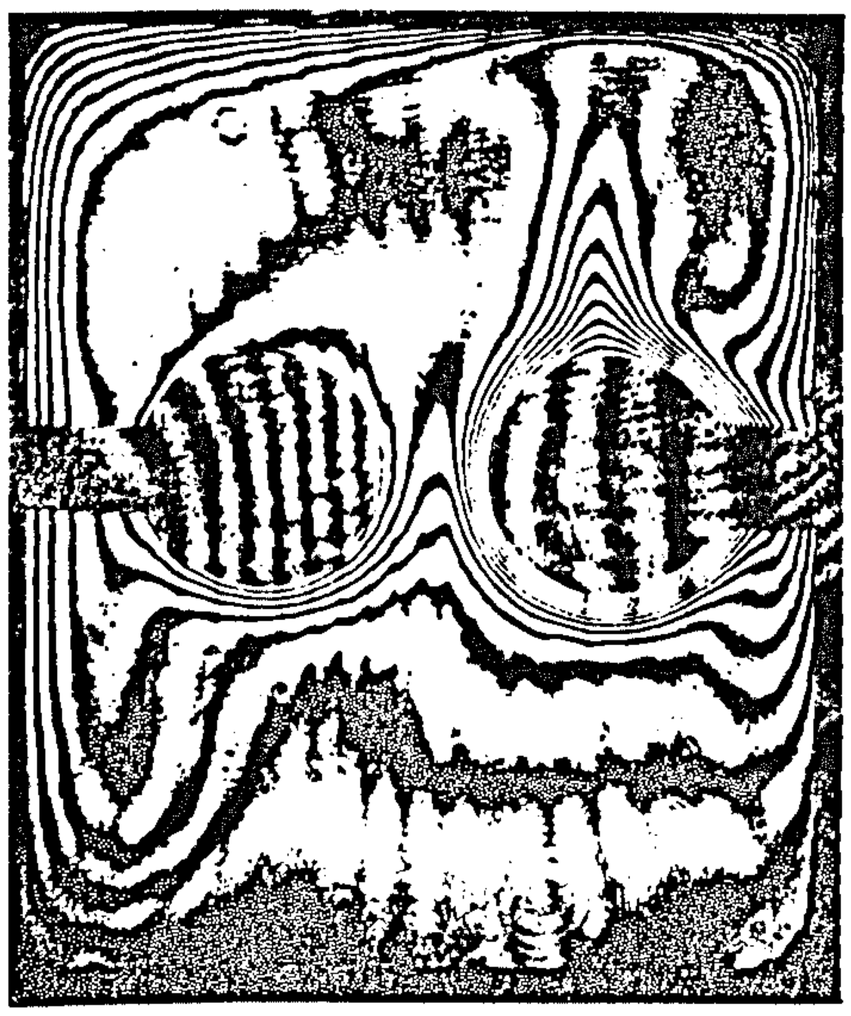

(g)

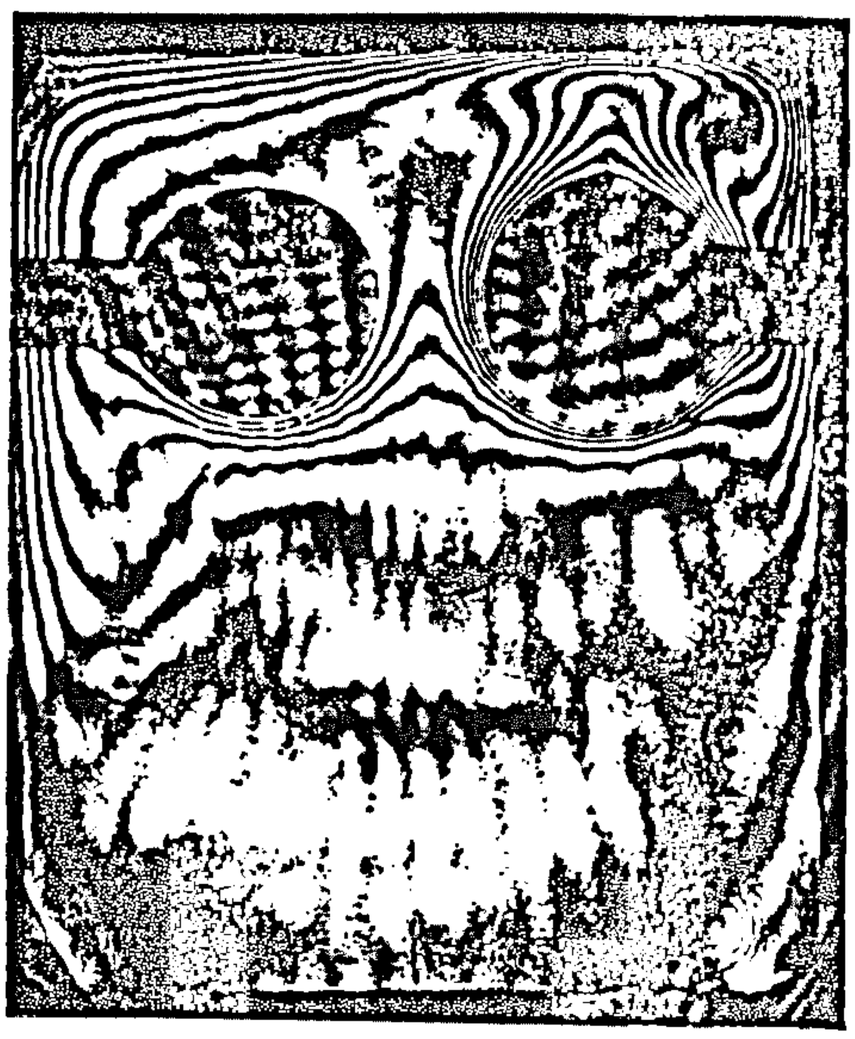

(h)

intense mixing: an oscillating plume between the two pipes, as well as large vortices, were produced above the cooler pipe. Consequently, relatively high rates of heat transfer occurred (see Fig. 7b).

Flow patterns for the side-by-side arrangement—having $E_R = E_S = 0$ (see configuration 3 of Fig. 4), that is current conventional practice—could be considered as consisting of three zones (see Fig. 7c). Firstly, there was an approximately triangular-shaped eddy circulating around the cooler pipe; secondly, a well-defined eddy ensued between the hotter pipe and the wall of the trench; and thirdly, in the lower half of the trench, a weak, irregularly shaped vortex occurred. If $E_R = E_S = 0.7$, that is configuration 4 of Fig. 4, the flow consisted of two zones, divided approximately diagonally across the trench section. The flows in these two zones again circulated in a counter-rotating manner, with a larger core (compared with configuration 3) near the base of the cavity (see Fig. 7d).

The shapes of the eddies in the four previously mentioned configurations were almost independent of the differences between T_0, T_R and T_S for the temperature ranges considered (6).

Steady state contour maps of isotherms were obtained for the four different configurations examined, with various applied steady state temperature distributions (see typically Fig. 7e to h). The interferograms with the hot pipe below the relatively cooler pipe arrangement (that is configuration 2 of Fig. 4) were not analysed in detail because the flow visualization observations indicated that this was the worst 'thermal insulation' situation, that is the rate of heat transfer was enhanced, rather than reduced, compared with that

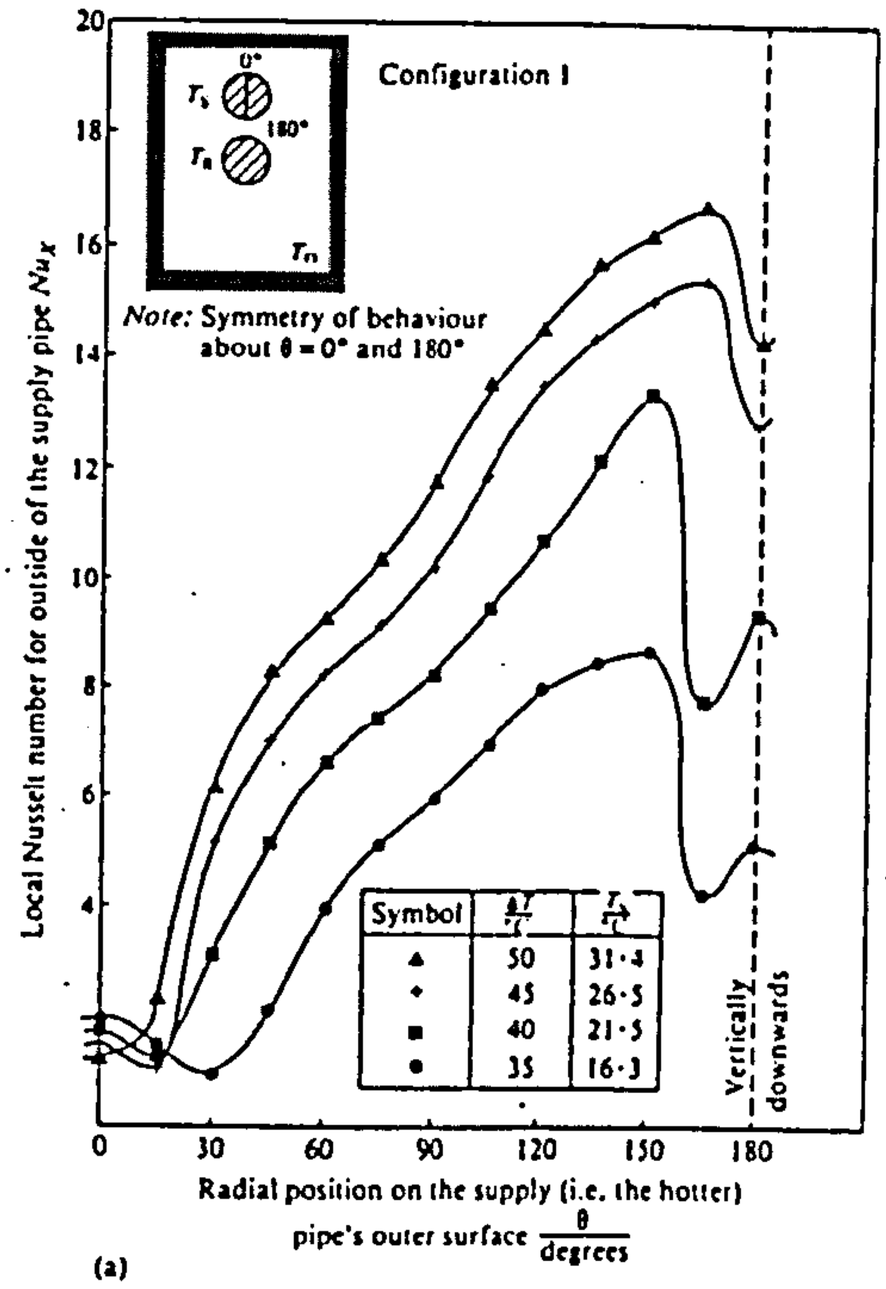

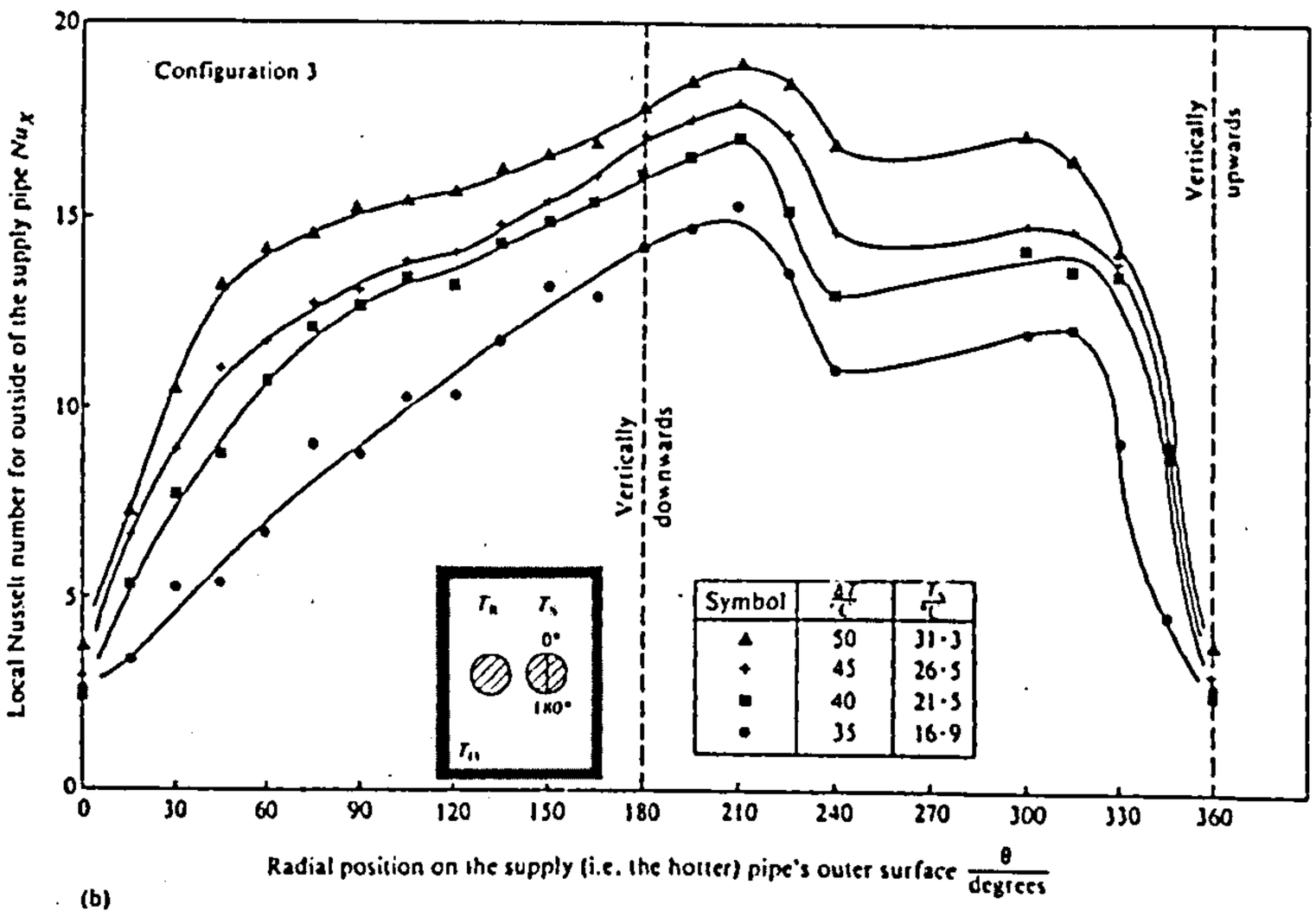

Fig. 8 Variation of the local Nusselt number Nu_x versus the angular coordinate θ for the supply pipe in the double-pipe system with $T_R = 30$ °C: (a) $E_R = -0.05$, $E_S = 0.7$; (b) $E_R = E_S = 0$

obtained with the conventional arrangement (that is configuration 3). The isotherms indicated the presence of severe convection instabilities and the plume was observed to be oscillating from side to side, with mixing occurring and hence relatively high rates of loss of heat ensued (6).

For the hot-above-cooler pipe arrangement (that is configuration 1 of Fig. 4), the supply (that is the hot) pipe position was kept constant at a displacement ratio E_s equal to 0.7 (which is the approximate value for the optimal location for a single-pipe system in a rectangular trench, as has been deduced previously). Five different displacement ratios, E_R, were then chosen for positioning the relatively less hot (that is the return) pipe directly below the hot pipe.

Similar steps (to those taken for the single-pipe system) were used to analyse the interferograms; except for the side-by-side arrangement (that is configurations 3 and 4 of Fig. 4), the range of θ covered was increased from 180 to 360° as no vertical symmetry for these configurations existed.

Figure 8 shows the variations of the local Nusselt number Nu_x with ΔT for selected arrangements. For configuration 1, the isotherms were packed most closely near the supply pipe's surface in the region $150° < \theta < 165°$ (see Fig. 8a). This zone experienced the greatest rate of combined convective and conductive steady state heat transfers through the air, that is $\dot{Q}_{conv+cond}$ for the $E_R = -0.05$ configuration under a specified ΔT. The value of θ corresponding to the surface zone having the greatest rate of heat transfer remained approximately unchanged as the return (that is the cooler) pipe was displaced relatively upwards or downwards (6). The maximum local rates of heat transfer for configurations 3 and 4 occurred near the bottom of the hot pipe, that is in the $180 \rightarrow 215°$ region (see Fig. 8b).

For the combined steady state convective plus conductive heat leaks through the air, it was suggested by Grigull and Hauf (2) that $\overline{Nu} = M(Gr)^n$. The value of M for this system (that is the double-pipe system) is a complicated function of geometry and the temperature distributions. It needs vastly more data than are at present available for its general form to be deduced. This needs to be investigated further!

The way in which the total steady state rate of heat loss $\dot{Q}_{total}$ from the supply pipe was dependent upon the temperature difference ΔT for different configurations is shown in Table 1, together with its radiation component $\dot{Q}_{rad}$ and its convective plus conductive component $\dot{Q}_{conv+cond}$ through the atmospheric pressure air in the cavity.

The $\dot{Q}_{total}$ values were plotted against the displacement ratio for the return pipe in order to deduce its optimal position. For the considered circumstances, the optimal position occurred with $E_R = -0.05$ (see Fig. 9). These optimal data (that is $E_R = -0.05$, $E_S = 0.70$) apply within the temperature range and for the component sizes employed. A reduction of approximately 14 per cent was obtained in the total rate of heat loss

Table 1 Steady state heat leaks from the 0.65 m long supply (that is the hot) pipe through the air across the considered cavity: $T_R = 30°C$

Configuration	Geometrical description	T_s °C	$\Delta T (= T_s - T_0)$ °C	$\dot{Q}_{conv+cond}$ W	$\dot{Q}_{rad}$* W	$\dot{Q}_{total}$ W
1	$E_R = 0.05$	35	16.5	1.6	4.2	5.8
	$E_S = 0.70$	40	21.4	3.0	5.7	8.7
		45	26.5	4.2	7.3	11.5
		50	31.6	5.9	9.0	14.9
1	$E_R = 0$	35	16.6	1.5	4.2	5.7
	$E_S = 0.70$	40	21.4	2.6	5.7	8.3
		45	26.4	4.1	7.3	11.4
		50	39.7	8.4	10.8	19.2
1	$E_R = -0.05$	35	16.3	1.2	4.2	5.4
	$E_S = 0.70$	40	21.5	2.4	5.8	8.2
		45	26.5	4.0	7.4	11.4
		50	31.4	5.4	9.1	14.5
1	$E_R = -0.10$	35	16.5	1.7	4.3	6.0
	$E_S = 0.70$	40	21.5	2.8	5.8	8.6
		45	29.2	4.7	8.0	12.7
		50	30.8	5.4	9.0	14.4
1	$E_R = -0.20$	35	15.9	1.7	4.2	5.9
	$E_S = 0.70$	40	20.7	3.0	5.7	8.7
		45	25.3	4.1	7.2	11.3
		50	30.2	5.8	8.8	14.6
3	$E_R = 0$	35	16.9	2.6	4.4	7.0
	$E_S = 0$	40	21.5	4.2	5.8	10.0
		45	26.5	5.5	7.5	13.0
		50	31.3	7.3	9.1	16.4
4	$E_R = 0.70$	35	15.7	1.8	4.1	5.9
	$E_S = 0.70$	40	20.4	3.2	5.6	8.8
		45	24.4	4.4	7.0	11.4
		50	31.1	6.6	9.1	15.7

* Deduced value based on $\varepsilon = 1$ for the trench surfaces and $\varepsilon = 0.78$ [that is oxidized copper (18)] for the return and supply pipes in the experimental rig.

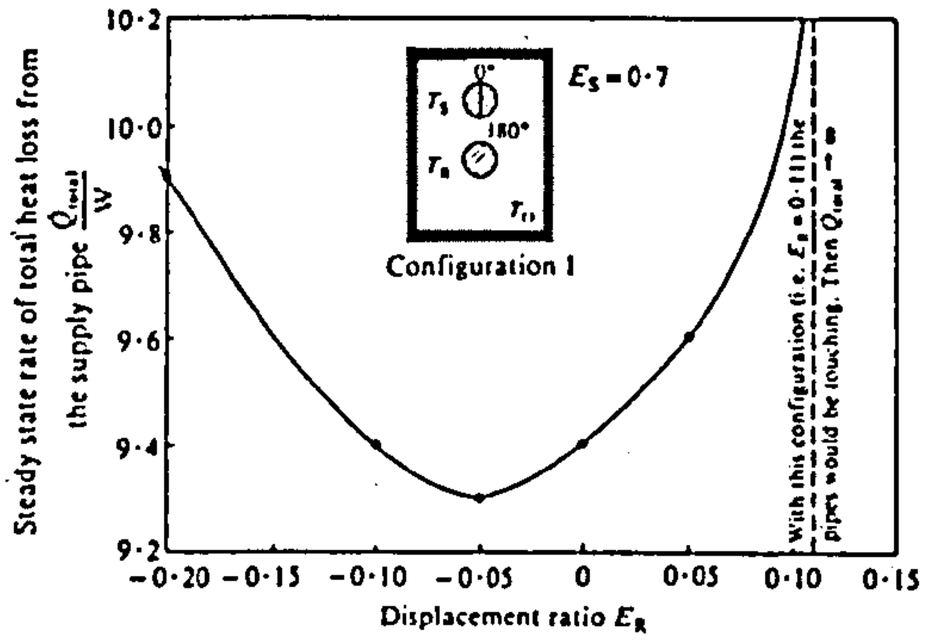

Fig. 9 Variation of the steady state total heat leak Q_{total} versus the displacement ratio E_R for configuration 1 of the double-pipe system with $T_R = 30°C$ and $\Delta T = 23°C$

through the air by using this optimal geometry of the hot-above-cooler configuration compared with that for the side-by-side arrangement under a selected steady state temperature difference of $\Delta T = 23°C$.

As this ΔT is reduced, the percentage reduction in steady state heat leak from the supply pipe, using the optimal geometry for configuration 1 of Fig. 4 rather than the side-by-side configuration, *increases*. Therefore, in practice, for well-insulated pipes, the percentage improvement in the thermal resistance of the air achieved by using the present recommendation rather than current conventional practice will possibly be significantly greater than the 14 per cent value suggested here.

5 CONCLUSIONS

There is an optimal configuration whose use leads to the least rate of heat being lost from the supply (that is the hot) pipe. With $E_S = 0.7$, an improvement of 13 per cent in the thermal resistance of the air-filled cavity was obtained compared with current conventional practice (that is the use of systems with $E_S = 0$); see Fig. 6. This improvement is smaller than that achieved for a similar sized pipe-in-pipe arrangement. This change is due to the influence that the shape of the external enclosure has on the fluid flows. The upward vertical displacement of a pipe-in-pipe arrangement restricts the convective flow in the region $90° < \theta < 180°$, the degree of this restriction being dependent upon the displacement ratio. In the rectangular trench, the flow zone is substantially affected only near $\theta = 180°$ by this displacement. This emphasizes the importance of the vertical separation between the tops of the inner and outer surfaces of the cavity on the steady state rate of convective heat transfer across the cavity.

Having a supply (that is the hot) pipe above a return (that is the cooler) pipe in a cold rectangular trench leads to lower steady state rates of heat loss than with any side-by-side arrangement or with the warm-above-hot pipe arrangement within the same trench under identical boundary temperature conditions. An optimal configuration (that is corresponding to least rate of heat loss from the supply pipe) occurred with $E_R = -0.05$ and $E_S = 0.70$.

A maximum reduction in the total rate of heat loss through the air of approximately 14 per cent was obtained with a temperature difference ΔT of 23°C between the wall of the trench and the outer surface of the supply pipe by using the optimal arrangement, compared with that for the conventional side-by-side arrangement (that is $E_R = E_S = 0$); see Fig. 9. The hot-above-cooler pipe arrangement had the added advantage that it would permit the use of narrower (and hence cheaper to excavate) trenches compared with the present conventional practice (19). Nevertheless, undertaking maintenance would require greater skills, for example with respect to the use of mirrors when repairing the lower pipe.

An overall loss of about 6 per cent of the distributed heat is usually acceptable (20), but frequently the losses are higher (8). For example, the district heating lines at Heathrow Airport suffer losses of about 9 per cent of the boiler-house output at peak loads, that is during January, whilst in July, due to the lower, intermittent loads then satisfied, this increased to 56 per cent (21). The latter figure was reduced subsequently to about 35 per cent by increasing the insulant thickness on the pipes.

In reality, for typically insulated pipelines, the 14 per cent improvement in the thermal resistance of the air-filled cavity would amount to only ~2 per cent gain in the overall insulation of the system (that is allowing for the presence of the insulant on the pipes and the insulation provided by the earth surrounding the air in the trench). Nevertheless, over the lifetime (>thirty years) of the pipelines system, this is still a very worthwhile benefit as its attainment incurs no additional capital expenditure, which could even be reduced.

REFERENCES

1 Liu, C., Mueller, W. K. and Landis, F. Natural convection heat transfer in long horizontal cylindrical annuli. *International developments in heat transfer*, International Heat Transfer Conference, Colorado, 1961, Paper 117, pp 976–984.
2 Grigull, U. and Hauf, W. Natural convection in horizontal cylindrical annuli. 3rd International Heat Transfer Conference, Chicago, 1966, Paper 60, pp 182–195 (Am. Instn Chem. Engrs).
3 Powe, R. E., Carley, G. T. and Carruth, S. L. A numerical solution for natural convection in cylindrical annuli. *Trans. ASME, J. Heat Transfer*, 1971, 93, 210–220.
4 Kuehn, T. H. and Goldstein, R. J. An experimental study of natural convection heat transfer in concentric and eccentric horizontal cylindrical annuli. *Trans. ASME, J. Heat Transfer*, 1978, 100, 635–640.
5 Schimmel, Jr W. P. Application of laser holographic interferometry to natural convection in enclosures. Sandia Laboratories, Fluid Mechanics and Heat Transfer Division, Albuquerque, 1979, pp 41–48.
6 Babus'Haq, R. F., Probert, S. D., Shilston, M. J. and Talati, A. Suggested design improvements concerning district-heating pipeline configurations. *Appl. Energy*, 1984, 17, 77–96.
7 Babus'Haq, R. F., Probert, S. D. and Shilston, M. J. Optimal location of a single horizontal pipeline in a rectangular, horizontal, air-filled enclosure to achieve maximum thermal insulation. *Appl. Energy*, 1984, 18, 239–259.
8 Courtney, R. G. and Hobson, P. J. The performance of 15 district-heating schemes. *Heating and Ventilating Engr*, 1977, 51, 4–11; 52, 24.
9. Quigg, J. S. Underground distribution systems. *Building Services Engineer*, 1976, 44, 40–41.

10 Union Nationale des Chambres Syndicales D'Enterprises en Genie Climatique. Règles professionnnelles UCH 26/78. *Promoclim A*, 1979, 10, 19–28.
11 Borger, H. A. Available types of underground heat distribution systems. *Symposium on Underground Heat and Chilled Water Distribution Systems*, 1973, Report NBS-BSS-66, pp 52–59 (National Bureau of Standards, Washington, DC).
12 CP 3009: 1970 *Code of practice for thermally-insulated underground piping system*, 1970 (British Standards Institution, London).
13 BS 5970: 1981 *Code of practice for thermal insulation of pipework and equipment (in the temperature range—100°C to 870°C)*, 1981 (British Standards Institution, London).
14 Hauf, W. and Grigull, U. Optical methods in heat transfer. *Advances in Heat Transfer*, Vol. 6, 1970, pp 133–366 (Academic Press, New York).
15 Brooks, R. G., Robert, S. D. and Maxwell, J. 18 cm field of view Mach–Zehnder interferometer for heat transfer studies. *Trans. Inst. Measurement and Control*, 1968, 1, T9–T16.
16 Mehta, J. M. and Black, W. Z. Errors associated with the measurement of convective heat transfer coefficients. *Appl. Optics*, 1977, 16, 1720–1726.
17 Feingold, A. and Gupta, K. G. New analytical approach to the evaluation of configuration factors in radiation from spheres and infinitely-long cylinders. *Trans. ASME, J. Heat Transfer*, 1970, 92, 69–76.
18 Gröber, H., Erk, S. and Grigull, U. *Fundamentals of heat transfer*, 3rd edition, 1961 (McGraw-Hill, New York).
19 Orchard, W. R. H. Personal communication, 1984, Orchard Partners, Southampton Row, London.
20 Mackenzie-Kennedy, C. *District-heating: thermal generation and distribution*, 1979 (Pergamon Press, Oxford).
21 British Airports, Authority. Boiler house 523: cargo terminal area. BAA leaflet, 1975, pp 1–2.

CHAPTER 5

OPTIMISING THE LOCATION OF A DISTRICT-COOLING PIPELINE IN A RECTANGULAR TRENCH

SUMMARY

Steady-state rates of heat transfer to a cold horizontal pipeline within an atmospheric pressure, air-filled, horizontal rectangular cavity (see Fig. 1) with relatively hot isothermal walls, have been determined experimentally. The optimal geometrical arrangement, i.e. that for which the least rate of heat is gained by the supply pipeline, occurs with a displacement ratio approximately equal to 0.67, the pipe being in the lower half of the cavity and mid-way between the vertical walls. The use of this configuration leads to significant energy savings (relative to employing the traditional arrangement with the pipe placed at half depth in the trench) without incurring any additional insulation costs.

NOMENCLATURE

D	Diameter of the supply (i.e. the cold) horizontal pipe, (m).
E	Displacement ratio { = [2H/(Y-D)] - 1 , see Fig. 1 } ; Y = Y_A or Y_B according to the system 'A' or 'B' tested; $-1 \leq E \leq 1$.
G	Average vertical gap [= (Y-D)/2] , (m).
Gr_D	Local Grashof number, based on the diameter, D, of the pipe.

H — Minimum gap, i.e. the shortest vertical distance between the supply horizontal pipe and the upper horizontal surface of the trench, see Fig. 1, (m).

k — Thermal conductivity of air, ($W\ m^{-1}\ K^{-1}$).

L — Axial length of the considered horizontal air-filled cavity, see Fig. 2, (m).

M — Dimensionless parameter, in the convective plus conductive steady-state heat transfer through the air relationship: it is dependent upon the geometry and temperature distribution of the considered system [$= \overline{Nu}_G / Gr_D^{\ n}$] .

n — Power index of the Grashof number in the Nu_G versus Gr relationship.

$Nu_G, \overline{Nu}_G$ — Local (i.e. at position Θ) and average Nusselt numbers respectively, for the steady-state heat transfers to the cold supply pipe, based on the average vertical gap, G.

T_o — Steady-state uniform temperature of the inner surfaces of the model outer surrounding isothermal rectangular trench, as used in the present set of experiments -- see Fig. 1, (°C).

T_s — Steady-state temperature of the outer surface of the supply pipe, see Fig. 1, (°C).

X, Y — Horizontal width and vertical extent respectively of the considered rectangular cavity, see Fig. 1, (m).

ΔT — Steady-state difference between the temperatures of the inner surfaces of the trench and the outer surface of the supply pipe: i.e. [$= T_o - T_s$], (°C).

Θ — Angular co-ordinate, measured from zero for the vertically downwards radius vector emanating from the horizontal centre-line of the supply pipe and increasing for counter-clockwise rotations - see Fig. 3, (degrees).

Suffixes

D — with respect to the diameter of the supply pipe.

G — with respect to the average vertical gap dimension.

o — of the inner surfaces of the rectangular trench.

s — for the cold-water supply pipe.

Abbreviation

DHC — District heating and cooling.

DISTRICT COOLING

Due to the increasing demand for air conditioning, district cooling is gradually becoming popular: it involves a centralised system supplying chilled water to the consumers[1]. Both district-heating and cooling (DHC), because of economies of scale, allow greater benefits to be derived per unit energy expenditure from the use of energy by reducing the consumptions of, and so dependence upon, the no-longer cheap, scarce or imported fuels[2,3].

However, district cooling is not as technically advanced as district heating. Nevertheless, more than fifty systems are already in operation or being installed in various cities of the USA[4-12], Europe[13-17], Japan[18,19], Australia[20], Nigeria[21], and the USSR[22]. District cooling is economically attractive only for high-intensity demand areas, e.g. for high-density occupation of tall government buildings or high population, small university campuses in tropical countries where comfortable conditions need to be maintained throughout the year.

District-cooling schemes have several advantages over local or individual cooling systems, each of which serves only one small building: these benefits include lower capital costs, less noise and vibration, and greater cleanliness[23-28]. In addition, a district-cooling system can often be used to distribute "waste" heat during winter[22].

The extent of the delivery area alone cannot be used as the sole criterion for assessing the economic feasibility of district heating or cooling potential. A small project can be worthwhile if a sufficiently large heating or cooling demand exists on the site, whereas conversely it will probably be uneconomic to serve a large area with only low demands[12].

UNDERGROUND DISTRIBUTION SYSTEMS

These systems for district-cooling pipelines can be classified as: either (i) thermally-insulated pipes in air-filled trenches; (ii) pipes in trenches, which are packed with loose-fill thermal insulants; or (iii) pipes in trenches with poured-in-place concrete. The most frequently recommended and widely-used system is group (i)[29-32]. The outer surface of any insulant applied to the cold pipe, as in (i), should be designed when operating to be at a temperature above the dew point so that condensation on this surface does not ensue. In the event of such a trench flooding, which occurs intermittently in Britain because of its maritime climate, the drainage and evaporation from around the pipe would be more likely to ensue automatically than with distribution systems of types (ii) or (iii). If allowed to remain damp, the moisture reduces the insulant's effectiveness (sometimes permanently) as well as promotes corrosion of the underlying steel pipe which is being protected by the insulant. The prime requirements therefore of the outer case of the trench in whatever form, are to protect the pipework and its thermal insulation against attack by water and chemical action during the

anticipated life of the system[29]. However, the air in the cavity also serves to thermally insulate the pipes. By optimising the geometry of such a system, the thermal insulation provided by the air in the trench can be maximised. An optimal position for the inner pipe occurs because the convective and conductive contributions to the steady-state total heat leak vary in different ways as the displacement ratio is changed. For example, as E tends to unity, for relatively large values of E, the conductive component increases whereas the convective component decreases.

THERMALLY-INSULATED PIPELINES

District-cooling involves refrigerating water at a central location, usually using steam-driven centrifugal or absorption type chillers. This cooled water is then pumped to the consumers at a temperature of about 40 °C through well-insulated pipelines and returned to the plant at about 13 °C[1]. The district-cooling pipelines are protected thermally by an insulant, which should be impervious to water but usually has little mechanical strength[29]. Unfortunately (from an energy-thrift viewpoint) some underground chilled-water pipes are installed uninsulated, in order to reduce the required initial capital investment and subsequent maintenance problems: this practice is particularly prevalent with large district-cooling systems[33,34].

Much time, effort, and money have been devoted to producing reliable, cheap thermally-insulated underground pipelines -- but

to date[30], these have not been compleltely successful. A thermally-insulating internal lining applied to pipes possesses some advantages for the conveyance of chilled water[35], but it needs considerable further research and development.

SCOPE OF THIS INVESTIGATION

For the air-filled trench system, the aim is to optimise the location of the supply pipeline within the cavity in order to minimise the rate of heat gain by the pipe via conduction, convection and radiation through the surrounding air. In other words, by using this optimal position, the thermal insulation afforded by the surrounding air is maximised without incurring any additional material costs or the need for special constructional skills.

During the present investigation, the steady-state rate of heat transfer across the atmospheric pressure, air-filled gap between an isothermal hot horizontal rectangular sectioned trench enclosing a horizontal relatively-cold pipe (representing the supply pipeline of the district-cooling system) was measured. The influence upon the steady-state heat transfer rate of the position of the horizontal pipe (i.e. the displacement ratio) relative to the trench was determined. So its optimal lcoation corresponding to the least rate of steady-state heat gain for each prescribed set of conditions was deduced.

Flow visualisations for various steady-state temperatures of the surfaces of the pipe and trench, and for different displacement ratios, were used to stimulate, supplement and corroborate conclusions being drawn from interferometric observations indicating the temperature distributions across the air gap.

The Tested Systems

The values of the experimental parameters (see Fig. 1) chosen for this investigation were:-

(i) For system 'A'

$$X = 100 \text{ mm}, \; Y_A = 100 \text{ mm}, \; L = 630 \text{ mm}, \; D = 28.5 \text{ mm};$$

$$-0.75 \leq E \leq 0.8;$$

$$6 \text{ °C} \leq T_s \leq 10 \text{ °C} \leq T_o \leq 40 \text{ °C},$$

$$3 \text{ °C} \leq \Delta T \leq 30 \text{ °C}.$$

(ii) For system 'B'

$$X = 100 \text{ mm}, \; Y_B = 125 \text{ mm}, \; L = 650 \text{ mm}, \; D = 28.5 \text{ mm};$$

$$-1.0 \leq E \leq 1.0;$$

$$10 \text{ °C} \leq T_s \leq 35 \text{ °C} \leq T_o \leq 40 \text{ °C},$$

$$5 \text{ °C} \leq \Delta T \leq 25 \text{ °C}.$$

For all the tests undertaken in this investigation, the centre of the pipe was maintained at X/2 (= 50 mm) from both vertical walls of the trench.

Independent supplies of warm water were fed to each wall of the trench. This avoids the appreciable drop in the temperature of the water which would have occurred if it had been used for heating all the walls in succession. The copper pipe was cooled by passing cold water from a water chiller at a steady temperature, T_s, so that $T_o > T_s$. Steady-state flow visualisation patterns were observed -- e.g. see Figs. 4 and 5 -- and distinctive patterns of the isotherms -- e.g. see Figs. 6 and 7 -- were photographed[36].

FLOW VISUALISATIONS

Different displacement ratios, E - four for system 'A' and five for system 'B', were chosen and, for each different steady-state temperature differences between the hot trench and the enclosing relatively-cold pipe were applied. A small amount of smoke was injected very slowly into the cavity and photographs were taken of the resulting steady-state flow patterns in the illuminated rectangular trench. Such flow visualisations (e.g. see Figs. 4 and 5) indicated the presence of any instabilities, so that the conditions under which the latter occurred could be ascertained.

For the E = 1.0 arrangement (for system 'B'), the flow patterns exhibited two almost stable counter-rotating, approximately triangular-shaped eddies, which when averaged with respect to time were symmetrical about the vertical plane through the horizontal axes of the pipe, bisecting the trench (see Fig. 5(a)). There was also a relatively stagnant region in the upper half of the cavity between the two rotating eddies. Qualitatively similar flow patterns, but with improved stabilities resulted if the displacement ratio was decreased to E = 0.7 (for both systems 'A' and 'B') - see Figs. 4(a) and 5(b). However the stability of the vortex patterns decreased if the displacement ratio was further reduceud, e.g. to a value of E = 0.5 (for system 'A') - see Fig. 4(b).

For the E = 0 arrangement (for both systems 'A' and 'B'), the relatively fast, relatively cold air down-flow below the pipe (i.e. the plume) oscillated slowly (about the vertical symmetrical plane) through an angle Θ between 5 and 15° (see Figs. 4(c) and 5(c)), and resulted in an increased rate of heat transfer. Flow patterns for even lower relative positions of the inner pipe, e.g. for E = -0.7 (for both systems 'A' and 'B'), exhibited more rapid severe plume oscillations, as well as the counter-rotating vortices in the cavity (see Figs. 4(d) and 5(d)).

The flow patterns, for the E = -1.0 configuration (for system 'B') were of irregular shape: they exhibited severe instabilities with intense mixing and large vortices occurred in the cavity

(see Fig. 5(e)). Consequently, relatively high rates of heat transfer ensued.

The approximate shapes of the eddies in all the previously-mentioned arrangements were almost independent of the difference between T_o and T_s for the temperatures ranges considered. Most of the observed effects could be accounted for by the air circulation speed, as expected, rising as the temperature difference, ΔT, increased.

INTERFEROMETRIC STUDIES

The Mach-Zehnder interferometer[37] was adjusted so that initially (with the tested system at room temperature), the whole field-of-view was occupied by a single fringe, i.e. the infinite-fringe mode. Interference fringe which became apparent when a temperature difference, ΔT, was applied across the cavity, then represented average isothermal contours for the air.

Enlarged prints of the steady-state isothermal contour maps for the air in the cavity were obtained for the different geometrical configurations examined, with various applied steady-state temperature distributions (see Figs.6 and 7). The isotherms were of qualitatively similar shapes for each arrangement, but the fringes became more closely packed together as the temperature differences were increased. Detailed analysis was only necessary for half of each interferogram, because the pipe was always equidistant from the two vertical walls of the trench, i.e. vertical

symmetry appertained. The first five fringe displacements from the pipe wall were measured at 15° increments around the pipe, except where there were less fringes in the pipe's boundary layer (see Fig. 3). Hence the temperature gradients in the air adjacent to the wall could be deduced so that the variations of the local Nusselt number, Nu_G, versus the angular co-ordinate, Θ, could be evaluated -- see representative plots in Figs. 8 and 9 for systems 'A' and 'B' respectively, for selected values of the displacement ratio, E, and temperature difference ΔT. For $-0.75 \leq E \leq 0.6$, the minimum value of the local Nusselt number occurred near the bottom of the pipe (i.e. at $\Theta = 0°$). However, this optimal angular position, corresponding to the minimum Nu_G, moved to $\Theta = 40°$ and 60° approximately (for systems 'A' and 'B' respectively), for the largest positive displacement ratios of 0.8 and 0.9 respectively. This was because the bottom gap between the supply horizontal pipe and the lower horizontal internal surface of the trench decreased as the displacement ratio, E, increased and hence conduction became eventually the dominant heat transfer process across this gap. The position at which Nu_G exhibited a minimum was temperature dependent. As the temperature difference, ΔT, increased, the angular position, Θ, at which this minimum local Nusselt number occurred decreased because the fluid velocity in the boundary layer increased, and the flow penetrated further into what had formerly been the relatively stagnant region near the bottom of the cavity.

For the combined steady-state convective plus conductive heat leaks through the air, it was suggested by Grigull and Hauf[38]

that $\overline{Nu}_G = M\ Gr_D^{\ n}$, which if fully developed laminar-flow convection ensues throughout the region then n = 0.25 (see Figs. 10 and 11). However, n is not always equal to 0.25. For low Grashof numbers, Gr_D (i.e. at small values of ΔT), a relatively stagnant fluid exists in large regions of the cavity, and n takes values at the lower end of the range $0 < n < 0.25$. For large temperature differences, the flow penetrates further into the stagnant regions when fully developed flow occurs through the cavity, n equals 0.25.

For both systems 'A' and 'B' , the value of the parameter 'M' was deduced and plotted versus the displacement ratio, E -- see Fig. 12. For each of the systems tested, M is effectively a measure of the conductance of the air surrounding the pipe: for a constant Grashof number, all the parameters affecting the convective plus conductive heat transfer relationship except the surface heat transfer coefficient ($= k\overline{Nu}_G/G$) are constant. Hence the minimum rate heat transfer from the pipe is obtained for the system configuration with the minimum value of M, i.e. the system where the air provides the maximum thermal redsistance for the pipe. Minima of 'M' occurred at $E = 0.67 \pm 0.03$ for both systems 'A' and 'B'. This represents the approximate value for the optimal location of the cold pipe in the hot rectangular trenches considered, and for the temperature distributions tested. In an analogous investigation [37] using system 'A', a displacement ratio of $E = -0.70 \pm 0.03$ was found to be the optimal location of a hot pipe in a cold rectangular trench, i.e. as might be used

for district heating, so that the minimum rate of heat loss occurred from the pipe.

By using such optimal configurations, improvements of ~ 11% and ~ 23%, for systems 'A' and 'B' respectively in the thermal resistances (for heat transfers via convection and conduction through the air) of the air-filled cavity were obtained compared with current conventional practice, i.e. the use of systems with E = 0 -- see Fig. 12. Using the optimal displacement ratio, E, becomes more desirable the greater the trench is elongated vertically from its square section. The total heat flux from the duct to the enclosed pipe is proportional to the product of the surface heat transfer coefficient and the surface area. Increasing the height of the duct from 100 mm to 125 mm resulted in an increase in the total heat flux, for a given temperature difference, between the pipe and the duct. However, because the surface area of the pipe remained constant, this resulted in an increase in the pipe's surface heat transfer coefficient, which is reflected in a higher value of M for system 'B' than for system 'A' at an equal value of Gr_D.

The radiative component of the steady-state rate of heat transfer across the cavity is independent of the displacement ratio for an infinitely-long pipe and trench[39]. Thus for this investigation, the optimal location, as deduced from the convective plus conductive data, is within experimental error the same as that as if the total heat leak had been considered.

CONCLUSIONS

There is an optimal location for a horizontal cold pipeline in a horizontal relatively hot, air-filled rectangular trench, which leads to the least rate of heat being gained by the supply pipeline. With E = 0.67 for both systems 'A' and 'B', maximum increases in the thermal resistance of the cavity's air of ~ 11% and 23% respectively, were obtained compared with the current conventional systems (having E = 0) -- see Fig. 12. For an associated investigation[37] with geometrical system 'A', an improvement of 13% was obtained using an optimal location of E = -0.7 for a hot pipeline in a relatively cold rectangular trench. An improvement of ~ 15% in the air's convection and conduction thermal resistance has also been reported by using optimal eccentricities in air-filled cylindrical annuli with relatively cold pipes [40].

In practice, for district-cooling systems, there is likely to be another pipeline in the trench, i.e. that acting as the return pipeline carrying the relatively warm water back to the chiller. Then, by using the optimal location of the supply pipeline as identified above, the optimal location of the return pipeline may be determined experimentally, so that the least steady-state rate of heat gain by the supply pipe occurs. In view of the available results, undoubtedly the higher temperature pipeline above the lower temperature pipeline configuration will be the recommended energy-thrift choice for district-cooling and district-heating distribution systems[41].

Improvements in the thermal resistances of the air cavities achieved by using optimal locations of the pipelines are small, compared with the total resistances of the insulated buried pipes. However, this increase of insulation provided by optimising the configuration of the air gap, does not involve any extra financial expenditure. Also because the life-span of the district-cooling pipeline distribution network is estimated to be more than 35 years, the prospect of reducing the energy leaks by even a small fraction (~ 3%) should be attractive to designers.

REFERENCES

1. R.M.E. Diamant and D. Kut, District-heating and cooling for energy conservation, The Architectural Press, London, 1981, pp. 392-414.

2. R. Meador, Cogeneration and district heating, Ann Arbor Science Publishers, Michigan, 1981, pp. 172-173.

3. P. Kier, J. Feit, W. Henselman, R. Loube, C. Meek and W. Wilson, State and local regulations for district-heating and cooling systems : issues and options, Argonne National Laboratory, Argonne, Illinois, Report No. ANL/ES-126, 1981.

4. B.H. Smith and E.W. Kiss, Hartford urban redevelopment program illustrates boiler selection for central heating and cooling plants, District Heating, 50(10), (1964), pp. 53-56 and pp. 61-64.

5. R.L. Michaud, Super central plant supplies steam and chilled water to Minneapolis, Heating Piping and Air Conditioning, 44(12), (1972), pp. 43-51.

6. K. Hartmann, Wirtschaftliche betriebsweise von fernkaltezentralen, Klima-Kalte Ing., 7(7-8), (1979), pp. 273-278.

7. E.G. Hansen, Modular central plant to serve Capitol Hill, Heating Piping and Air Conditioning, 49(12), (1977), pp. 59-65.

8. L.A. Huygen, Amerikaanse ervaringen, Klimaatbeheersing, 9 (11), (1980), pp. 618-619.

9. Anon., New district-heating/cooling plant in Nashville, Tennessee, District Heating, 58(2), (1972), pp. 20-23.

10. Anon. Three rivers stadium in Pittsburgh, Pennsylvania, District Heating 56(1), (1970), p. 9.

11. J.E. Mesko, District-heating and cooling systems: planning by a computer, Proc. 1st. Int. District-Heating Convention, London, Session 4, Section F(5), 1970, pp. 3-12.

12. A.S. Kennedy and J.F. Tschanz, Disrrict-heating and cooling: a 28-city assessment, Argonne National Laboratory, Argonne, Illinois, Report No. ANL/CNSV-TM-119, 1983.

13. W. Braun and T. Pinter, Technische und wirtschaftliche aspekte der vernkalteversorgung, Proc. 2nd. Int. Convention on District Heating, Budapest, VI, 1973, pp. 5-20.

14. L.Emho, A tauhutes kifejlodesenek muszaki gazdasagi lehetosegei Magyarorszagon, Proc. 2nd. Int. Convention on District Heating, Budapest, VI, 1973, pp. 21-32.

15. G. Giaimo, N. Rossi and F. Siniscalco, District-heating and cooling systems for air conditioning and other facilities of Naples University polyclinic, Proc. 2nd. Int. Convention on District Heating, Budapest, VI, 1973, pp. 33-48.

16. H. Laakso, Losung von abwarmeproblemen fur fernkalteanlagen mittels nasser und trockener luftkuhlung, Proc. 2nd. Int. Convention on District Heating, Budapest, VI, 1973, pp. 63-72.

17. British Airport Authority, Boiler House 523, cargo terminal area -- Heathrow Airport, London, BAA leaflet, 1975.

18. S. Inukai and S. Sato, District heating of Champion village at Sapporo Winter Olympics 1972, Proc. 2nd. Int. Convention on District Heating, Budapest, III, 1973, pp. 81-94.

19. J. Ishida, Recent application of large absorption units in Japan, ASHRAE Trans., 85(1), (1979), pp. 395-405.

20. A.L. Kong, An Australian district-heating scheme, Australian Refrigeration Air Conditioning and Heating, 23(2), (1969), pp. 18-24.

21. M. Constantino and P. Zuccala, Progetto delle infrastrutture e ipotesi di un sistema di teleraffreddamento per Abuja, nouva capiutale federale della Nigeria, Condizionamento Dell'aria - Riscaldamento - Refrigerazione, 27(9), (1983), pp. 965-971.

22. Z.A. Melikyan, Large-scale centralised cooling systems, Heating and Ventilating Engineer, 48(7), (1974), pp. 3-7.

23. Carrier Air Conditioning Co., Chilled water as a utility, Carrier booklet, New York, 1968.

24. J.E. Mesko, Economic advantages of central heating and cooling systems,Proc. Symposium on Underground Heat and Chilled-Water Distribution Systems, Washington, D.C., 1973, Report No. NBS-BSS-66, 1975, pp. 9-17.

25. G.V.R. Holness, Designing a central chilled-water system, Heating, Piping and Air Conditioning, 50(9), (1978), pp. 111 -122.

26. G.F. Carlson, Central plant chilled-water systems: pumping and flow balance, ASHRAE J., 14(2), (1972), pp. 27-34; 14 (3), (1972), pp. 46-54; 14(4), (1972), pp. 42-48.

27. G.S. Farkas, The energy cost of comfort cooling, Proc. Int. District-Heating Association, New Hampshire, 70(10), 1979, pp. 1-14.

28. L.Lang, Tavhutes energia igenyet befolyasolo tenyezok, Proc. 2nd. Int. Convention on District Heating, Budapest, VI, 1973, pp. 73-86.

29. J.S. Quigg, Underground distribution systems, Building Services Engineer, 44(9), (1976), pp. A40-A41.

30. H.A. Borger, Available types of underground heat-distribution systems, Proc. Symposium on Underground Heat and Chilled-Water Distribution Systems, Washington D.C., 1973, Report No. NBS-BSS-66, 1975, pp. 52-59.

31. Union Nationmal Des Chambres Syndicales D'Entreprises En Genie Climatique, Regles professionnelles UCH 26/78, Promoclim A., 10(2), (1979), pp. 19-28.

32. BS5970, Code of practice for thermal insulation of pipework and equipment (in the temperature range -100°C to 870°C), British Standards Institution, London, 1981.

33. J.H. Henderson, Economic justification of thermal insulation of underground hot and chilled-water piping, Proc. 1st. Int. District Heating Convention, London, Session 4, Section G, (7), 1970, pp.1-8.

34. T. Kusuda, Heat transfer studies of underground chilled-water and heat-distribution systems, Proc. Symposium on Underground Heat and Chilled-Water Distribution Systems, Washington, D.C., 1973, Report No. NBS-BSS-66, 1975, pp. 18-41.

35. S.D. Probert, C.M. Yeung and C.Y. Chu, Internally-insulated pipes for district-cooling systems, Applied Energy, 12, (1982), pp. 99-115.

36. R.F. Babus'Haq, S.D. Probert, M.J. Shilston and A. Talati, Suggested design improvements concerning district-heating pipeline configurations, Applied Energy, 17, (1984), pp. 77-96.

37. R.F. Babus'Haq, S.D. Probert and M.J. Shilston, Optimal location of a single horizontal pipeline in a rectangular, horizontal, air-filled enclosure to achieve maximum thermal insulation, Applied Energy, 18, (1984), pp. 239-259.

38. U. Grigull and W. Hauf, Natural convection in horizontal cylindrical annuli, Proc. 3rd. Int. Heat Transfer Conf., Chicago, 2(60), 1966, pp. 182-195.

39. A. Feingold and K.G. Gupta, New analytical approach to the evaluation of configuration factors in radiation from spheres and infinitely-long cylinders, Trans. ASME, J. Heat Transfer, 92, (1970), pp. 69-76.

40. S. Chakrabarti, S.D. Probert and M.J. Shilston, Optimal eccentric annuli (containing atmospheric-pressure air) for thermally-insulating, horizontal, relatively cold pipes, Applied Energy, 14, (1983), pp. 257-293.

41. R.F. Babus'Haq, S.D. Probert and M.J. Shilston, Improved configurations for district-cooling pipelines, Applied Energy, 16, (1984), pp. 67-76.

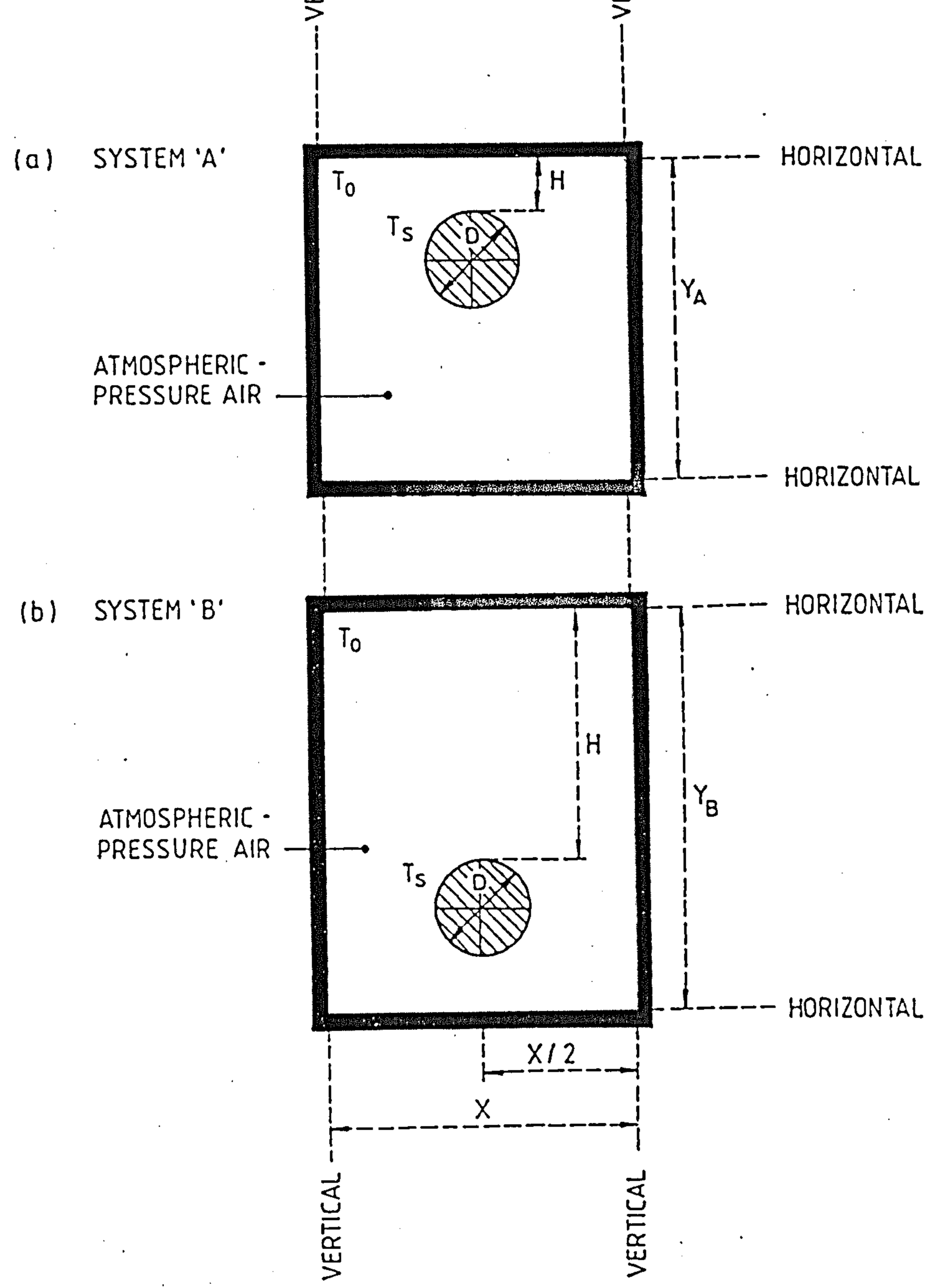

Fig. 5.1. Schematic representation of vertical sections through the considered horizontal pipes in the rectangular trenches: with(a) a negative displacement ratio and (b) a positive displacement ratio.

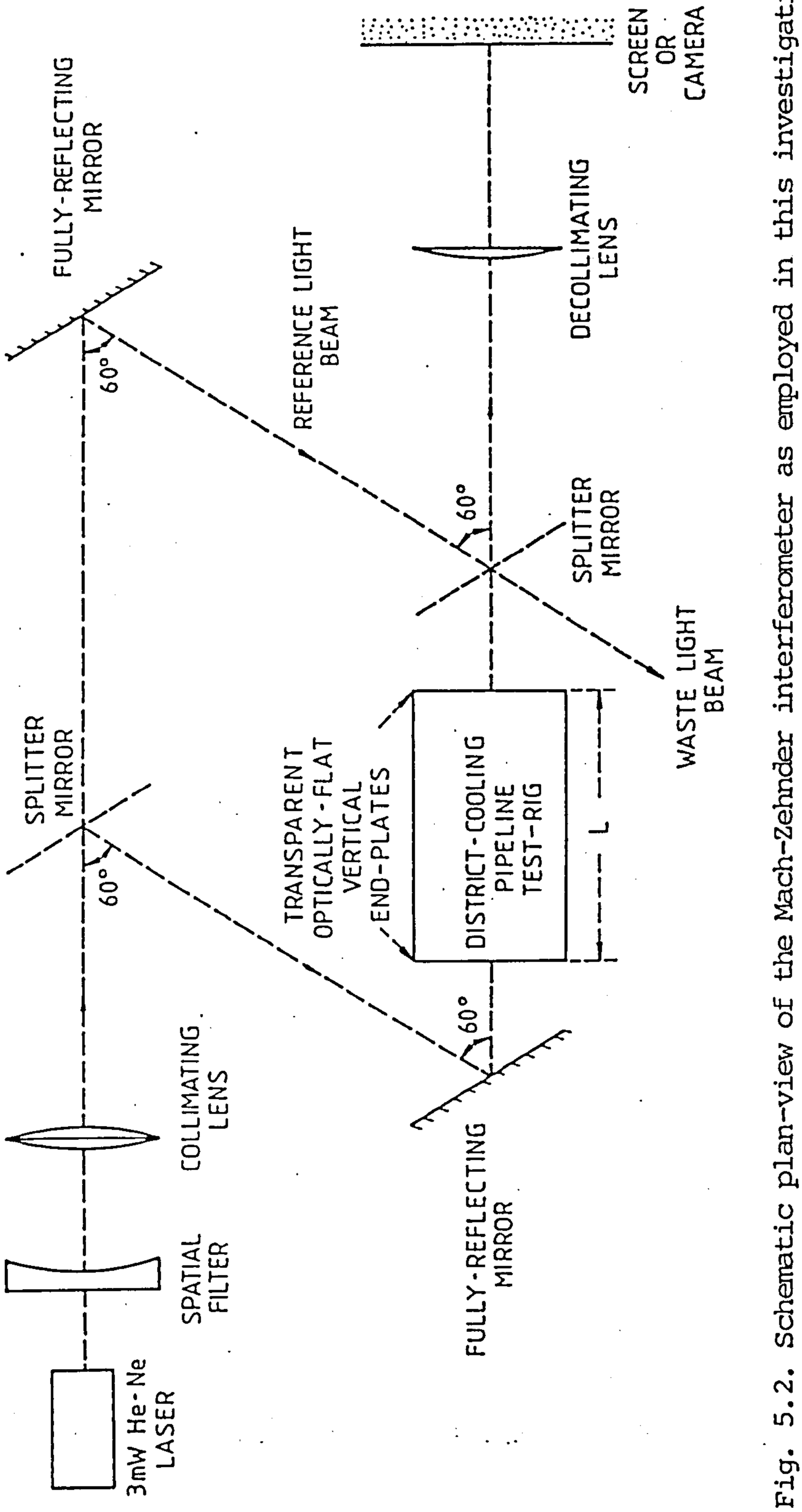

Fig. 5.2. Schematic plan-view of the Mach-Zehnder interferometer as employed in this investigation.

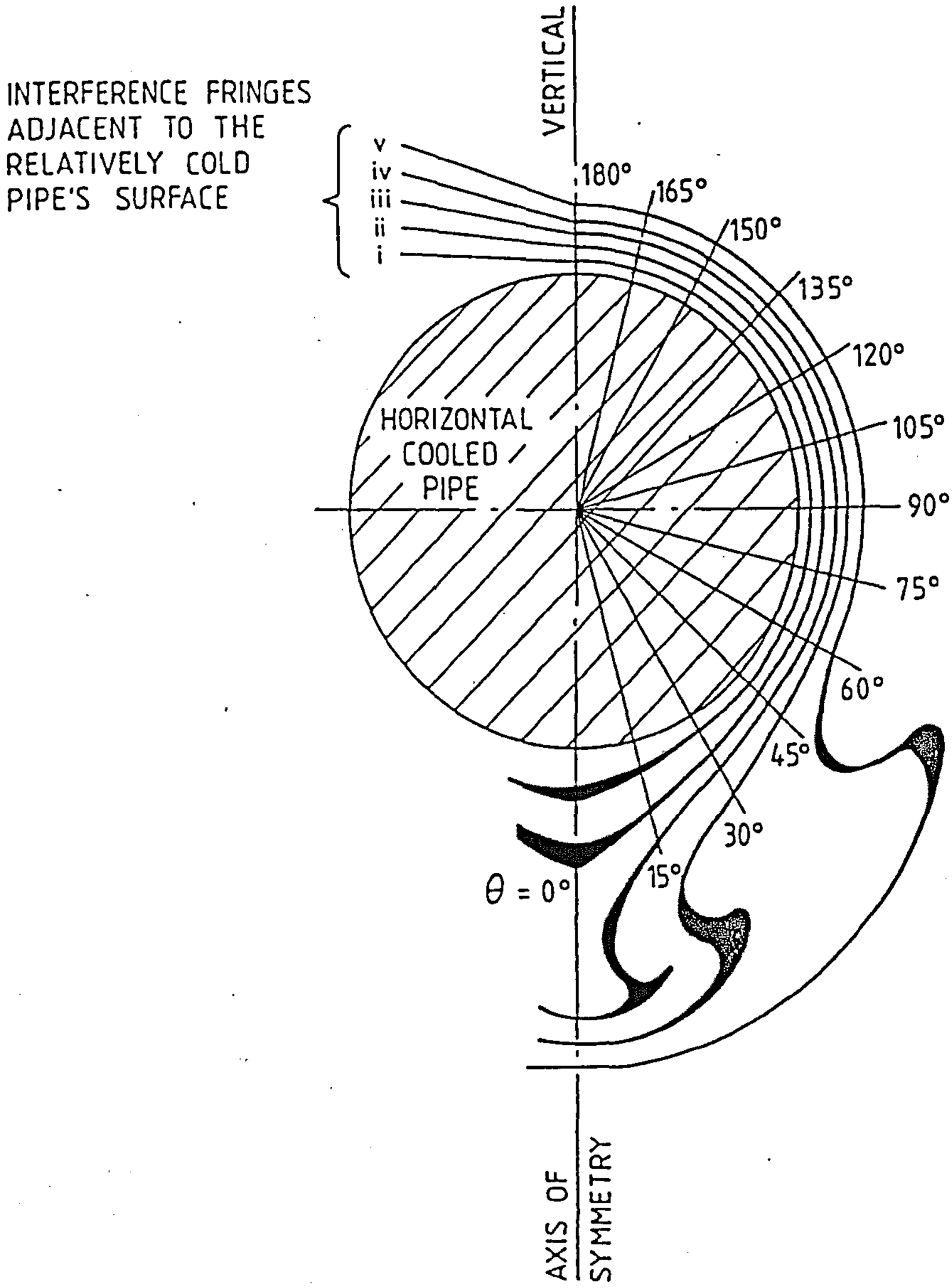

Fig. 5.3. A typical isothermal contour map of the region around a horizontal cooled pipe as obtained with the 18 cm field-of-view Mach-Zehnder interferometer The angular co-ordinate, 0, is measured relative to the vertically downwards radius vector from the centre of the pipe.

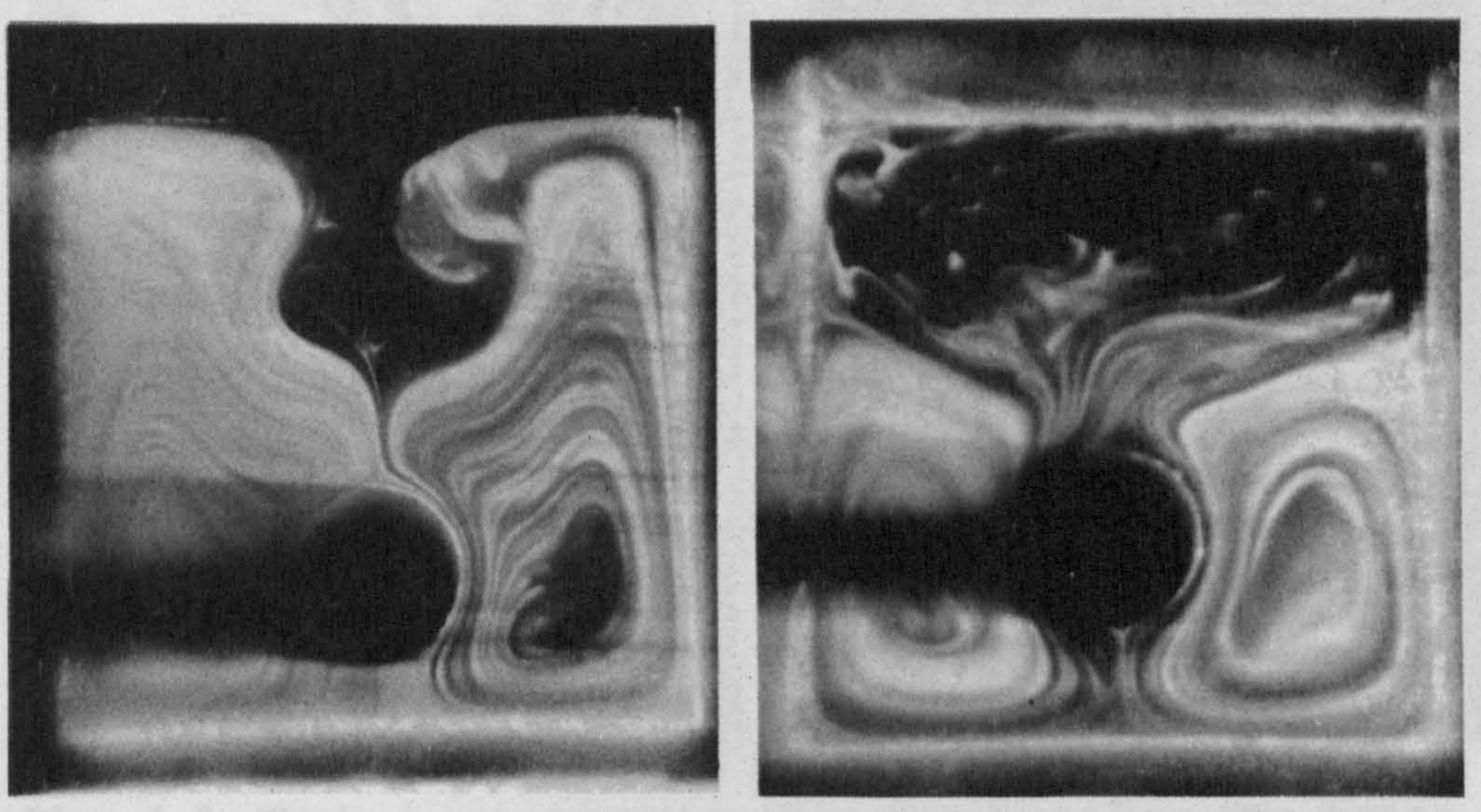

Fig. 5.4. Typical steady-state flow visualisations for system 'A':
T_s = 10 °C.

(a) E = 0.7, ΔT = 11 °C. (b) E = 0.5, ΔT = 20 °C.

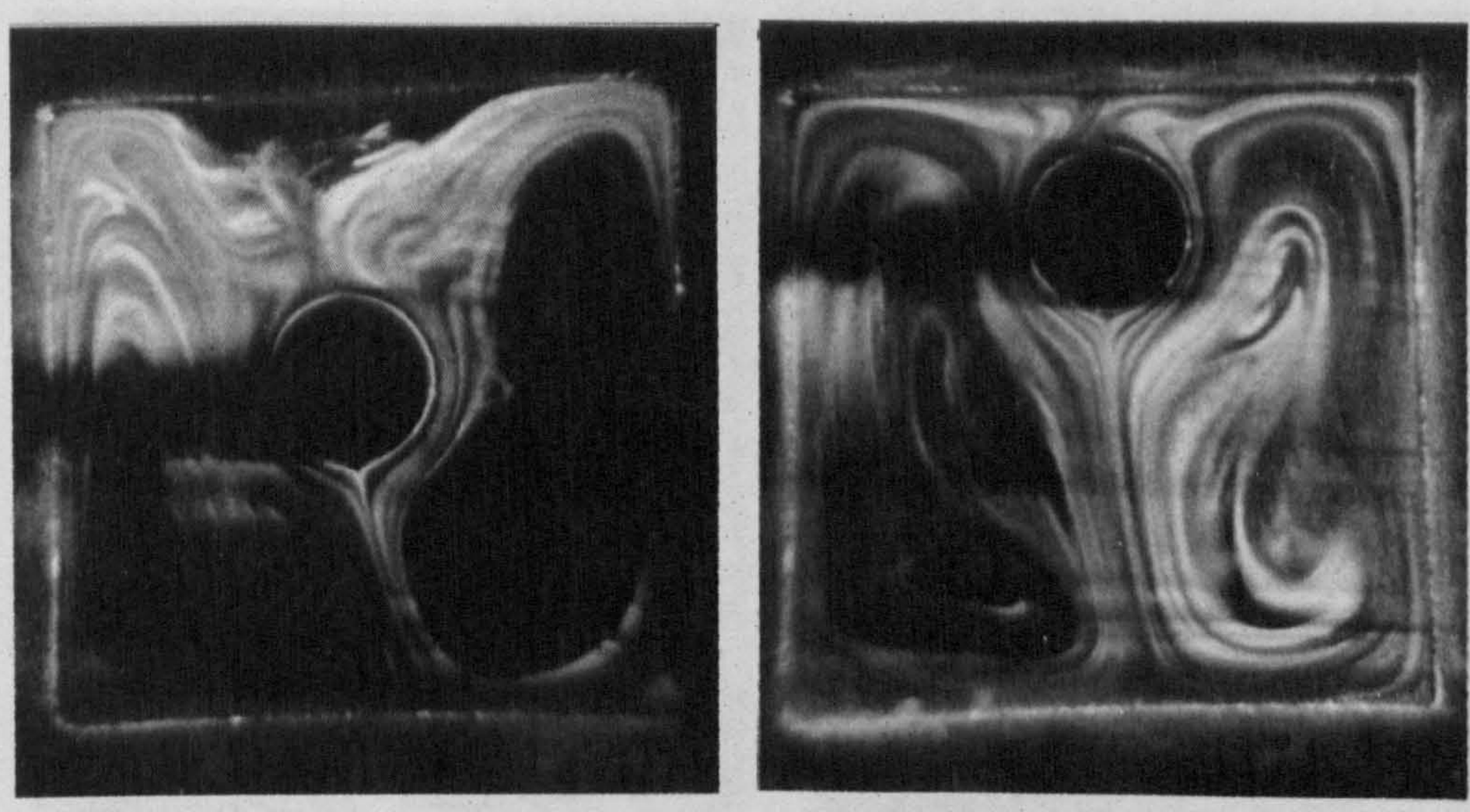

(c) E = 0, ΔT = 17 °C. (d) E = - 0.7, ΔT = 17 °C.

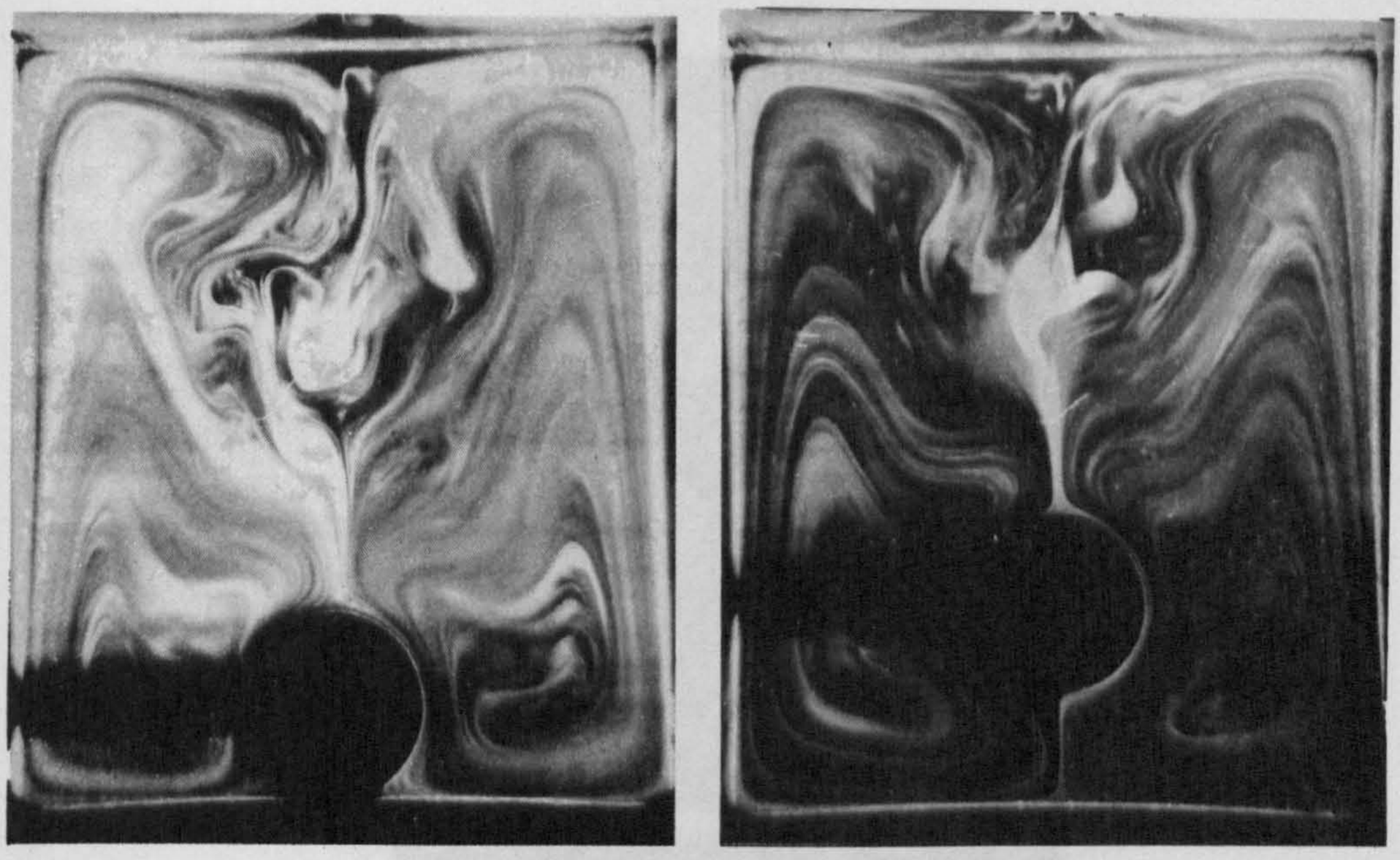

Fig. 5.5. Typical steady-state flow visualisations for system 'B': T_o = 35 °C, ΔT = 15 °C.

(a) E = 1.0 (b) E = 0.7

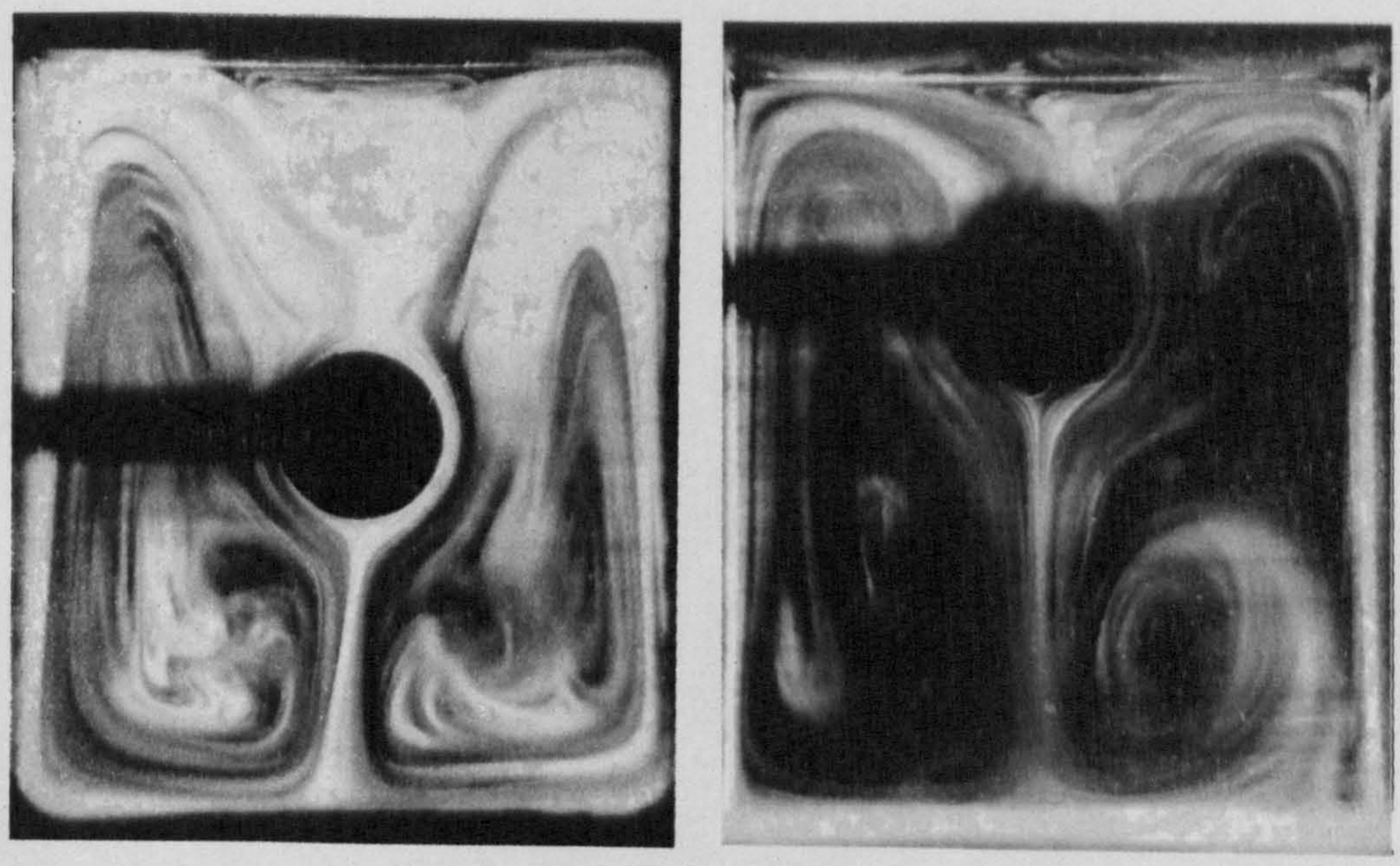

(c) E = 0 (d) E = - 0.7

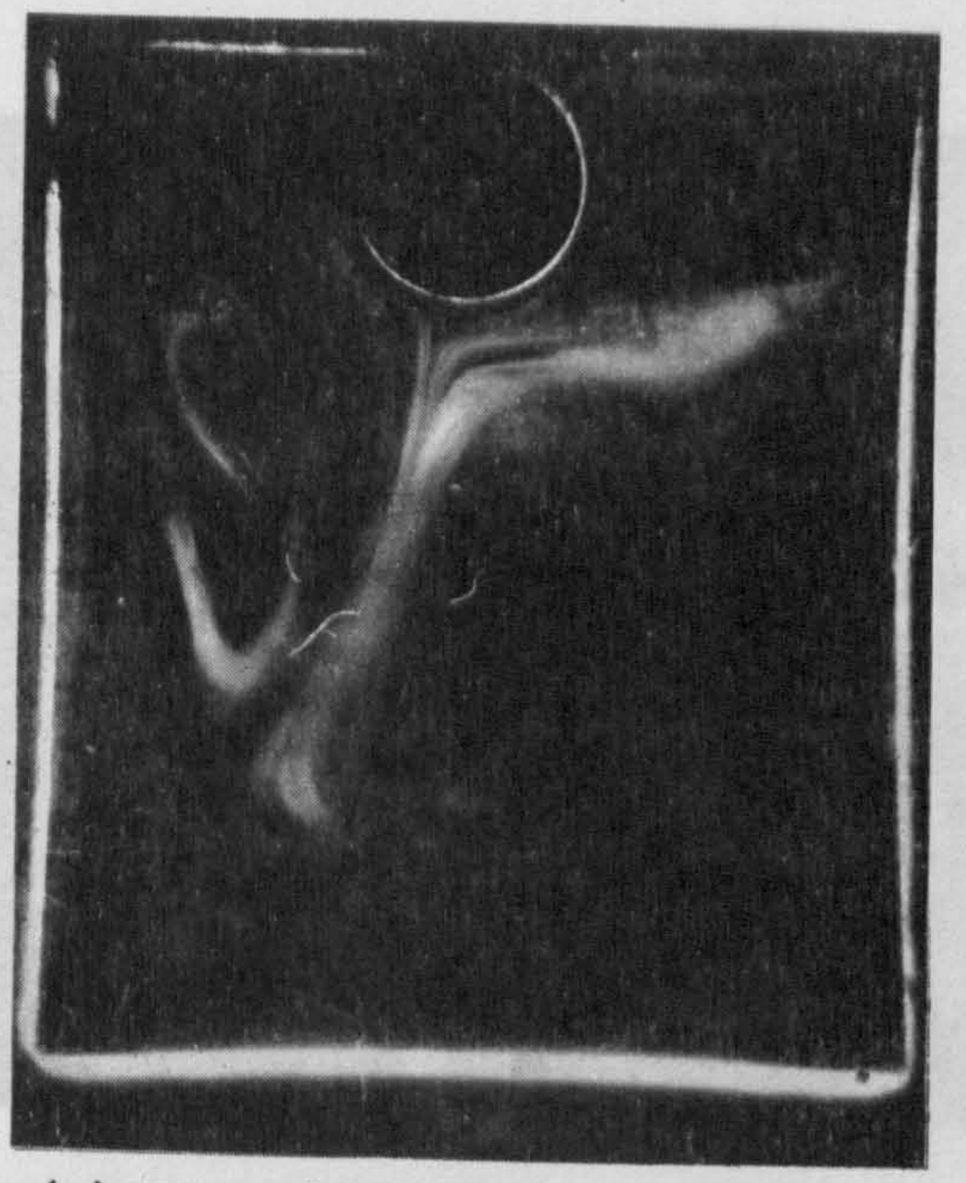

(e) E = -1.0

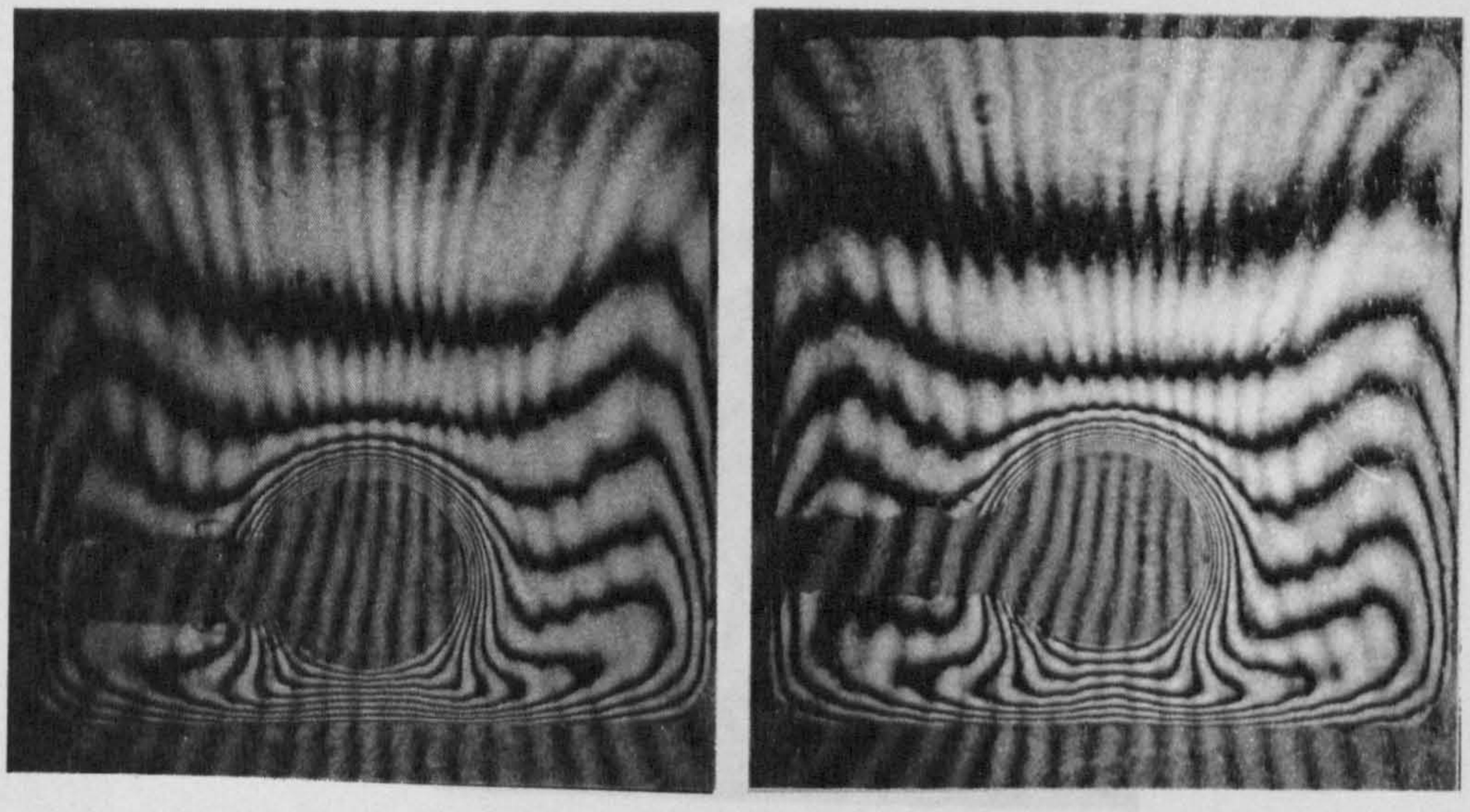

Fig. 5.6. Typical steady-state Mach-Zehnder interferograms for system 'A': T_s = 10 °C.

(a) E = 0.80, ΔT = 10.8 °C. (b) E = 0.70, ΔT = 10.4 °C.

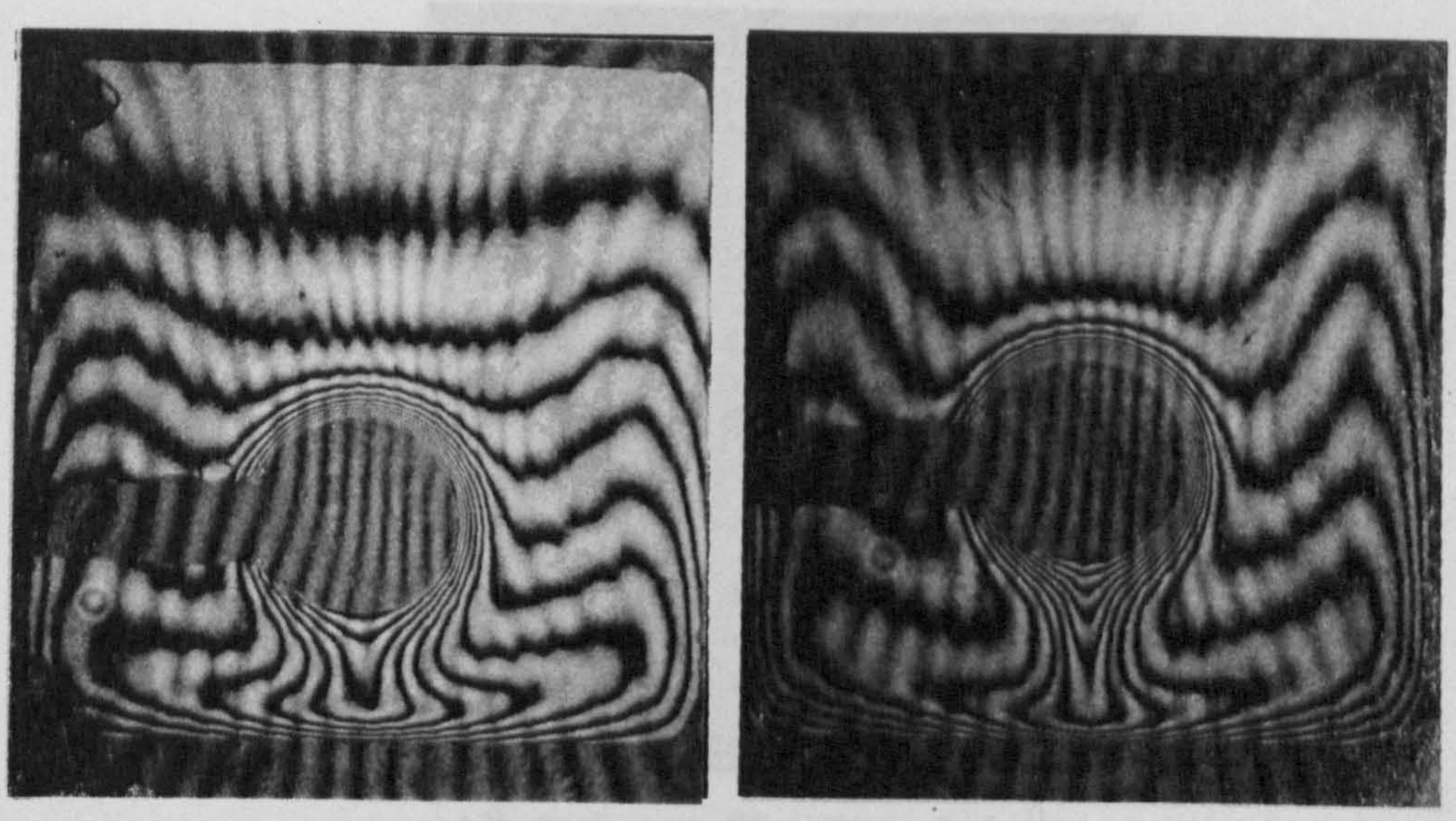

(c) E = 0.50, ΔT = 10.5 °C. (d) E = 0.25, ΔT = 9.8 °C.

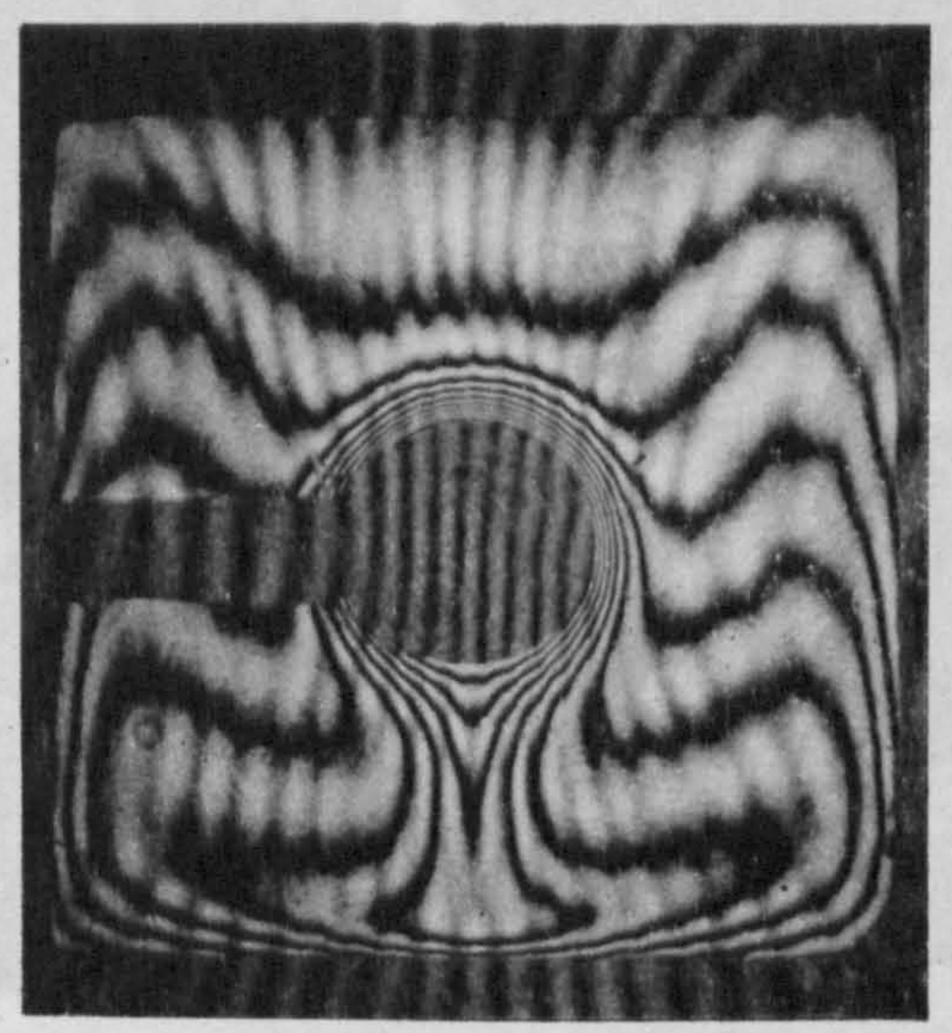

(e) E = 0, ΔT = 9.8 ^{o}C.

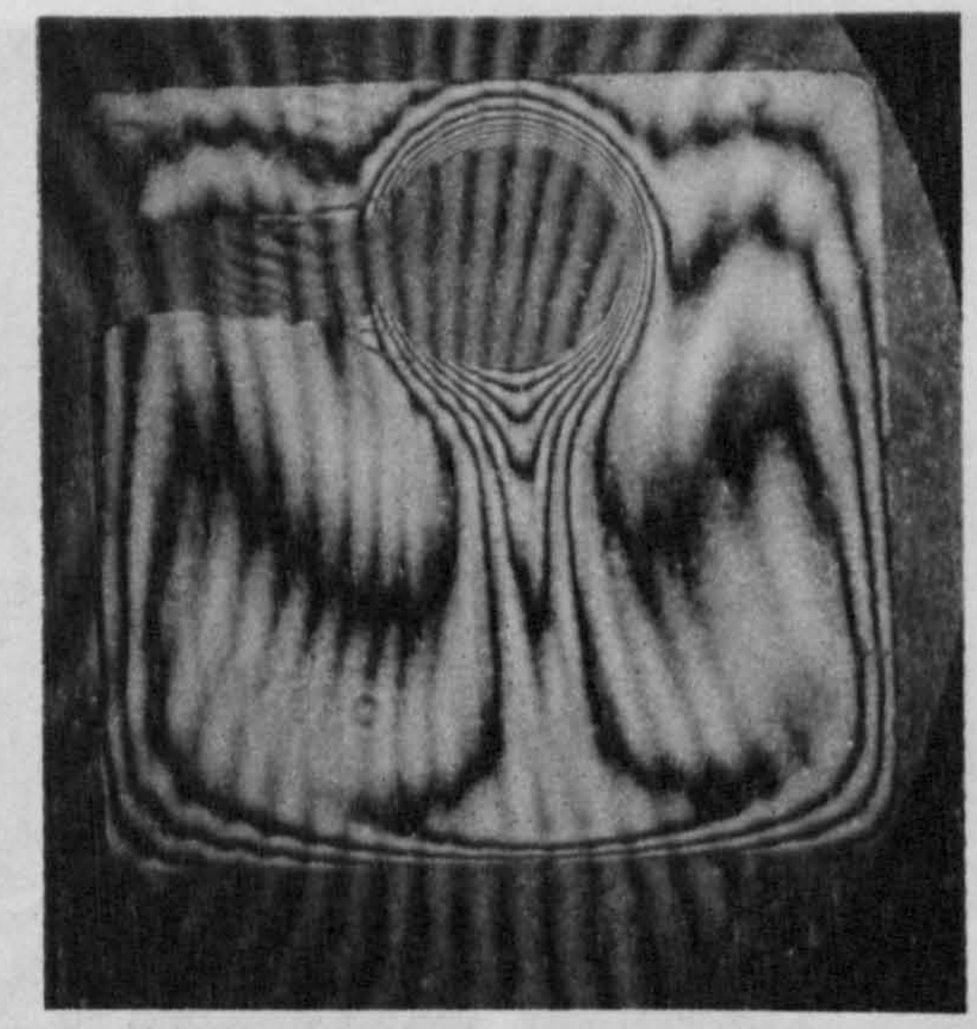

(f) E = - 0.75, ΔT = 9.0 ^{o}C.

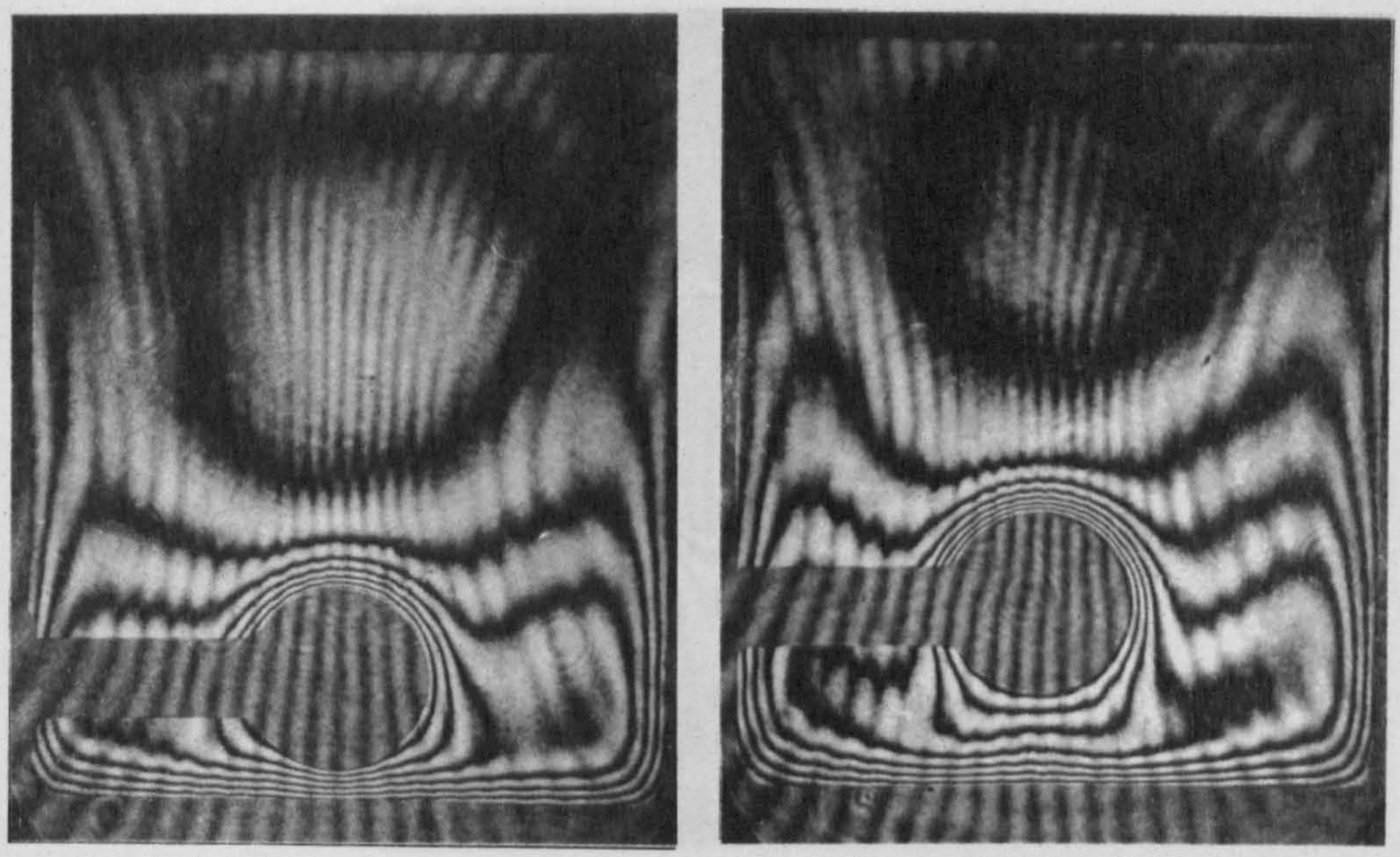

Fig. 5.7. Typical steady-state Mach-Zehnder interferograms for system 'B': T_o = 40 °C, ΔT = 10 °C.

(a) E = 0.9 (b) E = 0.7

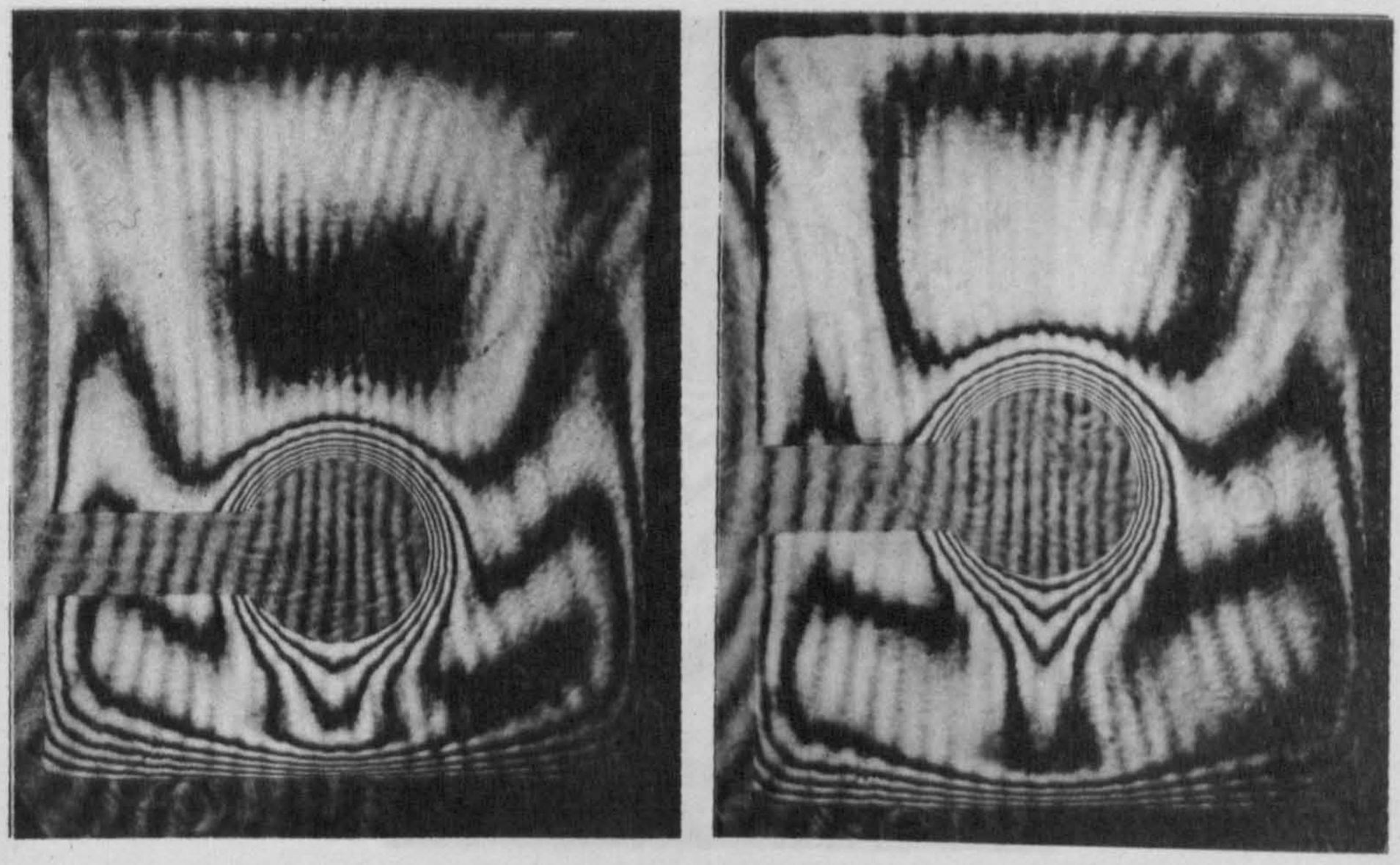

(c) E = 0.5 (d) E = 0.2

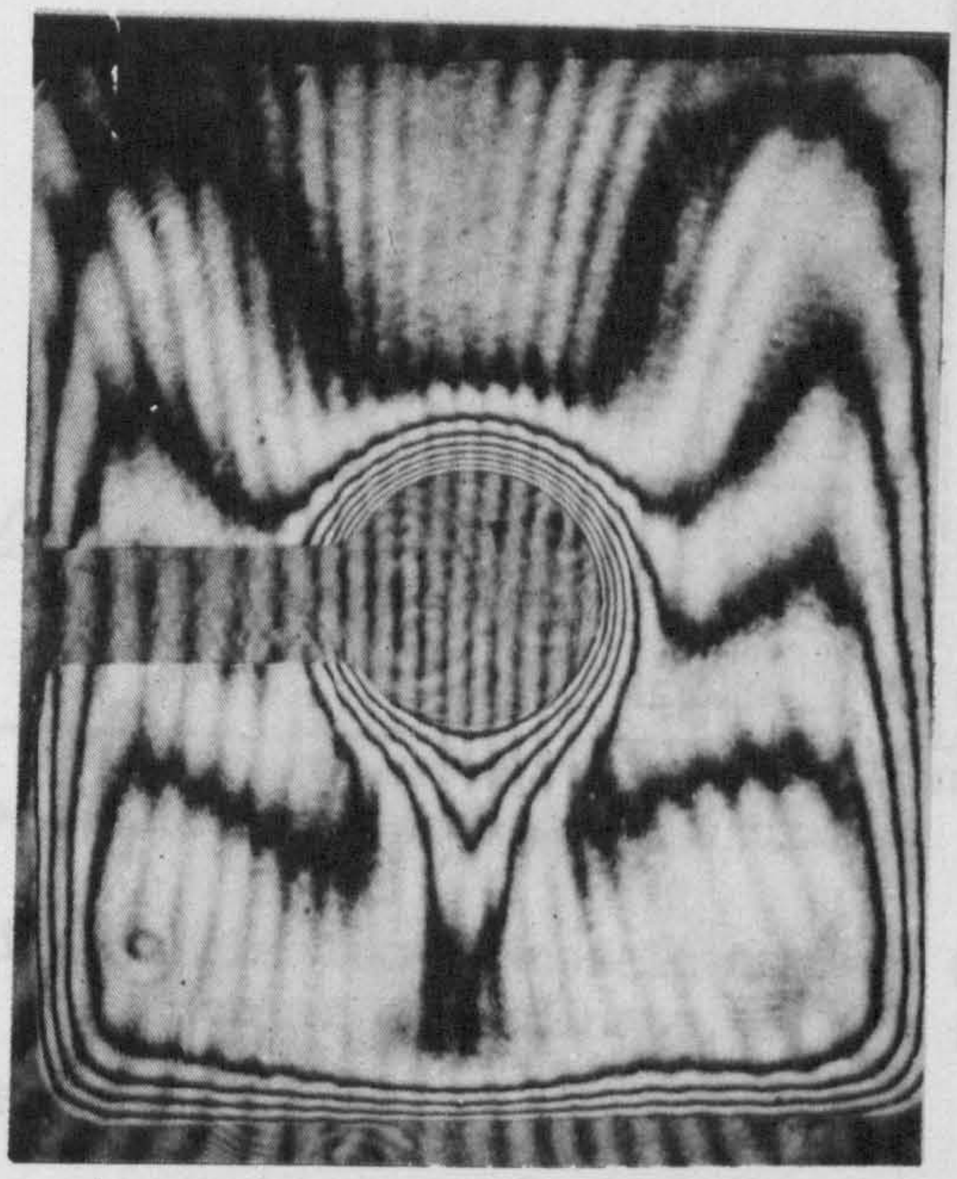

(e) E = 0

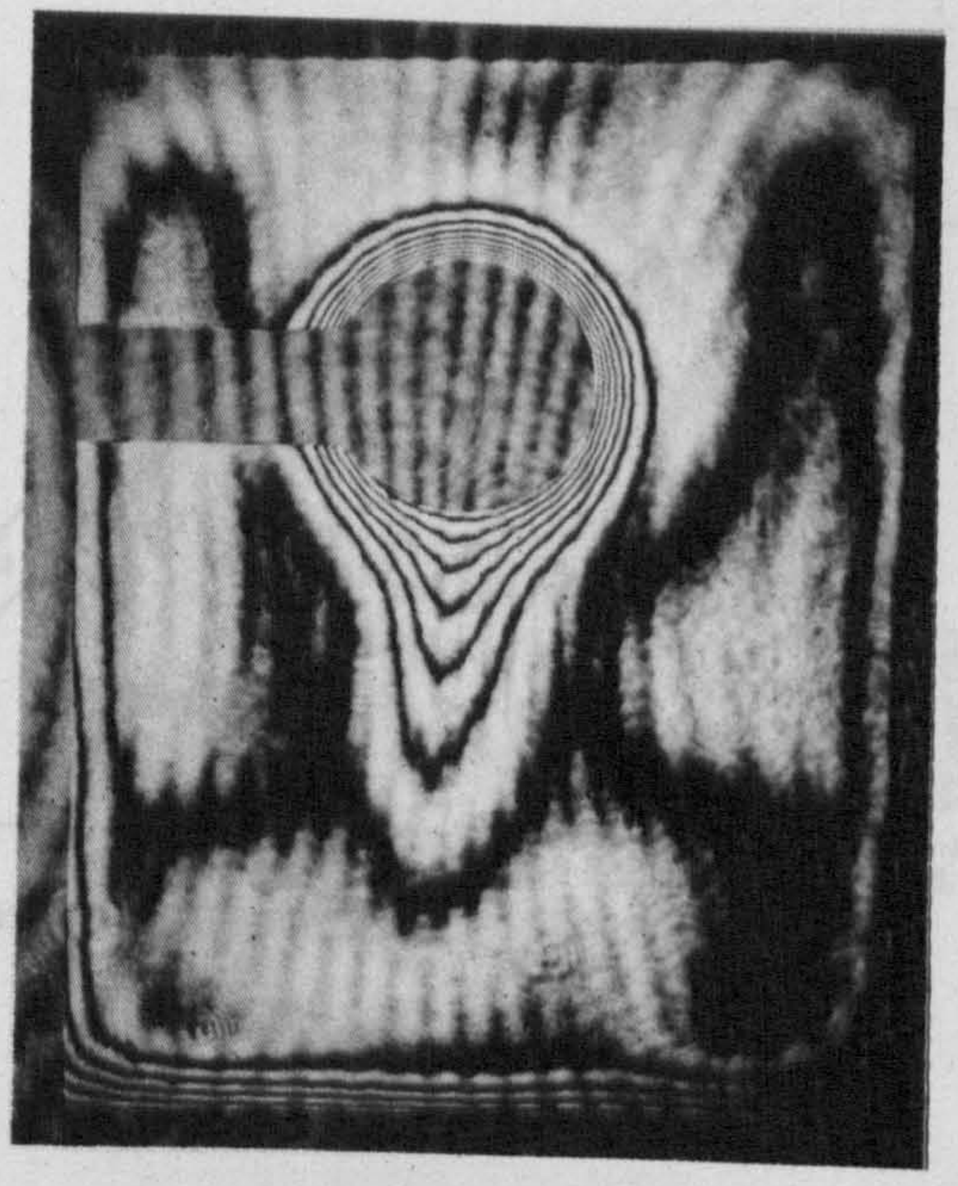

(f) E = - 0.5

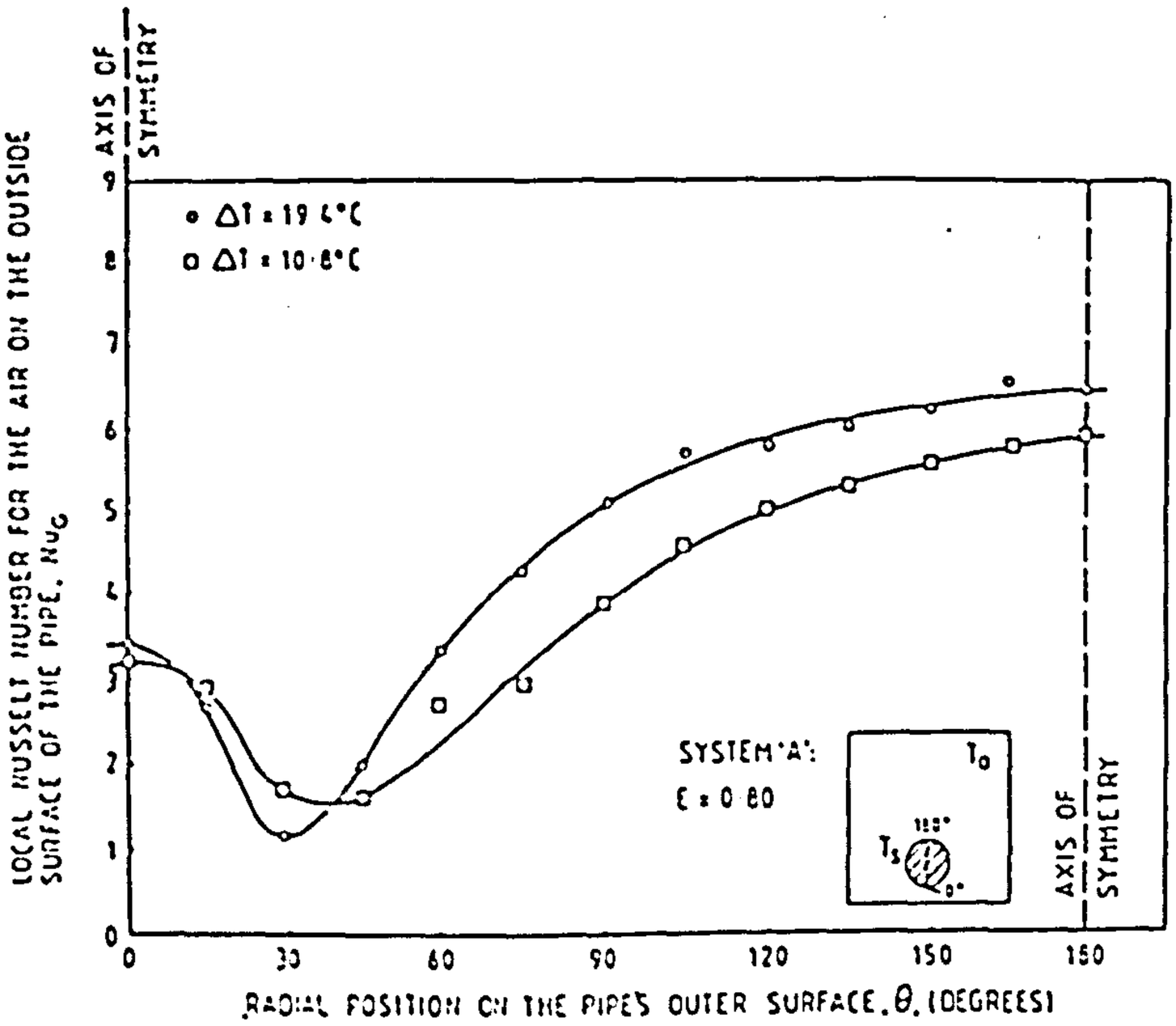

Fig. 5.8. Variation of the local Nusselt number, Nu_G, versus the angular co-ordinate, θ, for system 'A': T_s = 10 °C.

(a) E = 0.80

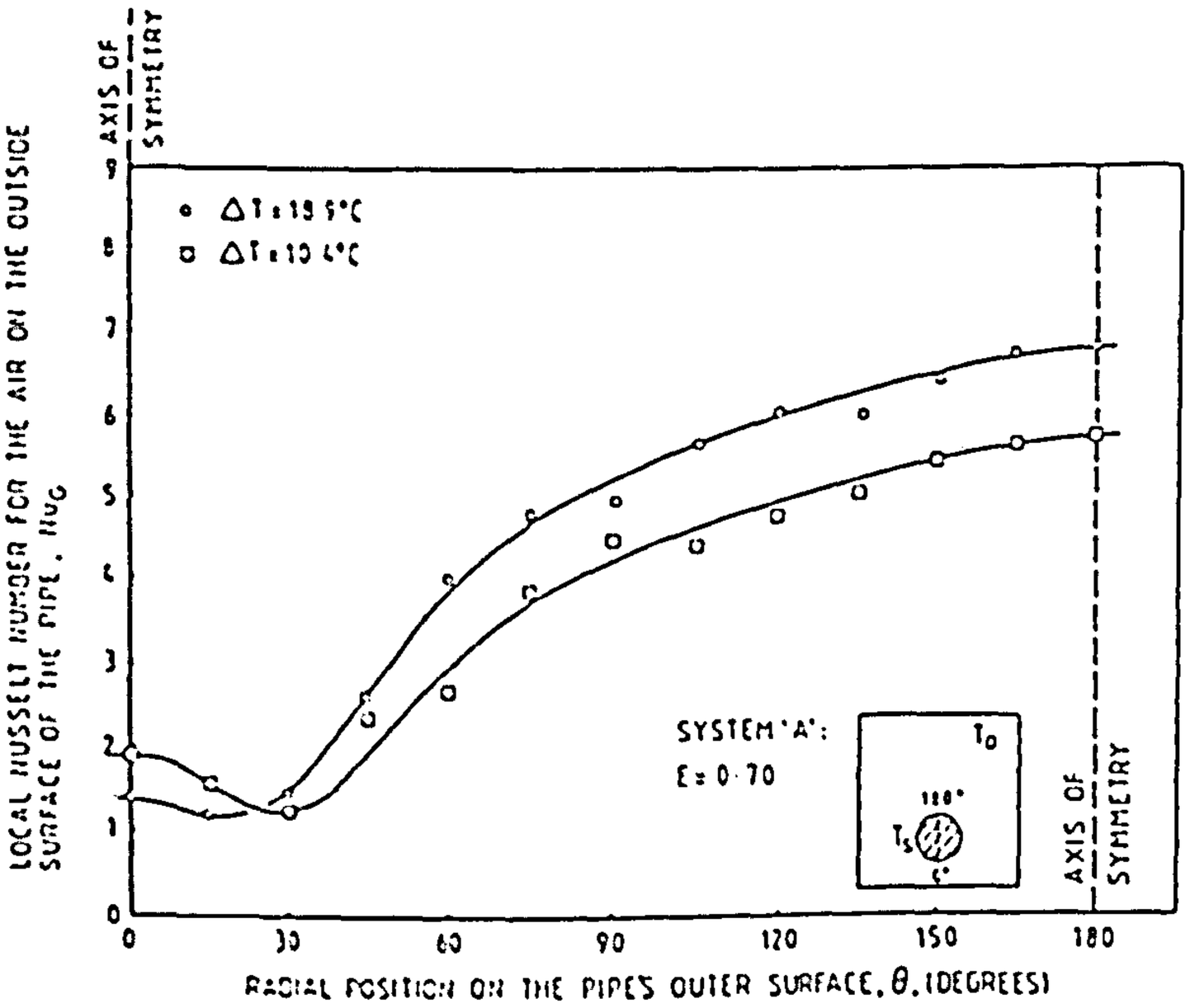

(b) E = 0.70

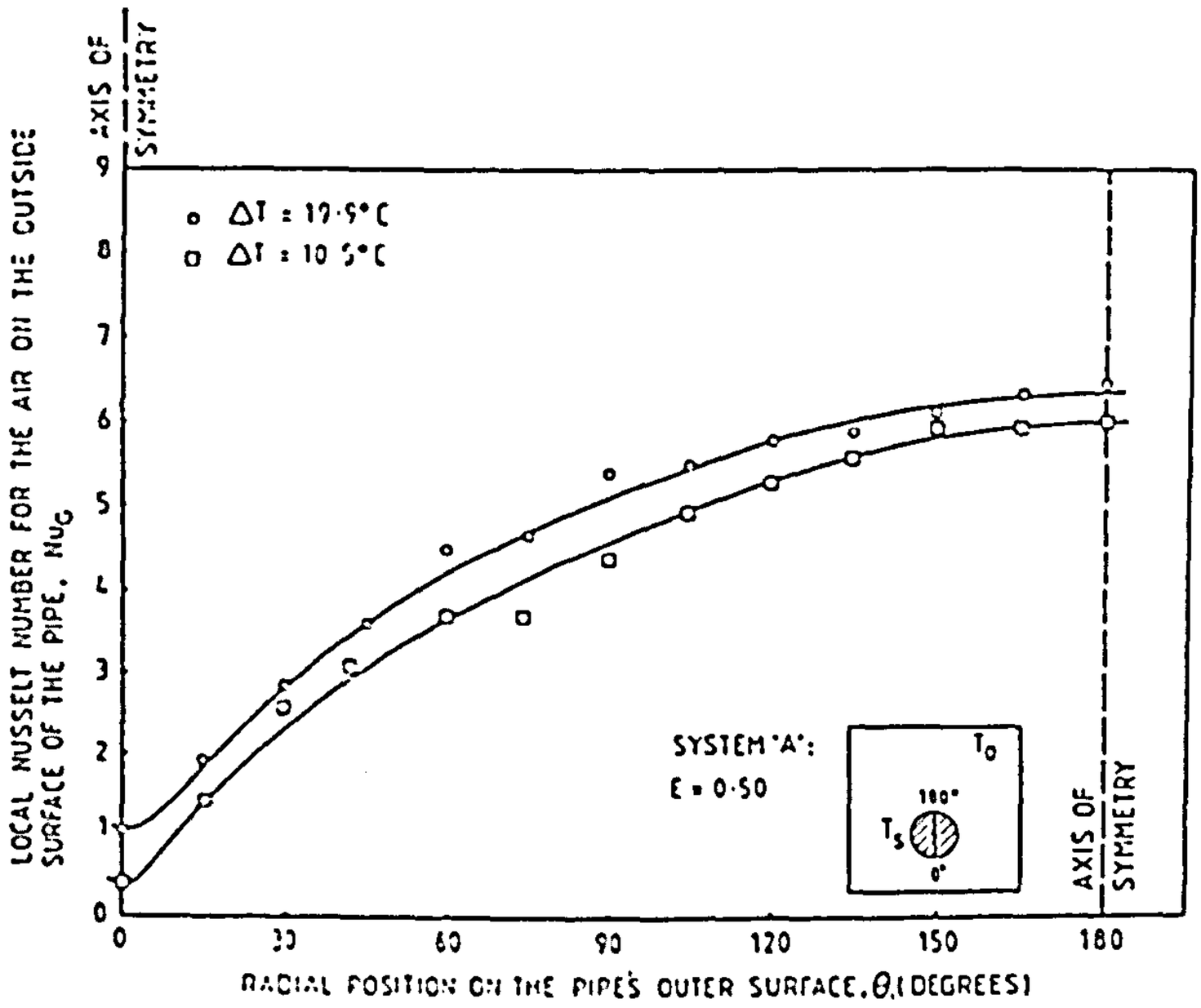
LOCAL NUSSELT NUMBER FOR THE AIR ON THE OUTSIDE SURFACE OF THE PIPE, Nu_θ
AXIS OF SYMMETRY
o ΔT = 19·9°C
□ ΔT = 10·5°C
SYSTEM 'A':
E = 0·50
T_o
180°
T_s
0°
AXIS OF SYMMETRY
0
1
2
3
4
5
6
7
8
9
0
30
60
90
120
150
180
RADIAL POSITION ON THE PIPE'S OUTER SURFACE, θ, (DEGREES)

(c) E = 0.50

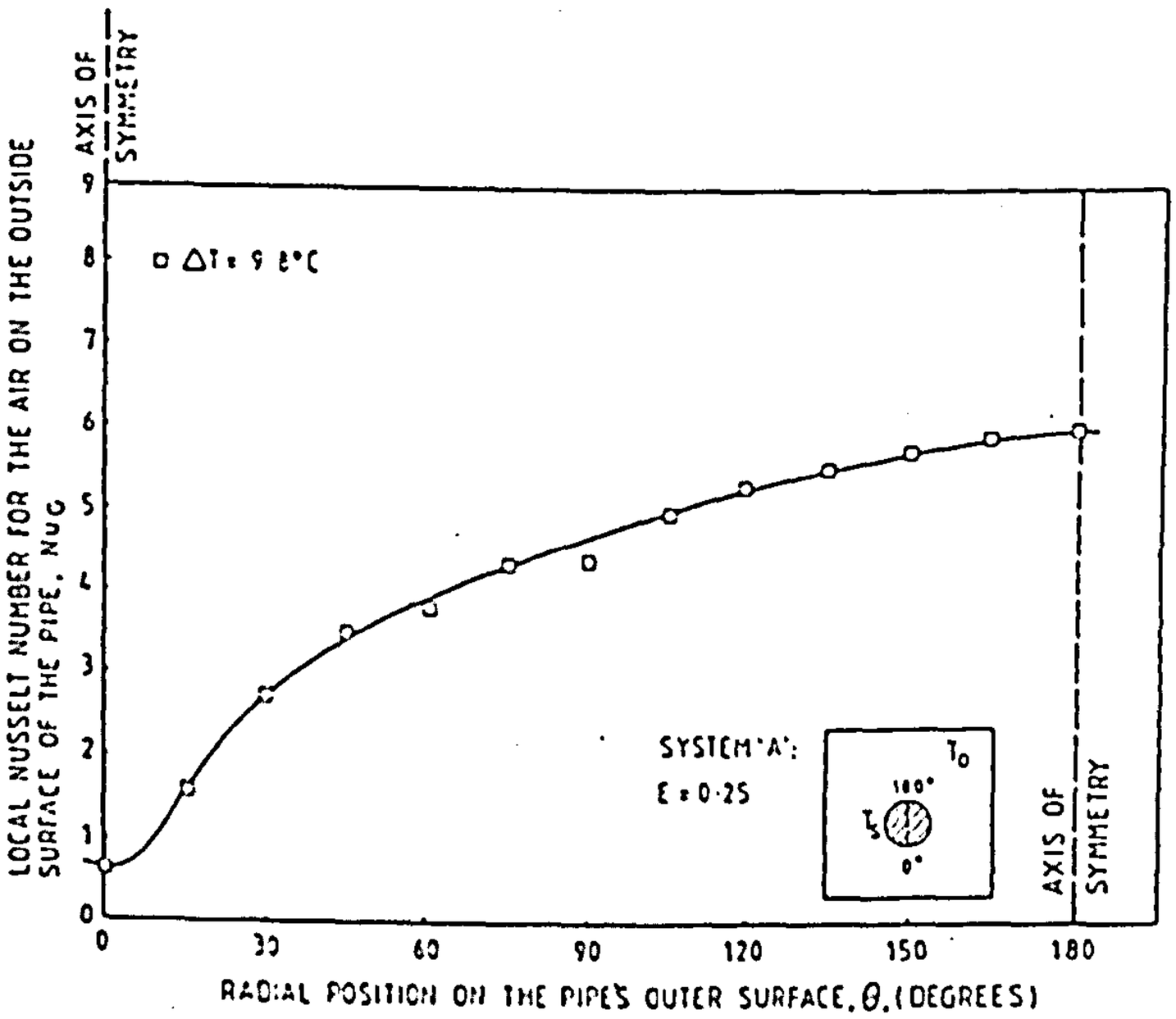
LOCAL NUSSELT NUMBER FOR THE AIR ON THE OUTSIDE SURFACE OF THE PIPE, Nu_θ
AXIS OF SYMMETRY
□ ΔT = 9·8°C
SYSTEM 'A':
E = 0·25
T_o
180°
T_s
0°
AXIS OF SYMMETRY
0
1
2
3
4
5
6
7
8
9
0
30
60
90
120
150
180
RADIAL POSITION ON THE PIPE'S OUTER SURFACE, θ, (DEGREES)

(d) E = 0.25

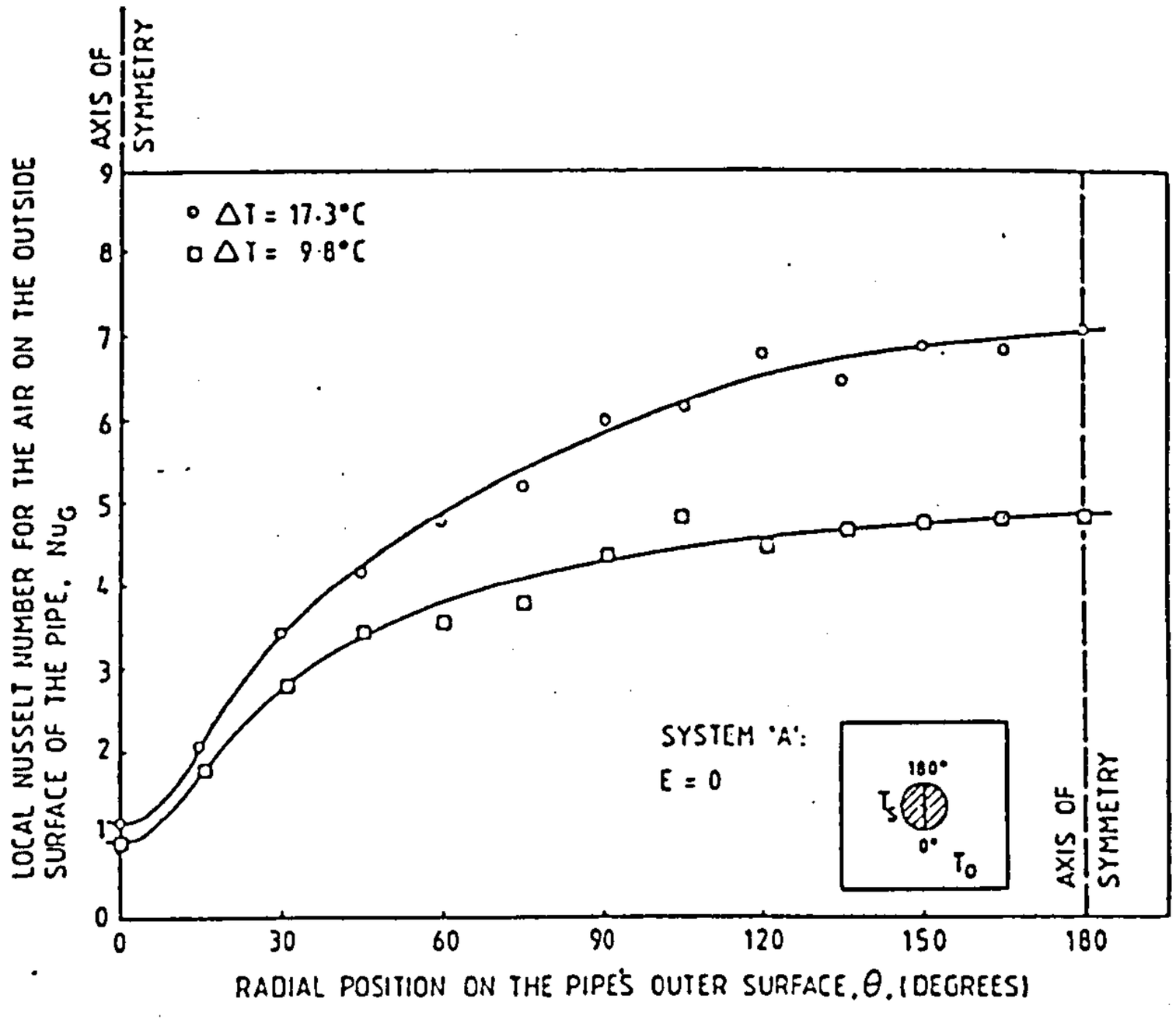
LOCAL NUSSELT NUMBER FOR THE AIR ON THE OUTSIDE SURFACE OF THE PIPE, Nu_G
AXIS OF SYMMETRY
o ΔT = 17·3°C
□ ΔT = 9·8°C
SYSTEM 'A':
E = 0
180°
T_S
0°
T_O
AXIS OF SYMMETRY
0
1
2
3
4
5
6
7
8
9
0
30
60
90
120
150
180
RADIAL POSITION ON THE PIPE'S OUTER SURFACE, θ, (DEGREES)

(e) E = 0

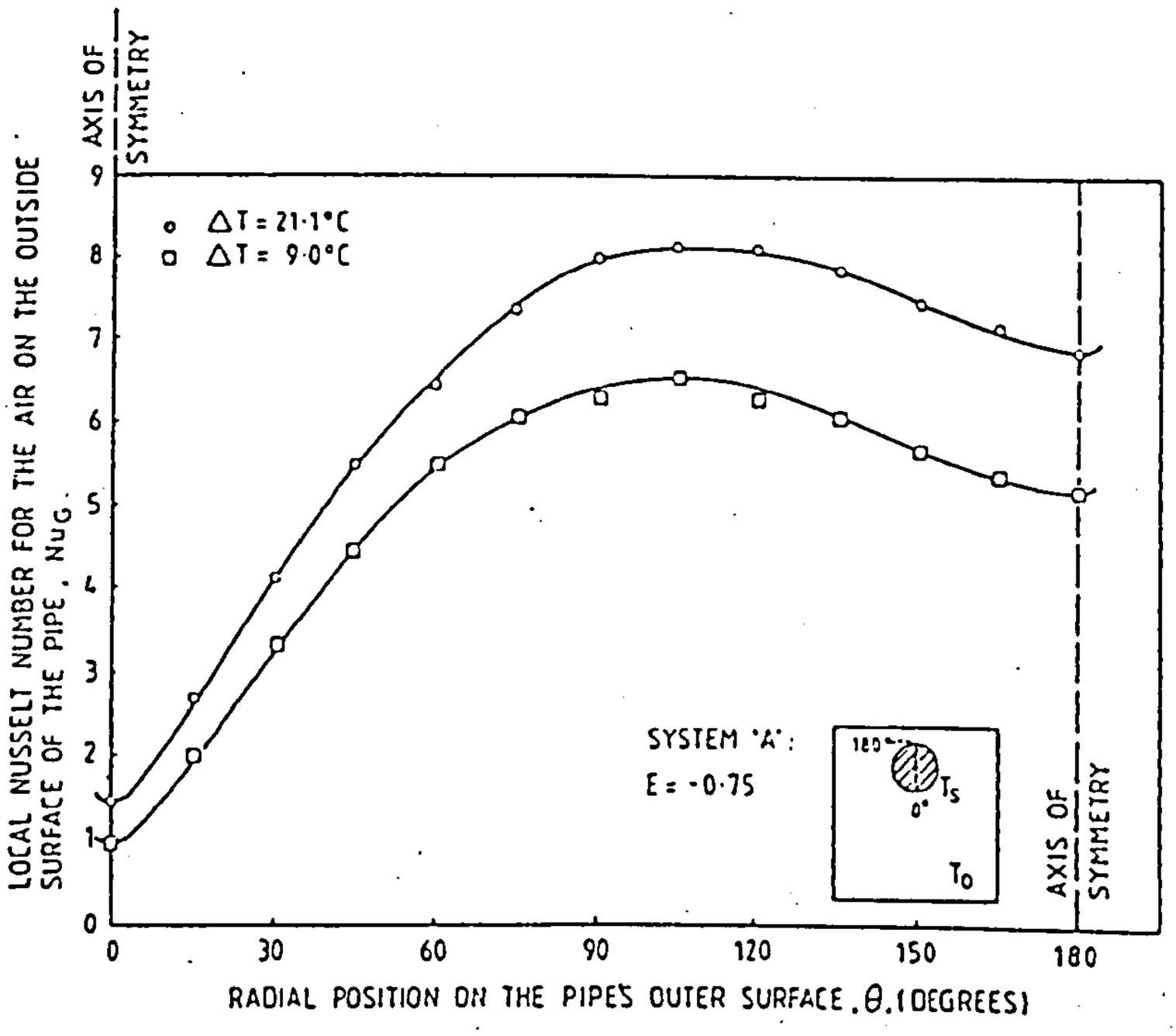
LOCAL NUSSELT NUMBER FOR THE AIR ON THE OUTSIDE SURFACE OF THE PIPE, Nu_G
AXIS OF SYMMETRY
o ΔT = 21·1°C
□ ΔT = 9·0°C
SYSTEM 'A':
E = -0·75
180°
T_S
0°
T_O
AXIS OF SYMMETRY
0
1
2
3
4
5
6
7
8
9
0
30
60
90
120
150
180
RADIAL POSITION ON THE PIPE'S OUTER SURFACE, θ, (DEGREES)

(f) E = - 0.75

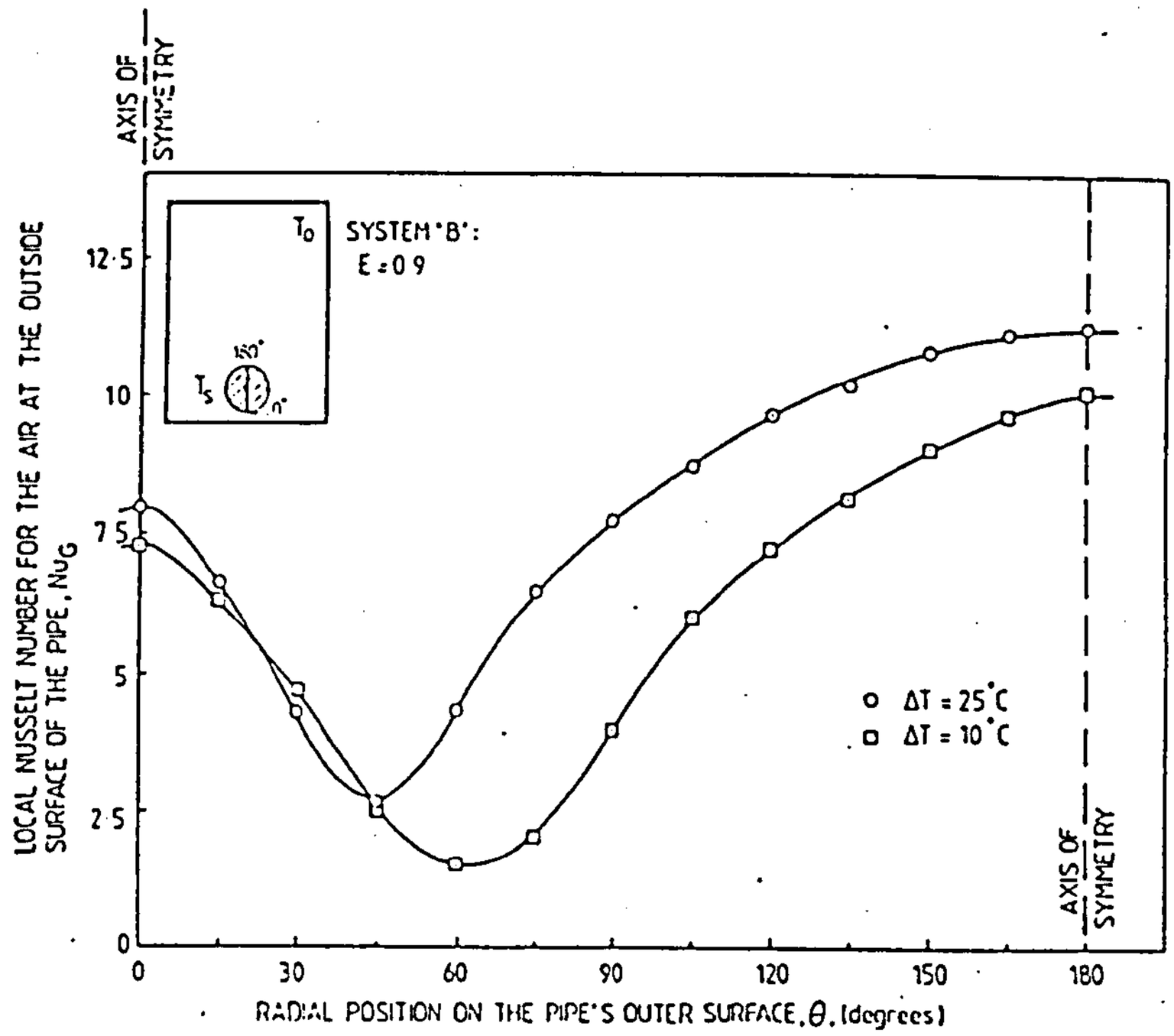

Fig. 5.9. Variation of the local Nusselt number, Nu_G, versus the angular co-ordinate, θ, for system 'B': T_o = 40 °C.

(a) E = 0.9

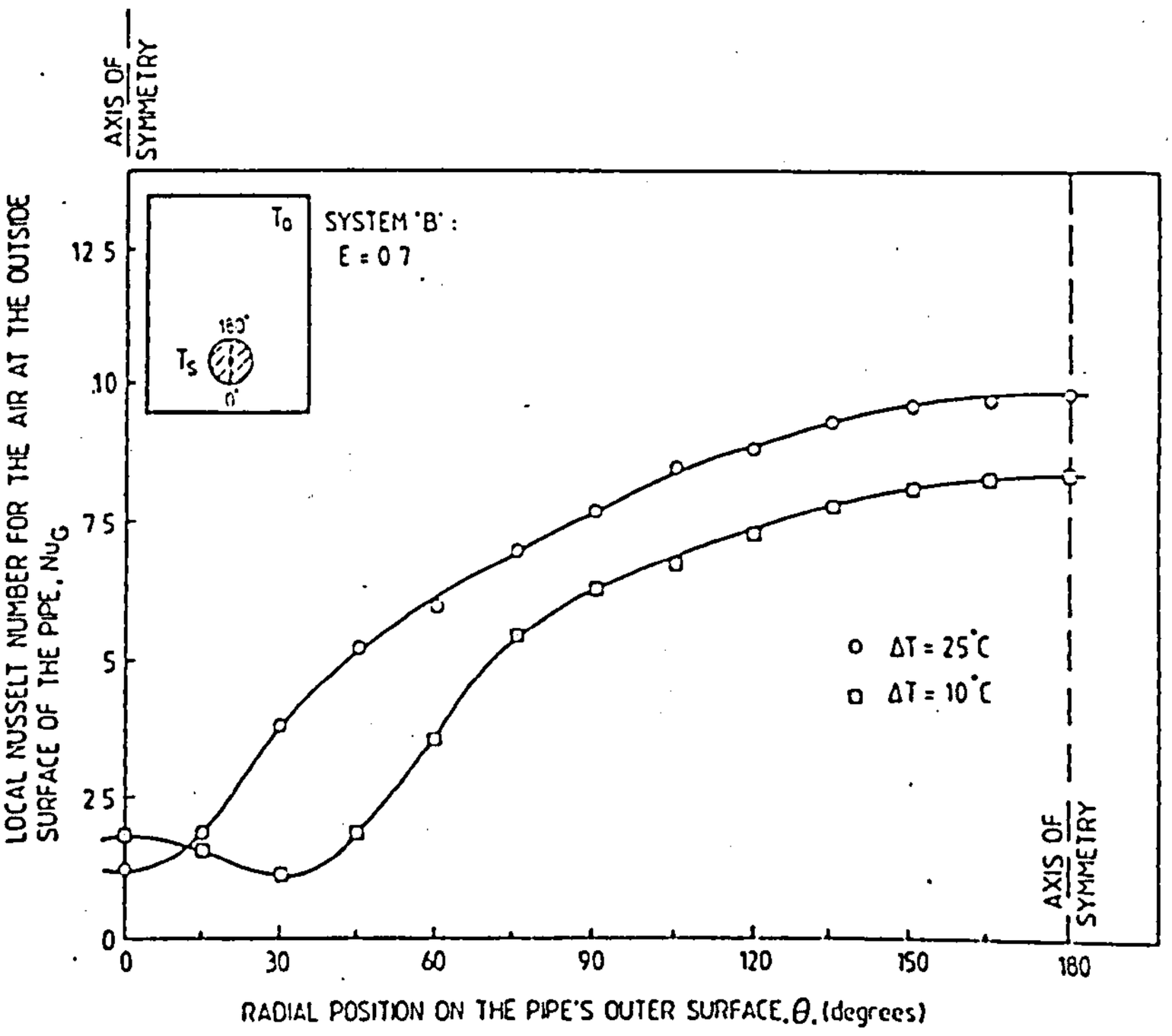

(b) E = 0.7

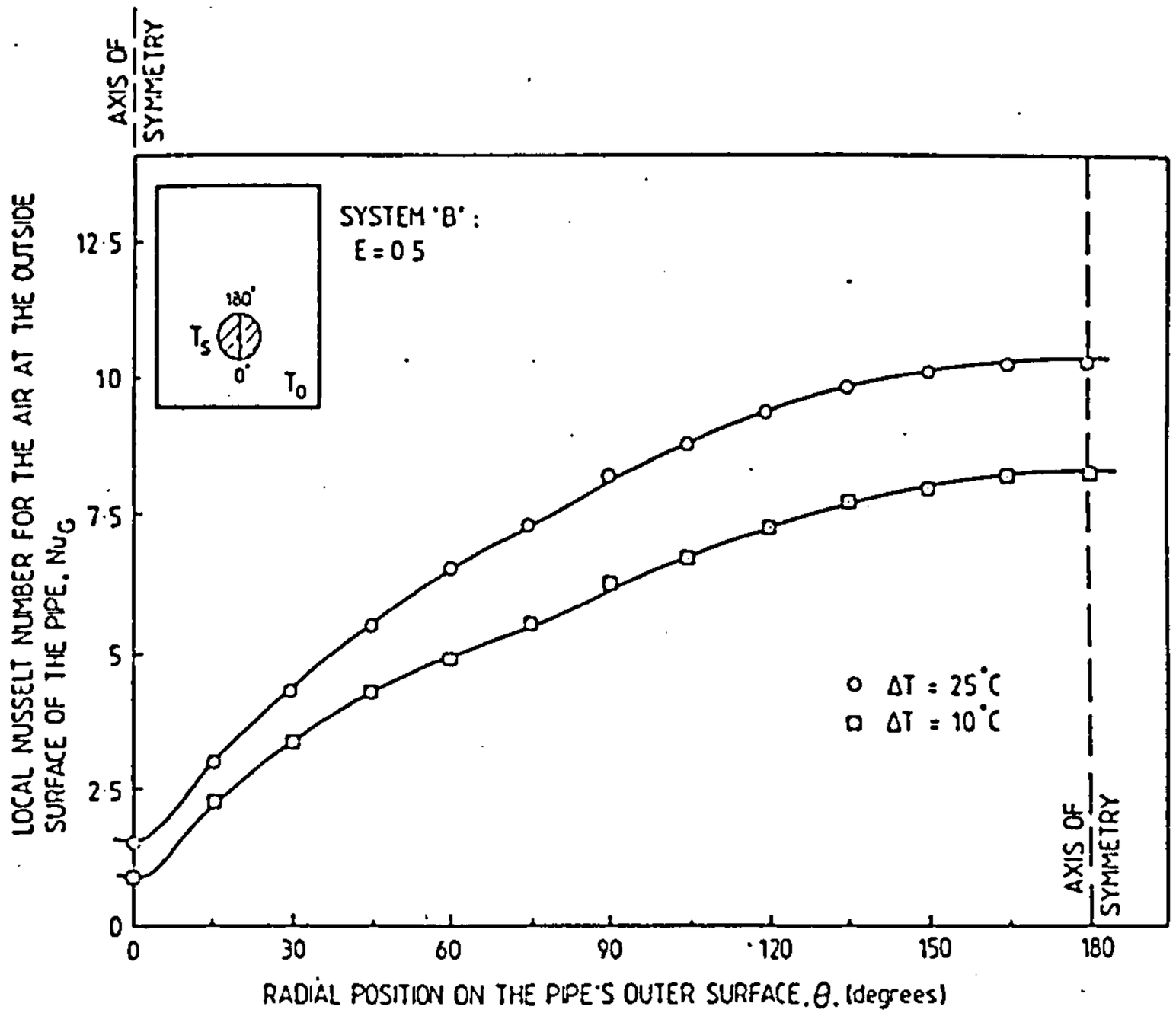
AXIS OF SYMMETRY
SYSTEM 'B':
E = 0.5
180°
T_s
0°
T_o
LOCAL NUSSELT NUMBER FOR THE AIR AT THE OUTSIDE SURFACE OF THE PIPE, Nu_G
12·5
10
7·5
5
2·5
0
0
30
60
90
120
150
180
RADIAL POSITION ON THE PIPE'S OUTER SURFACE, θ, (degrees)
o ΔT = 25°C
□ ΔT = 10°C
AXIS OF SYMMETRY

(c) E = 0.5

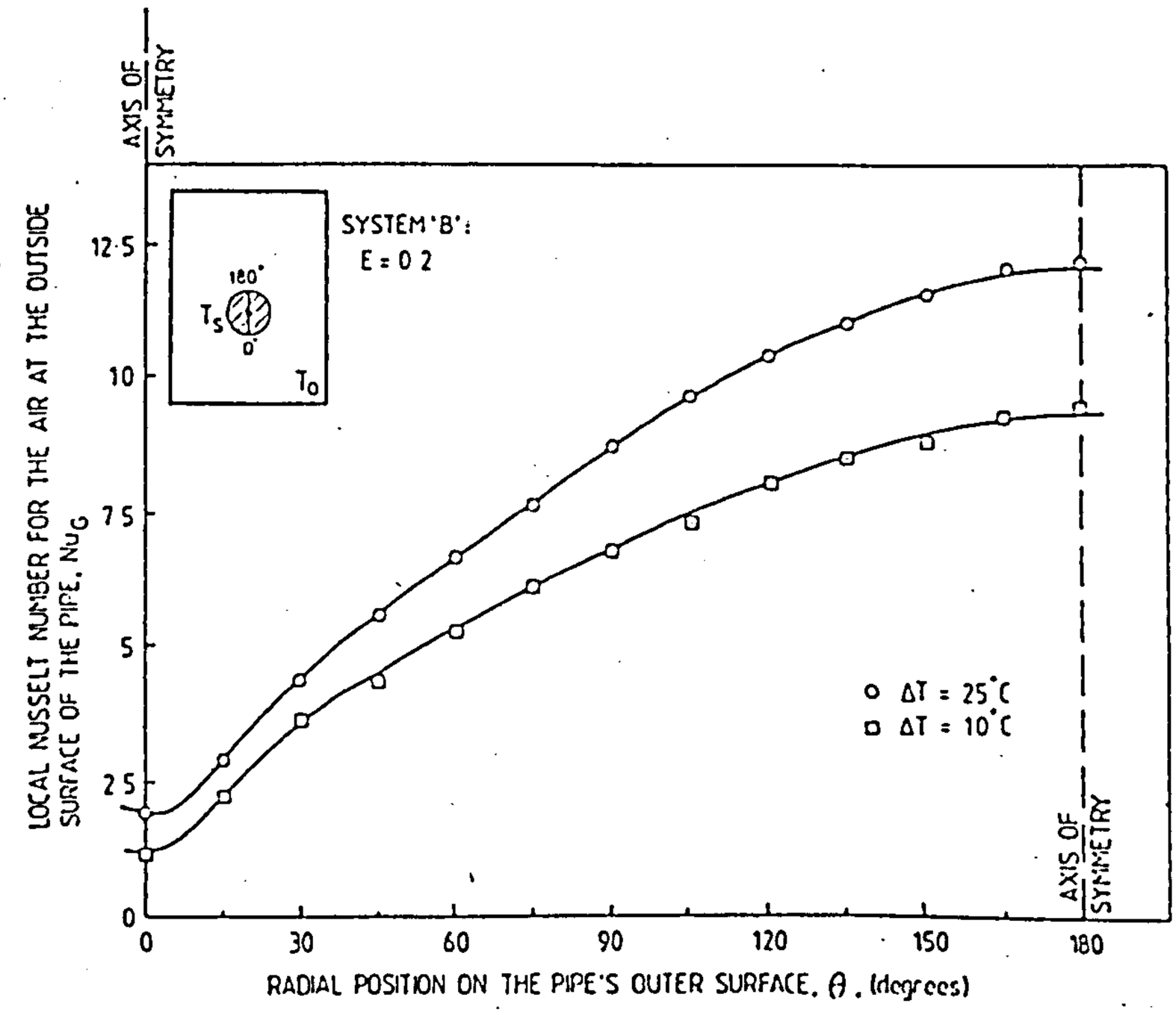
AXIS OF SYMMETRY
SYSTEM 'B':
E = 0.2
180°
T_s
0°
T_o
LOCAL NUSSELT NUMBER FOR THE AIR AT THE OUTSIDE SURFACE OF THE PIPE, Nu_G
12·5
10
7·5
5
2·5
0
0
30
60
90
120
150
180
RADIAL POSITION ON THE PIPE'S OUTER SURFACE, θ, (degrees)
o ΔT = 25°C
□ ΔT = 10°C
AXIS OF SYMMETRY

(d) E = 0.2

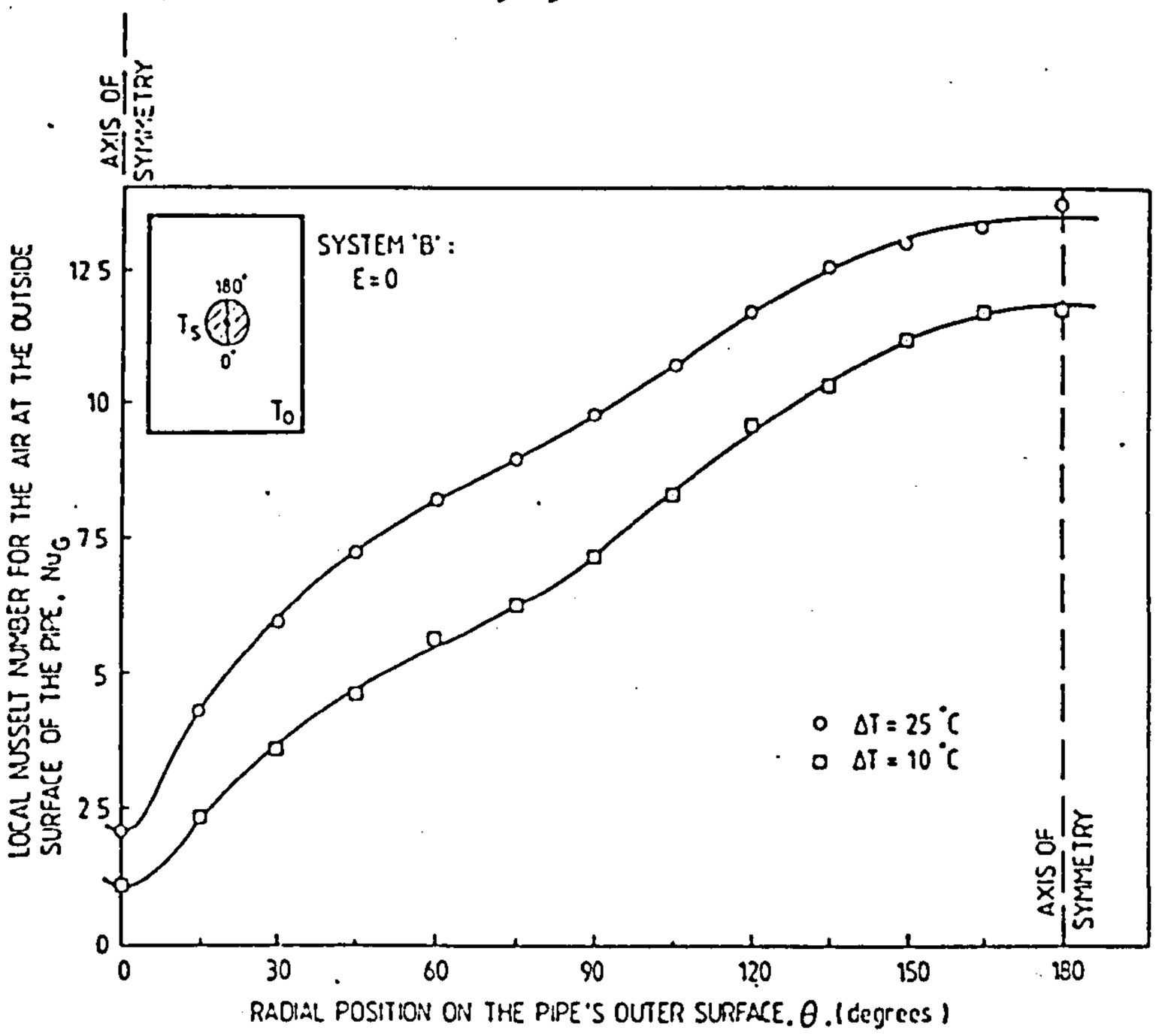
AXIS OF SYMMETRY
SYSTEM 'B' :
E = 0
180°
T_S
0°
T_O
LOCAL NUSSELT NUMBER FOR THE AIR AT THE OUTSIDE SURFACE OF THE PIPE, Nu_θ
0
25
5
75
10
125
0
30
60
90
120
150
180
AXIS OF SYMMETRY
o ΔT = 25 °C
□ ΔT = 10 °C
RADIAL POSITION ON THE PIPE'S OUTER SURFACE, θ, (degrees)

(e) E = 0

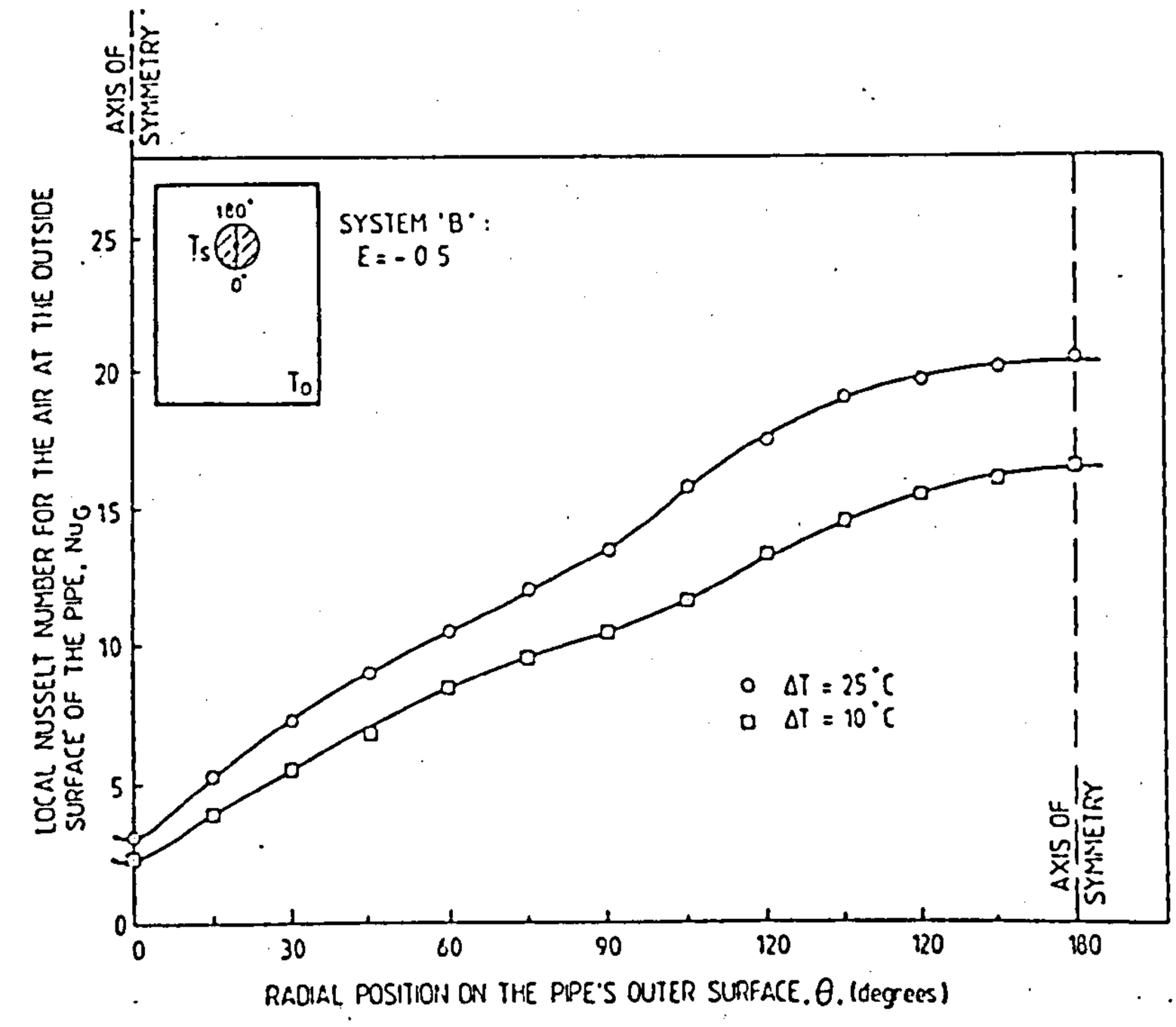
AXIS OF SYMMETRY
SYSTEM 'B' :
E = - 0 5
180°
T_S
0°
T_O
LOCAL NUSSELT NUMBER FOR THE AIR AT THE OUTSIDE SURFACE OF THE PIPE, Nu_θ
0
25
5
20
10
15
0
30
60
90
120
120
180
AXIS OF SYMMETRY
o ΔT = 25 °C
□ ΔT = 10 °C
RADIAL POSITION ON THE PIPE'S OUTER SURFACE, θ, (degrees)

(f) E = - 0.5

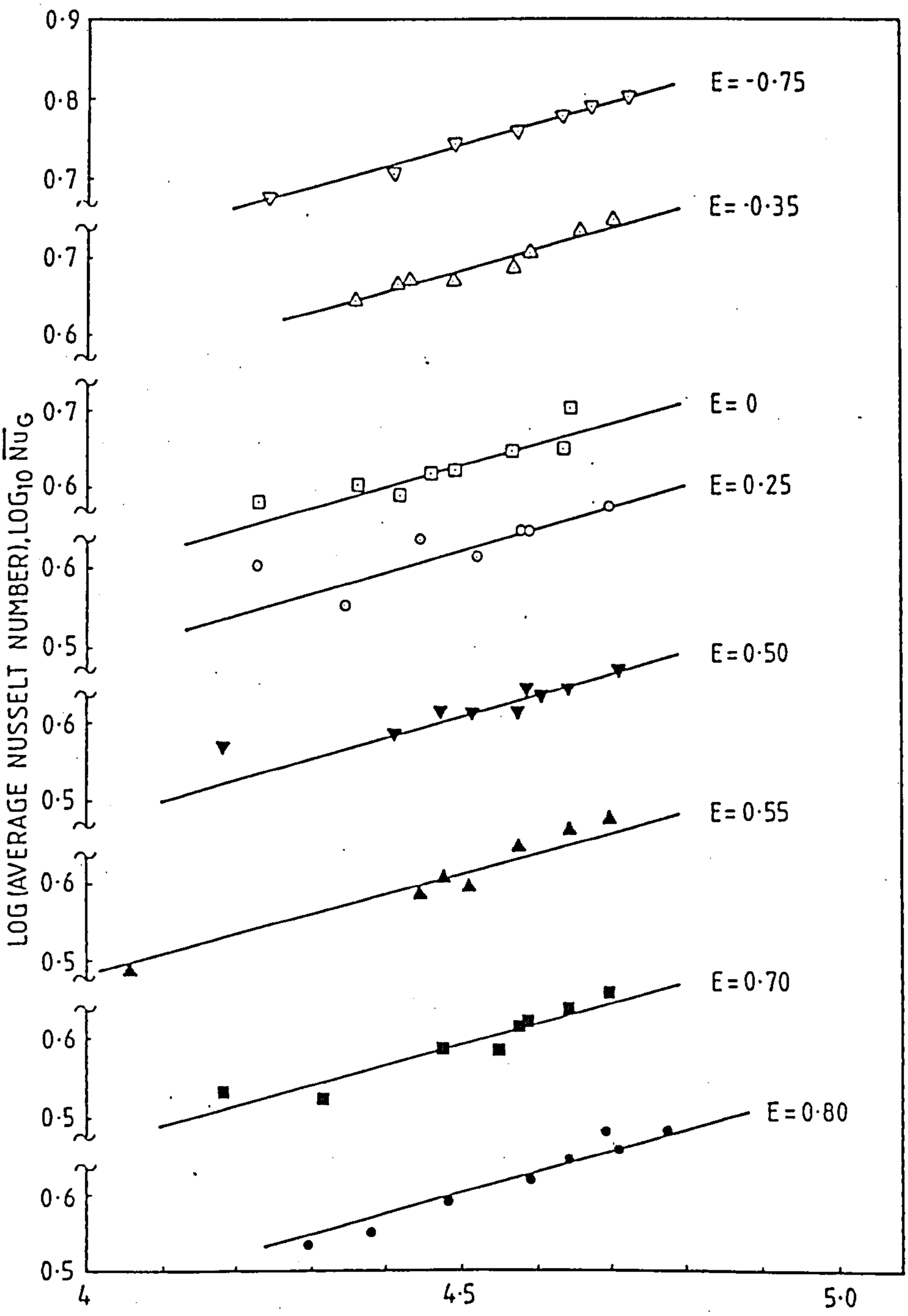

Fig. 5.10. Variation of the average Nusselt number, $\overline{Nu}_G$, versus Grashof number, Gr_D, for system 'A'.

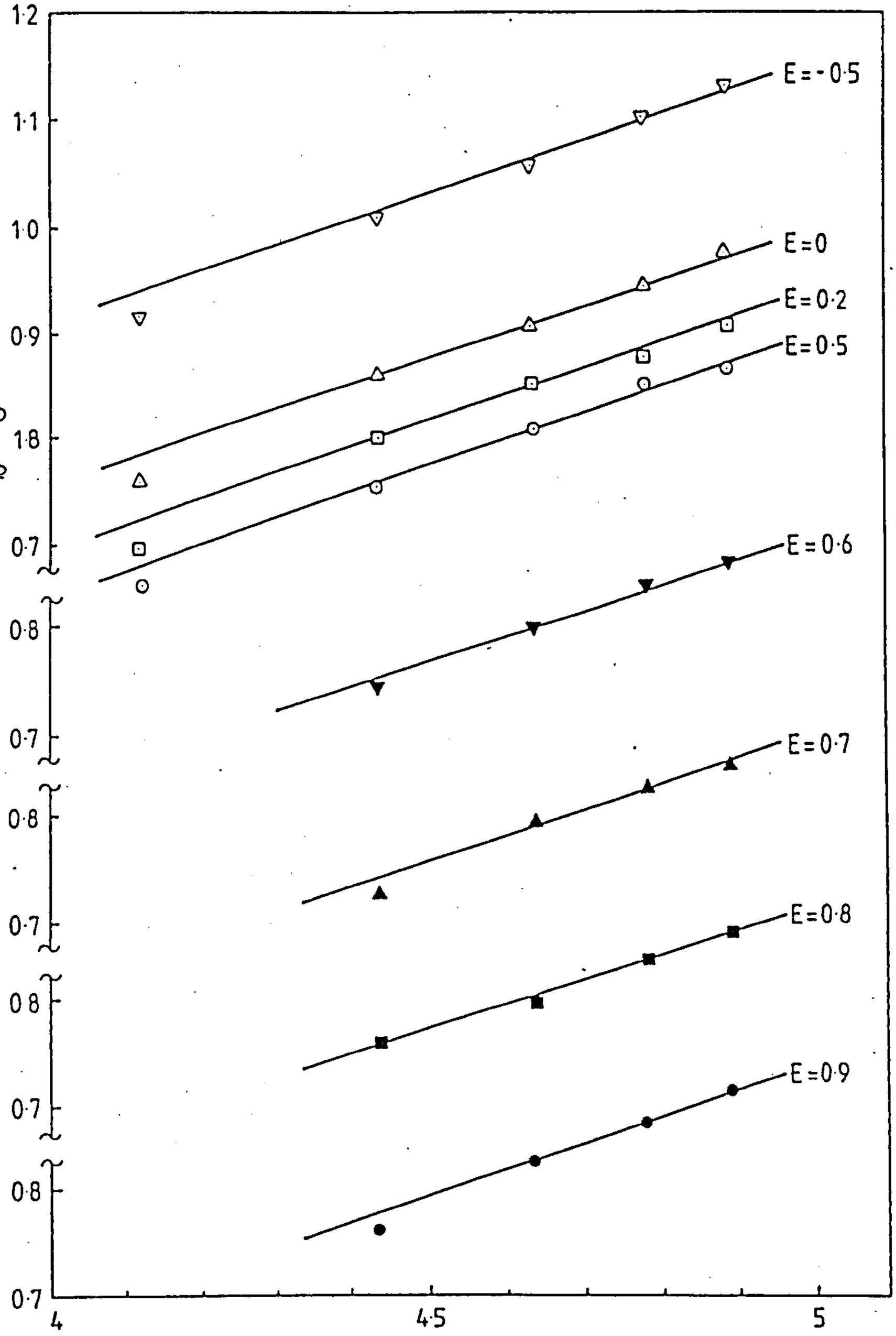

Fig. 5.11. As Fig. 10 but for system 'B'.

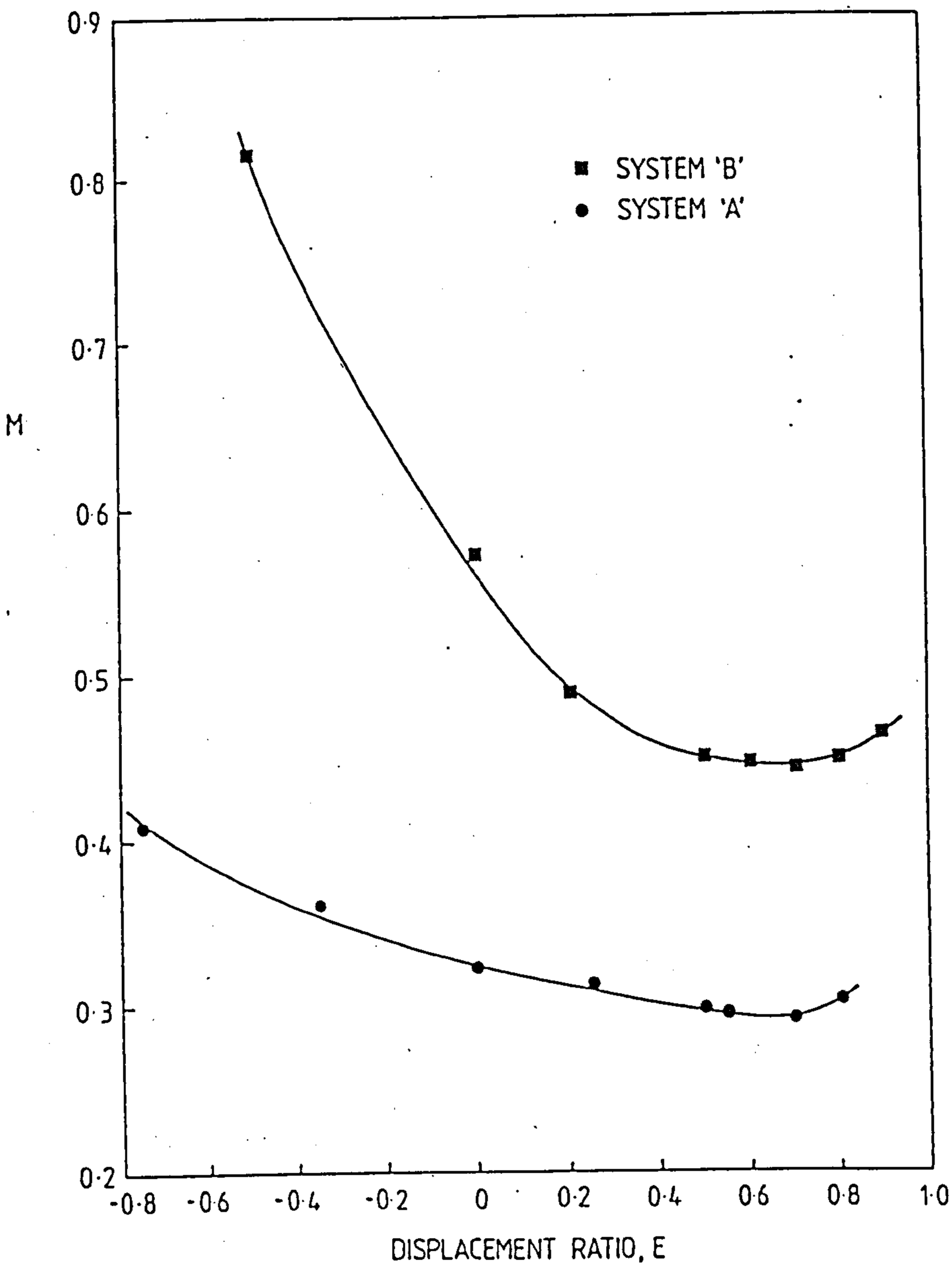

Fig. 5.12. Variation of the dimensionless parameter, M, versus the displacement ratio for systems 'A' and 'B': X = 100 mm, Y_A = 100 mm, Y_B = 125 mm and D = 28.5 mm.

CHAPTER 6

IMPROVED CONFIGURATIONS FOR DISTRICT-COOLING PIPELINES

Applied Energy 16 (1984)

Improved Configurations for District-Cooling Pipelines

SUMMARY

Visualisation of the air flows in the gaps between horizontal cylindrical pipes surrounding relatively cooler pipes has been undertaken, and the corresponding steady-state heat losses measured. Consequently, preliminary recommendations concerning how to improve the thermal insulation performances of district-cooling pipeline assemblies are presented.

NOMENCLATURE

D_o	Inner diameter of the horizontal outer cylinder (mm).
D_R, D_s	Outer diameters, respectively of the horizontal chilled-water return and supply pipes (mm).
L	Axial length of the considered horizontal air-filled cavity (mm) ($L = 610$ mm).
$\dot{Q}_R$, $\dot{Q}_s$	Net rates of heat gain, respectively by the horizontal chilled-water return and supply pipes (W).
T_o	Steady-state average temperature of the inner surface of the outer surrounding 'isothermal' cylinder (°C).
T_R, T_s	Steady-state average temperatures, respectively of the outer surfaces of the chilled-water return and supply pipes (°C).

Applied Energy 0306-2619/84/$03·00

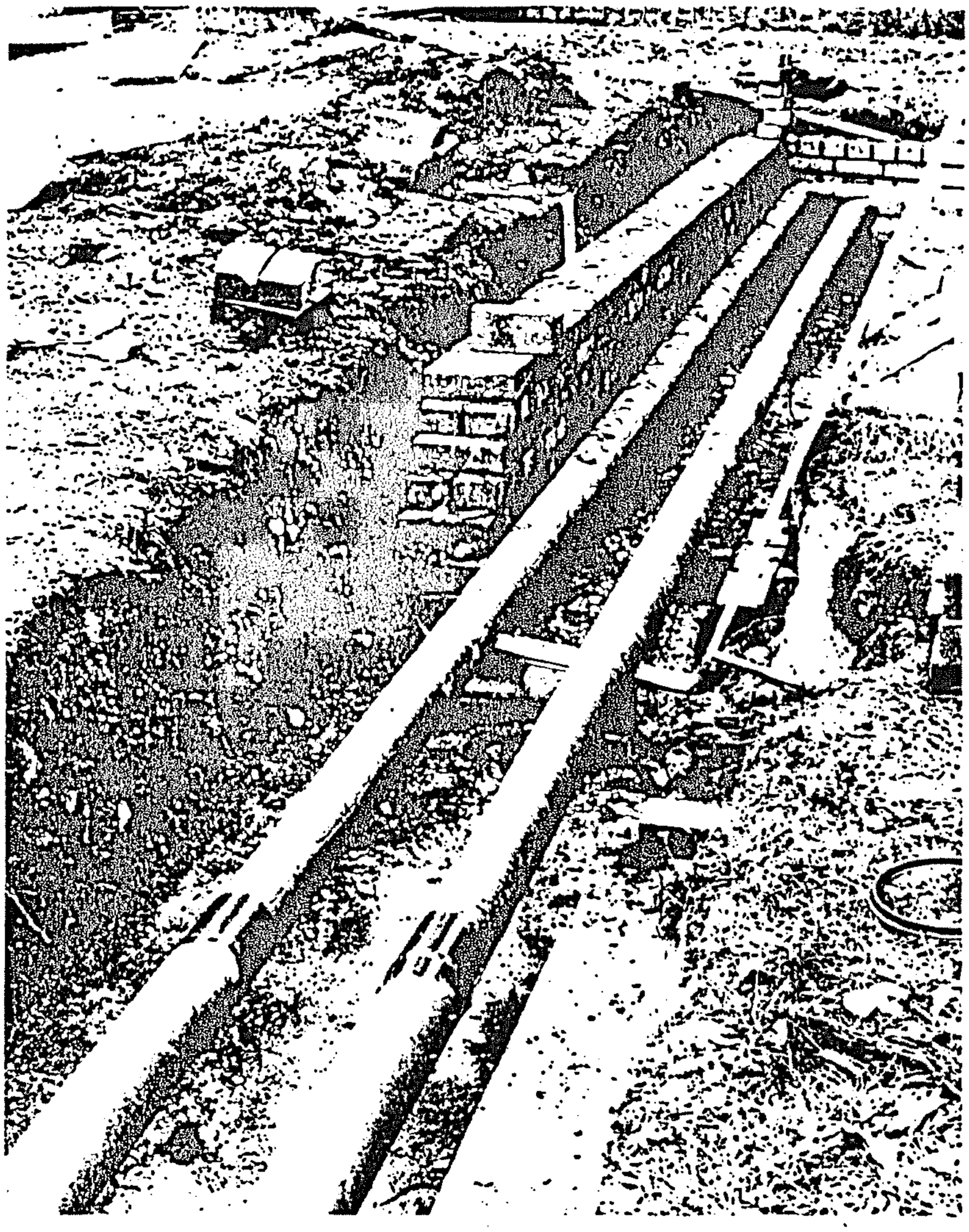

Fig. 1. Current conventional practice for district-heating pipework mains: the supply and return pipes are placed side-by-side in a relatively wide trench, without any endeavour to optimise (from an energy conservation viewpoint) the location of the pipes in that trench.

DISTRICT COOLING

This is becoming more popular, not only in 'hot' countries, but even in temperate climates where large local cooling requirements exist (e.g. in large buildings). District cooling is a socially acceptable means of reducing the consumptions of scarce or imported fuels.[1] It is already commonplace in Europe, Japan, the USA and the USSR. The chilled water so circulated is normally pumped to the consumers at a temperature of about 4 °C.[2-10] Unfortunately, some underground chilled water pipes are installed uninsulated in order to reduce the required initial capital investment: this practice is particularly prevalent with large district-cooling systems.[11,12]

THERMAL INSULATION

In any system, thermal insulation is usually achieved via the use of stagnant or near-stagnant air (or relatively high-density gas). Frequently, the district-heating or district-cooling pipes are surrounded by air and located conventionally in rectangular trenches as shown in Fig. 1: these trenches facilitate the evaporation or drainage necessary in the event of 'flash' flooding.[13] Otherwise, the insulant applied to the cool pipes would remain damp, thereby having its insulating effectiveness reduced and possibly suffering permanent damage. Thus it appears logical to employ air-filled trenches and also to try to maximise the thermal insulation provided by this air trapped around the district-cooling pipes. Arranging the pipes in their optimal configuration for minimum rates of energy dissipation should not incur extra initial capital investment, but lead to lower running costs. At present, for conventional practice, in general, a gap of 50 mm clear spacing between supply and return pipes is recommended for all pipe sizes, with the pipes placed *side-by-side*.[14]

THE PRESENT INVESTIGATION

For constructional simplicity and for a true comparison to be achieved easily, a single assembly (hereafter referred to as 'the system') has been employed to investigate how its orientation—and hence the relative

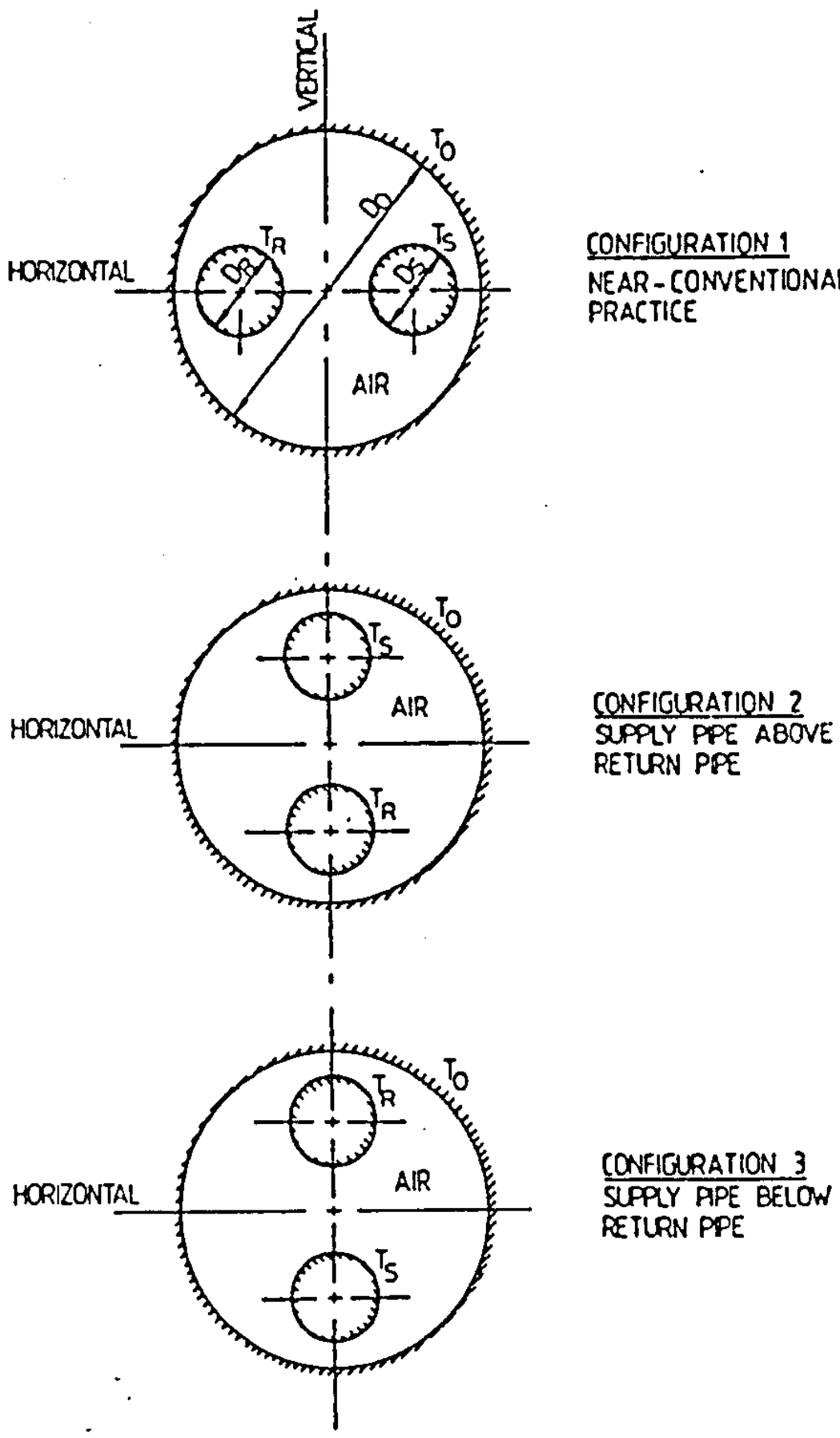

Fig. 2. The experimental model 'district-cooling' pipeline system tested: schematic representations of the vertical sections through the horizontal pipes are presented.

positions of its horizontal supply and return chilled-water pipes—affects the rates of heat transfer across the air gap. Three different configurations of this one system were tested. As a preliminary choice, the optimal eccentricity for a single supply pipe alone of diameter, D_s ($=28{\cdot}5$ mm), within the outer pipe of diameter, D_o ($=108{\cdot}5$ mm), has been selected to conform with the recommendation of Chakrabarti *et al.*[15] The other (i.e. the return) pipe, with $D_R = 28{\cdot}5$ mm, was symmetrically placed in the system (see Fig. 2). A *cylindrical* outer enclosure was used in this scientific investigation, because it ensured that the only factor which is different,

for each of the three configurations tested, was the relative position of the two inner pipes. In practice, rectangular (rather than circular) sectioned enclosures or trenches are commonly used, but the presently adopted abstraction from reality ensures that the observed changes of performance are due solely to variations of the relative position of the two inner pipes.

Steady-state natural-convective flow visualisations of the air around the relatively cold and slightly warmer horizontal cylinders (representing the supply and return pipes, respectively) within the surrounding, slightly heated, horizontal cylinder have been undertaken. The present study also measured the steady-state heat transfers across the horizontal air gap.

EXPERIMENTAL SYSTEM

In order to simulate, relatively easily, the warm environment surrounding the 'cold' pipes, the ranges of temperatures employed experimentally were:

$$25\,^{\circ}\mathrm{C} < T_o < 35\,^{\circ}\mathrm{C};\quad 12\,^{\circ}\mathrm{C} < T_R < 20\,^{\circ}\mathrm{C} \quad \text{and} \quad 8\,^{\circ}\mathrm{C} < T_s < 11\,^{\circ}\mathrm{C}$$

The horizontal outer Perspex cylinder was heated by circulating hot water at a constant temperature, T_o, through a polythene tube, which was wrapped uniformly around the cylinder. The inner copper pipes for the experimental rig were supported by means of horizontal hollow tubular extensions at their two ends: these tubes also conveyed the relatively cold and slightly warmer water, at their respective controlled temperatures, T_s and T_R, into and out of the pipes. Separate controlled-temperature water supplies—one for the outer cylinder and one each for the chilled-water supply and return pipes—were used. The tubular extensions were clamped to four vertical steel rods, two at each end, along which the clamps could be moved, up or down together, by identical amounts. The cavity was closed at one end by means of a vertical Perspex plate and at the other end with a uniformly thick, homogeneous, vertical glass plate.

A small amount of smoke (smoke tubes were obtained from MSA Britain Ltd, Queenslie Estate, Glasgow, E3) was injected into the cavity and photographs were taken of the steady-state flow patterns, the appropriate illumination being introduced from projectors via a thin circumferential slit window in the outer cylinder.

SET A. $\begin{cases} T_o = 35\,^{\circ}\mathrm{C} \\ T_R = 13\,^{\circ}\mathrm{C} \\ T_s = 8\,^{\circ}\mathrm{C} \end{cases}$

SET B. $\begin{cases} T_o = 25\,^{\circ}\mathrm{C} \\ T_R = 13\,^{\circ}\mathrm{C} \\ T_s = 8\,^{\circ}\mathrm{C} \end{cases}$

CONFIGURATION 1 →

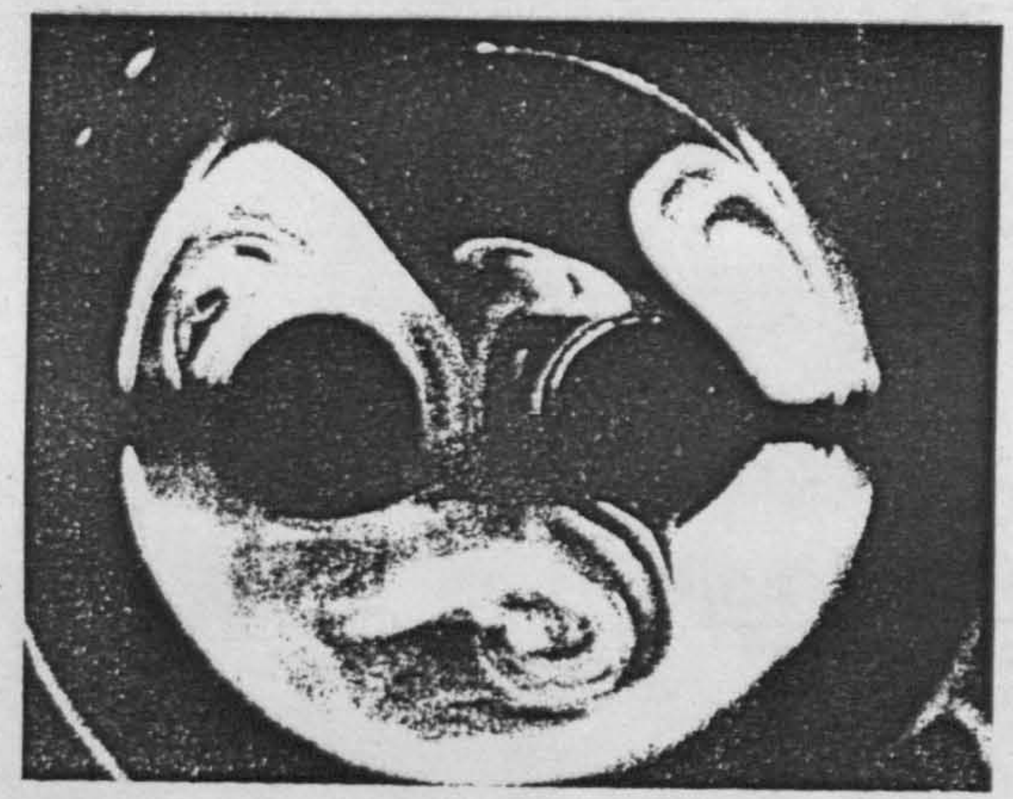

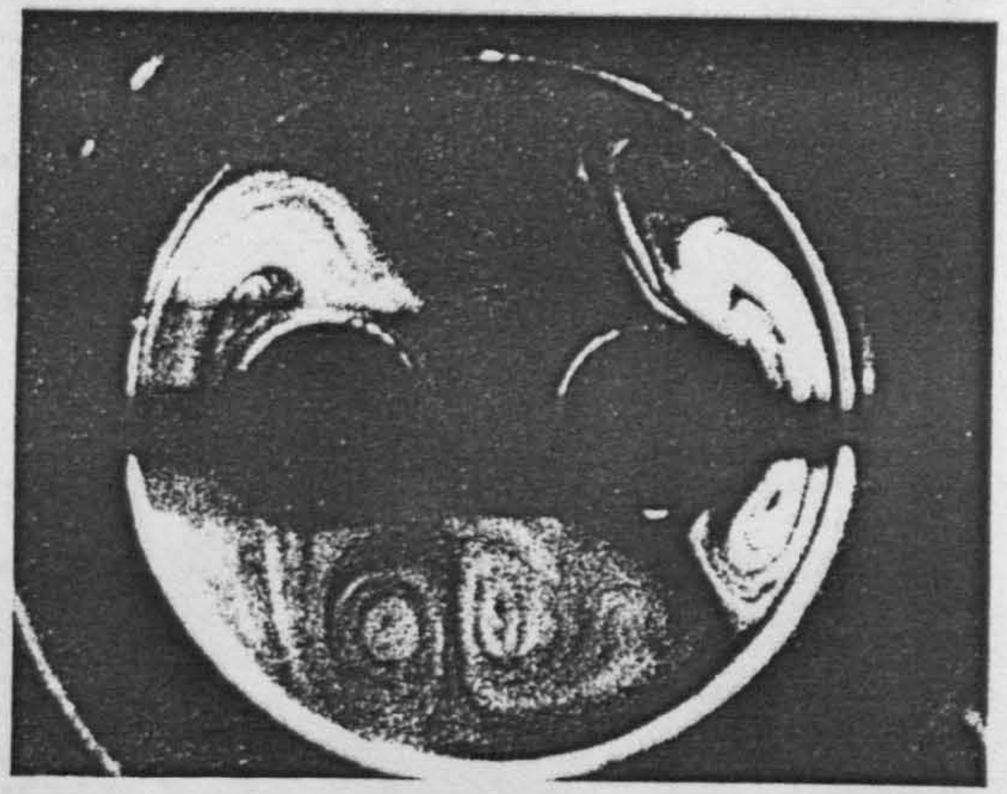

CONFIGURATION 2 →

CONFIGURATION 3 →

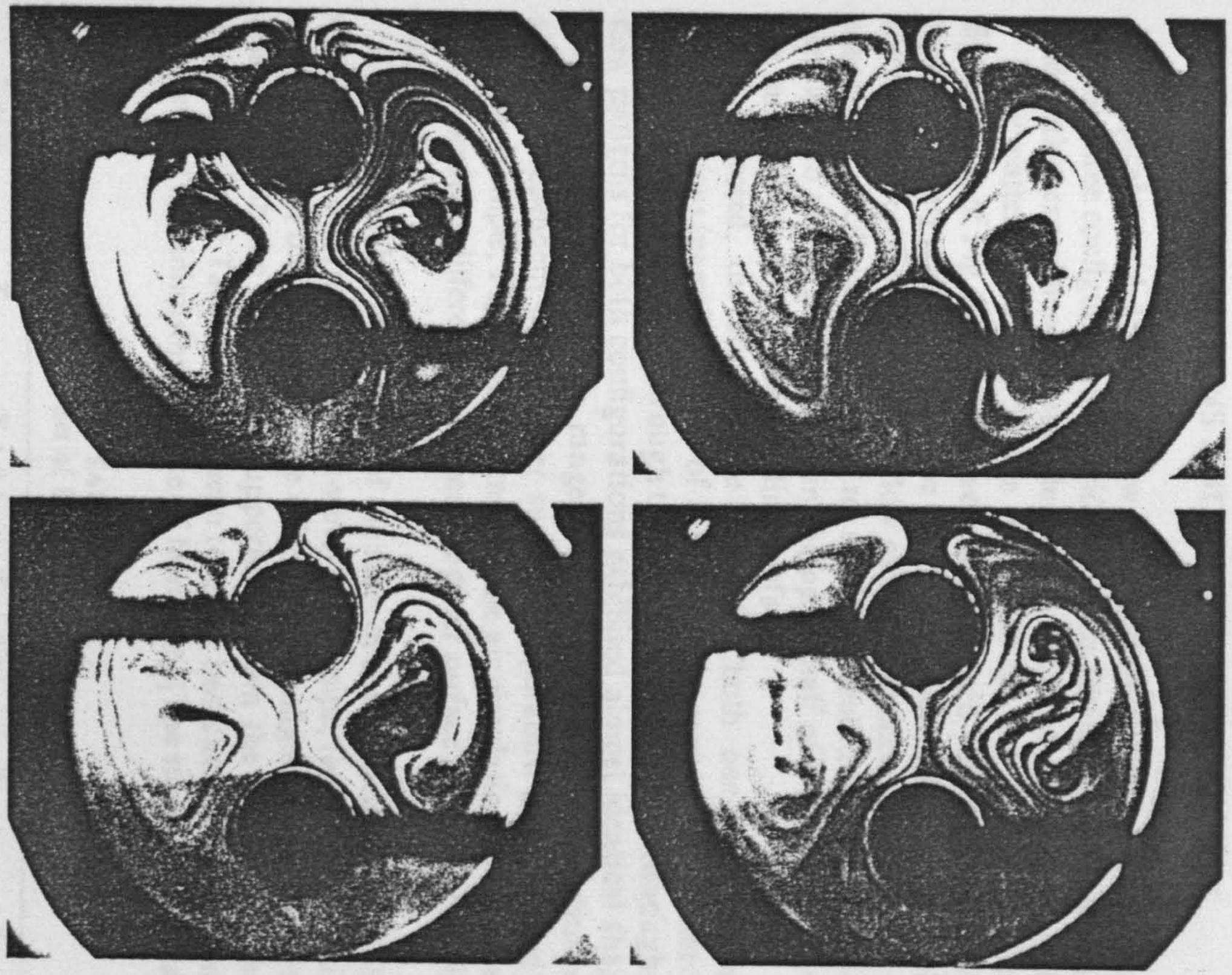

Fig. 3. Typical steady-state flow visualisations.

OBSERVATIONS AND RECOMMENDATIONS

Two typical sets (A and B) of flow visualisations are presented in Fig. 3, for the three configurations considered, each having the same geometry and, within experimental error, identical temperature conditions applied.

Flow patterns (see Fig. 3, sets A and B) for the '*side-by-side*' configuration 1 of Fig. 2 exhibited two kidney-shaped eddies. The flow-core was apparently undisturbed by the oscillating plume in the bottom half of the cavity. However, the intense flow mixing that occurred there and the associated oscillation gave rise to small recirculating vortices which ascended to the stagnation zone in the upper half of the cavity between the inner pipes and the surrounding surface.

As expected, the steady-state flows for both *one-above-the-other configurations* (namely 2 and 3 of Fig. 2), can be seen to be symmetrical around the vertical plane through the axes of the cylinders. Although the flow patterns for both configurations exhibited almost identical shapes, which, for the temperature ranges considered, remained qualitatively almost independent of the outer surface temperature or of T_s and T_R (see, for example, Fig. 3, sets A and B), the air circulation speed rose as the temperature differences between the outer surface and the inner pipes increased.

A comparison has been made of the rates of heat gained by the chilled-water supply pipe, and the chilled-water return pipe, for the side-by-side, compared with the one-above-the other, pipe configurations. The latter assembly, with the return pipe uppermost, from the steady-state heat transfer data (see Table 1) can be seen to be the best choice of those tested with respect to minimising the rate of heat gain. (The supply pipe acts as

TABLE 1
Typical Set of Experimental Data

System	T_∞ (°C)	$T_s \pm 0{\cdot}1$ (°C)	$T_R \pm 0{\cdot}1$ (°C)	$\dot{Q}_s$ (W)	$\dot{Q}_R$ (W)
Configuration 1	35	10·2	17·8	33·1	−14·9
	25	10·0	17·7	23·9	−22·0
Configuration 2	35	10·1	17·8	40·6	−29·8
	25	9·9	17·7	31·9	−30·3
Configuration 3	35	10·0	17·8	20·5	−7·9
	25	10·0	17·8	15·9	−15·5

the overall heat sink for the system, and therefore automatically absorbs $\dot{Q}_R$.) An improvement of approximately 35% was achieved in the insulating performance of the air by using configuration 3 rather than the current standard practice (namely configuration 1).

Thus, for district cooling, the recommended arrangement is with the return above the supply pipe, i.e. configuration 3. This would permit the use of narrower (and hence cheaper) trenches compared with the current conventional practice (which recommends the 'side-by-side' configuration as in Fig. 1). In practice, the return and supply pipes would be externally insulated and thus their surface temperatures would be nearer that of the environment. So the difference in the rates of heat transfer for the three configurations considered would be less dramatic than in the present tests. Nevertheless, the use of the best configuration for any particular set of insulated pipes would be economically worth while as no additional insulants would be required to achieve the improved performance.

A detailed investigation is needed to determine the optimal locations of the supply and return pipes within the outer pipe or rectangular trench for the variety of conditions likely to be encountered in practice. Also, filling the trench with rubble around the supply and return pipes would lessen the influence of the different orientations of the pipes, because convection would then be inhibited. Nevertheless, qualitatively identical conclusions would be drawn for such systems.

REFERENCES

1. P. Kier, J. Feit, W. Henselman, R. Loube and C. Meek, *State and local regulations for district-heating and cooling systems: issues and options*, Department of Energy, Washington DC, Report No. ANL/ES-126, Nov., 1981.
2. M. J. Wilson, District-cooling—Campus chilled water plants, *Heating, Piping and Air-Conditioning*, 38(11) (1966), pp. 106–9.
3. F. P. Sullivan, Co-op city gets unified energy system, *Power* (March, 1968), pp. 72–7.
4. Anon., Piggybacked district-cooling for California's Capitol Mall, *Heating, Piping and Air-Conditioning*, 42(3) (1970), pp. 75–82.
5. T. Ojima and T. Saito, District cooling system in Expo-70, *2nd Int. Convention on District Heating, Budapest*, 1973, pp.(VI). 87–(VI). 102.
6. S. Yoshida, District heating and cooling for eleven sky-scrapers in Tokyo, Japan, *Proc. 2nd. Int. Convention on District Heating, Budapest*, 1973, pp.(VI). 103–(VI). 124.

7. T. Gosling, District cooling, *Consulting Engineer*, 38(11) (1974), pp. 53–5.
8. C. E. Avers, Nashville confronts technical, economic problems in refuse-to-energy, *Professional Eng.*, 45(11) (1975), p. 32.
9. C. Piemonte and G. Scalvi, Considerations regarding modern district-cooling plants, *Termotecnica* (*Milan*), 31(6) (1977), pp. 286–94.
10. R. M. E. Diamant, District cooling: Parts I and II, *Heating and Air-Conditioning Journal*, 49(574) (1979), pp. 42–46 and pp. 60–66.
11. J. H. Henderson, Economic justification of thermal insulation of underground hot and chilled-water piping, *Proc. Ist. Int. District Heating Convention, Session 4, Section G*(7), London, 1970, pp. 1–8.
12. T. Kusuda, Heat transfer studies of underground chilled water and heat distribution systems, *Proc. of Symposium on Underground Heat and Chilled-Water Distribution Systems, Washington, DC, 1973*, Report No. NBS-BSS-66, May, 1975, pp. 18–41.
13. BS. 4508, Specifications for thermally insulated underground piping systems: Part 1: steel-cased systems with air gap, 1969.
14. J. H. Henderson, Combined installation of pipelines in different services, e.g. heating/cooling, *Proc. 2nd. Int. Convention on District Heating, Budapest*, 1973, pp. (VI). 49–(VI). 61.
15. S. Chakrabarti, S. D. Probert and M. J. Shilston, Optimal eccentric annuli (containing atmospheric-pressure air) for thermally-insulating, horizontal, cold pipes, *Applied Energy*, 14 (1983), pp. 257–93.

CHAPTER 7

DISTRICT-COOLING DISTRIBUTION NETWORK: OPTIMAL CONFIGURATION OF A DOUBLE-PIPE SYSTEM IN A RECTANGULAR TRENCH

SUMMARY

The optimal configuration, i.e. that which achieves the minimum steady-state rate of heat gain by the supply (i.e. the colder) pipe for the considered conditions, has been determined experimentally. By using the displacement ratios of the two pipes as the experimental variables, the optimal configuration of the supply and return (i.e. the warmer of the two) pipes was deduced to occur at displacement ratios of 0.67 and -0.08 respectively, i.e. with the supply pipe in the lower region of the atmospheric-pressure air-filled relatively hot trench and the return pipe vertically above it, both symmetrically placed with respect to the side walls. This optimal configuration differs significantly from the traditional side-by-side arrangement of district-cooling pipe-lines and should prompt designers to become more aware of prospective energy and financial savings which can be achieved.

NOMENCLATURE

D	Diameter of both the considered supply (i.e. the colder) and return (i.e. the relatively warmer) pipes (see Fig. 1), (m).
E	Displacement ratio {= $[2H_R/(Y - D)] - 1$} or {$[2H_S/(Y - D)] - 1$} for the return or supply pipe respectively (see Fig. 1).

Gr_X Local Grashof number for the convecting air flow, based on the width, X, of the trench.

H_R, H_S Shortest vertical distances between the return and supply horizontal pipes respectively and the upper horizontal internal plane surface of the trench (see Fig. 1), (m).

L Axial length of the considered horizontal air-filled cavity, (m).

Nu_X Local Nusselt number for the steady-state rate of heat transfer to the supply pipe, based on the width, X, of the trench.

$\dot{Q}_{conv.+cond.}, \dot{Q}_{rad.}$ Heat transfer contributions to the total steady-state rate of heat gain by the horizontal supply pipe due to convection plus conduction, and radiation respectively via the surrounding air, (W).

$\dot{Q}_{total}$ Total steady-state rate of heat gain by the supply pipe, (W).

T_o Uniform steady-state temperature of the inner surfaces of the outer surrounding isothermal model rectangular trench, as used in the present set of experiments (see Fig. 1): in practice T_o would vary over these surfaces, (°C).

T_R, T_S Steady-state temperatures of the outer surfaces of the return and supply pipes respectively (see Fig. 1), (°C).

X,Y, Horizontal width and vertical extent respectively of the rectangular cavity (see Fig. 1), (m).

ΔT Steady-state difference between the temperatures of the inner surfaces of the trench and the outer surfaces of the supply pipe: ($= T_o - T_S$), (°C).

ε Emissivity of the appropriately identified surface.

Θ Angular coordinate measured from zero for the vertically downwards radius vector emanating from the horizontal centre-line of the supply pipe and increasing with clockwise rotations (see Fig. 2), (degrees).

Suffixes

cond	due to conduction through the air.
conv	due to convection via the air.
o	of the inner surface of the rectangular trench.
R	for the pipe along which the chilled water returns to the refrigerator.
rad	due to the net thermal radiation gain by the supply pipe.
S	for the chilled-water supply pipe.

Abbreviations

CHP	Combined heat and power
DC	District cooling
DH	District heating
DHC	District heating and cooling

DISTRICT-COOLING (DC) NETWORKS

These distribute chilled water through insulated pipes to serve commercial, residential, and industrial energy needs for

space cooling and industrial purposes. DC systems permit energy, as distinguished from fuel, to be bought and sold as a commodity.

For some customers, such systems possess several advantages relative to rival energy systems. By replacing many individual refrigerators with a single, central, cooling source, the available effective space for occupants within the building is increased, building construction and operating costs reduced and air quality improved(1). In general, satisfying several criteria will contribute to the success of DC systems. These include serving a densely-populated area or core of frequently fully-used buildings, a source of relatively cheap fuel available nearby, and the desire to reduce dependence on imported oil. In plants where cogeneration (i.e. of heat and electricity) is practical, the absence of a heat load during the warm months may result in the operation being altered to produce a surplus of electric power. This power can be utilized to drive large-scale conventional refrigeration machines for the production of chilled water(2). However, the successful implementation of a large DC system will requires political initiative, wise management and a commitment from all participants.

There are five major alternative ways of obtaining the required chilled water at the central plant: (i) steam is generated locally and then is used to drive the refrigeration plant; (ii) the refrigeration plant is installed in close proximity to a DH network, and is driven by steam produced at the DH central-system; (iii) electricity-driven equipment is employed to produce

the chilled water; (iv) an absorption refrigerator (e.g. operating on a lithium bromide/water mixture is used; and (v) natural cold-water supplies of fresh water sources such as lakes, reservoirs, rivers, an ice pond or ground water, are employed.

In the UK and in other parts of Europe, there is a tendency to use system (i) unless there is a large air-chilling load demand. In many parts of the USA, the air conditioning demand is so large, that system (ii) is preferred, although the transition to system (iii) is being made in some cases where the cooling demand is so great that it is commercially feasible[3,4].

DC has not been so widely adopted as DH, but it is being advocated, and so is being introduced slowly as a financially-attractive process. However, DHC systems can be employed together successfully because many modern office and other commercial buildings require simultaneous heating in one part yet cooling in another. In addition, modern office buildings need to be cooled even on days when most domestic residences do not, because their windows are often sealed shut to prevent dust and pollution infiltration and to satisfy the requirements of high internal energy loads caused by lighting equipment and high-occupation patterns.

There are few DC systems operating, or being installed, in Europe. Some small DC, but no city-wide systems exist at present. Europeans neither expect nor are as accustomed to, air conditioning as are citizens of the USA. Nevertheless, air conditioning

has been installed in many new European office buildings, particularly in southern Europe. This suggests that DC is becoming more economically viable in many European cities and the USSR[5]. In the UK, DC is employed at the Heathrow international airport complex and also at a major shopping precinct in Chatham, Kent. One of the biggest systems in the world, outside Japan, is located in Hartford, Connecticut, USA: it was, in 1962, the first utility-operated district plant to market both chilled water and steam. Nevertheless, fewer than sixty urban DC systems are in current use in the USA[1]. Japan has been somewhat of a pioneer in the field of DC: even in 1981, it was estimated that about ninety different systems were in operation there[3].

DISTRIBUTION NETWORK

This thermally-insulated pipe-loop conveys chilled water at about 4 °C to consumers: separate pipe returns the slightly-heated water (at about 13 °C) for recooling. The pipes are usually either buried directly in the ground, placed in tunnels or concrete culverts, or located above ground. Communities with large space-cooling requirements and high densities may choose to distribute both hot and chilled water, according to the different seasonal demands[1,2].

The most frequently-recommended and widely-used design in the UK is that with thermally-insulated pipelines, located side-by-side about half-way down an atmospheric-pressure, air-filled, rectangular trench[4,6,7]. In the event of such a trench becoming

flooded (which occurs intermittently in Britain, because of its maritime climate, high humidities and relatively high water-table levels), subsequently drainage and evaporation from around the pipelines can then ensue automatically. Otherwise, if the insulant is allowed to remain damp, e.g. by being in intimate contact with the earth, the moisture may reduce the insulant's effectiveness and its mechanical strength (sometimes permanently), as well as possibly promoting corrosion of the underlying steel pipelines, which are supposedly being protected by the insulant.

DHC line-networks are expensive: they constitute at least 50% of the capital costs for DHC supply systems. Several design studies and behavioural tests have been undertaken[8-21]. Much time, effort and money have been devoted to producing reliable, cheap, well thermally- insulated underground pipelines, but unfortunately to date, these endeavours have <u>not</u> been completely successful[22].

The amount of water to be circulated will have a significant bearing on the magnitude of the distribution loop costs: in practice it is desirable to have the minimum water flow-rate with the smallest practical pipe size. The water flow in the mains distribution loop must always exceed the total flow in all the secondary circuits, i.e. the building loops. This is necessary to assure a constant supply temperature to each building. In general, the most economical distribution system lay-out will result if the mains are run by the shortest convenient route to the terminal equipment in the building or group of buildings

having the largest flow-rate requirements. The branch or secondary circuits are then laid out to connect with these mains[2].

THE EXPERIMENTS

The present investigation was aimed at determining the energy-thrift prospects with respect to what can be achieved through better design of a double-pipe DC system. It involved measuring the steady-state rates of heat transfer across the atmospheric-pressure air-filled gap between an isothermal hot horizontal, rectangular sectioned, trench enclosing two horizontal pipes, the first carrying cold water (i.e. the supply pipe), and the other slightly warmer water (i.e. the return pipe) — see Fig. 1.

By employing the optimal position of the supply pipe as indicated by previous investigations[5], the optimal position of the return pipe, so that the least steady-state rate of heat gain by the supply pipe for a prescribed ΔT occurs, was determined experimentally.

The convective flow patterns (as indicated by the presence of a small amount of smoke) within the enclosed air space, for various steady-state temperatures of the surface of the return pipe were observed. These patterns stimulate, supplement, and corroborate conclusions being drawn from interferometric observations of the steady-state isotherms in the air gap. [Measurements with such systems (i.e. with a completely air-filled cavity)

indicate the upper limits which convective contributions could make to the rate of heat transfer for the same geometrical system, with the same temperature distribution, but with pebbles packed around the pipes, an arrangement which is sometimes adopted in practice].

In this investigation, only the gains by the supply pipe were considered, because the prime aim of controllers of DC schemes is to distribute chilled water to their customers. Thus they are concerned primarily with reducing the heat gains by the supply pipelines during transmission. In practice, both the supply and return pipes would be well insulated thermally.

THE HEAT-TRANSFER RIG

The chosen values of the experimental variables were:-

$$X = 100 \text{ mm}, \quad Y = 125 \text{ mm}, \quad L = 650 \text{ mm}, \quad D = 28.5 \text{ mm}$$

$$-0.3 \leq E_R \text{ or } E_S \leq 0.67$$

$$15\ ^{\circ}C \leq T_R \leq 30\ ^{\circ}C$$

$$T_S = 10\ ^{\circ}C$$

$$T_o = 35\ ^{\circ}C$$

$$Gr_X = 3.3 \times 10^6$$

Each of the measured temperatures was accurate to $\pm$ 0.2°C, and the stated dimensions to $\pm$ 0.2 mm. The experimental rig

employed for investigating the steady-state rate of heat loss from a DH double-pipe system[23] was modified slightly to undertake the present heat gain and flow-visualisation tests.

FLOW VISUALISATIONS

These were obtained for three different displacement ratios of the DC system. The flows so observed indicated the occurrences of flow instabilities and helped in the interpretations of the heat-transfer phenomena resulting in the steady-state temperature field distributions indicated by the interferograms (see typical examples as shown in Fig. 4).

The flow patterns for the side-by-side arrangement (i.e. current conventional practice) -- with $E_R = E_S = 0$ (see configuration 1 of Fig.3) -- exhibited three zones of eddies (see Fig. 4(a)). Firstly, there was an approximately triangular-shaped eddy circulating around the warm (i.e. the return) pipe and having the longest path compared with those of the three other zones; secondly, two well-defined eddies ensued between the cold (i.e. the supply) pipe and the wall of the trench; and thirdly, in the upper half of the trench, a weak irregularly-shaped vortex occurred.

For the warm-above-cold pipe arrangement (see configuration 2 of Fig. 3), the flow patterns exhibited two, almost stable, counter-rotating, approximately triangular-shaped eddies, which when averaged with respect to time were symmetrical about the

vertical plane through the horizontal axes of the pipes, bisecting the trench (see Fig. 4(b)).

The flow patterns for the cold-above-warm pipe arrangement (see configuration 3 of Fig. 3) were of an irregular shape. Severe instabilities, with intense mixing, were also observed. The relatively fast air-flow between the two pipes (i.e. the plume) oscillated frequently -- this was corroborated by the relatively high rates of heat transfer occurring (see Fig. 4(c)).

As expected the shapes of eddies in the previously mentioned configurations were almost independent of the differences between T_o, T_R and T_S for the temperature ranges considered.

The observations drawn from the present flow visualisations agreed qualitatively well with those for a double-pipe DH system[23] under the conditions tested.

INTERFEROMETRY

The steady-state isothermal contour maps for the temperature distributions of the air in the cavity were obtained for the side-by-side and the warm-above-cold geometrical configurations, with various applied steady-state temperature distributions (see Fig. 5). The arrangement with the cold pipe above the warm pipe (that is configuration 3 of Fig. 3) was not considered because the flow visualisation observations indicated clearly that this was the worst configuration with respect to thermal insulation

(i.e. the steady-state rate of heat transfer was enhanced, rather than reduced) compared with that obtained with the side-by-side configuration (i.e. the current conventional practice).

For the warm-above-cold arrangement (that is configuration 2 of Fig. 3), the supply (i.e. the cold) pipe position was kept constant at a displacement ratio E_S equal to 0.67 (which is the optimal location for a DC single-pipe system in a relatively hot rectangular trench)[5]. Seven values of the displacement ratio, E_R, were then chosen successively for positioning the relatively warm (i.e. the return) pipe directly above the cold pipe. Appropriate measurements were made corresponding to each configuration, and the interferograms analysed[23].

The variations of the local Nusselt number Nu_x with the temperature difference ΔT for two of the selected arrangements are shown in Fig. 6. For configuration 1, the maximum local rates of heat transfer occurred near the top of the cold pipe (i.e. in the 180 → 215° region) -- see Fig. 6(a). However, for configuration 2, the isotherms were packed most closely near the supply pipe's surface in the region $150° < \Theta < 165°$ (see Fig. 6(b)), so indicating that high local rates of combined convective and conductive steady-state heat transfer ensued there.

The evaluated total steady-state rates of heat gain, $\dot{Q}_{total}$, by the supply pipe are shown in Table 1 for the different configurations considered. The radiation component, $\dot{Q}_{rad}$, as well as

Table 1. Steady-state heat gains by the supply (i.e. the cold) pipe through the air across the considered cavity: T_S = 10 °C, ΔT = 25 °C.

Configuration	Geometrical description	T_R (°C)	$\dot{Q}_{rad.}$* (W)	$\dot{Q}_{conv.+cond.}$ (W)	$\dot{Q}_{total}$ (W)
1	$E_R = E_S = 0$	30	6.5	4.1	10.6
		25	6.4	4.0	10.4
		20	6.3	3.9	10.2
		15	6.2	3.8	10.0
2	$E_R = -0.30$ $E_S = 0.67$	30	6.5	3.9	10.4
		25	6.4	3.7	10.1
		20	6.3	3.5	9.8
		15	6.2	3.4	9.6
2	$E_R = -0.25$ $E_S = 0.67$	30	6.5	3.7	10.2
		25	6.4	3.5	9.9
		20	6.3	3.4	9.7
		15	6.2	3.2	9.4
2	$E_R = -0.20$ $E_S = 0.67$	30	6.5	3.5	10.0
		25	6.4	3.3	9.7
		20	6.3	3.2	9.5
		15	6.2	3.0	9.2
2	$E_R = -0.15$ $E_S = 0.67$	30	6.5	3.3	9.8
		25	6.4	3.1	9.5
		20	6.2	3.0	9.2
		15	6.1	2.8	8.9
2	$E_R = -0.10$ $E_S = 0.67$	30	6.5	3.2	9.7
		25	6.3	3.0	9.3
		20	6.2	2.8	9.0
		15	6.1	2.6	8.7
2	$E_R = -0.05$ $E_S = 0.67$	30	6.5	3.2	9.7
		25	6.3	3.0	9.3
		20	6.2	2.8	9.0
		15	6.0	2.7	8.7
2	$E_R = 0$ $E_S = 0.67$	30	6.5	3.3	9.8
		25	6.3	3.1	9.4
		20	6.1	3.0	9.1
		15	6.0	2.8	8.8

* Based on $\varepsilon = 1$ for the trench surfaces and $\varepsilon = 0.78$ (i.e. oxidised copper[24] for the return and supply pipes in the experimental rig.

the convective plus conductive component, $\dot{Q}_{conv+cond}$, are also presented.

In order to determine the optimal position of the return pipe, the Q_{total} values were plotted against the displacement ratio for the return pipe, E_R, for different values of T_R -- see Fig. 7. The optimal position occurred with $E_R = -0.08 \pm 0.005$ for the temperature range and the component sizes employed. This optimal value was almost independent of the return pipe temperature. By employing these optimal data (i.e. $E_R = -0.08$ and $E_S = 0.67$), a reduction of approximately 11% was obtained in the total rate of heat gain through the air compared with that for the side-by-side arrangement.

CONCLUSIONS

An optimal configuration (i.e. corresponding to the least rate of heat gain by the supply pipe) was achieved with $E_R = -0.08$ and $E_S = 0.67$. This means that having the return (i.e. the warm) pipe above the supply (i.e. the cold) pipe in a hot rectangular trench leads to lower steady-state rates of heat gain than with any side-by-side arrangement or with the cold-above-warm pipe arrangement, within the same trench under identical boundary temperature conditions.

A maximum reduction of 11% was obtained by using the optimal arrangement, compared with that for the traditional side-by-side arrangement (i.e. $E_R = E_S = 0$) -- see Fig. 7. It has the added

advantage that it would permit the use of narrower (and hence cheaper to excavate) trenches compared with the present conventional practice. The pipe-over-pipe configuration has already been assessed to be cheaper to install than the pipe-beside-pipe system[25].

The 11% improvement in the convective/conductive thermal resistance of the air-filled cavity would amount to only ~ 3% gain in the overall thermal insulation of the system (i.e. allowing for the slight variations of the radiation exchange between the pipes as their proximity changes and for the presence of the insulant on the pipes and the insulation provided by the earth surrounding the trench). Nevertheless over the expected lifetime (> 30 years) of a pipeline network, the lower refrigeration costs incurred represent a very worthwhile benefit because its attainment incurs no additional capital expenditure. Also, from an independent viewpoint, because narrower trenches can be used and hence lower capital investment costs incurred, the configuration of pipes suggested in this investigation possesses economic advantages over current traditional practice, and so deserves further attention by designers and contractors.

REFERENCES

1. D.O. Meeker, Jr., DHC in the USA: prospects and issues, National Academy of Sciences, National Academy Press, Washington DC, USA, 1985.

2. IDHA, District heating handbook — a design guide : Vol. 1, 4th ed., Int. District Heating Association, Washington DC, USA, 1983.

3. R.M.E. Diamant and D. Kut, DHC for energy conservation, The Architectural Press, London, England, 1981.

4. R.F. Babus'Haq, S.D. Probert and M.J. Shilston, Envolvement of CHP with DHC, Applied Energy, 1987, in press.

5. R.F. Babus'Haq, S.D. Probert M.J. Shilston and S. Chakrabarti, Optimising the location of a DC pipeline in a rectangular trench, Applied Energy, 23(2), 1986, pp. 109-141.

6. R.K. McLaughlin, R.C. McLean and W.J. Bonthron, Heating services design, Butterworth & Co. Ltd., London, England, 1984.

7. D.R. Killpack, The role of polymers in DH, Shell Polymers, 7 (1), 1983, pp. 6-10.

8. K. Okada and E. Asano, An application of the finite-element method to the problem of underground temperature distribution around a buried heat source, Trans. Society of Heating, Air Conditioning and Sanitary Engineers of Japan, (3), 1977, pp. 27-37.

9. W.W. Martin and S.S. Sadhal, Bounds on transient temperature distribution due to a buried cylindrical heat source, Int. J. Heat Mass Transfer, 21(6), 1978, pp. 783-789.

10. R.M. Fand, T.E. Steinberger and P. Cheng, Natural convection heat transfer from a horizontal cylinder embedded in a porous medium, Int. J. Heat Mass Transfer, 29(1), 1986, pp. 119-133.

11. Anon, Central heating: a hot market for a pipe that can take the heat, Modern Plastics Int., 5(11), 1975, pp. 21-23.

12. G. Beckmann and P.V. Gill, Thermal energy storage, Springer-Verlag, Vienna, Austria, 1984.

13. J.R.R. Pelfrey and D.R. Pitts, Geothermal DH using existing potable-water piping systems, Trans. ASME, J. Energy Resources Technology, 105(2), 1983, pp. 162-164.

14. C. Mackenzie-Kennedy, DH of a British residential area in Germany, Heating and Ventilating Eng., 48(567), 1974, pp. 129-134.

15. Anon., Flexible distribution pipes from rigid PUR foam?, Modern Plastics Int., 15(5), 1985, p. 20; p. 24.

16. Anon., Rigid insulation is kept flexible by snap-fit collars, Plastics and Rubber Weekly, (1084), 1985, p. 15.

17. R.M.E. Diamant, Insulation of underground DH pipelines, Heating and Ventilating Eng., 46(540), 1972, pp. 24-26.

18. J. Christiansen and J.R. James, A new technique in the design and installation of large distribution systems, 3rd. Nat. Conf. DHA, A National Plan for Heat, Eastbourne, England, 1979.

19. S. Anderson, Developments in insulated pipework in Scandinavia, 6th Nat. Conf. CHPA, CHP -- Development and Decisions, Torquay, England, 1985.

20. D. Bublitz, General Report of the Study Committee for Heat Transport and Distribution, 22nd. Unichal Congress, Copenhagen, Denmark, 1985, Fernwarme Int., Address Book and Supplier Directory, FBV 4th. ed. 1985, pp. 48-68.

21. J.W. Sutton, A.J.B. Whitelocke, P. Farr, W.S. Isherwood and R.F. Angel, Pipe insulation and heating, Pipes and Pipelines Int., 16(9), 1971, pp. 14-36.

22. W.T. Huber, Piping systems are the key, ASHRAE J., 27(2), 1985, pp. 27-35.

23. R.F. Babus'Haq, S.D. Probert and M.J. Shilston, Steady-state heat losses from horizontal pipes in an air-filled rectangular concrete duct, Proc. I.Mech.E., 199(C3), 1985, pp. 203-213.

24. H. Grober, S. Erk and U. Grigull, Fundamentals of heat transfer, McGraw-Hill Book Co., Inc., New York, USA, 1961.

25. P.S. Woods, The design and costs of large-scale DH networks, Pipework Design and Operation Conf., I.Mech.E., London, England, 1985.

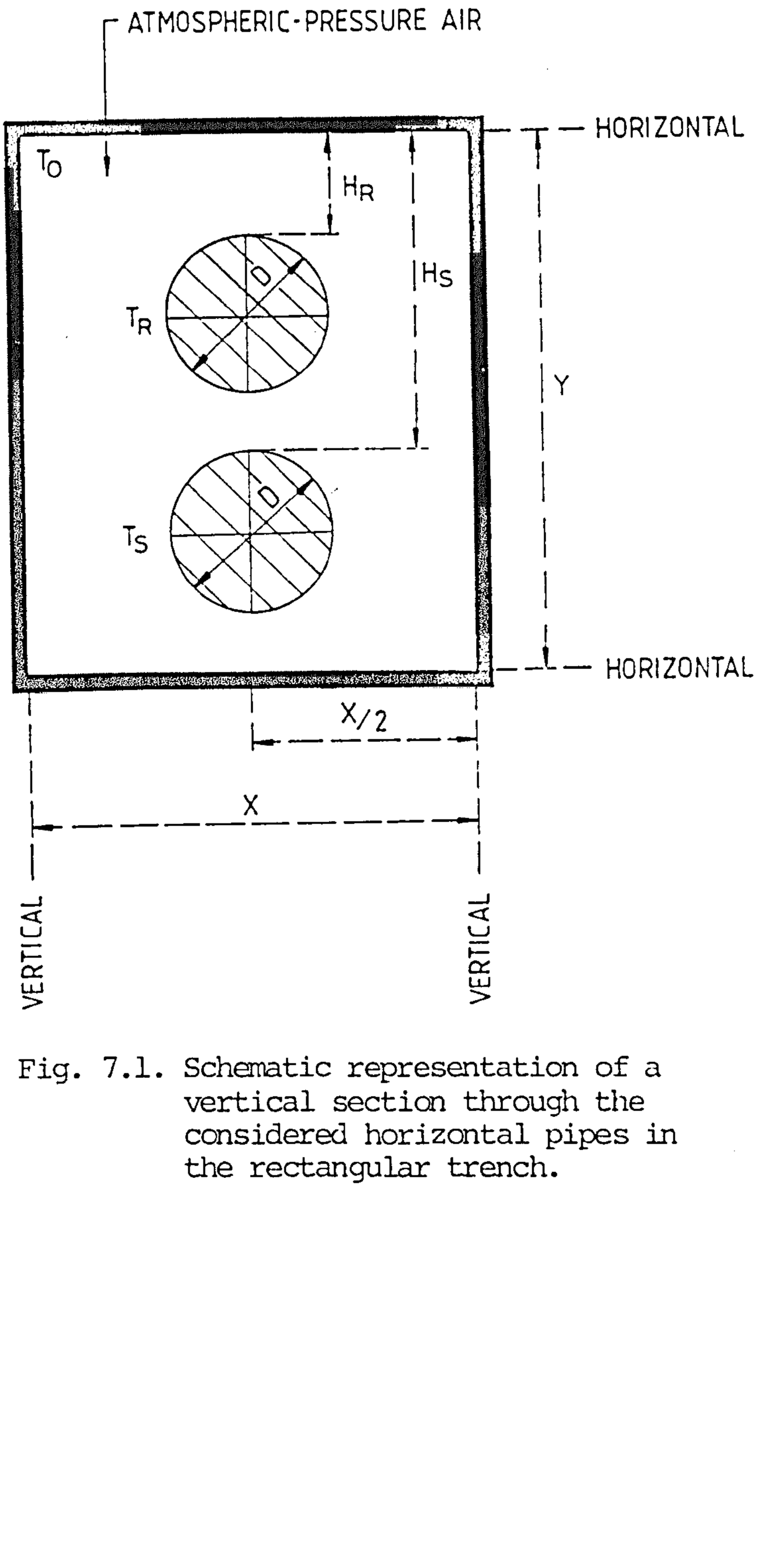

Fig. 7.1. Schematic representation of a vertical section through the considered horizontal pipes in the rectangular trench.

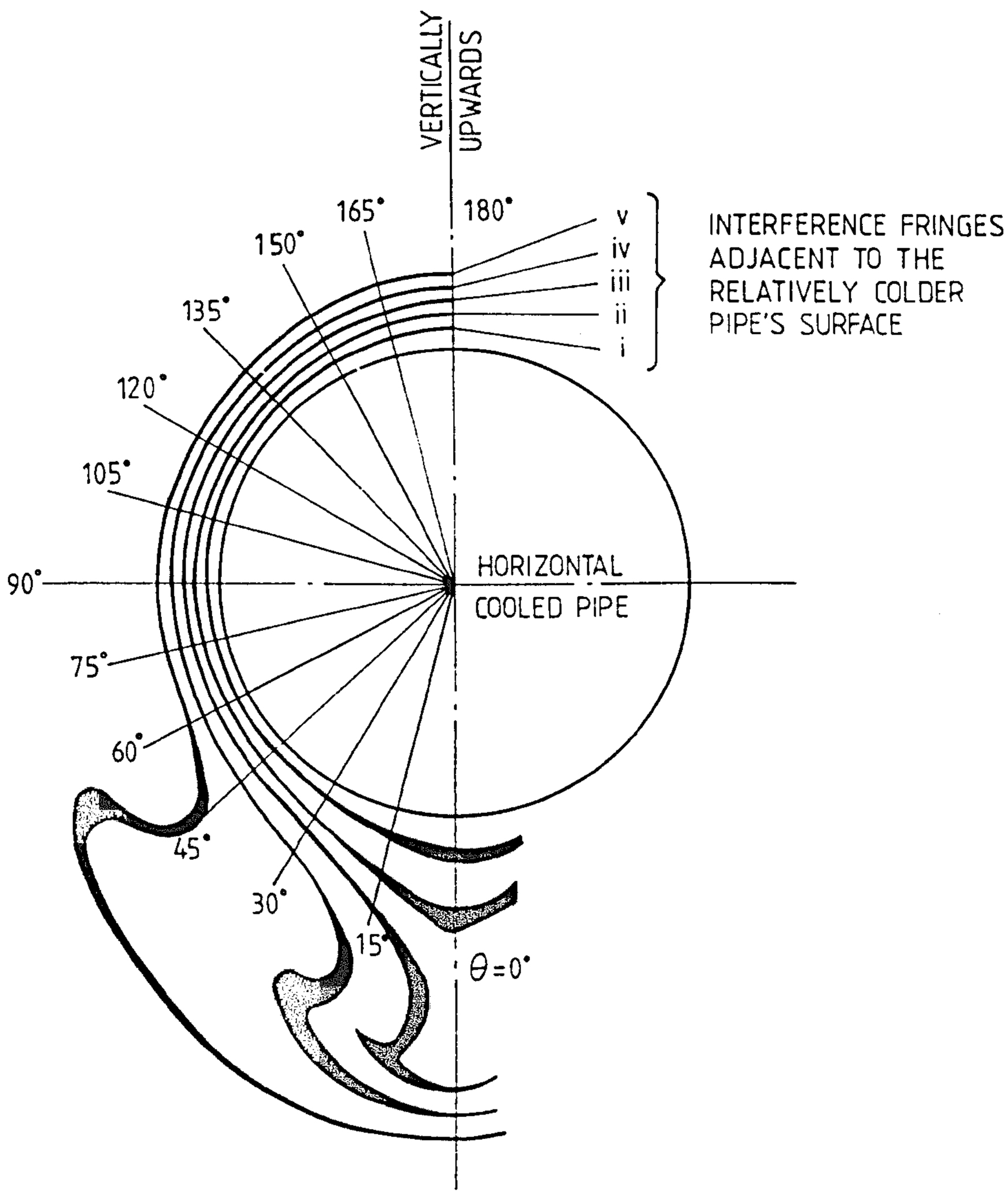

Fig. 7.2. A typical contour map of steady-state isotherms around a horizontal cooled pipe as revealed by Mach-Zehnder interferometry. The angular co-ordinate, θ, is measured from the vertically downwards radius vector for the supply pipe.

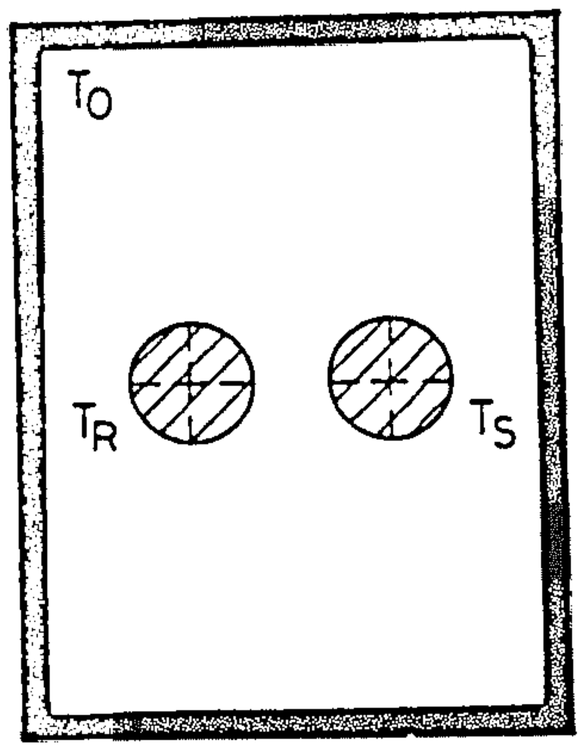

CONFIGURATION 1
($E_R = E_S = 0$)

$T_O > T_R > T_S$

HORIZONTAL

VERTICAL

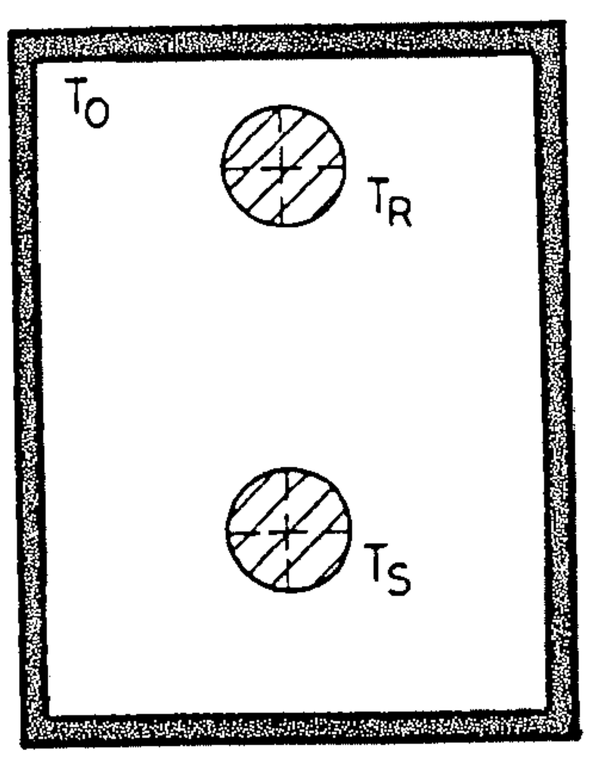

CONFIGURATION 2
($-0{\cdot}30 \leq E_R \leq 0$, $E_S = 0{\cdot}67$)

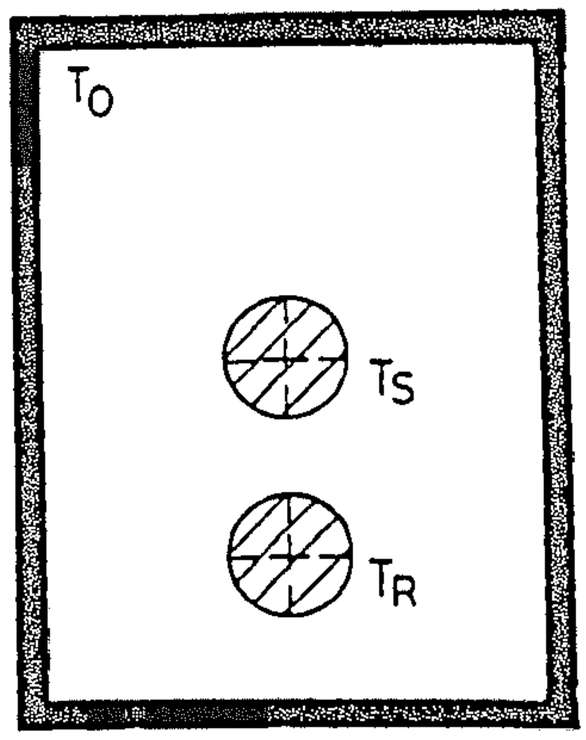

CONFIGURATION 3
($E_R = 0{\cdot}67$, $E_S = 0$)

Fig. 7.3. Schematic vertical sections perpendicular to the lengths of the experimental 'district cooling' horizontal pipeline systems tested.

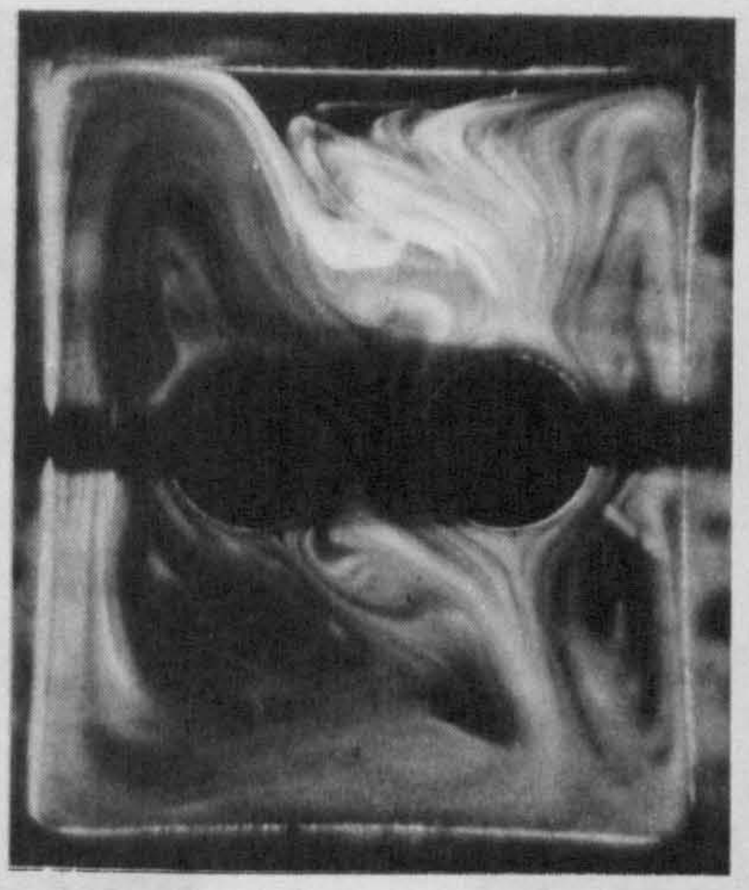

Fig. 7.4. Typical steady-state flow visualisations with, T_S = 10 °C, and T_R = 20 °C.

(a) $E_R = E_S = 0$

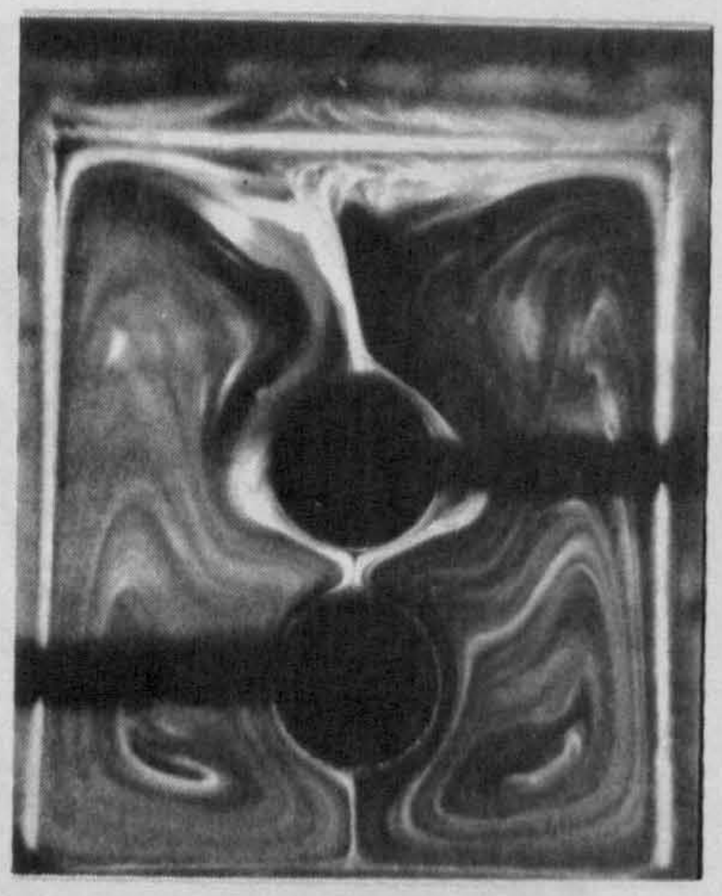

(b) $E_R = 0$, $E_S = 0.67$

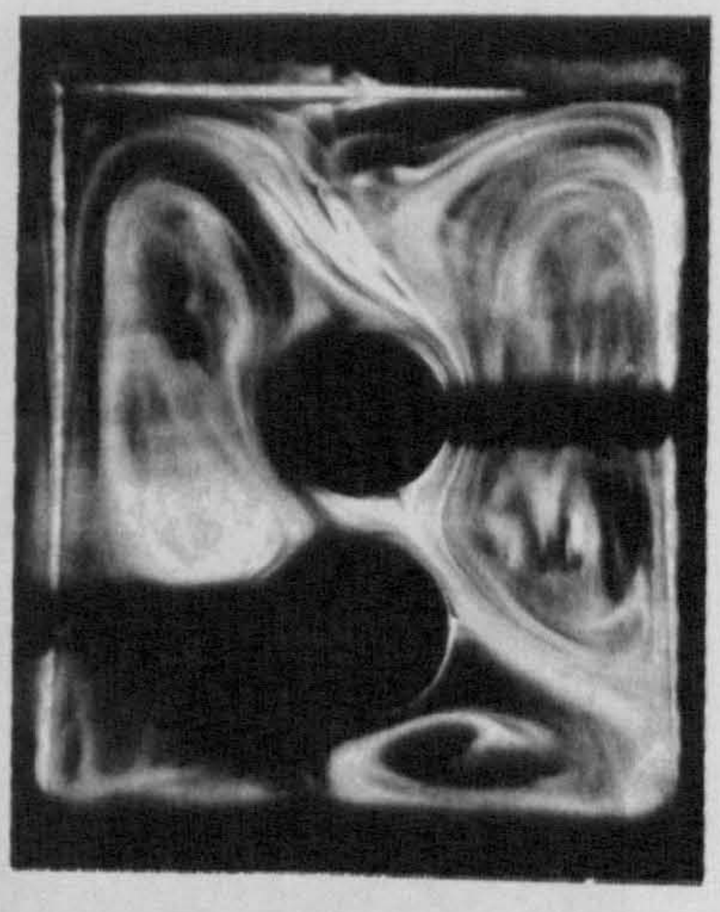

(c) $E_R = 0.67$, $E_S = 0$

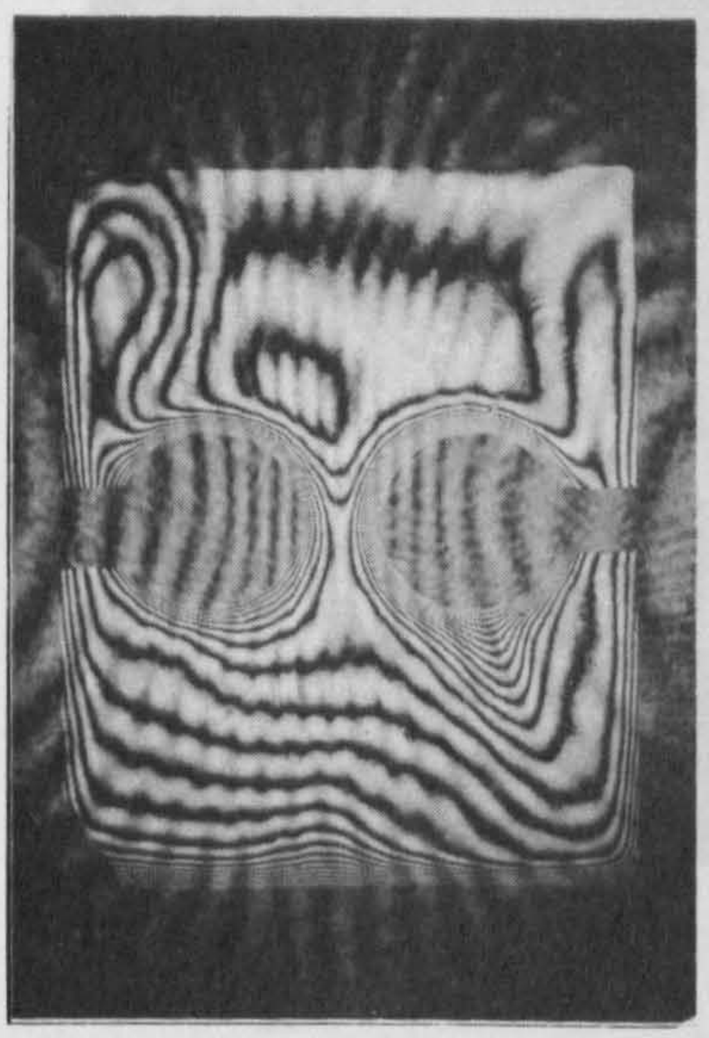

(a) $E_R = E_S = 0$

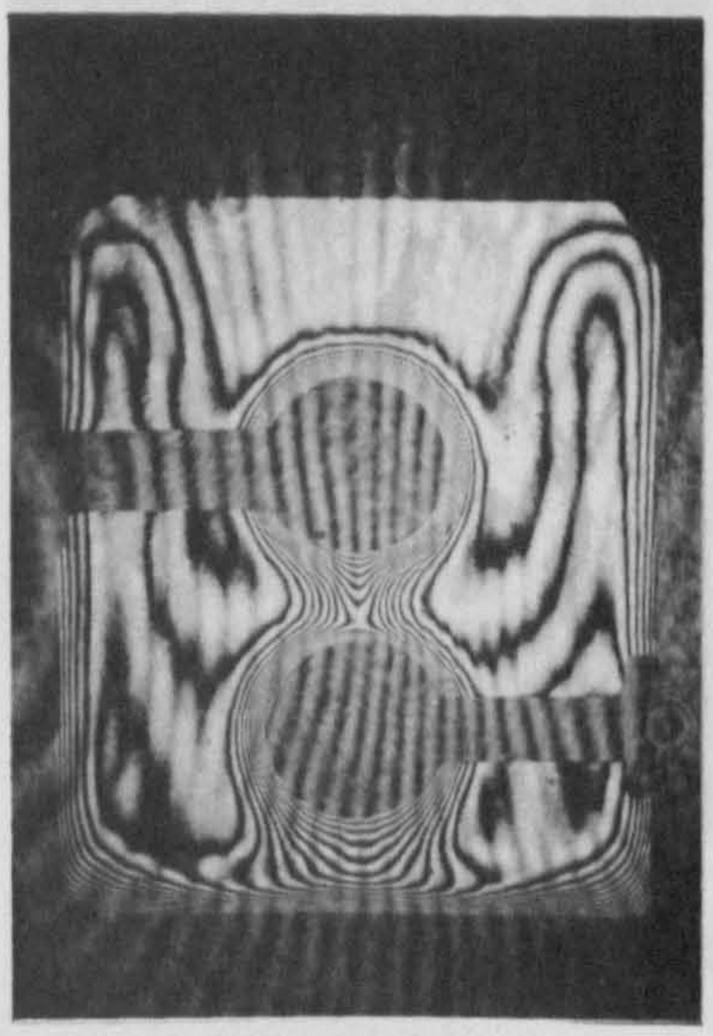

(b) $E_R = -0.30$, $E_S = 0.67$

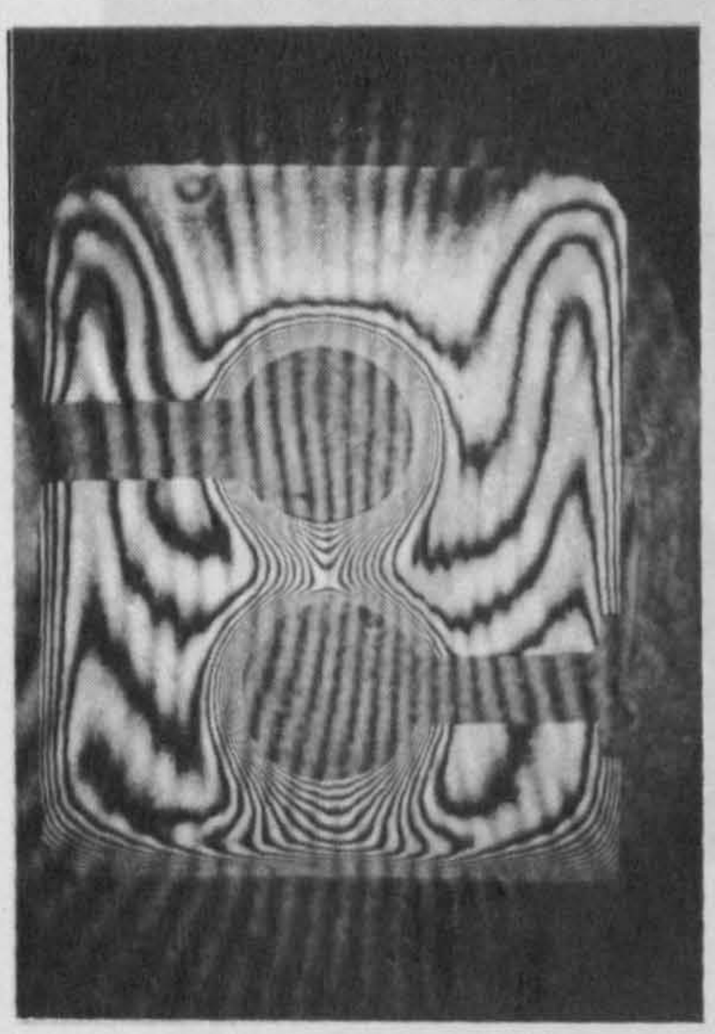

(c) $E_R = -0.25$, $E_S = 0.67$

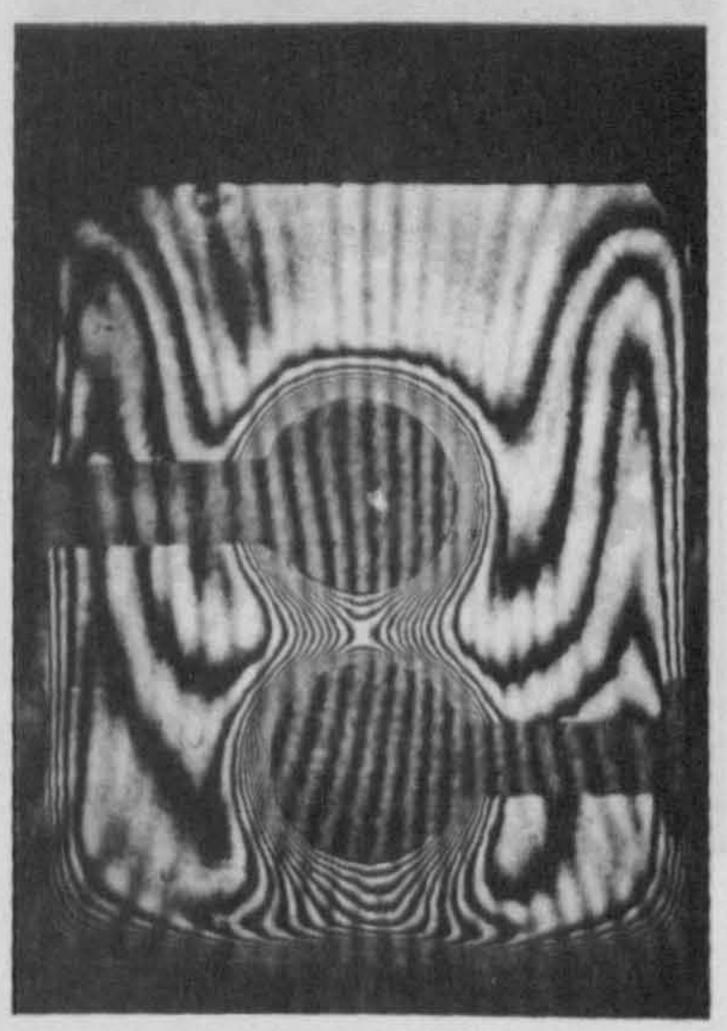

(d) $E_R = -0.20$, $E_S = 0.67$

Fig. 7.5. Typical steady-state Mach-Zehnder interferograms with, $T_S = 10\ ^{o}C$, and $T_R = 15\ ^{o}C$:

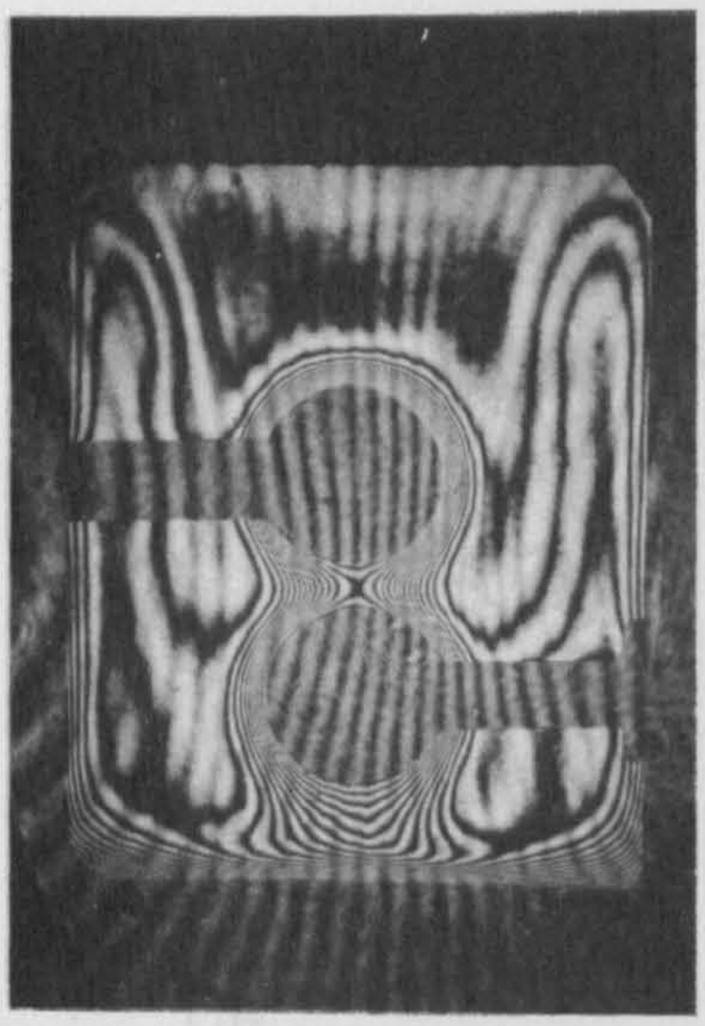

(e) $E_R = -0.15$, $E_S = 0.67$

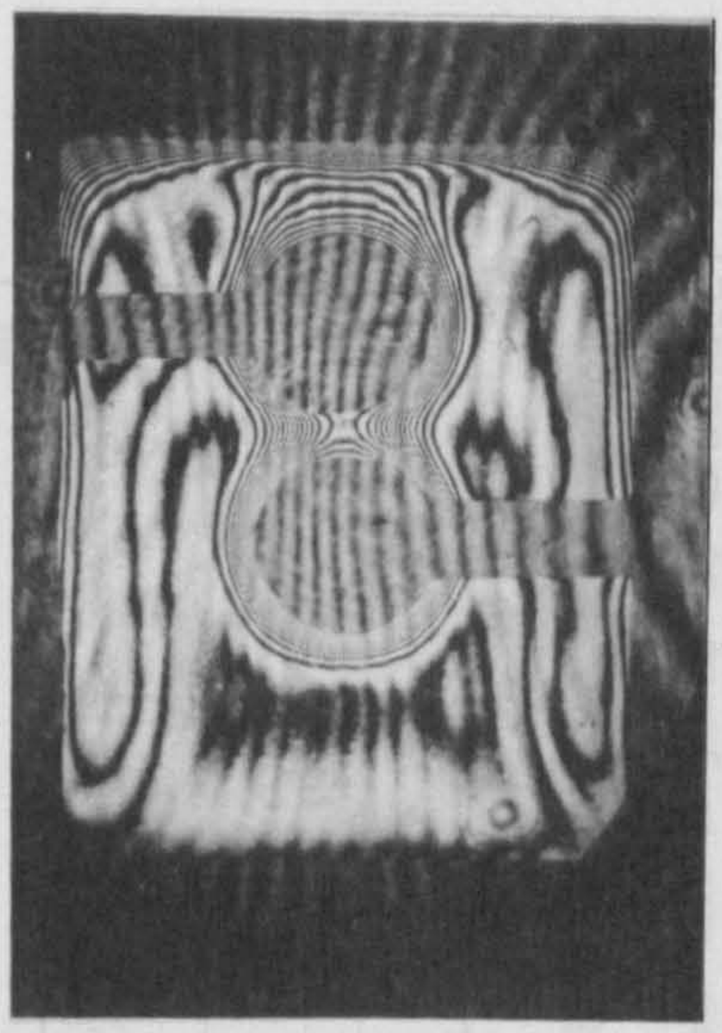

(f) $E_R = -0.10$, $E_S = 0.67$

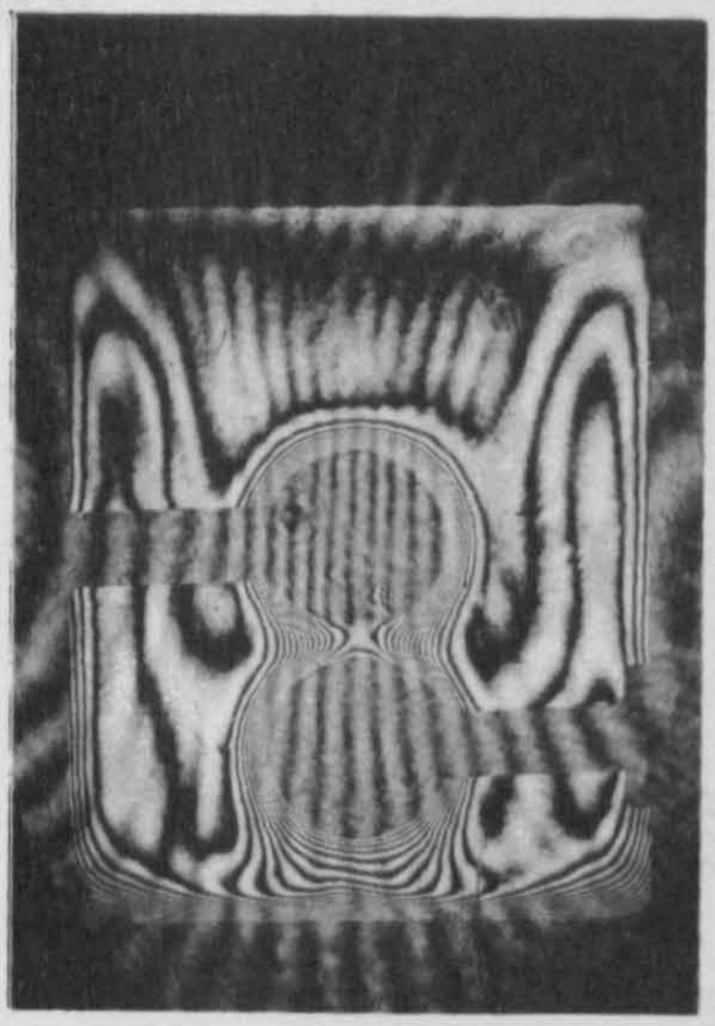

(g) $E_R = -0.05$, $E_S = 0.67$

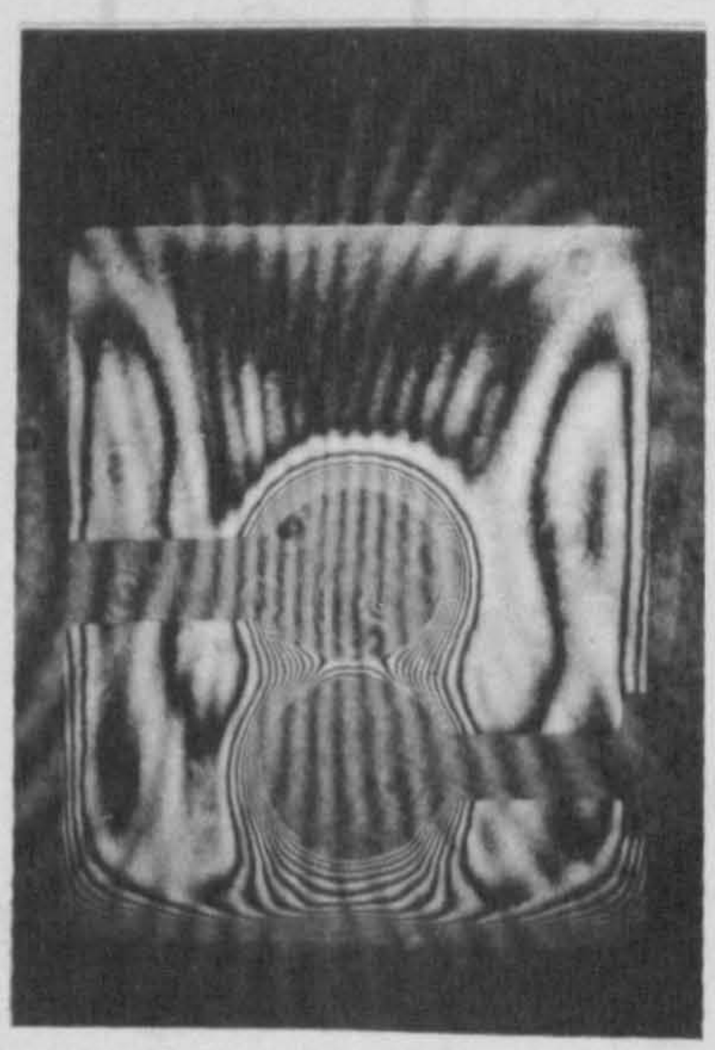

(h) $E_R = 0$, $E_S = 0.67$

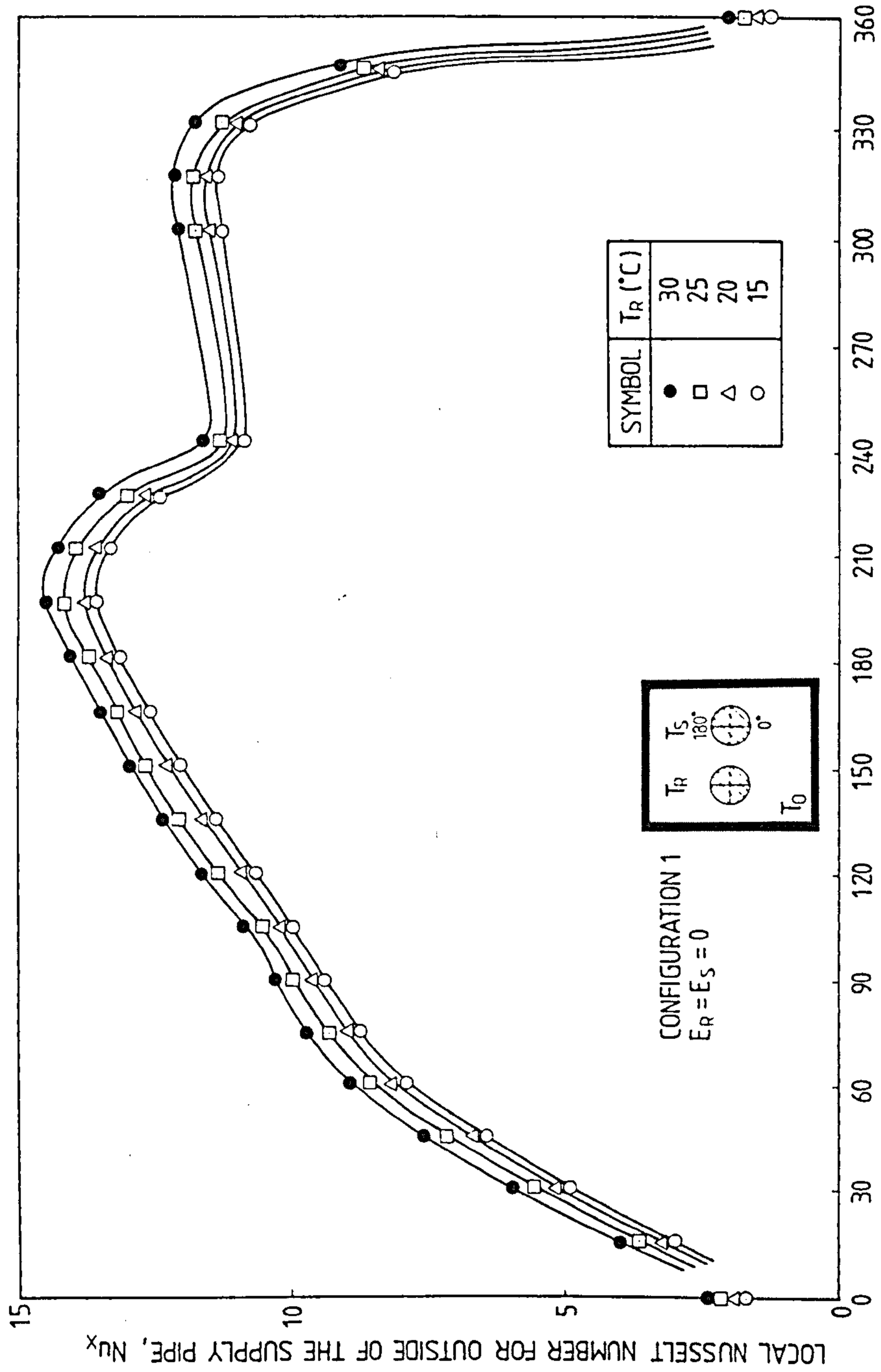

Fig. 7.6. Variation of the local Nusselt number, Nu_x, versus the angular co-ordinate θ, for the supply pipe, with $T_S = 10\ ^oC$:

(a) $E_R = E_S = 0$

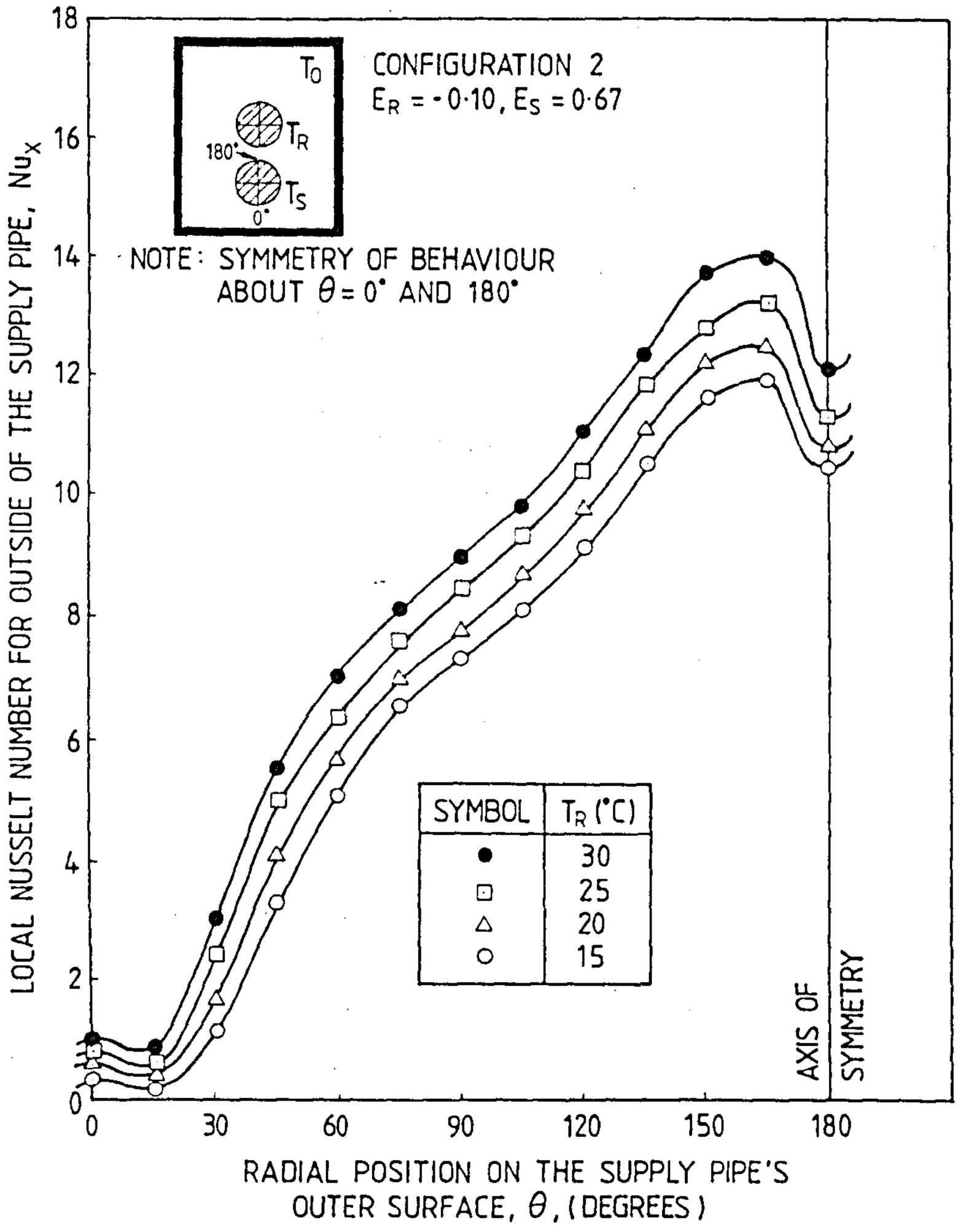

(b) $E_R = -0.10$, $E_S = 0.67$

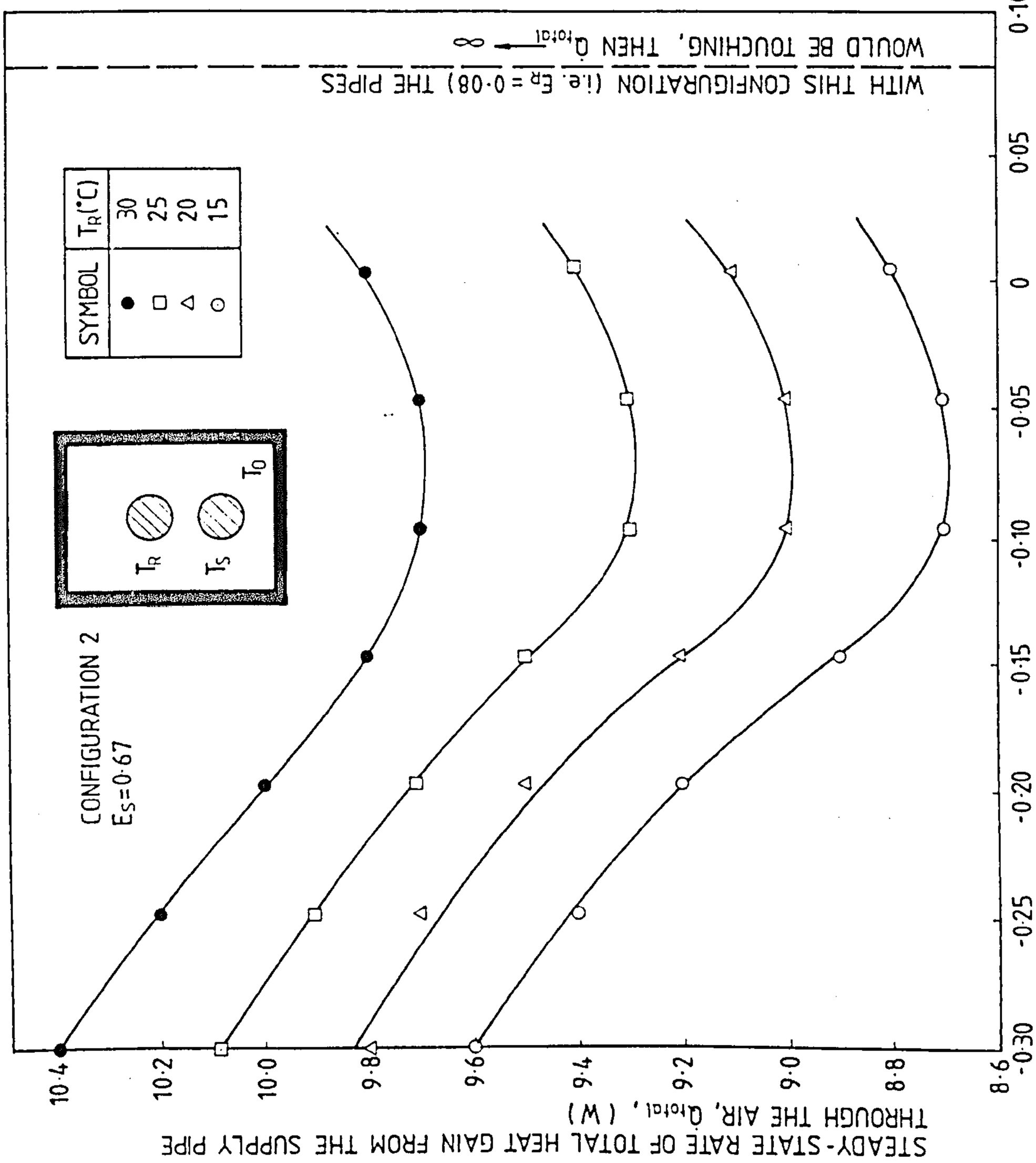

Fig. 7.7. Variation of the steady-state total heat gain, Q_{total}, versus the displacement ratio E_R for the warm-above-cold configuration, with T_S = 10 °C, and T_O = 35 °C.

CHAPTER 8

INFLUENCE OF BAFFLES UPON NATURAL-CONVECTIVE STEADY-STATE HEAT TRANSFERS INWARDS ACROSS HORIZONTAL ECCENTRIC ANNULI

SUMMARY

Flow patterns, temperature distributions and steady-state heat transfers inwards across a horizontal annular, atmospheric-pressure, air-filled eccentric cavity have been determined. Several different configurations of two, low-conductivity, baffles (arranged symmetrically with respect to the vertical plane through the centre lines of the pipes) inserted across the cavity and extending its whole length, were tested. With the horizontal inner pipe located at a vertical eccentricity of -0.65 (i.e. in the lower region of the outer pipe), the optimal inclination of the two baffles, corresponding to the least rate of convective heat exchange, was achieved at ± 140° from the vertically-downwards radius vector emanating from the centre of the inner pipe. This enabled a reduction of ~ 6 per cent in the steady-state convective heat leak to be achieved compared with that for the plain eccentric annulus under similar temperature differences between the pipes. However, by using a vertical baffle (i.e. at an angle of 0°), an increase of ~ 14 per cent in the convective heat leak through the air occurred. The results agree qualitatively with those expected on the basis of previous studies for the inverse case (of a concentric annulus) with the heat flowing outwards.

NOMENCLATURE

D Diameter of the outer (i.e. relatively hot) horizontal pipe, see Fig. 1, (m).

d — Diameter of the inner (i.e. relatively cold) horizontal pipe, see Fig. 1, (m).

e — Eccentricity of the configuration [= (H/G)], see Fig. 1: $-1 \leq e \leq 1$.

G — Mean gap size [= (D - d)/2], (m).

Gr_d — Grashof number for the convecting air, based on the diameter, d, of the inner pipe.

H — Vertical distance between the horizontal centre-lines of the two eccentric pipes, see Fig. 1, (m).

L — Axial length of the considered horizontal cavity, see Fig. 2, (m).

$Nu_G, \overline{Nu}_G$ — Local and average Nusselt numbers, respectively, for the steady-state heat transfers to the inner pipe, based on the average gap size, G.

Ra_G — Rayleigh number for the air flow, based on the average gap size, G.

T_o, T_s — Steady-state uniform temperatures of the inner surface of the outer pipe, and the outer surface of the inner pipe respectively, see Fig. 1, (°C).

ΔT Steady-state temperature difference [$=(T_o - T_s)$], (°C).

Θ Inclination of the baffles (or spacers), measured from zero for the vertically downwards radius vector, emanating from the centre of the inner pipe -- see Fig. 1, (degrees).

Suffixes

d with respect to the diameter of the inner pipe.

G with respect to the mean gap between the pipes.

o of the inner surface of the outer pipe.

s of the outer surface of the inner pipe.

HEAT TRANSFERS ACROSS THE ANNULUS, WITH BAFFLES ALONG ITS WHOLE LENGTH

In an annulus bounded by two horizontal pipes, which are maintained at different steady-state temperatures, radiation, conduction and natural convection through the air occur; the magnitudes of these heat-transfer components depending on the geometry of the annulus (e.g. the gap size, G, and the diameter ratio, D/d), the bounding surface finishes, as well as the temperatures of the pipes (i.e. T_o and T_s). The inner pipe is sometimes supported within the outer pipe by means of radial,

conical, or axial baffles. However the resulting obstructions of the annular space by such baffles will influence all three heat transfer modes: the effects of the baffles upon the radiation contributions for the range of temperatures considered in this investigation, however are relatively small.

Extensive experimental and theoretical studies concerning natural convection across plain annular cavities, between horizontal concentric or eccentric pipes, have been reported[1]. Unfortunately there is a dearth of available published information about the heat-transfer changes which result from the presence of baffles across air-filled cavities[2-6]. Nevertheless, such baffles are used in solar-energy collectors[7], compressed-gas insulated electric power cables[8], fusion-reactor blankets[9], and district-heating and cooling pipelines[10,11].

Grigull and Hauf[2] considered a concentric annulus, containing air, with three equally-spaced balsa wood baffles (i.e. either at $\Theta = 0°$, 120° and 240°, or at $\Theta = 60°$, 180° and 300°) between an inner and an outer pipe. Turbulent flows in the obstructed annular cavities, of diameter ratios of 2, 3 and 4 were investigated by Lis[3] using either six evenly-spced (i.e. at $\Theta =$ 30°, 90°, ... etc.) longitudinal baffles or a single helical spacer; the cavity being filled with various $SF_6 - N_2$ gas mixtures. Both designs, it was alleged, reduced the natural convection rate by ~ 20% compared with that for the same annulus when unobstructed, across which the same temperature difference was applied. No satisfactory explanations were given to justify

either the observed reduction of the heat transfer rate at mode-rate Rayleigh numbers, or the subsequent ineffectiveness of the baffles at high values of Ra_G.

Shilston and Probert[4] concluded that a reduction by ~ 11% of the steady-state convective plus conductive rate of heat flow through the air occurred as a result of using two horizontal radial co-planar spacers at $\Theta = \pm 90°$, across an open-ended con-centric annular cavity (with D/d = 1.5). Because the flows in the steady-state are symmetric with respect to the vertical plume through the centre-lines of the pipes, it was expected erroneous-ly that the presence of vertical spacers should not affect the convective contribution to the heat transfer. However, it was found that the use of vertical spacers increased this heat trans-fer rate by ~ 8%.

To optimise the performance of a solar collector, the differ-ence between the rates of insolation absorbed and heat lost in-effectively by the collector tube has to be maximised. Minimising the latter requires that the thermal resistance of the air surrounding the collector tube should be a maximum. So, to achieve the least steady-state rate of heat loss across the atmospheric-pressure air in a concentric horizontal cavity between a heated inner pipe and a naturally-cooled surrounding pipe (with D/d = 1.6), Norton and Probert[5], following a series of experimental tests, concluded that the radial supports along the length of the cavity should be at approximately $\Theta = \pm 30°$ from the vertically downwards position. A maximum reduction of

~ 25% in the convective heat leak was achieved by employing such a design compared with that for the plain cavity, under the identical small values of ΔT considered.

Kwon et al[6] studies, both experimentally and theoretically, the natural convcction which ensue across an annulus between concentric horizontal pipes (for $1.5 \leq D/d \leq 3.6$) using three equally-spaced (i.e. either at $\Theta = 0°$, 120° and 240°, or at $\Theta =$ 60°, 180° and 300°) axial spacers. A thin-fin approximation was used to predict (via two-dimensional finite-difference numerical computations) the temperature distributions in the air boundary layers along the surfaces of the spacers. It was concluded that the presence of low-conductivity spacers could lead to decreases in the natural convection by as much as 20% (according to the configuration adopted) below that for the corresponding plain unobstructed annulus aross which the same ΔT was applied: the rate of heat transfer being less for the " 3-spacers Λ " configuration than for the " 3-spacers Y " type for heat travelling outwards across the air cavity. Nevertheless even with significant reductions in convection, the use of high thermal conductivity baffles, and the resulting conduction through them, can lead to a rise in the total heat leak across the cavities.

THE PRESENT INVESTIGATION

It has been established[12] that the optimal location, to achieve maximum thermal insulation, of a cold pipe when enclosed by a relatively warm annular cavity occurs for an eccentricity,

e, equal to -0.65. The aim of this study was to determine the optiml position of a pair of radial wooden spacers (or baffles) bridging the gap between the isothermally heated outer pipe and the optimal-eccentricity placed, relatively cool isothermal inner pipe. This system could simulate a buried, insulated, pipe-in-pipe district-cooling assembly. Several configurations were examined and investigations were carried out to determine if such spacers could improve the thermal resistance of the optimal air-filled cavity over that of the unobstructed annulus. Steady-state isothermal contour maps (i.e. inerferograms with the Mach-Zehnder interferometer used in the infinite-fringe manner) were photographed. Qualitative analyses of the flow visualisations were used to suggest and to substantiate the quantitative explanations obtained from the corresponding interferograms.

THE TEST RIGS

The chosen values of the experimental parameters were:-

$$D = 140.5 \text{ or } 108.0 \text{ mm}$$

$$d = 42.5 \text{ or } 28.5 \text{ mm}$$

$$e = -0.65$$

$$L = 610.0 \text{ mm}$$

$$15 \text{ °C} \leq T_o \leq 42 \text{ °C}$$

$$7 \text{ °C} \leq T_s \leq 19 \text{ °C}$$

$$3 \text{ °C} \leq \Delta T \leq 30 \text{ °C}$$

Each of the measured temperatures was accurate to ± 0.2 °C, and the stated dimensions to ± 0.2 mm.

(i) Interferometry

The experimental assembly consisted of two hollow pipes, one within the other, mounted rigidly, but with a means for changing the vertical position of the inner pipe relative to the outer one. The latter (with D = 140.5 mm) was rolled from a 1.2 mm thickness (18 SWG) mild-steel sheet. Shellac-insulated copper wires were wound uniformly in a tightly-grouped helical spiral around its external surface. A second layer of such wires was wound on top of the first, and connected in series electrically so that the same electric current passed through it in the reverse direction to that in the first layer. Thereby non-inductive heating was achieved.

A guard-heater, also in the form of a cylindrical coil around the outside of the heater on the outer pipe, was used to help maintain a uniform temperature distribution over the surface of that pipe. Two variable transformers (each of 750 VA), one for the main heating coil, and the other for the guard heater were employed, together with two transformers (each of 750 VA), to control the power dissipations in the heating wires, and consequently the rate of inward heat transfer to the inner pipe. The outer pipe was protected by a further coat of shellac.

The inner copper pipe (having d = 42.5 mm) was supported by means of horizontal hollow tubular extensions at its two ends: these tubes also conveyed the relatively cold water (at temperature T_s) into and out of the inner pipe. A controlled-temperature water supply was used. The tubular extensions were clamped to two vertical brackets, along which the clamps could be moved up or down in unison, by identical amounts, thus altering the eccentricity, e, of the horizontal inner pipe relative to the horizontal outer pipe.

Sixteen copper-constantan thermocouples were introduced through 1.5 mm holes in the outer pipe, so that the leads and thermojunctions remained flush with its inner surface. Ten of the thermojunctions were located on a circumferential helix at approximately equal radial intervals, so permitting the temperature distribution over the inner surface of the outer cavity wall to be determined. The inner pipe was similarly instrumented.

The thin radial baffles or spacers (3mm thick at their edges touching the outer pipe and tapering off to 1 mm at their tips touching the inner pipe) were made of balsa wood which has a low thermal conductivity (~ 0.12 W/mK): they were positioned to span the eccentric (e = -0.65) air-gap along its whole length (see Fig. 3). The horizontal atmospheric-pressure air-filled cavity was closed at its two ends by means of two vertical, optically-flat, uniformly-thick, homogeneous glass plates -- the so-called 'end-plates' (see Fig. 2).

An 18 cm field-of-view, 3 mW He-Ne laser-stimulated, Mach-Zehnder interferometer was used as the temperature-field indicating instrument[13] -- see Fig. 2. This, when employed in the infinite-fringe mode, produced distinctive interferograms, which are isotherm maps of the air-filled cavity, for each two-dimensional configuration examined with each set of values of T_o and T_s employed. (These interferograms indicated the refractive index, and hence the density and consequently the temperature, variations of the air integrated over the axial length of the considered cavity). The effects of image distortion, due to the refraction of the laser beam through the test cell, were reduced by focussing the camera on the vertical plane at 0.33L from the end-plate nearer the camera[14].

(ii) Flow Visualisations

These were obtained with a rig having a horizonal outer cylindrical Perspex pipe (with D = 108 mm), which had been painted matt black, except for a narrow circumferential slit window (~ 5 mm wide at 0.33L from the end-plate nearer the camera). This pipe was heated by circulating hot water at a constant temperature (T_o) through a polythene tube, which was wrapped uniformly, in the form of a single layer closely-wound spiral, around the pipe. The design and construction of the inner copper pipe (d = 28.5 mm) were qualitatively similar to those for the pipe used in the interferometric measurements.

Steady-state tempertures of the surfaces of the pipes were monitored by eight copper-constantan thermocouples embedded, as previously indicated, in the inner surface of the outer pipe and four similar thermojunctions embedded on the outer surface of the inner pipe, so that the air flows in the annulus were not disrupted by their presence.

The end plane, which was remote from the camera, of the cavity was sealed with a vertical opaque Perspex plate, whereas the front end (through which the observations were made) was blocked by a uniformly-thick, homogeneous, vertical transparent glass plate. A small amount of smoke was injected very slowly into the cavity and photographs were taken of the resulting steady-state flow patterns, the appropriate illumination being introduced transversely from three halogen projectors via the thin circumferential slit window in the outer pipe. In order to avoid the inner cylinder partially obscurring the flow patterns, the camera was aligned so as to make a small angle with the horizontal axis of the inner cylinder. This nevertheless results in some distortion of the images.

THE OBSERVATIONS

(i) Flow-Visualisation Studies

Baffles, when introduced into a natural-convective flow field, can obstruct the paths of the air currents and so distort the shapes of the vortex patterns. The main flow cores rotated

symmetrically, about the vertical plane through the centre-lines of the pipes, in opposite directions, one in each half of the annulus.

With the baffles at $\Theta = \pm 30°$ (see Fig. 4(a)), the flow indicated the presence of a weaker than normal (i.e. with no spacers present) flow-circulation in the top sectorial cell. However this minor reduction in the flow intensity (and hence in the rate of heat transfer) was more than compensated for by a stronger recirculating flow in the relatively small lower compartment (i.e. between the baffles). For baffle positions throughout $\pm 45° \leq \Theta \leq \pm 120°$, the intensity of the recirculating eddies decreased in the lower sector as Θ increased, so leading to a reduction in the rate of heat transfer, while the flow weakened in the upper sector (see Fig. 4(b)).

With the baffles at $\Theta = \pm 140°$, the air movements observed in the lower compartment approximated to the flows in the unobstructed eccentric annulus under similar temperature differences across the air-filled gap. Simultaneously, the circulating flow in the upper compartment of the annulus was relatively weak (see Fig. 4(c)).

With the pair of baffles arranged vertically (i.e. at $\Theta = 0°$ and 180°), two small, almost stagnant zones adjacent to the middle of the upper baffle on its two sides were observed (see Fig. 4(d)).

(ii) Interferometric Studies

For all the arrangements of baffles tested, the fringe-patterns (i.e. the steady-state temperature contour maps) were different from those for the plain unobstructed annulus under identical values of ΔT. Selected samples of these interferograms, along with that for the plain annulus, are presented in Fig. 5. Such results indicate that the distribution of the local Nusselt number, Nu_G, around the cold inner pipe varied significantly near the baffles.

Generally, for configurations of baffles such that $\pm 45° \leq \Theta \leq \pm 120°$, the values of the local Nusselt number were relatively small for regions adjacent to the upper part of the spacers, whereas near the undersides of the spacers, they attained higher values (see Fig. 6(a→c)). This behaviour was caused by the differences of strengths of the recirculating flows above and below the spacers.

As the inclination of the spacers was increased to $\Theta = \pm 150°$ from $\Theta = \pm 120°$, no major qualitative changes, in the steady-state fringe patterns of the interferograms were observed. The weak recirculating flow in the upper sector kept the local Nusselt numbers (i.e. the rates of heat transfer) relatively small. However in the lower sector of the air-filled cavity, the local Nusselt numbers gradually approached those for a plain unobstructed annulus (see Fig. 6(d)).

When the pair of baffles were arranged vertically (i.e. at Θ = 0° and 180°), the interferograms do not show significant deviations from those for the upper part of the plain annulus -- see Fig. 5(a) and (f). However, the presence of boundary layers on the baffles tends to affect the convective heat leaks. This phenomenon coupled with the air flow deflection by the baffles, result in them having significant influence on the local heat transfer coefficients (see Fig. 6(e)).

The effect of the inclination Θ of the spacers, upon the total rate of convective heat transfer travelling inwards across an eccentric, horizontal, air-filled annulus can be seen in Fig. 7. The optimal location for a pair of radial spacers occurred approximately at $\Theta = \pm$ 140°. By employing such a configuration, a saving of ~ 6% in the steady-state convective heat transfer across the annulus was achieved compared with that for a plain annulus. However, by using one vertical spacer (i.e. at Θ = 0°), an increase of ~ 14% in the convective heat leak was observed compared with that for the plain annulus under otherwise identical conditions.

Conclusions drawn from the present set of results corroborate those from previous studies for the case of concentric annulus with the heat flowing outwards, i.e. for the inverse, vertically-inverted heat transfer system. For example, for a solar-energy collector, Norton and Probert[5], concluded that the optimal location of the spacers should be at $\Theta = \pm$ 30°.

CONCLUSIONS

There is an optimal configuration, for two, low-conductivity baffles (spacers or supports) inserted symmetrically across the whole length of an eccentric annulus, whose use leads to the least rate of convective heat gain being achieved by the cold inner pipe. With the two baffles inclined at an angle of $\Theta = \pm 140°$, improvements of ~ 6 per cent in the thermal resistance of the air-filled cavity were obtained compared with that for a plain annulus. However, with the baffle placed vertically (i.e. at $\Theta = 0°$), an increase of ~ 14 per cent in the heat leak was observed, once again compared with that for the plain annulus under an almost identical ΔT (see Fig. 7). Results from the present study agree qualitatively with those for a concentric annulus, with the heat flowing outwards. In practice, there is often likely to be another pipe in the cavity, i.e. that acting as the return pipe for the non-ambient temperature fluid, and the external enclosure may be rectangular rather than cylindrical. Then somewhat different flow patterns and isothermal contours in the cavity would be expected, and so further investigations in order to determine the optimal placements of both sets of baffles would be needed.

REFERENCES

1. R.F. Babus'Haq, S.D. Probert and M.J. Shilston, Natural convection across cavities: design advice, Applied Energy, 20(3), 1985, pp. 161-188.

2. U. Grigull and W. Hauf, Authors' rebuttal, Natural convection in horizontal cylindrical annuli, Proc. 3rd. Int. Heat Transfer Conf., Chicago, Discussion Volume, 1966, pp. 159-160.

3. J. Lis, Experimental investigation of natural convection heat transfer in simple and obstructed horizontal annuli, Proc. 3rd. Int. Heat Transfer Conf., Chicago, Paper 61, 2, 1966, pp. 196-204.

4. M.J. Shilston and S.D. Probert, Effects of horizontal and vertical spacers on the heat transfer across a horizontal, annular, air-filled cavity, Applied Energy, 4(1), 1978, pp. 21-37.

5. B. Norton and S.D. Probert, Thermal insulation of a low capital cost solar-energy collector, Applied Energy, 6(4), 1980, pp. 323-327.

6. S.S. Kwon, T.H. Kuehn and T.S. Lee, Natural convection in the annulus between horizontal circular cylinders with three axial spacers, Trans. ASME, J. Heat Transfer, 104(1), 1982, pp. 118-124.

7. A.C. Ratzel, C.E. Hickox and D.K. Gartling, Techniques for reducing thermal conduction and natural convection heat losses in annular receiver geometries, Trans. ASME, J. Heat Transfer, 101(1), 1979, pp. 108-113.

8. J.A. Hitchcock and M.J. Thelwell, The cooling of underground EHV transmission cables, Trans. IEEE, Power Apparatus and Systems, 87(1), 1968, pp. 129-134.

9. P.J. Gierszewski, B. Mikic and N.E. Todreas, Natural circulation in fusion reactor blankets, ASME paper 80-HT-69, 1980.

10. R.F. Babus'Haq, S.D. Probert and M.J. Shilston, Steady-state heat losses from horizontal pipes in an air-filled rectangular concrete duct, Proc. I. Mech. E., Eng. Sci., 199(C3), 1985, pp. 203-213.

11. R.F. Babus'Haq, S.D. Probert, M.J. Shilston and S. Chakrabarti, Optimising the location of a district-cooling pipeline in a rectangular trench, Applied Energy, 23(2), 1986, pp. 109-141.

12. S. Chakrabarti, S.D. Probert and M.J. Shilston, Optimal eccentric annuli (containing atmospheric-pressure air) for thermally-insulating, horizontal, relatively cold pipes, Applied Energy, 14(4), 1983, pp. 257-293.

13. R.F. Babus'Haq, S.D. Probert and M.J. Shilston, Optimal location of a single horizontal pipeline in a rectangular, horizontal, air-filled enclosure to achieve maximum thermal insulation, Applied Energy, 18(4), 1984, pp. 239-259.

14. J.M. Mehta and W.Z. Black, Errors associated with the measurement of convective heat transfer coefficients, Applied Optics, 16(6), 1977, pp. 1720-1726.

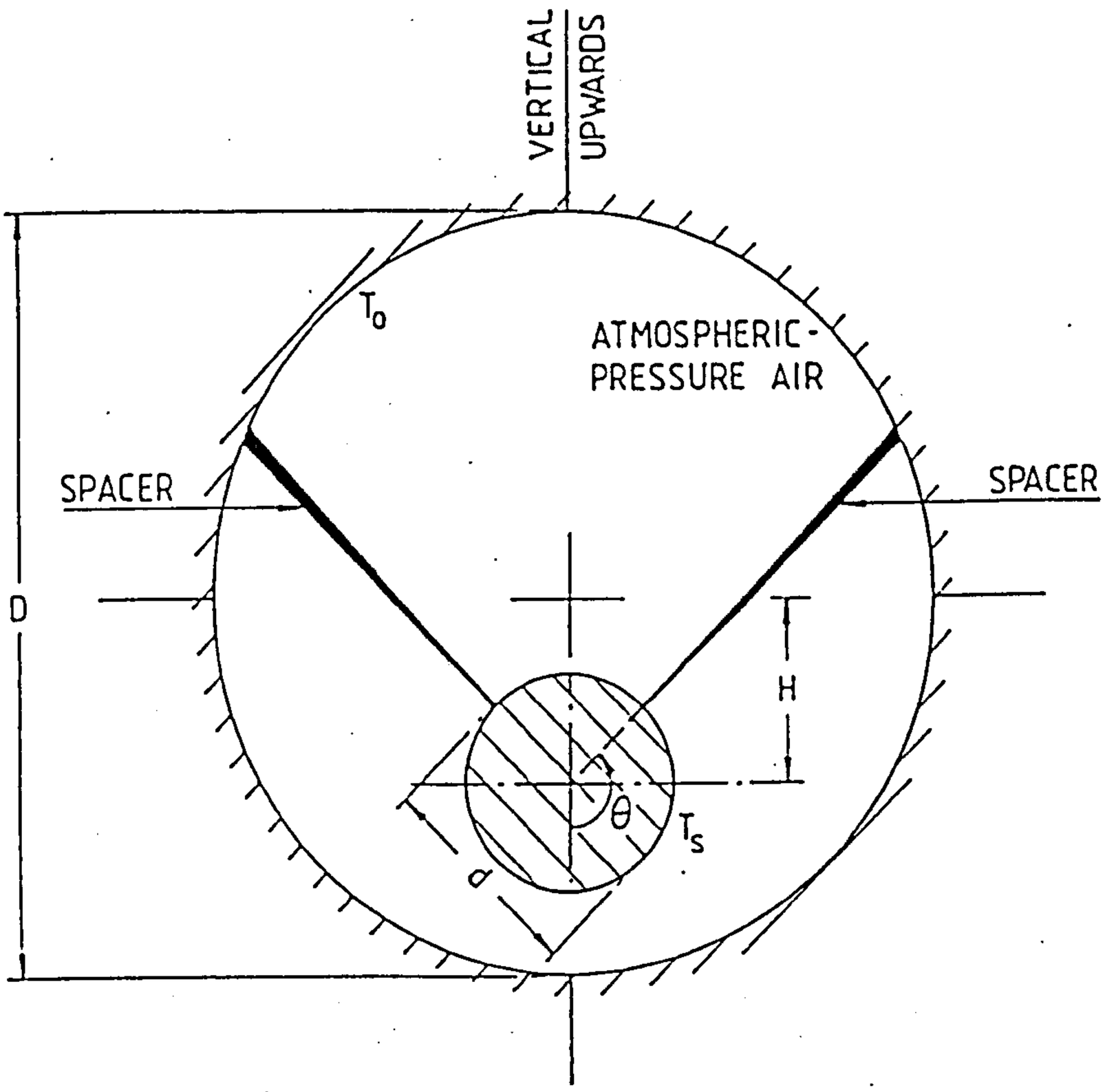

Fig. 8.1. Schematic representation of a vertical cross-section through the considered horizontal pipe aligned with a negative eccentricity relative to its horizontal circular enclosure.

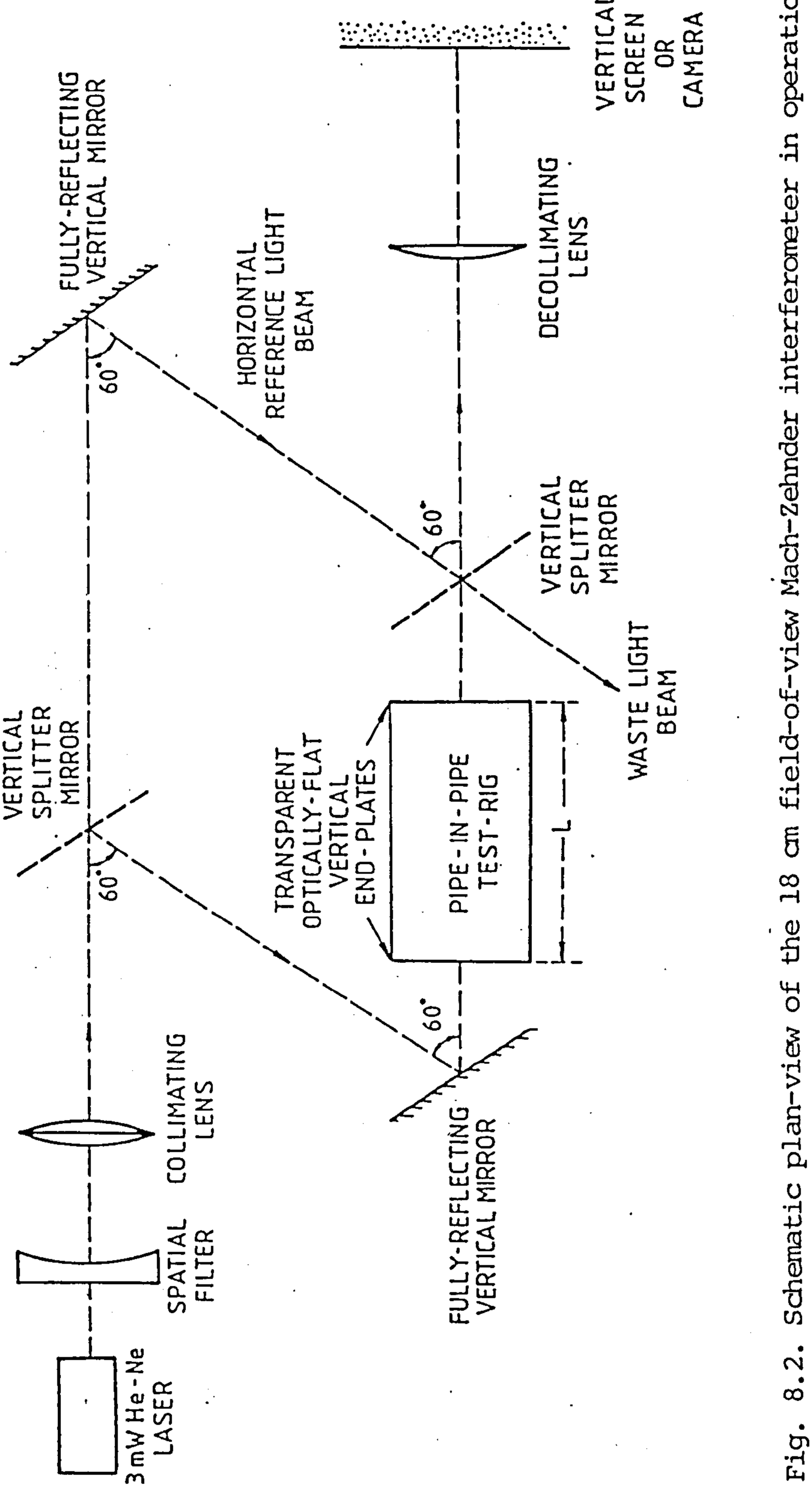

Fig. 8.2. Schematic plan-view of the 18 cm field-of-view Mach-Zehnder interferometer in operation.

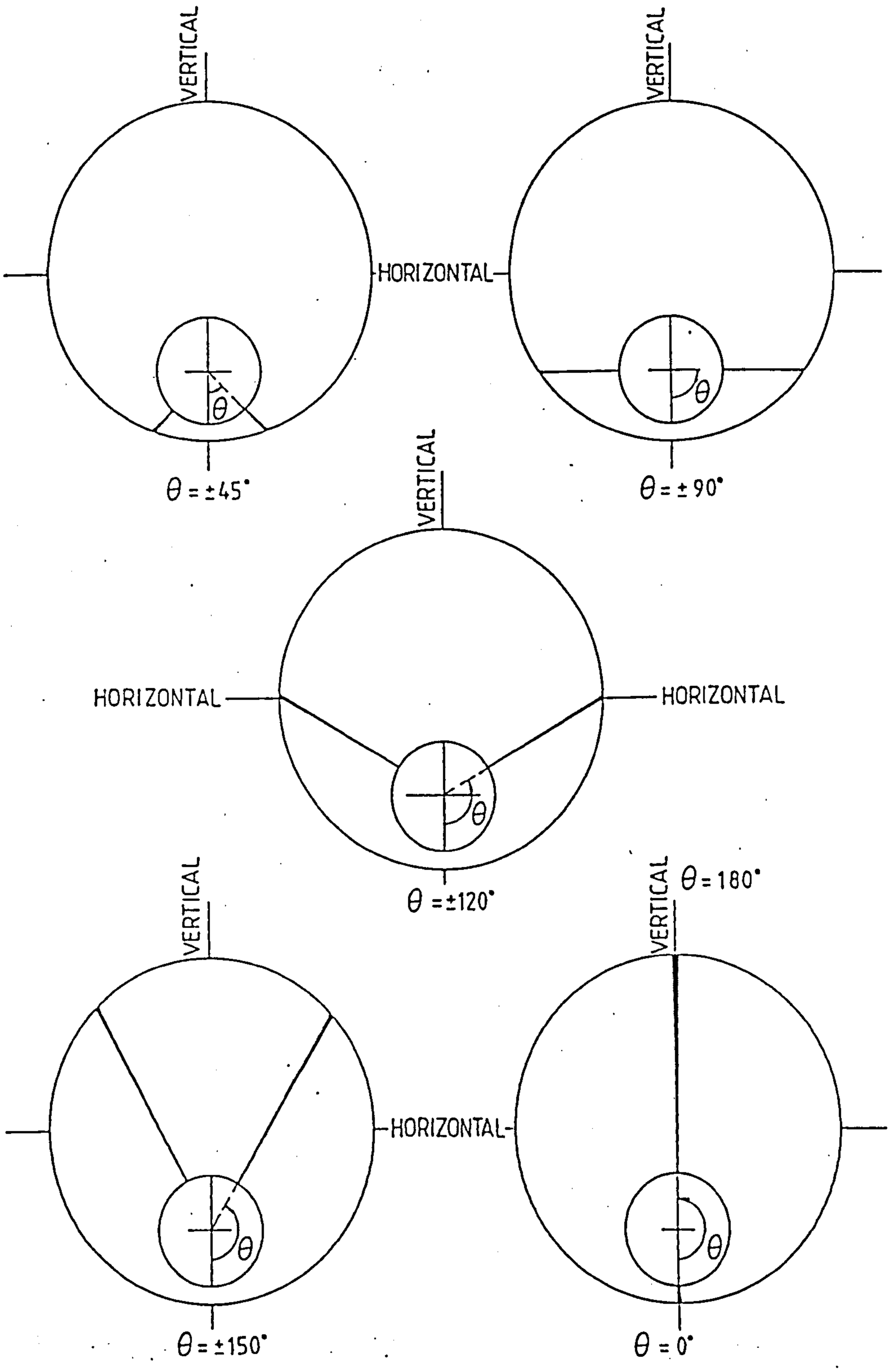

Fig. 8.3. Vertical cross-sections perpendicular to the lengths of some of the considered horizontal pipeline systems (all with e = - 0.65).

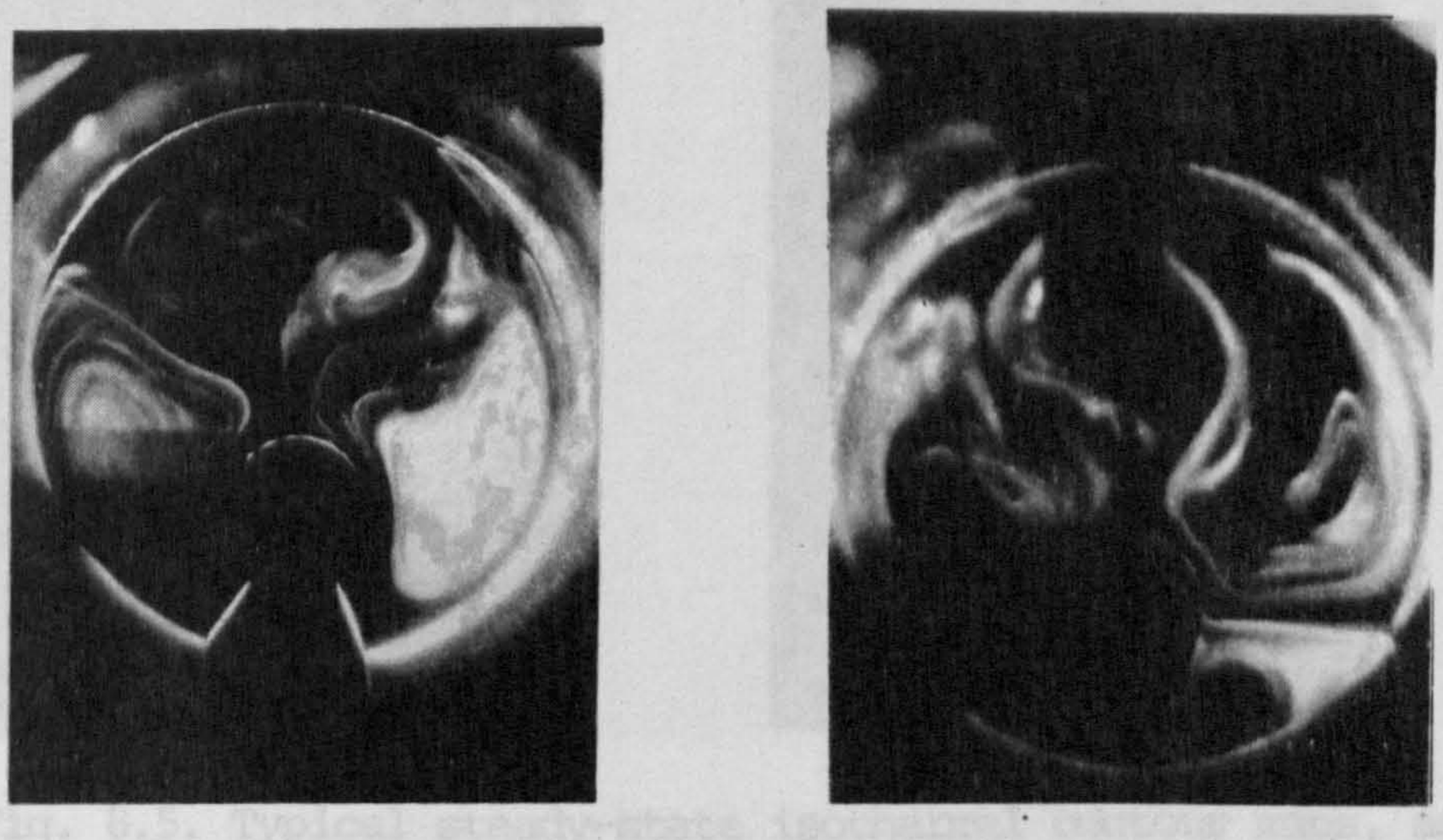

Fig. 8.4. Typical steady-state flow visualisations for some of the considered systems with e = - 0.65:
(a) $\Theta = \pm 30^{o}$, $T_s = 14.3\ ^{o}C$, $\Delta T = 4.0\ ^{o}C$.
(b) $\Theta = \pm 85^{o}$, $T_s = 13.7\ ^{o}C$. $\Delta T = 11.3\ ^{o}C$.
(c) $\Theta = \pm 140^{o}$, $T_s = 11.8\ ^{o}C$, $\Delta T = 12.9\ ^{o}C$.
(d) $\Theta = 0^{o}$ and 180^{o}, $T_s = 12.5\ ^{o}C$, $\Delta T = 6.0\ ^{o}C$.

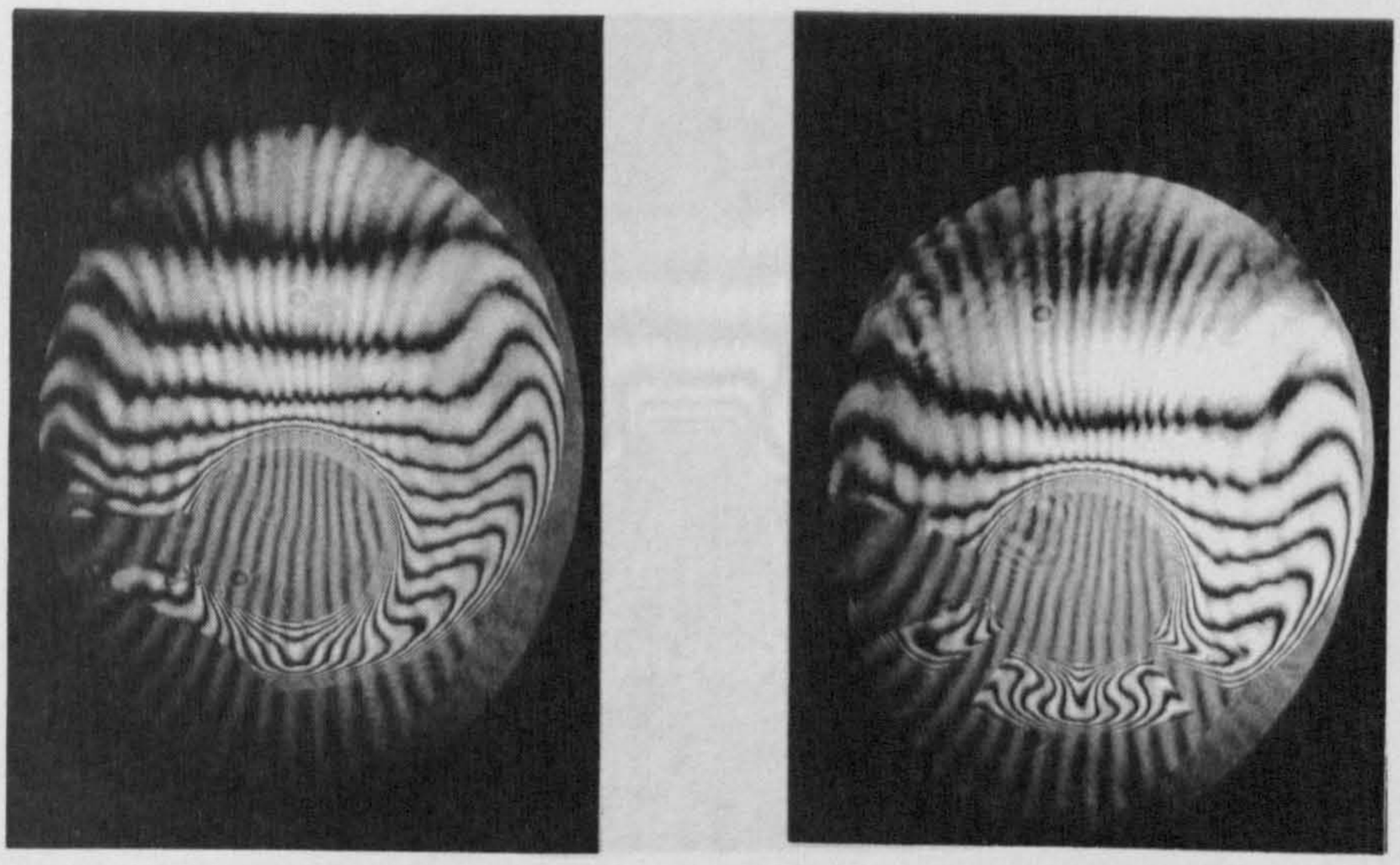

Fig. 8.5. Typical steady-state isothermal contour maps, as indicated by infinite-field Mach-Zehnder interferograms for the considered systems with e = - 0.65: (a) Plain cavity, T_s = 7.7 °C, ΔT = 15.6 °C. (b) $\theta = \pm 45^{\circ}$, T_s = 7.7 °C, ΔT = 9.7 °C. (c) $\theta = \pm 95^{\circ}$, T_s = 7.4 °C, ΔT = 15.8 °C. (d) $\theta = \pm 120^{\circ}$, T_s = 7.6 °C. ΔT = 16.1 °C.

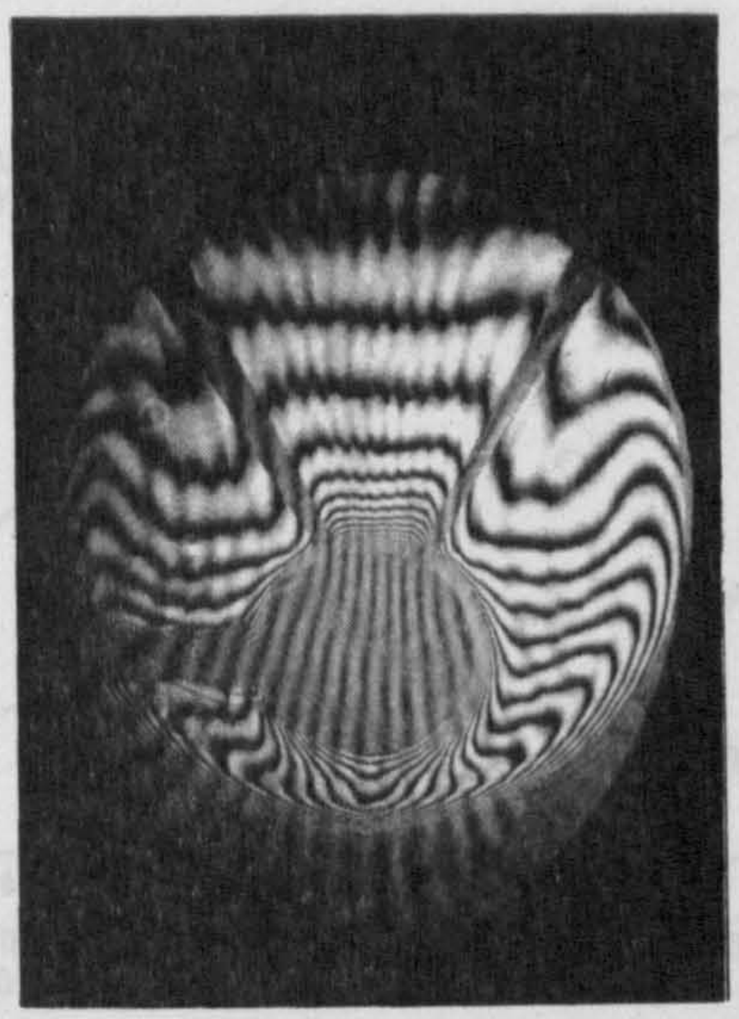

(e) $\Theta = \pm 150^{\circ}$, $T_s = 7.2\ ^{\circ}C$, $\Delta T = 15.0\ ^{\circ}C$.

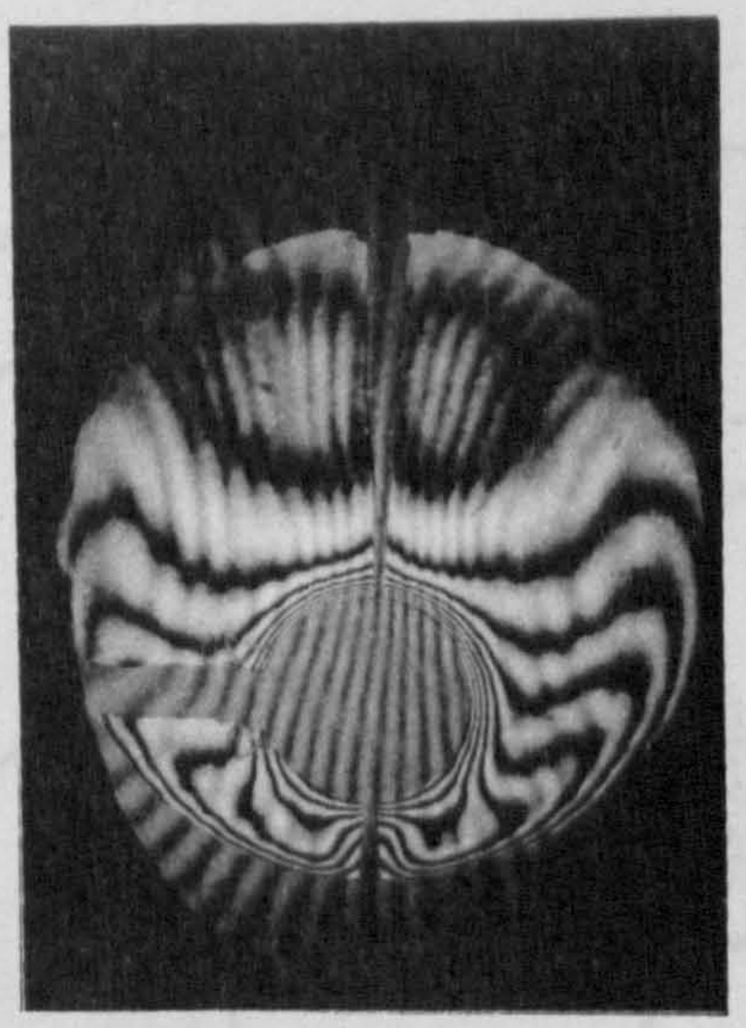

(f) $\Theta = 0^{\circ}$ and 180°, $T_s = 7.6\ ^{\circ}C$, $\Delta T = 8.3\ ^{\circ}C$.

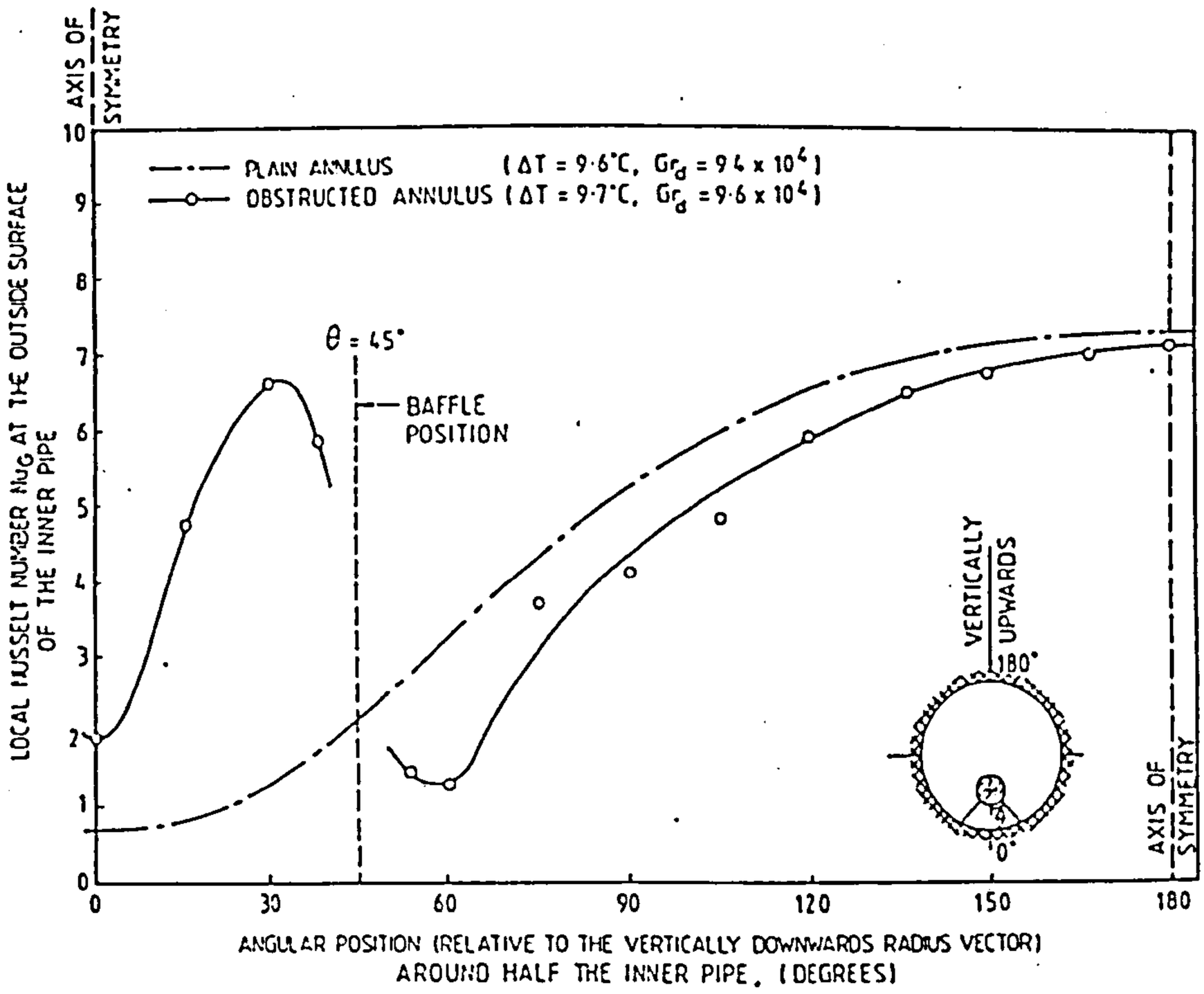

Fig. 8.6. The variation of the local Nusselt number over the surface of the inner pipe, which is aligned at an eccentricity of - 0.65 with its horizontal outer pipe:

(a) $\Theta = \pm 45^{o}$

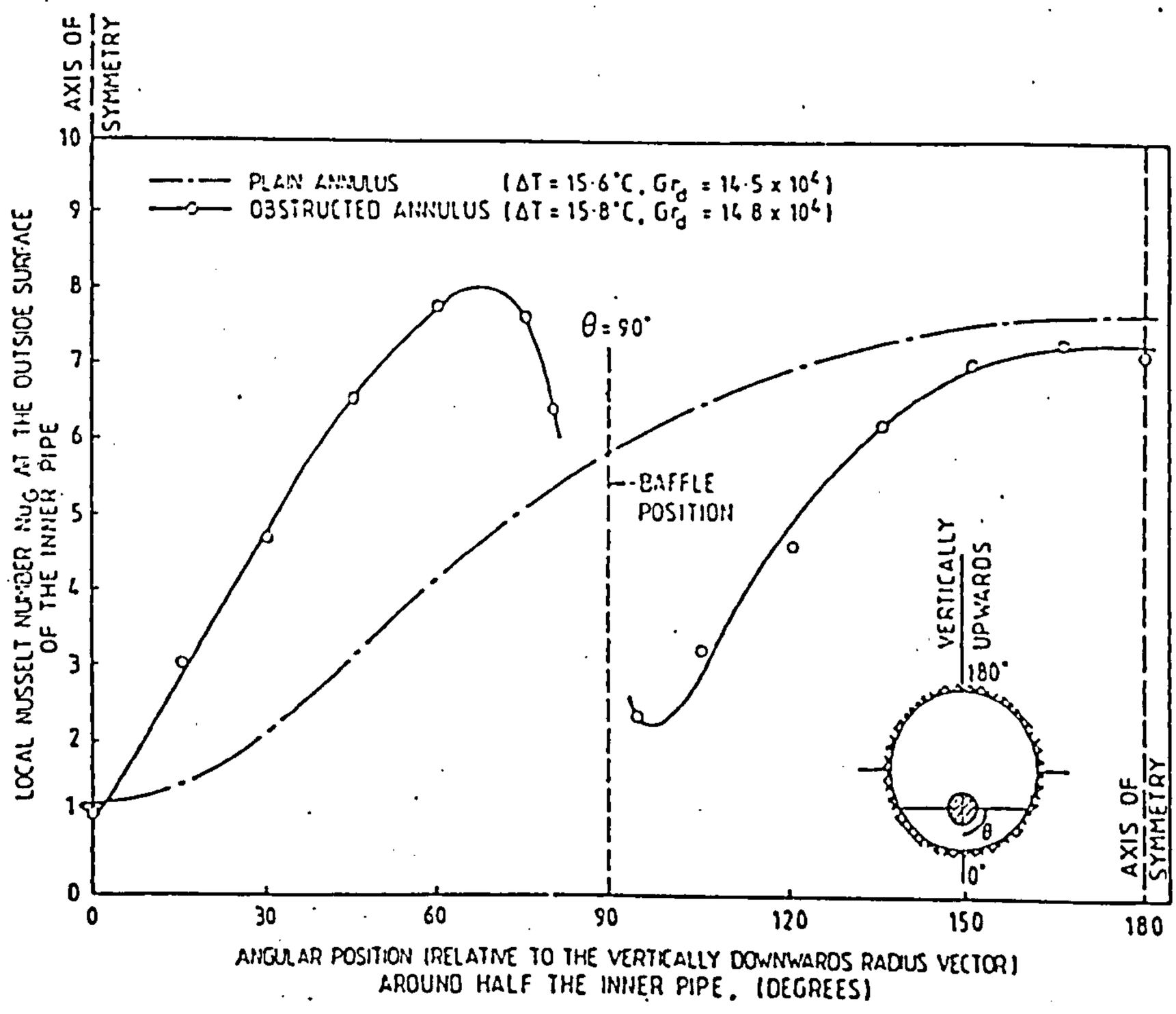

(b) $\Theta = \pm 90^{o}$

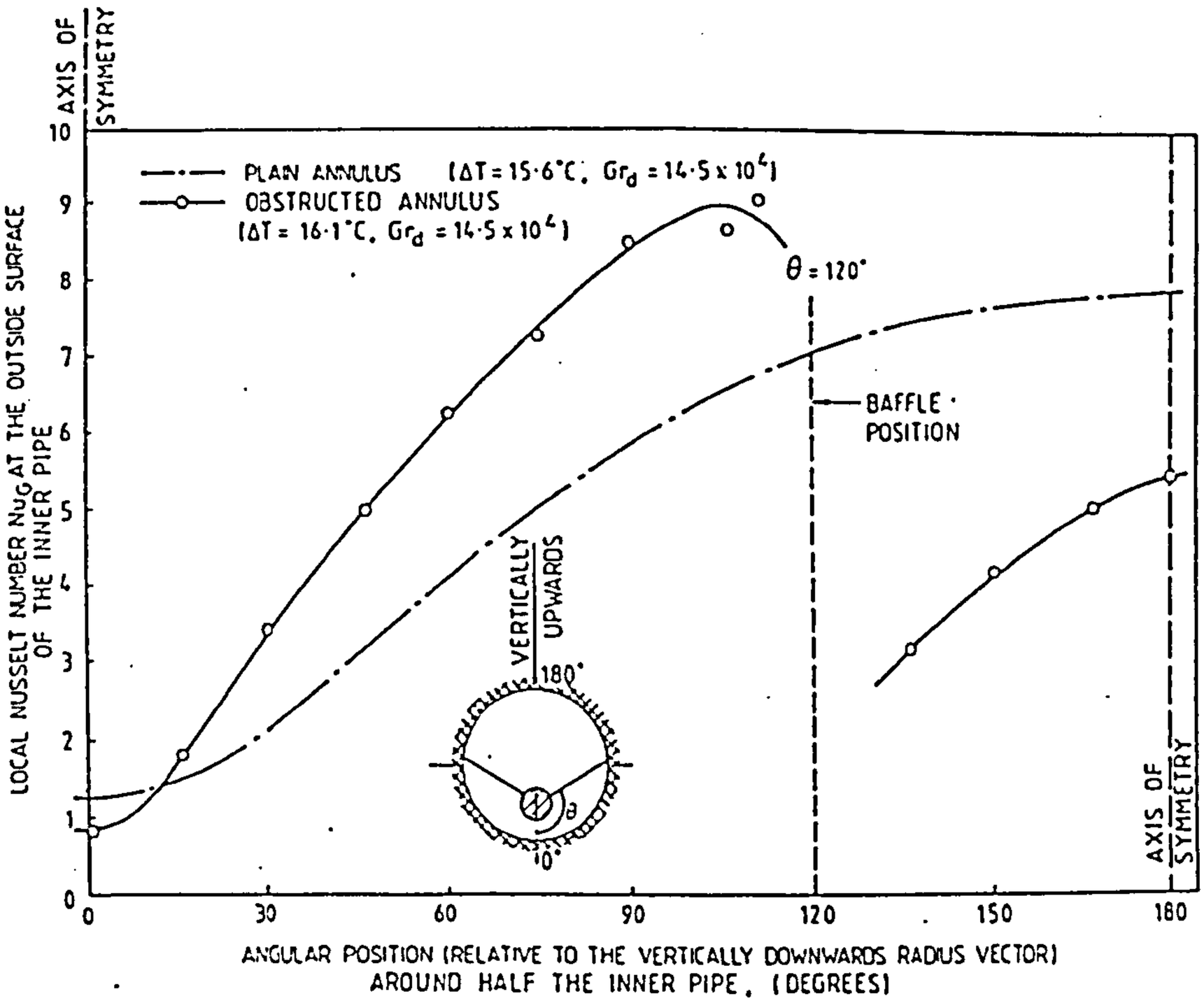

(c) $\Theta = \pm 120^{0}$

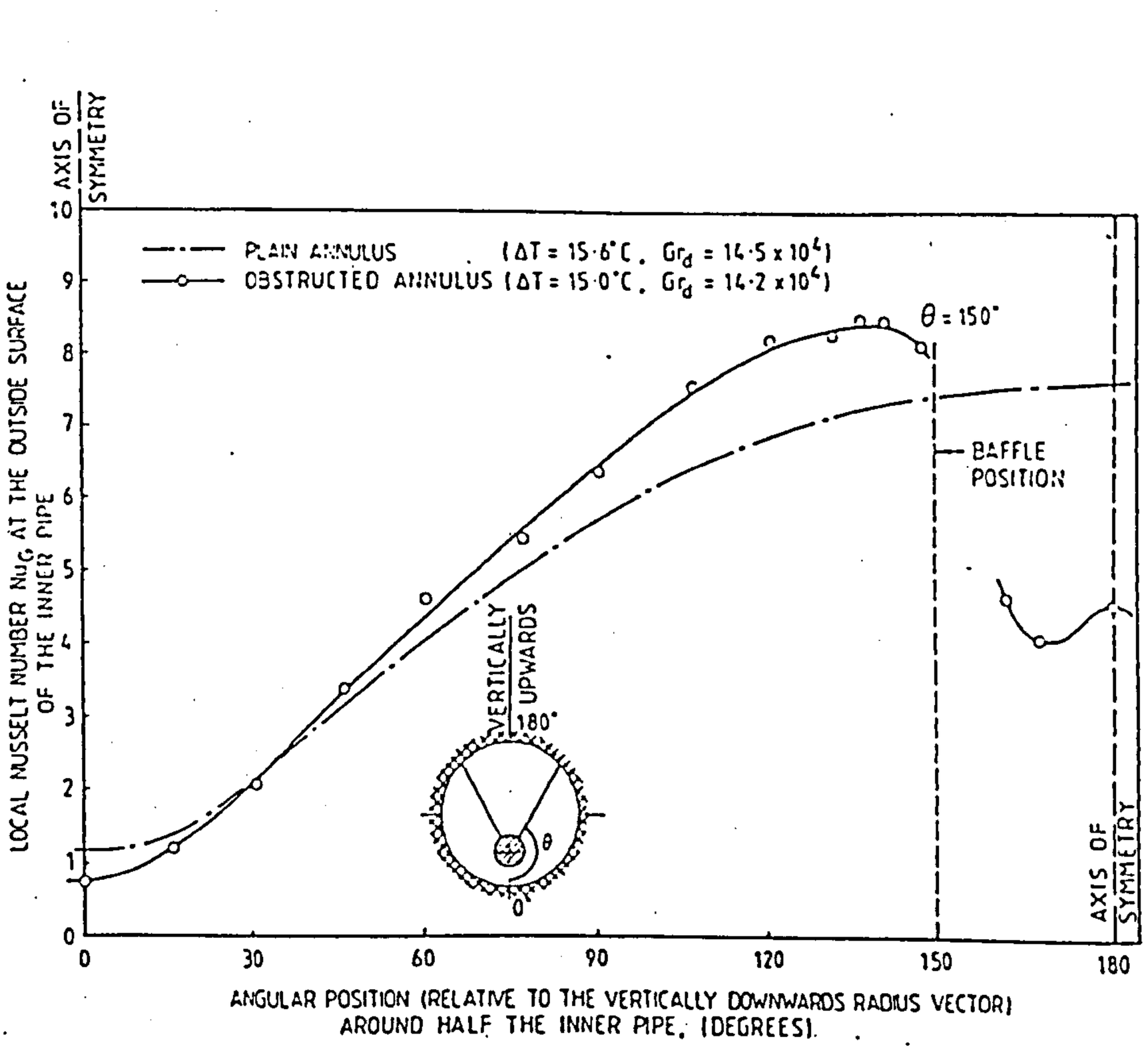

(d) $\Theta = \pm 150^{0}$

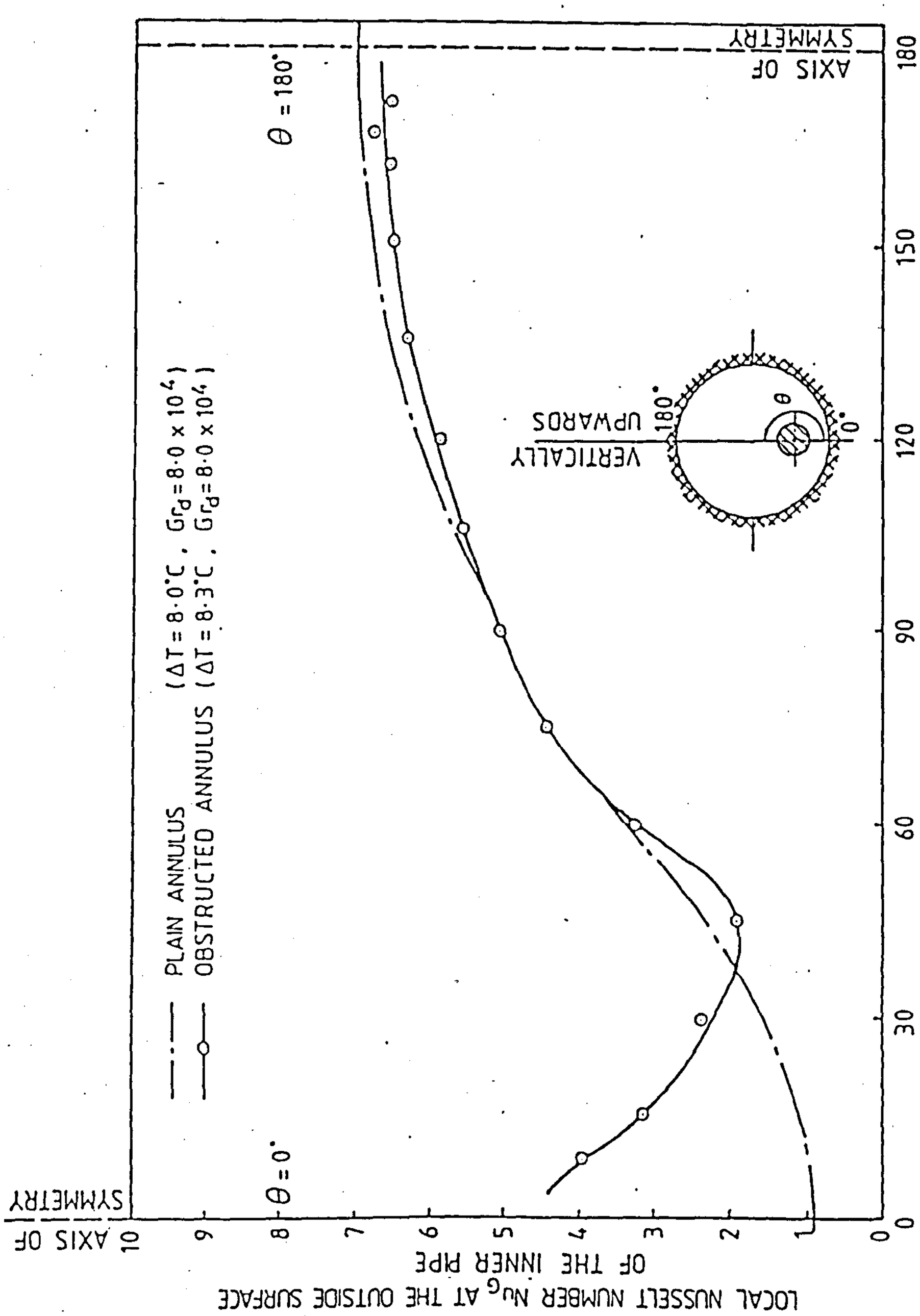
LOCAL NUSSELT NUMBER Nu_G AT THE OUTSIDE SURFACE OF THE INNER PIPE
(e) $\Theta = 0^o$ and 180^o
ANGULAR POSITION (RELATIVE TO THE VERTICALLY DOWNWARDS RADIUS VECTOR AROUND HALF THE INNER PIPE, (DEGREES)
PLAIN ANNULUS (ΔT = 8·0°C, $Gr_d = 8·0 \times 10^4$)
OBSTRUCTED ANNULUS (ΔT = 8·3°C, $Gr_d = 8·0 \times 10^4$)
$\Theta = 180°$
AXIS OF SYMMETRY
VERTICALLY UPWARDS
Θ
$180°$
$0°$
$\Theta = 0°$
AXIS OF SYMMETRY

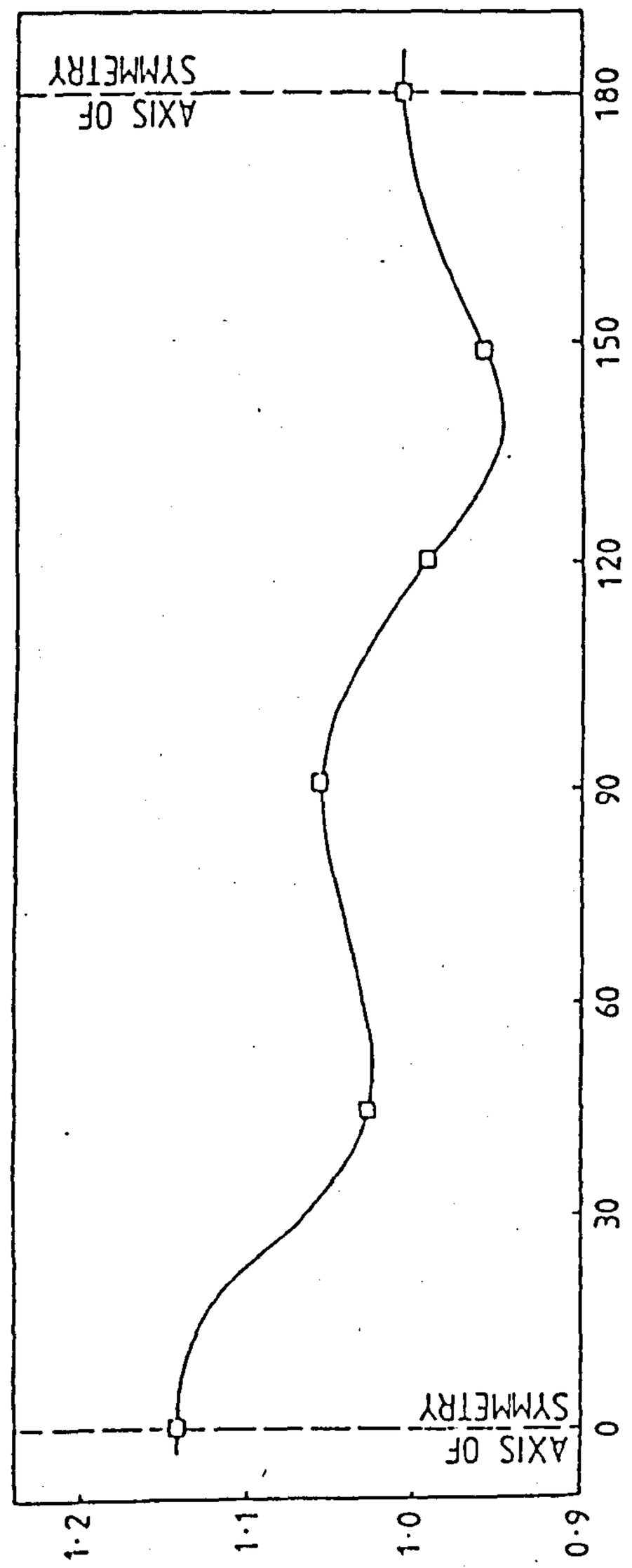

Fig. 8.7. Variation of the ratio of the average Nusselt numbers for the inner pipe with and without baffles present for e = - 0.65. With respect to the 0^0 and 180^0 data presented, only one baffle (rather than two) was employed in order to obtain these measurements.

APPENDIX 1

GEOMETRIC VIEW FACTORS FOR RADIATION EXCHANGES BETWEEN AN INFINITELY-LONG CYLINDER AND A PARALLEL INFINITELY-LONG ENCLOSURE OF EITHER CYLINDRICAL OR RECTANGULAR CROSS-SECTION

SUMMARY

The view (or shape) factor for an infinitely-long cylinder, enclosed in either a parallel cylindrical or rectangular enclosure, is independent of the relative disposition of the inner cylinder with respect to the enclosure or the dimensions of the system. Its value is unity.

NOMENCLATURE

A Surface area of the considered length of cylinder, see Fig. 1., (m^2).

e Eccentricity of the inner cylinder relative to its parallel surrounding outer cylinder [= s/(R-r)], see Fig. 1.

E Displacement ratio of the inner cylinder in the parallel rectangular enclosure { = S/[(Y/2) - r]}, see Fig. 2.

F View (or shape) factor for radiation between the inner cylinder and its enclosure.

m Strip parameter [= s sin $\propto$], see Fig. 1, (m).

n Strip parameter [= R - s cos $\propto$], see Fig. 1, (m).

r Radius of the inner cylinder, see Fig. 1, (m).

R Radius of the outer cylinder, see Fig. 1, (m).

s,S Distances between the centre of the inner cylinder and the centre of the cylindrical or rectangular enclosure respectively [= (Y/2) - y], see Figs. 1 and 2, (m).

X Dimension of the rectangular cavity, see Fig. 2, (m).

y Space parameter defining the position of the centre of the inner cylinder with respect to an inner surface of the rectangular enclosure, see Fig. 2, (m).

Y Dimension, of the rectangular enclosure, orthogonal to the direction of the X dimension, see Fig. 2, (m).

$\propto$ Radial co-ordinate, see Figs. 1 and 3, (degrees).

Suffixes

cyl for the inner cylinder.

rect for the rectangular enclosure.

1,2 for the first and second considered surfaces respectively.

INTRODUCTION

Heat transfers by radiation can be thought of as photon fluxes released from excited atoms and travelling usually in straight paths until they are absorbed by other atoms. Such exchanges can also be interpretted as energy transports via electromagnetic waves [1]. The heat radiated from a substance depends upon the fourth power of the absolute temperature of the emitting surface. As a consequence, the radiative exchange becomes large and eventually the dominant heat transfer mechanism, at high temperatures. However, as part of the design process for equipment which is to be used even at moderate temperatures, it is desirable to be able to predict accurately the magnitudes of the thermal radiation exchanges likely to occur[2].

Radiation heat-transfer predictions for engineering systems are usually carried out under the following assumptions[3]. Firstly, the enclosure surfaces are divided into what can be represenred as a large (but finite) number of isothermal regions at different temperatures. Secondly, the surfaces are regarded as "thermally grey-body" emitters, absorbers, or reflectors. Thirdly, the magnitude of the radiant energy flux leaving any considered isothermal surface is uniform over that surface.

The fraction of the radiant energy which leaves surface 1 and reaches surface 2 is termed the view factor of surface 1 with respect to surface 2. An analytical techniques has been developed to permit the prediction of the view factors for radiation from

spheres and infinitely-long cylinders to certain classes of surfaces[4]. Such factors were found to be independent of the validity of Lambert's cosine law, and appropriate shape factor formulae for several other geometries have been deduced.

The present analysis considered the effects of changing the eccentricity, e, or the displacement ratio, E, on the view factors (and consequently the net rate of radiation) from a hot infinitely-long cylinder enclosed, respectively, in either a cylindrical or a rectangular sectioned, parallel, relatively cooler duct.

INFINITELY-LONG CYLINDER ENCLOSED ECCENTRICALLY IN A PARALLEL INFINITELY-LONG CYLINDER

For an eccentrically-placed (i.e. e = 0), infinitely-long cylinder in relation to a portion of the outer cylinder[4],

$$F_{cyl \to m} = (1/2\Pi) \tan^{-1} (m/n) \quad \ldots\ldots\ldots\ldots\ldots\ldots (1)$$

$$\therefore F_{cyl \to m}/dm = n/2\Pi(n^2 + m^2) \quad \ldots\ldots\ldots\ldots\ldots\ldots (2)$$

This represents the factor for an arbitrary, infinitely-long strip of width dm, identified by the variables m and n as shown in Fig. 1. But m, dm and n are functions of the angle α, and dA_2 is the area of the incremental strip dm. Therefore equation (2) becomes,

$$F_{A1\rightarrow dA2} = R\, d\alpha\, (R - s\cos\alpha)/2\Pi(R^2 - 2Rs\cos\alpha + s^2) \quad . . (3)$$

By integrating from α_1 to α_2, the view factor for the inner cylinder relative to the portion PQ of the outer cylinder can be seen to be,

$$F_{A1\rightarrow A2} = (1/2\Pi)\{[(\alpha_2 - \alpha_1)/2] + \tan^{-1}\{[(R + s)/(R - s)]\tan(\alpha_2/2)\} - \tan^{-1}\{[(R + s)/(R - s)]\tan(\alpha_1/2)\}\} \quad . (4)$$

This factor is independent of the radius of the inner cylinder. But, for the whole cylindrical cavity, $\alpha_1 = -\Pi$ and $\alpha_2 = \Pi$. So,

$$F_{cyl1\rightarrow cyl2} = (1/2\Pi)[\Pi + \tan^{-1}(\infty) - \tan^{-1}(-\infty)]$$

$$\therefore F_{cyl1\rightarrow cyl2} = 1 \quad . . . . . (5)$$

INFINITELY-LONG CYLINDER ENCLOSED IN A PARALLEL INFINITELY-LONG RECTANGULAR CAVITY

(i) E = 0 : see Fig. 3

Let AEB be an arc of the circumscribed circle concentric with the cylinder (i.e. e = 0) -- see Fig. 3. Provided that AB does not intersect the cylinder, the view factor from the radiating cylinder to the rectangular enclosure is the same as the factor from the cylinder to the portion AEB of the outer cylinder. Irrespective of the validity of Lambert's law, this factor equals

α/Π and does not depend on the radius of the radiating cylinder[4].

Because,

$$\alpha = \tan^{-1} (X/Y)$$

$$\therefore F_{cyl \to AB} = (1/\Pi) \tan^{-1} (X/Y) \quad \ldots\ldots\ldots\ldots\ldots\ldots (6)$$

Because the view factor for the rectangular enclosure ABCD equals the sum of the factors for all the four sides of the cavity, then,

$$F_{cyl \to rect} = (2/\Pi)[\tan^{-1} (X/Y)] + (2/\Pi)[\tan^{-1} (Y/X)]$$

$$= (2/\Pi)\tan^{-1} \{(X/Y + Y/X)/[1 - (X/Y)(Y/X)]\}$$

$$= (2/\Pi)\tan^{-1} (\infty)$$

$$\therefore F_{cyl \to rect} = 1 \quad \ldots\ldots\ldots\ldots\ldots\ldots\ldots\ldots (7)$$

(ii) $\underline{E \neq 0}$: see Fig. 2.

Once again the analytical method for evaluating the view factor can be employed. For the sides AB and CD of the rectangular cavity, see Fig. 2,

$$F_{cyl \to AB,CD} = (1/\Pi)[\tan^{-1} (X/2y)] + (1/\Pi)\{\tan^{-1} [X/2(Y-y)]\}$$

$$\ldots (8)$$

For the sides AD and BC of the rectangular cavity,

$$F_{cyl\rightarrow rect} = (1/\Pi)[\tan^{-1}\ (2y/X)] + (1/\Pi)\{\tan^{-1}\ [2(Y-y)/X]\} \quad \ldots (9)$$

So for the rectangular cavity ABCD,

$$F_{cyl\rightarrow rect} = (1/\Pi)[\tan^{-1}\ (X/2y) + \tan^{-1}\ (2y/X)] + (1/\Pi)\{\tan^{-1}\ [X/2(Y-y)] + \tan^{-1}[2(Y-y)/X]\}$$

$$= (1/\Pi)\ \tan^{-1}\ (\infty) + (1/\Pi)\ \tan^{-1}\ (\infty)$$

$$= (2/\Pi)\ \tan^{-1}\ (\infty)$$

$$\therefore F_{cyl\rightarrow rect} = 1 \quad \ldots (10)$$

CONCLUSIONS

An analytical technique has been used to derive the view (or shape) factors for a hot infinitely-long cylinder enclosed in either a cylindrical or a rectangular, relatively-cool, infinitely-long duct. Their values are unity, i.e. independent of the geometries or the dimensions of the systems.

REFERENCES

1. E.R.G. Eckert, Radiation: relations and properties, Handbook of Heat Transfer, Edited by W.M. Rohsenow and J.P. Hartnett, McGraw-Hill Book Co. Inc., New York, 1973, 15(A), p. 15.1.

2. E.R.G. Eckert and R.M. Drake, Jr., Analysis of heat and mass transfer, McGraw-Hill Book Co. Inc., New York, 1972, p. 569.

3. E.M. Sparrow, Radiant interchange between surfaces separated by non-absorbing and non-emitting media, Handbook of Heat Transfer, Edited by W.M. Rohsenow and J.P. Hartnett, McGraw-Hill Book Co. Inc., New York, 1973, 15(B), p. 125.31.

4. A. Feingold and K.G. Gupta, New Analytical approach to the evaluation of configuration factors in radiation from spheres and infinitely-long cylinders, Trans. ASME, J. Heat Transfer, 92(1), 1970, pp. 69-76.

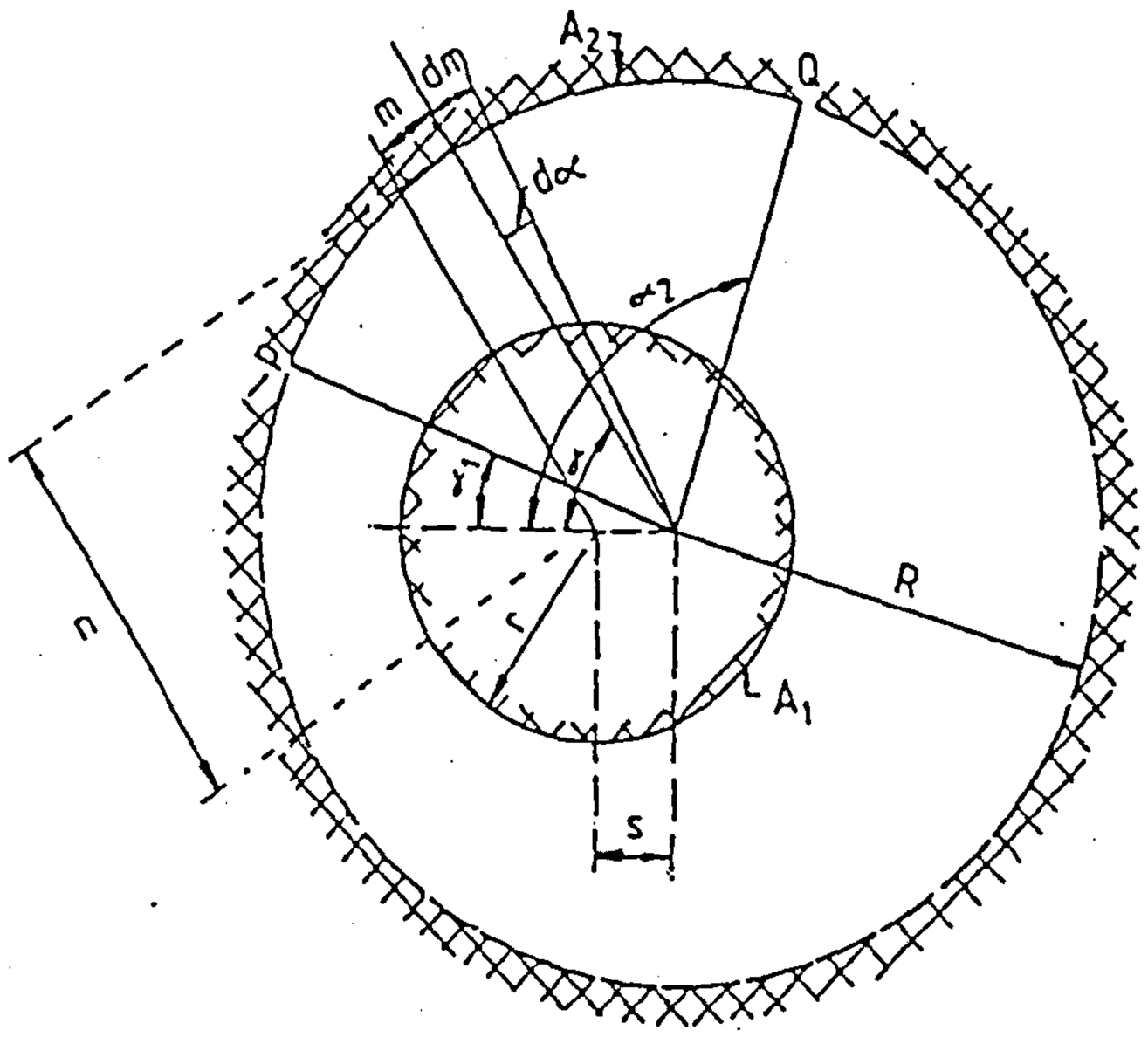

Fig. A1.1. Schematic representation of a pipe-in-pipe infinitely-long assembly.

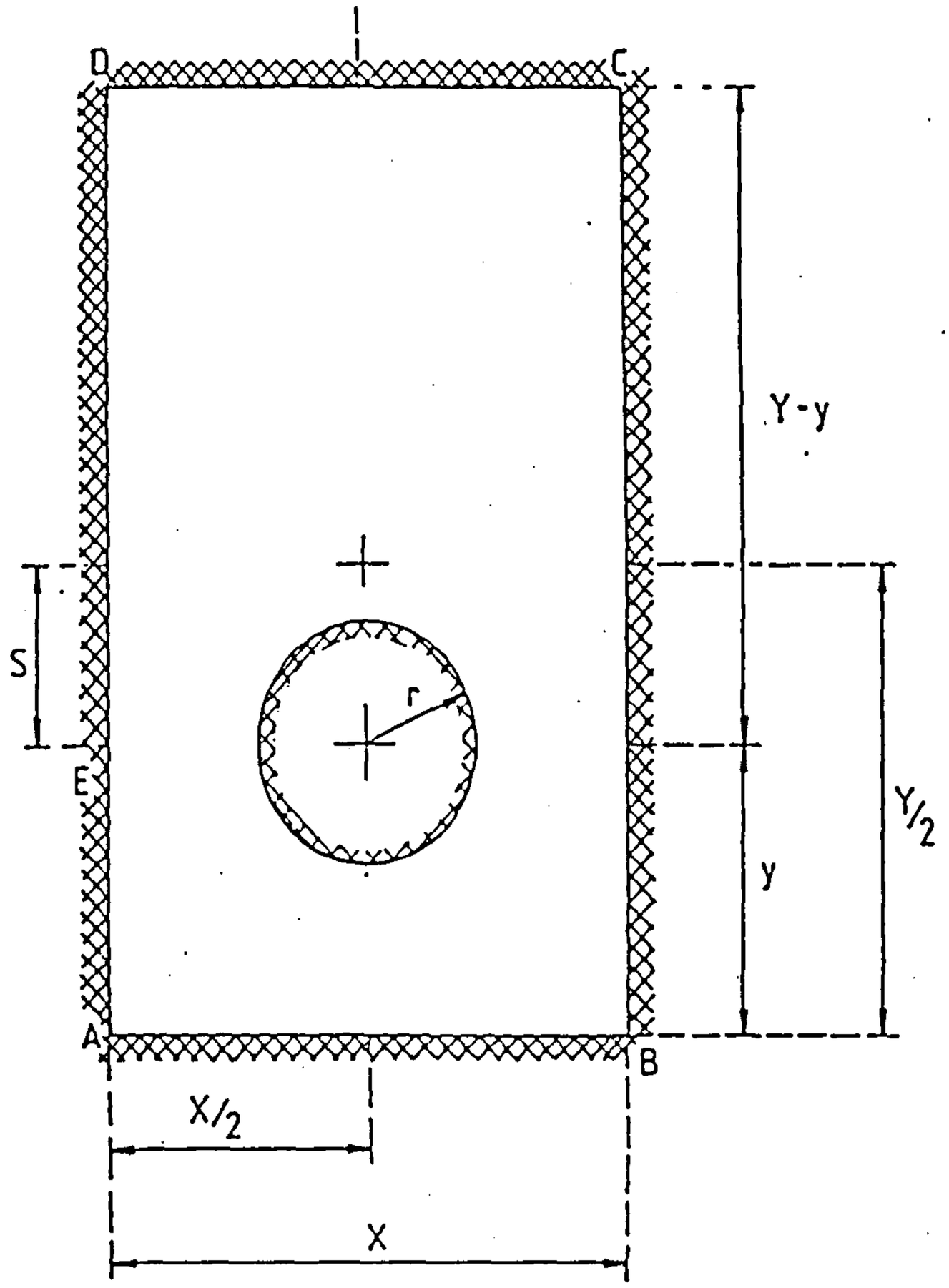

Fig. A1.2. Cross-section of a cylinder aligned with, but not centrally placed in, a rectangular sectioned duct.

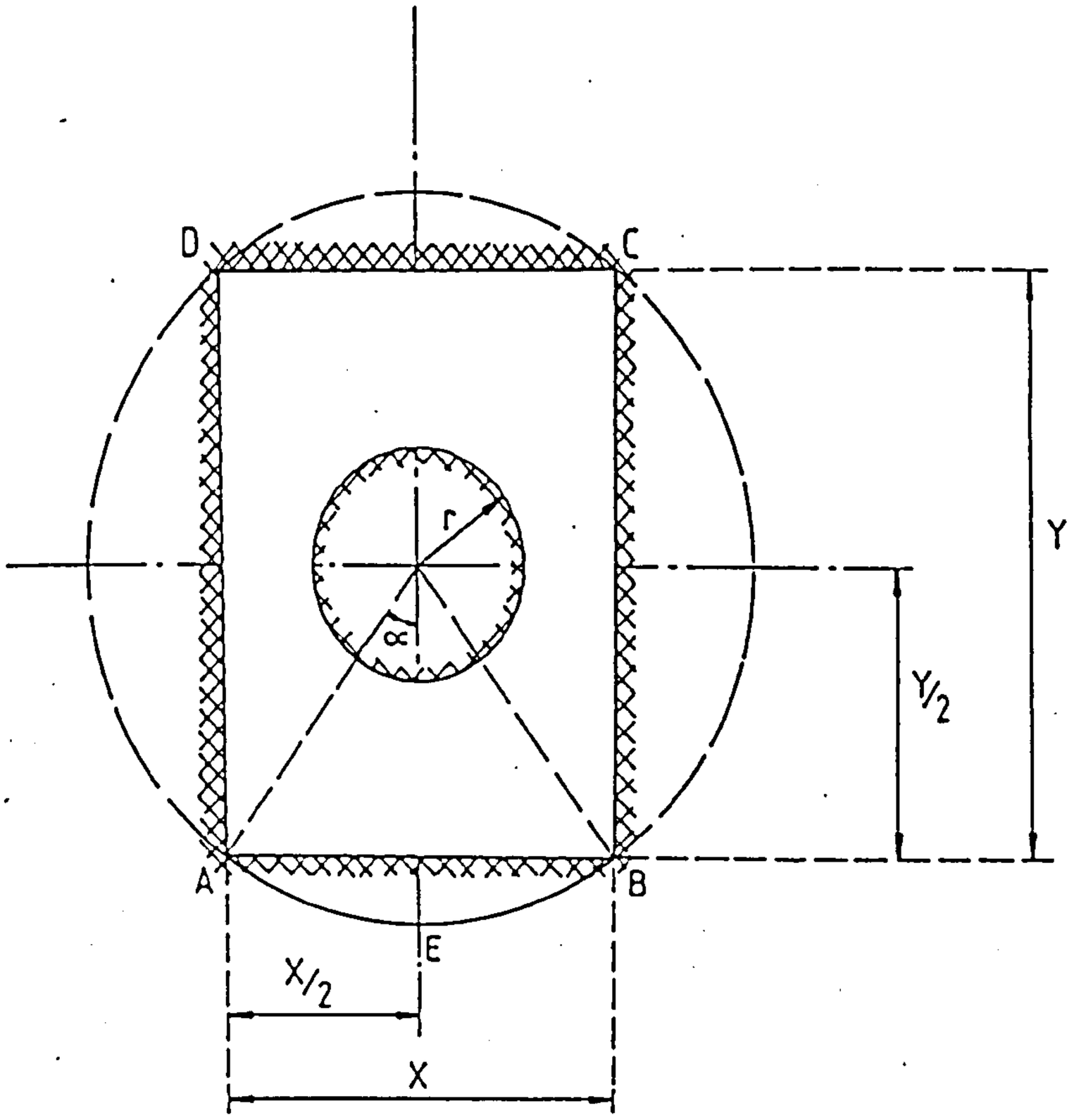

Fig. A1.3. As for Fig. A1.2, but with the cylinder placed centrally in its rectangular enclosure.

APPENDIX 2

IMPROVED PIPELINE CONFIGURATIONS FOR DISTRICT-HEATING AND COOLING DISTRIBUTION SYSTEMS

SUMMARY

Factors influencing the steady-state heat transfers to horizontal chilled-water or from hot-water pipelines, within an atmospheric-pressure, air-filled, relatively hot or cold respectively, horizontal rectangular trench, have been considered. An experimental investigation, using the displacement ratio of the pipe as the experimental variable, revealed the optimal configuration, i.e. that which achieves the minimum steady-state rate of heat exchange between the pipe and its surroundings under the considered conditions. For a set of temperatures for the pipe and the trench walls, corresponding closely with those likely to occur in practice, it has been deduced that the optimal configuration of the "supply" pipe occurred at displacement ratios of + 0.67 and - 0.73, for district-cooling and district-heating systems respectively, i.e. with the horizontal pipe placed equidistant between the vertical walls in the lower region of the cavity in the case of district cooling and in the upper region for district heating. Such conclusions are of significance with respect to achieving maximum energy thrift, because these recommended configurations differ radically from the arrangements of the pipes traditionally adopted in district-cooling or district-heating designs.

DISTRICT-HEATING AND COOLING (DHC)

By these processes, a heated or cooled fluid (usually water) from a central source is distributed to residential, commercial

or industrial consumers in high-intensity demand areas, e.g. for high-density of occupation tall buildings, in which comfortable conditions need to be maintained. The central source may be either a chiller, a boiler (Neil, 1976), a refuse incinerator (Griffin, 1980), a geothermal source (Reistad and Lawrence, 1984), solar energy (Lund and Routti, 1983), or "waste-heat", e.g. as a by-product of electricity generation (Mahini and Schrock, 1982). The extent of the delivery zone should not be specified alone as the sole criterion for assessing the economic feasibilities of proposed district-heating or district-cooling schemes. However it can be asserted with confidence that a small zone project can be worthwhile if a sufficiently large heating or cooling demand exists there, whereas it will probably be uneconomic to serve a large area having only low demands (Kennedy and Tschanz, 1983).

The use of piped heating systems is a very old concept. Nearly 2000 years ago, such systems were employed by the Romans for heating dwellings as well as baths. In more modern times, Sir William Cook in 1745 used pipe coils for conveying steam to heat his home in Manchester, England: he also attempted to warm a group of buildings from a single source of heat (Collins, 1976). Subsequently in 1748, Benjamin Franklin used an underground iron stove-furnace to heat a row of houses via a small districtheating scheme at Philadelphia, USA (Meador, 1981).

Birdsill Holly, in 1877, deserves the credit for being the first person to put district heating on a successful commercial

basis (Collins, 1976). However as economies of scale began to be achieved in the generation of electricity during the early part of the twentieth centry, the total-energy approach was abandoned, and so district heating then failed to gain popularity.

Significant installations of district-heating systems in Europe did not occur until after World War II. Since then, numerous sytems have been introduced mainly in Northern European countries, the USSR (the largest user of district-heating in the world) and the other communist block, centralised-planning, countries. This was usually feasible because of the development of compact housing blocks, a policy which is favoured in many of these countries. District heating in some European countries has not grown in popularity because of the low unit fuel costs during the last 40 years and the abundance of fossil fuels locally. However, in the USA, it has been adopted frequently for college/university campuses, and for commercial mixed-use buildings (Meeker et al, 1985). Such systems (e.g. in New York, NY, St. Louis, MO, Nashville, TN, Youngstown, OH, Baltimore, MD, Duluth, MN, and Pittsburgh, PA) are operating satisfactorily and increasing in number: the Philadelphia, PA system is currently under consideration for sale to new commercial owners.

Due to the 1973/74 and 1979/80 oil crises and the political reluctance to permit nuclear power to substitute for other fuels, the problem of energy thrift has, intermittently, been regarded as urgent during the last decade (McMullan et al, 1983). Thus the terms "district heating" (DH) , "district cooling" (DC), and

"combined heat and power" (CHP) or "cogeneration" have become increasingly accepted as essential concepts in energy-thrift policies, rather than as just economically or socially desirable, by many engineers, architects, planners and even politicians. For instance, district heating is included in the US Government's energy-conservation programme and is now regularly commended in the British Parliament as an important means of saving fuel (Haseler, 1975). Yet surprisingly few of the good intentions have been translated into positive actions. However in the USA, new systems have recently been put into service in St. Paul, MN, and Trenton, NJ, as a direct consequence of US government contribution. In addition, more than 36 cities are actively considering or planning new DH systems as part of the US Department of Energy and US Department of Housing and Urban Development grants and technical support.

District cooling is not as technically advanced as district heating. Nevertheless more than fifty systems are already in operation, or are being installed, in various cities of Europe, USA, USSR and Japan (Diamant and Kut, 1981; Meeker et al, 1985).

UNDERGROUND PIPELINE DISTRIBUTION SYSTEMS

The most expensive component of any DH system is the distribution-pipework network. In older steam-based systems and in higher temperature hot-water systems, the distribution system can account for up to 75 per cent of the total system cost (Center for Renewable Resources, 1984).

Traditional district heating and cooling (DHC) distribution systems can be classified as either (i) thermally-insulated clad pipelines, located in atmospheric-pressure air-filled rectangular trenches, which are slightly beneath ground level; (ii) insulated pipelines in such trenches, which are packed with loose-fill thermal insulants or pebbles around the pipes; (iii) insulated pipelines in trenches with poured-in-place concrete; or (iv) field-insulated, or pre-insulated directly-buried pipelines. For a pre-insulated or field-insulated buried district-heating pipeline, there is an optimal burial depth for which the rate of heat losses from the pipe will be a minimum (Bau, 1984).

The most frequently recommended and widely-used system in the UK and West Germany is that of group (i) (Quigg, 1976; Kell and Martin, 1984; Orchard, 1985). In the event of such a trench becoming flooded (which occurs intermittently in Britain, because of its maritime climate), drainage and evaporation from around the pipeline would be more likely to ensue automatically than with distribution systems of types (ii) or (iii). If the insulant is allowed to remain damp, the moisture often reduces the insulant's effectiveness and strength (sometimes permanently) as well as promotes corrosion of the underlying steel pipelilne, which is supposedly being protected by the insulant. However ventilation of the trench reduces the effective thermal resistance of this air cavity, and so usually should be constrained to the minimum which is likely to be necessary to permit the moisture to disperse readily by diffusion from the cavity.

The modern "pipe-in-pipe", pre-insulated systems (e.g. fibre-glass-reinforced plastic, cross-linked polyethylene or poly-butylene pipelines) are now accepted in some schemes as reliable and economical means of distribution (Quigg, 1976). The apparent disadvantages are the widely different coefficients of expansion of their components and the ($\leq$ 120 °C) operating temperature limitation (Haseler, 1970). In addition, such systems are more expensive than the trenched systems for pipelines with diameters exceeding ~ 700mm (Robinson, 1979). It is the author's conclusion that locating the pipelines in an air-filled rectangular trench should more frequently be the favoured choice for systems at high supply temperatures using large diameter pipes.

THERMALLY-INSULATED PIPELINES

DH pipelines in the USA, supply steam (at up to 215 °C), or hot water from a centralised plant to the consumers under a wide range of pressures (Strauss, 1979). In Europe, the heat-transfer medium almost universally adopted is water. It is pumped out, at an over-pressure, and returned to the plant at about 60 °C (IDHA, 1983). However, for DC systems, the chilled water is initially at about 4 °C and returns at about 13 °C (Diamant and Kut, 1981).

In the USSR, where pumping distances are immense, and in Iceland, where the heat sources are often geothermal springs, single pipeline systems have been used (Gromov, 1967; Kell and Martin, 1984). In such cases, the single flow-pipe conveys hot water to the buildings, the maximum use is made of the exergy by

satisfying initially the domestic hot-water demands, and the heat losses from these will, where desirable, be employed for space heating: any residual is conveyed to swimming pools, greenhouses, or to waste. Single pipelines are also used in steam-based DH networks in various cities in the USA -- e.g. in New York and Baltimore (IDHA, 1983).

Unfortunately from an anergy-thrift viewpoint, some underground DHC pipelines are still installed uninsulated in order to reduce the required initial capital investments and subsequent maintenance problems, but then the running costs are appropriately higher. Much time, effort and money have been devoted to producing reliable, cheap thermally-insulated underground pipelines, but regrettably to date, these have not been completely successful (Borger, 1975).

Currently, most analysts tend to assume that a high "heat-demand density" alone is the key to reducing distribution costs. But, lowering the heat-supply temperatures can also lessen the cost of distribution system materials. Adopting innovative routing practices and installation techniques can reduce significantly the capital costs and the unit heating costs to consumers. Nevertheless attention has not so far been focussed upon the financial savings, which can be achieved by reducing the rates of heat loss resulting from choosing the optimal configuration for such pipes in a trench.

An optimal position for the supply pipe occurs because the convective and conductive contributions to the steady-state total heat leak (or gain) through the air vary in different ways as the proximities of the pipelines to one another and to the walls of the trench are changed. The "displacement ratio", as defined in the nomenclature, indicates the position of the considered pipe in its rectangular trench and is analogous to the "eccentricity" for the case of concentric pipes (see Fig. 1).

SCOPE OF THIS INVESTIGATION

The tests involved measuring the steady-state rates of heat transfer across an atmospheric-pressure air-filled gap for the:-

DC SYSTEM, which is an isothermal hot horizontal rectangular sectioned, trench enclosing a single horizontal cold cylindrical pipe - see Fig. 1; and

DH SYSTEM, which is an isothermal cold horizontal, rectangular sectioned trench enclosing a single horizontal hot cylindrical pipe - see Fig. 1.

For each system, the aim was to determine the optimal position of the supply pipe, which results in the minimum rate of heat gain or loss for the DC and DH systems respectively, under a specified steady-state temperature difference, ΔT $(= T_o - T_s)$, between the pipe and its rectangular trench.

Airflow visualisations (for the various chosen steady-state temperatures of the surfaces of the pipe and the trench, and for different displacement ratios), were used to stimulate, supplement and corroborate conclusions being drawn from interferometric observations indicating the temperature distributions across the air gap.

THE TESTED SYSTEMS

The values of the experimental parameters (see Fig. 1) chosen for this investigation were:

$$X = 100 \text{ mm}, \; Y = 100 \text{ mm}, \; L = 630 \text{ m}, \text{ and } D = 28.5 \text{ mm}.$$

For the DC System

$$-0.75 \leq E \leq 0.80;$$

$$6 \text{ °C} \leq T_s \leq 10 \text{ °C} \leq T_o \leq 40 \text{ °C}; \text{ and}$$

$$3 \text{ °C} \leq \Delta T \leq 30 \text{ °C}.$$

For the DH System

$$-0.90 \leq E \leq 0.50;$$

$$13 \text{ °C} \leq T_o \leq 17 \text{ °C} \leq T_s \leq 40 \text{ °C}; \text{ and}$$

$$-25 \text{ °C} \leq \Delta T \leq -4 \text{ °C}.$$

Each of the temperatures stated was accurate to $\pm$ 0.2 °C, and the dimensions to $\pm$ 0.2 mm.

For all tests undertaken in this investigation, the centre-line of the pipe was maintained at X/2 (= 50 mm) from both vertical walls of the trench, with which it is parallel.

Hauf and Grigull (1970), stated that the length, L, of the test cavity should exceed 500 mm in order to justify disregarding the three-dimensional heat transfer effects in the air near the end plates (see Fig. 2). Taking R as the radius of the circle passing through the four corners of a cross-section of the rectangular trench perpendicular to its length, this implied that, for $L/R > 8$, three-dimensional motions in the annular cavity had only negligible influences upon the recorded steady-state rates of heat transfer (Grigull and Hauf, 1966). For the present system, $L/R = 8.9$, and so complied with this criterion.

The walls of the trench for the experimental simulation were manufactured from polymerised methyl methacrylate (trade names for which are Perspex, Plexiglas, or Lucite) and were water-cooled for the DH system (or heated to simulate the desired net heat-flow direction being inwards for the DC system), each wall containing a series of enclosed channels through which water ran from the mains supply. Each wall was cooled (or heated for the DC system simulation) independently, so as to avoid an appreciable rise (or drop respectively) in the temperature of the water, which would thereby lead to a significantly non-uniform temperature distribution over the inner surfaces of the rectangular walls forming the cavity. Vertical, optically-flat, uniformly-thick, homogeneous glass plates — i.e. the end plates, see Fig.

2 -- were fixed flush to both ends of the trench in order to seal the cavity from the surrounding ambient air. The copper pipe was cooled by passing cold water from a water chiller at a steady temperature T_s (< T_o). Alternatively it could be heated by passing a low-voltage, high amperage, alternating current between its two ends. The eddy-current dissipation resulted in uniform heating along the pipe, and thus $T_s > T_o$.

The main instrument used was an 18 cm field-of-view, 3 mW He-Ne laser stimulated, Mach-Zehnder interferometer (Babus'Haq et al, 1984). This, when employed in the infinite-fringe mode, produced a distinctive pattern of interference fringes which correspond to an isothermal contour map of the air-filled cavity for the chosen two-dimensional configuration and set of values of T_o and T_s. {These interferograms indicated the refractive index (and hence density and consequently temperature) variations of the air integrated over the axial length of the considered cavity}. This means of measurement permits the <u>whole</u> temperature field to be visualised simultaneously. As a non-contact method of measurement, it avoids the dileterious effects of the presence of any disturbing thermometry (e.g. thermocouple leads), whose associated heat leaks influence adversely the system being measured. Also by means of the Mach-Zehnder interferometer, the heat-transfer consequences of design changes in the DH or DC pipleine systems, can be seen easily.

FLOW VISUALISATIONS

These were undertaken for four different displacement ratios of the DC system. A small amount of smoke was injected very slowly into the cavity and photographs were taken of the resulting steady-state flow patterns in the illuminated trench. A thin (~ 5 mm wide) slit, parallel to the end plates and one-third the way along the trench, completely around the cavity, was employed to facilitate the introduction of adequate illumination from three projectors. The flow visualisations so observed indicated the occurrence of flow instabilities, and helped in the heat-transfer interpretations of the phenomena leading to the temperature field distributions as indicated by the interferograms (Babus'Haq et al, 1986).

For E = 0.7, the flow patterns exhibited two, almost stable, counter-rotating, approximately triangular-shaped eddies, which when averaged with respect to time, were symmetrical about the vertical plane through the horizontal axis of the pipe — see Fig. 4(a). However the stabilities of the vortex patterns decreased if the displacement ratio was further reduced, e.g. to a value of E = 0.5.

The relatively fast, cooled air down-flow below the cold pipe (i.e. the plume), for the E = 0 arrangement, oscillated slowly (about the vertical symmetrical plane) through an angle θ of between 5 and 15°, so resulting in an increased rate of heat transfer. Flow patterns for even lower positions of the inner

pipe relative to the trench, e.g. for E = -0.7, exhibited more rapid plume oscillations as well as the counter-rotating vortices in the cavity (see Fig. 4(b)). Most of the observed effects could be accounted for by the air circulation mean speed, which as expected, rose as the temperature difference, ΔT, increased.

INTERFEROMETRIC STUDIES

Enlarged prints of the steady-state isothermal contour maps for the air in the cavity were obtained for the different geometrical configurations examined, with various applied steady state temperature distributions (see Fig. 5). The isotherms were of qualitatively similar shapes for each arrangement, but the fringes became more closely-packed together as the temperature gradients were increased. The first five fringe-displacements from the pipe wall were measured at 15° increments around the pipe's circumference except where there were less fringes representing the pipe's boundary layer (see Fig. 3). Hence the temperature gradients in the air adjacent to the wall could be deduced so that the variation of the local Nusselt number, Nu_G, versus the angular co-ordinate, Θ, could be evaluated — see representative plots in Fig. 6 for the tested DC and DH systems with selected values of the displacement ratio, E, and temperature difference, ΔT.

If $-0.75 \leq E \leq 0.6$ for the DC system, and $-0.5 \leq E \leq 0.5$ for the DH system, the minimum value of the local Nusselt number occurred at $\Theta = 0°$ and 180° respectively. However, this optimal

angular position, corresponding to the minimum value of Nu_G, moved to Θ = 40° and 135° approximately (for the DC and DH systems respectively), for the extreme positive and negative displacement ratios of 0.8 and -0.9 respectively. This was because the gap between the horizontal pipe and horizontal internal surface of the trench decreased as the displacement ratio, E, increased for the DC system, or decreased for the DH system respectively, and hence conduction became eventually the dominant heat transfer process across this gap. As the temperature difference, ΔT increased, the angular position, Θ, at which the minimum local Nusselt number occurred decreased for the DC system and increased for the DH system. This is because the fluid velocity in the boundary layer increased and the flow penetrated further into what had formerly been the relatively stagnant region.

It was suggested (by Grigull and Hauf, 1966) that for the combined steady-state conductive plus convective heat leaks through the air, $\overline{Nu}_G = M\ Gr_D^{\ n}$, which if fully-developed laminar flow convection ensues throughout the region, then n = 0.25. For both the DC and DH systems, the magnitude of M provides an indication of the effective conductance of the air surrounding the pipe, because for a constant Grashof number, Gr_D, all the parameters affecting the conductive plus convective heat relationship except the overall heat transfer coefficient, $\overline{h}$, are constant. Thus the minimum rate of heat transfer from the pipe is obtained for the system configuration with the minimum value of

M, i.e. this is the configuration for which the air provides the maximum thermal resistance of the pipe.

The values of M for both the DC and DH systems were deduced and plotted versus the displacement ratio, E (see Fig. 7). For the DC system, the value of M was a maximum at the least displacement ratio employed, i.e. at E = -0.8, and decreased slowly as the value of E was increased. The minimum occurred at E = 0.67 $\pm$ 0.03 (i.e. with the pipe in the lower region of the cavity), which represents the approximate value for the optimal location for the single horizontal cold pipe in the rectangular, relatively-warm trench considered, and for the temperature distribution tested.

However, for the DH system, the value of M was a maximum at the highest displacement ratio used, i.e. E = 0.5 and decreased slowly as the value of E was decreased. The minimum occurred at E = -0.73 $\pm$ 0.03 (i.e. with the pipe in the upper region of the cavity), representing the approximate optimal location for the single horizontal hot pipe in the rectangular, relatively-cold trench considered.

By using such optimal configurations, increases of ~ 11% and ~ 13%, for the DC and DH systems respectively, in the thermal resistances (for heat transfers via conduction and convection through the air) of the air-filled cavity were obtained compared with current conventional practice, i.e. the use of systems with E = 0 -- see Fig. 7.

The radiative component of the steady-state rate of heat flux across the cavity would be independent of the displacement ratio for an infinitely-long pipe and trench (Feingold and Gupta, 1970). So the optimal position, as deduced from the "conduction plus convection through the air" data, is to a good first approximation also that for a long system when the total heat leak through the air is considered.

CONCLUSIONS

For air-filled trench installations there is an optimal configuration, whose use leads to the least rate of heat being lost or gained from the supply pipeline. With E = 0.67 for the DC system and E = -0.73 for the DH system, increases of 11% and 13% respectively, in the thermal resistance of the air-filled cavity were obtained compared with current conventional practice (i.e. the use of systems with E = 0). Even greater percentage benefits would be achieved if smaller ΔTs are employed, as would be the case with thick layers of insulants on the pipes.

In practice, for both the DH and DC systems, there is likely to be another pipeline in the trench, i.e. that acting as the return pipeline carrying the water back to the central plant. Therefore for DHC systems, by having the hot pipeline above the cooler pipeline in a rectangular trench, lower steady-state rates of heat loss from the supply pipe than with any "side-by-side" arrangement under identical boundary temperature conditions can be achieved. The "hot-above-cooler" pipe configuration has the

added advantage that it would permit the use of narrower (and hence cheaper to excavate) trenches compared with the present conventional practice (Orchard, 1985). Also this same system is the optimal one for district heating in winter and for district cooling in summer, the higher temperature pipe always being uppermost. Such a configuration is now employed in the DH system in the city of Rotterdam, The Netherlands. However, factors other than heat loss or gain will influence the practical choice of the selected position of the pipe in the trench, namely ease of access for repairing joints and the effects of the presence of supports structures on the optimal location. However, for no extra capital cost,with the optimal arrangement of the thermally insulated (or non-insulated) pipe, enhanced thermal insulation of the system can be achieved. Obviously the greater the amount of insulant applied to the pipe, the less the percentage increase in the overall insulation of the system which can be achieved by employing the optimal location.

In reality, for typically insulated pipelines, the 11% and 13% increases in the thermal resistance of the air-filled cavity mentioned previously would amount to only ~ 3% gain in the overall thermal insulation of the system (i.e. allowing for the presence of the insulant cladding on the pipes and the insulation provided by the earth surrounding the air in the trench). Nevertheless, over the life-time (> 30 years) of the pipeline system, this is still a very worthwhile benefit as its attainment incurs no additional capital expenditure, which could even be reduced by using the narrower trenches suggested.

NOMENCLATURE

D Diameter of the supply horizontal pipe, (m).

E Displacement ratio {= [2H/(Y - D)] - 1}, see Fig. 1, $-1 < E < 1$.

G Average vertical gap [= (Y - D)/2], (m).

Gr_D Local Grashof number for the air flows in the rectangular trench, based on the diameter, D, of the supply pipe [$Gr_D = \beta\ g\ \Delta T\ D^3/\nu^2$].

g Local gravitational acceleration, (m/s^2).

H The shortest vertical distance between the supply horizontal pipe and the upper horizontal internal surface of the trench, see Fig. 1, (m).

$\overline{h}$ Overall heat transfer coefficient, ($W/m^2\ °C$).

k Thermal conductivity of the air, (W/m °C).

L Axial length of the considered horizontal air-filled cavity, see Fig. 2, (m).

M — A dimensionless coefficient in the steady-state conductive and convective heat transfer through the air equation: it is dependent upon the geometry and temperature distribution of the considered system [= $\overline{Nu}_G/Gr_D^n$].

Nu_G, $\overline{Nu}_G$ — Local (i.e. at position θ) and average Nusselt numbers respectively, for the steady-state heat transfers from or to the supply pipe, based on the average vertical gap, G, [$\overline{Nu}_G = \overline{h}\ G/k$].

n — Power index of the Grashof number in the Nu versus Gr relationship -- describing the conductive and convective steady-state heat transfers through the air.

R — Radius of the circle passing through the four corners of a cross-section of the outer rectangular trench perpendicular to its length [= $\sqrt{X^2 + Y^2}$], (m).

T_o — Steady-state uniform temperature of the inner surfaces of the model outer rectangular trench, as used in the present set of experiments, see Fig. 1, (°C).

T_s — Steady-state temperature of the outer surface of the supply pipe, see Fig. 1, (°C).

X,Y — Horizontal width and vertical extent respectively, of the rectangular cavity, see Fig. 1, (m).

β Coefficient of volumetric thermal expansion of air at $[(T_o + T_s)/2]$, (K^{-1}).

ΔT Uniform steady-state difference between the temperatures of the inner surfaces of the rectangular trench and the outer surface of the supply pipe $[= T_o - T_s]$, (°C)

ν Kinematic viscosity of the air, (m^2/s)

Θ Angular co-ordinate, measured from zero for the vertically downwards radius vector emanating from the horizontal centre-line of the supply pipe and increasing for counter-clockwise rotations, see Fig. 3, (degrees)

Suffixes

D for the outer diameter of the pipe.

G based on the average vertical gap dimension.

o of the inner surface of the rectangular trench.

s for the supply pipe.

Abbreviations

CHP	Combined heat and power
DC	District cooling
DH	District heating
DHC	District heating and cooling

REFERENCES

Babus'Haq, R.F., Probert, S.D., and Shilston, M.J. 1984, "Optimal location of a single horizontal pipeline in a rectangular, horizontal air-filled enclosure to achieve maximum thermal insulation", Applied Energy, 18(4): 239-259.

Babus'Haq, R.F., Probert, S.D., Shilston, M.J., and Chakrabarti, S. 1986, "Optimising the location of a district-cooling pipeline in a rectangular trench", Applied Energy. 23(2): 109-141.

Bau H.H. 1984, "Convective heat losses from a pipe buried in a semi-infinite porous medium", Int. J. Heat and Mass Transfer, 27(11); 2047-2056.

Borger, H.A. 1975, "Available types of underground heat-distribution systems", Proc. Symposium on Underground Heat and Chilled Water Distribution Systems, Washington D.C., NBS-BSS-66 : 52-59.

Center for Renewable Resources, 1984, Renewable energy in cities, New York : Van Nostrand Reinhold Co. Inc.

Collins, Jr., J.F., 1976, "The history of district-heating", District Heating, 62(1) : 18-23.

Diamant, R.M.E., and Kut, D., 1981, District heating and cooling for energy conservation, London : The Architectural Press.

Feingold, A., and Gupta, K.G., 1970, "New analytical approach to the evaluation of configuration factors for radiation from spheres and infinitely-long cylinders", Trans. ASME, J.Heat Transfer, 92(1) : 69-76.

Griffin, S., 1980, "Waste equals grist for the mill as Swiss take up recycling", Smithsonian, 11(8) : 143-148.

Grigull, U., and Hauf, W., 1966, "Natural convection in horizontal cylindrical annuli", Proc. 3rd. Int. Heat Transfer Conf., Chicago, 2(60) : 182-195.

Gromov, N.K., 1967, Single-pipe systems for district-heating networks, Translation obtainable from:- England: National Lending Library for Science and Technology, Boston Spa.

Haseler, A.E., 1970, "New heat mains techniques for tele-thermics", JIHVE, 38(Dec) : 194-214.

Haseler, A.E., 1975, "District heating and telethermics -- new data on heat mains", Building Services Eng., 42 (Feb): 257-272, 42(Mar) : 273-285.

Hauf, W., and Grigull, U., 1970, "Optical methods in heat transfer", Advances in Heat Transfer, New York : Academic Press, 6 : 133-366.

IDHA, 1983, District heating handbook -- a design guide : Vol 1, 4th.Ed. Washington D.C.: International District Heating Association.

Kell, J.R., and Martin, P.L., 1984 Heating and air-conditioning of buildings, 6th Ed., London : The Architectural Press.

Kennedy, A.S., and Tschanz, J.F., 1983, District-heating and cooling -- a 28 city assessment, Illinois : Argonne Nat. Lab. ANL/CNSV-TM-119.

Lund, P.D., and Routti, J.T., 1983, "An analysis of district solar ponds with heat pump", Int.J. Ambient Energy, 4(4) : 187-192.

Mahini, R.T., and Schrock, V.E., 1982, The use of waste heat in district systems with consideration of seasonal heat-demand variations, Berkeley: University of California, UCB-NE-4022.

McMullan, J.T., Morgan, R.; and Murray R.B., 1983, Energy resources, 2nd Ed., London : Edward Arnold Publishers Ltd.

Meador, R., 1981, Cogeneration and district heating -- an energy efficiency partnership, Michigan : Ann Arbor Science Publishers, Inc.

Meeker, Jr., D.O. et al., 1985, District heating and cooling in the United States, prospects and issues, National Academy of Sciences, Washington D.C., National Academy Press.

Neil, D., 1976, "The role of the boiler in district heating", Building Services Eng, 44 (Sept.) : 50-51, 53-55.

Orchard, W.R.H., 1985, Personal communication, Orchard Partners, 67-69, Southampton Row, London WC1B 4ET.

Quigg, J.S., 1976, "Underground distribution systems", Building Services Eng., 44 (Sept) : 40-41.

Reistad, G.M., and Lawrence, T., 1984, "Geothermal district-heating models : a review of compatibility and validity, ASHRAE Transactions, 90(1B) : 313-344.

Robinson, P.J., 1979, "Transmission and distribution networks and the consumer -- the potential for development, Whole City Heating Conf., London.

Strauss, S.D., 1979. "District heating links with cogeneration", Power, 123(8) : 72-75

ACKNOWLEDGEMENTS

The authors wish to thank the University of Technology, Baghdad, Iraq for the award of a Research Fellowship to R.F. Babus'Haq.

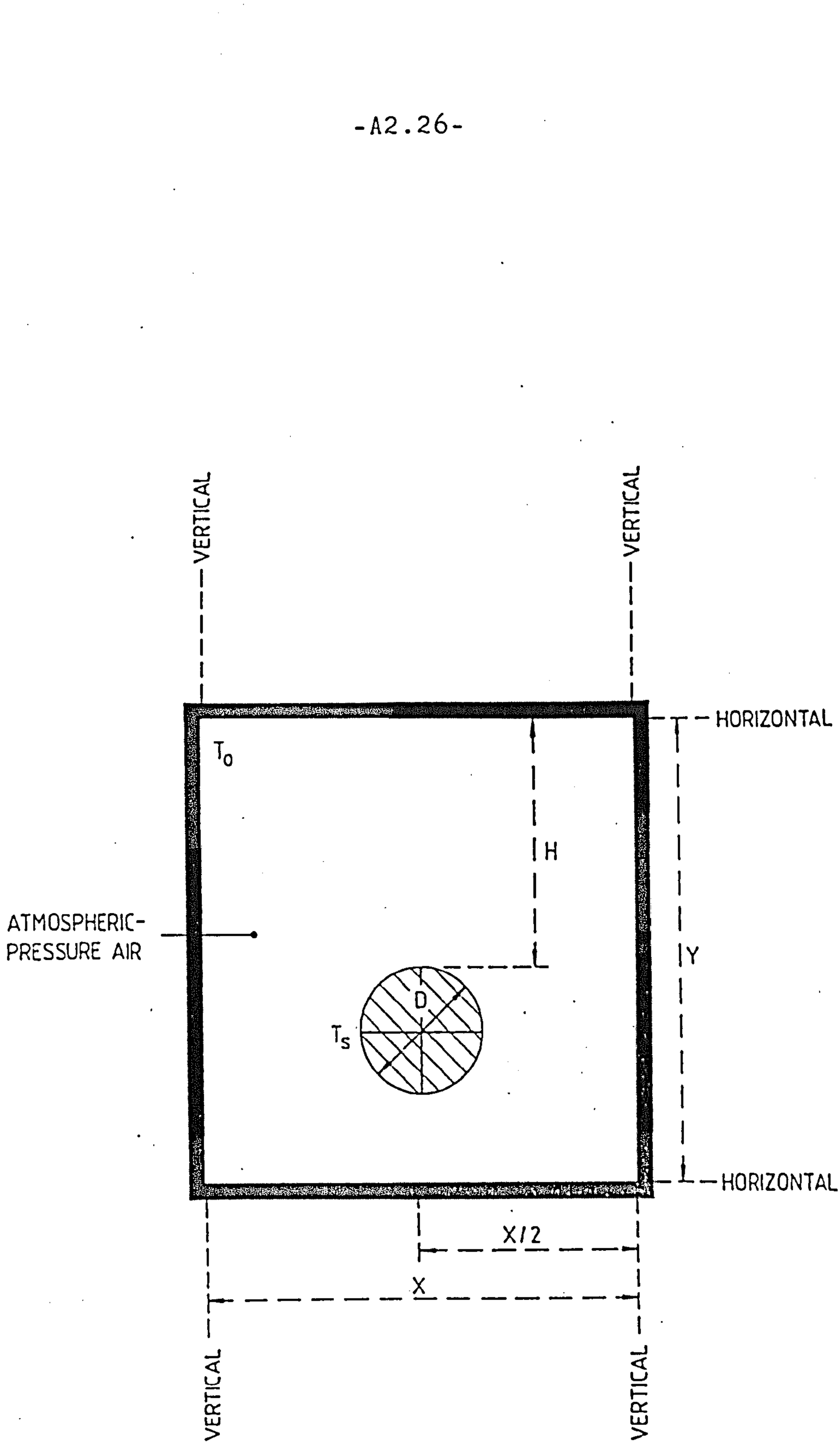

Fig. A2.1. Schematic representation of vertical section through the considered horizontal pipe (with a positive displacement ratio) in its rectangular trench.

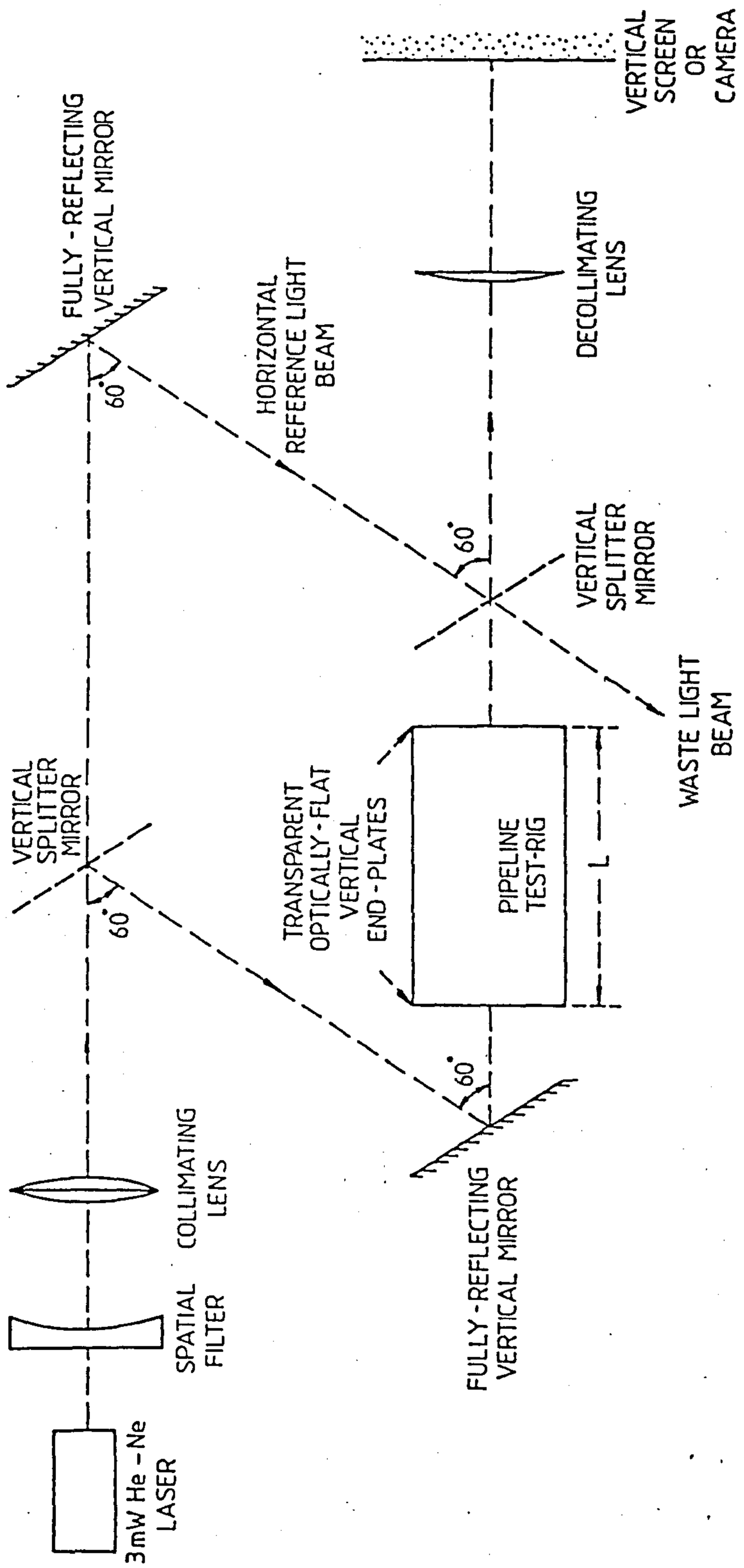

Fig. A2.2. Schematic plan-view of the 18 cm field-of-view Mach-Zehnder interferometer.

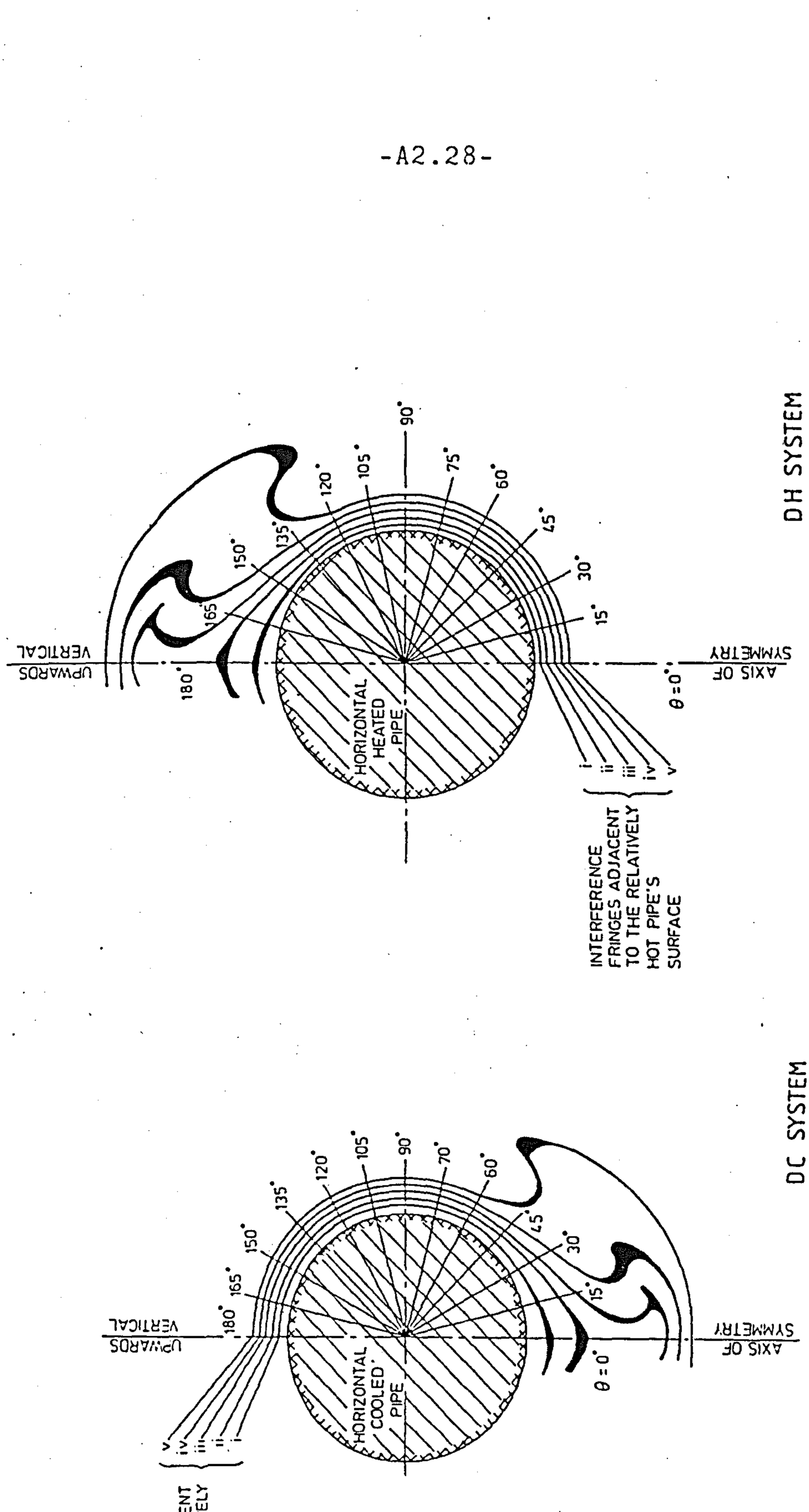

Fig. A2.3. Typical contour maps of isotherms around horizontal cooled or heated pipes in free space as revealed by Mach-Zehnder interferometry. The angular co-ordinate, θ, is measured from the vertically-downwards radius vector from the centre of the pipe.

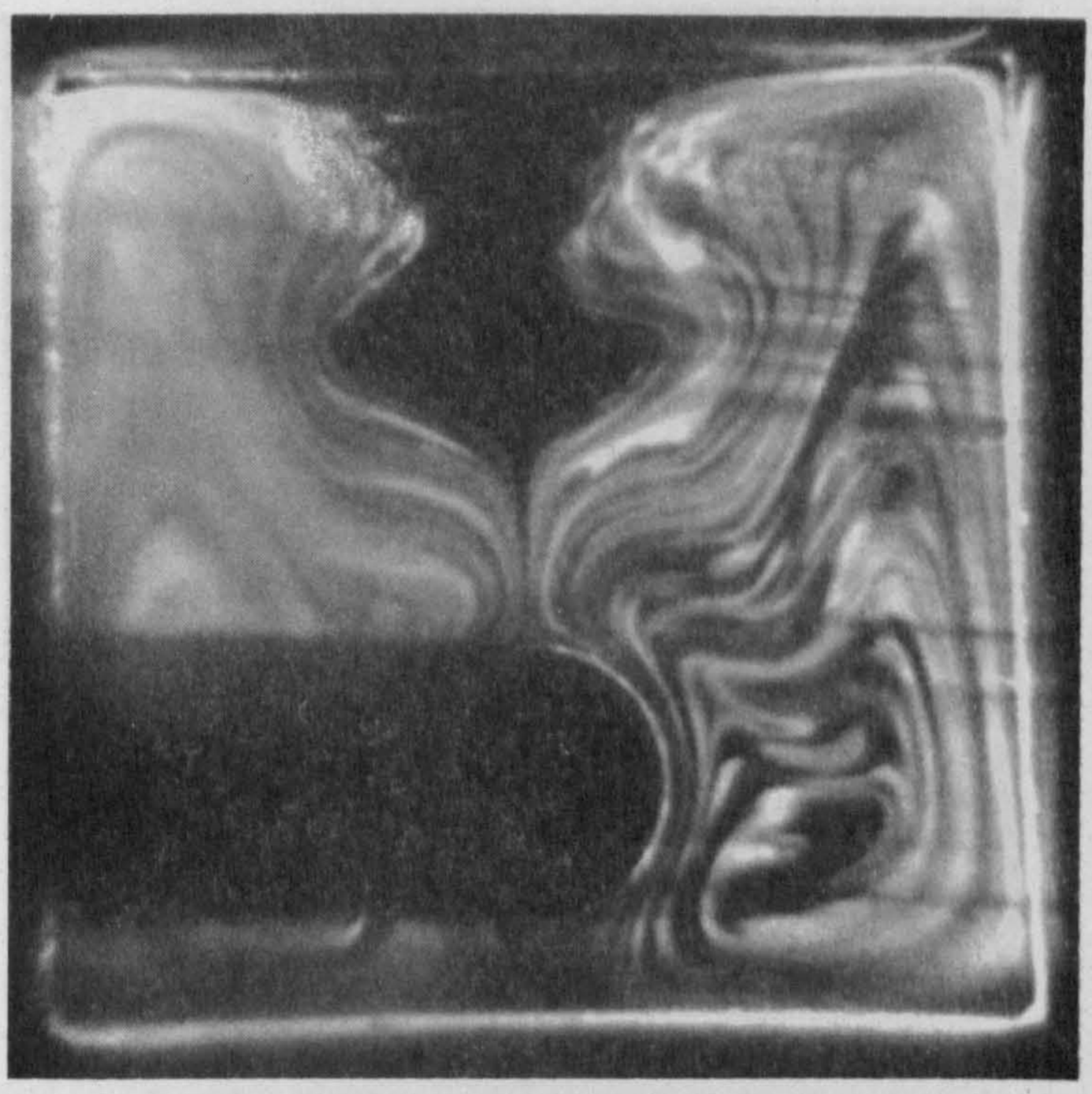

Fig. A2.4. Typical steady-state flow visualisations for a simulated district-cooling pipeline: T_s = 10 °C.

(a) E = 0.7, ΔT = 23 °C.

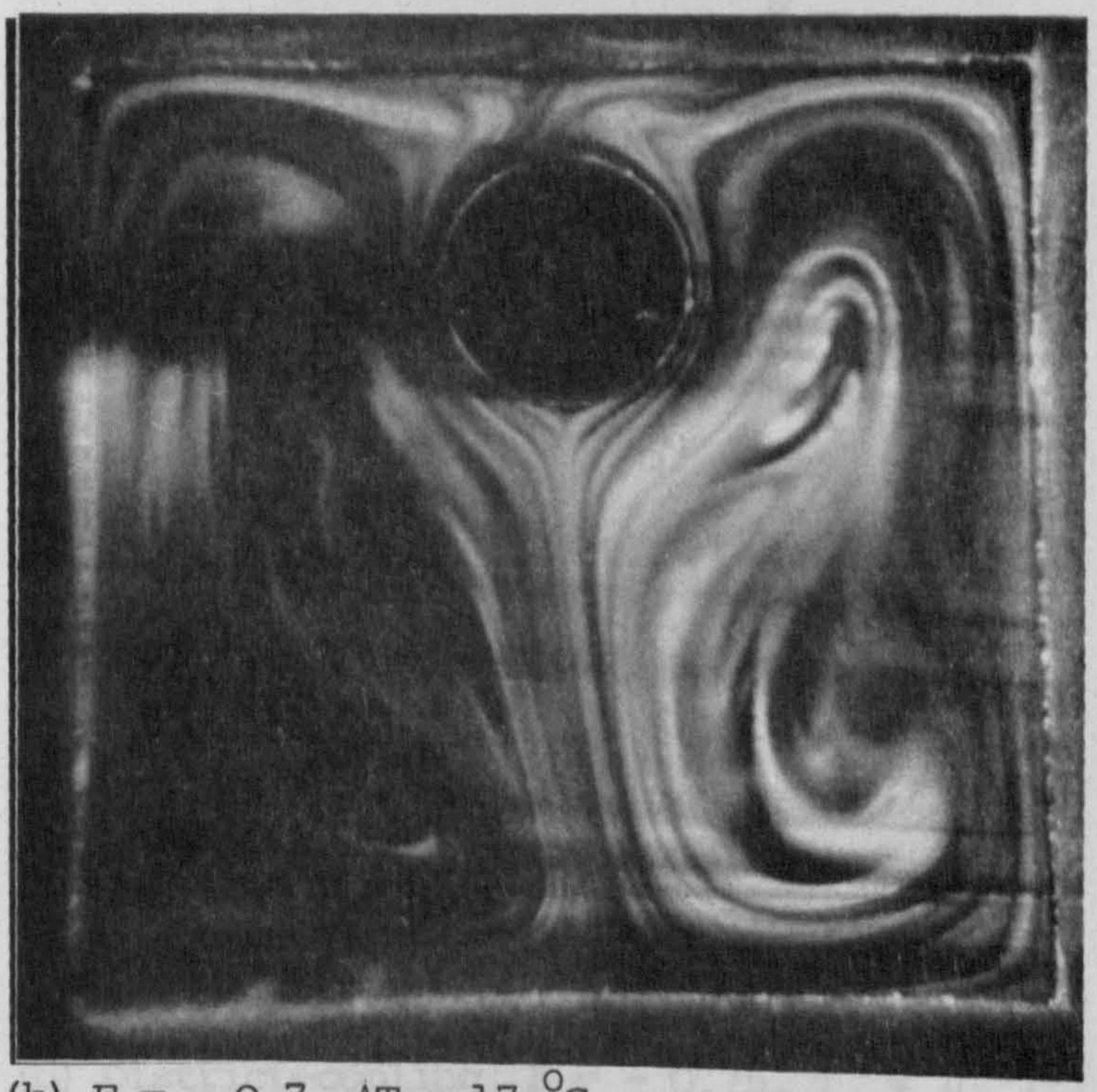

(b) E = - 0.7, ΔT = 17 °C.

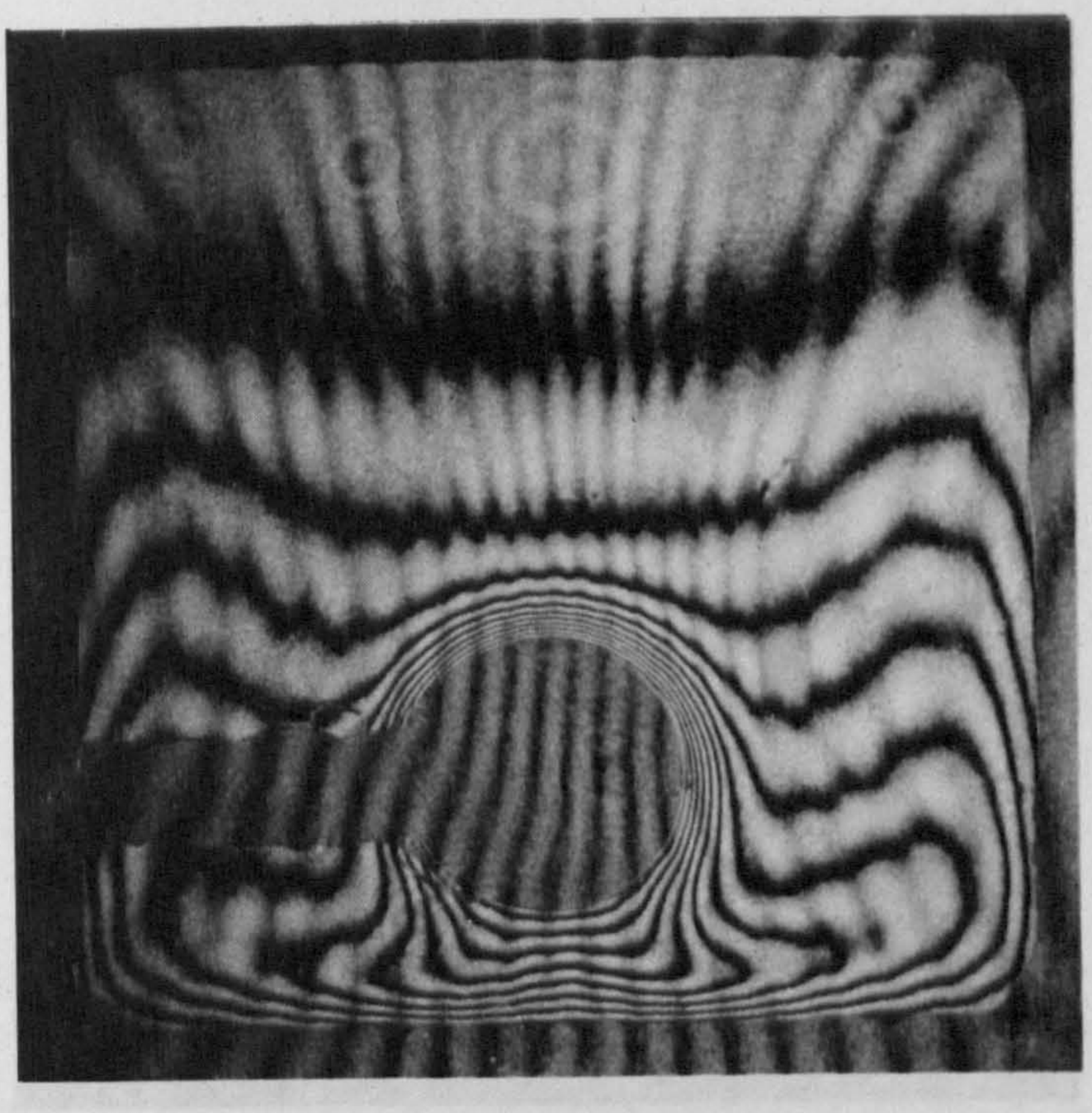

Fig. A2.5. Mach-Zehnder interferograms for district-cooling and heating systems, indicating the steady-state isotherms in the air-filled plain cavity:

(a) District-cooling, $E = 0.7$, $T_s = 10\ ^{\circ}C$, $\Delta T = 10.3\ ^{\circ}C$.

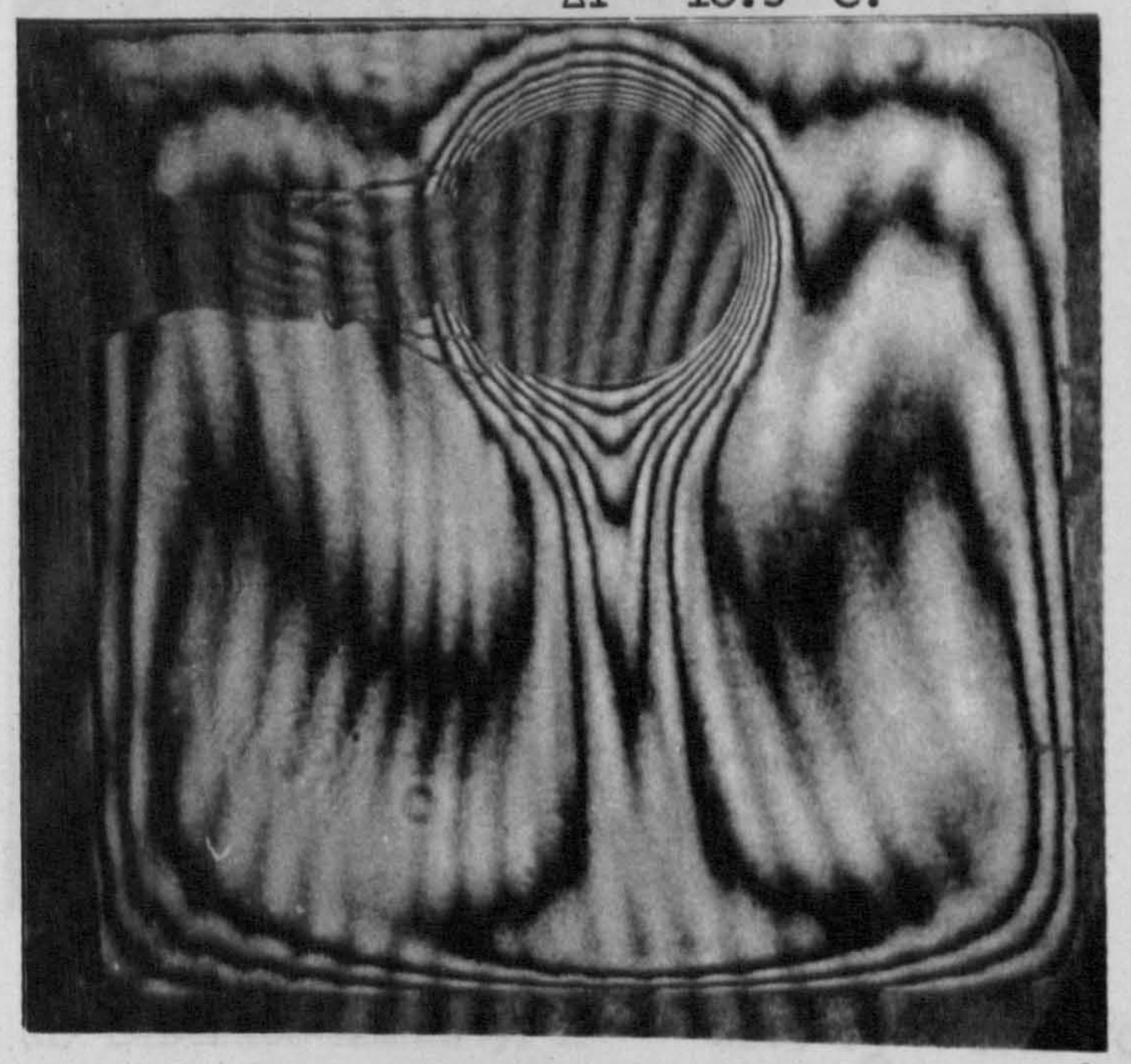

(b) District-cooling, $E = -0.75$, $T_s = 10\ ^{\circ}C$, $\Delta T = 10.3\ ^{\circ}C$.

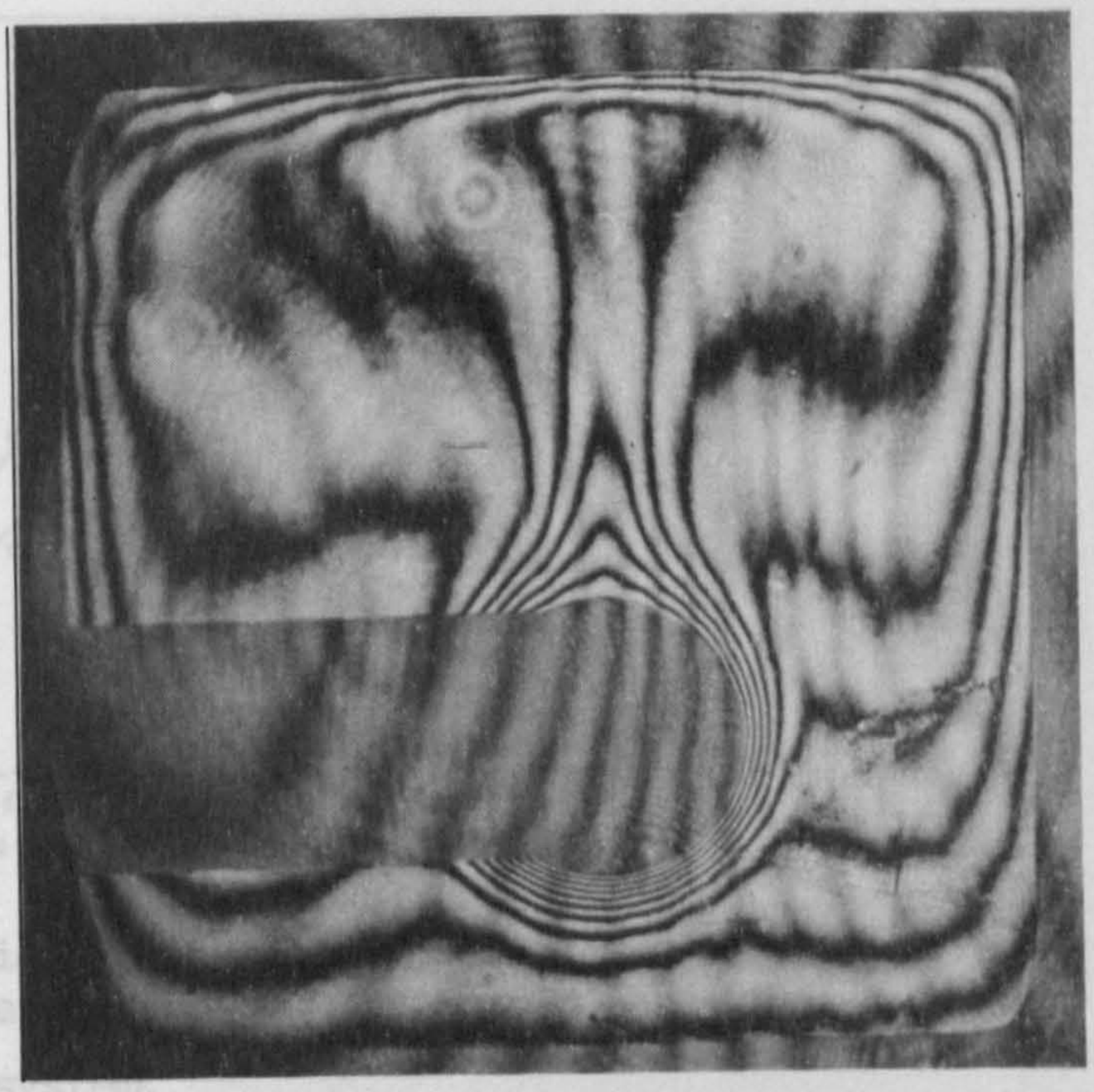

(c) District-heating, $E = 0.5$, $T_o = 16.3\ ^{o}C$, $\Delta T = -\ 9.9\ ^{o}C$.

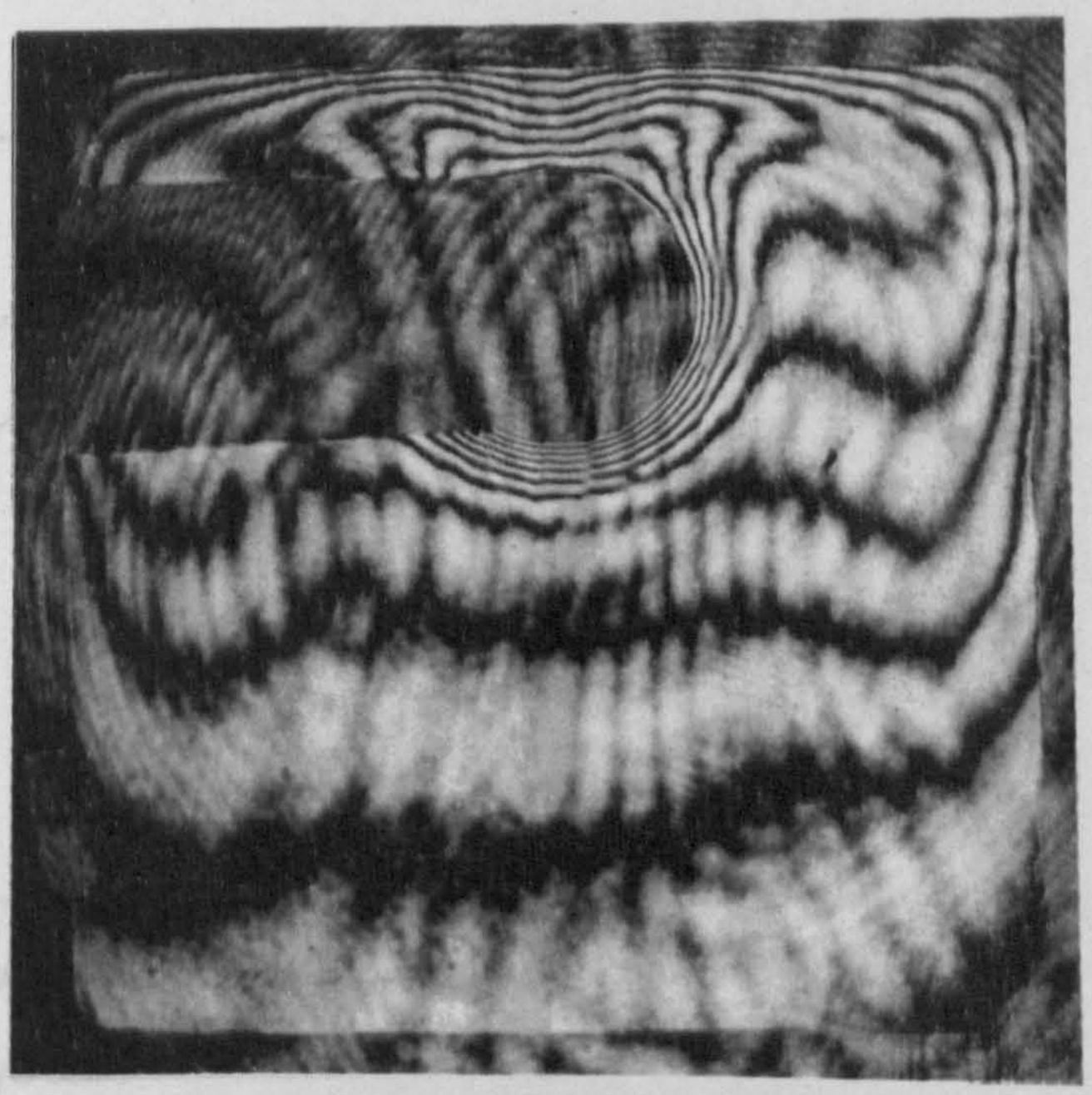

(d) District-heating, $E = -\ 0.7$, $T_o = 15.3\ ^{o}C$, $\Delta T = -\ 9.2\ ^{o}C$.

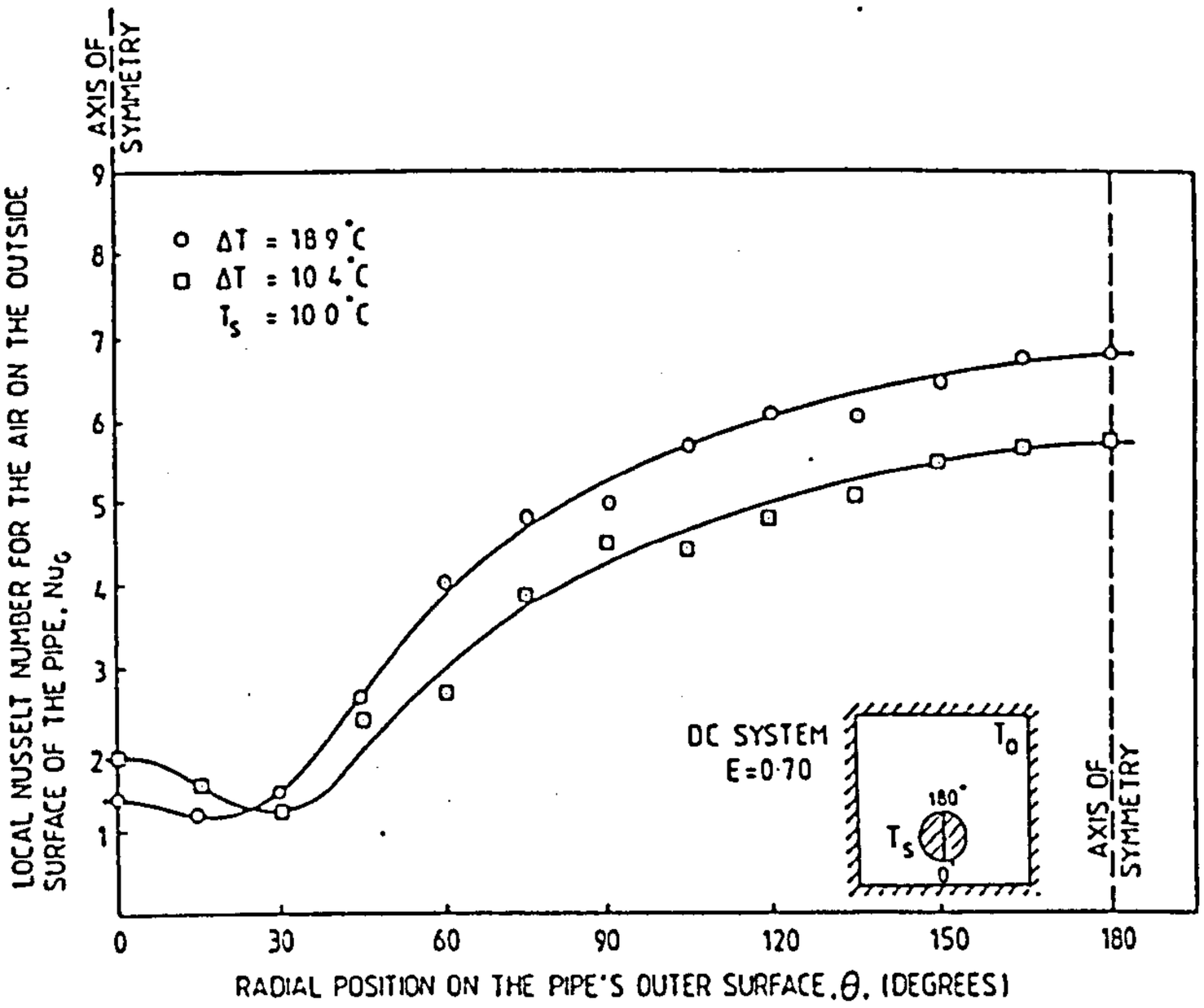

Fig. A2.6. Variations of the local Nusselt number, Nu_G, versus the angular co-ordinate, Θ:

(a) Simulated DC system.

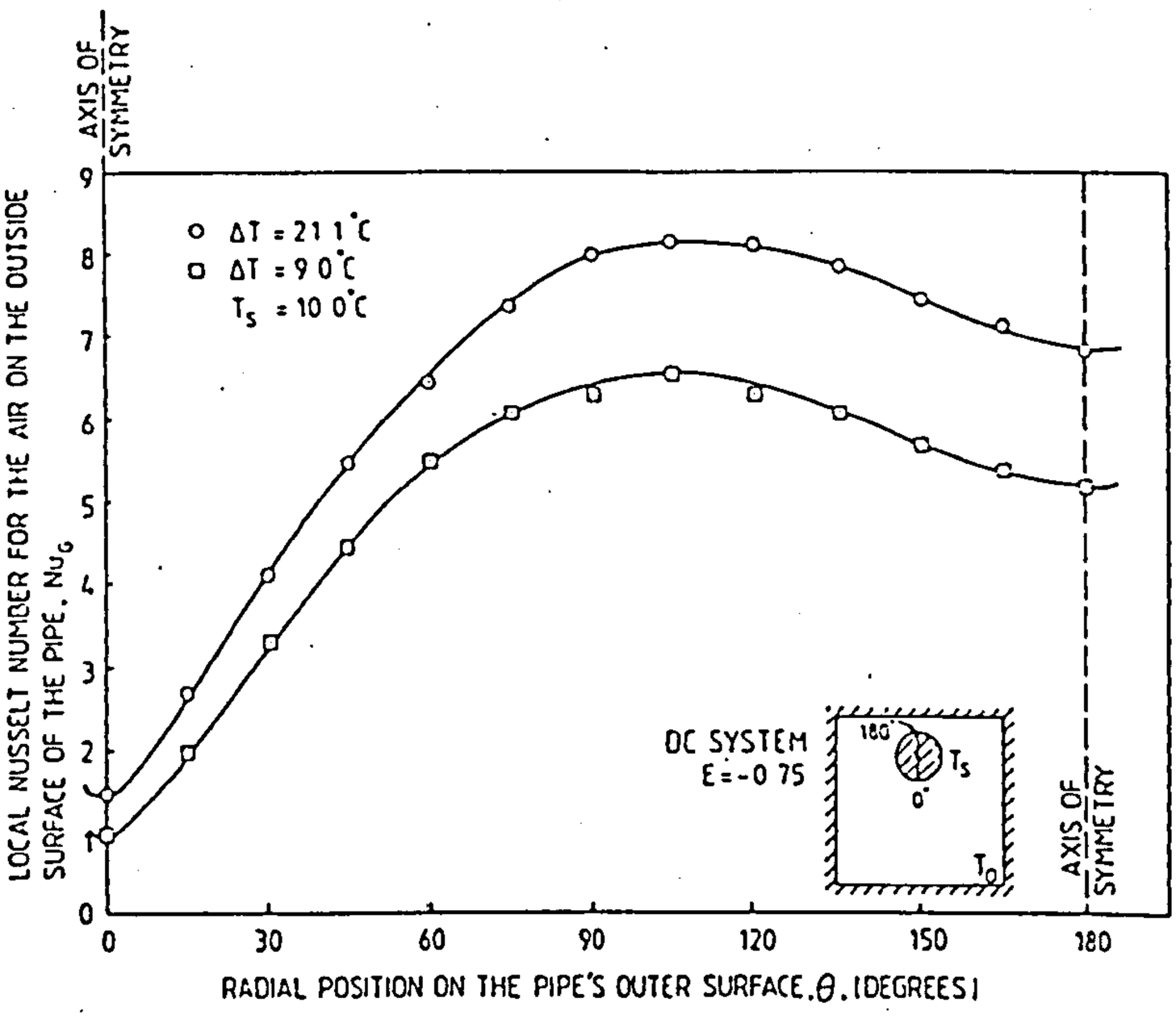

(b) Simulated DC system.

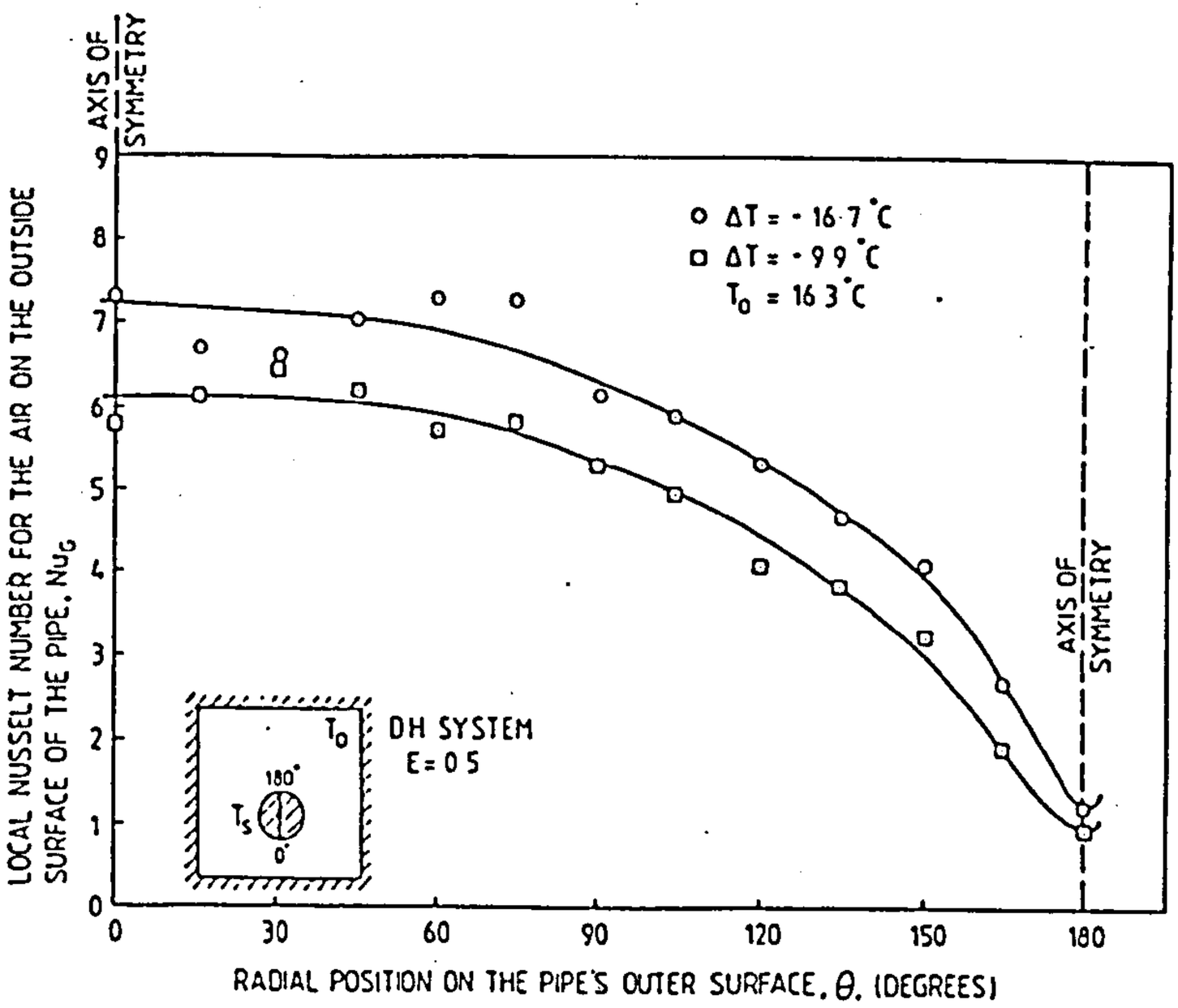

(c) Simulated DH system.

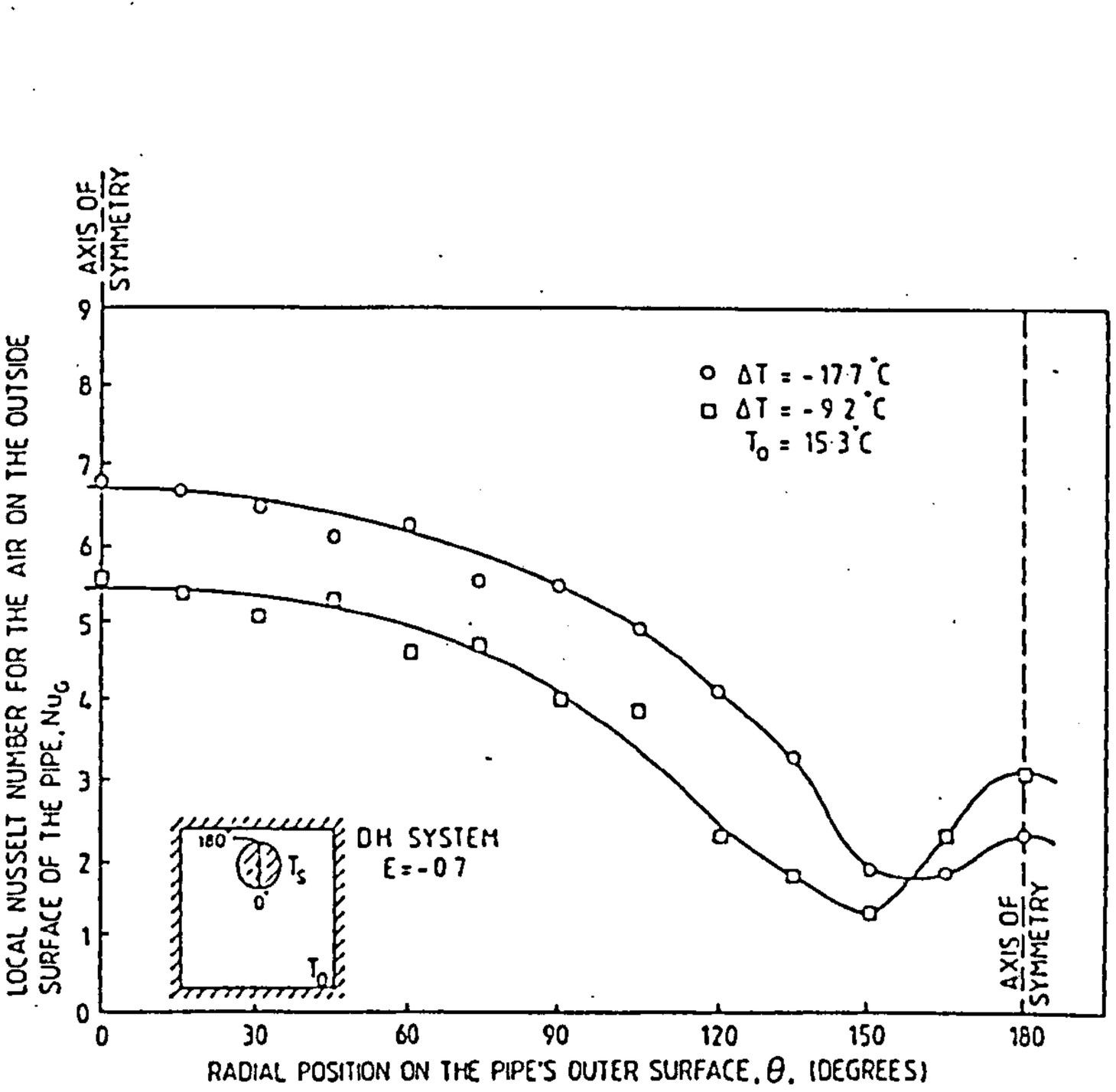

(d) Simulated DH system

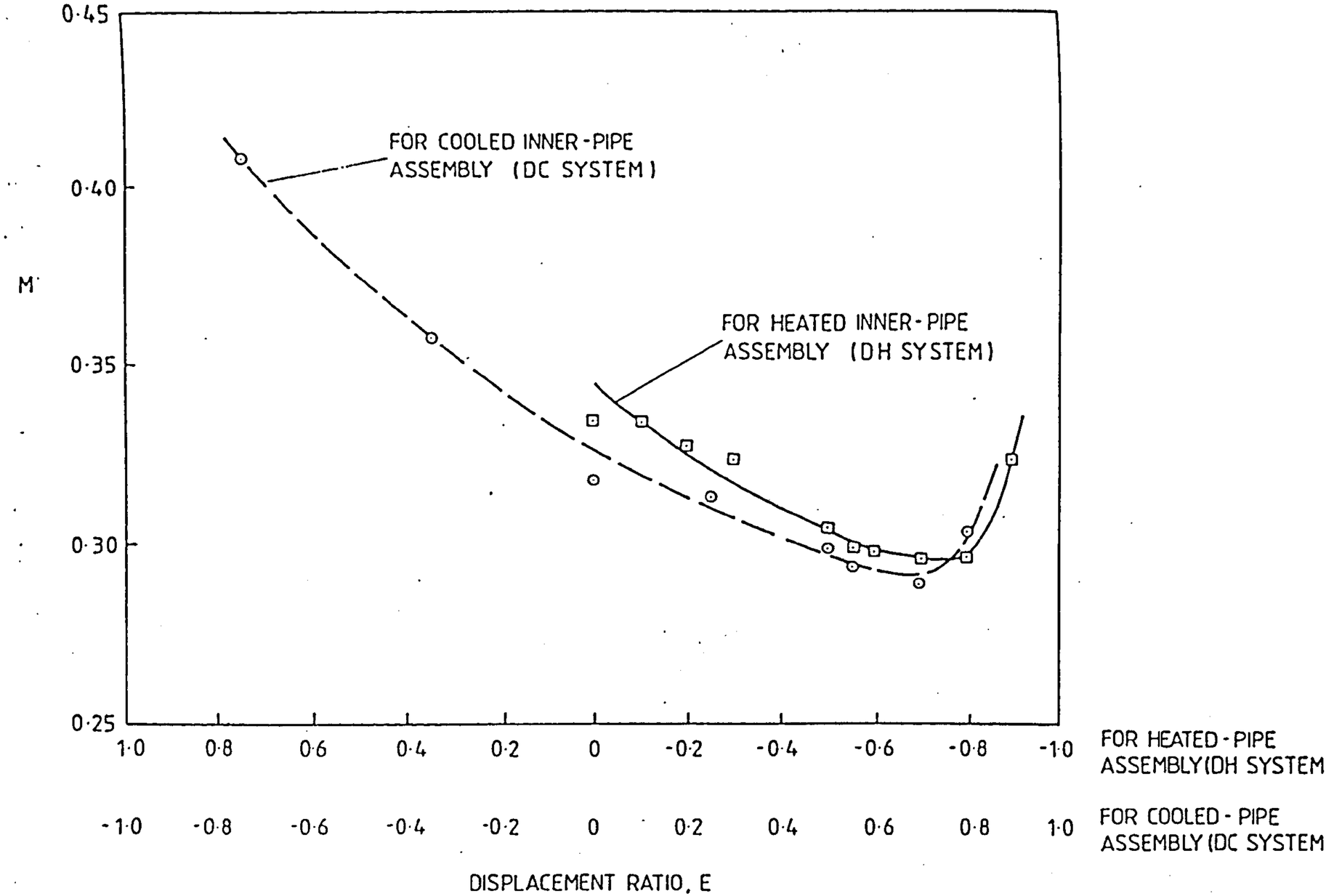

Fig. A2.7. Variations of M for the horizontal pipe in the horizontal rectangular-sectioned trench for DHC systems.

APPENDIX 3

SUGGESTED DESIGN IMPROVEMENTS CONCERNING DISTRICT-HEATING PIPELINE CONFIGURATIONS

Applied Energy 17 (1984)

Suggested Design Improvements Concerning District-Heating Pipeline Configurations

SUMMARY

Factors influencing the heat loss behaviours of horizontal 'supply' and 'return' hot-water pipes, within a rectangular trench, are considered (see Fig. 1). The use of such atmospheric-pressure air channels for district-heating systems is prevalent in the UK in order to facilitate drainage and evaporation. By optimising the location of the two pipes within the rectangular-sectioned trench, it is possible to achieve considerable reductions in the steady-state rate of heat loss from the supply pipe compared with conventional practice. Recommendations for future designs are presented.

NOMENCLATURE

D	Identical diameters of both the considered supply (i.e. the hot) and the considered return (i.e. the relatively cooler) pipes (mm).
E	Displacement ratio $\left\{ = 1 - \frac{2U_l}{(y-D)} \quad \text{or } 1 - \frac{2U_u}{(y-D)} \right.$ for the lower or upper pipes, respectively (see Fig. 2) $\left. \right\}$

Applied Energy 0306-2619/84/S03·00

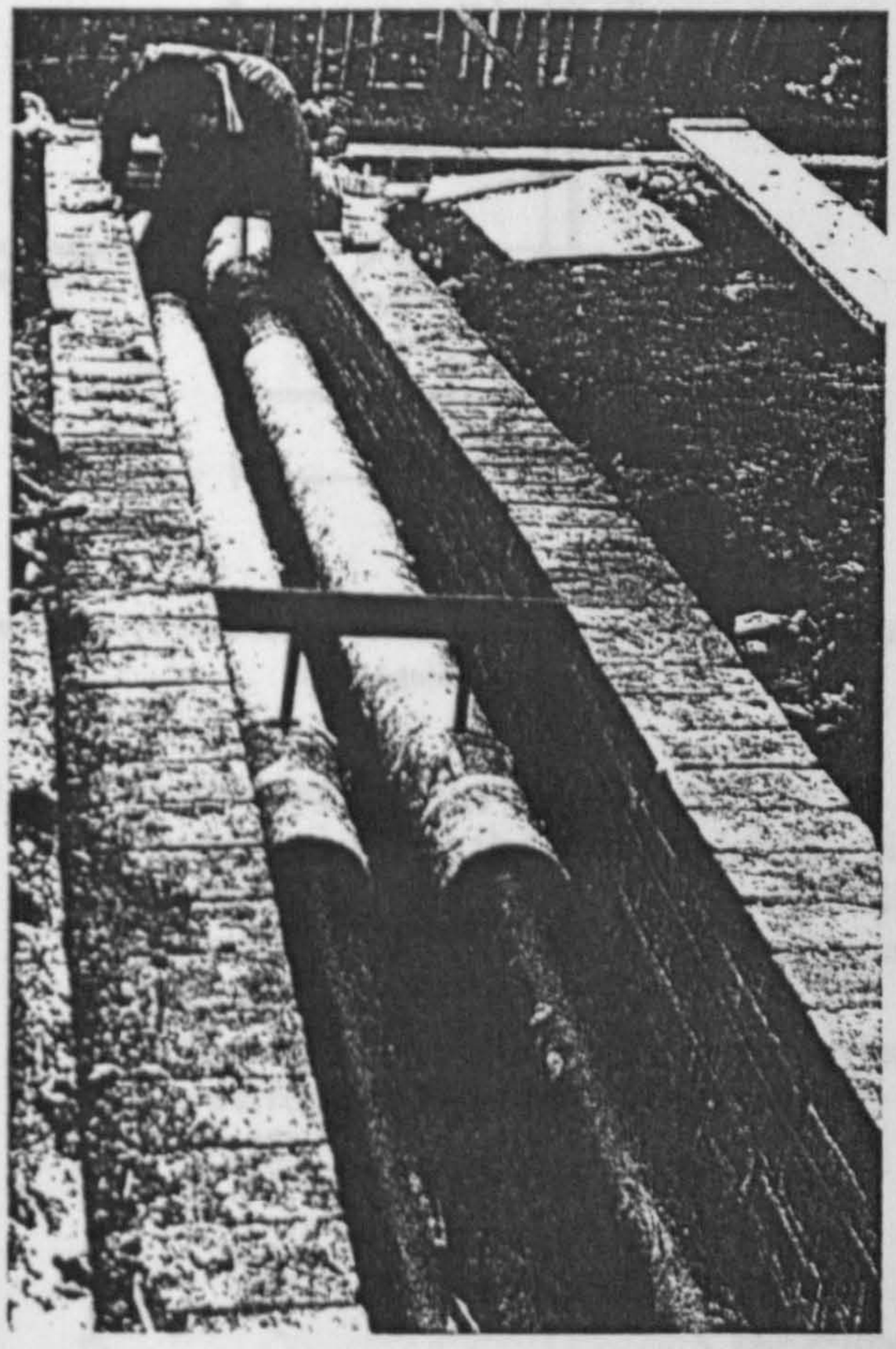

Fig. 1. Current conventional practice, i.e. the 'side-by-side' arrangement of district-heating pipelines in a trench.

L Axial length of the considered horizontal air-filled cavity (see Fig. 3) (mm)

M Dimensionless parameter dependent upon the geometry and temperature distribution of the system

$$\left\{ = \frac{\mathrm{Nu}_\theta}{\mathrm{Gr}_\theta^n} \right\}$$

n Power index of the Grashof number in the $\overline{\mathrm{Nu}_\theta}$ versus Gr_θ relationship

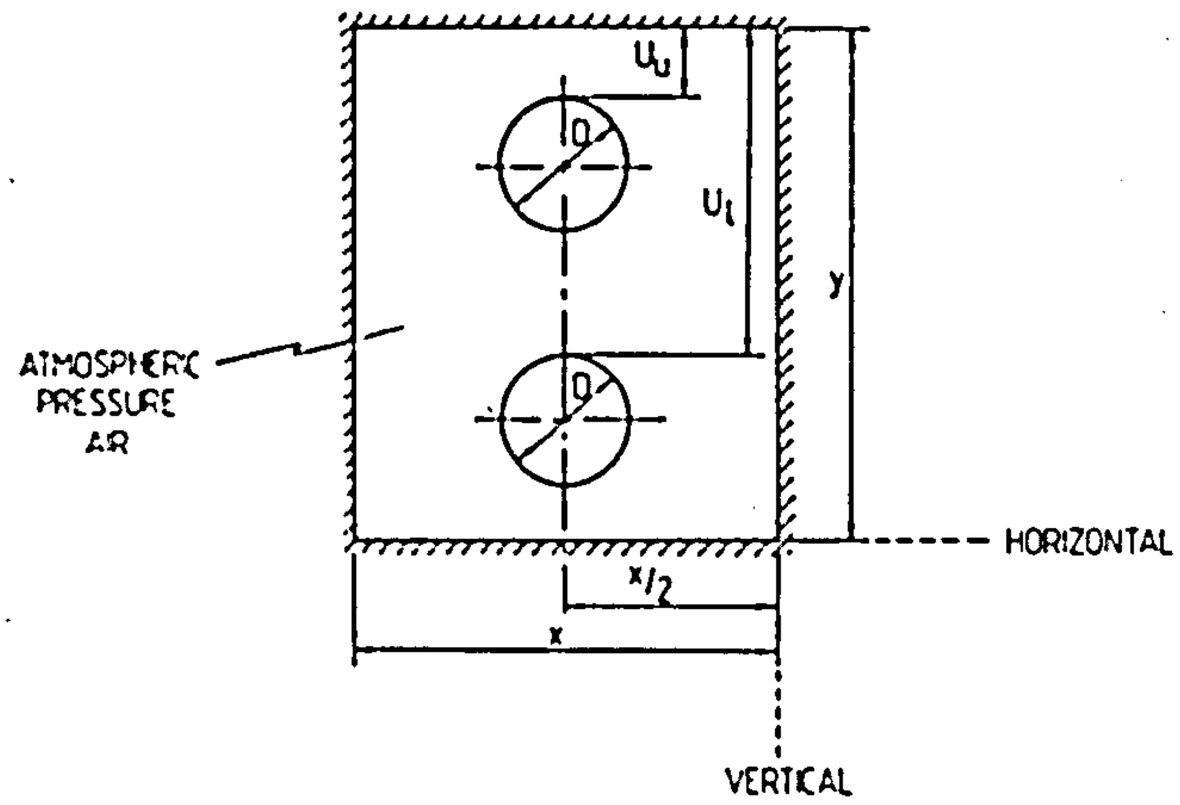

Fig. 2. Schematic representation of a vertical section through the horizontal pipes in the rectangular duct.

$\dot{Q}_{conv+cond}, \dot{Q}_{rad}$ Contributions to the steady-state rate of heat leak through the air from the horizontal supply pipe due to, respectively, convection + conduction and radiation (W)

$\dot{Q}_{total}$ Total steady-state rate of heat loss from the supply (i.e. the hotter) pipe (W)

T_0 Steady-state temperature of the inner surfaces of the outer surrounding 'isothermal' rectangular duct (see Fig. 4) (°C)

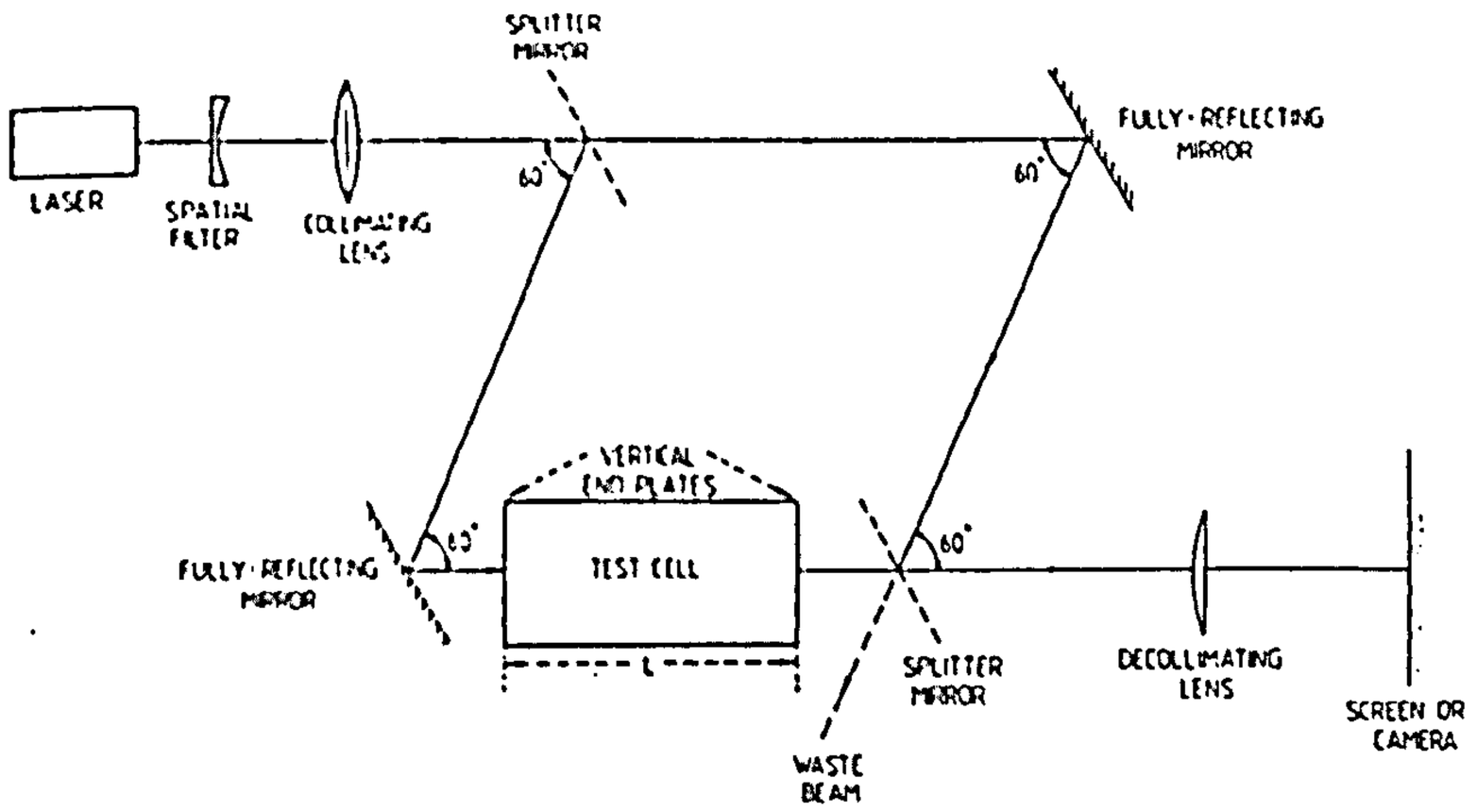

Fig. 3. Schematic plan-view of the Mach-Zehnder interferometer.

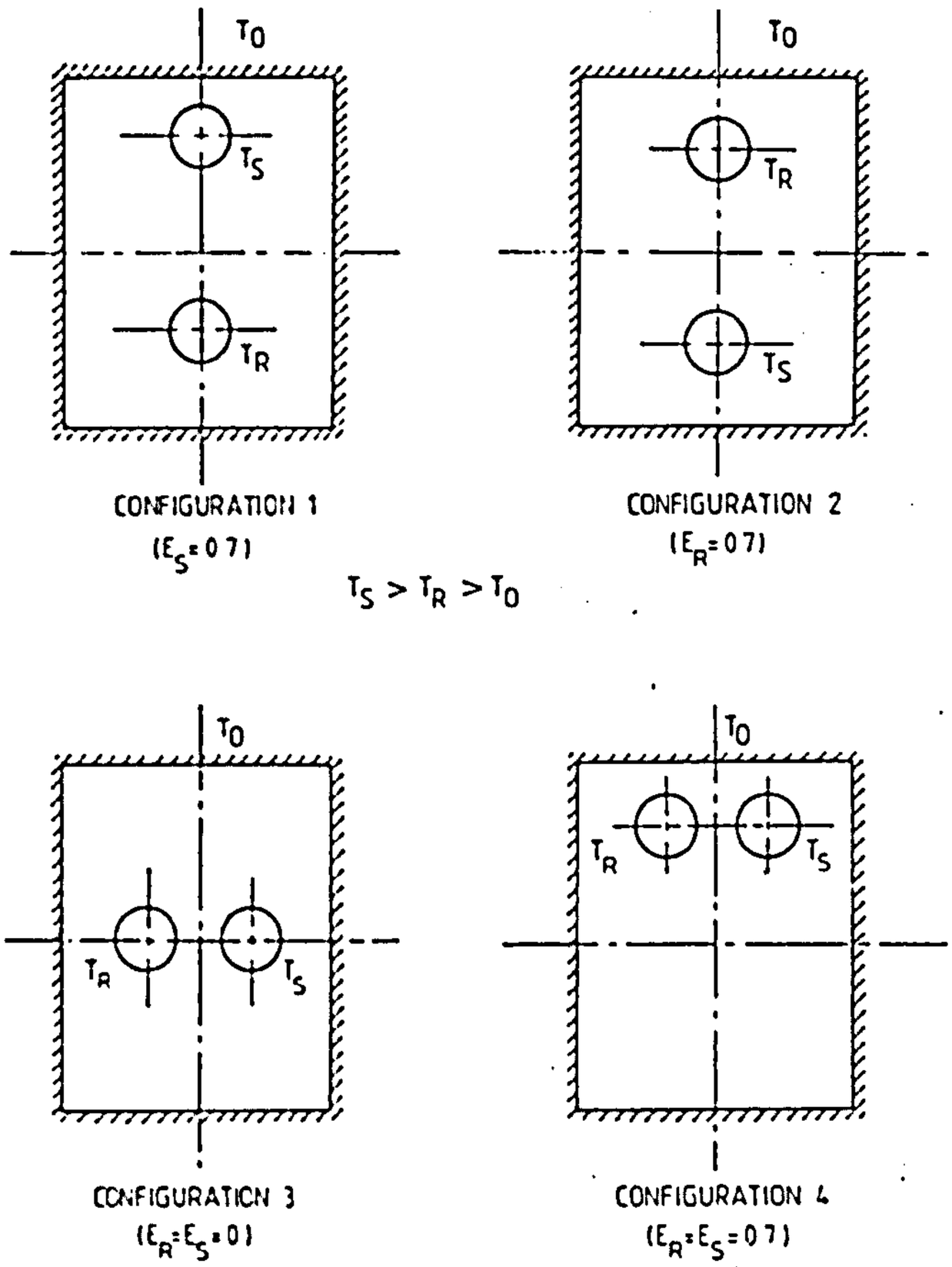

Fig. 4. Schematic vertical sections of the experimental model 'district-heating' horizontal pipeline systems tested.

T_R, T_S Steady-state temperatures of the outer surfaces of the return and supply pipes, respectively (see Fig. 4) (°C)

U_l, U_u Minimum gaps, i.e. the shortest vertical distances between the lower and upper horizontal pipes and the upper horizontal internal surface of the duct, respectively (see Fig. 2) (mm)

x Horizontal width of the rectangular cavity (see Fig. 2) (mm)

y Vertical dimension of the rectangular air-filled cavity (see Fig. 2) (mm)

Gr_0	Local Grashof number, based on the width x of the rectangular cavity
Nu_0 and $\overline{Nu_0}$	Local and average Nusselt numbers, for the steady-state heat transfers from the hot supply pipe, based on the width x of the rectangular cavity
ΔT	Temperature difference between the outer surface of the supply (i.e. the hot) pipe, at T_s, and the inner surface of the duct, at T_0
ε	Emissivity of the appropriately identified surface
θ	Angular co-ordinate, measured from zero for the vertically upwards radius vector emanating from the centre of the supply pipe (see Fig. 5) (degrees)

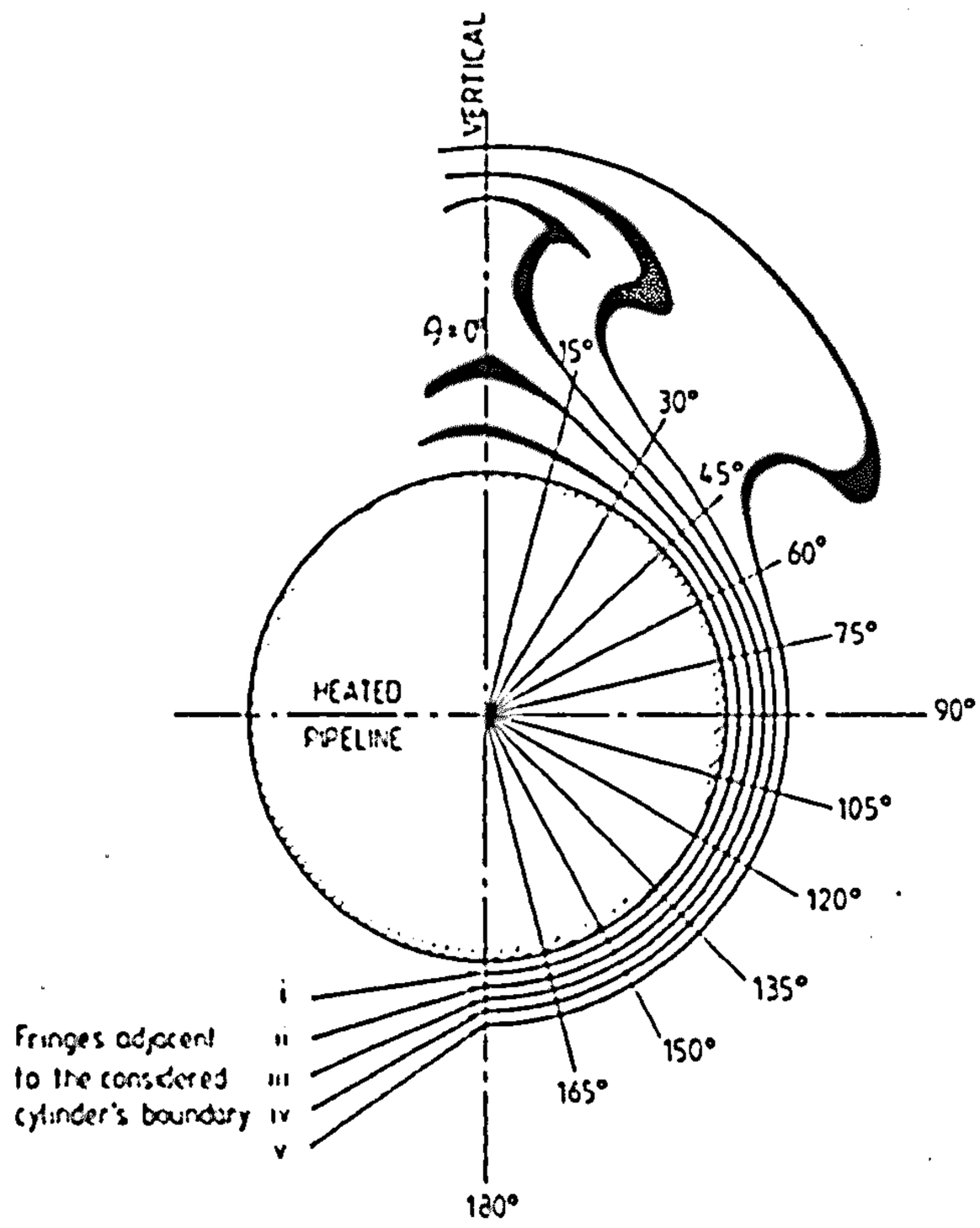

Fig. 5. Isotherms around a horizontal heated pipeline as revealed by Mach-Zehnder interferometry. The angular co-ordinate, θ, is measured from the top of the supply pipe.

Suffixes

cond	Due to conduction through the air
conv	Due to convection of the air
l	Referring to the lower pipe
o	Of the inner surface of the rectangular enclosure
R	For the return pipe
rad	Due to net radiation loss from the supply pipe
S	For the supply pipe
total	Referring to the total steady-state heat leak through the air
u	Referring to the upper pipe
θ	At angle *θ*

CURRENT PRACTICE AND THE PRESENT INVESTIGATION

District heating usually refers to the distribution of heat from a centralised source to many different customers within a small locality, i.e. to a high density of big demand customers for the heat.[1] Employing a single pipeline for the distribution of heat is usually unsatisfactory, both technically and economically. It is preferable to use twin-pipe systems, comprising of a 'return' pipe containing water at a lower temperature than that in the 'supply' pipe but still much higher than the environmental temperature. Most hot-water distribution systems nowadays are based on the two-pipe, *side-by-side* layout. Unfortunately, little attention has so far been devoted to the financial savings which can be achieved in reducing the heat losses by choosing the optimal configuration for such pipes.

It is normal practice for district-heating pipes to be clad with insulants. These insulated pipes are then located in air-filled rectangular trenches. Thus, in the event of flooding of such trenches, which occurs intermittently in Britain because of its maritime climate (i.e. almost continuous high humidity and large rainfall), drainage and evaporation from around the pipes would ensue automatically.[2] Otherwise, if allowed to remain damp, the effective conductivity of the applied insulant increases significantly: it would probably also suffer irreversible structural damage. As this atmospheric pressure air-filled cavity is often adopted for moisture removal purposes, it appears desirable to employ the air in the trench to achieve maximum energy thrift, i.e. to use its thermally insulating properties (air being the commonest thermal

insulant) to minimise the rate of heat loss from the supply pipeline. Because of the conflicting dependences of the radiative, conductive and convective contributions through the air to the total steady-state heat leak from the supply pipeline, there are optimal positions for the pipelines. By choosing this optimal configuration rather than the conventional system (see Fig. 1), the thermal insulation provided by the air can be increased without any extra financial expenditure being incurred.[3,4]

Current conventional practice recommends a gap of 50 mm clear spacing between the supply and return pipes for all pipe sizes, with the pipes being placed *side-by-side*.[5]

The present investigation was aimed at studying the following:

(i) The steady-state heat transfers across the atmospheric-pressure air-filled gap between an isothermal 'cold' horizontal rectangular sectioned Perspex duct enclosing two horizontal pipes, the first carrying hot water (i.e. the supply line) and the other, slightly cooler water (i.e. the return line), were measured—see Fig. 4.

In particular, the effects of position changes of the horizontal pipes were examined, with a view to determining the optimal positions of the inner pipes in order to achieve the least rate of steady-state heat loss from the *supply* pipe.

Because the owners of district-heating schemes are mainly interested in distributing hot water to their customers with the least heat loss from the supply (i.e. the hotter) pipe as possible during transmission, only losses from this pipe were considered in the present investigation.

(ii) The convective flow patterns within the enclosed air-space were observed by injecting smoke particles slowly into the illuminated rectangular duct. Flow visualisations for different steady-state temperatures of the pipes and enclosure, for different geometric configurations, were needed to supplement and corroborate conclusions drawn from interferometric observations of the steady-state isotherms in the air gap.

THE EXPERIMENTAL RIG

The main instrument used in this investigation was the 18 cm field-of-view, 3 mW He–Ne laser-stimulated Mach-Zehnder interferometer (see Fig. 3). This, when employed in the infinite-fringe mode, produced a

distinctive characteristic interferogram for each two-dimensional steady-state temperature distribution in the cavity examined. These interferograms indicated the refractive index (and hence density) variations integrated over the axial length of the considered cavity. The map of interference fringes so obtained represented isothermal contours within the cavity. The main benefit using Mach-Zehnder interferometry is that it enables the temperature distribution of the whole field-of-view to be measured without the disturbing influences of temperature probes or concomitant leads having to be present in the cavity. Thereby it satisfies the basic principle of measurement—the measuring system should not affect the system being examined.

The horizontal rectangular cavity considered experimentally was closed at its two ends by means of two vertical, optically flat, uniformly thick, homogeneous glass plates, i.e. the end-plates (see Fig. 3). The effects of image distortion due to refraction of the beam through the test cell, and also at the ends of the cavity, were reduced by focusing the camera on a vertical plane (at $0{\cdot}33L$) from the end-plate nearer to the camera, as recommended by Mehta and Black.[6]

EXPERIMENTAL TEST CELL

The values of the experimental parameters chosen for this investigation were:

$$x = 100\,\text{mm},\ y = 125\,\text{mm},\ L = 650\,\text{mm},\ D = 28{\cdot}5\,\text{mm}$$

$$-0{\cdot}6 < E_R \text{ or } E_s < 0{\cdot}7$$

and

$$10\,^{\circ}\text{C} < T_0 < 20\,^{\circ}\text{C} < T_R < 30\,^{\circ}\text{C} < T_s < 50\,^{\circ}\text{C}$$

The cold outer duct, manufactured from transparent Perspex, was painted matt black except for a thin (~ 5 mm) slit (in the previously considered vertical cross-sectional plane at $0{\cdot}33L$ from the end plate) to facilitate the introduction of adequate illumination from three projectors, so enabling the convecting airflows within the duct to be observed. The duct walls were cooled by passing water, at mains pressure and temperature, through a series of enclosed channels within each wall in order to simulate approximately the conditions occurring in underground trenches. Thirty-six thermojunctions were attached flush with the duct's

inner surface, so permitting the temperature distribution over the inner surface of the cavity wall to be determined. The two contained copper pipes were heated by passing hot water through them at their respective steady temperatures, T_R and T_S, so that $T_R < T_S$. Both pipes were supported at their ends by means of horizontal hollow tubular extensions, which also served to introduce and remove the hot and the relatively cooler water: the water passed into and out of these pipes in a counter-flow manner. The tubular extensions were clamped to four vertical brackets, two at each end, along which the clamps could be moved, up or down, together by identical amounts, thus altering the displacement ratio, E_R or E_s, of the horizontal pipes.

FLOW VISUALISATION

This was undertaken for several different geometrical configurations (see Fig. 4). A small amount of smoke was injected slowly into the cavity and photographs were taken of the resulting steady-state flow patterns. Flow visualisations provided qualitative indications of the convecting air flows that occur in the cavity and also indicated the presence of any flow instabilities, so that the conditions under which the latter occurred could be ascertained.

Four different configurations were examined, each for two different steady-state temperature differences between the hot and the relatively cooler pipes (see Fig. 6).

Flow patterns for the 'hot-above-cooler' pipe system (i.e. configuration 1 of Fig. 4) exhibited two stable counter-rotating, approximately triangular shaped, eddies, which were symmetrical about the vertical plane, through the horizontal axes of the cylinders, bisecting the duct (see Fig. 6(i) and (ii)). There was also a stagnant layer near the bottom of the air-filled cavity. For the two temperature differences tested (i.e. $\Delta T =$ 17·5 °C and 27·5 °C), the patterns were of almost identical shapes and qualitatively independent of T_0, T_S and T_R. The air circulation speed, as expected, rose as the temperature difference between the duct and the contained pipes increased.

For the 'warm-above-hot' pipe system (i.e. configuration 2 of Fig. 4), the flow pattern was of an irregular shape. It also exhibited severe instabilities with intense mixing: an oscillating plume between the two pipes, as well as large vortices, were produced above the cooler pipe (see

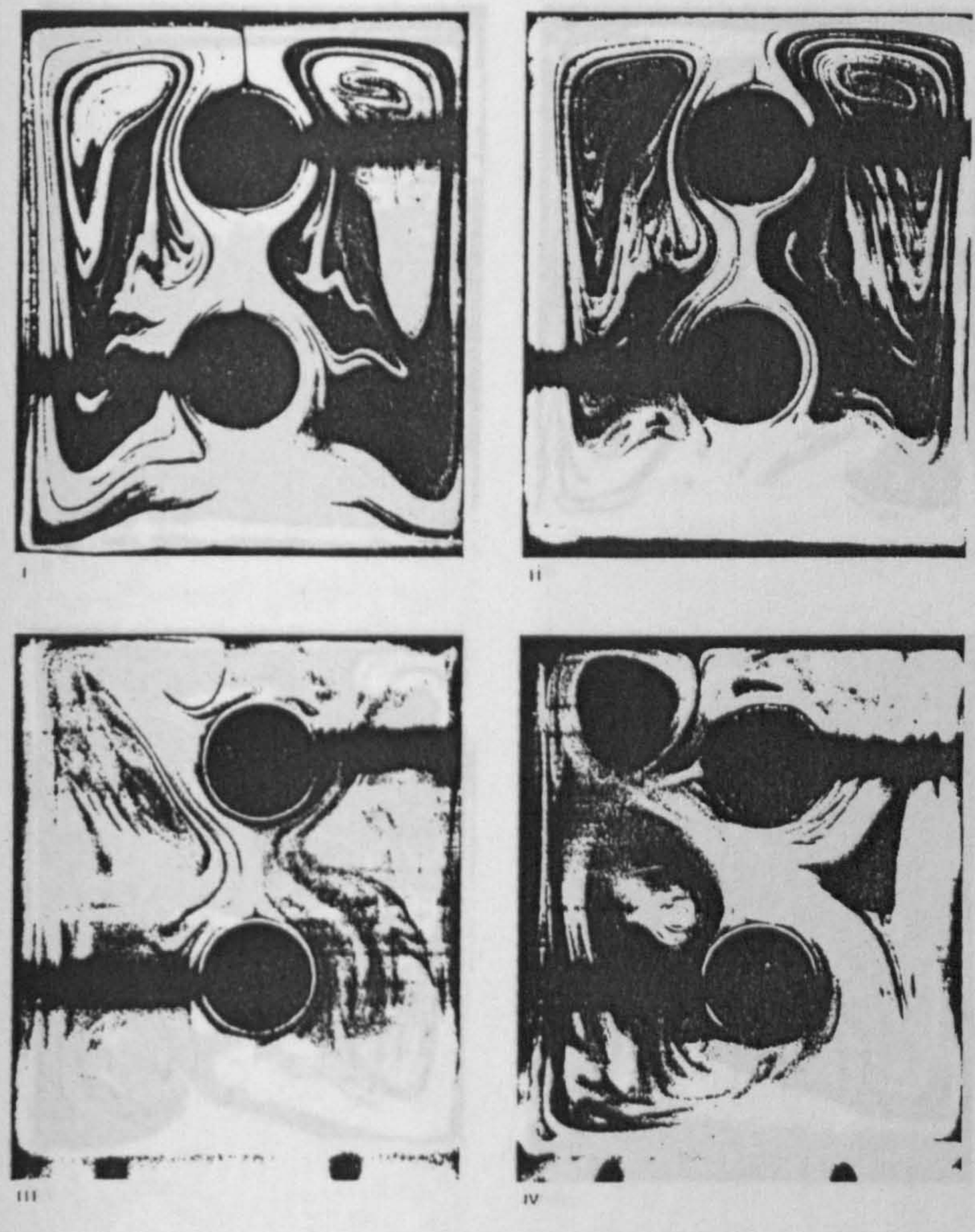

Fig. 6. Typical steady-state flow visualisations: $T_0 = 12{\cdot}7\,°C$. (i) and (ii) Configuration 1 ($E_R = -0{\cdot}65$, $E_S = 0{\cdot}7$). (iii) and (iv) Configuration 2 ($E_R = 0{\cdot}7$, $E_S = -0{\cdot}65$). (i) and (iii) $\Delta T = 17{\cdot}5\,°C$; (ii) and (iv) $\Delta T = 27{\cdot}5\,°C$. (v) and (vi) Configuration 3 ($E_R = E_S = 0$). (vii) and (viii) Configuration 4 ($E_R = E_S = 0{\cdot}7$). (v) and (vii) $\Delta T = 17{\cdot}5\,°C$; (vi) and (viii) $\Delta T = 27{\cdot}5\,°C$.

Fig. 6(iii) and (iv)). Consequently, relatively high rates of heat transfer occurred. The shapes of the eddies were again almost independent of the differences between T_0, T_R and T_S.

Flow patterns for the '*side-by-side*' system, having $E = 0$ (i.e. configuration 3 of Fig. 4), could be considered as consisting of three zones (see Fig. 6(v) and (vi)). First, there was an approximately triangular-

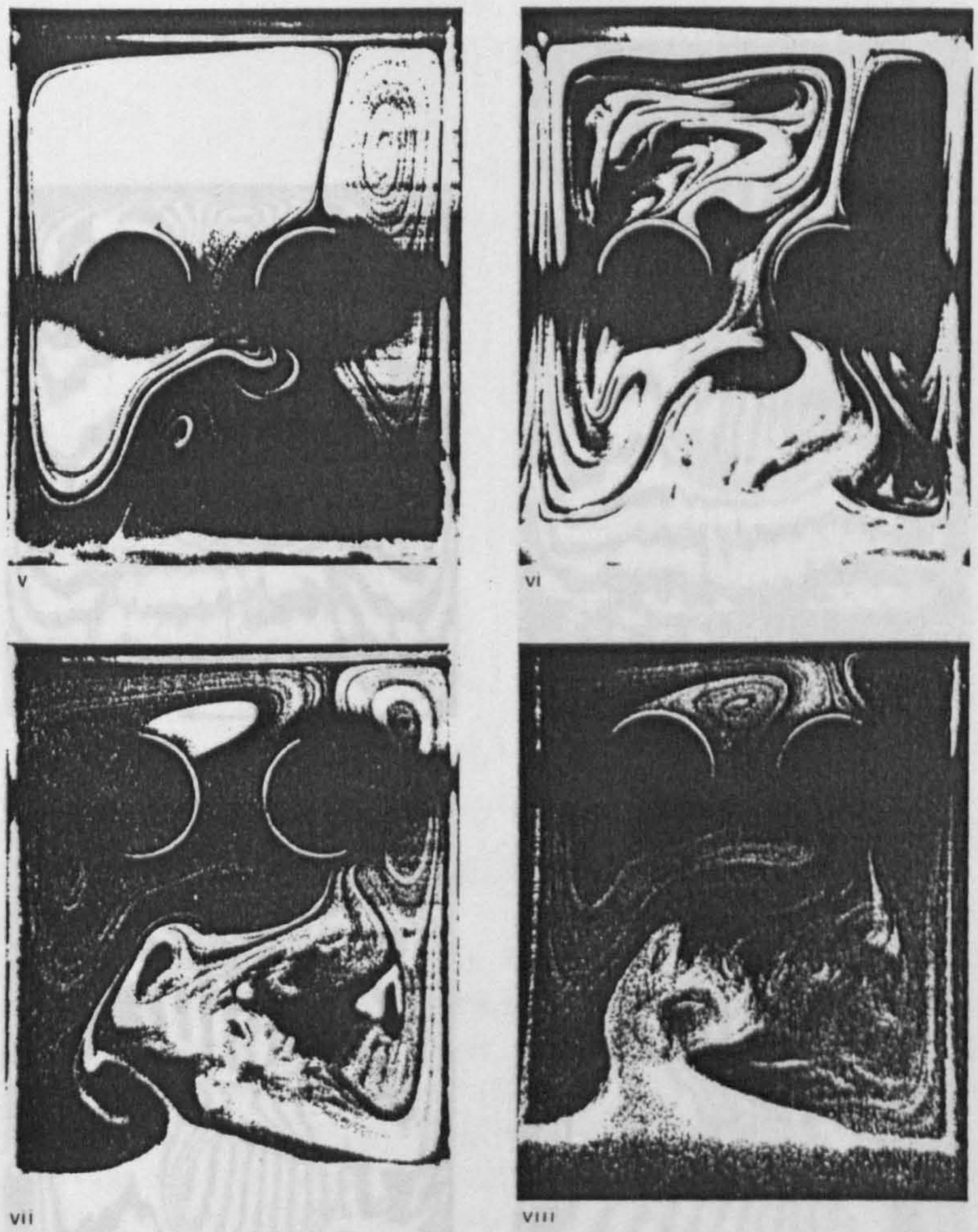

Fig. 6.—*contd.*

shaped eddy circulating around the cooler pipe and this had the longest flow path of the three zones; secondly, a well-defined eddy ensued between the hotter pipe and the wall of the enclosure and, thirdly, in the lower half of the duct, a weak, irregularly shaped vortex occurred.

If $E = 0{\cdot}7$, i.e. configuration 4 of Fig. 4, the flow was observed to consist of two zones divided approximately diagonally across the duct section (see Fig. 6(vii) and (viii)). The flows in these two zones again circulated in a counter-rotating manner, with a larger stagnant core (than that which occurred if $E = 0$, i.e. for configuration 3) near the base of the cavity.

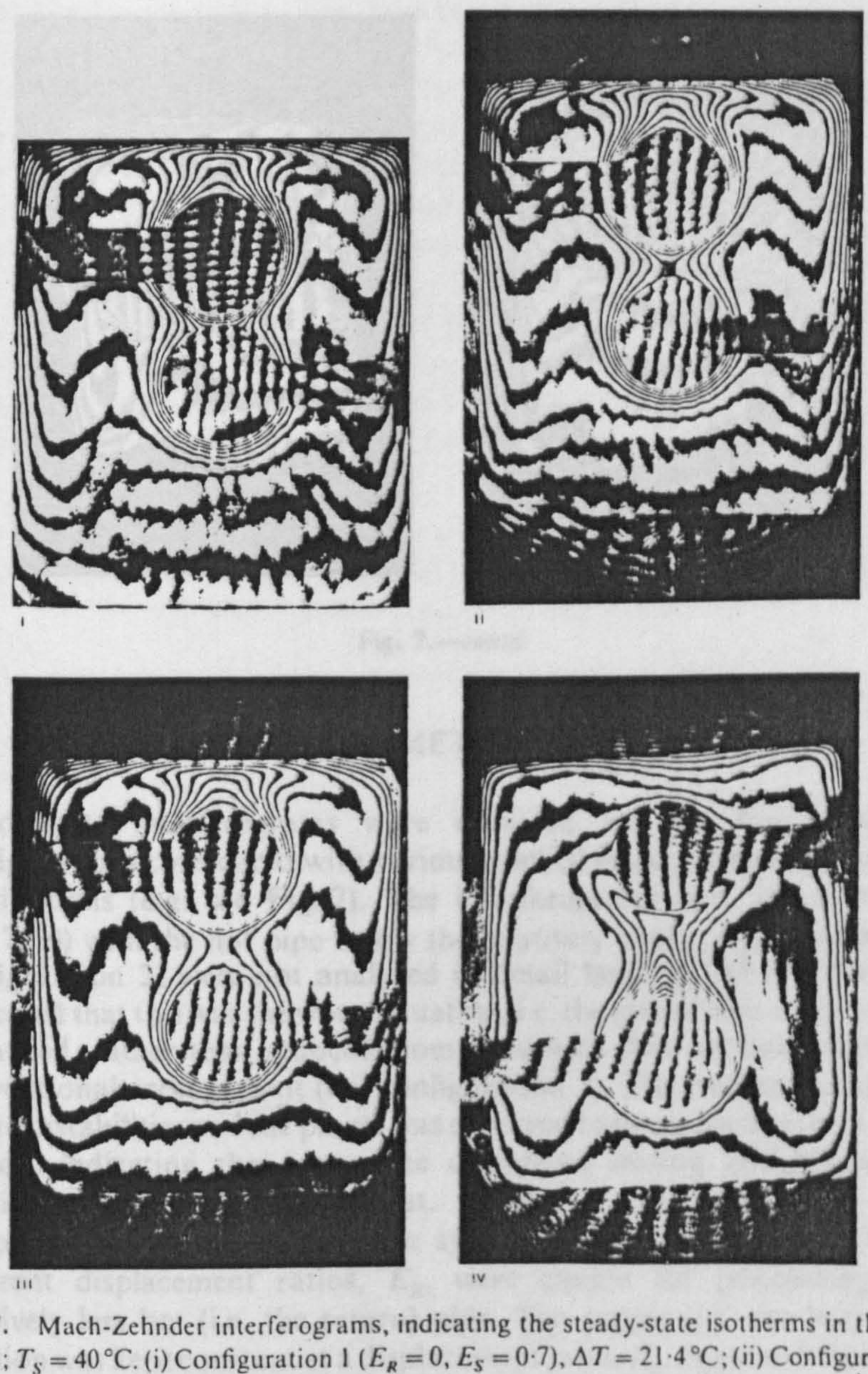

Fig. 7. Mach-Zehnder interferograms, indicating the steady-state isotherms in the air cavity; $T_S = 40\,°C$. (i) Configuration 1 ($E_R = 0$, $E_S = 0{\cdot}7$), $\Delta T = 21{\cdot}4\,°C$; (ii) Configuration 1 ($E_R = -0{\cdot}1$, $E_S = 0{\cdot}7$), $\Delta T = 21{\cdot}5\,°C$; (iii) Configuration 1 ($E_R = -0{\cdot}2$, $E_S = 0{\cdot}7$), $\Delta T = 20{\cdot}7\,°C$; (iv) Configuration 2 ($E_R = 0{\cdot}7$, $E_S = -0{\cdot}65$), $\Delta T = 20{\cdot}4\,°C$; (v) Configuration 3 ($E_R = E_S = 0$), $\Delta T = 21{\cdot}5\,°C$; (vi) Configuration 4 ($E_R = E_S = 0{\cdot}7$), $\Delta T = 20{\cdot}4\,°C$.

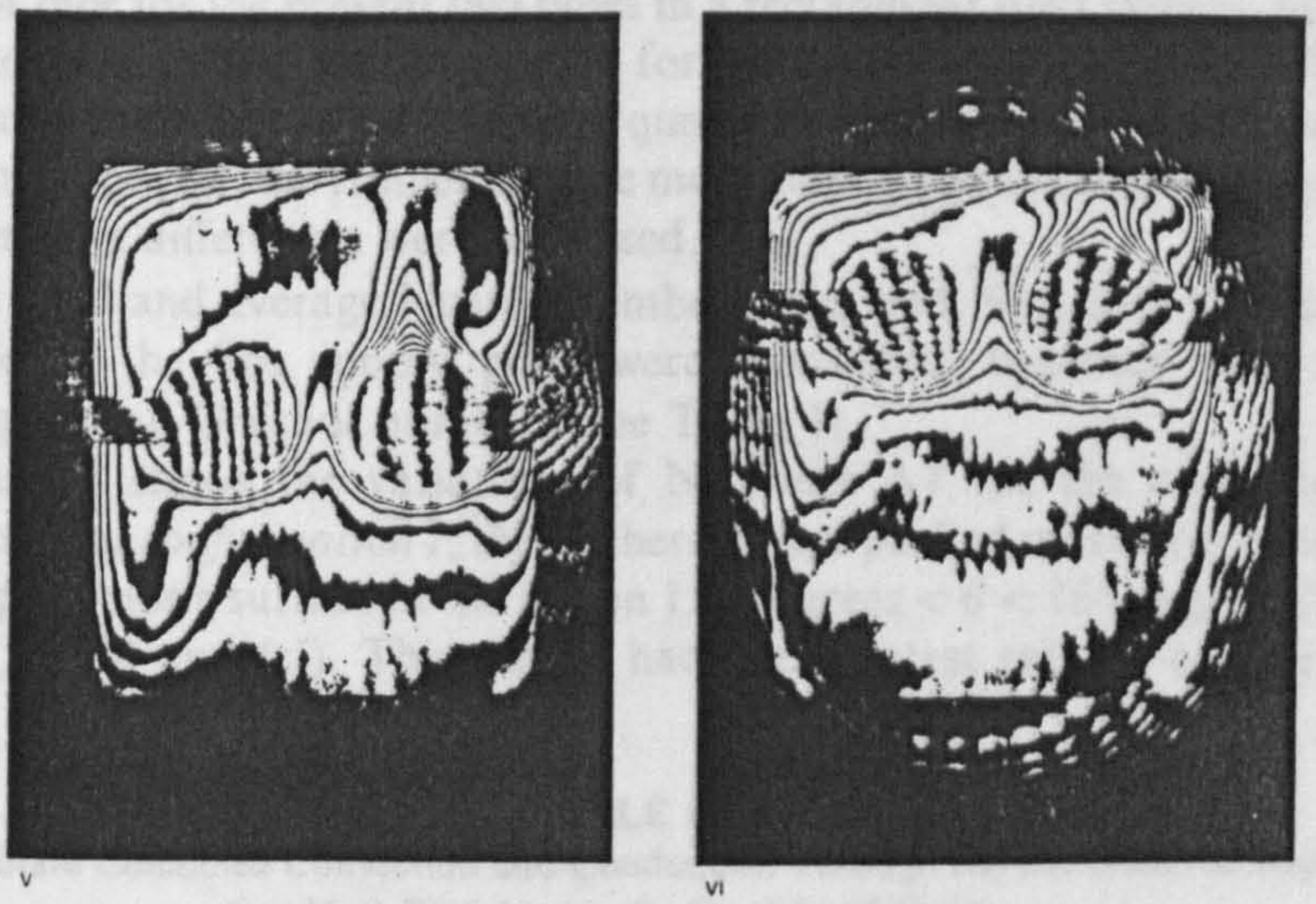

Fig. 7.—*contd.*

INTERFEROMETRIC STUDIES

Steady-state interferograms were obtained for the four different configurations considered with various applied steady-state temperature distributions (e.g. see Fig. 7). The interferograms (see, for example, Fig. 7(iv)) with the hot pipe below the relatively cooler pipe system (i.e. configuration 2) were not analysed in detail because the observations indicated that this was the worst situation, i.e. the rate of heat transfer was enhanced, rather than reduced, compared with that obtained with the conventional arrangement (i.e. configuration 3). The isotherms showed severe instabilities and the plume was observed to be oscillating from side-to-side, indicating the occurrence of intense mixing and hence the relatively high rates of loss of heat.

For the '*hot-above-cooler*' pipe system (i.e. configuration 1), three different displacement ratios, E_R, were chosen for positioning the relatively less hot (i.e. the return) pipe. The supply (i.e. the hot) pipe position was kept constant at a displacement ratio, E_S, equal to 0·7 (which is the approximate value for the optimal location for a single horizontal pipe in a rectangular duct, as recently established in another series of experiments at Cranfield). This may not be the overall optimal position of

the hot pipe for the present two pipes in a rectangular duct system, but it represents a logical starting point for the present investigation. The isotherms for different ΔT's were of qualitatively similar shapes for each configuration, but the fringes became more closely packed together as the temperature differences were increased.

The local and average Nusselt numbers, Nu_θ and $\overline{Nu}_\theta$, over the outer surface of the hot supply pipe, were calculated, together with the corresponding Grashof numbers (see Table 1).

Figure 8 shows the variations of Nu_θ with ΔT for the considered systems. For *configuration 1*, the isotherms were packed most closely near the supply pipe's surface in the region 150 degrees $< \theta <$ 165 degrees (see Fig. 8(a), (b) and (c)). This region had the greatest rate of combined

TABLE 1
Steady-State Combined Convection and Conduction Through the Air from the Supply (i.e. Hot) Pipe Across the Considered Cavity
($T_R = 30°C$)

Qualitative configuration description	*Geometrical description*	T_s (°C)	ΔT $(= T_s - T_0)$, (°C)	$10^{-6} Gr_\theta$	$\overline{Nu}_\theta$
1	$E_R = 0$	35	16·6	2·2	6·0
	$E_s = 0{\cdot}7$	40	21·4	2·8	8·0
		45	26·4	3·5	10·1
		50	39·7	5·2	13·8
1	$E_R = -0{\cdot}1$	35	16·5	2·2	6·9
	$E_s = 0{\cdot}7$	40	21·5	2·8	8·6
		45	29·2	3·8	10·5
		50	30·8	4·0	11·2
1	$E_R = -0{\cdot}2$	35	15·9	2·1	7·1
	$E_s = 0{\cdot}7$	40	20·7	2·7	9·5
		45	25·3	3·3	10·6
		50	30·2	3·9	12·2
3	$E_R = 0$	35	16·9	2·3	10·1
	$E_s = 0$	40	21·5	2·8	12·6
		45	26·5	3·5	13·4
		50	31·3	4·1	15·0
4	$E_R = 0{\cdot}7$	35	15·7	2·1	7·7
	$E_s = 0{\cdot}7$	40	20·4	2·7	10·1
		45	24·4	3·2	11·8
		50	31·1	4·0	13·7

convective and conductive steady-state heat transfer $\dot{Q}_{conv+cond}$ for the $E_R = 0$ configuration under a specified ΔT. As the return (i.e. the cooler) pipe was displaced relatively downwards (E_R becoming $-0{\cdot}1$ and subsequently $-0{\cdot}2$), the value of θ, corresponding to the surface zone having the greatest rate of heat transfer, remained approximately unchanged. All the isotherms were symmetrical about the zero and 180 degree axes (see Fig. 8(a), (b) and (c)).

The maximum rate of heat transfer for *configurations 3 and 4* occurred near the bottom of the hot pipe, i.e. in the 180 to 215 degree region (see Fig. 8(d) and (e)). For configuration 1, the flow pattern was observed to be stable with a stagnant region near the base of the air-filled cavity.

The value of M in the standard equation describing the combined steady-state conduction plus convection through the air—$\overline{Nu}_\theta = M Gr_\theta^n$—

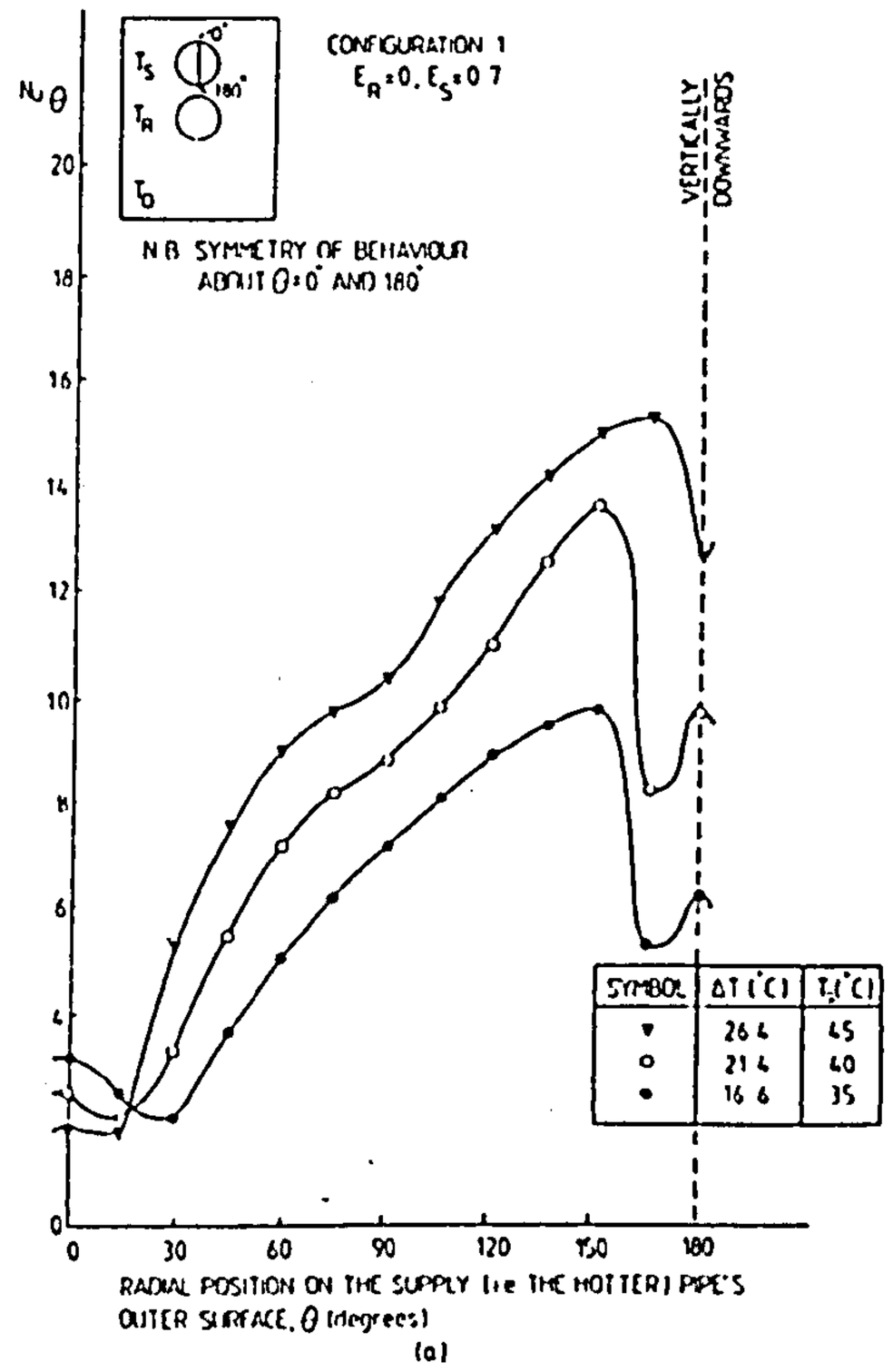

Fig. 8. Variation of the local Nusselt number, Nu_θ, versus angular co-ordinate, θ, for the supply pipeline: θ increases in this instance from 0° to 180° (and thence to 360° for (d) and e)) in a *counter-clockwise* direction.

VERTICALLY DOWNWARDS
CONFIGURATION 1
$\varepsilon_R = 0.2$, $\varepsilon_S = 0.7$
NB SYMMETRY OF BEHAVIOUR ABOUT $\theta = 0^\circ$ AND 180°
T_S $\phi^{0^\circ}_{180^\circ}$
T_R ○
T_O
SYMBOL | ΔT (°C) | T_S (°C)
△ | 30·2 | 50
▲ | 25·3 | 45
○ | 20·7 | 40
● | 15·9 | 35
Nu_θ
RADIAL POSITION ON THE SUPPLY (i.e. THE HOTTER) PIPE'S OUTER SURFACE, θ (degrees)
(c)

VERTICALLY DOWNWARDS
CONFIGURATION 1
$\varepsilon_R = 0.1$, $\varepsilon_S = 0.7$
NB SYMMETRY OF BEHAVIOUR ABOUT $\theta = 0^\circ$ AND 180°
T_S $\phi^{0^\circ}_{180^\circ}$
T_R ○
T_O
SYMBOL | ΔT (°C) | T_S (°C)
△ | 30·8 |
▲ | 27·2 |
○ | 21·5 |
● | 16·5 |
Nu_θ
RADIAL POSITION ON THE SUPPLY (i.e. THE HOTTER) PIPE'S OUTER SURFACE, θ (degrees)
(b)

Fig. 8.—*contd.*

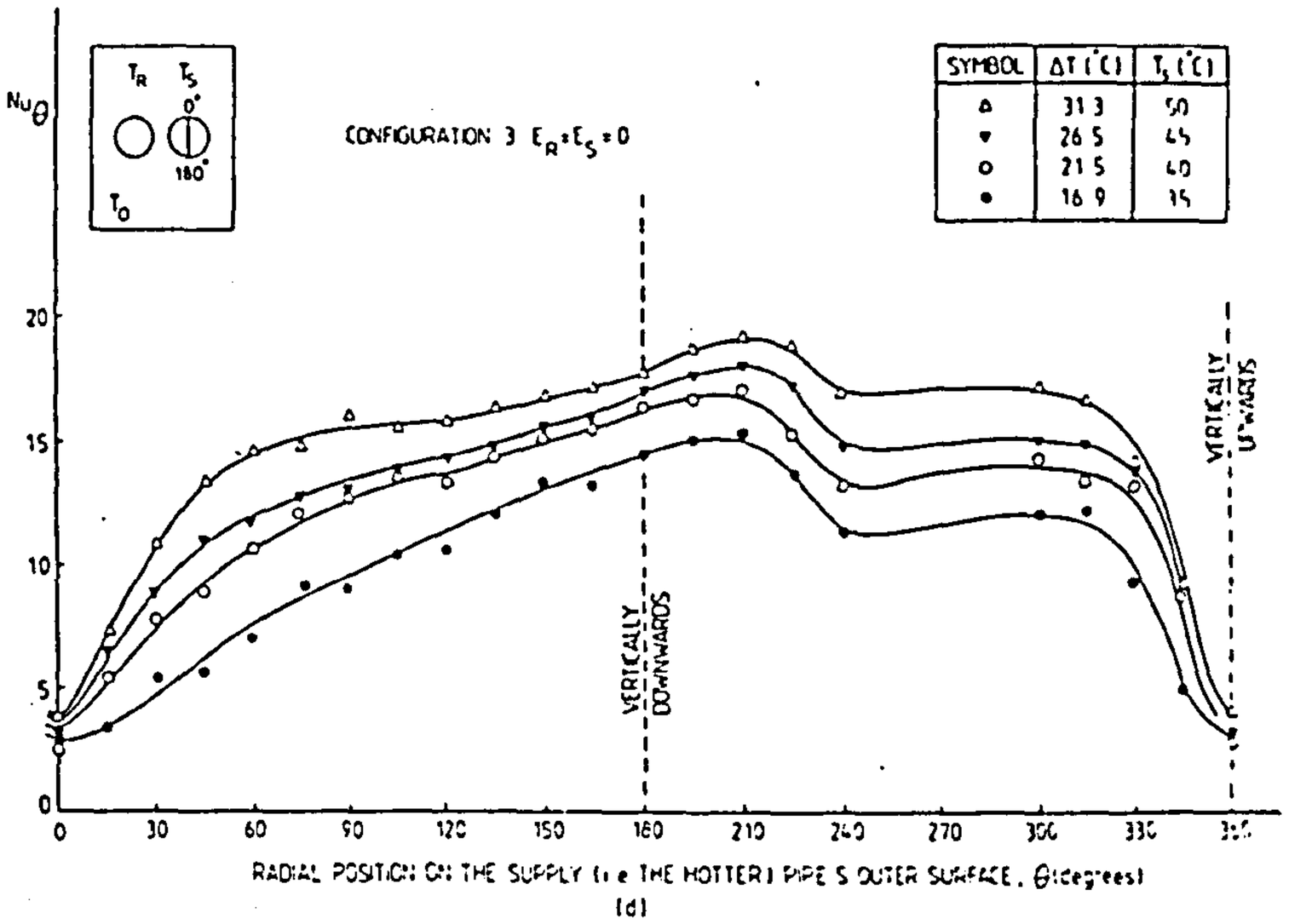
Nu_θ
T_R
T_S
0°
180°
T_0
CONFIGURATION 3 $E_R = E_S = 0$
SYMBOL | ΔT (°C) | T_S (°C)
Δ | 31 3 | 50
▼ | 26 5 | 45
○ | 21 5 | 40
● | 16 9 | 35
VERTICALLY DOWNWARDS
VERTICALLY UPWARDS
0 30 60 90 120 150 180 210 240 270 300 330 360
RADIAL POSITION ON THE SUPPLY (i e THE HOTTER) PIPE S OUTER SURFACE, θ (degrees)
(d)

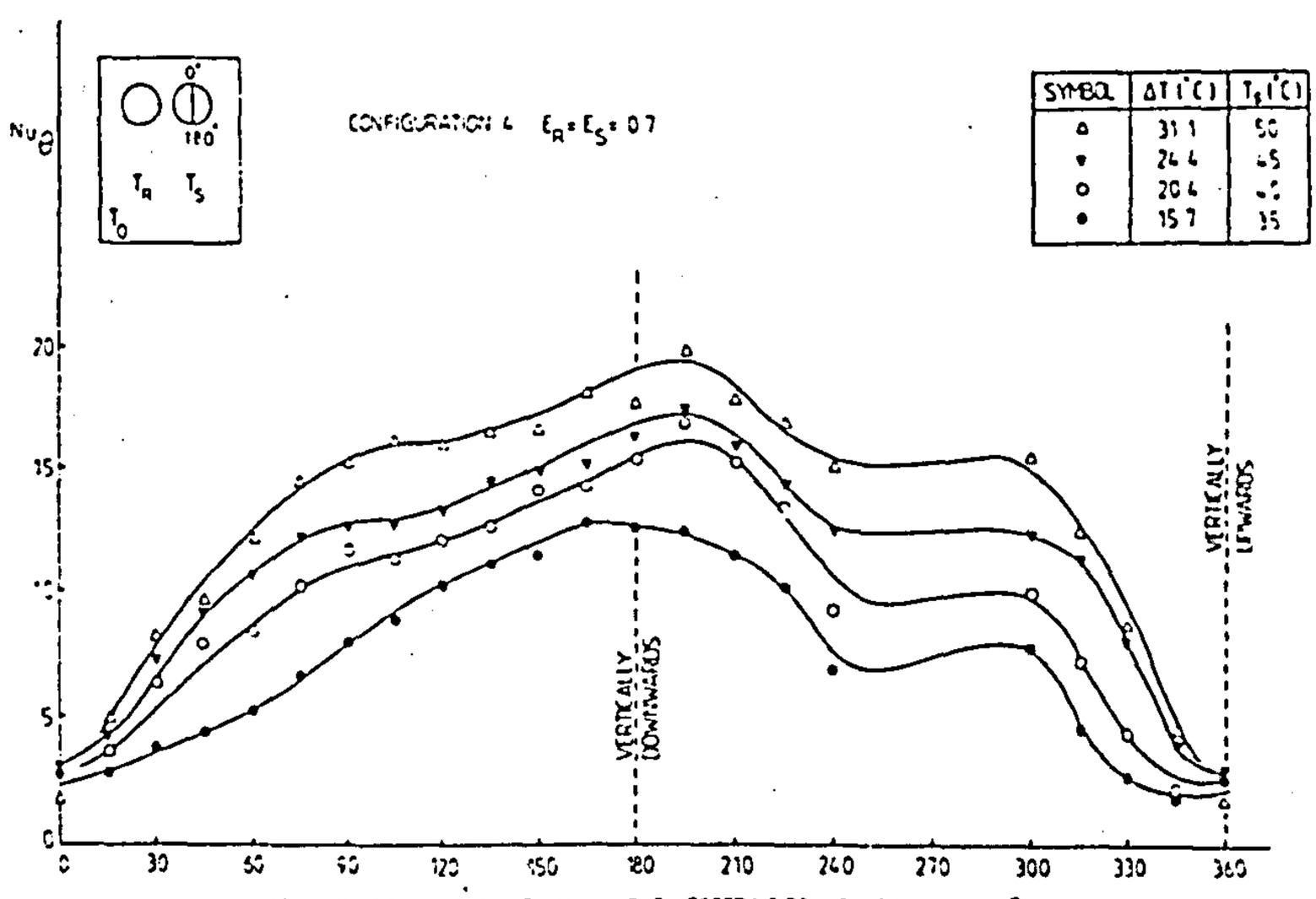
Nu_θ
0°
180°
T_R
T_S
T_0
CONFIGURATION 4 $E_R = E_S = 0.7$
SYMBOL | ΔT (°C) | T_S (°C)
Δ | 31 1 | 50
▼ | 24 4 | 45
○ | 20 4 | 40
● | 15 7 | 35
VERTICALLY DOWNWARDS
VERTICALLY UPWARDS
0 30 60 90 120 150 180 210 240 270 300 330 360
RADIAL POSITION ON THE SUPPLY (i e THE HOTTER) PIPE'S OUTER SURFACE, θ (degrees)
(e)

Fig. 8.—*contd.*

for this system is a complicated function of geometry and the temperature distributions. It needs more data than are at present available for its general form to be deduced.

The way in which the total steady-state rate of heat loss Q_{total} from the supply pipe was dependent upon the temperature difference, ΔT, for different configurations is shown in Table 2, together with its radiation component, $\dot{Q}_{rad}$, and its convective plus conductive component, $\dot{Q}_{conv+cond}$, through the atmospheric pressure air in the cavity. It can be seen that, for the hot pipe above the relatively cooler pipe, $\dot{Q}_{rad}$ is relatively insensitive to changes in T_R, but $\dot{Q}_{conv+cond}$ increases slightly as E_R decreases from $-0{\cdot}1$ to $-0{\cdot}2$, all conditions remaining invariant. For

TABLE 2

Steady-State Heat Leaks from the 0·65 m Long Supply (i.e. Hot) Pipe Through the Air Across the Considered Cavity

($T_R = 30°C$)

Configuration	*Geometrical description*	T_s (°C)	ΔT ($= T_s - T_0$), (°C)	$\dot{Q}_{conv+cond}$ (W)	$\dot{Q}_{rad}$* (W)	$\dot{Q}_{total}$ (W)
1	$E_R = 0$ $E_s = 0{\cdot}7$	35	16·6	1·5	4·2	5·7
		40	21·4	2·6	5·7	8·3
		45	26·4	4·1	7·3	11·4
		50	39·7	8·4	10·8	19·2
1	$E_R = -0{\cdot}1$ $E_s = 0{\cdot}7$	35	16·5	1·7	4·3	6·0
		40	21·5	2·8	5·8	8·6
		45	29·2	4·7	8·0	12·7
		50	30·8	5·4	8·9	14·3
1	$E_R = -0{\cdot}2$ $E_s = 0{\cdot}7$	35	15·9	1·7	4·2	5·9
		40	20·7	3·0	5·6	8·6
		45	25·3	4·1	7·2	11·3
		50	30·2	5·8	8·8	14·6
3	$E_R = 0$ $E_s = 0$	35	16·9	2·6	4·4	7·0
		40	21·5	4·2	5·8	10·0
		45	26·5	5·5	7·4	12·9
		50	31·3	7·3	9·1	16·4
4	$E_R = 0{\cdot}7$ $E_s = 0{\cdot}7$	35	15·7	1·8	4·1	5·9
		40	20·4	3·2	5·6	8·8
		45	24·4	4·4	6·9	11·3
		50	31·1	6·6	9·0	15·6

* Based on $\varepsilon = 1$ for the trench surfaces and $\varepsilon = 0{\cdot}78$ (i.e. oxidised copper[7]) for the return and supply pipes in the experimental rig.

the side-by-side configuration, relative to the hot above the warm pipe, the convective plus conductive contribution is significantly increased whereas the radiation component remains relatively unchanged.

CONCLUSIONS

There is an optimal configuration which leads to the least rate of heat being lost from the supply (i.e. the hot) pipe. Having a supply pipe above a return (i.e. the cooler) pipe in cold rectangular enclosures leads to lower rates of steady-state heat loss than with any 'side-by-side' (i.e. the conventional practice) arrangement or with the warm-above-hot pipe configuration within that same enclosure under identical boundary temperature conditions. A maximum reduction in the total rate of heat loss through the air of approximately 17 per cent was obtained with a temperature difference, ΔT, of 20 °C between the wall of the trench and the outer surface of the supply pipe by using the optimal configuration, compared with that for the near conventional side-by-side configuration (i.e. $E_R = E_S = 0$). The 'hot-above-cooler' pipe configuration has the added advantage that it would permit the use of narrower (and hence cheaper) trenches compared with present conventional practice.

The return and supply pipes should, in a real system, be externally insulated, and their surface temperatures would be nearer that of the environment than has been adopted in the present series of simulation tests. The percentage differences in the rates of heat transfer for the considered configurations would then be even greater than indicated by the present results. Thus, the use of the optimal configuration for any particular set of insulated pipes would be economically worth while, because no additional insulants, compared with those used in present practice, would be required to achieve the improved insulation performances.

It is apparent that British Standard 4508 needs to be extended in order to include a recommendation with respect to the optimal location of district-heating pipelines in trenches.

If the trenches were filled with pebbles, the improvements obtained by using the hot above the relatively cooler pipe, rather than the conventional side-by-side system, would be less than for the present air filled cavity but, nevertheless, qualitatively the proposed configuration would still be preferred as smaller heat leaks would occur.

ACKNOWLEDGEMENT

Part of this paper was presented at the Pipetech '84 Conference in January 1984, held at Birmingham's Metropole Hotel and organised by Access Conferences Ltd. It is reprinted here with the organiser's permission.

REFERENCES

1. C. Mackenzie-Kennedy, *District heating: Thermal generation and distribution*, Pergamon Press, Oxford, 1979, pp. 2–3.
2. BS 4508, 'Specifications for thermally insulated underground piping systems: Part I: Steel cased systems with air gap', British Standards Institution, London, 1969.
3. S. Chakrabarti, S. D. Probert and M. J. Shilston, Optimal eccentric annuli (containing atmospheric-pressure air) for thermally insulating horizontal, relatively cold pipes, *Applied Energy*, 14 (1983), pp. 257–93.
4. R. F. Babus'Haq, S. D. Probert and M. J. Shilston, Improved configurations for district-cooling pipelines, *Applied Energy* 16 (1984), pp. 67–76.
5. J. H. Henderson, Combined installation of pipelines in different services, e.g., heating/cooling, *Proc. 2nd. Int. Convention on District Heating, Budapest*, VI (1973), pp. 49–61.
6. J. M. Mehta and W. Z. Black, Errors associated with the measurement of convective heat transfer coefficients, *Applied Optics*, 16(6), (1977), pp. 1720–26.
7. H. Grober, S. Erk and U. Grigull, *Fundamentals of heat transfer*, McGraw-Hill Book Co. Inc., New York, 1961, pp. 448–9.

APPENDIX 4

IMPROVED PIPELINE CONFIGURATIONS FOR DISTRICT-HEATING IN GREAT BRITAIN

COMBINED HEAT AND POWER ASSOCIATION – CHP '85

'CHP-DEVELOPMENTS AND DECISIONS'

'IMPROVED PIPELINE CONFIGURATIONS FOR DISTRICT-HEATING IN GREAT BRITAIN'

'IMPROVED PIPELINE CONFIGURATIONS FOR DISTRICT-HEATING IN GREAT BRITAIN'

SUMMARY

Factors influencing the heat losses from horizontal 'supply' and 'return' hot-water pipes, within an atmospheric-pressure air-filled, relatively cold, horizontal, rectangular sectioned, ground duct or trench are considered. This deliberately contentious paper has been written as a challenge to traditional practice, in order to prompt designers to become more aware of prospective energy and financial savings.

An experimental investigation, using the displacement ratios for the two pipes as the experimental variables, revealed the optimal configuration, i.e. that which achieves the minimum steady-state rate of heat loss from the supply pipe for the considered conditions. For a representative set of temperatures for the pipes and the inner surfaces of the trench, corresponding closely but approximately with those likely to occur in practice for district-heating systems, the optimal configuration of the supply and return pipes occurred at displacement ratios of +0.70 and -0.05, i.e. with the horizontal supply pipe in the upper region of the cavity, and the horizontal return pipe vertically below it; the pipes being equidistant from the vertical walls of the trench. This configuration is of significance with respect to achieving maximum energy thrift for district-heating pipelines, because it differs radically from the 'side-by-side' arrangement of pipes adopted traditionally in district-heating pipeline designs.

NOTATION

D — The common diameter of both the considered supply (i.e. the hot) and return (i.e. the *relatively* cooler) pipes, (m). [For the present tests $D = 28.5 \times 10^{-3}$ m].

E — Displacement ratio

$\{E_R = \left(1 - \frac{2H_R}{Y-D}\right)$ and $E_S = \left(1 - \frac{2H_S}{Y-D}\right)$ for the return and supply pipelines respectively, see Fig. 1.$\}$

G — Average vertical gap size $[= (Y-D)/2]$, (m).

g — Gravitational acceleration, (m/s^2).

Gr_D — Local Grashof number for the air flows in the rectangular trench, based on the diameter, D, of the supply pipe $[Gr_D = \beta g \Delta T D^3/\nu^2]$.

H_R, H_S — Minimum depths, i.e. the shortest vertical distances, below the upper horizontal internal surface of the trench of the return and supply horizontal pipes respectively, see Fig. 1, (m).

$\bar{h}$ — Overall heat-transfer coefficient, $(W/m^2\,°C)$

k — Thermal conductivity of the air, $(W/m\,°C)$

L — Axial length of the considered horizontal air-filled cavity, (m).

M — A dimensionless coefficient in the steady-state rate of conductive plus convective heat transfers through the air equation: it is dependent upon the geometry and temperature distribution of the system $[= \overline{Nu}_G/Gr_D^n]$.

$\overline{Nu}_G$ — Average Nusselt number for the steady-state conductive plus convective rate of heat loss through the air from the supply (i.e. the hot) pipe $[\overline{Nu}_G = \bar{h} G/k]$.

n — Power index of the Grashof number in the $\overline{Nu}$ versus Gr relationship, which describes the conductive and convective steady-state heat loss through the air.

$\dot{Q}_{cond+conv}, \dot{Q}_{rad}$ — Components of the steady-state rate of heat leak through the air from the horizontal supply pipe due, respectively, to conduction plus convection, and radiation, (W).

$\dot{Q}_{total}$ — Total steady-state rate of heat loss from the supply (i.e. the hotter) pipe through the air $[= \dot{Q}_{cond+conv} + \dot{Q}_{rad}]$, (W).

T_o — Steady-state temperature of the inner surfaces of the outer surrounding isothermal rectangular trench, as used in the present series of experiemntal tests - see Fig. 1, (°C)

T_R, T_S — Steady-state temperatures of the outer surfaces of the horizontal return and supply pipes respectively, see Fig. 1, (°C).

X, Y — Horizontal width and vertical extent, respectively, of the rectangular cavity as shown in Fig. 1, (m).

ΔT — Steady-state difference between the temperature of the outer surface of the supply pipe and the inner surface of the trench: i.e. $\Delta T = T_S - T_o$, (°C).

β — Coefficient of volumetric thermal expansion of the air, (K^{-1}).

ϵ — Emissivity of the appropriately identified surface.

ν — Kinematic viscosity of the air, (m^2/s).

Suffixes

cond — Due to conduction through the air.
conv — Due to convection of the air.
D — For the diameter of the pipes.
G — For the average gap size.
o — Of the inner surface of the rectangular trench.
R — For the pipe along which the hot water returns.
rad — Due to the net radiation loss from the supply pipe.
S — For the hot-water supply pipe.
total — Referring to the total steady-state heat leak through the air from the hot-water supply pipe.

Abbreviations

CHP — Combined heat and power
DH — District heating
SNG — Synthetic natural gas

1. DISTRICT HEATING

This is a method by which heat from a central source is distributed to residential, commercial or industrial consumers for space, water or process heating. The central source may be a boiler, a refuse incinerator, a geothermal source, solar energy, or 'waste'-heat, e.g. as a by-product of electricity generation [1-5].

The first district-heating schemes to be introduced in the U.K. were at Gorton and Blackley in Manchester during 1919, but they failed due to pipeline corrosion. Since then, various other systems have been installed, the best known of which is probably the Pimlico scheme using waste-heat from Battersea power station in London. When completed in 1956, hot water was pumped to 2403 apartments spread over 31 acres[6]. But the widespread installation of district heating has not occurred in the U.K. partly because of the high capital costs, as well as the abundance and still relatively low unit costs of fossil fuels.

Due to the 1973/74 and 1979/80 oil crises, and the political reluctance to permit nuclear power to substitute for other fuels as rapidly in the U.K. as in other countries (e.g. France), the problem of achieving energy thrift has become more urgent during the last decade[7]. In particular, the terms 'district heating' (DH) and 'combined heat and power' (CHP) have become increasingly familiar to many engineers, architects, planners and even to politicians [8,9]. However, unfortunately less than 1 per cent of the U.K. space-heating demand is at present supplied by district heating compared with more than 10 per cent in countries such as Denmark and Sweden[10]. In the USSR (the largest user of district heating in the world) and Eastern Block countries, it has proved to be extremely successful because of the compact, but boring, development of housing estates which results from centralised planning. It has been estimated that 55 per cent of the population of Europe could be supplied economically from district-heating plants, and this figure will probably rise during the next two decades, because the world's urban population is growing at a faster percentage rate than that for the total population[11]. By the time natural gas prices will have risen sufficiently for coal-derived synthetic natural gas (SNG) to become economic and available commercially, combined heat and power, together with district-heating schemes (CHP/DH), will probably have the potential to serve economically almost 30 per cent of the existing buildings in the U.K. [12]. However, pertinent experience to date [13,14] has often been less than satisfactory, although these predominantly employ mains heat-delivery systems *not* conforming to the relevant British Standards.

2. DISTRICT-HEATING PIPELINE DISTRIBUTION SYSTEMS

These can be classified as either (I) thermally-insulated clad pipes located in atmospheric-pressure air-filled rectangular trenches, which are slightly beneath ground level; (II) insulated pipes in such trenches, which are packed with loose-fill thermal insulants around the pipes; or (III) insulated pipes in trenches with poured-in-place concrete. The most frequently recommended and widely used system is that described in group (I) [15,16]. In the event of such a trench flooding, which occurs intermittently in Britain because of its maritime climate, possibly poor detailing of the trench or high water table, the drainage and evaporation from around the pipe would be more likely to ensue automatically than with distribution systems of types (II) or (III). If the insulant is allowed to remain damp, the moisture often reduces the insulant's effectiveness (sometimes permanently) as well as promotes corrosion of the underlying steel pipe, which is supposedly being protected by the insulant. The prime purpose of the outer case of the trench, in whatever form, is to protect the pipework and its thermal insulation against attack by water and chemical action during the anticipated life of the system [15]. However, excessive ventilation of the trench reduces the effective thermal resistance of the air cavity, and so usually should be constrained to the minimum, which is likely to be necessary to permit the moisture to disperse readily by diffusion via the air from the cavity.

3. THERMALLY-INSULATED PIPELINES

Unfortunately (from an energy-thrift viewpoint), in the past, some underground cross-country hot-water pipelines have occasionally been installed uninsulated but with corrosion-protection wrapping, in order to reduce the required initial capital investments and the subsequent maintenance problems, but then the running costs are relatively high[17]. Nevertheless much time, effort and money have been devoted to producing reliable, cheap thermally-insulated underground pipelines but, regrettably to date [16], these have not been completely successful.

In the USSR, where pumping distances are immense, and in Iceland, where the heat sources are often geothermal springs, single-pipeline DH systems have been used [18]. On the continent of Europe, it is most common to use double-pipe systems, comprising of a 'supply' pipe conveying the hot water (at ~90°C) to the customer, and a 'return' pipe taking the water from which heat has been extracted by the customer (but which is still much higher in temperature than the environment) back to the central boilers.

Most hot-water distribution systems nowadays are based on the 'side-by-side' two-pipe layout[19]. Unfortunately, attention has not so far been focussed upon the financial savings which can be achieved by reducing the heat losses resulting from choosing the optimal configuration for such pipes in a duct.

4. SCOPE OF THE PRESENT TESTS

The present investigation is an abstraction from reality, in order to comprehend the energy-thrift

possibilities of what can be achieved through better design of a double-pipe DH system. It involved measuring the steady-state rates of heat transfer across the atmospheric-pressure air-filled gap between an isothermal 'cold' horizontal, rectangular sectioned, trench enclosing:

i) initially, a single horizontal hot pipe (i.e. the supply pipeline) - see Fig. 1; and subsequently

ii) two horizontal pipes, the first carrying hot water (i.e. the supply pipe), and the other, slightly cooler water (i.e. the return pipe) - see Fig. 2.

These systems involved air-filled cavities rather than having pebbles, for instance, around the pipes (as frequently occurs in practice) because the tested arrangements indicate the upper limits of convection effects upon the rate of heat transfer. With system (i), the aim was to determine the optimal position of the hot (i.e. the supply) pipe, which results in the minimum rate of heat loss for a specified steady-state temperature difference $\Delta T (= T_S - T_O)$ between the pipe and its rectangular trench. Then for system (ii), using this optimal position of the supply pipe as identified from experiments with system (i), the optimal position of the return pipe was identified experimentally, so that the least steady-state rate of heat loss from the supply pipe, for a prescribed ΔT, occurs.

The convective flow patterns within the enclosed air-space were observed by injecting smoke particles very slowly into the illuminated rectangular trench. Flow visualisations for different steady-state surface temperatures of the pipes and trench, and for different geometric configurations, were needed to stimulate the development of, supplement and corroborate conclusions being drawn from interferometric indications of the steady-state isotherms in the air gap[20].

In practice, T_O is likely to be less on the upper surface of the trench than at its base, because during winter the ambient environment air temperature will probably be low compared with the ground temperature. However when the district-heating system is in operation, the temperature gradients along the vertical surfaces of an actual trench in such circumstances will be very small because of the compensating effect of convective losses from the hot pipes in the trench leading to the upper top strata of air being the hotest air region. Thus the isothermal assumption is a reasonable first approximation for the present design-optimisation exercise. In practice, there would be a small non-uniform vertical temperature gradient along the sides of the concrete duct, but the relatively small effect of this would have to be assesssed as a separate investigation when the probable magnitude of the gradient for each particular application is known.

Because controllers of district-heating schemes aim to distribute the maximum amount of heat to their customers, they are concerned primarily with recucing the heat losses from the supply pipelines during transmission. So, only losses from these pipes were considered in the present experimental investigation. Nevertheless, in practice, the return pipe would also be well insulated thermally.

5. THE EXPERIMENTAL RIG

The values of the experimental parameters (see Figs. 1 and 2) chosen for this investigation were:

i) **For the single-pipe system:**

$X = 100$ mm, $Y = 100$ mm, $L = 630$ mm,
$D = 28.5$ mm

$$-0.5 \leq E_S \leq 0.9$$
$$17^\circ C \leq T_S \leq 40^\circ C$$
$$4^\circ C \leq \Delta T \leq 25^\circ C$$

ii) **For the double-pipe system:**

$X = 100$ mm, $Y = 125$ mm, $L = 650$ mm
$D = 28.5$ mm

$$-0.6 \leq E_R \text{ or } E_S \leq 0.7$$
$$10^\circ C \leq T_O \leq 20^\circ C \leq T_R \leq 30^\circ C \leq T_S \leq 50^\circ C$$

Each of the temperatures stated were accurate to $\pm 0.2^\circ C$, and the dimensions to 0.2 mm.

The main instrument used was an 18 cm field-of-view, 3 mW He-Ne laser-stimulated, Mach Zehnder interferometer[21]. This, when employed in the infinite-fringe mode, produced distinctive interferograms which are isothermal maps of the air-filled cavity for each two-dimensional configuration examined and set of values of T_O, T_R and T_S. (These interferograms indicated the refractive index, and hence density and consequently temperature, variations of the air integrated over the axial length of the considered cavity).

6. THE OBSERVATIONS

(i) For the Single-Pipe System

A4 enlarged photographic prints of the steady-state interferograms were produced for analysis[21]. It was suggested[22] that for the combined conductive plus convective heat leaks through the air, $\overline{Nu}_G = M\, Gr_D^n$. However for this system, M is effectively an indication of the conductance of the air surrounding the pipe: for a constant Grashof number, Gr_D, all the parameters affecting the conductive plus convective heat transfer relationship except the overall heat-transfer coefficient, $\bar{h}$, are constant. Thus the minimum rate of heat transfer from the pipe is obtained for the system configuration with the minimum value of M, i.e. the configuration for which the air provides the maximum thermal resistance of the pipe. The value of M for this system was deduced and plotted versus the displacement ratio, E_S (see Fig. 3). The value of 'M' was a maximum at the least displacement ratio employed, i.e. at $E_S = -0.5$, and decreased slowly to its value at $E_S = 0.3$, where

it began to decrease more rapidly. The minimum occurs at $E_S = 0.70 \pm 0.03$, which represents the approximate value for the optimal location of the single horizontal pipe in the rectangular trench considered, and for the temperature distribution tested. The radiative component of the steady-state rate of heat flux across the cavity would be independent of the displacement ratio for an infinitely-long pipe and trench. So the optimal position, as deduced from the 'conduction plus convection through the air' data, is to a good first approximation also that if the total heat leak through the air had been considered.

(ii) For the Double-Pipe System

Flow visualisations were undertaken for several different geometrical configurations. These indicated the occurrences of flow instabilities, and helped in the heat transfer interpretations of the interferograms [20]

Steady-state contour maps of isotherms were obtained for the four different configurations examined (see Fig. 2), with various values of ΔT. The interferograms with the hot horizontal pipe below the relatively cooler horizontal pipe arrangement (i.e. configuration 2) were not analysed in detail because the flow visualisation observations as well as experience indicated that this was the worst 'thermal insulation' situation (i.e. the rate of heat transfer was enhanced, rather than reduced, compared with that obtained with the conventional arrangement - i.e. configuration 3). Severe convective instabilities, as well as the plume oscillating from side-to-side, occurred and hence the relatively high rates of loss of heat that ensued.

For the 'hot-above-cooler' pipe arrangement (i.e. configuration 1), the supply (i.e. the hot) pipe was positioned at a constant displacement ratio, E_S, equal to 0.7 (which corresponds to the optimal location for a single-pipe in a rectangular trench, as had been deduced previously). Five different displacement ratios, E_R, were then chosen for positioning the relatively cooler (i.e. the return) pipe directly below the hot pipe.

The value of 'M' for this system (i.e. the double-pipe system) is a complicated function of geometry and the surface temperatures. It needs vastly more data than are at present available for its general form to be deduced. This needs to be investigated further!

The way in which the total steady-state rate of heat loss, $\dot{Q}_{total}$, from the supply pipe was dependent upon the temperature difference, ΔT, for different configurations is shown in Table 1, together with its radiation component, $\dot{Q}_{rad}$, (which for this system depends on the location of the two pipes in the cavity). Its convective plus conductive component, $\dot{Q}_{conv + cond}$, through the atmospheric-pressure air in the cavity is also evaluated.

The $\dot{Q}_{total}$ values were plotted against the displacement ratio for the return pipe in order to determine its optimal position. For the considered circumstances, the optimal position occurred with $E_R = -0.05$ (see Fig. 4). These optimal data (i.e. $E_R = -0.05$, $E_S = 0.70$) apply within the temperature range and for the componnent sizes employed. A reduction of approximately 14% was obtained in the total rate of heat loss through the air, by using this optimal geometry for the 'hot-above-cooler' configuration compared with that for the 'side-by-side' arrangement, under a selected steady-state temperature difference of $\Delta T = 23^{\circ}C$.

As this ΔT is reduced, the percentage reduction in steady-state heat leak from the supply pipe, using the optimal geometry for configuration 1 rather than the 'side-by-side' configuration, increases. Therefore, in practice, for well-insulated pipes, the percentage improvement in the thermal resistance of the air achieved by using the present recommendation rather than the current conventional practice will probably be greater than the 14% value suggested here.

7. CONCLUSIONS

There is an optimal configuration, adherence to which leads to the least rate of heat being lost from the supply (i.e. the hot) pipe. With $E_S = 0.7$, an improvement of 13% in the thermal resistance of the air-filled cavity was obtained compared with current conventional practice (i.e. the use of systems with $E_S = 0$) - see Fig. 3.

Having a supply (i.e. the hot) pipe above a return (i.e. the cooler) pipe in a cold rectangular trench leads to lower steady-state rates of heat loss than with any 'side-by-side' arrangement or with the 'warm-above-hot' pipe arrangement, within the same trench under identical boundary temperature conditions. An optimal configuration (i.e. corresponding to least rate of heat loss from the supply pipe) occurred with $E_R = -0.05$ and $E_S = 0.70$.

A maximum reduction in the total rate of heat loss through the air of approximately 14% was obtained with a temperature difference, ΔT, of $23^{\circ}C$ between the wall of the trench and the outer surface of the supply pipe, by using this optimal arrangement, compared with that for the traditional 'side-by-side' arrangement (i.e. $E_R = E_S = 0$), see Fig. 4. The 'hot-above-cooler' pipe configuration has the added advantage that it would permit the use of narrower (and hence cheaper to excavate) trenches compared with the present conventional practice. Also the pipe-over-pipe configuration has already been assessed to be cheaper to install than the pipe-beside-pipe system.[24] Nevertheless, undertaking maintenance would be somewhat more difficult, e.g. requiring the use of mirrors when repairing the lower pipe. However, the average annual repair and preventative maintenance costs combined represent only ~1.2 per cent of the installed cost of underground district-heating pipelines[25]. Therefore installation and running costs are the main factors influencing the use of this optimal configuration.

TABLE 1 Steady-state heat leaks from the 0.65 m long supply (i.e. the hot) pipe through the air across the considered cavity: T_R = 30°C

Configuration	Geometrical Description Parameters	T_S (°C)	ΔT $(=T_S-T_o)$, (°C)	$\phi_{conv + cond}$ (W)	ϕ_{rad}* (W)	ϕ_{total} (W)
1	E_R = 0.05 E_S = 0.70	35	16.5	1.6	4.2	5.8
		40	21.4	3.0	5.7	8.7
		45	26.5	4.2	7.3	11.5
		50	31.6	5.9	9.0	14.9
1	E_R = 0 E_S = 0.70	35	16.6	1.5	4.2	5.7
		40	21.4	2.6	5.7	8.3
		45	26.4	4.1	7.3	11.4
		50	39.7	8.4	10.8	19.2
1	E_R = -0.05 E_S = 0.70	35	16.3	1.2	4.2	5.4
		40	21.5	2.4	5.8	8.2
		45	26.5	4.0	7.4	11.4
		50	31.4	5.4	9.1	14.5
1	E_R = -0.10 E_S = 0.70	35	16.5	1.7	4.3	6.0
		40	21.5	2.8	5.8	8.6
		45	29.2	4.7	8.0	12.7
		50	30.8	5.4	9.0	14.4
1	E_R = -0.20 E_S = 0.70	35	15.9	1.7	4.2	5.9
		40	20.7	3.0	5.7	8.7
		45	25.3	4.1	7.2	11.3
		50	30.2	5.8	8.8	14.6
3	E_R = 0 E_S = 0	35	16.9	2.6	4.4	7.0
		40	21.5	4.2	5.8	10.0
		45	26.5	5.5	7.5	13.0
		50	31.3	7.3	9.1	16.4
4	E_R = 0.70 E_S = 0.70	35	15.7	1.8	4.1	5.9
		40	20.4	3.2	5.6	8.8
		45	24.4	4.4	7.0	11.4
		50	31.1	6.6	9.1	15.7

* Deduced values based on ϵ = 1 for the trench surfaces and ϵ = 0.78 (i.e. for oxidised copper[23]) for the return and supply pipes' surfaces in the experimental rig.

An overall loss of about 6 per cent of the distributed heat is usually acceptable[26], but frequently the losses are higher. For example, the district-heating pipelines at Heathrow Airport suffered losses of about 9 per cent of the boiler-house output at peak loads, i.e. during January, whilst in July, due to the lower intermittent load demands then satisfied, this increased to 56 per cent[27]. The latter figure was reduced subsequently to about 35 per cent by increasing the insulant thickness on the pipes.

In reality for typically insulated pipelines, the 14% improvement in the thermal resistance of the air-filled cavity would amount to only ~ 3% gain in the overall thermal insulation of the system (i.e. allowing for the presence of the insulant on the pipes and the insulation provided by the earth surrounding the air in the trench). Nevertheless, over the life-time (> 30 years) of the pipeline system, this is still a very worthwhile benefit as its attainment incurs no additional capital expenditure, which could even be reduced by the measures suggested in this investigation.

Thus, from two completely independent viewpoints, (i.e. capital investment costs, and heat loss costs in operation), the configuration of pipes suggested in this paper has economic advantages over current traditional practice, and so deserves further attention by contractors.

ACKNOWLEDGEMENTS

The authors wish to thank the University of Technology, Baghdad, Iraq, for the award of a Research Fellowship to R.F. Babus'Haq.

REFERENCES

1. Int. District-Heating Assoc., District heating handbook: a design guide, Vol. 1, 4th ed., 1983, pp. 1-11.
2. W.R.H. Orchard, CHP: The nine-star energy option, Chartered Mech. Eng., 32(1), 1985, pp. 34-37
3. F. Nash, Waste heat and CHP, Heating and Ventilating Eng., 58(666), 1984, pp.5-9.
4. J.O. Kolb, Use of municipal solid waste for district-heating in St. Paul, Minnesota, Oak Ridge Nat. Lab., Tennessee, ORNL/TM-8076, 1982.
5. W. Kamler, Adaptation of municipal district-heating network to snow melting, Proc. 2nd. Int. District-Heating Convention, Budapest, 1, 1973, pp 143-168.
6. J.T. McMullan, R. Morgan and R.B. Murray, Energy resources, 2nd ed., Edward Arnold Publishers Ltd., London, 1983.
7. A. Grimes, The socio-economic aspects of district heating, Proc. Practical Aspects of DH and CHP Conf., Glasgow, 1981, pp. 27-32
8. D.J. Bennet, District heating and combined heat and power, Proc. Practical Aspects of DH and CHP Conf., Glasgow, 1981, pp. 5-9.
9. D.L. Williams, The architect's role in the design of district heating, Conf. District Heating for the Community, Bristol, 1969, pp. 19/1-19/4.
10. A.F. Postlethwaite, Combined heat and power activities in the U.K., Central Electricity Generating Board, Generation Development and Construction Division, Barnwood, Gloucestershire, 1981, pp. 1-6.
11. J.E. Mesko, Economic advantages of central heating and cooling systems, Proc. Symposium on Underground Heat and Chilled Water Distribution Systems, Washington DC, 1973, Report No. NBS-BSS-66, 1975, pp. 9-17.
12. W.R.H. Orchard and J.A. MacAdam, The potential of CHP/DH as a major energy-supply option for the U.K., Proc. District-Heating Association, 5th Nat. Conf., Torquay, Paper No. 14, 1983.
13. Anon., Planning for CHP heat, Heating and Ventilating Eng., 57 (660), 1983, pp. 22-24.
14. E.F. O'Sullivan, District-heating mains, J. Chartered Inst. Building Services, 6 (10), 1984, p. 73.
15. J.S. Quigg, Underground distribution systems, Building Services Eng., 44(9), 1976, pp. 40-41.
16. H.A. Borger, Available types of underground heat-distribution systems, Proc. Symposium on Underground Heat and Chilled Water Distribution Systems, Washington DC, 1973, Report No. NBS-BSS-66, 1975, pp. 52-59.
17. J.H. Henderson, Economic justification of thermal insulation of underground hot and chilled water piping. Proc. 1st. Int. District Heating Conv., Session 4, Section G(7), London, 1970, pp. 1-8.
18. J.R. Kell and P.L. Martin, Heating and air-conditioning of buildings, 6th ed., Architectural Press, London, 1984.
19. Union National Des Chambres Syndicales D'Entreprises En Genie Climatique, Règles professionnelles UCH 26/78, Promoclim A., 10(2) 1979, pp. 19-28.
20. R.F. Babus'Haq, S.D. Probert and M.J. Shilston, Steady-state heat losses from horizontal pipes in an air-filled rectangular concrete duct, Proc. I.Mech.E., Eng. Sci., Paper No. C090/84, Accepted for publication.
21. R.F. Babus'Haq, S.D. Probert and M.J. Shilston, Optimal location of a single horizontal pipeline in a rectangular, horizontal, air filled enclosure to achieve maximum thermal insulation, Applied Energy, 18(4), 1984, pp. 239-259.
22. U. Grigull and W. Hauf, Natural convection in horizontal cylindrical annuli, Proc. 3rd. Int. Heat Transfer Conf., Chicago, 2(60), 1966, pp. 182-195.
23. H. Gröber, S. S.Erk and U. Grigull, Fundamentals of heat transfer, 3rd. Ed., McGraw-Hill Book Co. Inc., New York, 1961, pp. 448-449.
24. P.S. Woods, The development of CHP/DH in London, Report 4, The costs of local heat distribution and building connections, Orchard Partners for the GLC, London, 1983.
25. A.B. Birtles and E.F. O'Sullivan, Operator experience of underground heat mains reliability in the U.K., Proc. District Heating Assoc., 5th. Nat. Conf., Torquay, Paper No. 9, 1983.
26. C. Mackenzie-Kennedy, District heating: thermal generation and distribution, Pergamon Press Ltd., Oxford, 1979, p. 136.
27. British Airport Authority, Boiler House 523: Cargo terminal area - Heathrow Airport, London, BAA leaflet, 1975, pp. 1-2.

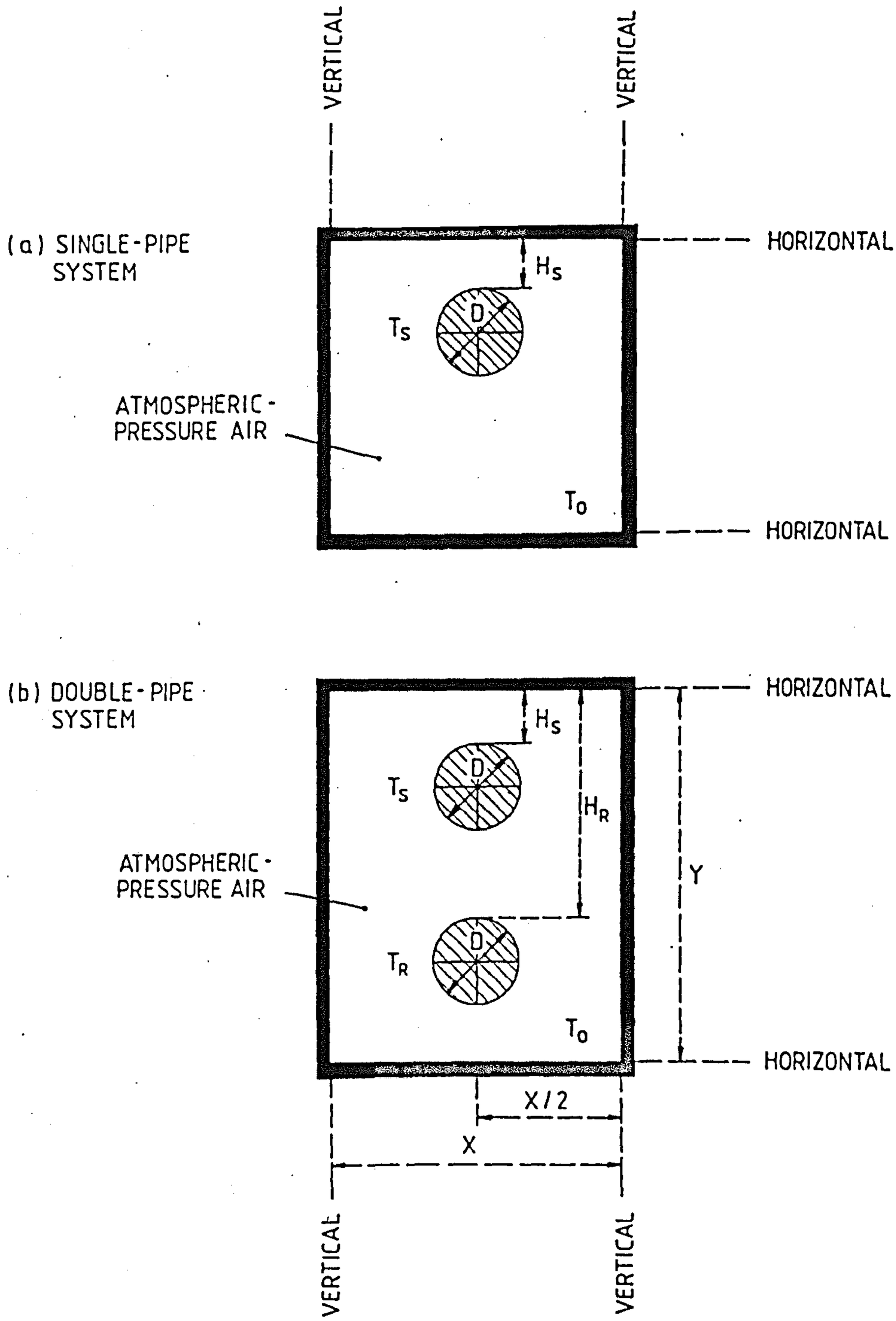

FIG. 1 Schematic representations of vertical sections through the considered horizontal pipes in their respective rectangular trenches

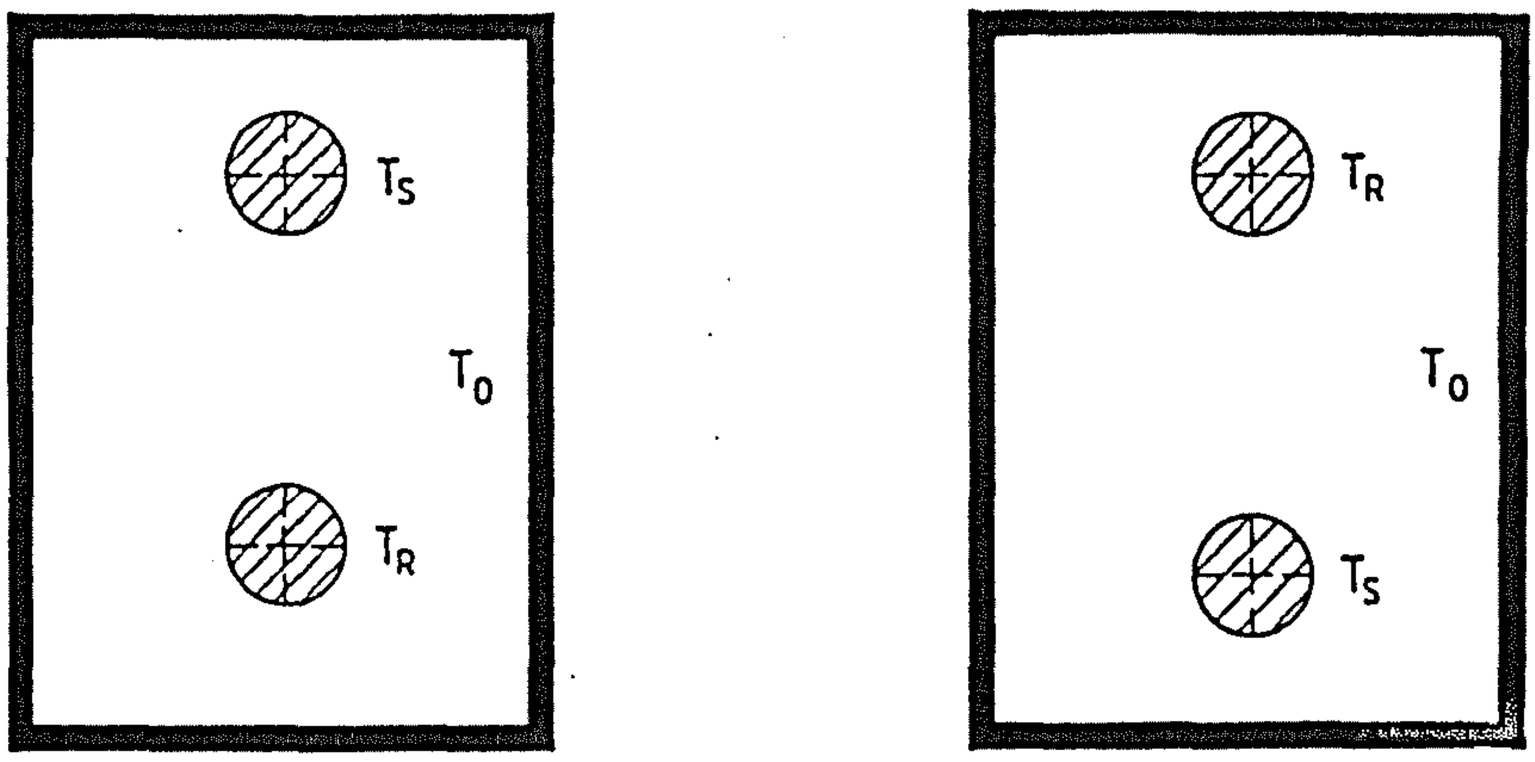

CONFIGURATION 1
$(-0{\cdot}65 < E_R \leqslant 0{\cdot}05, E_S = 0{\cdot}7)$

CONFIGURATION 2
$(E_R = 0{\cdot}7, E_S = -0{\cdot}65)$

CONFIGURATION 3
$(E_R = E_S = 0)$

CONFIGURATION 4
$(E_R = E_S = 0{\cdot}7)$

FIG. 2 Schematic vertical sections, perpendicular to the lengths, of the experimental 'district-heating' horizontal pipeline systems tested.

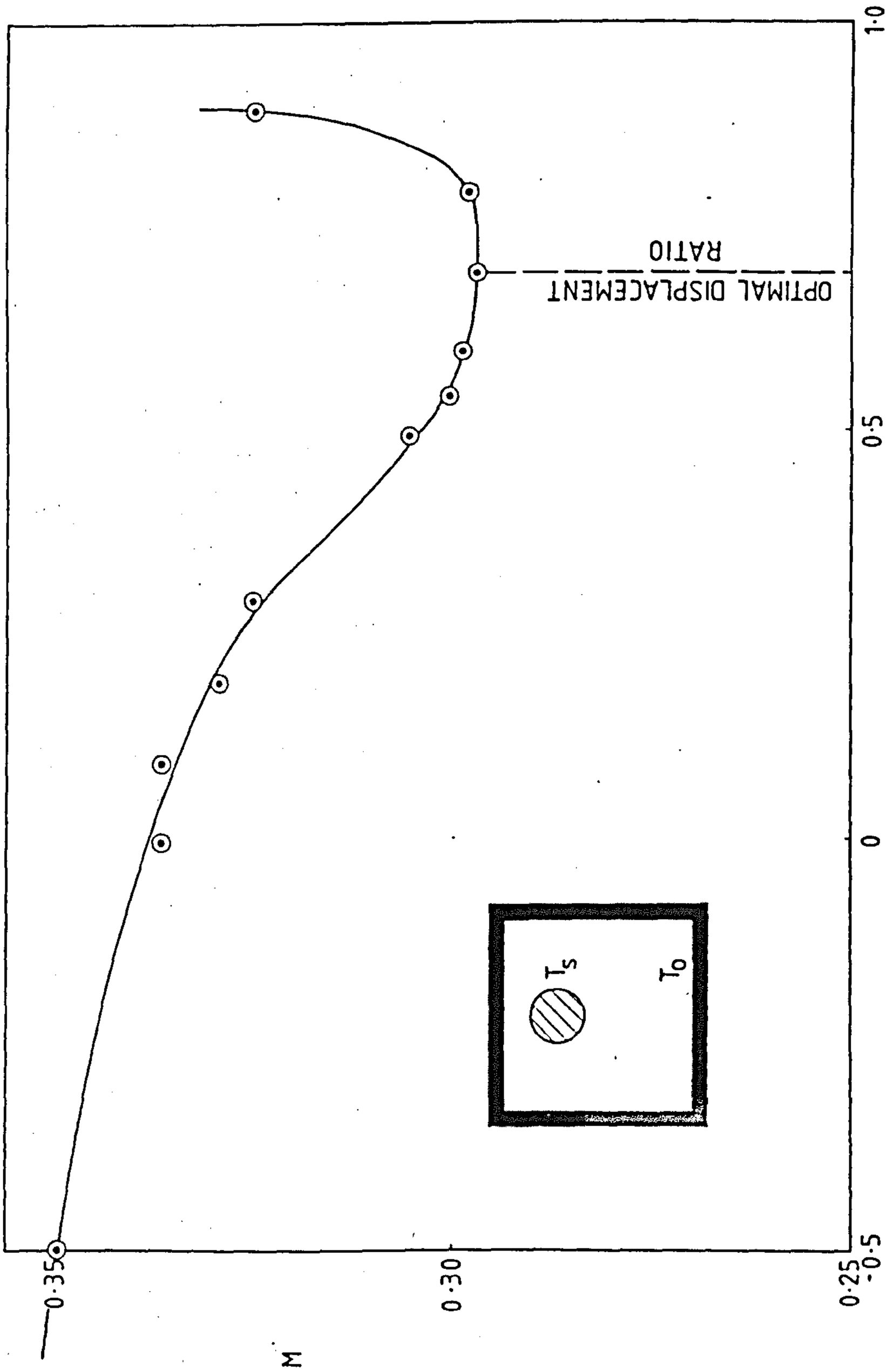

FIG. 3 Variation of M for the horizontal supply pipe in the horizontal rectangular section trench

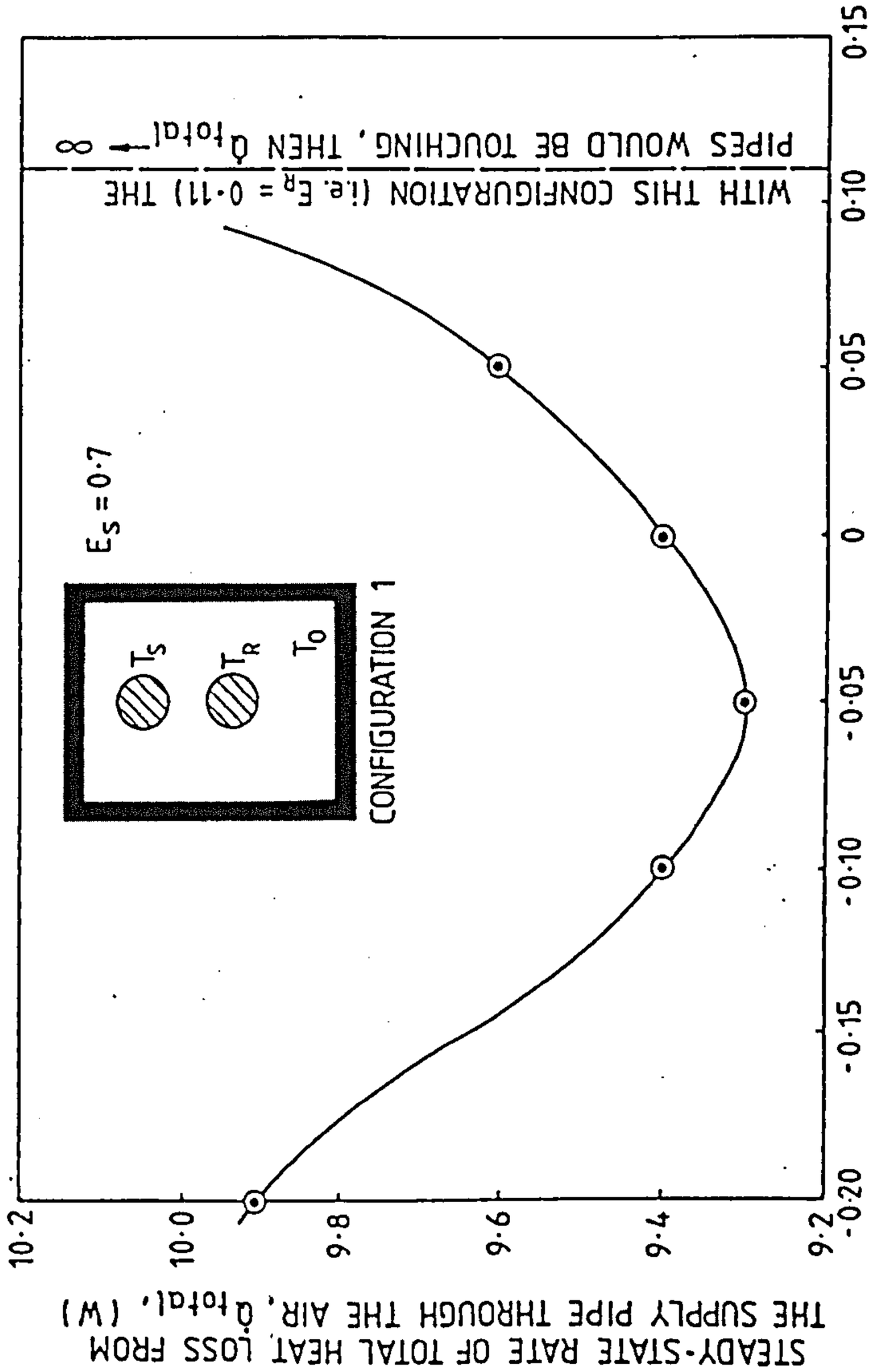

FIG. 4 Tot[illegible] steady-state heat leak, $\dot{Q}_{total}$, through the air for configuration 1 of the double-pipe system, with T_R = 30°C and ΔT = 23°C.

APPENDIX 5

INFLUENCE OF BAFFLES UPON NATURAL-CONVECTIVE STEADY-STATE HEAT TRANSFERS ACROSS HORIZONTAL AIR-FILLED ANNULI

SUMMARY

Flow patterns, temperature distributions and steady-state rates of heat transfer across horizontal, atmospheric-pressure, air-filled annuli have been determined. The optimal positions of two, low-conductivity, radial baffles inserted across (i) a concentric cavity with the heat flowing outwards, and (ii) an eccentric cavity with the heat flowing inwards were identified. It is feasible to interpolate from the way in which the results for these two quite different heat-transfer systems are presented, what will happen for other pipe-in-pipe configurations.

1. INTRODUCTION

Air (or a high molecular-weight gas) has frequently been employed as the insulant in the annular gap of some underground pipe-in-pipe systems for distributing hot or chilled fluids (i.e. for district-heating or cooling systems respectively, or horizontal cylindrical solar-energy collectors). Such gases, because of their low effective thermal conductivities, inhibit the heat transfers between the surfaces: the magnitude of the rate of heat leak depends on the geometry of the system (i.e. the gap width, G, and the diameter ratio, D/d), the bounding surface finishes, as well as upon the isothermal temperatures of the pipes (i.e. T_o and T_s).

The inner pipe is supported within the outer pipe by means of radial, conical, or axial baffles (or spacers). The resulting

obstructions of the annular space by such baffles will influence all three heat transfer modes (i.e. radiation, conduction, and natural convection). However, the effects of such baffles (in the considered systems) upon the radiation contributions over the range of temperatures considered for this investigation, are relatively small.

Extensive experimental and theoretical studies concerning natural convections across plain annular cavities, between horizontal concentric or eccentric pipes at uniform temperatures, have been reported[1,2]. Unfortunately there is a dearth of available published information about the heat-transfer perturbations, which result from the presence of baffles (or spacers) across air-filled cavities[3-8].

The aim of the present investigation was to determine the optimal position of a pair of radial balsa-wood baffles bridging the gap between:- (i) an isothermally hot inner pipe, placed concentrically in a relatively cold isothermal outer pipe, and (ii) an isothermally cold inner pipe placed at an optimal eccentricity (i.e. to achieve maximum thermal insulation of the plain cavity) of -0.65, i.e. in the lower half of the cavity[9], in a relatively hot isothermal outer pipe — see Figure 1. Several configurations were examined and investigations were carried out to determine if such baffles could improve the thermal resistance of the air-filled cavity over that of the unobstructed annulus. Steady-state isothermal contour maps (i.e. interferograms obtained with the Mach-Zehnder interferometer used in the infinite-

fringe adjustment -- see Figure 2) were photographed. Qualitatively interpreted flow visualisations were used to suggest and to substantiate the quantitative explanations obtained from the corresponding temperature-field interferograms - see Figure 3.

2. THE EXPERIMENTAL RIG

The chosen values of the experimental variables were:-

$$108.0 \text{ mm} \leq D \leq 140.5 \text{ mm}$$

$$28.5 \text{ mm} \leq d \leq 82.5 \text{ mm}$$

$$e = -0.65 \text{ or zero}$$

$$L = 610.0 \text{ or } 660.0 \text{ mm}$$

$$-30\ ^{\circ}C \leq \Delta T \leq 50\ ^{\circ}C$$

$$6.0 \times 10^4 \leq Gr_d \leq 1.3 \times 10^6$$

Each of the measured temperatures was accurate to $\pm$ 0.2 °C, and the stated dimensions to $\pm$ 0.2 mm.

2.1. Flow Visualisations

These were obtained with a rig having a horizontal, outer, cylindrical, polymerised methyl methacrylate (trade names for which are Perspex, Plexiglass, or Lucite), pipe (with D = 114.0 mm or 108.0 mm for heat flowing outwards or inwards respectively) which had been painted matt black, except for a narrow circumferential transparent slit window (~ 5 mm wide) in an axial direction at 0.33L from the end-plate nearer the camera. This

pipe was cooled or heated as required by circulating chilled or hot water *respectively* through a polythene tube, which was wrapped uniformly, in the form of a single-layer *closely-wound* spiral around the pipe. The steady-state temperature (T_o) of the inner surface was monitored by copper-constantan thermojunctions embedded in the outer surface, so that the thermocouple leads and thermojunctions remained flush with the inner surface.

For the heat flowing outwards experiments, the hot inner stainless-steel pipe (having d = 76.0 mm) was located concentrically (i.e. e = zero) with the outer pipe. The inner pipe was heated by an eddy-current dissipation induced from a low voltage, high amperage transformer. Guard heaters were incorporated at the ends of the pipe-in-pipe configuration in order to inhibit axial heat losses. Copper constantan thermocouples were used to indicate the inner pipe's temperature (T_s).

The cold inner copper pipe (having d = 28.5 mm) for the heat flowing inwards, was supported at an optimal eccentricity e of -0.65 by means of horizontal hollow tubular extensions at its two ends: these tubes also conveyed the relatively cold water (at approximately T_s) into and out of the inner pipe.

The thin radial baffles(3 mm thick at their outer extremities and tapering off to 1 mm at their tips touching the inner pipe) were of balsa-wood, which has a thermal conductivity (~ 0.12 W/mK): they were positioned to span the air gap along its whole length L -- see Figures 1 and 2 . The cavity was sealed by means

of the end-plates (see Figure 2), and a small amount of smoke was injected very slowly into it: photographs were taken of the resulting steady-state flow patterns which became fully observable ~ 15 seconds later -- see *Figure 3. The appropriate illumination* was introduced transversely from three halogen projectors via the thin circumferential slit window in the outer pipe.

2.2. Interferometry

The design of the test cell (with D = 127.0 mm and d = 82.5 mm) in the case of heat flowing outwards was qualitatively similar to that for the system used for the flow visualisations tests.

For the heat flowing inwards, shellac-insulated copper wires were wound uniformly in a tightly-grouped helical spiral around the external surface of a stainless-steel outer pipe (having D = 140.5 mm). A second layer of such wires was wound on top of the first, and connected in series electrically, so that the same electric current passed through it in the reverse direction to that in the first layer. Thereby non-inductive heating was achieved, so avoiding eddy current induced heating of the inner pipe. A guard heater, also in the form of a cylindrical coil around the outer pipe, and variable transformers were employed to permit one to select accurately the rate of inward heat transfer to the inner pipe. Copper-constantan thermocouples were employed to determine the temperature T_o of the inner surface. The inner

copper pipe (with d = 42.5 mm) was similar in its construction to that used in the flow visualisations studies.

An 18 cm field-of-view, 3mW He - Ne laser stimulated, Mach-Zehnder interferometer was used as the temperature-field indicating instrument -- see Figure 2. The effects of image distortion, due to the refraction of the laser beam through the test cell, were reduced by focusing the camera on the vertical plane at 0.33L from the end-plate nearer the camera[10].

3. DISCUSSION

3.1. Heat Flowing Outwards

Baffles, when introduced into a natural-convective flow field, can obstruct the paths of the air currents or by the establishment of slower moving air boundary layers, distort the shapes of the vortex patterns. Because of the geometries tested, vertical symmetry about the vertical plane through the centres of the pipes existed. The main flow cores rotated symmetrically, about the vertical plane through the centre-lines of the pipes, in opposite directions, one in each half of the annulus. With the pair of baffles arranged vertically(i.e. at $\Theta = 0°$ and $180°$), a stable coil-like vortex was observed adjacent to the upper baffle (i.e. at $\Theta = 180°$)[5], and so the rate of the convective heat transfer and consequently local Nusselt numbers were greater than those for the plain cavity (i.e. with no baffles present) with identical values of T_o and T_s.

As the inclination of the baffles was reduced to $\Theta = \pm 150°$, the local Nusselt numbers gradually approached those for the corresponding unobstructed annulus. However, for baffles positions throughout $\pm 60° \leq \Theta \leq \pm 120°$, a very stable crescent-shaped flow pattern ensued[5]. The fluid moved much more slowly around the bottom half of the annulus than it did in both the plain cavity or that containing the vertical baffles, so corroborating the quantitative results deduced from the heat-transfer measurements.

The effect of changing the inclination, Θ, of the baffles, upon the total rate of convective heat transfer travelling outwards across the air-filled cavity can be seen in Figure 4. The optimal location for a pair of radial baffles occurred at $\Theta = \pm 60°$ approximately. By employing this configuration, a reduction of ~ 20% in the steady-state convective heat transfer was achieved compared with that for a plain annulus. However, by using one vertical baffle (i.e. at $\Theta = 0°$), an increase of ~ 8% in the convective heat leak was observed compared with that for the unobstructed cavity under identical conditions. Conclusions drawn from the present set of results agree well with that of Kwon et. al.[7] for the "3-spacers Λ " configuration.

In addition, results drawn for two concentric pipes agree quantitatively with those of previous studies[2].

3.2. Heat Flowing Inwards

The flow pattern at the top of the annulus was considerably changed by the introduction of baffles at $\Theta = \pm 30°$: it indicated the presence of weaker than normal (i.e. with no baffles present) flow circulations. However, this beneficial reduction in the flow intensity (and hence in the rate of heat transfer) was more than off-set by a stronger recirculating flow in the relatively small lower compartment.

Generally, for configurations of baffles such that $\pm 45° \leq \Theta \leq \pm 120°$, the intensities of the recirculating eddies decreased in the lower sector as Θ increased, while the flow weakened in the upper sector. However, local Nusselt numbers were relatively small for regions adjacent to the upper part of the baffles, whereas near the undersides of the baffles, they attained higher values[8].

The air movements in the lower compartment, approximated to the flows in the unobstructed eccentric annulus with the baffles at $\Theta = \pm 150°$, under similar temperature differences across the air-filled gap, and no major qualitative changes in the steady-state fringe patterns of the interferograms were observed. However, local Nusselt numbers gradually approached those for the corresponding plain annulus.

When the pair of baffles was arranged vertically (i.e. at $\Theta = 0°$ and $180°$), two almost-stagnant zones adjacent to the middle

of the upper baffle, on its two sides, were observed. The presence of boundary layers on the baffles affected the convective heat leaks. This phenomenon coupled with the air flow deflection by the baffles, resulted in them having significant influences on the observed local heat-transfer coefficients.

The variation of the total rate of convective heat transfer travelling inwards across the annulus with the angle of inclination, Θ , of the baffles is shown in Figure 4. The optimal location for the pair of baffles occurred at $\Theta = \pm 140°$ approximately. By adopting such an arrangement, an increase of ~ 6% in the thermal resistance of the annulus compared with that for a plain unobstructed cavity could be achieved. However by employing a vertical baffle (i.e. at $\Theta = 0°$), an increase of ~ 14% in the convective heat leak was observed compared with that for the plain annulus under similar conditions.

4. CONCLUSIONS

There is an optimal configuration for two, low-conductivity baffles (or spacers) inserted symmetrically across the whole length of an annular, atmospheric-pressure, air-filled cavity, whose use leads to the least rate of convective heat transfer being achieved.

For the heat flowing outwards in the concentric annulus, with the two baffles inclined at an angle of $\pm 60°$, an improvement of ~ 20% in the thermal resistance was obtained compared with that

for a plain annulus. However, an increase of ~ 8% in the heat leak was observed, when the sole baffle was placed vertically (i.e. at $\Theta = 180°$).

By adjusting the two baffles to be inclined at $\pm$ 140° in an optimally eccentric cavity with the heat flowing inwards, an increse of ~ 6% in the thermal insulation across the cavity was achieved compared with that for an unobstructed annulus. However, an increase of ~ 14% was obtained in the convective heat leak if a vertical baffle at $\Theta = 0°$ was employed. It is preferable if the inclined insulating baffles appear tangentially from the upper surface of the inner pipe, then less convective currents upwords in the top sector will occur.

As the radiation contributions for the range of temperatures considered are less than 20% of the total heat flux, the 20% and 6% increases in the thermal resistance of the air-filled cavity mentioned previously would amount to only ~ 10% and ~ 3% gains respectively in the overall thermal insulation of the system. Nevertheless, these are very worthwhile benefits as their attainment involves no additional capital expenditures.

Results drawn from the present investigation agree qualitatively with those of previous studies[2,6,7].

NOMENCLATURE

d,D	Diameters of the outer surface of the inner pipe and the inner surface of the outer horizontal pipe respectively, see Figure 1, (m).
e	Eccentricity of the inner pipe relative to the outer one [= (H/G)]: $-1 \leq e \leq 1$.
G	Mean gap width [= (D - d)/2], (m).
Gr_d	Grashof number for the convecting air, based on the diameter, d, of the inner pipe.
H	Vertical distance between the horizontal centre-lines of the two eccentric pipes, see Figure 1, (m).
L	Axial length of the considered horizontal cavity, see *Figure 2, (m).*
$\overline{Nu}_G$	Average Nusselt numbers respectively, for the steady-state heat transfers from or to the inner pipe, according to the stipulated circumstances, based on the average gap width, G.
T_o, T_s	Steady-state uniform temperatures of the inner surface of the outer pipe, and the outer surface of the inner pipe respectively, see Figure 1, (°C).

ΔT Steady-state temperature difference[$=(T_o - T_s)$], (°C).

Θ Inclination of the baffles (or spacers), measured from zero for the vertically downwards radius vector, emanating from the centre of the inner pipe -- see Figure 1, (degrees).

REFERENCES

1. Kuehn, T. H., and Goldstein, R. J., An Experimental and Theoretical Study of Natural Convection in the Annulus Between Horizontal Concentric Cylinders, J. Fluid Mech., vol. 74, pp. 695-719, 1976.

2. Babus'Haq, R. F., Probert, S. D., and Shilston, M. J., Natural Convection Across Cavities : Design Advice, Applied Energy, vol. 20, pp. 161-188, 1985.

3. Grigull, U., and Hauf, W., Authors' Rebuttal, Natural Convection in Horizontal Cylindrical Annuli, Proc. 3rd. Int. Heat Transfer Conf., discussion volume, pp. 159-160,1966.

4. Lis, J., Experimental Investigation of Natural-Convection Heat Transfer in Simple and Obstructed Horizontal Annuli, Proc. 3rd. Int. Heat Transfer Conf., vol. 2, pp. 196-204, 1966.

5. Shilston, M. J., and Probert, S. D., Effects of Horizontal and Vertical Spacers on the Heat Transfer Across a Horizontal, Annular, Air-Filled Cavity, Applied Energy, vol. 4, pp. 21-37, 1978.

6. Norton, B., and Probert, S. D., Thermal Insulation of a Low Capital Cost Solar-Energy Collector, Applied Energy, vol. 6, pp. 323-327, 1980.

7. Kwon, S. S., Kuehn T. H., and Lee, T. S., Natural Convection in the Annulus Between Horizontal Circular Cylinders with Three Axial Spacers, Trans. ASME, J. Heat Transfer, vol. 104, pp. 118-124, 1982.

8. Babus'Haq, R. F., Probert, S. D., Shilston, M. J., and Chakrabarti, S., Influence of Baffles Upon Natural-Convective Steady-State Heat Transfers Inwards Across Horizontal Eccentric Annuli, Applied Energy, in press, 1986.

9. Chakrabarti, S., Probert, S. D., and Shilston, M. J., Optimal Eccentric Annuli (Containing Atmospheric-Pressure Air) For Thermally-Insulating, Horizontal, Relatively Cold Pipes, Applied Energy, vol. 14, pp. 257-293, 1983.

10. Mehta, J. M., and Black, W. Z., Errors Associated with the Measurement of Convective Heat-Transfer Coefficients, Applied Optics, vol. 16, pp. 1720-1726, 1977.

ACKNOWLEDGEMENTS

The authors wish to thank the University of Technology, Baghdad, Iraq, for the award of a Research Fellowship to R.F. Babus'Haq.

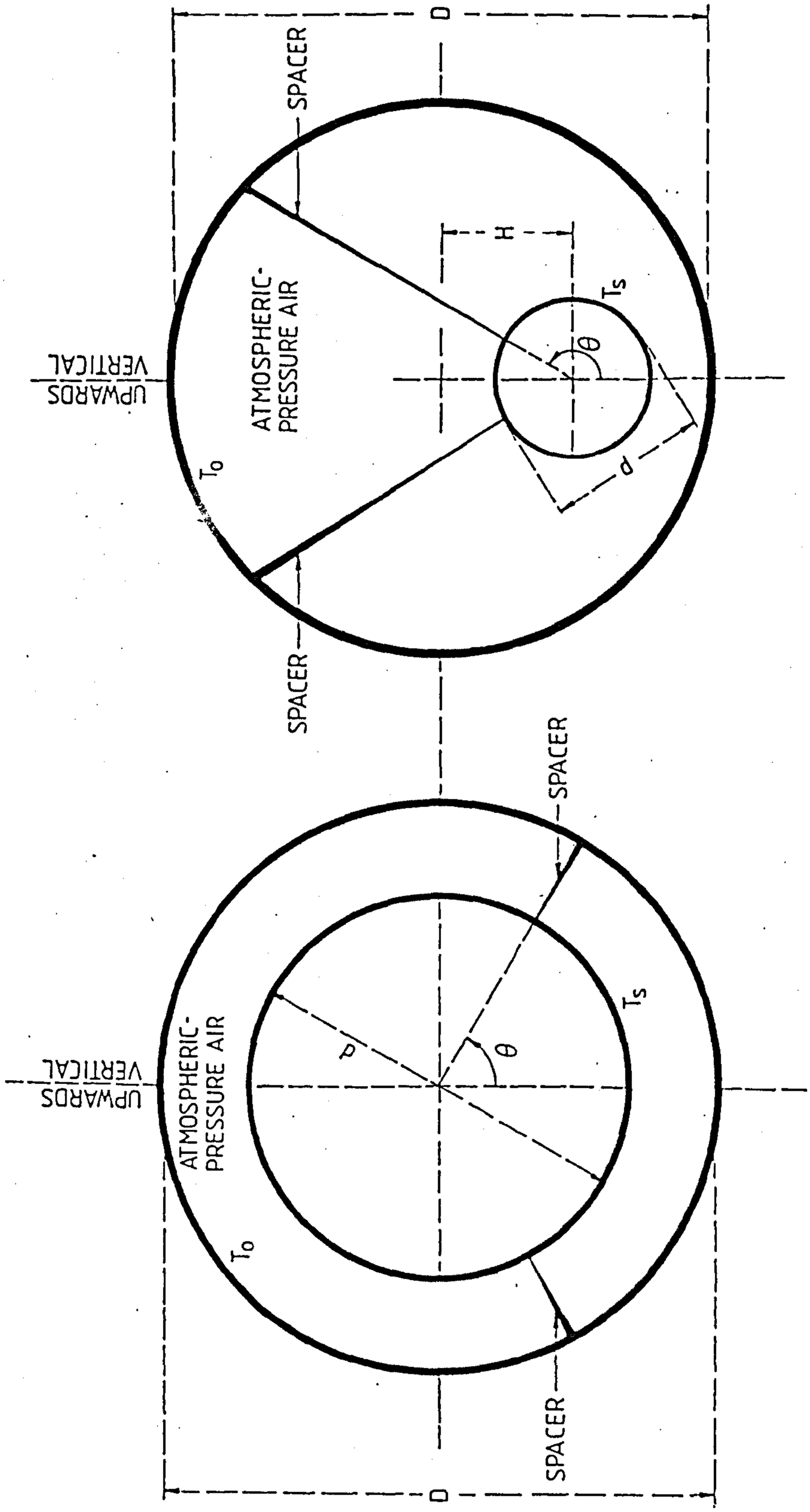

(A) CONCENTRIC SYSTEM :
HEAT FLOWING OUTWARDS ($T_s > T_o$)

(B) ECCENTRIC SYSTEM :
HEAT FLOWING INWARDS ($T_o > T_s$)

Fig. A5.1. Schematic representation of vertical cross-sections through the considered horizontal pipes.

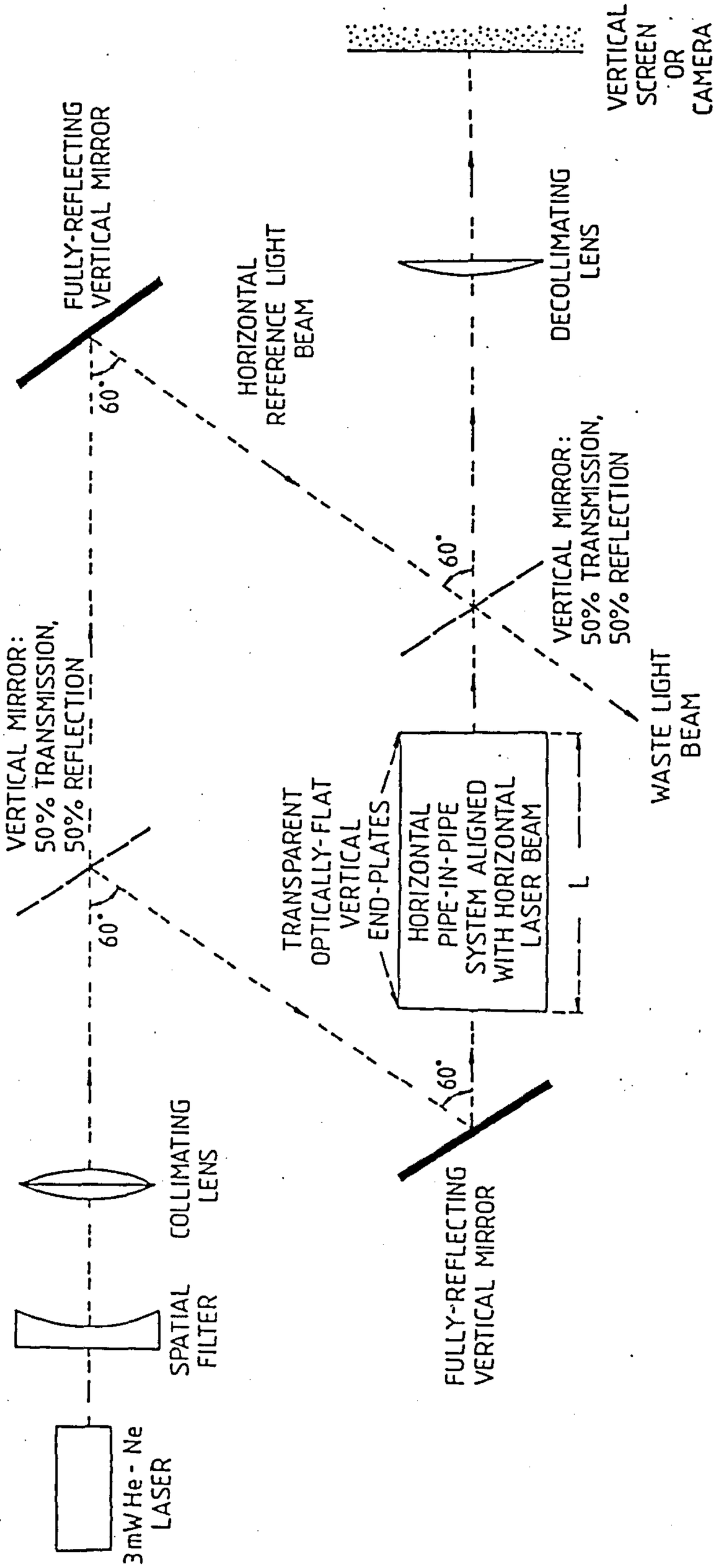

Fig. A5.2. Schematic horizontal plan of the 18 cm vertical field-of-view Mach-Zehnder interferometer.

Fig. A5.3. Typical steady-state flow visualisations for some of the considered systems, with e = - 0.65 and the heat flowing <u>inwards</u>:

(a) $\Theta = \pm 30^{o}$, $T_s = 14.3\ ^{o}C$, $\Delta T = 4.0\ ^{o}C$.

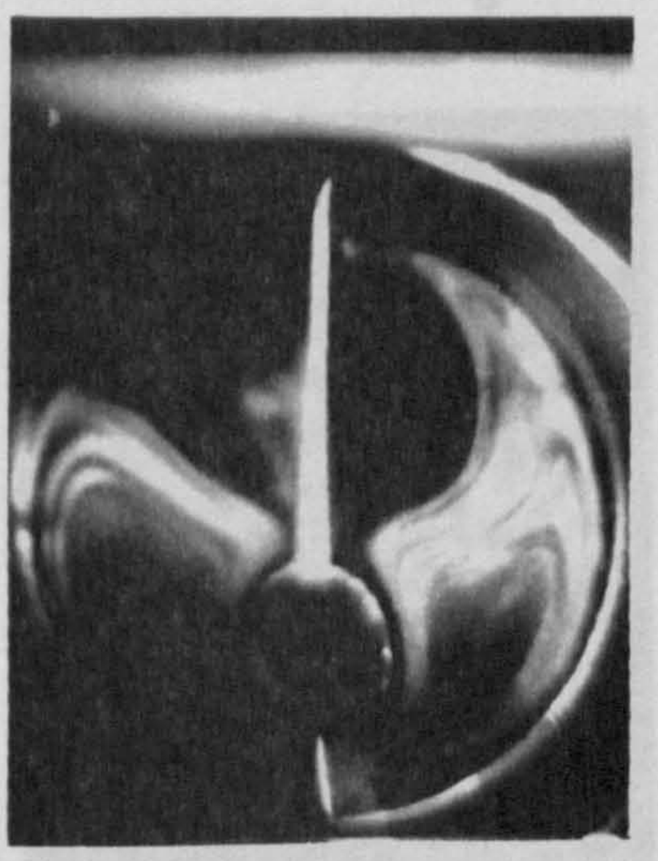

(b) $\Theta = 0^{o}$ and 180^{o}, $T_s = 12.5\ ^{o}C$.
$\Delta T = 6.0\ ^{o}C$.

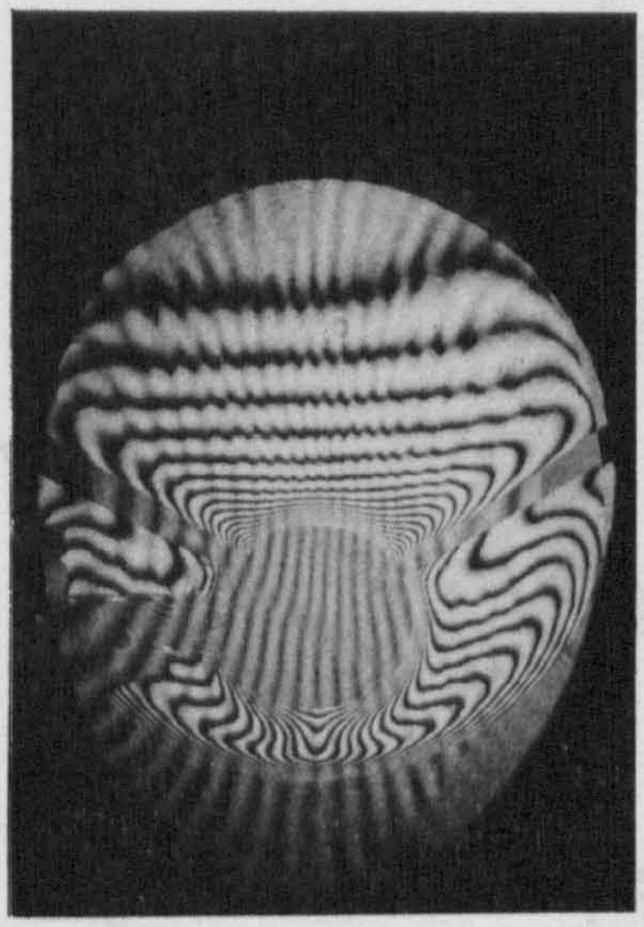

Fig. A5.4. Typical steady-state Mach-Zehnder interferograms for some of the considered systems, with e = - 0.65 and the heat flowing <u>inwards</u>:

(a) $\Theta = \pm 120^{o}$, $T_s = 7.6\ ^{o}C$, $\Delta T = 16.1\ ^{o}C$.

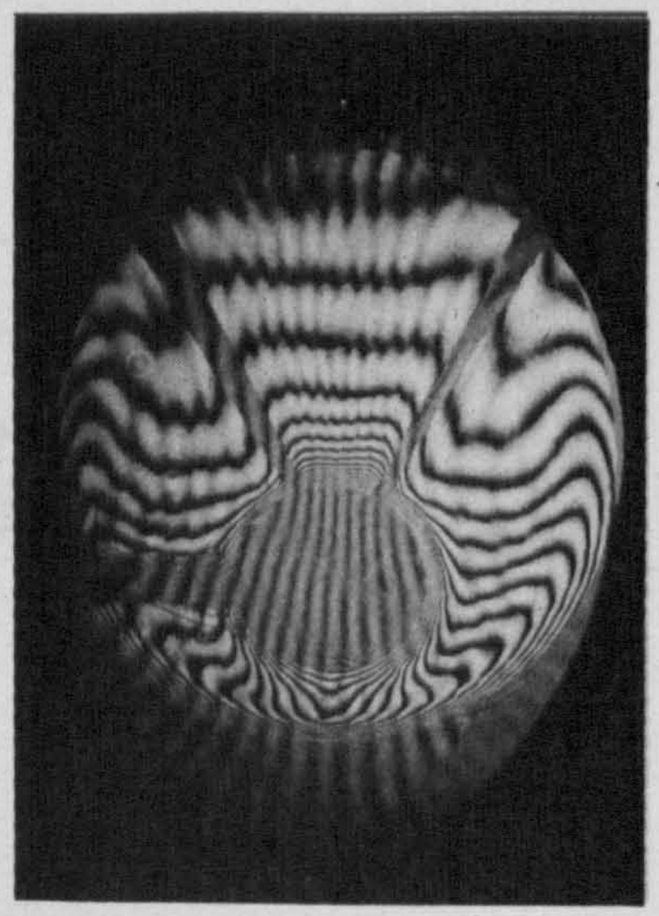

(b) $\Theta = \pm 150^{o}$, $T_s = 7.2\ ^{o}C$, $\Delta T = 15.0\ ^{o}C$.

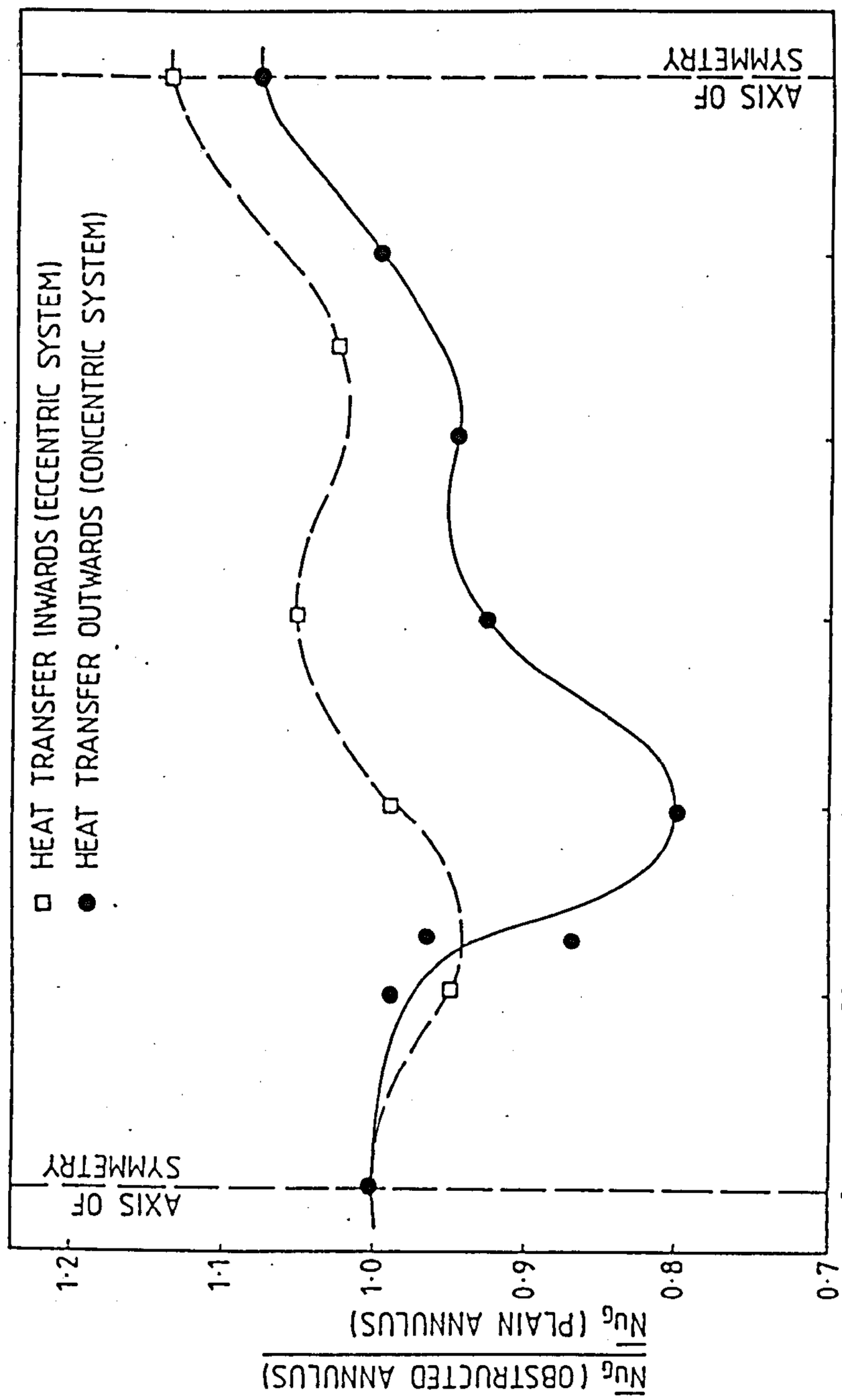

Fig. A5.5. Variations of the ratio of the average Nusselt numbers for the inner pipe with and without baffles present. For the 0^{o} and 180^{o} data presented, only one baffle (rather than two) was employed.